Ph 260 C1 (Magasin)

Peri-Tethys Memoir 4

Epicratonic Basins of Peri-Tethyan Platforms

Edited by
Sylvie CRASQUIN-SOLEAU
& Éric BARRIER

MÉMOIRES DU MUSÉUM NATIONAL D'HISTOIRE NATURELLE
TOME 179
1998

CCM

Source MNHN, Paris

Source : MNHN, Paris

BIBL. DU MUSÉUM PARIS

Bibliothèque Centrale Muséum
3 3001 00023269 3

Source : MNHN, Paris

MÉMOIRES DU MUSÉUM NATIONAL D'HISTOIRE NATURELLE

Rédacteur en chef *(Editor-in-Chief)* : Jean-Lou JUSTINE
Rédacteurs (*Editors*) : Jean-Marie BETSCH, Philippe BOUCHET, Christian ÉRARD & Jean-Lou JUSTINE
Assistantes de rédaction (*Copy editors*) : Bernadette GOTTINI-CHARLES & Laurence BÉNICHOU

Adresse (*Address*)
Mémoires du Muséum national d'Histoire naturelle
57, rue Cuvier
F-75005 Paris
Tél. : [33] 01 40 79 34 37
Fax. : [33] 01 40 79 38 08
e-mail : memoires@mnhn.fr

Les *Mémoires du Muséum national d'Histoire naturelle* publient des travaux originaux majeurs, tels que des monographies ou des volumes à auteurs multiples. Les auteurs sont invités, pour toutes les questions éditoriales, à prendre contact avec le directeur de la publication. Les manuscrits peuvent être en français ou en anglais.

The Mémoires du Muséum national d'Histoire naturelle *publishes major original contributions, such as monographs or multi-authored volumes. Prospective authors should contact the Editor-in-Chief. Manuscripts in French or English will be considered.*

Vente en France :

MUSÉUM NATIONAL D'HISTOIRE NATURELLE
SERVICE DES PUBLICATIONS SCIENTIFIQUES
Diffusion : Delphine HENRY
57, rue Cuvier
F-75005 Paris
Tél. : [33] 01 40 79 37 00
Fax : [33] 01 40 79 38 40
e-mail : dhenry@mnhn.fr

Sales Office:

UNIVERSAL BOOK SERVICES
Dr W. BACKHUYS
P.O. Box 321
NL-2300 AH Leiden
The Netherlands
Tel. : [31] (71) 517 02 08
Fax : [31] (71) 517 18 56
e-mail: backhuys@euronet.nl

Parution et prix irréguliers. Les ordres permanents d'achat et les commandes de volumes séparés sont reçus par le **Service des Publications Scientifiques, Diffusion** (pour la France et les DOM-TOM uniquement), ou par **Backhuys Publishers**. Catalogue sur demande. Une liste des derniers titres parus figure en page 3 de couverture.

Volumes are published at irregular intervals, and at irregular prices. Standing orders and orders for single volumes should be directed to the ***Service des Publications Scientifiques du Muséum****, (France and DOM-TOM only) or* ***Backhuys Publishers****. Price list and catalogues are available on request. Recently published memoirs are listed on page 3 of the cover.*

Printed on acid-free paper
Imprimé sur papier non acide

Source : MNHN, Paris

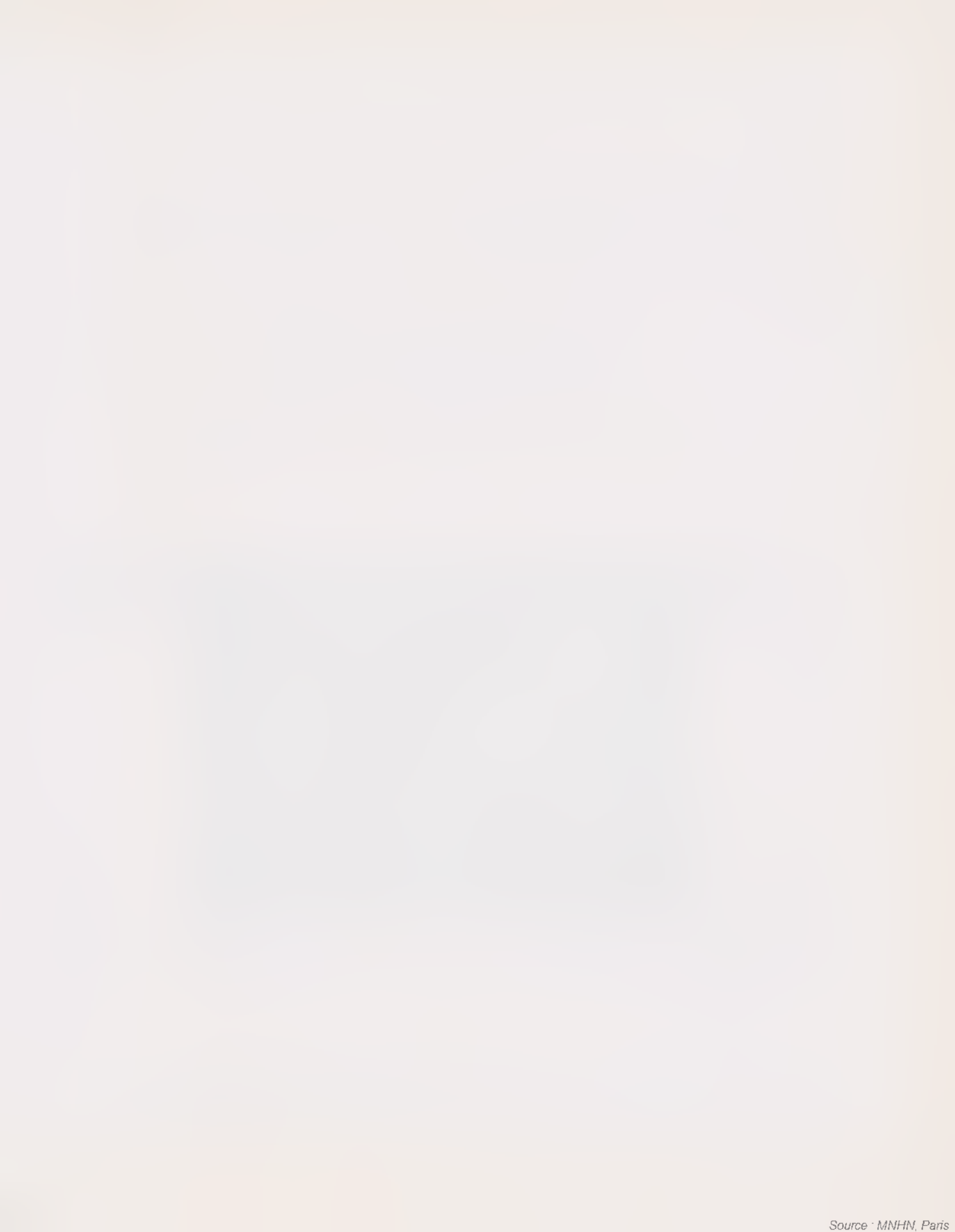

Source : MNHN, Paris

Cover photograph / *Photographie de couverture:*

Semenoviceras fauna, Akmysh, North side of west Karatau, Mangyshlak. Late Albian (see GAETANI *et al.*, this volume).

Faune à Semenoviceras, *Akmysh, versant nord de l'ouest Karatau, Mangyshlak. Albien supérieur (*GAETANI et al., *ce volume).*

The Peri-Tethys Program, sponsored by international industries (AGIP, ARCO, BRGM, CHEVRON, CONOCO, EAP(ELF), EXXON, SHELL, SONATRACH, TOTAL), research centres (CNRS, IFP), and a university (UPMC), started in 1993. It examines the influence of Tethyan evolution on the bordering cratons since its birth (through the break-up of Pangea), its life (by the extension and formation of oceanic seaways) and finally its death (by collision between the main bordering plates which led to inversion within the epicratonic basins).

Volumes déjà parus/*Previously published volumes*:

Peri-Tethys Memoir 1 (1994): *Peri-Tethyan platforms. Proceedings of the IFP/Peri-Tethys Research Conference.* Technip, Paris: 1-275. ISBN: 2-7108-0679-7.

Peri-Tethys Memoir 2 (1996): Structure and Prospects of Alpine Basins and Forelands. *Mém. Mus. natn. Hist. nat.*, **170**: 1-550 (+ Atlas). ISBN: 2-85653-507-0.

Peri-Tethys Memoir 3 (1998): Stratigraphy and Evolution of Peri-Tethyan Platforms. *Mém. Mus. natn. Hist. nat.*, **177**: 1-262. ISBN: 2-85653-512-7.

Peri-Tethys Memoir 4 (1998): Epicratonic Basins of Peri-Tethyan Platforms. *Mém. Mus. natn. Hist. nat.*, **179**: 1-294. ISBN: 2-85653-518-4.

Aussi/*Also:*

Peri-Tethys: stratigraphic correlations 1 (1997). 330 pp. *Geodiversitas*, **19** (2): 169-499. ISSN: 1280-9659.

Peri-Tethys: stratigraphic correlations 2 (1998). 224 pp. *Geodiversitas*, **20** (4): 515-738. ISSN: 1280-9659.

Source : MNHN, Paris

Peri-Tethys Memoir 4

Epicratonic Basins of Peri-Tethyan Platforms

Source : MNHN, Paris

ISBN : 2-85653-518-4
ISSN : 1243-4442
© Publications Scientifiques du Muséum, Paris, 1998

PHOTOCOPIES :

Les *Publications Scientifiques du Muséum* adhèrent au Centre Français d'Exploitation du Droit de Copie (CFC), 20, rue des Grands Augustins, 75006 Paris. Le CFC est membre de l'International Federation of Reproduction Rights Organisations (IFRRO). Aux États-Unis d'Amérique, contacter le Copyright Clearance Center, 27, Congress Street, Salem, Massachusetts 01970.

PHOTOCOPIES:

The Scientific Publications of the Muséum *adhere to the Centre Français d'Exploitation du Droit de Copie (CFC), 20, rue des Grands Augustins, 75006 Paris. The CFC is a member of International Federation of Reproduction Rights Organisations (IFRRO). In USA, contact the Copyright Clearance Center, 27, Congress Street, Salem, Massachusetts 01970.*

Source : MNHN, Paris

MÉMOIRES DU MUSÉUM NATIONAL D'HISTOIRE NATURELLE

TOME 179
GÉOLOGIE

Peri-Tethys Memoir 4

Epicratonic Basins of Peri-Tethyan Platforms

edited by

Sylvie CRASQUIN-SOLEAU [1] & Éric BARRIER [2]

[1] Université Pierre et Marie Curie / CNRS
Département de Géologie Sédimentaire
T15-25, E.4, case 104
4, Place Jussieu
F-75252 Paris Cedex 05

[2] Université Pierre et Marie Curie / CNRS
Département de Géotectonique
T.25-26, E.1, case 129
4, Place Jussieu
F-75252 Paris Cedex 05

PUBLICATIONS SCIENTIFIQUES
DU MUSÉUM
PARIS

1998

Source : MNHN, Paris

Source : MNHN, Paris

CONTENTS
SOMMAIRE

Pages

NORTHERN PLATFORM

1. **The Upper Jurassic of the Volga basin: ammonite biostratigraphy and occurrence of organic-carbon rich facies. Correlations between boreal-subboreal and submediterranean provinces** 9
Pierre HANTZPERGUE, François BAUDIN, Vassili MITTA, Alexander OLFERIEV & Victor ZAKHAROV

2. **Mesozoic of tbe Mangyshlak (West Kazakhstan)** 35
Maurizio GAETANI, Marco BALINI, Valery J. VUKS, Vera A. GAVRILOVA, Eduardo GARZANTI, Alda NICORA, Elisabetta ERBA, Élie CARIOU, Fabrizio CECCA, Isabella PREMOLI SILVA, Maria Rose PETRIZZO, Simonetta CIRILLI & Raffaella BUCEFALO PALLIANI

3. **Development and deformation of a Mesozoic basin adjacent to the Teisseyre-Tornquist Zone: The Holy Cross Mountains (Poland)** 75
Juliette LAMARCHE, Jolanta SWIDROWSKA, Françoise BERGERAT, Maciej HAKENBERG, Jean-Louis MANSY, Josef WIECZOREK, Ewa STUPNICKA & Thierry DUMONT

4. **The Mid-Cretaceous events in eastern Europe: development and palaeogeographical significance** 93
Evgenij J. BARABOSHKIN, Ludmila F. KOPAEVICH & Alexander G. OLFERIEV

5. **Evolution of the eastern Fore-Caucasus basinduring the Cenozoic collision: burial history and flexural modelling** 111
Andrei V. ERSHOV, Marie-Françoise BRUNET, Anatoly M. NIKISHIN, Sergey N. BOLOTOV, Maxim V. KOROTAEV & Svetlana S. KOSOVA

SOUTHERN PLATFORM

6. **Stratigrapbic analysis of the Upper Jurassic (Oxfordian-Kimmeridgian) Antalo limestone in the Mekele outlier (Tigrai, Northern Ethiopia): preliminary data** 131
Luca MARTIRE, Pierangelo CLARI & Giulio PAVIA

Source : MNHN, Paris

7. **Stratigraphic and palaeogeographie survey of the Lower and Middle Jurassie along a north-south transeet in western Algeria** 145
Serge ELMI, Yves ALMÉRAS, M'Hamed AMEUR, Jean-Paul BASSOULLET, Mohamed BOUTAKIOUT, Miloud BENHAMOU, Abbés MAROK, Larbi MEKAHLI, Abderrahmane MEKKAOUI & René MOUTERDE

8. **The Jurassie of the southern Levant. Biostratigraphy, palaeogeography and eyelie events** 213
Francis HIRSCH, Jean-Paul BASSOULLET, Élie CARIOU, Brian CONWAY, Howard R. FELDMAN, Lydia GROSSOWICZ, Avraham HONIGSTEIN, Ellis F. OWEN & Amnon ROSENFELD

9. **The central High-Atlas (Morocco). Litho- and chrono-stratigraphie eorrelations during Jurassic times between Tinjdad and Tounfite. Origin of subsidence** 237
André POISSON, Majid HADRI, Ahmed MILHI, Myriam JULIEN & Jean ANDRIEUX

10. **The Permian hasins of Tiddas, Bou Achoueh and Khenifra (central Morocco). Biostratigraphic and palaeophytogeographie implieations** 257
Jean BROUTIN, Habiba AASSOUMI, Mohammed EL WARTITI, Pierre FREYTET, Hans KERP, Cecilio QUESADA & Nadège TOUTIN-MORIN

INDEX 279

Source : MNHN, Paris

The Upper Jurassic of the Volga basin: ammonite biostratigraphy and occurrence of organic-carbon rich facies. Correlations between boreal-subboreal and submediterranean provinces

Pierre HANTZPERGUE [1], *François* BAUDIN [2], *Vassili* MITTA [3], *Alexander* OLFERIEV [4] & *Victor* ZAKHAROV [5]

[1] Université Claude Bernard, Centre des Sciences de la Terre, CNRS-UMR 5565
27-43, boulevard du 11 Novembre, F-69622 Villeurbanne Cedex, France

[2] CNRS-ESA 7073 & FR32, Département de Géologie Sédimentaire, Université Pierre et Marie Curie
case 117, 4 place Jussieu, F-75252 Paris Cedex 05, France

[3] Research Geological Oil Institute, VNIGNI, Shosse Entuziastov 36, 10581 Moscow, Russia

[4] Geosintez, Washavskoje Shosse 39A, 113525 Moscow, Russia

[5] Institute of Geology and Geophysics, Siberian Branch ofAcademy of Science, Novosibirsk 90, Russia

ABSTRACT

A detailed litho-biostratigraphic succession of the Upper Jurassic deposits of the middle Volga basin is described using six sections, including the lectostratotype of the Volgian. A new biostratigraphic scheme, displaying nineteen ammonite zones, is completed for the Russian Platform. Many biostratigraphic equivalencies between the Russian Platform and both the boreal-subboreal and the submediterranean provinces are proposed and discussed. Seven common horizons (*Pictonia densicostata, Pictonia baylei, Orthaspidoceras lallierianum, Aspidoceras caletanum, Aulacostephanus contejeani, Aulacostephanus yo* and *Aulacostephanus autissiodorensis*) are recognized for the Kimmeridgian Stage, that allow a remarkably precise correlation between the Russian Platform and the western european area. The equivalencies between Volgian, Portlandian and Tithonian are discussed. Correspondences can be only suggested by affinities of the endemic russian ammonites and the boreal faunas. Up to now, the local scheme appears still necessary. Bulk geochemical characterization of the Upper Jurassic series from the Russian Platform shows six main intervals with high organic content (Corg. >10%) and good petroleum potentials. Nevertheless, the stratigraphical distribution of black shales of the Russian Platform is different from those of the Kimmeridge Clay Formation. This clearly indicates that oil shale bands cannot be taken as marker beds at a large scale.

HANTZPERGUE, P., BAUDIN, F., MITTA, A., OLFERIEV, A. & ZAKHAROV, V., 1998. — The Upper Jurassic of the Volga basin: ammonite biostratigraphy and occurrence of organic-carbon rich facies. Correlations between boreal-subboreal and submediterranean provinces. *In*: S. CRASQUIN-SOLEAU & É. BARRIER (eds), Peri-Tethys Memoir 4: epicratonic basins of Peri-Tethyan platforms, *Mém. Mus. natn. Hist. nat.*, **179** : 9-33. Paris ISBN : 2-85653-518-4.

Source : MNHN, Paris

RÉSUMÉ

Le Jurassique supérieur du bassin de la Volga: biostratigraphie des ammonites et distribution des faciès riches en carbone organique. Corrélations entre les provinces boréale-subboréale et subméditerranéenne.

Une description litho-biostratigraphique détaillée des dépôts du Jurassique supérieur de la moyenne vallée de la Volga est établie à partir de six coupes, dont celle du lectostratotype du Volgien. Une nouvelle succession des faunes d'ammonites, comprenant dix-neuf zones, est proposée pour la plate-forme russe. De nombreuses corrélations entre les échelles biostratigraphiques de la plate-forme russe et celles des provinces boréale-subboréale et subméditerranéenne sont proposées et discutées. Sept horizons (*Pictonia densicostata, Pictonia baylei, Orthaspidoceras lallierianum, Aspidoceras caletanum, Aulacostephanus contejeani, Aulacostephanus yo* et *Aulacostephanus autissiodorensis*) sont communs pour le Kimméridgien, ce qui permet des corrélations très précises entre la plate-forme russe et l'Europe occidentale. Les équivalences entre Volgien, Portlandien et Tithonien sont discutées. Des correspondances peuvent juste être suggérées compte tenu des affinités entre les faunes endémiques russes et les faunes boréales. L'utilisation d'un schéma biostratigraphique local est encore nécessaire à ce niveau de l'étude. La caractérisation géochimique globale de la série du Jurassique de la plate-forme russe montre six intervalles principaux d'enrichissement en matière organique (Corg. > 10%), avec d'excellents potentiels pétroliers. La distribution stratigraphique des black shales de la plate-forme russe est différente de celle des principaux intervalles riches en matière organique de la Formation de Kimmeridge Clay. Ceci indique clairement que ces "bandes organiques" ne peuvent être utilisées comme des marqueurs lithostratigraphiques à une grande échelle.

INTRODUCTION

During Upper Jurassic, precise stratigraphical correlations present many difficulties because of the well known provincialism of ammonite faunas. They become acute progressively from the middle Oxfordian to the Tithonian, and it is necessary to separate schemes of standard ammonites zones for each province and to describe the succession that are to be correlated.

In the Russian Platform, the dominant faunas present boreal or sub-boreal affinities during the Oxfordian and lower Kimmeridgian times. Progressively, endemic ammonites occur in upper Kimmeridgian and in the Volgian faunal sequence.

Correlations with the primary standard of reference of the submediterranean province are the most imprecise. In the recent compilation of the parallel ammonites scales for tethyan northern margin (CARIOU *et al.*,1997; HANTZPERGUE *et al.*, 1997; GEYSSANT, 1997), the equivalence with russian faunal sequences was not taken into consideration. On the contrary, the faunal affinities between Oxfordian and/or Kimmeridgian of the Russian Platform allow best correlations with boreal and sub-boreal provinces. But the "Volgian province" named by NIKITIN (1881a) for the condensed and incomplete uppermost Jurassic sequences require a local faunal scheme. The established ammonite succession in the middle Volga basin should provide useful alternative standard of reference in an area in which another standard cannot be easily applied.

Though most of the sedimentary rocks contain dispersed organic matter from different origins, only a few of them can be considered as organic-rich (> 5% Corg.). Those having a high amount of marine organic matter (> 10 % Corg.) appropriate to generate hydrocarbons and presenting a high degree of immaturity can be considered as "oil shales". Such facies are widespread distributed in the Upper Jurassic succession of the Russian Platform.

The purpose of this paper is to precise the litho-biostratigraphic succession of Upper Jurassic of the Russian Platform, to propose correlations with other Late Jurassic ammonite zonations and to situate the black shales deposits in the stratigraphic framework in order to check their possible synchronicity with the main organic-rich intervals from the North Sea area.

SECTIONS

Five sections were studied in the Moscow basin and the Ulyanovsk-Saratov trough along the Volga River (Fig. 1). The precise location of each section is given in Fig. 2:

Source : MNHN, Paris

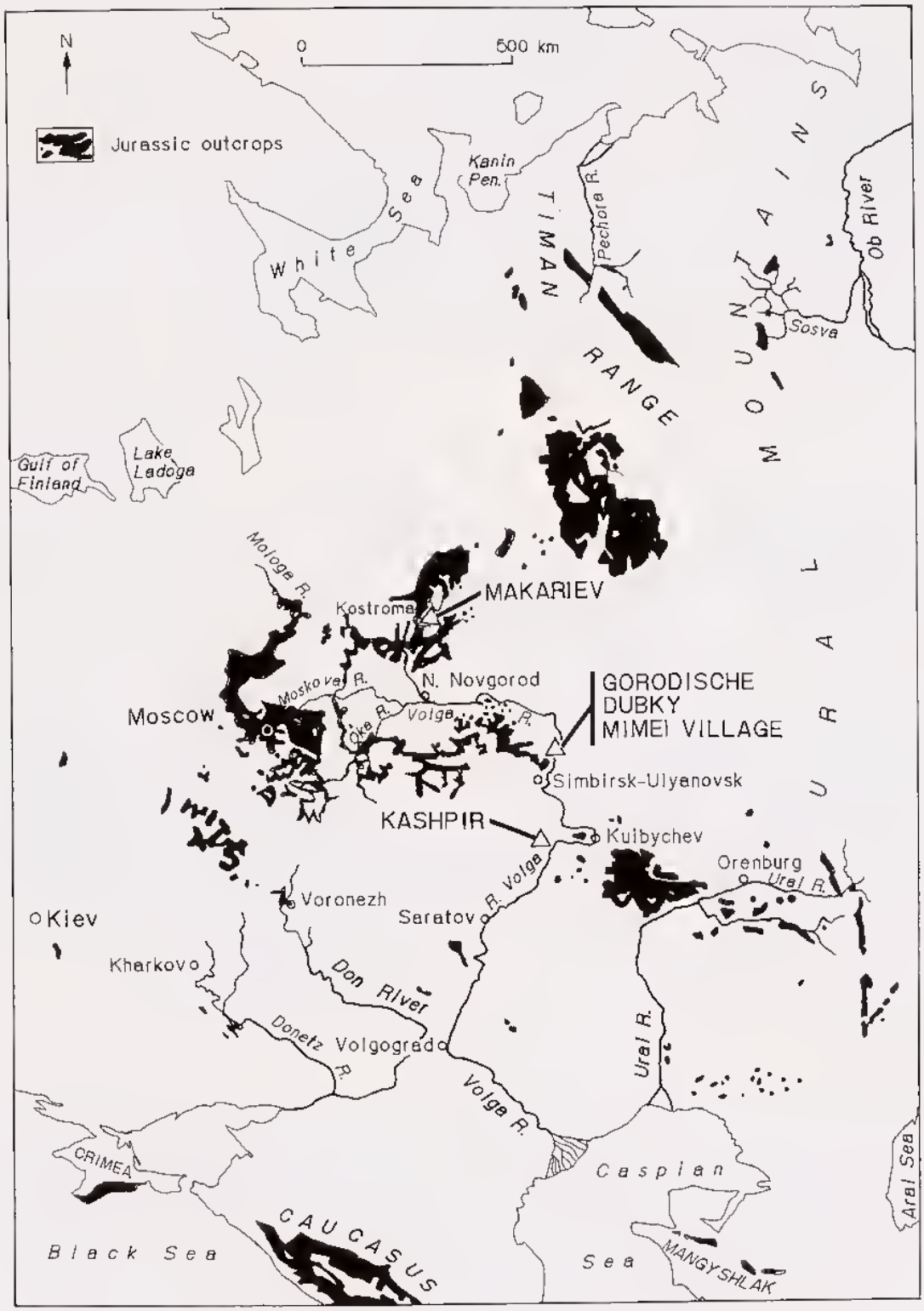

FIG. 1.— Jurassic outcrops of the Russian Platform and location of the studied sections.

FIG. 1.— Affleurements jurassiques sur la plate-forme russe et localisation des coupes étudiées.

Source : MNHN, Paris

— the Oxfordian deposits are detailled in the sections described by NIKITIN (1884) near the town of Makariev on the Unzha River (Fig. 2A). They consist of 5.90 m grey to dark clays with a characteristic horizon of bituminous shales in the middle part and phosphatic pebbles in the upper part. The Makariev section ends with the base of the Kimmeridgian Stage;

— the Kimmeridgian crops out on the waterside of the Kuibyshev reservoir (Volga River, 25 km north of the town of Ulyanovsk), north-east of Undory, between Dubky and Mimei localities (Fig. 2B). It is a thick alternance (54 m and visual gap) of marls and argillaceous limestones containing only one black shales horizon;

— the Volgian Formation are studied in the shore of the Kuibyshev reservoir, between Gorodische village and Dubky locality (Undory village, Fig. 2B). This section corresponds to the Volgian lectostratotype proposed by GERASSIMOV & MIKHAILOV (1966). The upper Volgian Formation is also described in Kashpir, directly south of Syzran, on the Kuibyshev reservoir (Fig. 2C). It corresponds to 18 m of terrigenous deposits, argillaceous in the lower part and sandy in the upper part, with intercalations of four major black shales horizons.

BIOSTRATIGRAPHICAL ELEMENTS

Ammonites were collected bed by bed which allow to characterize the faunal succession for the Upper Jurassic of the middle Volga basin. The observed scheme shows three major biogeographic influences and requires the use of three different zonal scales:

— the Oxfordian Zones are used throughout the boreal province which extends from northern Britain to Greenland through Spitzbergen into the Russian Platform. This scheme is based on Cardioceratids faunas;

— the Kimmeridgian zonal scheme is that of subboreal province which extends from southern Britain across Poland and the middle Volgian basin. Aulacostephanids are the dominant elements. Endemic ammonites of the Franco-German Bioma (HANTZPERGUE, 1989) occur in this subboreal faunal sequence and are common elements between Russian and western european series.

The endemic Volgian ammonites belong to a biogeographic unit which extends from northern Siberia, Russian Platform and Poland across the circum-Arctic shelf, including Barents shelf and northern Canada. This faunal sequence can be compared to the English zonal standard based on boreal Perisphinctids. The correlations with the Tithonian stage are hypothetical (GEYSSANT, 1997); only the genus *Gravesia* allows, according to MESEZHNIKOV *et al.* (1984) an equivalence between the base of the Submediterranean Tithonian and the lowermost beds of the "English upper Kimmeridgian".

ORGANIC MATTER DATA

All the 175 collected rock-samples were open air-dried and crushed in a metallic mortar to obtain a fine (2 µm) powder. Calcium carbonate content (% $CaCO_3$) was measured using a calcimetric bomb. The total carbon content (% Ctot.) was measured using a WR 12 LECO analyser. The organic carbon content (% Corg.) is estimated as the difference between total carbon and mineral carbon, assuming that all the mineral carbon is represented by pure calcite. The C org. concentration describes the quantity of organic carbon, although it should be kept in mind that organically bound hydrogen, oxygen, nitrogen and sulphur can contribute up to 50% of the total sedimentary organic matter. In immature samples, 1 wt% C org. corresponds to 1.5 to 2.0 wt% organic matter. The source and thermal maturation of the organic matter were estimated on 65 samples using a Rock-Eval instrument (ESPITALIÉ *et al.*, 1985-86).

Source : MNHN, Paris

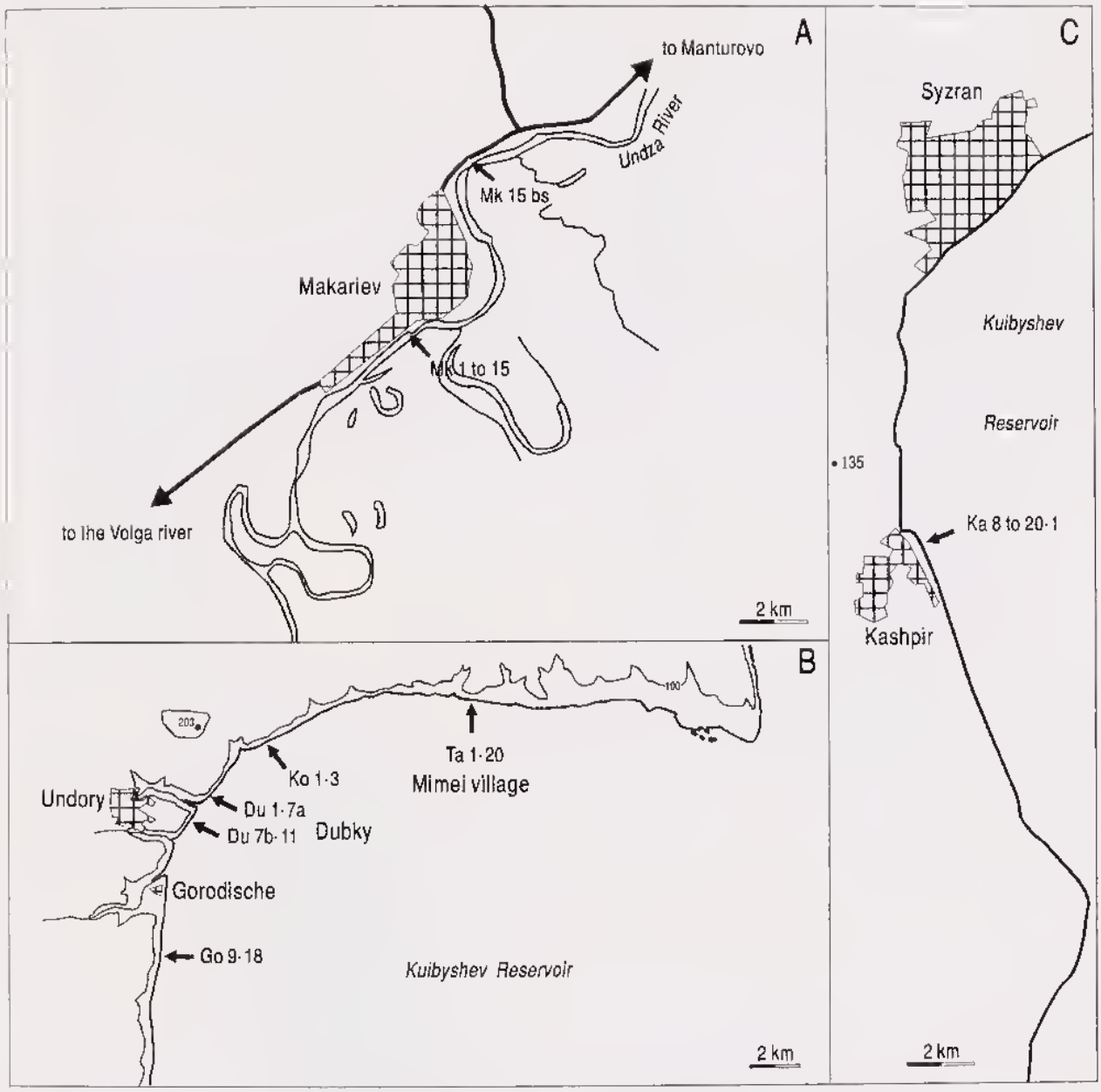

FIG. 2.— Precise location of the studied sections.

FIG. 2.— Localisation précise des coupes étudiées.

UPPER JURASSIC SYNTHETIC SECTION OF THE VOLGA BASIN

OXFORDIAN: MAKARIEV SECTION (MK) (Fig. 3)

LOWER OXFORDIAN

Cordatum Zone d'ORBIGNY (1852).

Mk 16- Compact grey clays, highly bioturbated, showing a 10 to 20 cm-thick bedding with planar surfaces. Centimetric phosphatic nodules are present, and large pieces of wood occur at 20 cm from the

Source : MNHN, Paris

bottom. *Pleuromia* sp., *Dentalium* sp., *Astarte* sp., *Entolium* sp., *Nucnloma* sp., *Oxytoma* sp., *Grammatodon* sp., rhynchonellids, belemnites and *Cardioceras (Cardioceras)* gr. *cordatum* (Sow.), *Cardioceras* sp., *Perisphinctes* sp. 1.40 m.

MIDDLE OXFORDIAN

Densiplicatum Zone SYKES (1975) and Tenuiserratum Zone CARTOU (1966).

Mk 15- compact grey clays, bioturbated, starting with a 10 to 15 cm-thick layer rich in glauconite and containing a lot of reworked and non-oriented belemnites. The boundary with the previous unit is underlined by a thin level with crushed ammonites. A lumachellic bed with ammonites, belemnites, gastropods (*Pleurotomaria* sp.) and bivalves (*Gryphaea dilatata, Cosmetodon* sp.) occurs 40 cm below the top. The top of this unit is marked by a yellowish to greenish 10 cm-thick layer of argillaceous pyritic sand with belemnites. *Cardioceras (Subvertebriceras) densiplicatum* Boden, *Cardioceras (Plasmatoceras) tenuistriatum* Borissiak, *Cardioceras (Plasmatoceras) popilanieuse* Boden, *Cardioceras (Snbvertebriceras) zenaidae* Ilov., *Cardioceras (Plasmatoceras) tenuicostatum* (Nik.), *Cardioceras (Maltoniceras) kokeni* Boden, *Cardioceras* cf. *mauntjoi* Freb. and in upper part: *Cardioceras (Subvertebriceras) zenaidae* Ilov., *Cardioceras (Cawtoniceras) tenuiserratum* (Oppel), *Perisphinctes (Arisphinctes)* gr. *plicatilis* (Sow.). 1.80 m.

UPPER OXFORDIAN

Glosense Zone SYKES (1975).

— Ilovaiskii Subzone SYKES (1975).

Mk 14- finely laminated black shales, with some planar traces (trails ?) at the bottom. Gastropods (*Aporrhais, Dicroloma*), bivalves (*Entolium* sp.) and ammonites: *Amoeboceras ilovaiskii* (Sok.), *Amoeboceras alternoides* (Nik.), Perisphinctidae ind. 0.12 m.

Mk 13- black bioturbated clays (Chondrites) with a thin layer of crushed ammonites, bivalves and gastropods at 2 cm from the base. Rare pieces of crinoids at the top. *Amoeboceras ilovaiskii* (Sok.), *Amoeboceras alternoides* (Nik.), Perisphinctidae ind. 0.15 m.

Mk 12- grey silty clays with *Trautscholdia cordata* and debris of ammonites: *Amoeboceras alternoides* (Nik.), *Amoeboceras transitorium* Spath, *Amoeboceras* cf. *glosense* (Bigot & Brasil), *Amoeboceras ilovaiskii* (Sok.). 0.30 m.

Serratum Zone SYKES (1975).

— Koldewcyense Subzone Sykes (1975).

Mk 11d- compact grey clays with belemnites: *Pachytheutis panderiana* (d'Orb.), *Hibolites* sp. and ammonites: *Amoeboceras alternoides* (Nik.), *Amoeboceras* cf. *damoni* Spath, *Amoeboceras* cf. *koldewevense* Sykes & Callomon, *Amoeboceras ilovaiskii* (Sok.). 0.30 m.

Mk 11c- greenish clays having a yellowish to rust-coloured alteration, containing pyritic and phosphatic nodules, glauconite, belemnites and ammonites: *Amoeboceras koldeweyense* Sykes & Callomon, *Amoeboceras* gr. *serratum* (Sow.), *Amoeboceras* cf. *talbejense* Kal. & Mesezhn. 0.10 m.

— Serratum Subzone SYKES (1975).

Mk 11b- compact grey clays with: *Amoeboceras* cf. *ovale* (Quenst.), *Amoeboceras* cf. *tuberculatoalternans* (Nik.), *Amoeboceras* gr. *serratum* (Sow.). 0.10 m.

Mk 11a- greenish clays having a yellowish to rust-coloured alteration, containing bivalves (*Bnchia, Meleagrinella, Astarte*) and belemnites. 0.08 m.

Mk 10b- grey clays becoming glauconitic to the top with belemnites, bivalves (*Trautscholdia cordata*), and *Amoeboceras* cf. *ovale* (Quenst.), *Amoeboceras* gr. *serratum* (Sow.). The upper surface is bioturbated and burrows filled by the glauconitic clays. 0.20 m.

Source : MNHN, Paris

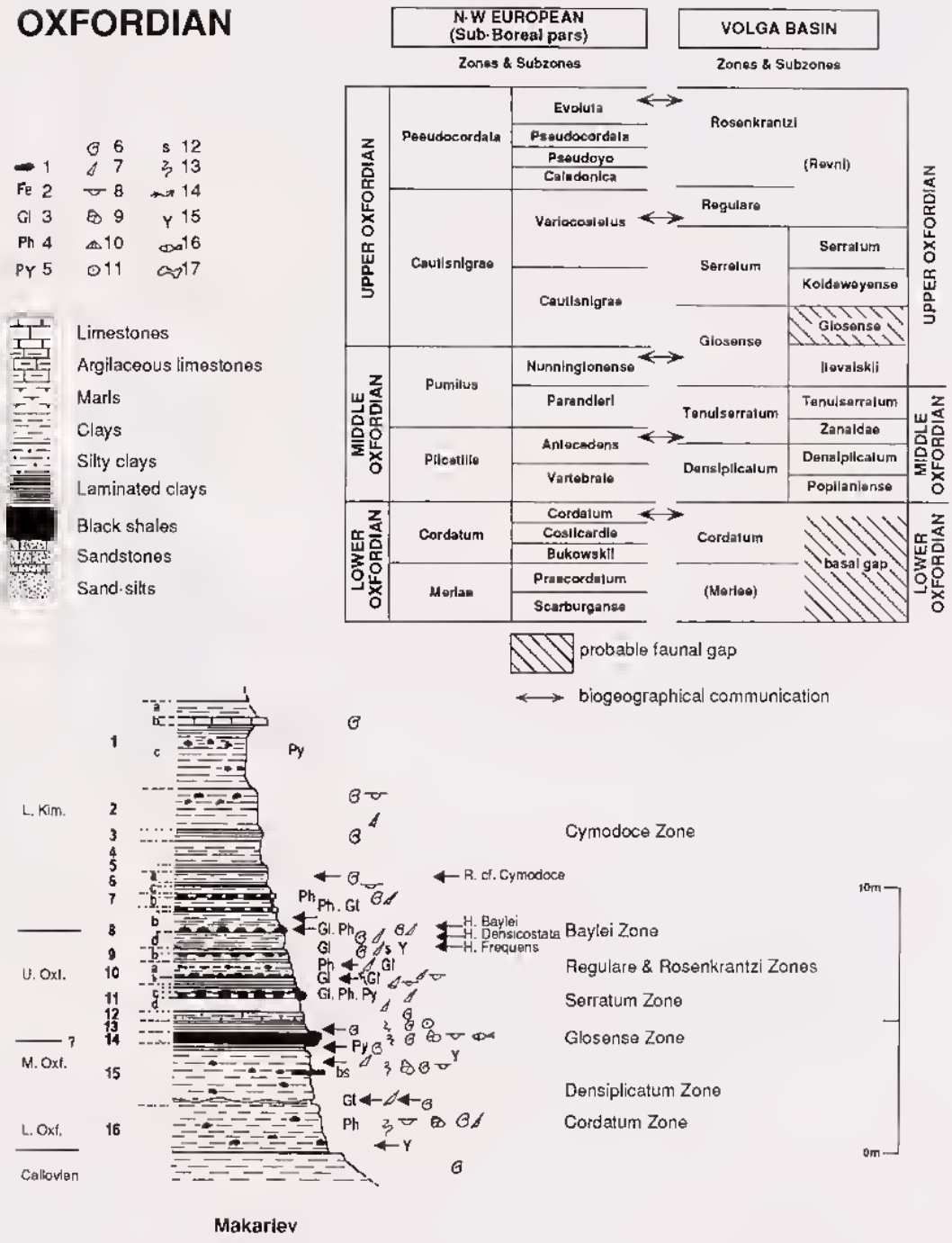

FIG. 3.— Oxfordian lithostratigraphy and biostratigraphy: Makariev (Mk) section. **1**, Nodules; **2**, Oxidized surface; **3**, Glauconite; **4**, Phosphate; **5**, Pyrite; **6**, Ammonite; **7**, Belemnite; **8**, Bivalve; **9**, Gastropod; **10**, Brachiopod; **11**, Crinoid; **12**, Serpule; **13**, Bioturbation; **14**, Trail; **15**, Larges wood fragments; **16**, Fish; **17**, Vertebrates remains.

*FIG. 3.— Lithostratigraphie et biostratigraphie de l'Oxfordien : coupe de Makariev (Mk). **1**, Nodules ; **2**, Surface oxydée ; **3**, Glauconie ; **4**, Phosphate ; **5**, Pyrite ; **6**, Ammonite ; **7**, Bélemnite ; **8**, Bivalve ; **9**, Gastéropode ; **10**, Brachiopode ; **11**, Crinoïde ; **12**, Serpule ; **13**, Bioturbation ; **14**, Piste ; **15**, Grands fragments de bois ; **16**, Poisson ; **17**, Restes de vertébrés.*

Source : MNHN, Paris

Regulare and Rosenkrantzi Zones SYKES (1975).

Mk 10a- grey clays with phosphatic pebbles, becoming intensely biotubated with reworked belemnites at the top. *Amoeboceras* cf. *ovale* (Quenst.), *Amoeboceras tuberculatoalternans* (Nik.), *Amoeboceras* cf. *lineatum* (Quenst.), *Amoeboceras* gr. *serratum* (Sow.), *Amoeboceras gerassimovi* Kal. & Mesezhn., *Amoeboceras* cf. *freboldi* Spath, *Amoeboceras leucuni* Spath. 0.40 m.

Mk 9b- grey clays with ammonites, belemnites and some phosphatic concretions at the top. *Amoeboceras* cf. *lineatum* (Salf.). 0.40 m.

Mk 9a- glauconitic clays with phosphatic concretions, belemnites, bivalves and serpulids. Floated wood appears on the upper surface of this unit. 0.05 m.

Mk 8d- grey clays with belemnites and ammonites: *Amoeboceras* cf. *lineatum* (Salf.) and *Ringsteadia* cf. *frequens* Salf. at the top. 0.50 m.

KIMMERIDGIAN (Fig. 4)

LOWER KIMMERIDGIAN: MAKARIEV (MK) AND MIMEI VILLAGE (TA) SECTIONS

Baylei Zone SALFELD (1913).

Mk 8c- glauconitic and ferrugineous clays with phosphatic nodules, bivalves (*Nuculona* sp.), belemnites and ammonites: *Pictonia densicostata* Salfeld. 0.05 m.

Mk 8b- grey clays with ammonites (*Pictonia baylei* Salfeld) appearing at 20 cm from the base. *Amoeboceras (Amoebites)* cf. *kitchini* (Salfeld), *Amoeboceras* sp., *Desmosphinctes* cf. *mniovnikensis* Nik. 0.50 m.

Mk 8a- altered glauconitic clays with oyster fragments, phosphatic nodules and small crystal of (secondary ?) gypsum. 0.05 m.

Cymodoce Zone DOUVILLÉ (1881).

Mk 7b- dark laminated clays with belemnites, fish-scales, gastropods (*Aporrhais*) and bivalves (*Loripes* sp., *Nannogyra* sp.), *Perisphinces* sp. juv. 0.50 m.

Mk 7a- glauconitic clays with nodules and large crushed ammonites and oysters. 0.05 m.

Mk 6c- grey clays having a cubic cutting up. 0.20 m.

Mk 6b- dark laminated clays with bivalves (*Loripes* sp.). 0.10 m.

Mk 6a- grey clays with large shells of ammonites: *Rasenia* cf. *uralensis* (d'Orb.) and *Raseuia* cf. *cymodoce* (d'Orb.). 0.30 m.

Mk 5- dark laminated clays, *Amoeboceras (Amoebites)* gr. *kitchini* (Salf.) 0.20 m.

Mk 4- clays having a cubic cutting up and containing large crushed shells of ammonites (*Amoeboceras* sp.) and bivalves (*Nuculoma* sp. ind.). 0.70 m.

Mk 3- dark laminated clays with *Rasenia* sp. 0.30 m.

Mk 2- grey clays, deeply altered toward the top, with rare ammonites, belemnites at the base, bivalves (*Nuculoma* sp.) and phosphatic nodules at the top. 1.10 m.

Mk 1c- grey clays, bioturbated near the bottom, with numerous shelly debris (ammonites, bivalves) at the middle part. Centimetric limestone nodules appear 30 cm below the top. *Amoeboceras* cf. *cricki* (Salf.). 1.80 m.

Source : MNHN, Paris

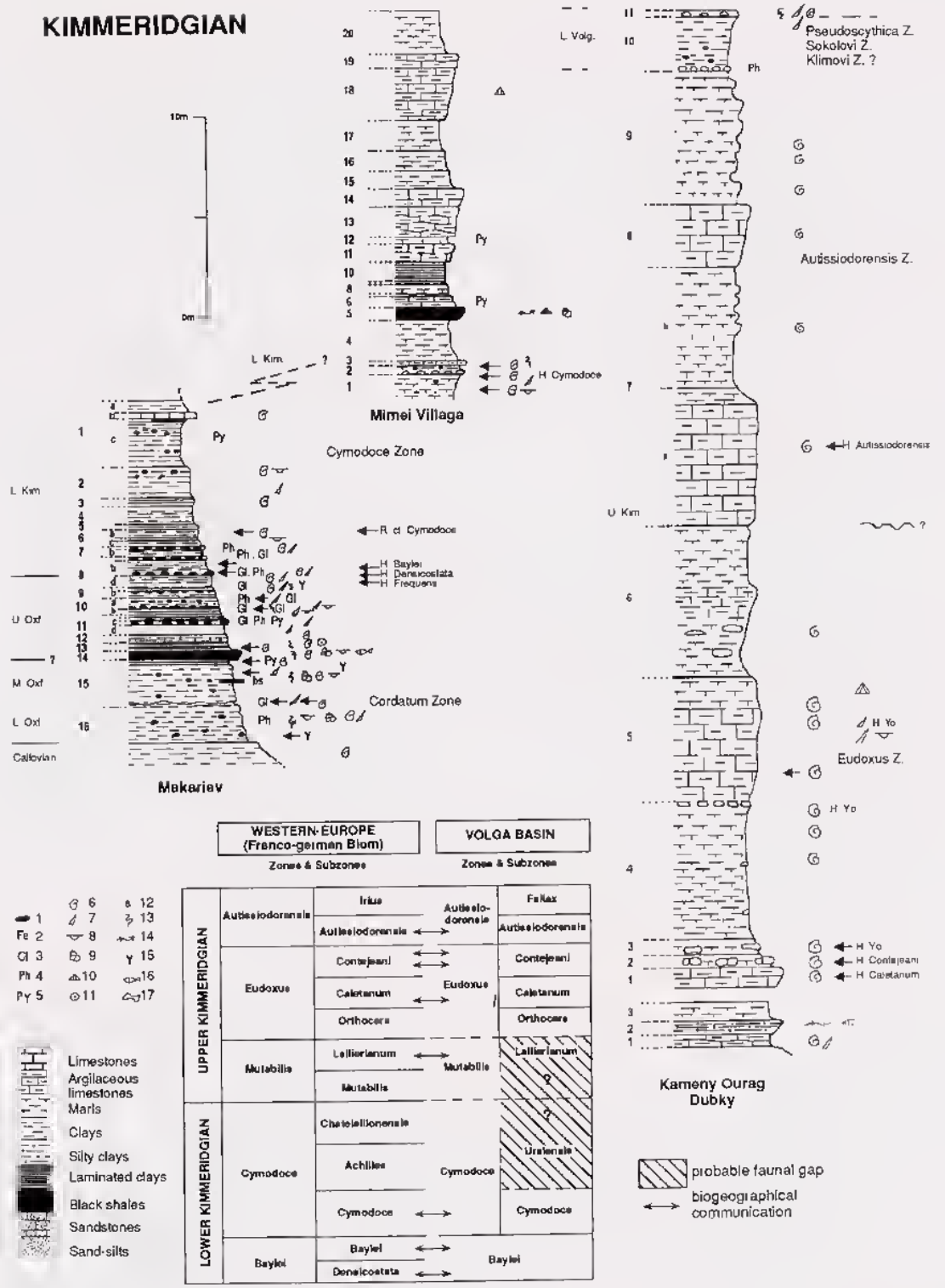

FIG. 4.— Kimmeridgian lithostratigraphy and biostratigraphy: Makariev (Mk), Mimei village (Ta), Dubky (Du) and Kameny Ourag (KO) sections.

FIG. 4.— Lithostratigraphie et biostratigraphie du Kimméridgien : coupes de Makariev (Mk), Mimei village (Ta), Dubky (Du) et Kameny Ourag (KO).

Source : MNHN, Paris

Mk 1b- grey micritic limestone with a rust-coloured alteration in the middle part containing *Rasenia* cf. *uralensis* (d'Orb.) at the top. 0.20 m.

Mk 1a- clays, deeply altered by the proximity of soil. 0.40 m.

Hiatus.

Ta 1- grey marls with phosphatic nodules. At the bottom, large debris of wood. Bivalves: *Buchia concentrica*, *Malletia* sp., and ammonites: *Rasenia* cf. *uralensis* (d'Orb.), *Amoeboceras* sp. At the top, ammonites, *Rasenia* cf. *cymodoce* (d'Orb.) and belemnites. 2.00 m.

Ta 2- grey marls with phosphatic nodules and ammonites (Perisphinctids). The base is marked by a more or less continuous level of whitish nodules. 0.30 m.

Ta 3- grey argillaceous limestone, intensely bioturbated. 0.20 m.

Ta 4- grey marls becoming darker to the top. 1.60 m.

Ta 5- brownish finely laminated black shales with planar traces (trails ?) and rare fauna of brachiopods and gastropods (*Meleagrinella*, *Aporrhais* sp.). 0.50 m.

Ta 6- dark-grey platy argilaceous limestones with pyritic nodules. 0.45 m.

Ta 7- dark-grey laminated marls. 0.03 m.

Ta 8- light-grey marls. 0.40 m.

Ta 9- greyish to brownish laminated clays. 0.10 m.

Ta 10- dark-grey laminated clays. 0.70 m.

Ta 11- light-grey argillaceous limestones. 0.75 m.

Ta 12- marls more or less laminated. 0.25 m.

Ta 13- grey to beige argillaceous limestones. 1.10 m.

Ta 14- compact beige argillaceous limestones. 0.70 m.

Ta 15- grey to beige platy marls. 0.70 m.

Ta 16- grey marls. 0.80 m.

Ta 17- compact beige marls. 1.10 m.

Ta 18- light-beige argillaceous limestones containing rare *Lingula* sp. 2.00 m.

Ta 19- light-grey argillaceous limestones. 0.50 m.

Ta 20- marls, deeply altered due to the proximity of soil. 1.50 m.

Hiatus.

UPPER KIMMERIDGIAN: DUBKY AND KAMENYI OURAG SECTIONS (DU AND KO)

Hiatus.

Eudoxus Zone NEUMAYR (1873).

Ko 1- grey argillaceous limestones with belemnites and ammonites: *Pararasenia hybridus* Ziegler, *Aspidoceras caletanum* (Opp.). 0.50 m.

Ko 2- greyish to greenish silty clays with planar burrows, numerous fish-scales and remains. 0.40 m.

Ko 3- grey marls. 1.00 m.

Du 1- light-grey argillaceous limestones containing some ferrugineous nodules with belemnites and ammonites: *Aulacostephanus eudoxus* (d'Orb.), *Aspidoceras caletanum* (Opp.), *Aspidoceras* gr. *longispinum* (Sow.), and *Amoeboceras* sp. 0.60 m.

Source : MNHN, Paris

Du 2- marls containing light-grey calcareous lenses and numerous limonitic ammonites: *Aulacostephanus coutejeani* (Thur.), *Aspidoceras quercynum* Hantzpergue, and *Tolvericeras sevogodense* (Contini & Hantzpergue). 0.50 m.

Du 3- marls containing light-grey calcareous lenses and numerous limonitic ammonites: *Aulacostephanus yo* (d'Orb.), *Aspidoceras* gr. *quercynum* Hantzpergue. 0.50 m.

Du 4- light-grey marls containing some calcareous nodules and small belemnites. A 50 cm thick more clayey bed lies 2 m from the base. Ammonites, *Aspidoceras* sp. and *Aulacostephanus* cf. *yo* (d'Orb.) appear at 3 m and 4 m. The top of this units is marked by a layer of calcareous nodules. 4.00 m.

Du 5- beige massive argillaceous limestones, with rare phosphatic nodules, becoming grey and marly within the uppermost 1 m. Aptychus (*Laevaptychus*), belemnites, brachiopods (Zeillerids), bivalves (*Loripes*) and large pyritic disc containing ammonites: *Aspidoceras* sp. and *Aulacostephanus* cf. *yo* (d'Orb.). 4.00 m.

Du 6- grey to beige bioturbated marls and argillaceous limestone with calcareous nodules containing ammonites, *Tolvericeras* gr. *sevogodense* (Contini & Hantzpergue). 5.00 m.

Autissiodorensis Zone ZtEGLER (1961).

Du 7a- beige argillaceous limestones becoming marly in the topmost 50 cm. *Amoeboceras* sp., *Aulacostephanus autissiodorensis* (Cotteau), *Aulacostepanus kirghisensis* (d'Orb.), *Aulacostephanus volgensis* (d'Orb.), *Aulacostephanus undorae* (Pavl.), *Amoeboceras (Nannocardioceras) volgae* (Pavl.), *Amoeboceras (Nannocardioceras) subtilicostatum* (Pavl.), *Sutneria* sp., *Virgataxioceras* sp. 4.50 m.

Du 7b1- grey to grey-greenish marls with phosphatic nodules and pyritic disc. 2.00 m.

Du 7b2- alternation of dark-grey to light-grey marls with ammonites: *Aulacostephanus autissiodorensis* (Cotteau), *Aulacostephanus kirghisensis* (d'Orb.), *Aulacostephanus volgensis* (d'Orb.), *Aulacostephanus undorae* (Pavl.), *Virgataxioceras fallax* (Ilov.). 2.00 m.

Du 8- grey to light-beige argillaceous limestone with ammonites: *Aulacostephanus autissiodorensis* (Cotteau), *Aulacostephanus kirghisensis* (d'Orb.), *Aulacostephanus volgensis* (d'Orb.), *Aulacostephanus undorae* (Pavl.), *Virgataxioceras fallax* (Ilov.) 2.20 m.

Du 9- alternation of dark-grey to light-grey marls with ammonites concentrated at the base of dark-grey beds, *Aulacostephanus autissiodorensis* (Cotteau), *Virgataxioceras fallax* (Ilov.), small *Aspidoceras* (?) and *Sutneria* sp. 4.50 m.

VOLGIAN (Fig. 5)

LOWER VOLGIAN: DUBKY SECTION (DU)

Klimovi Zone MtKHAtLOV (1962 a).

Ammonite fauna, after MESEZHNIKOV *et al.* (1984): *Ilowaiskya klimovi* (Ilov & Flor.), *Gravesia* cf. *gigas* (Zieten), *Gravesia* cf. *gravesiana* (d'Orb.) *Neochetoceras* cf. *steraspis* (Opp.), *Glochiceras* cf. *lithographicum* (Opp.) and *Sutneria* cf. *subeumela* (Schneid).

Du 10a- grey clay with phosphatic nodules at the base. *Ilowaiskya klimovi* (Ilov.), *Neochetoceras* sp., *Glochiceras* sp. 0.80 m.

Sokolovi Zone ILOVAtSKY & FLORENSKY (1941).

Ammonite fauna, after MESEZttNtKOV (1988): *Ilowaiskya sokolovi* (Ilov. & Flor.), *Ilowaiskya pavida* (Ilov. & Flor.), *Sutneria* sp., *Haploceras* cf. *elimatum* (Opp.), *Glochiceras* (*Paralingulaticeras*) cf. *lithographicum* (Opp.), *Glochiceras* (*Paralingulaticeras*) cf. *parcevali* (Font.)

Source : MNHN, Paris

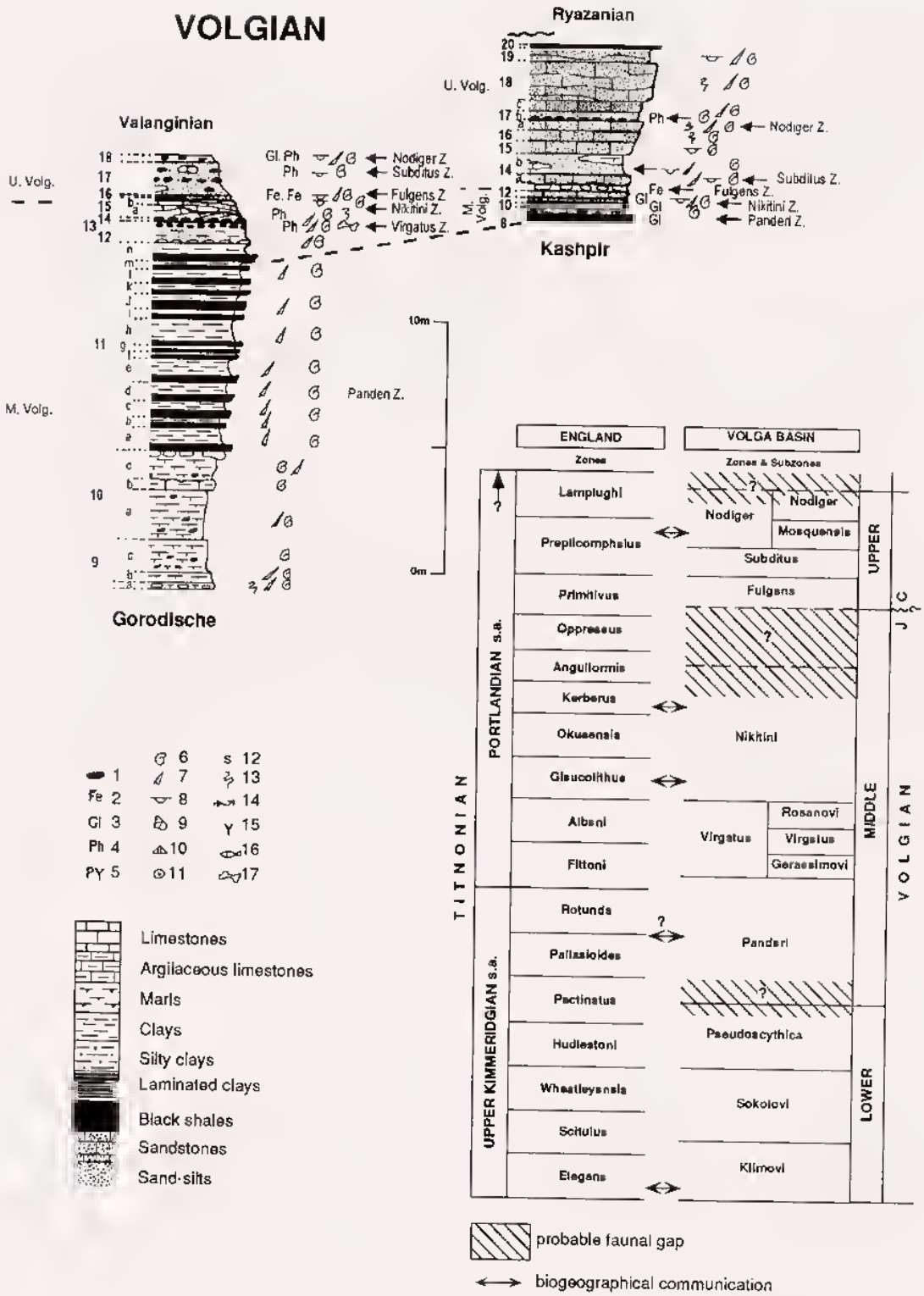

FIG. 5.— Volgian lithostratigraphy and biostratigraphy: Dubky (Du), Gorodische (Go) and Kashpir (Ka) sections.

FIG. 5.— Lithostratigraphie et biostratigraphie du Volgien : coupes de Dubky (Du), Gorodische (Go) et Kashpir (Ka).

Source : MNHN, Paris

Du 10b- dark-grey clay with small carbonates nodules, *Ilowaiskya sokolovi* Ilov., *Ilowaiskya pavida* Ilov. 1.00 m.

Pseudoscythica Zone ILOVAISKY & FLORENSKY (1941).

Ammonite fauna, after MESEZHNIKOV (1988): *Ilowaiskya schaschkovae* (Ilov. & Flor.), *Ilowaiskya pseudoscythica* (Ilov. & Flor.), *Pectinatites ianschini* (Ilov.), *Pectinatites tenuicostatus* Mikhailov, *Glochiceras* sp., *Sutneria* sp., *Haploceras* sp.

Du.10c- grey clay with ammonites and belemnites concentrated at the top, *Ilowaiskya pseudoscythica* Ilov., *Ilowaiskya pavida* Ilov. 0.80 m.

MIDDLE VOLGIAN: GORODISCHE (GO) AND KASHPIR(KA) SECTIONS

Panderi Zone ROZANOV (1906).

Ammonite fauna, after MESEZHNIKOV *et al.* (1984) and MITTA (1993): *Dorsoplanites dorsoplanus* (Vischniakoff), *Dorsoplanites panderi* (d'Orb.), *Pavlovia pavlovi* (Michalski), *Zaraiskites scythicus* (Vischniakoff), *Zaraiskites michalskii* Mitta, *Zaraiskites quenstedti* (Rouillier & Fahrenkohl), *Zaraiskites tschernyschovi* (Michalski), *Zaraiskites zarajskensis* (Michalsky), *Acuticostites acuticostatus* (Michalski), *Acuticostites bitrifurcatus* Mitta.

Go 9a- grey marls, intensely bioturbated (*Chondrites*), with pyrite concretions. Perforated calcareous nodules occur at the base, ammonites and belemnites at the top. 0.20 m.

Go 9b- dark-grey marls with ammonites and belemnites. 0.25 m.

Go 9c- grey marls, intensely bioturbated, with phosphatic nodules, belemnites and ammonites. 1.00 m.

Go 10a- grey marls, intensely bioturbated, with phosphatic nodules, belemnites and ammonites. 1.50 m.

Go 10b- nodular argillaceous limestones with ammonites. 0.15 m.

Go 10c- bioturbated grey marls being dark-grey in the middle part with ammonites, belemnites and phosphatic nodules. Within the last 20 cm, a white argillaceous millstone level is visible. 0.85 m.

Go 11- alternation of black shales and dark-grey calcareous clays with ammonites, belemnites, rare bivalves and pyritic nodules. Toward the top, the clays appear lighter in colour: grey to brownish with some yellowish level due to alteration of pyritic layer (jarosite ?). This unit is subdivided into 14 decimetric black shale/calcareous clays doublets. 6.10 m.

Virgatus Zone ROUILLIER (1845).

Ammonite fauna, after MESEZHNIKOV *et al.* (1984) and MITTA (1993): *Virgatites virgatus* (Buch), *Virgatites* cf. *sosia* (Vischniakoff), *Virgatites pallasianus* (d'Orb.), *Virgatites pusillus* (Mich.), *Virgatites gerassimovi* Mitta, *Lomonossovella lomonossovi* (Vischniakoff), *Acuticostites acuticostatus* (Michalski), *Acuticostites bitrifurcatus* Mitta.

Go 12- conglomerate of red to black phosphatic nodules and pebbles, belemnites and ammonites: *Virgatites virgatus* (Buch). 0.10 m.

Go 13- yellowish to greenish argillaceous silts with dispersed phosphatic pebbles and belemnites. 14 cm below the top, phosphatic pebbles, belemnites and vertebrate remains (*Icthyosaurus, Pleisiosaurus*) are concentrated. 0.50 m.

Go 14- conglomerate of black phosphatic pebbles, belemnites and ammonites (*Virgatites virgatus* (Buch)) in a sandy matrix. The top of this unit has an irregular surface. 0.10 m.

Nikitini Zone LAHUSEN (1883).

Ammonite fauna, after Mitta (1993): *Epivirgatites nikitini* (Michalsky), *Epivirgatites bipliciformis* (Nikitin), *Laugeites stscliurowskii* (Nikitin), *Laugeites aeutivanovi* Mitta, *Lomonossovella lomonossovi* (Vischniakoff).

Source : MNHN, Paris

Go 15- yellowish to greenish argillaceous sands passing laterally to sandstones with ammonites, *Paracraspedites* sp., *Epivirgatites nikitini* (Michalsky), bivalves (*Buchia* sp.) and concentration of belemnites to the top. The upper limit is an undulated oxidised surface with a rust-colour. 0.60 m.

UPPER VOLGIAN: KASHPIR SECTION (KA)

Fulgens Zone NIKITIN (1888).

Ammonite fauna, after GERASIMOV (1969): *Kashpurites fulgens* (Trautschold), *Kashpurites subfulgens* (Nikitin), *Garniericeras catenulatum* (Fischer), *Craspedites okensis* (d'Orb.), *Craspedites nekrassovi* Prigorovski.

Ka 13- brownish to greyish clayey sandstones with calcareous seams containing ammonites, *Kashpurites fulgens* (Trautschold), *Garniericeras catenulatum* (Fischer), belemnites (*Acrotheutis mosquensis*) and bivalves (*Buchia* sp.). At the top of the unit occurs a thin level (2 cm) of strongly ferrugineous carbonate. 0.50 m.

Subditus Zone NIKITIN (1888).

Ammonite fauna after MESEZHNIKOV *et al.* (1984): *Craspedites okensis* (d'Orb.), *Craspedites subditus* (Trautsch.), *Craspedites subditoides* (Nikitin), *Garniericeras catenulatum* (Fischer).

Ka 14a- light-grey fine-grained glauconitic sandstones with belemnites, ammonites and bivalves. 0.25 m.

Ka 14b- light-grey sands poorly cemented with calcareous patches. This unit is rich in ammonites, *Craspedites okensis* (d'Orb.), *Craspedites subditus* (Trautsch.), broken belemnites and *Buchia* sp. 0.60 m.

Ka 15- light-grey fine-grained sandstone with calcareous cement containing ammonites and *Buchia* sp. 0.35 m.

Ka 16- dark-grey bioturbated sandstones with numerous ammonites and bivalves. 0.30 m.

Nodiger Zone NIKITIN (1888).

Ammonite fauna, after GERASIMOV (1969): *Craspedites nodiger* (Eichwald), *Craspedites kaschpuricus* (Trautsch.), *Craspedites parakaschpuricus* Gerassimov, *Craspedites milkovensis* Stremooukhov, *Craspedites kuznetzovi* (Sokolov), *Craspedites mosquensis* Gerassimov, *Garniericeras subclypeiforme* (Milaschevitsch).

Ka 17a- light-grey fine-grained sandstones, strongly bioturbated, with dark-grey burrows, ammonites, *Craspedites nodiger* (Eichwald) and belemnites. 0.35 m.

Ka 17b- fine-grained calcareous sandstones starting by a level containing cm-long phosphatic pebbles and ammonites. 0.20 m.

Ka 17c- light-grey calcareous sandstones with lumachellic lenses rich in belemnites, ammonites and bivalves. 0.30 m.

Ka 18- massive light-grey fine-grained calcareous sandstones, strongly bioturbated, with numerous and non-oriented shells, belemnites and ammonites. 1.10 m.

Ka 19- light-grey to greenish bioclastic sandstones having a nodular appearance. Numerous ammonites: *Craspedites nodiger* (Eichwald), *Craspedites kaschpuricus* (Trautsch.), *Garniericeras subclypeiforme* (Milaschevitsch). 0.40 m.

Ka 20- brown finely laminated black shale overlain by Ryazanian deposits. 0.15 m.

Source : MNHN, Paris

AMMONITES ZONATION AND CORRELATIONS

OXFORDIAN

On the central part of the Russian Platform (middle Volga basin), the Oxfordian stage is characterized by boreal Cardioceratids. This ammonite faunas allow a precise correlation with the standard zonation of the boreal Oxfordian (SYKES & SURLYK, 1976) and with the *Amoeboceras* zonation of the boreal upper Oxfordian (SYKES & CALLOMON, 1979).

The equivalence between sub-boreal and tethyan zonations is yet imperfect: the base of Cordatum Zone is only correlated with the Claromontanus Zone of the tethyan scheme (CARIOU *et al.*, 1997).

In the excellent sections of Makariev, on the Unzha River (NIKITIN, 1884), the Oxfordian shows likely a hiatus of the lower part. The first Oxfordian ammonite faunas is a Cardioceratid assemblage, including *Cardioceras* gr. *cordatum* (Sow.), typical form of the standard Cordatum Subzone (Cordatum Zone). Although the species ranges are not precisely determined, it seems that Bukowskii and/or Gloriosum Subzones, and Costicardia and/or Percaelatum Subzones are included in the basal Oxfordian gap.

The middle Oxfordian Cardiocerartid faunas, dominated in lower part by *C. (Subvertebriceras) densiplicatum* Boden, *C. (Plasmatoceras) popilaniense* Boden, *C. (Subvertebriceras) zenaidae* Ilov. and *C. (Plasmatoceras) tennistriatum* Borissiak, indicate the Densiplicatum Zone. The occurrence of *C. (Cawtoniceras) tenuiserratum* (Opp.) and *P. (Arisphinctes)* gr. *plicatilis* (Sow.) in upper part of Mk 15 level, suggest the Tenuiserratum Zone. A Tenuiseratum Horizon was defined at the top of the Antecedens Subzone (Plicatilis Zone) of the submediterranean province (CARIOU, 1966; MALINOWSKA, 1966). This unit allows a precise correlation between the top of the boreal middle Oxfordian and the medium part of this substage in Tethyan realm (CARIOU *et al.*, 1997; MESEZHNIKOV, 1988, 1989).

In the upper Oxfordian boreal series, an *Amoeboceras* faunal sequence allows to subdivide this part of the Stage into four zones: Glosense, Serratum, Regulare and Rosenkrantzi Zones (SYKES & SURLYK, 1976). In Makariev sections, the Glosense Zone contains a typical fauna of the Ilovaiskii Subzone. The upper Glosense Subzone is not clearly identified. These boreal unit is approximately equivalent to the lower part of the Submediterranean Bifurcatus Zone (Stenocycloides Subzone, CARIOU *et al.*, 1997). The assemblage of *Amoeboceras ilovaiskii* (Sok.) and *A.* cf. *glosense* (Bigot & Brasil) (Mk 12) possibly indicates the nearby of the Ilovaiskii/Glosense boundary. A hiatus of the Glosense Subzone seems probable.

The Koldeweyense and Serratum Subzones (Serratum Zone) are indicated by the occurrence of their index. The assemblage of different *Amoeboceras* with *A. leucum* Spath and *A. tuberculatoalternans* (Nik.) indicate the upper Oxfordian Regulare and Rosenkrantzi Zones. It should be noted that the ammonite ranges in this section need to be worked out more precisely. The occurrence of *Ringsteadia cuneata* (Trautsch.) (MESEZHNIKOV, 1988) and *R. frequens* Salf. in Mk 8d level indicates the uppermost Oxfordian. This *Ringsteadia* fauna is directly followed by Kimmeridgian *Pictonia* (Mk 8c). Consequently, the Oxfordian/Kimmeridgian boundary can be precisely correlated between Russian Platform and sub-boreal western-european series.

Concerning a possible correlation with tethyan series, an equivalence is suggested between boreal Serratum and Regulare Zones and the tethyan Bifurcatus Zone (CARIOU *et al.*, 1997). The correspondence of the Oxfordian/Kimmeridgian boundary for this two realms is still imprecise. Recent propositions (ATROPS *et al.*, 1993) suggest that the usual tethyan Planula Zone belongs partly or totally into the Kimmeridgian stage.

Source : MNHN, Paris

KIMMERIDGIAN

During the Kimmeridgian, the ammonites provincialism is more pronounced in the north tethyan margin. The Tethyan and Boreal Realms are separated by an intermediate area: the Franco-German Bioma (HANTZPERGUE, 1979, 1989 ; HANTZPERGUE *et al.*, 1997 ; ENAY, 1966, 1980 ; HAUG, 1898). The subboreal province is characterized by Cardioceratids and Aulacostephanids with respectively the genus *Amoeboceras* and *Pictonia*, *Rasenia*, *Aulacostephanus*. In an other hand, the Franco-German Bioma is an overlapping area for the sub-boreal and tethyan faunas but above all, a differentiated area with endemic forms of Aspidoceratids, Aulacostephanids and Perisphinctids (HANTZPERGUE, 1989). The middle Volga Kimmeridgian series show the same particularities and the best biostratigraphical correlations can be made with the Kimmeridgian stage.

The lowermost Russian usual zone, the Evoluta Zone (MESEZHNIKOV, 1988) contains a *Pictonia* fauna. The Densicostata and Baylei Horizons located in Mk 8c-8b levels of Makariev section define the standard Baylei Zone.

The "kitchini beds" (MESEZHNIKOV, 1988) are characterized by *Amoeboceras* faunas with *A. (Amoebites) kitchini* (Salf.) and *A. (Amoebites) cricki* (Salf.). *Rasenia* gr. *cymodoce* (d'Orb.) and *Rasenia* gr. *uralensis* (d'Orb.) occur in Mk 7a-6a levels of the Makariev section. They indicate a Cymodoce Horizon located at the lower part of the Cymodoce Subzone (HANTZPERGUE *et al.*, 1997), and the "Zonovia" uralensis Subzone corresponds probably with the upper part of the standard Cymodoce Zone. Consequently, the classic "*Amoeboceras kitchini* Beds" of the Russian Platform are equivalent or partially equivalent to Baylei and Cymodoce Zones of the western european standard biostratigraphical scale.

The lower Kimmeridgian of middle Volga area is not complete: Makariev and Mimei village outcrops are relatively poor in ammonite faunas and incomplete for the middle and upper part of Cymodoce Zone.

Upper Kimmeridgian is most fully developed on these area, but lower Mutabilis Zone, (equivalent to the Sosvaensis Zone (MESEZHNIKOV, 1988) or to the Acanthicum Zone *auct.*), is no more visible. *Orthaspidoceras liparum* (Opp.) is mentioned by Meseznikov below the lake level of the Kuyibishev reservoir. This ammonite is the dimorphic form of *O. lallierianum* (d'Orb.), index of a Lallierianum Horizon and a Lallierianum Subzone, located at the upper part of the standard Mutabilis Zone (HANTZPERGUE, 1989).

In compensation, the Eudoxus and Autissiodorensis Zones show the most biostratigraphical accuracy. Three western european horizons of the Eudoxus Zone are present in the Dubky section:

— Caletanum Horizon, Caletanum Subzone (HANTZPERGUE, 1979), with *Aspidoceras caletanum* (Opp.), *Aspidoceras* gr. *longispinum* (Sow.), *Aulacostephanus endoxus* (d'Orb.), *Pararasenia* cf. *hybridus* Ziegler and *Amoeboceras* sp., levels Ko 1-3, Du 1;

— Contejeani Horizon, Contejeani Subzone (HANTZPERGUE, 1979), with *Aspidoceras* gr. *quercynum* Hantzpergue, *Aulacostephanus contejeani* (Thurmann), *Tolvericeras sevogodense* (Contini & Hantzpergue), Du 2 level;

— Yo Horizon, Contejeani Subzone, with *Aulacostephanus yo* (d'Orb.), *Aspidoceras* gr. *quercynum* Hantzpergue, *Aspidoceras* sp. and *Tolvericeras* gr. *sevogodense* (Contini & Hantzpergue), levels Du 3-6.

The Autissiodorensis Zone corresponds to the occurrence of the index *Aulacostephanus autissiodorensis* (Cott.) and its dimorphs, *A. volgensis* (Vischn.), *A. kirghisensis* (d'Orb.), *A. undore* (Pavl.). In the upper part, was defined the Fallax Subzone (MITKHAILOV, 1962 b) with dominant *Virgataxioceras fallax* (Ilov.) constantly accompanied by the zonal index. The Kimmeridgian/Volgian boundary is setting at the last apparition datum of *A. autissiodorensis* (Cott.).

Source : MNHN, Paris

VOLGIAN

The deposits of the "Volgian stage" of the typical region (central part of the Russian Platform) are subdivided into three substages (MIKHAILOV, 1962 a, 1964, GERASIMOV & MIKHAILOV, 1966): lower Volgian, (SOKOLOV, 1901, "Wetlianian" horizon), middle Volgian (NIKITIN, 1881 a, "lower Volgian stage"), and upper Volgian (NIKITIN, 1881 b, "upper Volgian stage").

Traditionally, the Volgian crowned the Jurassic system and was considered to an equivalent of the Tithonian stage. However, many data, in several areas of the world, contradict the correlation adopted in Russia (SEY & KALACHEVA, 1993). A recent resolution of standing commission of the Interdepartmental Stratigraphic Committee of Russia (ISC) on the Jurassic and Cretaceous systems (1996, unpublished) proposed to draw the Jurassic/Cretaceous boundary in the Boreal realm between the middle and upper substage of the Volgian (Nikitini/Fulgens Zones). In that way, the upper Volgian is correlated with two lower zones of the Berriasian stage. In the subboreal province, such a break corresponds to the boundary between marine series with ammonites of the Dorset Portland Beds and lagoonal-lacustrine facies of the Purbeck Beds. The top of Portlandian *sensu anglico* is putting above the Oppressus Zone (BIRKELUND, *et al.*, 1984) and the Portlandian last zones (Primitivus, Preplicomphalus and Lamplughi Zones) can be an equivalent to the upper Volgian.

At the All-Russian Conference in Saint Petersbourg in 1988 (Resolution, 1993), on the development of an unified stratigraphic scheme of the Mesozoic deposits of the Russian Platform, the Volgian stage was subdivided into the following substages, zones and subzones: lower substage (Klimovi Zone, Sokolovi Zone, Pseudoscythica Zone), middle substage (Panderi Zone with Pavlovi and Zarajskensis Subzones, Virgatus Zone with Gerassimovi, Virgatus and Rosanovi Subzones, Nikitini Zone with Blakei and Nikitini Subzones, Oppressus Zone), and upper substage (Fulgens Zone, Subditus Zone, Nodiger Zone with Mosquensis and Nodiger Subzones).

Today Volgian is differently subdivided (MESEZHNIKOV, 1982; MITTA, 1993 ; GERASIMOV *et al.*, 1995):

— Klimovi Zone MICHAILOV (1962 a): *Ilowaiskya klimovi* Ilovaisky, *Neochetoceras* aff. *steraspis* (Opp.), *Glochiceras* sp., *Gravesia* cf. *gigas* (d'Orb.), *Sutneria* aff. *subeumela* (Schneid).

— Sokolovi Zone ILOVAISKY & FLORENSKY (1941): *Ilowaiskya sokolovi* Ilovaisky, *I. pavida* Ilovaisky, *Haploceras* aff. *elimatum* (Opp.), *Glochiceras* aff. *lithographicum* (Opp.), *Glochiceras* aff. *parcevali* (Font.).

— Pseudoscythica Zone ILOVAISKY & FLORENSKY (1941): *Ilowaiskya schaschkovae* Ilovaisky, *I. pseudoscythica* Ilovaisky, *Pectinatites* aff. *pectinatus* (Phillips), *P. ianschini* (Ilovaisky), *P. tenuicostatus* Mikhailov, *Weatleyites* aff. *aestlecotteusis* (Salfeld), *W. arkelli* Michailov, *W. spathi* Mikhailov, *Physodoceras neuburgense* (Oppel).

— Panderi Zone ROZANOV (1906): *Zaraiskites zarajskensis* (Michalski), *Z. scythicus* (Vischniakoff), *Z. michalskii* Mitta, *Z. quenstedti* (Rouillier & Fahrenkohl), *Z. tschernyschovi* (Michalski), *Acuticostites acuticostatus* (Michalski), *A. bitrifurcatus* Mitta, *Dorsoplanites dorsoplanus* (Vischniakoff), *Dorsoplanites panderi* (d'Orbigny), *Pavlovia pavlovi* (Michalski).

Subdivision of Panderi Zone into two Subzones is impossible. The same ammonite species occur in lower and upper parts of zone; there are not biostratigraphicaly or lithostratigraphicaly limited. MIKHAILOV (1962 a) who proposed the subdivision of the Panderi Zone into two subzones, as ILOVAISKY (ILOVAISKY & FLORENSKY, 1941) which proposed such subdivision, have based his suppositions on Rozanov's indications. He was the first, who believed in the compound composition Panderi Zone. However, ILOVAISKY & MIKHAILOV did not take into account that the greater part of Rozanov's "lower Subzone Panderi-Zone" was included by the latest workers into the lower Volgian "Wetlianian horizon".

Virgatus Zone ROUILLIER (1845) (emend. by LAHUSEN, 1883 and ROSANOV, 1906): *Virgatites virgatus* (Buch), *V. sosia* (Vischniakoff), *V. pusillus* (Michalski), *V. pallasianus* (d'Orb.), *V. larisae*

Source : MNHN, Paris

Mitta, *V. gerassimovi* Mitta, *V. rosanovi* Michailov, *V. crassicostatus* Mitta, *Dorsoplanites serus* Gerasimov, *D. rosanovi* Gerasimov, *Serbarinovella serbarinovi* Mitta, *S. ringsteadiaeformis* (Gerasimov), *Lomonossovella lomonossovi* (Vischniakoff), *Craspedites ivanovi* Gerasimov, *C. pseudofragilis* Gerasimov, *Acuticostites acuticostatus* (Michalski), *Laugeites stschurowskii* (Nikitin), *Craspedites kuncevi* Michailov.

The subdivision of the Virgatus Zone is based on the species and succession of the genus *Virgatites* and *Dorsoplanites:*

— Gerassimovi Subzone ROZANOV (1919) *Virgatites gerassimovi* Mitta, *V. pusillus* (Michalski), *V. pallasianus* (d'Orb.), *V. sosia* (Vischniakoff). *Dorsoplanites serus* Gerasimov, *D. rosanovi* Gerasimov, *Lomonossovella lomonossovi* (Vischniakoff), *Acuticostites acuticostatus* (Michalski).

— Virgatus Subzone ROUILLIER (1845) (emend. by ROSANOV, 1919): *Virgatites virgatus* (Buch), *V. pallasianus* (d'Orbigny), *V. sosia* Vischniakoff, *V. larisae* Mitta, *V. crassicostatus* Mitta., *Dorsoplanites serus* Gerasimov, *D. rosanovi* Gerasimov, *Lomonossovella lomonossovi* (Vischniakoff), *Serbarinovella serbarinovi* Mitta, *S. ringsteadiaeformis* (Gerasimov), *Craspedites ivanovi* Gerasimov, *C. pseudofragilis* Gerasimov.

— Rosanovi Subzone ROZANOV (1913) (= Ivanovi Subzone): *Virgatites virgatus* (Buch), *V. rosanovi* Michailov, *V. pallasianus* (d'Orbigny), *V. sosia* (Vischniakoff), *Dorsoplanites serus* Gerasimov, *D. rosanovi* Gerasimov, *Lomonossovella lomonossovi* (Vischniakoff), *Craspedites ivanovi* Gerasimov, *C. pseudofragilis* Gerasimov, *Craspedites kuncevi* Michailov, *Laugeites stschurowskii* (Nikitin).

— Nikitini Zone LAHUSEN (1883): *Epivirgatites nikitini* (Michalski), *E. bipliciformis* (Nikitin), *E. lahuseni* (Nikitin) *Laugeites stschurowskii* (Nikitin), *L. aenivanovi* Mitta, *Lomonossovella lomonossovi* (Vischniakoff). *Craspedites ivanovi* Gerasimov, *Craspedites pseudofragilis* Gerasimov.

The separation of the upper part of formerly Nikitini Zone as Oppressus Zone by CASEY & MESEZHNIKOV (1986) cannot be adopted. Nikitini Zone is the interval of distribution of *Epivirgatites nikitini* (Michalski), which is found in complete section of zone in its formerly volume. The separation of "the beds with *Paracraspedites oppressus*", as upper subzone of Nikitini Zone, is also impossible. The presence of the western-european genus *Paracraspedites* is not confirmed in middle Volgian.

The separation of the lower part Nikitini Zone into Blakei Subzone cannot be also adopted. The name *Lomonossovella blakei* (Pavlow) *emend.* MIKHAILOV is the younger synonym of *L. lomonossovi* (Vischniakoff). There are no data which allow to distinguish the complexes of "Blakei and Nikitini Subzones". The differences shown by CASEY & MESEZHNIKOV (1986) had geographical nature. They cannot be adopted as evidence of more older Nikitini Zone age in near-Moscow and upper Volga than the age of the beds in middle Volgian.

Fulgens Zone NIKITIN (1888): *Craspedites fragilis* (Trautschold), *C. okensis* (d'Orb.), *C. nekrassovi* Prigorovsky, *C. krilovi* Prigorovsky, *C. subditoides* (Nikitin), *Garnericeras catenulatum* (Fischer), *G. interjectum* (Nikitin), *Kachpurites fulgens* (Trautschold), *K. subfulgens* (Nikitin).

Subditus Zone NIKITIN (1888): *Craspedites okensis* (d'Orb.), *C. nekrassovi* Prigorovsky, *C. jugensis* Prigorovsky, *C. subditus* (Trautschold), *C. subditoides* (Nikitin), *Garnericeras catenulatum* (Fischer). *G. interjectum* (Nikitin).

Nodiger Zone NIKITIN (1888): *Craspedites nodiger* (Eichwald), *C. triptychus* (Nikitin), *C. kaschpuricus* (Trautschold), *C. parakaschpuricus* Gerasimov, *C. milkovensis* Strmooukhov, *C. kuznetzovi* (Sokolov), *C. mosquensis* Gerasimov, *Garnericeras subclypeiforme* (Milaschevitsch).

The Nodiger Zone admits two subdivisions: Subzone of *Craspedites mosquensis* (lower) and Subzone of *Craspedites nodiger* (upper). These subzones differ by the distribution of species *Craspedites mosquensis* Gerasimov and *C. triptychus* (Nikitin) in the lower part (subzone) of Nodiger Zone.

The correlations of the base of the lower Volgian with the Kimmeridgian/Tithonian boundary of western-Europe area could be assured, on the basis of genus *Gravesia* found in the Klimovi Zone on the Gorodische lectostratotypical section (MESEZHNIKOV, 1988). On a same way, *Neochetoceras* and *Glochiceras*, mentioned by GERASIMOV & MIKHAILOV (1966), could be a possible equivalent with the lowermost Tithonian (Hybonotum Zone).

Source : MNHN, Paris

The correlation of the base of the middle Volgian (Panderi Zone) is much less certain. The pavlovids of the Panderi Zone, suggest a rough parallel with the Pallasioides/Rotunda boundary in Britain (CALLOMON & BIRKELUND, 1982).

Higher in the succession, the group of *Epivirgatites nikitini* (MICHALSKI, 1890), has been equated with the Albani-Glaucolithus Zones of the English Portlandian (WIMBLEDON & COPE, 1978). *"Lomonossovella" lomonossovi* (Vishniakov, 1882) appears to be a true *Kerberites* Buckmann from the Kerberus Zone (CALLOMON & BIRKELUND, 1982). The upper Volgian begins everywhere with the appearance of *Craspedites*. The closest correspondence which can suggest is between the Nodiger Zone and the English Preplicomphalus Zone, in which the *Craspedites* has also been found (CASEY, 1973, CALLOMON & BIRKELUND, 1982).

STRATIGRAPHICAL DISTRIBUTION OF RUSSIAN PLATFORM "OIL SHALE BANDS" AND THEIR GEOCHEMICAL TRENDS

The background facies of the Upper Jurassic deposits from the Russian Platform are mainly mudstone and marlstone with $CaCO_3$ content lower than 40% (25% in average). Carbonate-free sandstone and siltstone, as subordinate facies, are mainly related to upper Volgian deposits. Some samples show higher carbonate content (50-80%), and correspond either to sandstone with calcitic cement or carbonate-nodules within the mudstone. The background facies show a very variable Corg. content, from about 1 wt% (higher than the average for shales) to very high values (10 wt%), that are elevated compared to recent and ancient marine sediments. Some levels show higher Corg. (up to 50%) and correspond to finely laminated shales, here called oil shales (Fig. 6). Such a richness is exceptional and the corresponding sediment could be regarded as pure organic matter.

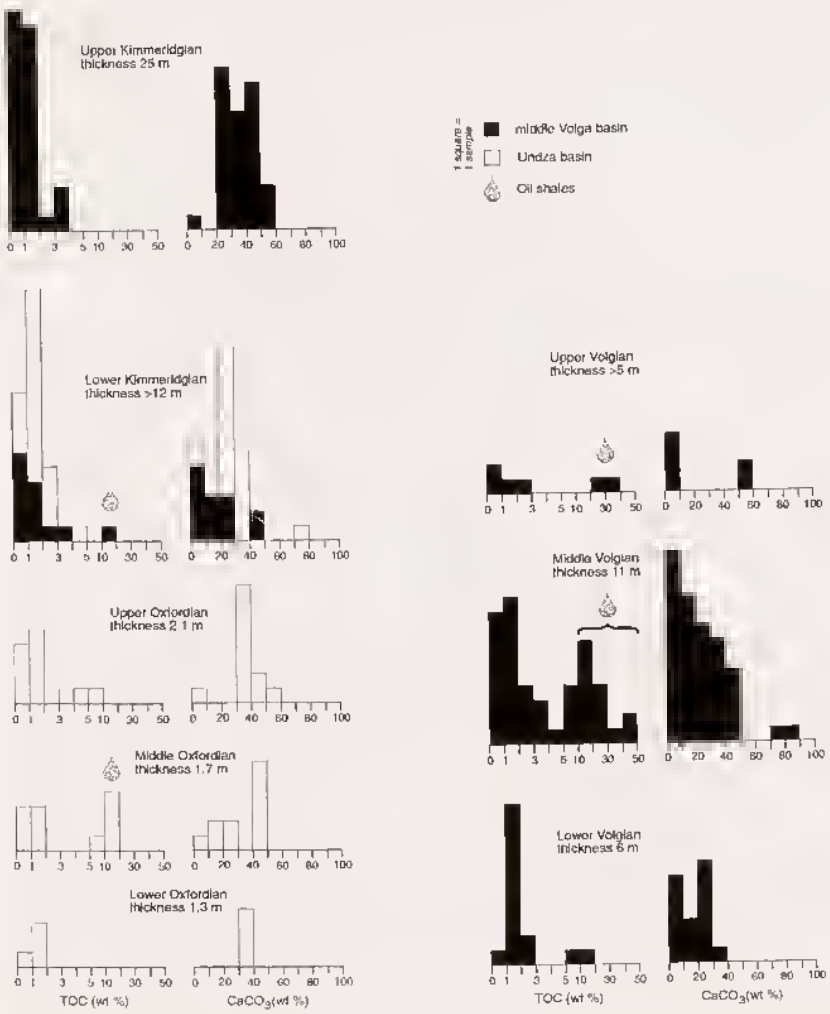

FIG. 6.— Frequency distribution for TOC and $CaCO_3$ content of samples from the Upper Jurassic of the Russian Platform. Samples with larges wood fragments are here disregarded (Note change in TOC scale axis for values above 5 and 10 % TOC).

FIG. 6.— Histogrammes des fréquences du contenu en COT et $CaCO_3$ des échantillons du Jurassique supérieur de la plate-forme russe. Les échantillons contenant de grands fragments de bois sont ici négligés. (Noter le changement d'échelle des abscisses pour les valeurs au dessus de 5 et 10% de COT).

Source : MNHN, Paris

The pyrolytic measurements show that the organic matter is widely distributed between type II (marine) and type IV (altered organic matter), according to the broad distribution of hydrogen index (HI) values, ranging from 10 to 700 mg HC/g TOC (Fig. 7). Oil shales show the higher HI values and are related to type II organic matter. Nevertheless, such facies may likewise contain organic matter with HI values less than 150. Most of the mudstone and marlstone show likewise low to medium HI values (23 to 250). These low values, associated with low organic carbon content, support the hypothesis of strong alteration of the organic matter. HI-values in organic-lean sediments, however, can be due to mineral matrix effect, e.g. adsorption of pyrolytically generated hydrocarbons on clay mineral surfaces (ESPITALIÉ *et al.*, 1985-86). Detailed organic geochemical studies are in progress in order to carefully determined the type of organic matter and to characterized the depositional environment by the mean of biomarkers.

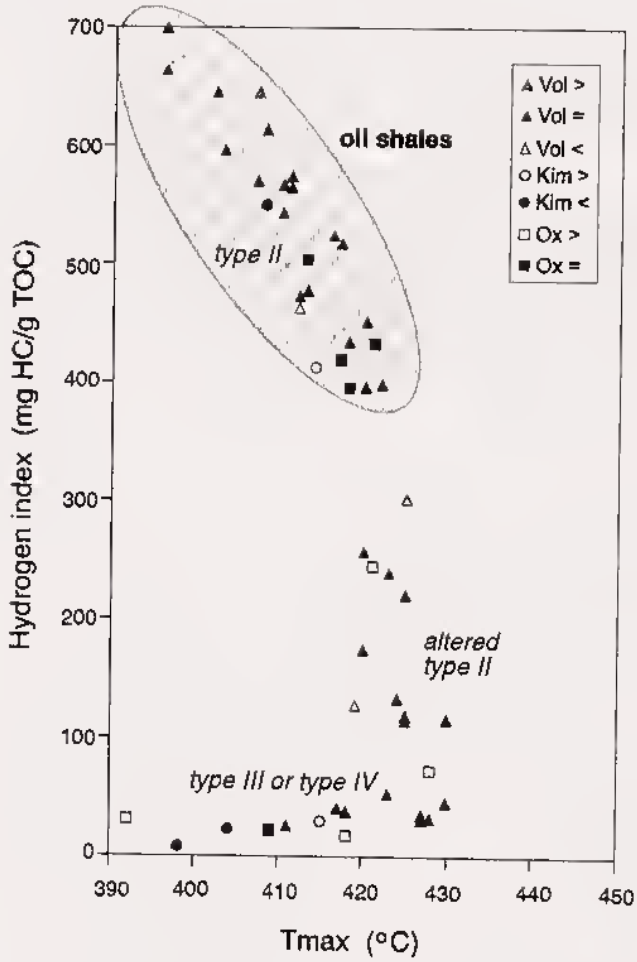

FIG. 7.— Hydrogen index vs Tmax diagram of selected samples from the Upper Jurassic of the Russian Platform.

FIG. 7.— Diagramme Index d'hydrogène vs. Tmax d'échantillons sélectionnés dans le Jurassique supérieur de la plate-forme russe.

Petroleum potentials of the oil shales are very good with an average of 95 kg HC/t of rock and some exceptional potentials ranging from 200 to 300 kg/t for the Volgian oil shale bands.

The oil shales show a variable frequency through the studied interval and are mostly concentrated in six bands, separated by the background mudstone and marlstone with less Corg. content. They are by stratigraphic order (Fig. 8):

— a 12 cm-thick band, occurring close to the middle-upper Oxfordian boundary (Glosense Zone) in the Makariev section (level Mk 14). Its organic content varies from 11 to 19% TOC. This level is overlain by 15 cm of dark claystones with bioturbations (level Mk 13), containing up to 6.5% TOC. A discontinuous, cm-thick oil shale level exists locally below this first horizon. This first oil shale band is well known in subsurface as far as Moscow, where its thickness increases up to 1 m, whereas its organic richness is decreasing (only 3% Corg, according to authors unpublished measurements);

Source : MNHN, Paris

— a lower Kimmeridgian (Cymodoce Zone) oil shale band is described here for the first time in the Russian Platform. This level is 50 cm thick in the Mimei village section (level Ta 5) and its organic richness is 15% TOC;

— the most famous and widespread oil shale band is of middle Volgian age and is more precisely related to the Panderi Zone. This band was investigated in detail along the 6 m-thick profile of Gorodische (level Go 11). It is made by alternation of black shales and dark claystones. The organic richness of black shales varies from 2.3 to 44.5% TOC with a 16.5% mean value. The dark claystones contain between 0.5 and 5.4% TOC;

— the next band belongs to the same Substage but has a Virgatus Zone dating. This level was not recognised along the Gorodische section because of the predominance of sandy facies;

— the fifth band, from the base of upper Volgian (Fulgens Zone), was not recognised along the Gorodishche or Kashpir sections because of the predominance of sandy and calcareous-sandy facies;

— the last band belongs to the uppermost Volgian (Nodiger Zone), equivalent to the lower Berriasian. This level has a thickness ranging between 6 to 15 cm in the Kasphir section (level Ka 20) and an organic richness fluctuating from 22 to 33% TOC.

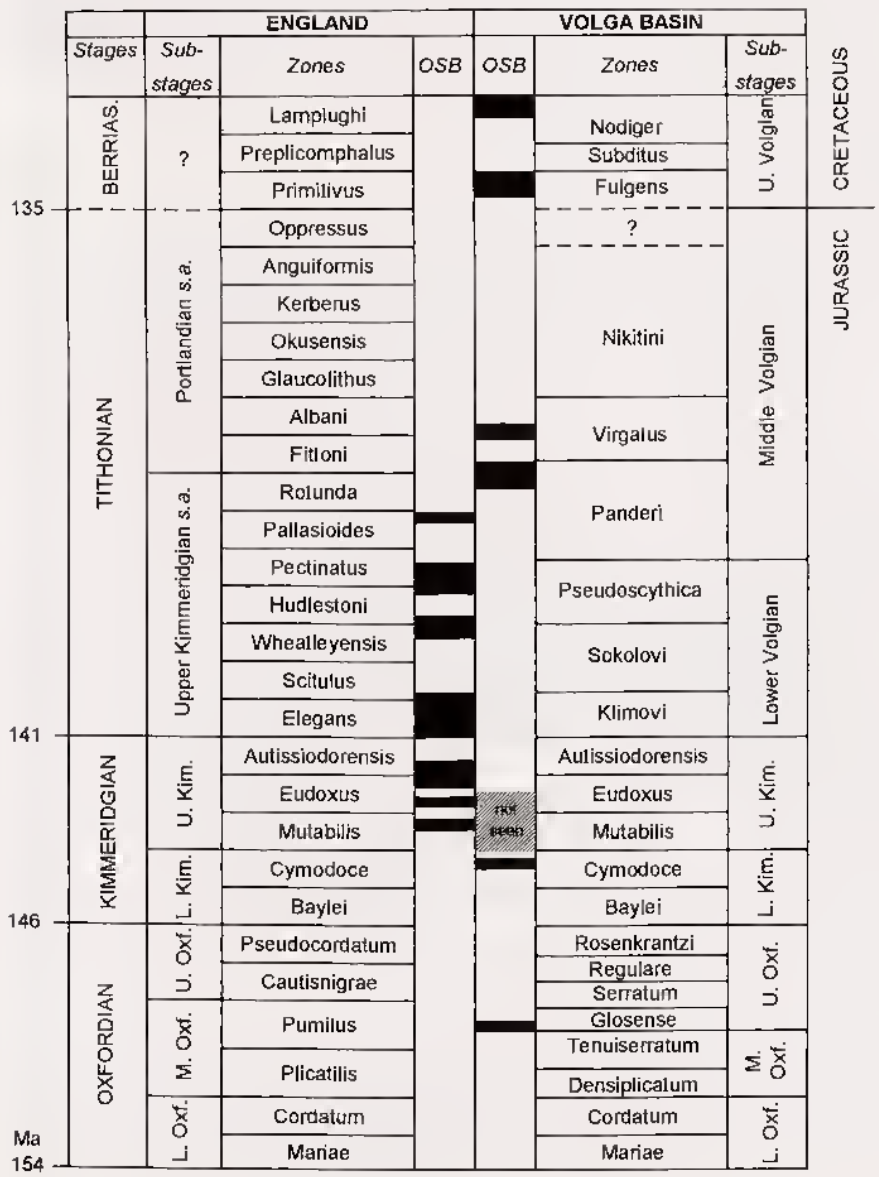

FIG. 8.— Stratigraphical distribution of the oil shale band (OSB) in both England and Volga basins. Time scale according to ODIN & ODIN (1990). See text for explanation.

FIG. 8.— Distribution temporelle des bandes de schistes bitumineux (OSB) en Angleterre et dans le bassin de la Volga. Échelle des temps d'après ODIN & ODIN (1990). Voir le texte pour les explications.

Source : MNHN, Paris

It should be noted that the upper Kimmeridgian deposits were not completely investigated during our field work and the Mutabilis Zone and basal part of the Eudoxus Zone was not recognised.

COMPARISON WITH THE KIMMERIDGE CLAY FORMATION

Late Jurassic is known to have been prone to the deposition of Corg.-rich series at a global scale and especially in the boreal domain (NORTH, 1979; ULMISHEK & KLEMME, 1990; BAUDIN, 1995). The Kimmeridge Clay Formation is one of the famous petroleum source rock which was deposited during this time interval. It extends onshore from the Wessex basin in southern England to the Cleveland basin of northern Yorkshire and is the main source rock in the North Sea basin. It has an homogeneous dark-coloured mudstone facies with a few, apparently isochronous, carbonate and oil-shale marker-beds that can be correlated all over the basin (COX & GALLOIS, 1981).

Because the age of the Kimmeridge Clay Formation ranges from Kimmeridgian to Volgian, that includes a large part of the studied interval on the Volga basin, we attempt to compare the stratigraphic distribution of oil shales between these two provinces.

According to the works of GALLOIS (1978), COX & GALLOIS (1981), WIGNALL (1991), HERBIN *et al.* (1991), HERBIN & GEYSSANT (1993) and RAMDANI (1996) five oil shale bands can be recognized in the Kimmeridge Clay Formation (Fig. 8):

— a middle Eudoxus band (BGS bed 29 *sensu* GALLOIS, 1979);

— an upper Eudoxus-lower Autissiodorensis band (BGS beds 32 and 33);

— an Elegans-basal Scitulus band (BGS beds 36 and 37);

— an upper Wheatleyensis-basal Hudlestoni band (BGS beds 42 and 43);

— an uppermost Hudlestoni-Pectinatus band (beds 45-47 *sensu* WIGNALL, 1991);

Although the frequency of oil shale bands is greater in the middle part of the Formation (Eudoxus to Pectinatus Zones), some oil shales are present in the Mutabilis and Pallasioides Zones (Fig. 8). The Mutabilis oil shale band is demonstrated by HERBIN *et al.* (1991) in the Yorkshire, whereas the Pallasioides band corresponds in the Dorset to beds 52-54 (Wignall, 1991).

It appears that the stratigraphic distribution of the oil shale bands from the Kimmeridge Clay Formation is completely different from those of the Volga basin (Fig. 8). As might be expected, the probably shallower environment in the Volga basin did not allow the preservation of organic matter during these time intervals. It appears that either these intervals were not associated with a relative change in water depth sufficient to allow dysoxic-anoxic conditions to be established or that other watermass factors were not suitable to organic matter preservation during the upper Kimmeridgian and lower Volgian. On the contrary, oil shale bands are present on the Russian Platform during upper Oxfordian, lower Kimmeridgian, middle and upper Volgian when the environments were more sandy and shallower in England and unfavourable to the organic matter preservation.

This lack of temporal correlation of the organic-rich deposits at a large scale during the Upper Jurassic has been mentioned previously for the Tethyan realm (BAUDIN, 1995). It seems that the Upper Jurassic was a suitable period for organic matter preservation, but any stratigraphic interval can be regarded as global time-slice prolific for source rock deposition. The oil shale bands discussed here are definitely not equivalent to oceanic anoxic events as the lower Toarcian (JENKYNS, 1988) or Cenomanian-Turonian (BUSSON & CORNÉE, 1996) events.

CONCLUSION

The above biostratigraphic study of the Upper Jurassic from middle Volgian basin has enabled the Russian series to he correlated more precisely with the western-european standard zonation. Concerning the Oxfordian Stage, the use of Cardioceratids faunas authorised some equivalencies with boreal and

Source : MNHN, Paris

sub-boreal successions. The Oxfordian/Kimmeridgian boundary is precisely identified with the basal Kimmeridgian Densicostata Horizon.

The best biostratigraphical correlations between the Russian Platform and western Europe are achieved for the Kimmeridgian stage. Seven ammonites horizons are common within these two areas: *P. densicostata, P. baylei, O. lallierianum, A. caletanum, A. contejeani, A. yo and A. autissiodorensis.* Morever, the levels with *R. uralensis* can be probably subdivided with various *Rasenia* species. Similarly, the "Acanthicum Zone *auct*" seats many suboreal Aulacostephanids and a more precise biostratigraphical scheme can be obtain with better correlations between Russian Platform and the subboreal province (North Sea basin, southern England, Aquitaine and Paris basins, northern Germany...).

On the other hand, the equivalences between the regional "Volgian stage" and/or Tithonian/Portlandian *sensu anglico*, are much less certain. Some difficulties proceeded of a pronounced faunal provincialism. Correspondences can be only suggested by affinities of the endemic Russian ammonites and the boreal faunas. Local scheme is still necessary.

Geochemical characterisation of the Upper Jurassic series from the Russian Platform show several intervals with high organic content (Corg >10%) and good petroleum potentials. Nevertheless, they are not synchronous with organic-rich intervals from the Kimmeridge Clay Formation. Further studies are needed to understand the depositional control of these oil shales at a small scale, but the present data clearly indicate that oil shale bands cannot be taken as marker beds at a large scale.

ACKNOWLEDGMENTS

We are indebted to the Peri-Tethys Program for providing financial support for this study (prop. 95-28 and 95/96-28). We grateful acknowledge J. SANFOURCHE for his helpful technical assistance for geochemical analyses. We are indebted to A.Y. HUC and J. THIERRY for their critical suggestions on an earlier draft of this paper.

REFERENCES

ATROPS, F., GYGI, R., MATYJA, B.A. & WIERZBOWSKI, A., 1993.— The *Amoeboceras* faunas in the Middle Oxfordian-lowermost Kimmeridgian Submediterranean succession and their correlation value. *Acta Geologica Polonica*, **43**, 3-4: 213-227.

BAUDIN, F., 1995.— Depositional controls on the Mesozoic source rocks in the Tethys. *In*: A.Y. HUC (ed.), Paleogeography, Paleoclimates and Source Rocks. *American Association of Petroleum Geologists, Studies in Geology*, **40**: 191-211.

BIRKELUND, T., CALLOMON, J.H. & FÜRSICH, F.T., 1984.— The stratigraphy of the Upper Jurassic-Cretaceous sediments of Milne Land, central East Greenland. *Grönlands Geologiske Undersogelse, Bulletin*, **153**: 1-56.

BUSSON, G. & CORNÉE A., 1996.— L'événement océanique anoxique du Cénomanien supérieur-terminal: une revue et une interprétation mettant en jeu une stratification des eaux marines par le CO_2 mantellique. *Publications de la Société géologique du Nord, Lille*, **23**: 1-144.

CALLOMON, J.H. & BIRKELUND, T., 1982.— The ammonite zones of the Boreal Volgian (Upper Jurassic) in East Greenland. *In*: A.F. EMBRY & H.R. BALKWILL (eds). Arctic geology and geophysics. *Memoir· Canadian Society of Petroleum Geologists*, **8**: 349-369.

CARIOU, É. 1966.— L'Oxfordien supérieur du synclinal de Lezay-Avon (Deux-Sèvres). *Comptes Rendus de l'Académie des Sciences, Paris*, **262**, D: 45-47.

CARIOU, É., ENAY, R., ATROPS, F., HANTZPERGUE, P., MARCHAND, D. & RIOULT, M., 1997.— Oxfordien. *In*: *f*. CARIOU & P. HANTZPERGUE (eds), Biostratigraphie du Jurassique ouest-européen et méditerranéen: zonations parallèles et distribution des invertébrés et microfossiles. *Elf Aquitaine Édition, Pau, Mémoire*, **17**: 144-147, tab. IX-X, pl. 21-22.

CASEY, R. & MESEZHNIKOV, M.S., 1986.— Upper horizons of Middle Volgian substage and English equivalents. *Izvestiya Akademiy Nauk SSSR, Seriya Geologicheskaya*, **10**: 69-81 (in Russian).

CASEY, R., 1973.— The position of the Middle Volgian in the English Jurassic. *Proceedings of the Geological Society of London*, **1650**: 128-133.

COX, B.M. & GALLOIS, R.W., 1981.— *The Stratigraphy of the Kimmeridge Clays of the Dorset Type Area and its Correlation with Some other Kimmeridgian Sequences*. Institute of Geological Sciences, London: 1-28.

Source : MNHN, Paris

DOUVILLÉ, R., 1881.— Note sur la partie moyenne du terrain jurassique dans le bassin de Paris et sur le terrain corallien en particulier. *Bulletin de la Société géologique de France, Paris*, (3), **9**: 439-474.

ENAY, R., 1966.— Le genre *Gravesia* (Ammonitina jurassique) dans le Jura français et les chaînes subalpines. *Annales de Paléontologie, Paris*, III, I: 96-116.

ENAY, R., 1980.— Paléobiogéographie et ammonites jurassiques: "rythmes fauniques" et variations du niveau marin; voies d'échanges, migrations et domaines biogéographiques. *Livre Jubilaire de la Société géologique de France, mémoire hors série*, **10**: 261-281.

ESPITALIÉ, J., DEROO, G. & MARQUIS, F., 1985-1986.—La pyrolyse Rock-Eval et ses applications. *Revue de l'Institut français du Pétrole*, **40**, 5: 563-579; **40**, 6: 755-784; **41**, 1: 73-89.

GALLOIS, R.W., 1979.— A pilot study of oil shale occurrences in the Kimmeridge Clay. *Institute of Geological Sciences Report*, **78**, 13: 1-44.

GERASIMOV, P. A., 1969.— *Upper substages of the Volgian Stage of the Central Part Russian Platform*. Nauka, Moscow: 1-144.

GERASIMOV, P.A. & MIKHAILOV, N.P., 1966.— Volgian stage and the geostratigraphical scale for the Upper series of the Jurassic system. *Izvestiya Akademiy Nauk SSSR, Seriya Geologicheskaya*, **2**: 118-138 (in Russian).

GERASIMOV, P.A., MITTA, V.V. & KOCHANOVA, M.D., 1995.— *Volgian Fossils of the Central Russia*. VNIGNI, Moscow: 1-116 (in Russian).

GEYSSANT, J.R., 1997.— Tithonien. *In*: É. CARIOU & P. HANTZPERGUE (eds), Biostratigraphie du Jurassique ouest-européen et méditerranéen: zonations parallèles et distribution des invertébrés et microfossiles. *Elf Aquitaine Édition, Pau, Mémoire*: 152-155, tab. XIII, pl. 25-26.

HANTZPERGUE, P., 1979.— Biostratigraphie du Jurassique supérieur nord-aquitain. *Bulletin de la Société géologique de France, Paris*, (7), XXI, 6: 715-726.

HANTZPERGUE, P., 1989.— Les Ammonites kimméridgiennes du Haut-fond d'Europe occidentale. *Cahiers de Paléontologie, Paris*: 1-428.

HANTZPERGUE, P., ATROPS, F. & ENAY, R., 1997.— Kimméridgien. *In*: É. CARIOU & P. HANTZPERGUE (eds), Biostratigraphie du Jurassique ouest-européen et méditerranéen: zonations parallèles et distribution des invertébrés et microfossiles. *Elf Aquitaine Édition, Pau, Mémoire*: 148-151, tab. XI-XII, pl. 23-24.

HAUG, E., 1898.— Portlandien, Tithonique et Volgien. *Bulletin de la Société géologique de France, Paris*, **3**, 26: 197-228.

HERBIN, J.P. & GEYSSANT, J.R., 1993.— "Ceintures organiques" au Kimméridgien/Tithonien en Angleterre (Yorkshire, Dorset) et en France (Boulonnais). *Comptes Rendus de l'Académie des Sciences, Paris*, **317**, II: 1309-1316.

HERBIN, J.P., MÜLLER, C., GEYSSANT, J.R., MÉLIÈRES, F. & PENN, I.E., 1991.— Hétérogénéité quantitative et qualitative de la matière organique dans les argiles du Kimméridgien du val de Pickering (Yorkshire, UK). Cadre sédimentologique et stratigraphique. *Revue de l'Institut français du Pétrole*, **46**, 6: 675-712.

ILOVAISKY, D.I. & FLORENSKY, K.P., 1941.— Les ammonites du Jura supérieur des bassins des rivières Oural et Ilek. Contribution à la connaissance géologique de l'URSS. *Bulletin de la Société des Naturalistes de Moscou, Nouvelle serie*, **1** (5): 1-196 (in Russian).

JENKYNS, H.C., 1988.— The early Toarcian (Jurassic) anoxic event: stratigraphic, sedimentary and geochemical evidence. *American Journal of Science*, **288**: 101-151.

LAHUSEN, J., 1883.— Die Fauna der jurassische Bildungen der Rjasanische Gouvernements. *Mémoire du Comité géologique*, vol. I, 1: 1-94.

MALINOWSKA, L., 1966.— Posttaway stratigrafii dolnego i srodkowego oksfor der polnaenej i polnocnozachodniej Polski. *Kwartalnik Geologiczny*, **10**, 3: 786-800.

MESEZHNIKOV, M.S., 1982.— Tithonien (Volgian) Stage. *In*: G. KRYMGALTS (ed.), *The Jurassic Zones of the USSR*. Nauka, Leningrad: 120-146.

MESEZHNIKOV, M.S., 1988.— Oxfordian, Kimmeridgian, Volgian. *In*: G.Y. KRYMHOLTS *et al.*, The Jurassic Ammonite Zones of the Soviet Union. *Geological Society of America*, Special papers, **223**: 39-62.

MESEZHNIKOV, M.S., 1989.— *The Middle and Upper Oxfordian of the Russian Platform*. Nauka, Leningrad: 1-183.

MESEZHNIKOV, M.S., BLOM, G.I., KUZNETSOVA, K.I., 1984.— Excursion 060 "Jurassic and Cretaceous Boundary Beds in the Middle Volga River area and Ryazan District". *In*: *Guidbook for excursion 059, 060, 066 for 27 th International Geological Congress*. Nauka, Moscow: 113-124.

MICHALSKI, A., 1890.— Die Ammoniten der unter Wolga-Stufe. *Mémoire du Comité géologique de Saint-Petersbourg*, 8, **2**: 1-159.

MIKHAILOV, N.P., 1962a.— Pavlovia and related groups of ammonites. *Bulletin de la Société des Naturalistes de Moscou, Section géologie*, **37**, 6: 3-30 (in Russian).

MIKHAILOV, N.P., 1962 b.— The upper boundary of the Kimmeridgian. *Report of the URSS Academy of Science*, **145**, 6: 1366-1368 (in Russian).

MIKHAILOV, N.P., 1964.— Boreal Late Jurassic (Lower Volgian) ammonites (Virgatosphinctinae). *Transactions of Geological Institute, Academy of Sciences USSR*, **107**: 5-88 (in Russian).

MITTA, V.V., 1993.— *Ammonites and Zonal Stratigraphy Middle Volgian Deposits of the Central Russia*. Geoprognoz, Kiev: 1-132 (in Russian).

Source : MNHN, Paris

NEUMAYR, M., 1873.— Die Fauna der Schichten mit *Aspidoceras acanthicum*. *Abhandlungen der Kaiserlich-koniglichen geologischen Reichsanstalt, Vienne*: 141-257.

NIKITIN, S.N., 1881a.— Jurassic formations between Rogbinsk., Mologa, and Myshkin. *In*: Materials on the Geology of Russia. *Mineralogical Society*, **10**: 1-194 (in Russian).

NIKITIN, S.N., 1881b.— Die Jura-Ablagerungen zwischen Rybinsk, Mologa und Myschkin an der oberen Volga. *Mémoires de l'Académie impériale des Sciences. Saint-Petersbourg*, série 7, livre 28, **5**: 1-98 (in Russian).

NIKITIN, S.N., 1884.— Allgemeine geologische Karte von Russland, feuille 56. *Mémoire du Comité géologique*, **1**, 2: 1-153.

NIKITIN, S.N., 1888.— Allgemeine geologische Karte von Russland, feuille 71. *Mémoire du Comité géologique*, **2**, 1: 1-218.

NORTH, F.K., 1979.— Episodes of source-sediment deposition (1). *Journal of Petroleum Geology*, **2**, 2: 199-218.

ODIN, G.S. & ODIN, C., 1990.— Échelle numérique des temps géologiques. *Géochronique*, **35**: 12-21.

ORBIGNY, A. D', 1852.— *Cours élémentaire de paléontologie et de géologie stratigraphique*. Vol. II, tome 2. Masson, Paris: 383-847.

RAMDANI, A., 1996.— *Les paramètres qui contrôlent la sédimentation cyclique de la "Kimmeridge Clay Formation" dans le bassin de Cleveland (Yorkshire, Grande-Bretagne): comparaison avec le Boulonnais (France)*. Thèse, Université Paris-Sud, Orsay, France, **4522**: 1-259.

RESOLUTION, 1993.— *The Standard Stratigraphical Scheme of The Jurassic of Russian Platform*. VNIGRI, Roskomnedra: 1-72, 28 tables.

ROUILLIER, CH., 1845.— Sur les animaux des gouvernements de Moscou. *Maskovskie vedomosty*: 1-96 (in Russian).

ROZANOV, A.N., 1906.— Sur la question de la subdivision des couches à Virgati dans les environs de Moscou. *L'Annuaire géologique et minéralogique de la Russie*, **8**, 6-7: 198-210 (in Russian).

ROZANOV, A.N., 1919.— Sur la division du Volgien inférieur du gouvernement de Simbirsk. *Nouvelles du Comité géologique de la section de Moscou*, **1**: 193-204 (in Russian).

SALFELD, H., 1913.— Certain Upper Jurassic strata of England. *Quarterly Journal of the Geological Society of London*, **69**: 423-430.

SEY, I.I. & KALACHEVA, E.D., 1993.— *Biostratigraphic Criteria of Jurassic/Cretaceous Boundary in Russia*. VSEGEI, Saint-Petersburg: 1-60.

SOKOLOV, D.N., 1901.— Sur la géologie des environs d'Ileizkaya Zastschita. *Bulletin de la Section d'Orenbourg, Société de Géographie de Russie*, **16**: 37-79 (in Russian).

SYKES, R.M. & CALLOMON, J.H., 1979.— The *Amoeboceras* zonation of the Boreal Oxfordian. *Palaeontology, Londres*, **22**, pt. 4: 839-903.

SYKES, R.M. & SURLYK, F., 1976.— A revised ammonite zonation of the Boreal Oxfordian and its application on northeast Greenland. *Lethaia*, **9**: 421-436.

SYKES, R.M., 1975.— The stratigraphy of the Callovian and Oxfordian stages (Middle-Upper Jurassic) in northern Scotland. *Scottish Journal of Geology*, **11**: 51-78.

ULMISHEK, G.F. & KLEMME, H.D., 1990.— Depositional controls, distribution, and effectiveness of World's Petroleum Source Rocks. *US Geological Survey Bulletin*, **1931**: 1-59.

VISHNIAKOV, N., 1882.— Description des Planulati (Perisphinctes) jurassiques de Moscou. 1ère partie. The author, Moscow: 9 pl. and legends.

WIGNALL, P.B., 1991.— Test of the concepts of sequence stratigraphy in the Kimmeridgian (Late Jurassic) of England and northern France. *Marine and Petroleum Geology, London*, **8**: 430-441.

WIMBLEDON, W.A. & COPE, J.C.W., 1978.— The ammonite faunas of the English Portland Beds and the Zones of the Portlandian Stage. *Journal of the Geological Society, London*, **135**: 183-190.

ZIEGLER, B., 1961.— Stratigraphische und zoogeographische Beobachtung an *Aulacostephanus* (Ammonoidea-Oberjura). *Palaeontographica, Stuttgart*, **35**: 79-89.

Source : MNHN, Paris

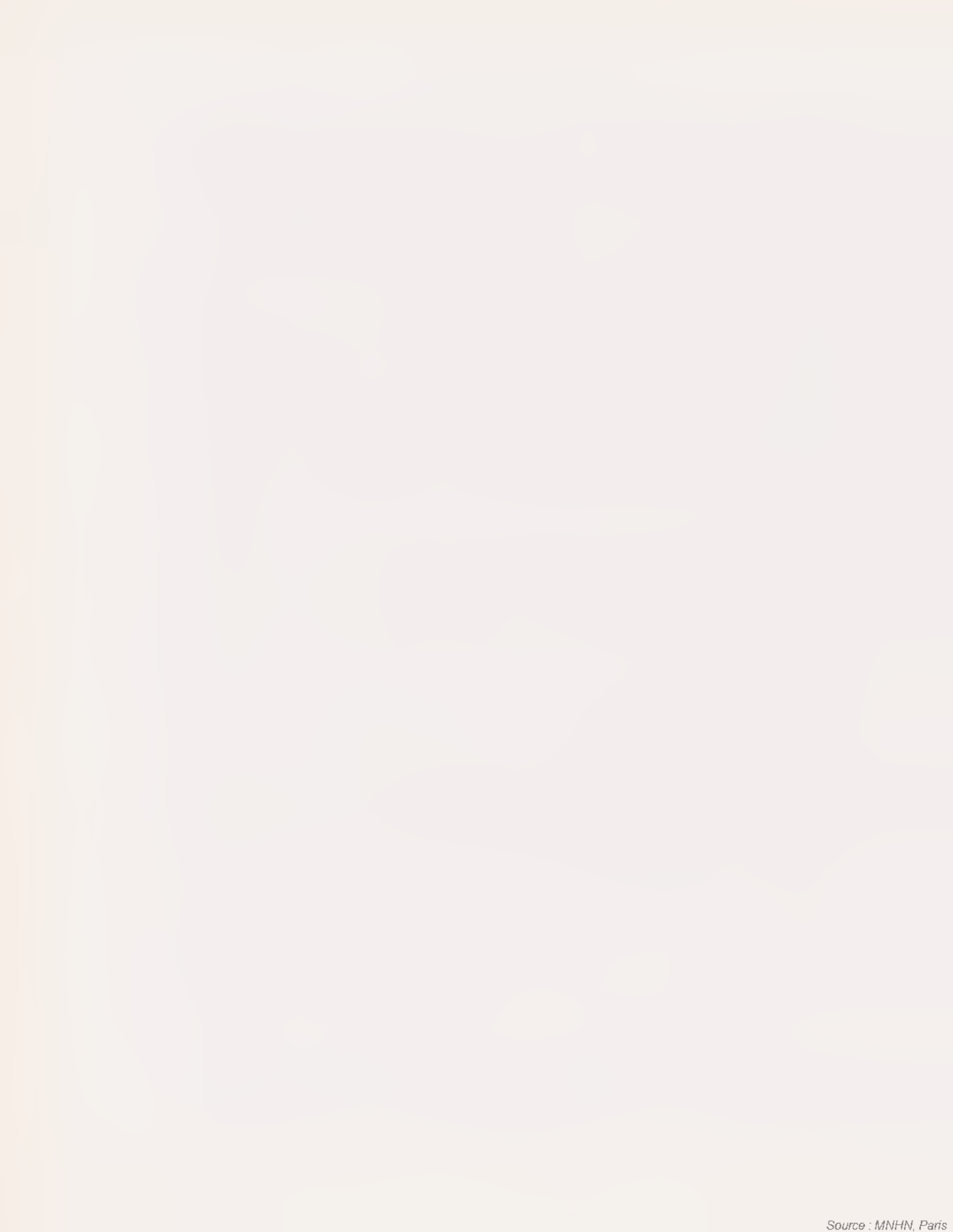

Source : MNHN, Paris

The Mesozoic of the Mangyshlak (West Kazakhstan)

Maurizio GAETANI [1], *Marco BALINI* [1], *Valery J. VUKS* [2], *Vera A. GAVRILOVA* [2], *Eduardo GARZANTI* [1], *Alda NICORA* [1], *Elisabetta ERBA* [1], *Élie CARIOU* [3], *Fabrizio CECCA* [4], *Isabella PREMOLI SILVA* [1], *Maria Rose PETRIZZO* [1], *Simonetta CIRILLI* [5] & *Raffaella BUCEFALO PALLIANI* [5]

[1] Dipartimento di Scienze della Terra, Via Mangiagalli 34, 20133 Milano, Italia

[2] VSEGEI, Sredny pr. 74, Saint-Petersburg 199106, Russia

[3] Université de Poitiers, UFR Sciences Fondamentales et Humaines, Laboratoire de Géobiologie, Biochronologie et Paléontologie, 40, avenue du Recteur Pineau, F-86022 Poitiers, France

[4] Istituto di Geologia, Università di Urbino, loc. Crocicchia, Urbino, Italia

[5] Università di Perugia, Dipartimento di Scienze della Terra, Piazza Università 1, Perugia, Italia

ABSTRACT

The Mesozoic succession of the Mangyshlak (W. Kazakhstan) starts with the Lower Triassic Birkut, Otpan, and Dolnapa Formations, representing an alluvial plain. Permian units were not detected. The marine ingression is recorded by the Tyururpa Group, which yielded ammonoid/conodont faunas, dated to the Olenekian. Towards the top of the Group, a resumption of terrigenous sedimentation and a shallowing-upward trend, is recorded. Sandstone petrography demonstrates fine-grained litharenites or feldspathic litharenites, largely derived from "dacite" volcanics. Accumulation exceed 200-300 m/Ma. The overlying Karaduan Formation is dominated by continental facies, possibly of Middle Triassic age. It is overlaid by the Carnian Akmysh Formation, with re-establishment of marine conditions. Several high-frequency cycles are present, often with a strong terrigenous input, which prevails upwards in the Shair Formation. The sandstone petrography indicates a persistent erosion of a volcanic arc. The 3000/4000 m-thick Triassic succession suggests a high sedimentation rate. The Mangyshlak area emerged and was deformed during the Norian, due to the Eo-Cimmerian orogeny. Subaerial conditions persisted for tens of Ma, because spectacular silcrete soils seal the Triassic beds. The generalized Jurassic transgression on an irregular topography occurred only with the Middle Jurassic, with lacustrine, marshy or fluvial deposits. Marine ingressions occurred episodically during the Middle Jurassic, becoming generalized during the early Callovian. Sedimentation continued with shales of Oxfordian age. They ends with an ironstone, unconformably overlain by Berriasian oyster banks. The Jurassic is characterized by low subsidence rate, with mostly terrigenous sedimentation. The mid Jurassic sandstones are feldspathic litharenites, derived from low-grade metamorphics, granitoids and mafic to felsic volcanics. The Cretaceous succession is 800-1000 m- thick and is divided into

GAETANI, M., BALINI, M., VUKS, V. J., GAVRILOVA, V. A., GARZANTI, E., NICORA, A., ERBA, E., CARIOU, É., CECCA, F., PREMOLI SILVA, I., PETRIZZO, M.R., CIRILLI, S. & BUCEFALO PALLIANI, R., 1998. — The Mesozoic of the Mangyshlak (West Kazakhstan). *In*: S. CRASQUIN-SOLEAU & É. BARRIER (eds), Peri-Tethys Memoir 4: epicratonic basins of Peri-Tethyan platforms, *Mém. Mus. natn. Hist. nat.*, **179** : 35-74. Paris ISBN : 2-85653-518-4.

Source : MNHN, Paris

three parts. In the lower part, three to four thin sequences may be recognized. They are controlled by the Neo-Cimmerian orogenic event, ending with a generalised emersion during the Barremian. The sandstones are lithic arkoses and feldspathic litharenites, originating from igneous rocks and low-grade metamorphics. The subsidence rate greatly increased from the upper Aptian up to the Turonian, and a clay to fine sandstone sequence was deposited, with phosphatic and ironstone horizons. With the Coniacian, a white chalk unit sedimented over the whole area, ending in the Palaeocene.

RÉSUMÉ

Le Mésozoïque du Mangyshlak (Ouest Kazakhstan).

La série mésozoïque du Mangyshlak (ouest du Kazakhstan) débute avec les formations Birkut, Otpan et Dolnapa du Trias inférieur, représentant une plaine alluviale. Les unités permiennes n'ont pas été détectées en surface. L'avancée marine est enregistrée par le groupe Tyururpa, qui a livré des ammonites et des conodontes, datés de l'Olénékien. La pétrographie des grès montre des litharénites à grains fins ou des litharénites feldspathiques largement dérivées de roches volcaniques dacitiques. L'accumulation dépasse 200-300 m/Ma. La formation Karaduan sus-jacente est dominée par des faciès continentaux, peut-être du Trias moyen. Elle est surmontée par la Formation carnienne Akmysh, avec le rétablissement des conditions marines. Plusieurs cycles de haute fréquence sont présents, souvent avec des apports terrigènes importants, qui dominent plus haut dans la Formation Shair. La pétrographie des grès indique l'érosion persistante d'un arc volcanique. La série triasique, épaisse de 3 à 4000 m, suggère un taux de sédimentation élevé. La région du Mangyshlak a émergé et a été déformée durant le Norien, sous l'effet de l'orogenèse Éo-Cimmérienne. Des conditions sub-aériennes persistent durant des dizaines de Ma car des sols siliceux spectaculaires scellent les dépôts du Trias. La transgression généralisée du Jurassique sur une topographie irrégulière se produit seulement au Jurassique moyen avec des dépôts fluviaux, lacustres ou marécageux. Des incursions marines ont lieu périodiquement durant le Jurassique moyen, devenant généralisées durant le Callovien inférieur. La sédimentation se poursuit avec les shales de l'Oxfordien. Ils se terminent avec un niveau riche en minerai de fer, recouverts en discordance par des bancs à huîtres bérriasiens. Le Jurassique est caractérisé par un faible taux de sédimentation essentiellement terrigène. Les grès du Jurassique moyen sont des litharénites feldspathiques dérivées de roches faiblement métamorphiques, de granitoïdes et de roches volcaniques mafiques à acides. La série crétacée est épaisse de 800 à 1000 m et est divisée en 3 parties. Dans la partie inférieure, 3 à 4 séquences fines peuvent être reconnues. Elles sont contrôlées par l'événement orogénique Néo-Cimmérien, et s'achèvent avec l'émersion généralisée durant le Barrémien. Les grès sont des arkoses lithiques et des litharénites feldspathiques, issues de roches magmatiques et faiblement métamorphiques. Le taux de subsidence augmente fortement de l'Aptien supérieur jusqu'au Turonien, et on observe une séquence d'argiles ou de grès fins avec des horizons phosphatés et ferrugineux. Avec le Coniacien, une unité de craie blanche se dépose sur l'ensemble de la région, se terminant au Paléocène.

INTRODUCTION

The Gorny Mangyshlak forms an alignment of hillocks on the east side of the Caspian Sea, reaching an altitude of 560 m (Fig. 1). The Triassic to Palaeogene succession was studied extensively by Soviet and Russian geologists, for its unique rock sequence exposed in isolated outcrops in the steppes of Central Asia. Towards the end of the Triassic, rocks were fairly strongly folded and the overlying units rest unconformably on them, folded in open asymmetric anticlines with a northward merging axial plane and a partially faulted southern limb (POLI, com. pers.). Consequently, the best outcrops and sections are preserved along the northern limb.

The aim of the present paper is to summarize the main features of the Mesozoic succession, focusing on the Triassic and Jurassic, with special attention to sandstone petrography, to the Lower Triassic ammonoid succession and to sequence stratigraphy interpretation. Field work was carried out in August-September 1995, during an expedition organised by N. Lyberis, UPMC, Paris and H. Yusufhocaev, Technical University of Tashkent. M. Gaetani, M. Balini, V.A. Gavrilova, and V.J. Vuks worked in the field, assisted by N. Lyberis, J.T. Poli (UPMC) and V.I. Troitzky (University of Tashkent).

THE TRIASSIC

The Triassic succession forms the core of the Mangyshlak anticlinorium, and crops out from west to east in three main areas: the Karatauchik, West Karatau and East Karatau (Fig. 1). Most field work was done in Karatauchik and West Karatau.

A basic lithostratigraphic scheme was proposed during the Samarkand Conference in 1971 (published in 1977 by the Interdepartimental Stratigraphic Commission, here called Samarkand Scheme) and was followed by later authors (TITOV *et al.*, 1985; LOZOWSKY *et al.*, 1986; GAVRILOVA, 1989, 1992

Source : MNHN, Paris

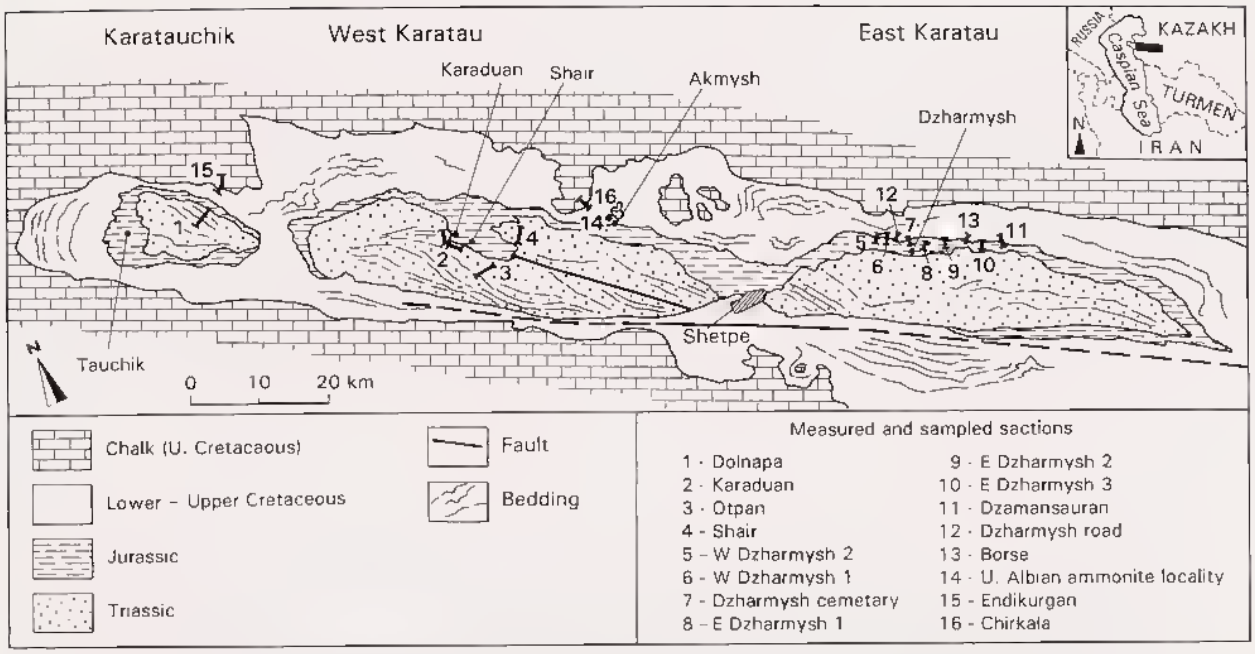

FIG. 1.— Index map of the Gorny Mangyshlak with position of the measured sections and isolated sampling localities.

FIG. 1.— Carte du Gorny Mangyshlak avec position des coupes levées et des localités échantillonnées.

and others). However, LITPATOVA (1984) and her co-workers split the previously proposed lithostratigraphic scheme, introducing more units and different chronostratigraphic attributions, especially for the central part of the succession. ZHIDOVINOV (1994) and VOLOZH *et al.* (subm.) recently followed this approach. The Samarkand Scheme is accepted in this paper, with the addition of some original age data, based on ammonoids, conodonts, palynomorphs and foraminifers (Fig. 2). In most cases the Russian "svita" is here considered equivalent to the western concept of formation.

The succession is as follows, bottom to top.

BIRKUT, OTPAN AND DOLNAPA FORMATIONS

These units were distinguished mostly in the western part of the area, where they reach an overall thickness of 2500 m (LOZOWSKY, 1974). However, internal folding probably accounts for several repetitions and thus the true stratigraphic thickness is considerably less. A figure between 1000 and 1500 m might be realistic, if seismostratigraphic data are also considered (VOLOZH *et al.*, submit.). The Birkut Formation consists of green-grey nodular shales, with rare siltstone layers, reddish in the upper part. It is gradually followed by the Otpan Formation with an increasing occurrence of siltstones and very fine sandstones, mostly dark grey or green in colour, with very rare, coarser intercalations. Sedimentary structures are rare with fine, parallel or low-angle laminations, and current ripple-marks. LOZOWSKY (1974) also recorded thin red siltitic intercalations. The transition to the mostly red sediments of the Dolnapa Formation is gradual. The best sections are around mount Otpan, south of Shair in West Karatau, whereas only the upper part of the unit crops out near Dolnapa, in Karatauchik. Red (rarely green) shales and siltstones dominate, with festoon-shaped medium-grained sandstone intercalations, and more laterally, persistent bodies of fine-grained sandstones in 10 m-thick packages. Sedimentary structures are rare, with mostly thin, parallel laminations. The upper boundary was drawn at the appearance of the first calcareous or dolostone bed, usually a grey shell-lag. However, in the shaly grey-red uppermost part of the Dolnapa Formation, VINYUKOV (1966) and LOZOWSKY (1974) reported several euryhaline pectinid bivalves, mostly *Eumorphotis*. The age of this fairly homogeneous

Source : MNHN, Paris

succession is disputed. The Samarkand Scheme by convention draws the Permian/Triassic boundary at the base of the Dolnapa Formation, without any paleontological evidence. LOZOWSKY *et al.* (1986) found megaplant remains (*Pleuromeia*) in the Birkut Formation, that they considered of Triassic age. Moreover, sporomorphs obtained in a borehole from the Otpan Formation in East Karatau were attributed to the Early Triassic by LOZOWSKY *et al.* (1986). On the contrary, ZHIDOVINOV (1994), followed by FEINBERG *et al.* (1996) and VOLOZH *et al.* (subm.), still drew the P/T boundary at the base of the Dolnapa Formation. Since the palaeontological evidence of LOZOWSKY *et al.* (1986) has not yet been challenged and no new palaeontological evidence has been presented, we concur with LOZOWSKY that all the terrigenous successions that crop out in West Karatau are Triassic in age. The environment was mostly continental, with large alluvial plains in which overbank deposits were predominant on low gradient rivers. Lakes and swamps were also identified by V.I. Zhelezko (Ekaterinburg University) within the Dolnapa Formation (pers. comm.). Red colour suggests oxic conditions in a semiarid climate. The top of the Dolnapa Formation indicates that brackish to euryhaline conditions were gradually established on the previous coastal plains.

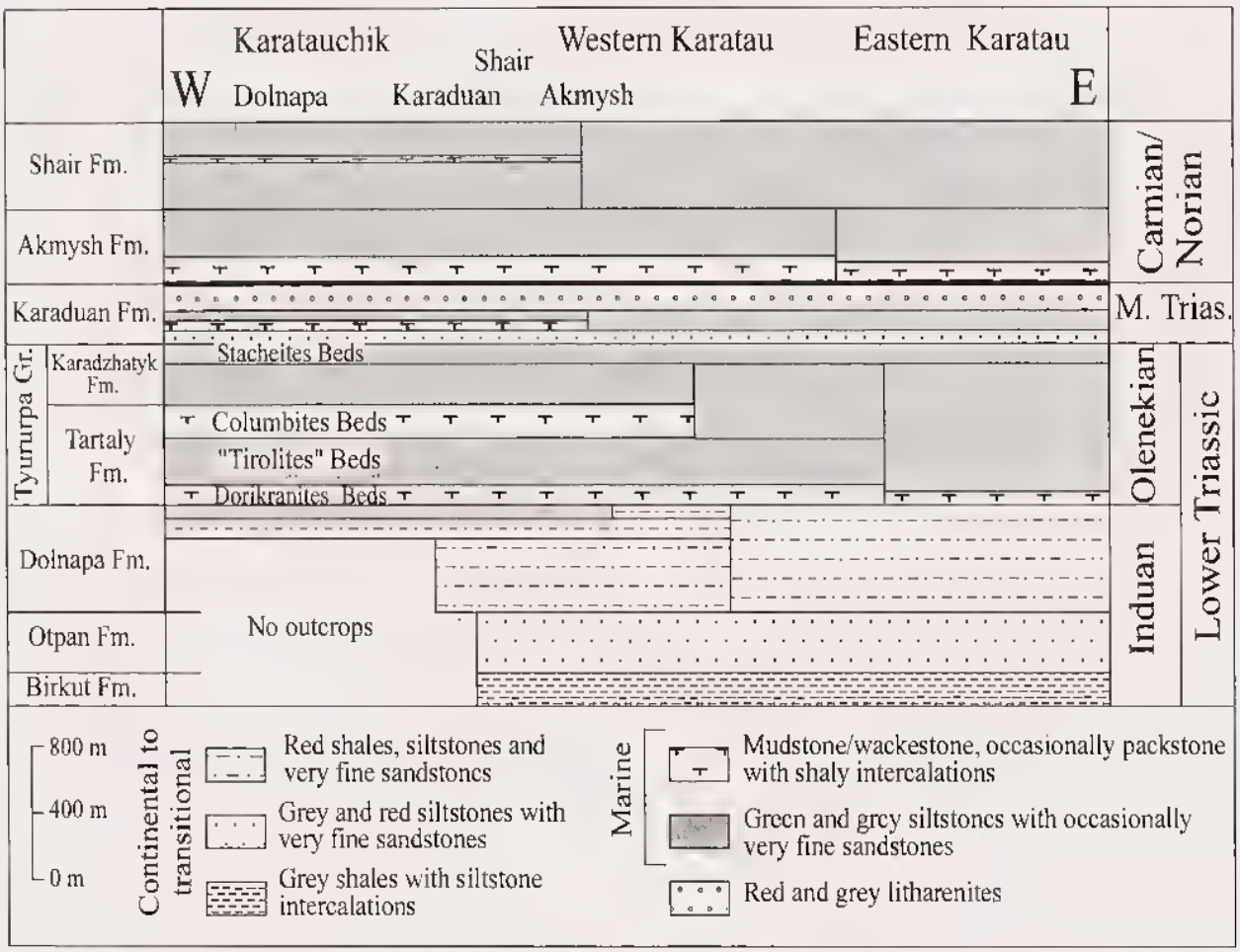

FIG. 2.— General scheme of Triassic formations with main continental to shallow marine environments and transgression/regressions.

FIG. 2.— Schéma général des formations du Trias avec les principaux environnements continentaux et marins et les transgressions - régressions.

Source : MNHN, Paris

TYURURPA GROUP (TARTALY AND KARADZHATYK FORMATIONS)

This group has been studied extensively, especially because of its fairly abundant ammonoid content (BAJARUNAS, 1936; ASTAKHOVA, 1960, 1964; SHEVYREV, 1968, 1990; KUMMEL, 1969; LIPATOVA, 1984; TITOV *et al.*, 1985; LOZOWSKY *et al.*, 1986; GAVRILOVA, 1989, 1992, 1995; ZHIDOVINOV, 1994). The best outcrops are in the western part of the range, whereas to the east the most typical facies are reduced in thickness and more difficult to distinguish from the other terrigenous units. We measured the Dolnapa section in Karatauchik and found it to have a total thickness of 732 m. LOZOWSKY (1974) reported a thickness of 840 m. This difference may be linked to the interpretation of minor faults.

The Group may be subdivided into three parts (Fig. 3). The lower part is dominated by siltstones and very fine-grained sandstones, in thin to medium-thick parallel-laminated beds. It contains significant calcareous intercalations, especially in the lowermost part, and reaches a thickness of about 250-300 m. In the middle part, about 300 m-thick, up to 2 m-thick local calcareous beds with brachiopods and small calcareous concretions, packed with ammonoids, are embedded in a grey-green shaly to silty succession. In the third part (200-250 m thick) that is attributed to the Karadzhatyk Formation, grey-green siltstones and very fine-grained sandstones dominate, always in thin beds with almost no sedimentary structures. The upper boundary is marked by the appearance of red siltstones and rare red-brown sandstones. The ammonoid and bivalve content was illustrated by ASTAKHOVA (1960, 1964), SHEVYREV (1968, 1990) and GAVRILOVA (1989, 1992, 1995), and the sequence of the ammonoid faunas was established in the sixty's (GAVRILOVA & KURUSHIN, 1986). However, a report of a bed-by-bed sampling was never published. In Fig. 3, we report the distribution of the ammonoids collected in two sections. The discovery of conodonts and the first finding of foraminifers from the Triassic of the Gorny Mangyshlak, allowed us to date these strata more precisely. The palynological content shows high thermal maturity. For this reason, the microflora is not always well preserved and its occurrence is discontinuous throughout the succession.

DORIKRANITES-TIROLITES BEDS

Conodonts in the upper part of the Dorikranites Beds, typical of the lower part of the Tyururpa Group, allowed this endemic ammonoid fauna to be dated. Sample MK 277 from the north side Otpan Mountain section yielded a few specimens of *Neospathodus* cf. *N. brevissimus* Orchard, whose range is possibly early Spathian (ORCHARD, 1995). In the Dorikranites Beds of the Otpan section, recrystallized fragments of macrofauna, microgastropods and the foraminifer *Limotuba* ? sp. are frequent. In the Dorikranites Beds of the Dolnapa section, only microgastropods occur. In the upper part of the Tirolites Beds the foraminifers *Tolypammina* ex. gr. *gregaria* Wendt and *Nodosaria* sp. are present.

Palynological assemblages from the base of the Dorikranites Beds to the top of the Tirolites Beds (Dolnapa section, samples MK 196 to MK 215), are characterized by *Endosporites papillatus* Jansonius associated with *Lunatisporites noviaulensis* (Leschik) Foster and *Lunatisporites* spp. (Table 1, Fig. 4). In the lower part of this interval, few specimens of *Krauselisporites* sp. were recorded, while rare *Corisaccites stradivarii* Utting and *Uvaesporites* sp. characterize the upper portion (MK 215). Stratigraphic analysis of the microflora indicates an Induan-early Olenekian age. For further discussion see the paragraph below on the Stacheites Beds.

COLUMBITES BEDS

In the Columbites Beds, the conodonts *Goudolella* cf. *jubata* Sweet, *Neospathodus symmetricus* Orchard, *N. abruptus* Orchard, and *N. homeri* (Bender) indicate a mid Spathian age (ORCHARD, 1995). Other microfossils, such as microgastropods, ostracods, and foraminifers, are also frequent. Amongst the latter, *Tolypammina* ex. gr. *gregaria* Wendt, *Planiinvoluta*? sp. (ex gr. *carinata* Leischner), *Nodosaria hoae* (Trifonova), *N.* aff. *hoae* (Trifonova), *N.* cf. *ordinata* Trifonova, *N.* aff. *pseudoprimitiva* Efimova, *N.* cf. *shablensis* Trifonova, *N.* sp., *"Froudicularia"* ex gr. *elegantula* K.M.-Maclay, *Lenticulina* ex gr.

Source : MNHN, Paris

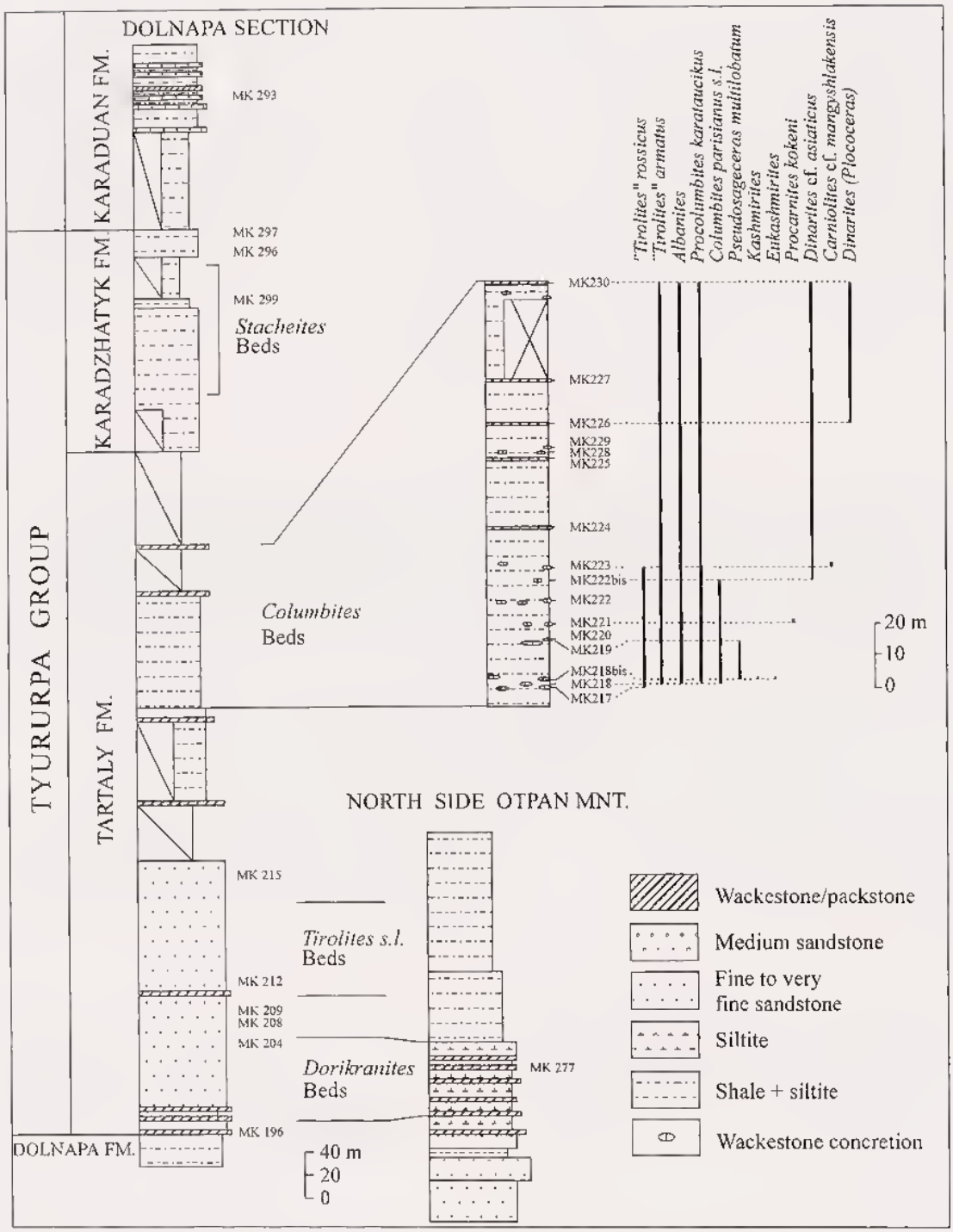

FIG. 3.— The two stratigraphic sections measured in the Tyururpa Group: North side Otpan Mountains and Dolnapa, with ammonoid range of the Columbites Beds in Dolnapa section. Species of *Tirolites* are in inverted commars, because the generic attribution needs revision.

FIG. 3.— Les deux coupes stratigraphiques levées dans le groupe de Tyururpa: versant nord des Montagnes Otpan et Dolnapa, avec les répartitions des ammonites des niveaux à Colombites pour la coupe de Dolnapa. Les espèces de Tirolites *sont entre guillemets car l'attribution générique nécessite une révision.*

Source : MNHN, Paris

TABLE 1.— Dolnapa section, Lower Triassic. Range chart of the most significant palynomorphs. The four semi-quantitative categories were established by averaging the number of palynomorphs counted for each taxon on three microscope slides. A form was classified as rare (R) if it averaged between 0 and 3 specimens, common (C) between 3 and10 specimens, frequent (F) between 10 and 20 specimens and abundant (A) if more than 20 specimens.

TABLEAU 1.— Coupe de Dolnapa, Trias inférieur. Répartition des palynomorphes les plus significatifs. Les quatre catégories semi-quantitatives ont été établies par moyennes du nombre de spécimens de palynomorphes pour chaque taxon sur trois lames minces. Une forme est qualifiée de rare (R) quand la moyenne est comprise entre 0 et 3 spécimens, commun (C) entre 3 et 10 spécimens, fréquent (F) entre 10 et 20 spécimens et abondant (A) si plus de 20 spécimens.

PERIOD	STAGE		SAMPLES	*Endosporites papillatus*	*Cycadopites follicularis*	*Lunatisporites noviaulensis*	*Lunatisporites pellucidus*	*Lunatisporites spp.*	*Krauselisporites sp.*	*Corisaccites stradivarii*	*Uvaesporites sp.*	*Densoisporites nejburgii*	*Densoisporites playfordii*	*Lundbladispora brevicula*	*Lundbladispora sp.*	*Gordonispora fossulata*	*Gordonispora sp.*	*Crinalites sabinensis*	*Grebeispora concentrica*	*Striatoabieites richterii*	*Protohaploxypinus limpidus*	*Protohaploxypinus sp.*	*Maculatisporites sp.*	*Calamospora sp.*	*Chordasporites singulichorda*	*Minutosaccus sp.*	*Alisporites tenuicorpus*	undetermined bisaccates	*Micrystridium sp.*	*Veryhachium sp.*
Early Triassic	OLENEKIAN	upper	MK293	R	C	R	C	R				C	R		R	R									R				R	
			MK297	C	F	A	C	F				A	C	A	F	F	R	C	C	F	F	F	R	R			C	F		R
			MK298	C	C	A	F	A	R			A	R	F	F	F	R	C	C	C	C	C	R	R		R	C	F		R
			MK299	R	F		F					A	C	C	C															
		lower	MK219									R	R																	R
			MK215	F	A	C		C		R	R														C					R
			MK212																											
			MK209	F	C	F		C													C	C		R			R			
			MK208	A	C	F		C													F	C		C	C	C				C
			MK204	A	F	A		C	R																		C			
			MK196	R																										

goettingensis (Franke), *Astacolus* spp. were identified. These foraminifers appear to be typical of the Olenekian of the West Caucasus and Precaucasus (EFIMOVA, 1991). The organic facies show high thermal maturity. The palynological content is very scarce. Only a few specimens of *Densoisporites* spp. and of acritarchs (*Veryhachium* sp.) were recognized (sample MK 219). In the basal part of the Columbites Beds, DAGYS (1974) reported the brachiopods *Piarorhynchella mangyshlakensis* Dagys, *Costispiriferina mansfieldi* Girty, *Spirigerellina pygmaea* Dagys and *Fletcherithyris margaritovi* (Bittner).

STACHEITES BEDS

No conodonts were found in the Stacheites Beds, and consequently the age of the top of the Tyurupa Group can be defined only with ammonoids and palynomorphs. The genus *Stacheites* was reported from

Source : MNHN, Paris

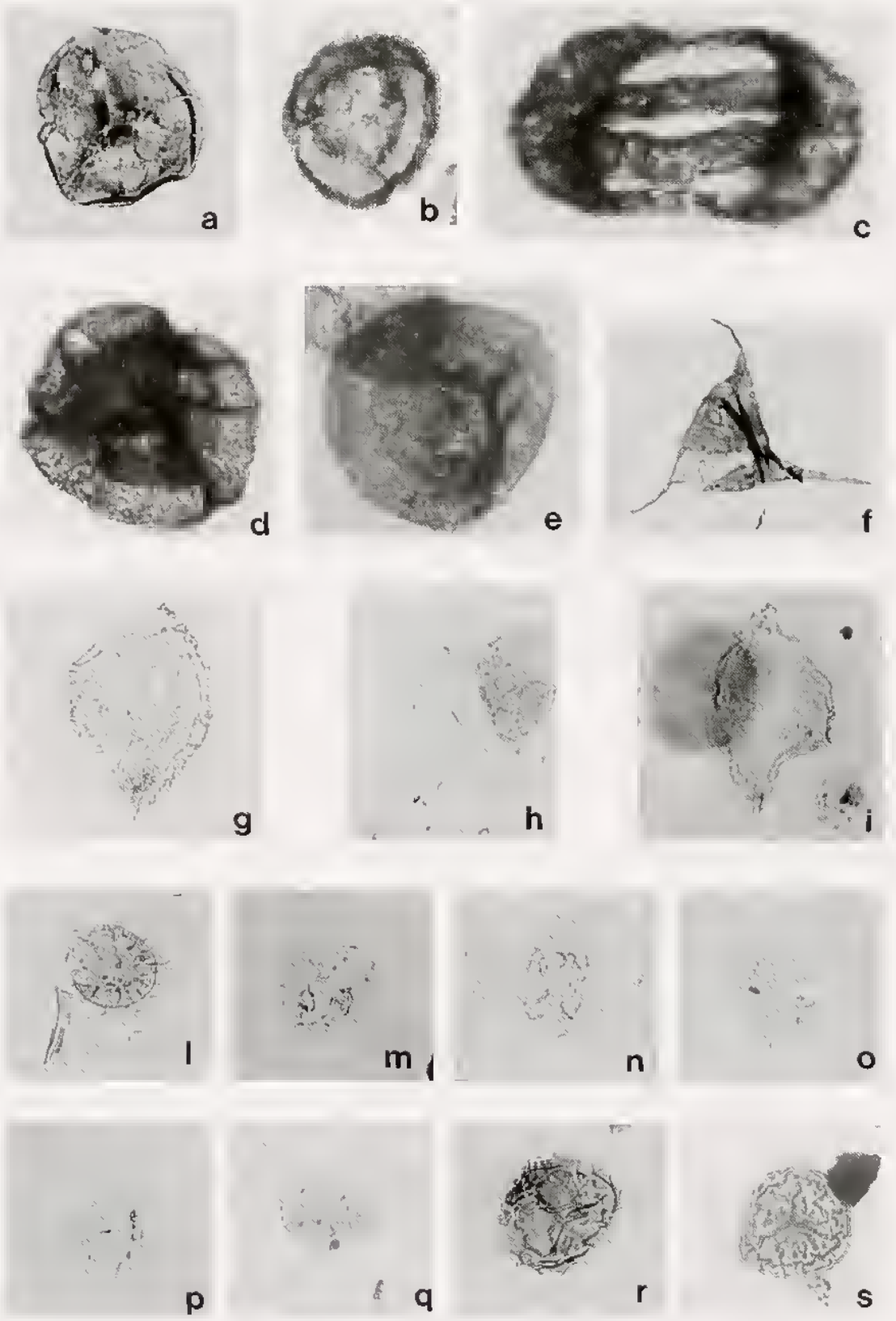

Source : MNHN, Paris

Nevada (Tobin Range, KUMMEL, 1969; Humboldt Range, SILBERLING & WALLACE, 1969), from the Anarak region in Iran (TOZER, 1972) and from Dalmatia (KITTL, 1903). Bed-by-bed data are available from the Anarak region where the genus was reported from the mid-upper Spathian, and from the Humboldt Range, where *Stacheites* was found in the next to the last zone of the Spathian. The mid-late Spathian age of the top of the Tyururpa Group is also supported by the occurrence of *Kazaklistanites*, which was found above *Stacheites*, but below the Anisian faunas, in the Anarak region (TOZER, 1972).

Above the Stacheites Beds, the microflora is represented by the first occurrences of *Densoisporites nejburgii* (Schulz) Balme, *Densoisporites playfordii* (Balme) Balme and *Lundbladispora* sp., along with a decrease in the abundance percentage of *Endosporites papillatus* (MK 299). The most diversified and abundant microfloral assemblage (samples MK 298 and MK 297) yielded *Densoisporites nejburgii*, *Endosporites papillatus*, *Lundbladispora* sp., *Lundbladispora brevicula* Balme, *Lunatisporites noviaulensis*, *L. pellucidus* (Goubin) De Jersey, *Lunatisporites* spp., *Krauselisporites* sp., *Gordonispora fossulata* (Balme) Van der Eem, *Gordonispora* sp.; undetermined bisaccates are common. Few specimens of *Crinalites sabiaensis* Utting, *Grebeispora concentrica* Jansonius, *Striatoabieites richterii* (Klaus) Hart, *Protohaploxypinus limpidus* (Balme & Hennelly) Balme & Playford, *Protohaploxypinus* sp., *Alisporites tenuicorpus* Balme were found. *Maculatisporites* sp. and *Calamospora* sp. are rare.

The presence of important stratigraphic taxa, such as *Endosporites papillatus* and *Densoisporites nejburgii*, allows a fairly precise correlation of the Stacheites Beds. According to FISHER (1979), *E. papillatus* and *L. singhii*, associated with several species of *Densoisporites* and *Lundbladispora*, together with *Lunatisporites* and *Protohaploxipinus*, are representative of Zone I and Zone II (Induan) in the North American Lower Triassic. In this zonation, the younger association (Zone II, upper Induan) is characterized by the presence of *Corisaccites alatus*, *Densoisporites nejburgii*, *Lundbladispora brevicula* and *L. echinata*. The overlying Zone III (lower Olenekian) is based on the appearance of the monolete cavate spores of lycopsids such as *Aratrisporites* and Zone IV (upper Olenekian) is defined by an assemblage which includes the previous taxa, plus the appearance of *Guttapollenites hannonicus*, but lacks *E. papillatus*.

The zonation of the Lower Triassic sequences in the Barents Sea, Svalbard, former USSR and Sovietic Arctic islands provides further data. HOCHULI *et al.* (1989) assigned:

— an early Olenekian age to Assemblage N containing abundant *P. fungosus*, a diversified association of cavate spores, and characterized by the LADs of *Densoisporites complicatus*, *D. playfordii* and *Naumovaspora striata*.

— a late Olenekian age to Assemblage M containing *D. nejburgii*, *Krauselisporites*, *Lundbladispora*, *Rewanispora*.

The distribution of *E. papillatus* in the Lower Triassic of Europe extends from the Induan to the upper Olenekian, while *D. neiburgi* is present only in the upper Olenekian (VISSCHER & BRUGMAN, 1981, 1986; BRUGMAN, 1986).

FIG. 4.— Selected taxa of sporomorphs and dinoflagellate cysts from the Triassic and Middle Jurassic rocks of Mangyshlak. Specimens photographed in plain transmitted light. Magnification x 350 (a-f) and x 525 (g-s).

FIG.4.— Quelques spécimens de microflore et de kystes de dinoflagellés du Trias et du Jurassique moyen du Mangyshlak. Spécimens photographiés en lumière transmise. Grossissement a-f:x 350; g-s: x 525.

a, *Endosporites papillatus* Jansonius, 1962 (MK 204); **b**, *Grebespora concentrica* Jansonius, 1962 (MK 298); **c**, *Lunatisporites pellucidus* (Goubin) De Jersey, 1971 (MK 298); **d**, *Densoisporites playfordii* (Balme) Balme, 1970 (MK 299); **e**, *Lundbladispora brevicula* Balme, 1970 (MK 298); **f**, *Verybachium* sp. (MK 215); **g**, *Nannoceratopsis gracilis* Alberti, 1961 emend. Evitt, 1962 (MK 17-1, England Finder coordinate V35-3); **h**, *Nannoceratopsis spiculata* Stover, 1966 (MK 17-1, England Finder coordinate K 36-2); **i**, *Nannoceratopsis gracilis* Alberti, 1961 emend. Evitt, 1962 (MK 64-2, England Finder coordinate F 29-2); **j**, *Mendicodinium spinosum* Bucefalo Palliani *et al.*, 1997 (MK 17-1, England Finder coordinate G 44-1); **m**, *Susadinium scrofoides* Dörhöfer & Davies, 1980 emend. Below, 1987 (MK 17-1, England Finder coordinate G 31-1); **n**, *Susadinium scrofoides* Dörhöfer & Davies, 1980 emend. Below, 1987 (MK 17-1, England Finder coordinate O 36-1); **o**, *Rentlingia cordobarbata* Below, 1987 (MK 17-1, England Finder coordinate J34-1); **p**, *Parvocysta nasuta* Bjaerke, 1980 (MK 17-1, England Finder coordinate G 35-1); **q**, *Mendicodinium semitabulatum* Morgenroth, 1970 (MK 17-2, England Finder coordinate D 29-3); **r**, *Lycopodiumsporites austroclavatoides* (Cookson) Potoni, 1956 (MK 17-1); **s**, *Coronatisporites valdensis* (Couper) Deltmann, 1963 (MK 17-1).

Source : MNHN, Paris

On the basis of the references cited, the presence of *E. papillatus* throughout the section allows the Tyururpa Group to be attributed to the Early Triassic, and possibly the base of the Group to the Olenekian. The first occurrence of *D. nejburgii* in sample MK 299 (upper part of the Stacheites beds) definitively indicates the upper Olenekian.

In conclusion, the age of the Tyururpa Group seems to be restricted to the Olenekian. The few conodonts found in the upper part of the Dorikranites Beds suggest a Spathian (late Olenekian) age, whilst the palynoflora hints to a slightly older age assignments. This is why we do not definitively rule out a possible early Olenekian age for the very base of the Tyururpa Group.

Environment

The occurrence of marine fauna decreases eastwards, and in the East Karatau and Kugusem Scarp in the Ustyurt Plateau only *Dorikranites* was recorded (Shevyrev, 1990, Lozowsky, 1974; Gavrilova, 1989, 1992). Lithological correlations made by Shleznger (1965) and Lozowsky (1974) tried to link the East Karatau to the better-constrained western parts of the range.

In Karatauchik and in part of West Karatau, the Tyururpa Group was deposited under marine conditions. Calcareous shell lags, that may be considered as storm deposits, are most typical. Also coquinoid levels at the base of Tirolites *s.l.* Beds suggest a shallow subtidal accumulation under a current regime. Most of the Columbites Beds were deposited instead in a quiet, poorly oxygenated environment, with ammonoid accumulation that allowed the formation of calcareous concretions, in which packed ammonoids were crushed during burial compaction. However, freshwater runoff was present, because Estherids and Labirintodonts were found (Lozowsky, 1974). A gradual return to more marginal conditions is indicated by the Karadzhatyk Formation, with the finding of terrestrial megaplants like *Pleuromeia sternbergii* (Muenster) Corda (Dobruskina, 1982). Occasional ammonoid remains still indicate local marine influence, at least in the westernmost part of Mangyshlak.

Organic facies

Due to the high thermal maturity, the organic facies are not a very useful tool for detailed palaeoenvironmental and palaeoecologic considerations. The percentage of terrestrial versus marine material, represented by few species of acritarchs, is high in the entire section.

The percentage of palynomacerals (inertinite and vitrinite) and palynomorphs is constantly high. Inertinite is mostly equidimensional and vitrinite particles are commonly unrounded and unsorted. Amorphous organic matter is present in very low percentage, or absent. These data suggest an oxygenated marine environment, probably characterized by high terrestrial input, and probably not far from the shoreline. The palynofacies suggest a depositional palaeoenvironment proximal to the continental area, where the parent floras developed. This proximal condition seems to be more evident in samples MK 298 and MK 297. These levels contain abundant and diversified (in number and species) microflora, suggesting a close proximity to the source area. Among the marine microorganisms, acritarchs are present in very low percentage throughout the section, with a relative increment in sample MK 208. The most represented genus is *Veryhachium*, and only at the top of the section the presence of *Micrhystridium* sp. was recorded.

Sequence stratigraphy

Three cycles may be identified in the Tyururpa Group. The first cycle starts with a transgression recorded by the dolostones, shell-lags and calcareous lenses of the Dorikranites Beds. It is followed by several parasequences of fine sandstones and siltstones suggesting a regression or an increased sediment supply. A second cycle may be identified with the Tirolites *s.l.* Beds, with a transgression marked by the basal coquinoid bed. The final cycle starts with a transgression recorded by the basal calcareous horizons, has the maximum flooding within the Columbites Beds, and the high standing with gradual filling of the basin at the time of the Karadzhatyk Formation.

Source : MNHN, Paris

KARADUAN FORMATION

The overlying succession is probably the most problematic. In the Dolnapa section (Karatauchik), the grey-green shales and siltstones of the Karadzhatyk Formation are overlain by red shales and very fine-grained sandstones, followed in turn by festooned, brown sandstones, rare calcareous beds, dark claystones and again shelly calcareous beds (Fig. 5). South of Karaduan, in the West Karatau, the absence of the Columbites Beds, which provide a firm base for correlation, makes it difficult to trace the lower boundary of the Karaduan Formation. Consequently, a 200 m-thick succession of grey-green siltstones, shales and fine grained sandstones, containing several calcareous shell lags, was tentatively attributed to the Karadzhatyk Formation. The portion displaying an increase of sandstones and disappearance of calcareous shell lags was chosen as the lower boundary of the Karaduan Formation. Positive correlations become increasingly difficult eastwards, where continental conditions were more prevalent. In the Karaduan area, above the last calcareous bed which yielded a few specimens of hakewelliids and modiolids, grey-green fine-grained sandstones in 10-20 m-thick packages follow, reaching a total thickness of about 300 m. They are overlain by at least five coarsening-up parasequences, each 20-40 m-thick, consisting of grey to red siltstones up to medium sandstones. In some cases, typical point bar and channel fluvial structures, each a few metres thick, may be observed. They are in turn overlain by the shale and limestone beds of the Akmysh Formation. This unit with calcareous shell lags yielded several euryhaline bivalves, mentioned in ANONYMUS (1973), the Samarkand Scheme (1977), and by LOZOWSKY (1974) and LIPATOVA (1984). A few foraminifers, common in the Middle and Upper Triassic, were observed in the lower part of the Karaduan Formation in the Dolnapa section, i.e. *Planiinvoluta carinata* (Leischner) and *Tolypammina gregaria* Wendt. They are euryhionthic forms which live attached to the bottom or to other faunal elements. A firm age assignment is difficult. Usually a Middle Triassic age is suggested. In the Dolnapa section, a microflora similar to that of the Stacheites Beds, suggesting still an Olenekian age, was found (sample MK 293). Recently, LIPATOVA (1984) and especially ZHIDOVINOV (1994) provided a different interpretation for the succession. They distinguished the lower unit as "Karaduan Svita" in which marine intercalations are still present, assigning it to the Early Triassic on the basis of charophytae specimens. They named the more arenaceous unit, in which ZHIDOVINOV (1994) recognized a large input of "tuffogenic" material, "Khozbulak Svita" and divided it into three parts. According to ZHIDOVINOV (1994), the age of Khozbulak is

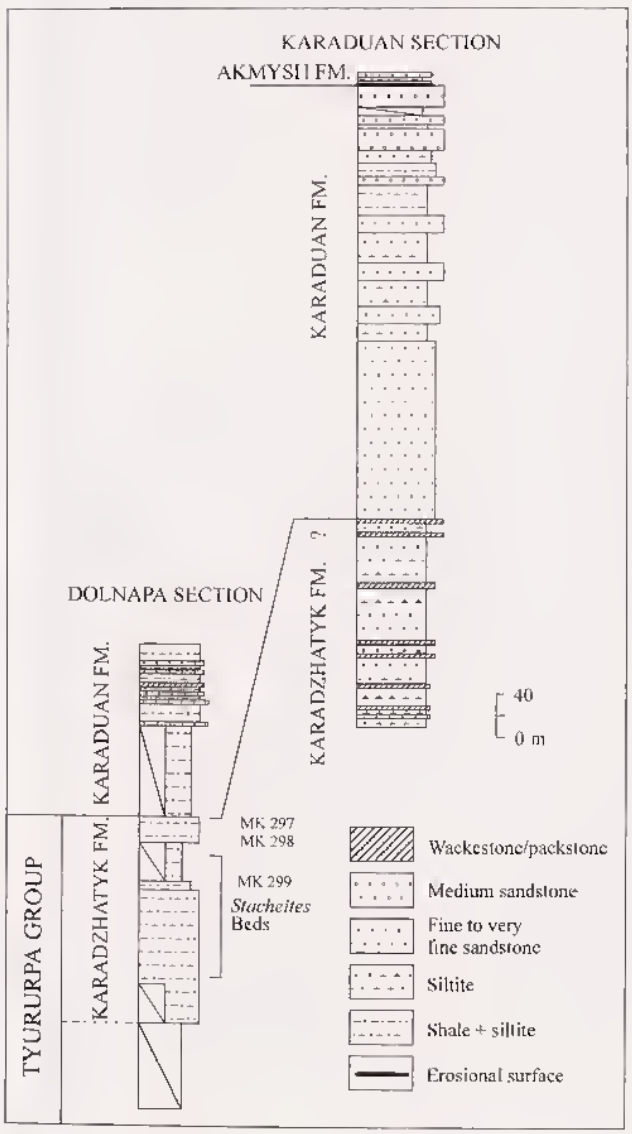

FIG. 5.— The Karaduan Formation at the top of the Dolnapa section and the SW Karaduan section.

FIG. 5.— La formation Karaduan au sommet de la coupe de Dolnapa et au sommet de la coupe de Karaduan sud ouest.

Source : MNHN, Paris

Middle Triassic. We think it is fairly hard to fit all of the Karaduan Formation *sensu* ZHtDOVtNOV in the Early Triassic, because the ammonoid beds of the underlying Tyurupa Group already represent most of the Spathian. Moreover, a firm correlation of the charophytae data to other more tested biostratigraphic scales is yet to be demonstrated. Consequently, we prefer to maintain a generic Middle Triassic age for most of the Karaduan succession *sensu lato*.

ENVIRONMENT

The lower part of the section contains several episodes of transitional to coastal sedimentation, with rare episodes of shelly storm deposits. The upper, thicker part, consists of alluvial plain cycles, with increasing energy and meandering river episodes.

SEQUENCE STRATIGRAPHY

In the lower part, a stratigraphic interpretation of the sequence may still be attempted. Two sequences are recognizable in which the calcareous horizons indicate the MFS. The lack of biostratigraphic control in the upper portion hampers any clear interpretation.

AKMYSH FORMATION

The fairly abrupt change of sedimentation may suggest a paraconformity at the scale of the outcrop (Fig. 6). The fine to medium-grained sandstones of the Karaduan Formation are overlain by dark grey mudstones-wackestones in 20-40 cm-thick beds, alternating with green-grey splintery shales and rarely, very fine-grained sandstones. Commonly, the top of the calcareous layers contains a gastropod/bivalve assemblage, with mud-supported shells. A few dark siliceous crusts and small nodules are also present. Burrowing is usually dense. In the first 310 m of the unit, the mudstone/wackestone to terrigenous ratio (usually shales) is about 1:2. Very fine-grained sandstones are very subordinate. On the contrary, the upper part of the unit, about 200 m-thick, is mostly shaly with rare marly intercalations. The fossil content is fairly abundant in the lower part, where density and low diversity of gastropod/bivalve assemblages indicate a restricted environment. Dasycladacean algae are significantly absent. A few foraminifers (*Ophthalmidium* sp.) were identified at about 145 m from the base of the unit. The finding of palynomorphs near the base of the unit is most important. All samples show a very high thermal maturity and palynomorphs are scattered and badly preserved. The most important palynomorphs found in these samples (MK 254, MK 257) are: *Camerosporites secatus* Leschik emend. Scheuring 1978, *Enzonalasporites vigens* Leschik, *Cycadopites* sp., *Partitisporites* spp., *Ovalipollis pseudoalatus* (Thiergart) Schuurman and very rare specimens of *Patinasporites densus* Leschik emend. Scheuring 1970.

This assemblage can be assigned to the *Camerosporites secatus* phase, which is generically considered as a Ladinian-Carnian event (SCHUURMAN, 1977, 1979; VtSSCHER & KRYSTYN, 1978; VISSCHER & BRUGMANN, 1981; VAN DER EEM, 1983 ; FtSHER & DUNAY, 1984). The presence of *Patinasporites densus* and *E. vigens* suggests a Carnian age (VISSCHER & KRYSTYN, 1978; VISSCHER & BRUGMANN, 1981; WARRINGTON, 1996). The scarcity of more age-specific microflora does not allow more precise dating at the substage level.

ENVIRONMENT

The lower part is considered a restricted, coastal marine flat, periodically invaded by fine-grained terrigenous detritus. Gradually the clay input becomes dominant and the upper part of the unit is interpreted as a muddy coastal flat.

Source : MNHN, Paris

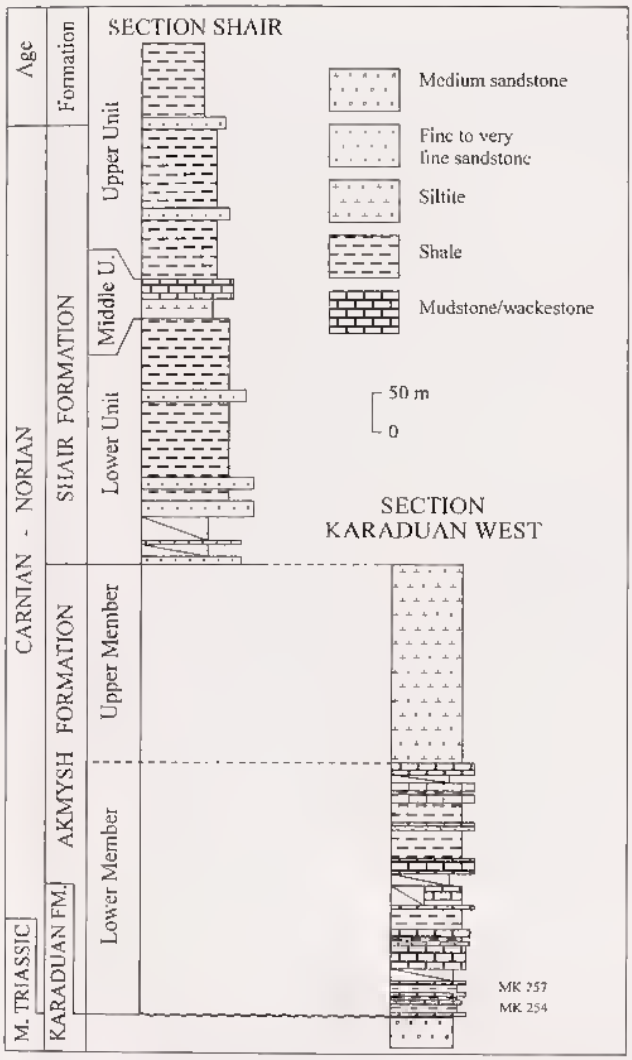

FIG. 6.— Akmysh and Shair Formations in the W Karaduan and Shair sections.

FIG. 6.— Les formations Akmysk et Shair dans les coupes du Karaduan ouest et de Shair.

SEQUENCE STRATIGRAPHY

The lower boundary of the Akmysh Formation is interpreted as a sequence boundary with the calcareous/shaly lower part as the transgressive system tract. All other parts of the sequence are difficult to recognize.

SHAIR FORMATION

The overlying Shair Formation may be subdivided into three parts, bottom to top (Fig. 6).

The lower unit consists of grey to green, fine-grained sandstones, forming 1-4 m-thick amalgamated packages, occasionally with faint parallel laminations. The sandstone layers are subdivided by thicker packages of splintery shales and siltstones. The basal 100 m are richer in sandstones and form cliffs. Gradually, the sandstone content and size decrease and siltstones and shales prevail for more than 200 m. The arenaceous layers, presenting very few parallel laminations, have a great lateral continuity.

The intermediate unit is characterized by a weak recovery of the carbonate sedimentation, with dark grey marly limestones, marls and marly siltstones, which form ridges, about 20 m-thick, with persistent lateral continuity. The total thickness of this unit is about 50-60 m. No foraminifers were detected, but only fragments of macrofauna. The bivalves *Trigonodus hornschuchi* Berg., *T. (?) roeperti* (Berg.), *Myophoriopsis gregariodes* (Philippi), *Mytilus (Falcimytilus) nasai* (Kobayashi & Ichikawa) were reported from this unit (LIPATOVA, 1984; ZHIDOVtNOV, 1994).

The upper part of the formation consists once more of dark grey to green shales and siltstones, with subordinate very fine-grained sandstones. The thickness is highly variable, depending on the subsequent Late Triassic and Early Jurassic erosion. The top of the unit may preserve an alteration cap, with a varicoloured silcrete, tens of m-thick, like in the two large gullies immediately to the east of Shair.

The thickness of the Shair Formation is usually more than 500 m, but we did not measure the topmost part.

ENVIRONMENT

The rare occurrence of euryhaline bivalves and the great lateral continuity of the very fine-grained arenaceous bodies suggest a quiet protected shelf, with euryhaline conditions. Notable is the absence of dasycladacean algae.

No new data about the age. According to the current literature, the Shair Formation is attributed to the Carnian-Norian (ZHIDOVINOV, 1994).

Source : MNHN, Paris

COMPOSITION OF TRIASSIC SANDSTONES

The samples studied are mostly very fine-grained (Lower Triassic) to fine-grained (Middle to Upper Triassic) feldspathic litharenites to lithic arkoses (average composition Q=35±9; F=30±7; L=34±6; point-counting method and parameters after DICKINSON, 1970) (Fig. 7). Detrital quartz increases significantly with grain size relative to feldspar grains (coeff. correl. GSZ vs. ln(Q/F) = 0.74; sign. lev. 1%); the Q/F ratio increases from as low as 0.5 in very fine sandstones, to as much as 4 in upper fine sandstones, within the Akmysh Formation. Monocrystalline quartz, rarely showing features diagnostic of volcanic origin, predominates over basement-derived polycrystalline grains (average C/Q = 15%). Plagioclase dominates among detrital feldspars (average P/F= 95%); alkali-feldspars are largely chessboard-albite, with rare orthoclase and perthite. Volcanic lithics are virtually exclusive (V/L = 100%), with predominant felsic types (felsites, microfelsites, spherulites, pumiceous clasts); microlitic grains are subordinate ≤ 10%. Metamorphic rock fragments (slates, micaschists, paragneisses) are rare and sedimentary rock fragments are negligible. Micas, opaques, apatite, rutile, zircon, and tourmaline, along with local silty mudclasts and greenish grains are also found; most significant is the occurrence of dark red to coffee brown chrome-rich chromian spinel in the Karaduan, Akmysh and Shair Formations. Quartzose and albitic syntaxial cements are common in most samples (up to 22% of the rock), as well as illitic to chloritic epimatrix (up to 17% of the rock). Intragranular porosity is therefore very low. Late diagenetic carbonates (locally poikilotopic calcite, siderite) are locally abundant (up to 55% of the rock); authigenic pyrite, chlorite or hematite are locally significant. Samples with abundant carbonate replacements tend to be depleted in rock fragments relative to quartz (coeff. correl. AUT vs. ln(Q/L) = 0.59; sign. lev. 5%).

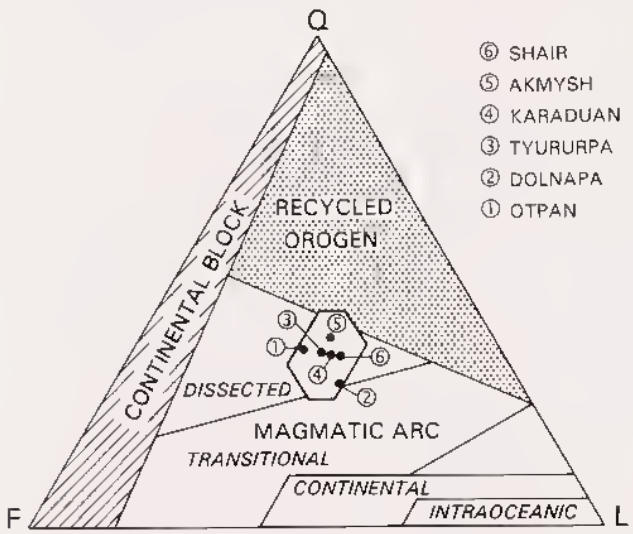

FIG. 7.— Average detrital modes for the six Triassic terrigenous units plot right in the middle of the QFL diagram and all within the "dissected magmatic arc provenance field" (DICKINSON, 1985), reflecting an excess of detrital quartz with respect to "normal" volcaniclastic continental arc suites (MARSAGLIA & INGERSOLL, 1992). Polygon refers to all studied Triassic samples, and is one standard deviation each side of the mean. Q= total quartz; F= feldspars; L= "aphanite" lithic fragments.

FIG. 7.— Le report du mode de moyenne détritique pour les six unités triasiques au milieu du diagramme QFL et tous à l'intérieur du "champ de provenance de l'arc magmatique" (DICKINSON, 1985) montre un excès de quartz détritique en ce qui concerne des suites d'arc volcaniques continentaux "normaux" (MARSAGLIA & INGERSOLL, 1992) Le polygone se rapporte à tous les échantillons triasiques et est une déviation standard de chaque cotés de la principale. Q : quartz ; F : feldspaths ; L : fragments de roches aphanitiques.

PROVENANCE OF TRIASSIC SANDSTONES

Volcanic detritus largely derived from erosion of intermediate to felsic products (e.g. dacites) is virtually exclusive in all Triassic sandstones of Mangyshlak, from the Induan Otpan Formation to the Carnian-Norian Shair Formation, suggesting an arc-related source terrane. Average detrital modes of all Triassic units plot right in the middle of the QFL triangle, within the "Dissected Arc" provenance field (Fig. 7; DICKINSON & SUCZEK, 1979; DICKINSON, 1985) but close to the boundary with the "Recycled Orogen" provenance field. The Mangyshlak sandstones are in fact notably enriched in quartz and feldspars relative to clastic suites typically found in modern fore-arc to back-arc basins and derived from oceanic to continental undissected volcanic arcs; they compare more closely with siliciclastics characterising triple junction to strike-slip settings (GERGEN & INGERSOLL, 1986; PACKER & INGERSOLL, 1986; MARSAGLIA & INGERSOLL, 1992). On the other hand, the invariably high P/F ratio indicates that the batholithic roots of the arc massif were never widely exposed, and deepening of erosion levels with time was slow. Evidence of unroofing of the volcanic source areas during the Triassic is

Source : MNHN, Paris

subtle, including a slight increase with time of polycrystalline quartz and alkali feldspars (coeff. correl. vs. C/Q and P/F 0.54 and -0.37 respectively; sign. lev. 10% or higher). Moreover, chessboard-albite is most abundant, granophyric and holocrystalline hypabissal grains are sporadically observed, and a few metasedimentary grains hint at a greater contribution from basement wallrocks in the Upper Triassic Shair Formation. The occurrence of chrome-rich Cr-spinel in several samples suggest provenance from protrusions of upper mantle rocks emplaced in strike-slip arc settings (HISADA & ARAI, 1993), rather than from slivers of oceanic lithosphere (DICK & BULLEN, 1984) tectonically incorporated within a subduction complex.

The geometry of the thick and invariably fine-grained deltaic volcaniclastic wedge, thinning rapidly towards the south, along with transition to more proximal continental facies in the east, suggest that the source area was located in the eastern qnadrants, at a distance of at least many tens of kilometres (SELF, 1975; DAVIES *et al.*, 1979).

The relative abundance of quartz and feldspars with respect to volcanic lithics cannot be totally ascribed to selective depletion of unstable volcanic grains, due to either pre-depositional (e.g. weathering, transport, hydraulic sorting) or post-depositional (e.g. carbonate replacement) processes (CAMERON & BLATT, 1971; MATHISEN, 1984; GARZANTI, 1986). Rather, dilution from polycyclic sources cannot be ruled out. An extremely attractive alternative hypothesis is that detritus was not directly fed from erosion of active volcanoes, but was largely paleovolcanic and derived from a relict arc terrane of Palaeozoic age (GRAHAM *et al.*, 1993). In fact, broadly comparable compositions characterize mainly continental Permian to Triassic clastic suites derived from erosion of largely Carboniferous volcaniclastic assemblages and accumulated in foreland-style basins in Central Asia after the Late Palaeozoic Altaid-Hercynian orogeny (e.g., CARROLL *et al.*, 1995; HENDRIX *et al.*, 1996).

The precise geodynamic setting thus cannot be discriminated by the compositional data alone. On one hand, strongly asymmetric sediment-thickness distribution is consistent with deposition in a retroarc foreland basin (as inferred by BAUD & STAMPFLI, 1989, for the Triassic of Aghdarband, which lies, however, some 1000 km to the SE). On the other hand, exclusiveness of homogeneous volcanic detritus for over 30 m.y. - P/F ratio ≥90; V/L ratio =100; microlitic/(microlitic + felsitic) lithic type ratio < 10% - is atypical for provenance from a fold-thrust belt.

THE JURASSIC

The Jurassic succession lies unconformably on several Triassic units, from the Akmysh to the Shair Formations, sealing a structured palaeotopography. East of Shair it rests almost flat on the Akmysh rocks, sealing a palaeovalley. Thickness rarely exceed 200 m in a context of low subsidence rate. The general depositional trend is from fluvial to lacustrine continental deposition in the lower part, onlapped with successive steps by open, shallow marine sediments.

After pioneering work, the basic stratigraphy of the Jurassic succession was established by the team of Mokrinsky (VSEGEI) and by the Geological Expedition to Mangyshlak of the VNIGRI (MUROMCHEV, 1968). This classification was adopted by the Samarkand Scheme (1977). Several papers dealing with ammonoids, foraminifers, palinostratigraphy, and brachiopods were published subsequently, i.e. TIMOSHKINA & MENSHIKOVA (1985), KIRICHKOVA *et al.* (1989) and KIRICHKOVA & DOLYDENKO (1996) on palynostratigraphy, AZBEL (1979) and AZBEL & HOFFMAN (1982) on foraminifers, and REPIN & RASHWAN(1996) on Callovian ammonoids.

We worked mostly west to east of the village of Dzharmysh and near Shair (Fig. 1). Most of the area studied falls in the east Karatau according to the Samarkand Scheme. The following units were measured and sampled from bottom to top (Fig. 8).

KARADJIRMEN FORMATION AND BAZARLY FORMATION

These two units consist entirely of terrigenous sediments, and present a very variable thickness because they seal the underlying palaeotopography. According to the Samarkand Scheme (1977) they

Source : MNHN, Paris

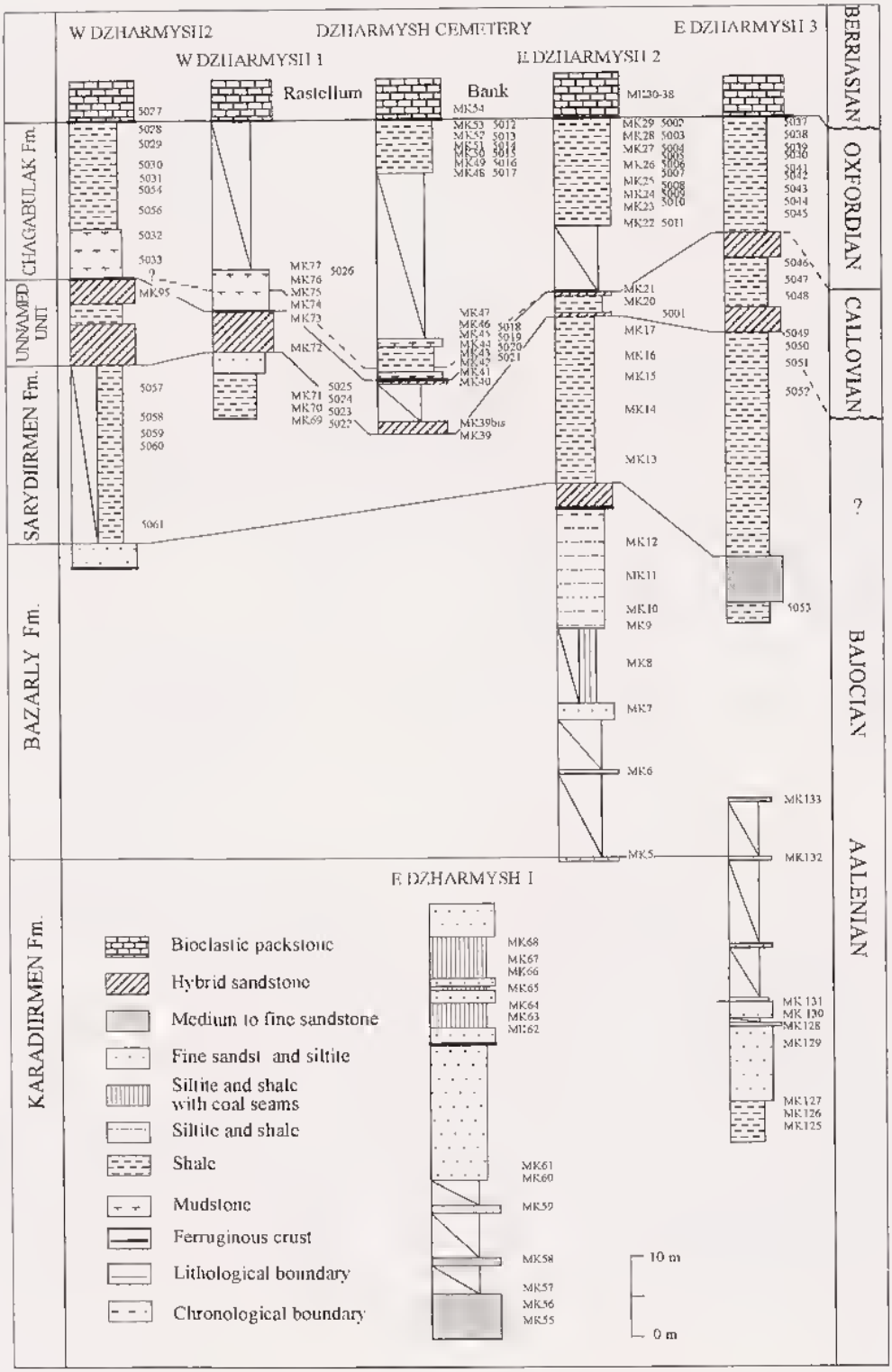

FIG. 8.— Measured sections in Jurassic formations in the district of the Dzharmysh village, Eastern Karatau.

FIG. 8.— Coupes levées dans les formations jurassiques du district de Dzharmysh, est Karatau.

Source : MNHN, Paris

may reach a thickness of up to 260 m, but usually are thinner than 200 m. Three main lithological assemblages were identified.

— Dark shales rich in organic matter with coal seams cm to dm-thick. These levels are more diffuse in the lower part of the unit and were observed mostly east of Shair, where they rest on the silcrete soils of the topmost Triassic succession. Sometimes this part is also distinguished as Kokala Formation Unfortunately, the coal seams did not yield any palynoflora, but only macerals with vitrinite and inertinite, indicating high sorting in a fairly high energy environment.

— Light grey to dark brown medium to fine sandstones, forming ledges a few m-thick, occasionally with high angle cross-lamination and flat top sets, a few cm-thick. Interference ripple-marks were also observed and frequent plant fragments, especially leaf imprints, are present. In a few levels, brackish-water bivalves (*Modiolus*-like) were observed. At the top of the sandstone ledges a ferruginous crust may be preserved, with vertical concretions interpreted as remnants of roots.

— Grey to dark grey very fine sandstones, siltites and shales, often poorly exposed, interbedded with the previous medium to fine sandstones and more abundant in the upper part of the unit. The clay content is very variable. These lithotypes are predominant over the sandstone with at least a 10:1 ratio. Cementation is not homogenous, with partially cemented grey sands. In the section E Dzharmysh 1, the base of a fossil tree in living position was observed.

AGE

According to MUROMCHEV (1968) and the Samarkand Scheme (1977), the Karadiirmen Formation contains vascular plants such as *Coniopteris* spp., *Ptylophyllum* spp. and *Nilssonia* spp. and brackish-water bivalves. The age is bracketed between the Aalenian and the Bajocian. The following Bazarly Formation may indicate a Bajocian age, with the first marine spells yielding a few ammonoids of the *Parkinsonia* group and trigoniid bivalves.

The E Dzharmysh 1 section was sampled for palynostratigraphy (samples MK 61 to 68) (Table 2). In the lower part (MK 61 to MK 63) samples are barren of palynomorphs and the palynofacies consists of vitrinite (about 80%) and inertinite (about 10%). Rare tracheids were observed. When pollens are present (MK 63), the most abundant constituents are trilete spores of Pteridophytae. Bisaccate pollens are rare. This organic composition is related to a very near-shore palaeoenvironment, where the heaviest pteridophytic spores are concentrated. The palynofacies records a significant change from sample MK 65 up to MK 68, where the marine influence becomes very strong. The most abundant organic constituents are *Botryococcus*, frequently associated with *Pediastrium* and *Tasmanites*, algae that are very tolerant of euryhaline conditions and typical of transitional environments. A significant feature of the sporomorph assemblages is the common occurrence of Araucariaceae-type pollen (*Araucariacites australis* Cookson and *Callialasporites minus* (Tralau) Guy). In the Lower Jurassic, a rapid distribution of Araucariaceae-type pollen coincided with the decline of *Classopollis*. This Toarcian event was

Period	Samples	*Araucariacites australis*	*Apiculisporites* sp.	*Alisporites* sp.	*Dyctiophyllidites* spp.	*Ischyosporites* sp.	*Leptolepidites major*	*Leptolepidites* spp.	*L. verrucatus/rotundus*	*Neoraistrickia taylorii*	*Paustpelliferites* sp.	*Tribuloporites* sp.	*Dyctiophyllidites harrisii*	*Callialasporites minus*	*Mendicodinium umbrense*	*Mendicodinium microscabratum*	*Moncodinium semitubulatum*	*Nannoceratopsis gracilis*	*Botryococcus*	Tasmanites	*Pediastrum*
Jurassic	MK 68																				
	MK 67		A																		
	MK 66															R					
	MK 65																		A		
	MK 64	C			A				R			R	R	A		R	R	R	F	R	R
	MK 63	C	C	R	A	R	R	C	A	A	R				R				R		
	MK 61																				

TABLE 2.— Semi-quantitative stratigraphical range of selected sporomorphs and dinoflagellate cysts from the Jurassic of the E Dzarmysh 1 and 2 sections. (A: abundant; F: frequent: C: common; R: rare).

TABLEAU 2.— Répartition stratigraphique semi-quantitative de palynomorphes sélectionnés et de kystes de dinoflagellés du Jurassique des coupes Est Dzarmysh 1 et 2 (A : abondant ; F : fréquent ; C : commun ; R : rare).

Source : MNHN, Paris

recorded in Europe (SCHULZ, 1967; HOELSTAD, 1985), Argentina (VOLKHEIMER & QUATTROCCHIO, 1981), Australia (FILATOFF, 1975), Greenland (LUND & PEDERSEN, 1985), the Netherlands (HERNGREEN & DE BOER, 1974) and Sweden (GUY-OHLSON, 1989). The first occurrence of *A. australis* in the Perth Basin was referred to the *E. tumulus* zone (Lower Jurassic). This taxon became abundant in the *C. dampieri* zone (late Toarcian and Middle Jurassic). *Leptolepidites* spp., recorded in the E Dzharmysh 1 section, is a typical Middle Jurassic taxon (TRALAU, 1968; GUY, 1971).

The Mangyshlakh sporomorph assemblage includes all the index taxa of phase VI of VISSCHER *et al.* (1980), such as *Ischyosporites* spp., *Callialasporites* sp. and *Leptolepidites* spp. *Callialasporites minus*, present in sample MK 64, was reported from Australia and Sweden. In Sweden, its range is from Bajocian to Bathonian (GUY, 1971). The sporomorphs assemblages from the E Dzharmysh 1 section may be referred to the transition between the E. tumulus zone (Hettangian-Bajocian) and the C. dampieri zone (Bajocian - Kimmeridgian) of FILATOFF (1975), due to the presence of *C. minus* associated with common *Araucariacites australis*, and the absence of *Classopollis* and *Callialasporites dampieri*.

Rare dinoflagellate cysts were found throughout the section. They are represented mainly by long-range taxa. *Mendicodinium umbrieuse* Bucefalo Palliani, Riding & Torricelli, a Toarcian taxon with Tethyan affinity was recorded. *Nannoceratopsis gracilis* Stover and *Mancodinium semitabulatum* Morgenroth, taxa with stratigraphic ranges from late Pliensbachian to Callovian and from late Pliensbachian to early Bajocian respectively, were also found.

In conclusion, our data confirm an earliest Middle Jurassic age for the Karadiirmen Formation

On the contrary, we failed to find ammonoids in the Bazarly Formation and palynomorphs were also not found in the E Dzharmysh 2 section. The content of organic matter is very low and the exclusive presence of inertinite suggests a strong oxidation of the palaeoenvironment.

ENVIRONMENT

The Karadiirmen Formation was deposited in a continental environment. The topographic relief on which it aggraded was not fully peneplaned, as indicated by palaeovalleys filled by the Karadiirmen Formation or by the the Kokala Formation where the last unit is present. However, the sandstone grain-size and the abundance of coaly shales deposited in water ponds and marshy flats in the lower part of the unit suggest that the topographic gradient was low. An alluvial plain with small meandering rivers and possibly coastal lagoons, where brackish bivalves might also dwell, was a likely environment. Due to the wandering course of the rivers, ferruginous crusts could develop during episodes of non deposition. The inertinite is blade-shaped and suggests selection processes during the sedimentation. The organic content reveals a well-oxygenated palaeoenvironment, where the degradation of the hydrogen-rich organic matter is complete. The climate was humid. The upper part of the Karadiirmen Formation suggests an increased marine influence. An environment similar to the overlying Bazarly Formation, where temporary ingressions produced thin levels with ammonoids, is hypothesized. However, the bulk of these two units was formed in a continental environment under well-oxygenated conditions.

SEQUENCE STRATIGRAPHY

Lack of sufficient biostratigraphic control does not allow sequences to be recognized.

SARYDIIRMEN FORMATION

The base of the formation was defined with the appearance of grey and brown shales, silty and sandy in the basal metres, that transgress over a condensed horizon with a siliceous brown crust. The Sarydiirmen Formation consists of grey shales in which very thin horizons of silts and very fine sands may occur. Pure claystones are rare.

This succession, about 20-25 m thick, ends with bioturbated shaly sands, gradually becoming more sandy, and is capped by a peculiar layer of grey/brown sandstones to hybrid sandstones with calcareous

Source : MNHN, Paris

cement, here attributed to an overlying unit. The total thickness of the Sarydiirmen that we measured is in contrast with the up to 100 m reported in the Samarkand Scheme (1977).

AGE

The shales were sampled for nannofossils but none were found. Palynomorphs are also scarce, even if at the base (sample MK 13) the palynofacies is dominated by terrestrial organic matter (palynomacerals and sporomorphs), while marine constituents are rare and dinoflagellate cysts are absent. Most interesting is the dinoflagellate cyst assemblages recorded in samples MK 14 and MK 17 (section E Dzharmysh 2). Both samples yielded taxa belonging to the *Parvocysta* suite of RIDING (1984). Rare specimens of *Parvocysta* ? *tricornata* Riding & Shaw were recorded in sample MK 14 while sample MK 17 contains a high percentage of *Susadinium scrofoides* Dörhöfer & Davies emend. Below and *Parvocysta nasuta* Bjaerke (Table 2).

In the Boreal Realm, this dinoflagellate suite shows a very restricted range, between the upper Toarcian (H. bifrons Zone) and the lower Aalenian (L. opalinum Zone) (RIDING & THOMAS, 1992). This stratigraphic range was recorded also in Russia (Siberia) by ILYINA *et al.* (1994). The specimens of *S. scrofoides* recorded in the assemblages are characterised by a spinose and/or granulose autophragm, a morphological feature typical of the Aalenian *S. scrofoides* (BUCEFALO PALLIANI & RIDING, in press). In sample MK 17, long-range species, such as *Nannoceratopsis spiculata* Stover, *Nannoceratopsis gracilis* Alberti emend. Evitt and *P. halosa* (Filatoff) emend. Prauss were recorded. On the basis of this assemblage the sample may be tentatively referred to the early Aalenian.

This finding, just below the layers with Callovian ammonoids, is somewhat puzzling and suggests the need for improvement of the Middle Jurassic stratigraphy in Gorny Mangyshlak. A gap at the top of the Sarydiirmen Formation was suggested also by KIRKHOVA *et al.* (1989) on the basis of palynomorphs.

ENVIRONMENT

The presence of dinocysts suggests a marine influence in the upper part of the terrigenous succession. The dominant shaly facies with rare fine siltitic intercalation indicate a marginal sheltered environment, where connections with the open ocean were episodic and sedimentation gaps could occur locally.

UNNAMED UNIT

A thin unit lies between the shales of the Sarydiirmen Formation and the overlying mudstones and shales of the Chagabulak Formation. The succession is not named in the Russian literature, and even in REPIN & RASHWAN (1996), it is reported by its age only.

It consists of two layers of grey/brown sandstones to hybrid sandstones with calcareous cement, separated by a silty/shaly bed containing isolated, well preserved zircon crystals. The total thickness of this unit varies from 2 to 6 m and it is sealed by a ferruginous crust, up to 20-30 cm thick, that forms a continuous horizon in the landscape.

The two sandy/hybrid layers contain an abundant marine fauna, with clusters of brachiopods, large isolated oysters and sparse ammonoids. The very abundant brachiopod *Rhynchonelloidella* sp. (det. B. Laurin, Dijon) forms clusters, possibly still in life position, whilst the shells of *Liostrea* sp., up to 10 cm-large, appear isolated and reworked. The two sandy/hybrid layers yielded ammonoids of the Calloviense Zone (top of the early Callovian; Fig. 9, Table 3). However, about 2 km west of Dzharmysh (section W Dzharmysh 2), the top of the sandy layers contains ammonoids from the Coronatum Subzone of the middle Callovian (MK 95). A very reduced or condensed middle Callovian is suggested also by REPIN & RASHWAN (1996), who were able to identify ammonoids from the Koenigi Zone, immediately underlying the Calloviense Zone. Amongst the microfossils, calcations nannofossils are very rare, with few *Watznaueria* sp. found at the top of the unit where foraminifers are also very rare. In section W

Source : MNHN, Paris

Dzharmysh 2. *Textularia jurassica* Guembel (sample N 5059) and *Ammobaculites* ? sp. (sample N 5061) were identified.

This unit is well constrained to the upper part of the early Callovian, locally to the middle Callovian in the condensed layer. On the contrary, according to KIRICHKOVA & DOLYDENKO (1996, fig. 6) the top of the Bathonian and the lower Callovian are missing in the Mangyshlak.

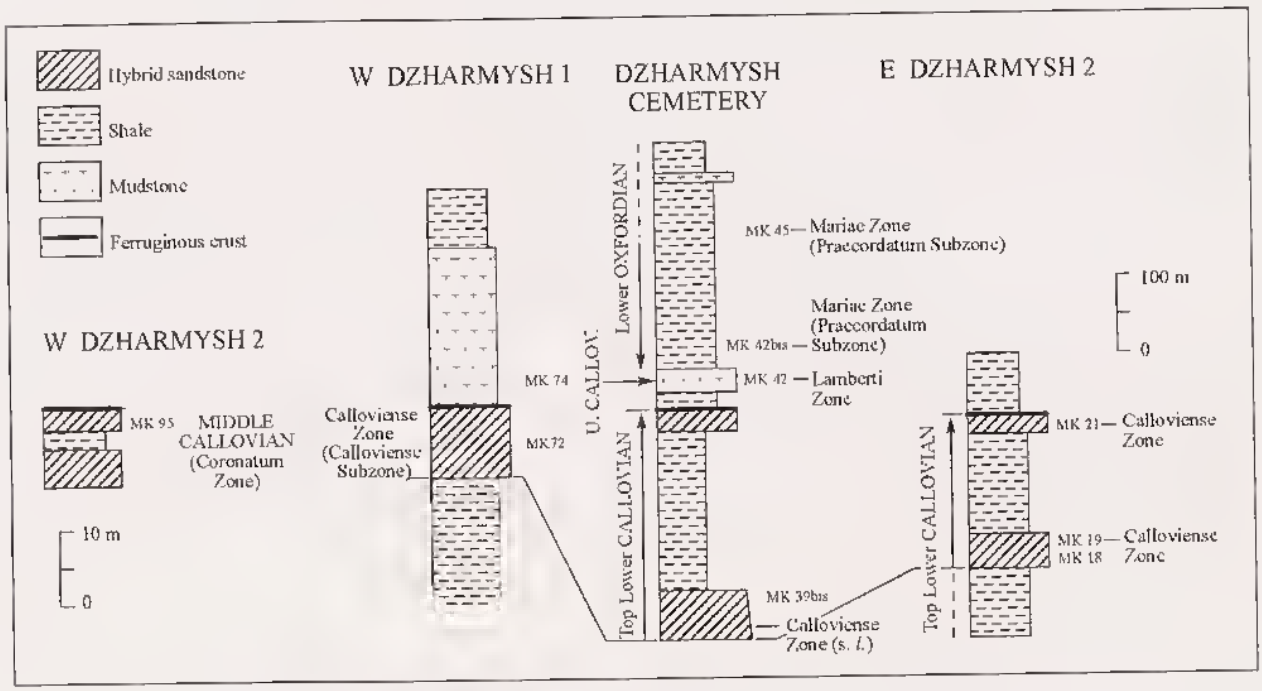

FIG. 9.— Ammonoid range in the Callovian-Oxfordian layers.

FIG. 9.— Répartition des ammonites dans les niveaux calloviens - oxfordiens.

ENVIRONMENT

This unnamed unit indicates the gradual but generalized ingression of an epicontinental sea on the peneplaned flat of the southern shores of Asia. The final drowning of the near shore coarser terrigenous sediments and the reduced and condensed chemical precipitation of the ferruginous crust are recorded during the middle Callovian. The well-preserved zircon crystals suggest a remote, contemporaneous volcanic activity.

SEQUENCE STRATIGRAPHY

The hybrid shelly sandstone layers are considered as the Transgressive Tract, whilst the ferruginous crust corresponds to the maximum flooding and starved basin stage. A similar condensed sedimentation and reduced layers were recognised throughout western Europe in the upper Callovian by NORRIS & HALLAM (1995).

COMPOSITION OF MIDDLE JURASSIC ARENITES

Several sandstone samples were collected in the previous Jurassic formations and 5 were point-counted (MK 6, MK 59, MK 131, MK 21, MK 41). The arenites studied are fine-grained feldspathic

Source : MNHN, Paris

TABLE 3.— List of the identified ammonites in the Callovian-Oxfordian of the area around Dzarmysh village.
TABLEAU 3.— Liste des ammonites reconnues dans le Callovien - Oxfordien de la région du village de Dzarmysh

Sample number	Age - zone	species
MK 95	Middle Callovian Coranatum zone	*Kosmoceras (Zugokosmoceras) obductum* (Buckman) *Kosmoceras (Zugokosmoceras)* aff. *crassum* Tintant *Grossouvria* sp. *Flabellisphinctes villanyensis* (Till)
MK 72	Top of lower Callovian Calloviense zone and subzone	*Sigaloceras (S.) calloviense* (Sowerby)
MK 73	Top of lower Callovian Calloviense zone and subzone	*Sigaloceras (S.) calloviense* (Sowerby)
MK 39bis	Top of lower Callovian	*Proplanulites* aff. *capistratus* Buckman
MK 42	Upper Callovian Lamberti Zone	*Quenstedtoceras* sp. *Peltoceras* sp. *Hecticoceras (Lunuloceras)* cf. *faurei* Fallot *Hecticoceras (Lunuloceras)* sp. *Kosmoceras annulatum* Quenstedt
MK 42bis	Lower Oxfordian	*Protocardioceras* cf. *praecordatum* (Douvillé)
MK 45	Lower Oxfordian	*Protocardioceras* sp.
MK 18	Top of lower Callovian	*Proplanulites* sp.
MK 19	Top of lower Callovian Calloviense zone	*Sigaloceras (S.) calloviense* (Sowerby) *Sigaloceras (Gulielmina) quinqueplicatum* Buckman *Proplanulites* aff. *koenigi* (Sowerby)
MK 21	Top of lower Callovian Calloviense zone	*Sigaloceras (S.) calloviense* (Sowerby) *Cadoceras* sp. *Proplanulites* cf. *trifurcatus* Buckman *Hectococeras (Lunuloceras)* sp. *Choffatia* sp.

litharenites to lithic arkoses (average composition Q = 32±11 ; F = 25±6 ; L = 43±11) (Fig. 10). Detrital quartz is mostly monocrystalline (average C/Q = 9%); several grains display straight extinction and may be of volcanic origin. Alkali feldspars (locally perthitic orthoclase, subordinate microcline and chessboard-albite) prevail over plagioclase (average P/F = 46%). Volcanic lithics are common and largely represented by felsitic and vitric types, with subordinate microlitic, fluidal and lathwork grains (V/L = 85%); plagioclase-bearing to granophyric hypabissal grains and granitoid rock fragments are also frequently recorded. Metasedimentary (slate, phyllite, quartzite, paragneiss) and sedimentary

Source : MNHN, Paris

(radiolarian chert, siltstone) rock fragments are both significant. Alterites are frequent in continental settings; bivalves, benthic foraminifers, glaucony and silicatic peloids commonly characterize the marine samples. Poikilotopic calcite or dolomite cements are widespread, but quartz or K-spar syntaxial cements are also found. Secondary porosity is very significant in several samples.

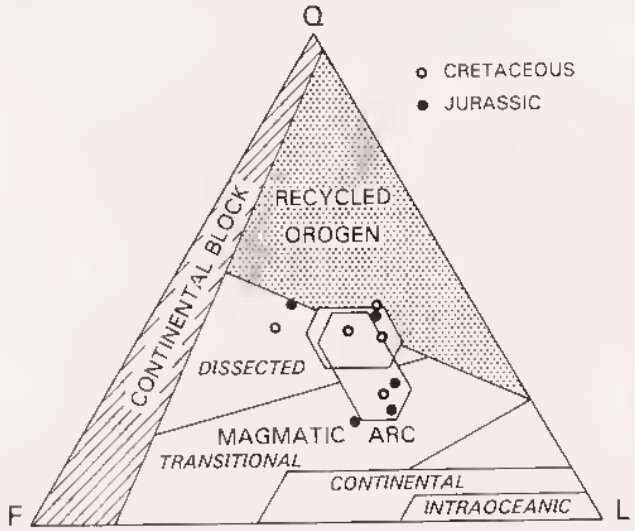

FIG. 10.— Detrital modes for studied Jurassic and Cretaceous samples are very close to Triassic samples (see Fig. 7; polygons are one standard deviation each side of the mean), but tend to be more dispersed. Sedimentary and metasedimentary rock fragments are also present, pointing to deposition in a collisional successor basin linked with Eo-Cimmerian and Neo-Cimmerian suture belts (GRAHAM *et al.*, 1993). Provenance fields are after DICKINSON (1985) and MARSAGLIA & INGERSOLL (1992).

FIG. 10.— Le contenu détritique des échantillons jurassiques et crétacés sont très proches de ceux du Trias (voir fig. 7 ; les polygones ont une déviation standard de chaque côté de la principale), mais tendent à être plus dispersés. Des fragments de roches sédimentaires et métasédimentaires sont aussi présents, montrant un dépôt dans un bassin en collision en liaison avec les ceintures de suture éo-cimmérienne et néo-cimmérienne (GRAHAM et al., *1993). Zones de provenance d'après DICKINSON (1985) et MARSAGLIA & INGERSOLL (1992).*

CHAGABULAK FORMATION

A mostly clayey unit, forming a recessive step in the landscape, overlies the ferruginous crust. Its basal part is often made by grey mudstones and clayey marls in poorly defined beds of 20-40 cm, for a total thickness of 4-5 m. The mudstones may end abruptly or continue with few lenticular layers followed by dark grey splintery shales, that form the monotonous remaining part of the unit, about 25-30 m-thick. The sequence is topped by a ferruginous crust, a few cm-thick.

AGE

The lowermost mudstone beds contain ammonoids of the top of the late Callovian (Lamberti Zone) (i.e. *Quenstedoceras* cf. *praelamberti*, *Quenstedoceras* sp., *Peltoceras* sp., *Hecticoreas* (*Lunuloceras*) cf. *fanrei*, *Kosmoceras annulatum*, *Enaspidoceras* sp.). In the middle-upper part of this lithozone, early Oxfordian ammonoids, with *Protocardioceras* cf. *praecordatum* were recovered. Coccoliths are fairly abundant with *Cyclagelosphaera wiedmanni*, *Stephanolithion hexum* and *S. bigoti maximum* marking the base of the Oxfordian, a few tens of cm from the base of the mudstone layer (Table 5).

In the overlying dark shales, nannofossils are scarce, being dominated by the resistant *Watznaueria* group, suggesting a generic Oxfordian age (Table 4). Benthic foraminifers are instead rather common.

Species identified are: *Haplophragmoides* sp., *Textularia jurassica* Guemb., *Tristix tutkowskii* Kapt., *Nodosaria* ex gr. *oxforea* Mjatl., *Geinzinita* ex gr. *crassata* (Gerke), *Ophthalmidium strumosum* (Guemb.), *Quinqeloculina* sp., *Lagena* ex. gr. *laevis* (Montagu), *Lingulina* ex gr. *belorussica* Mitjan., *Dentalina oppeli* Schw., *Dentalina turgida* Schw., *Dentalina* sp., *Lenticulina* cf. *tumida* (Mjatl.), *Lenticulina compressaeformis* (Paalz.), *Lenticulina comae* Byk & Azbel, *Lenticulina brueckmanni* (Mjatl.), *Lenticulina hyalina* (Mjatl.), *Lenticulina* aff. *sumensis* Pja, *Lenticulina* aff. *russiensis* (Mjatl.), *Lenticulina* spp., *Astacolus compressaeformis* (Paalz.), *Astacolus ectypa costata* Cordey, *Astacolus* sp., *Planularia colligata* (Brueckm.), *Planularia subcompressa* (Schw.), *Planularia contracta* (Trq.), *Planularia spatulata* (Wisn.), *Planularia tricarinella* Reuss, *Planularia* sp., *Marginulinopsis* aff. *procera* (Kapt.), *Saracenaria inclusa* Schw., *Saracenaria cornucopiae* (Schw.), *Falsopalmula inaequilateralis* (Terq.), *Eoguttulina* sp., *Globuligerina* sp., *Marginulina batrakiefornis* Azbel, *Marginulina minuta* Terquem, *Citharina sokolovae* (Mjatl.), *Citharinella spatha* (Lalicker), *Epistomina* sp.

Source : MNHN, Paris

TABLE 4.— Distribution of calcareous nannofossils in the Upper Jurassic.

TABLEAU 4.— Répartition des calcaires nannofossiles au Jurassique supérieur.

SAMPLE	Total Abundance	Preservation	Watznaueria britannica	Watznaueria communis	Watznaueria barnesae	Watznaueria contracta	Cyclagelosphaera margerelii	Watznaueria spp.	Lotharingius spp.	Zygodiscus erectus	Discorhabdus sp.	Cyclagelosphaera wiedmannii	Watznaueria aff. W. manivitae	Watznaueria crucicentralis	Schizosphaerella punctulata	Ethmorhabdus gallicus	Watznaueria fossacincta	Diazomatholithus lehmanii	Watznaueria biporta	Coccospheres	Stephanolithion bigotii bigotii	Stephanolithion hexum	Stephanolithion bigotii maximum	Watznaueria manivitae	Crepidolithus crassus	Biscutum constans	Ansulasphaera helvetica	Retecapsa incompta	Sollasites sp.	Clay	Dolomite	Micarbs	Calcite Fragments	Dark Minerals
MK78	FC	MP	F		A		C																								C		A	
MK77	A	M	AA	F	A		F			F			R		R	FC	R			F	C		R		R	R			R					
MK76	A	M	A	F	A		C			F		R	R	R		FC				F	FC		R	R		R	R	R	R					
MK75	C	M	A	F	A		F			R		R	R	R	R		R				F				R	R								
MK74	FC	MP	C	R	C		F					R			R	R															F	A		
MK73	FC	M	C	F	C	R	F					R		R											R						F	C		
MK71	B																															F		
MK70	B																												A					F
MK69	B																												A	F				
																													A					
MK54	RR				R		R	R					F	R			F													R		A		
MK53	C	M	C	R	C		F						A		R						R			F						RF		RF		
MK52	C	MP	CA	F	A		C			F			C		R							R								RF		RF		
MK51	CA	MP	A	F	A		CA			F			CA	R	R						R		R							RF		RF		
MK50	A	M	CA	F	A	R	F			C			R							R										F		F		
MK49	A	M	C	C	A		R			R					R						F	R	R	R								C		
MK48	A	M	A	C	CA	R	R																											
MK47	VB		RR					A																								A		
MK45	CA	P	A	C	C	R						F		R							F	R	R							A				C
MK44	A	M	A	C	A	R	F					R							R	R														
MK43	CA	M	A	C	A	R	F																											
MK 39	B																																	
MK38	RF	PM																														A		
MK37	RF	PM	F	R	R		R	R																						C		A		
MK36	VB							R																						C		A		
MK35	VB							R																						C		A		
MK34	RR	PM	R				R	R																						C		A		
MK33	RR	PM	R				R	R																						C		A		
MK32			R		F		F	F										R	R											C		A		
MK31	R	M					FC	F									R	R												C		A		
MK30	R	PM					F	F									R													C		A		
MK29	C	P	CA				CA			R					R															C		A		
MK28	C	P	CA	CA	CA		CA			R		R			R		R																	
MK27	C	P	CA	CA	CA		CA			F					F	F																		
MK26	C	P	C	A	A	R	R	R	R			R	FC		R																			
MK25	C	P	CA	A	A					FC				R	R																			
MK24	C	MP	CA	CA	C				R				R																					
MK23	C	MP	A	C	C	F	F	F	F	F		R																		F	F	F		
MK22	CA	MP	A	C	CA	CA	CA	F	F	F	R																							

In conclusion, the Chagabulak Formation extends from the latest Callovian at its base to the Oxfordian. It should be noted that no Kimmeridgian deposits are reported in the Gorny Mangyshlak and only a few tens of metres of Kimmeridgian sediments were drilled in the Southern Mangyshlak (MUROMCHEV, 1968).

ENVIRONMENT

Open marine with steady clay input in a low-subsidence regime.

SEQUENCE STRATIGRAPHY

The Chagabulak Formation represents the high-standing tract and the sequence is truncated at the top by a non-depositional or erosional surface.

Source : MNHN, Paris

THE CRETACEOUS

The Cretaceous succession crops out extensively all around the Gorny Mangyshlak and is especially well exposed on its northern slope. It was the object of several recent detailed studies (KOPAEVICH, 1989; LUPPOV *et al.*, 1988; MARCINOWSKI *et al.*, 1996; NAIDIN *et al.*, 1984,) and is presently under further study by a team from Moscow University directed by L. F. KOPAEVICH and E. J. BARABOSHKIN.

The succession may reach 1000 m in thickness and may be subdivided into three parts, bottom to top.

— Three to four sandy to shaly sequences, rarely including shallow water carbonates, with low subsidence rate. Berriasian-Barremian (part A).

— A complex pattern of shaly to sandy sequences in a higher subsidence regime, but also with many non-sedimentation gaps in the upper part. Aptian-Turonian (part B).

— A uniform, whitish chalky sedimentation in open marine environment in a low subsidence pattern. Coniacian to earliest Palaeocene (part C).

For logistic reasons, we had the opportunity to sample only a few sections and consequently we provide only sparse data and conclusions on the Cretaceous stratigraphy and evolution. We will present data on parts A and C. The upper Albian-Coniacian part was described exhaustively by MARCINOWSKI *et al.* (1996). The ammonoids collected from the Semenoviceras horizon (late Albian) were illustrated by CECCA (1997).

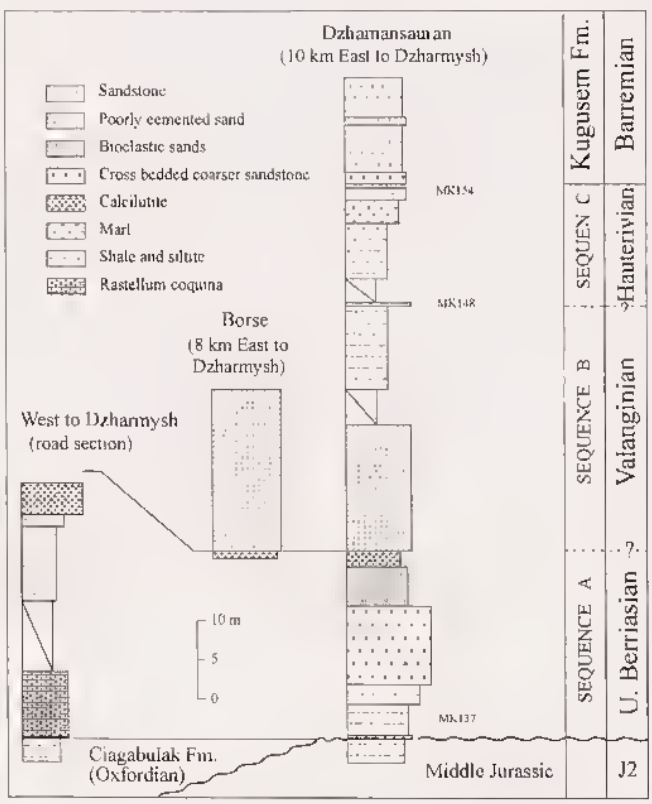

FIG. 11.— Lower Cretaceous sections measured on the north side of East Karatau, Gorny Mangyshlak.

FIG. 11.— Coupes levées dans le Crétacé inférieur du coté nord de l'est Karatau.

PART A

A lithostratigraphic scheme has not yet been published for the lower portion of this part, probably due to the large lateral variability and reduced thickness of this succession. Only the upper red siltstones and shales were grouped into the Kugusem Formation. A brief review follows, according to the sequences we identified (Fig. 11).

SEQUENCE 1.— From a few km west of Dzharmysh to 10 km east of the village, the succession is as follow, bottom to top:

— extremely dense accumulation of oyster-like (*Rastellum*) building mounds up to 9 m thick. At the top, a nannofossil assemblage was found (*Watznaueria* spp., *W. barnesae*, *W. britannica*, *Nannoconus* spp. (both narrow- and wide-canal forms), *Nannoconus steinmannii minor*, *Zygodiscus* spp., *Zygodiscus erectus*, *Cyclagelosphaera margerelii*, *C. deflandrei*, *Micrantolithus hoschulzii*, *M. obtusus*, *Biscutum constans* and *Lithraphidites carnioleusis* (sample MK 137, section Dzhamansauran);

— litharenites and poorly cemented sands, brown to greenish, locally with coarse, high-angle cross-bedding. Sparse brachiopods and bivalves. Up to 15 m;

Source : MNHN, Paris

— bioclastic hybrid sandstones, rich in bivalves, especially oysters, and few ammonoids (Ryazanites beds of LUPPOV *et al.*, 1988). 2 to 5 m;

— whitish to light grey chalky limestones. 1-2 m thick.

The development of this sequence was analysed in detail in the monograph of LUPPOV *et al.* (1988), who distinguished 5 types of possible successions.

AGE

According to LUPPOV *et al.* (1988) the upper part of the Berriasian, from the Neocosmoceras up to *Ryazinites* ammonoid zones, is represented. The age of the nannofossil assemblage is Berriasian-Valanginian, but the absence of latest Berriasian or younger markers restricts the sample to the Berriasian. Consequently, the gap between the Rastellum Bank and the top of the Chagabulak Formation includes Kimmeridgian, Tithonian and lower Berriasian, for a time span of at least 10-15 m.y.

ENVIRONMENT

The lithology suggests a shore-face environment with short-lived episodes of more open marine conditions. The relative abundance of nannoconids and braarudosphaerids suggests deposition in a marginal setting, with possible eutrophic conditions as inferred by the occurrence of *Biscutum* and *Zygodyscus*. All nannofossil specimens are characterized by small size. This is peculiar to lagoonal nannofloras from the modern oceans and the fossil record, suggesting a very restricted environment.

SEQUENCE 2.— Yellowish to olive-green, poorly cemented sandstones with high-angle cross-laminations and poorly defined bedding. They form a cliff about 20 m-high which is in turn overlain by 10 to 15 m of greyish to dark grey shales.

AGE

According to the Samarkand Scheme (1977) this sequence represents the Valanginian. No nannofossils were found in the shales.

ENVIRONMENT

The lower sandstone layer indicates a shore-face environment with coastal sands forming festooned bars. The overlying shales should represent the deepening of the sequence.

SEQUENCE 3.— Sequence 3 starts with a thin cross-laminated arenaceous bed 40 cm-thick (MK 148). It contains fragments of Trigoniancean bivalves. It is followed by about 10 m of grey-green shales and marls, in turn overlain by pinkish marls (3 m). This sequence is also capped by a cross-laminated sandstone with ostreid fragments 1.8 m-thick (MK 154). The total thickness is about 15 m.

AGE

According to the Samarkand Scheme, this sequence represents the lower Hauterivian. Samples analysed for coccoliths were negative.

ENVIRONMENT

Similar to sequence 2.

KUGUSEM FORMATION.— This sandy to shaly unit caps the first part of the Cretaceous succession. It consists of a basal layer of grey, high angle cross-laminated sandstones, with current direction towards WSW, followed by very fine sandstones, siltites and occasionally shales of red to pink colour. The top is made of pink siltites and grey fine sandstones with ripple-marks. This unit is cliff-forming and is several tens of m-thick.

AGE

According to the Samarkand Scheme (1977) this unit represents the upper Hauterivian and all but the upper part of the Barremian. No new data are available.

Source : MNHN, Paris

ENVIRONMENT

Coastal marine to continental alluvial plain in oxic conditions.

COMPOSITION OF LOWER CRETACEOUS ARENITES.— Very few sandstone samples were sufficiently coarse to be counted (MK 148, MK 154, MK 155, MK 157). The arenites studied are fine-grained feldspathic litharenites to lithic arkoses (average composition Q = 38±6 ; F = 24±8 ; L = 38±9) (Fig. 10). Detrital quartz is mostly monocrystalline (average C/Q = 10%); several grains display straight extinction or even bipyramidal outlines and may be of volcanic origin. Alkali feldspars (locally perthitic orthoclase, subordinate microcline and chessboard-albite) prevail over plagioclase (average P/F= 42%). Volcanic lithics are common and largely represented by felsitic and vitric types, with subordinate microlitic and lathwork grains (V/L = 83%); granophyric, myrmechitic and granitoid grains are common. Metasedimentary (slate, greenschist, chloritoschist, phyllite) and sedimentary (chert, siltstone, shale) rock fragments are both significant. Micas, zircon, and celadonite are frequently recorded. Alterites and soil fragments characterize fluviatile samples; glaucony, silicate peloids, bivalves, benthic foraminifers, ooids and peloids commonly occur in marine settings. Locally, poikilotopic calcite or dolomite cements and late diagenetic replacements are widespread; quartz or K-spar syntaxial cements also occur. Secondary porosity is significant in several samples.

PART B

This part is often very poorly exposed, especially in its lower portion, where the steppe hides large segments of the outcrops. Its base is transgressive with a few dm of hybrid siltstones and calcareous siltites and locally, like NW of Shetpe, along the road to Akmysh, it covers the underlying Kugusem formation with a gentle angular unconformity.

It may be subdivided roughly, bottom to top, as follows.

— black shale unit with thin siltitic layers and fine arenaceous nodules. Very faint interference ripples in the thin arenaceous layers. > 100 m thick. Aptian.

— monotonous succession of shales and siltitic shales with more arenaceous intercalations coarsening upwards. Very peculiar sandstone concretions m-sized, sometimes with high-angle cross-laminations. Not less than 300 m, but thickness difficult to assess. The lower Albian section has been extensively studied by SAVELIEV (1992). Aptian-? middle Albian.

— phosphatic sandstones, also forming m-thick concretions, alternating with shaly packages tens of m-thick. The sedimentation rate seems to decrease upwards where several phosphatic horizons, very useful tools for regional correlations (MARCINOWSKI *et al.*, 1996) are present. Sedimentation gaps are frequent in the Cenomanian-Turonian part, with the upper Turonian mostly represented by condensed phosphatic horizons. Overall thickness up to 120 m. Upper Albian-Turonian.

The succession No. 3 was monographed in detail by MARCINOWSKI *et al.* (1996). We collected 35 samples for calcareous nannofossils and all resulted barren. A rich ammonoid fauna was found in the sandy phosphatic concretions about 500 m northwest of the Akmysh Pioneer Camp and Spring (Fig. 1). Above a first level with *Semenoviceras mangyschlakensis* (Saveliev), a very rich horizon of phosphatized ammonoids and trigoniids is present. The ammonoids include *Semenoviceras uhligi* (Semenov), *S. litschkovi* (Saveliev), *S. pseudocoelonodosus* (Semenov), *S. michalskii* (Semenov) and indicate the S. litschkovi Zone of the upper Albian (= Semenovites michalskii Zone in MARCINOWSKI *et al.*, 1996), correlatable to the Dipoloceras cristatum Zone of Western Europe. Immediately above this horizon, which is about 5 m thick, poorly exposed grey sands follow. A single specimen of *Cunningtoniceras* aff. *inerme* (Pervinquière) was collected, suggesting a middle Cenomanian age. These specimens were described by CECCA (1997).

Source : MNHN, Paris

PART C = "CHALK-LIKE" UNIT

The Aktau (White Mountains) characterize the landscape around the Gorny Mangyshlak with white, cliff forming chalk. In this unit, consisting of light grey marls and marly limestone rithmites, and extending up to the early Palaeocene (NATDIN *et al.*, 1984), we sampled two sections at Chirkala and near Endikurgan (Figs 1 and 11), for foraminifers and nannofossils, which add new data to the paper of MARCINOWKI *et al.* (1996) and NATDIN *et al.* (1984).

CHIRKALA SECTION.— The section was measured probably slightly east of the Shyrkala section of MARCINOWSKI *et al.*, (1996), to date the base of the "Chalk-like" unit (Fig. 11). A few samples were also collected in the phosphatic horizons and yellowish quartzitic sands.

Calcareous nannofossils are common to abundant in samples MK 418 through 428. Preservation is poor in the bottom sample and increases in quality upwards. The assemblages are characterized by common to abundant *Prediscosphaera* spp., *Watznaueria barnesae*, *Eiffellithus eximius*, *Eiffellithus turriseiffelii*, *Eprolithus floralis*, *Tranolithus phacelosus*, *Zygodiscus* spp., *Zygodiscus diplogrammus*, *Zygodiscus erectus*, *Microrhabdulus decoratus*, *Lucianorhabdus maleformis*, *Ahnuellerella octoradiata*, *Cylindralithus* sp., *Cretarhabdus* spp., *Cribrosphaerella ehrenbergii* and *Manivitella pemmatoidea*. A few nannoconids (*N. multicadus*, *N. farinaccíae*, *N. minutus* and cross sections of narrow-canal forms) were observed in most samples.

AGE

The occurrence of *Lithastrinus septenarius* in samples MK 418 through 428 indicate a Coniacian to earliest Santonian age. A single specimen identified tentatively due to poor preservation as *Reinhardtites anthophorus* was observed in sample MK 420 and indicates the base of the Santonian. Samples MK 424 through 428 contain common *Micula decussata* which is indicative, along with *L. septenarius*, of the upper Coniacian-lowermost Santonian CC 14-15 zones of STSSTNGH (1977). It should be noted that our results suggest a younger age (i.e. Coniacian) for the top of the sands, instead of early Turonian as indicated by MARCINOWKI *et al.* (1996).

ENDIKURGAN SECTION.— The section was measured along the slope, west of the Endikurgan hamlet, and a few samples were collected in an isolated outcrop, directly below the main section, in the flat steppe to the SW.

The entire section lies within the "Chalk-like Unit" (Fig. 12).

CALCAREOUS NANNOFOSSILS

The lowermost part of the section (samples MK 412 through 417) contains common to abundant, moderately preserved nannofloras. The assemblages are characterized by common *Micula decussata* and *Prediscosphaera* spp. along with frequent *Lucianorhabdus cayeuxii*, *Lucianorhabdus maleformis*, *Calculites obscurus*, *Eiffellithus eximius*, *Nannoconus* spp., *Nannoconus multicadus* and *Watznaueria barnesae*. *Aspidolithus parcus parcus* and *Aspidolithus parcus constrictus* as well as *Ceratolithoides aculeus* were observed throughout the section. *Quadrum sissinghii* occurs in samples MK 413 and 414, whereas *Reinhardtites levis* was found in samples MK 416 and 417. Such an assemblage, together with the absence of *Quadrum trifidum*, are indicative of the mid-Campanian CC 20-21 zones of STSSINGH (1977) (ERBA *et al.*, 1995).

Calcareous nannofloras are common to abundant and poorly to moderately preserved in samples MK 300 through 411. Although both diversity and preservation slightly fluctuate, the assemblages are very similar in all samples. The most abundant taxa are: *Prediscopshaera* spp., *Watznaueria barnesae*, *Micula decussata*, *Lucianorhabdus cayeuxii*, *Calculites obscurus* and *Cylindralithus serratus*. *Quadrum gothicum*, *Cribrosphaerella ehrenbergii*, *Reinhardtites levis*, *Aspidolithus parcus constrictus* and *Microrhabdulus decoratus* are always present and their abundance fluctuates from rare to frequent. *Eiffellithus eximius* was observed only in the lower part of the section, from sample MK 300 through

Source : MNHN, Paris

SAMPLES	Hedbergella planispira	Hedbergella delrioensis	Marginotruncana marginata	Marginotruncana paraconcavata	Marginotruncana pseudolinneana	Heterohelix moremani	Globigerinelloides ultramicrus	Heterohelix globulosa	Heterohelicids	Globigerinelloids	Whiteinella baltica	Heterohelix reussi	Dicarinella imbricata	Hedbergella hoelzli	Archaeoglobigerina cretacea	Hedbergella simplex	Hedbergella llandrinl	Marginotruncana coronata	Hedbergella amabilis	Whiteinella paradubia	Whiteinella brittonensis	Globigerinelloides asper	Globigerinelloides prairiehillensis	Contusotruncana fornicata	Globotruncana ventricosa	Contusotruncana plummerae	Globotruncana arca	Globotruncana orientalis	PLANKTONIC FORAMINIFERA	BENTHIC FORAMINIFERA	Benthic foram. preservation	RADIOLARIANS	CALCISPHERES	Planktonic Foram ZONES	NANNOFOSSIL ZONES	AGE
MK353									C																				C	C/A		F/C	C			
MK352									C																				C	C/A		F/C	C			
MK351									C																				C	C/A		F/C	C			
MK350									C																				C	C/A		F/C	C			
MK349								F	C	C																		1	2	C	C/A		F/C	C			
MK348								F	C	F												F		1	1	1			C	C/A		F/C	C			
MK347								R	C	F												R							C	A		C	F			
MK346									C	F																			C	A		C	F			
MK345								R	C	F												R							C	A		C	F			
MK344								R	C	F												R							C	A		C	F			
MK343								R	C	F																			C	A		C	F			
MK342									C	F																			C	A		C	F			
MK341									C	F																			C	A		C	F			
MK340								R	C	F												1							C	A		C	F			
MK339									C	F																			C	A		C	F			
MK338									C	F																			C	A		C	R/F			
MK337									C	F																			C	A		C	R/F			
MK336								R	C	F												1							C	A		C	R/F			
MK335									C	F																			C	A		C	R/F			
MK334									C	F																			C	A		C	R/F			
MK333									C	F																			C	A		C	R/F			
MK332									C	F																			C	A		C	R/F			
MK331								R	C	F																			C	A		C	R/F			
MK330									C	F																			C	A		C	R/F			
MK329									C	F																			C	A		C	R/F			
MK328								R	C	F												1							C	A		C	R/F			
MK327									C	F																			C	A		C	R/F			
MK326									C	F																			C	A		C	R/F			
MK325								R	C	F																			C	A		C	R/F			
MK324									C	F																			C	A		C	R/F			
MK323									C	F																			C	A		C	R/F			
MK322								R	C	F																			C	A		C	R/F			
MK321									C	F																			C	A		C	R/F			
MK320									C	F																			C	A		C	R/F			
MK319									C	F																			C	A		C	R/F			
MK318								R	C	F																			C	A		C	R/F			
MK317									C	F																			C	A		C	R/F			
MK316									C	F																			C	A		C	R/F			
MK315								R	F													1							F	A	fragmented	A	R/F			
MK314								R	F																				F	A	fragmented	A	R/F			
MK313								R	F																				F	A	fragmented	A	R/F			
MK312								R	F																				F	A	fragmented	A	R/F			
MK311								R	F																				F	A	fragmented	A	R/F			
MK310								R	F	R																			F	A	fragmented	A	R/F			
MK309								R	F	R																			F	A	fragmented	A	R/F			
MK308								R	F	R																			F	A	fragmented	A	R/F			
MK307								R	F	R																			F	A	fragmented	A	R/F			
MK306								R	F	R																			F	A	fragmented	A	R/F			
MK305								R	F																				F	A		A	R/F			
MK304								R	F																				F	A		A	R/F			
MK303								R	F																				F	A		A	R/F			
MK302								R	F																				F	A		A				
MK301								R	F																				F	A		A				
MK 300								R	F																				F	A		A				
MK416								R	R													1	1						R	A		A				
MK415								R	R													1	1						R	A		A				
MK414								R	R																				R	A		A				
MK413								R	R																				R	A		A				
MK412								R	R																				R	A		A				
MK417								1	VR														1	1					R	A		A				
MK424	R	F/C	A		C/A	F	C	C		F	cf/F					cf/R					R								C	A				not zoned	Globotruncana ventricosa	
MK423		F	C	R	A	F/C		F/C			F							F	F		R	R							F/C	C						
MK421		F	F/C		F/C		F	F				F	R	R	F	cf/R	R	F/C	R										F/C	C						
MK428		R	C		C	F/C	F	C				F																	F	C						
MK420			C	R	C		R	C			R	F		R	R	F	F	R											R/F	R/F						
MK427	R	C	C		F	R	F	C		R	R	R	cf/R																F	A						
MK425	F	F	C	R	C	F	R/F	C	C																				F	C						

Source : MNHN, Paris

TABLE 5.— Distribution of planktonic foraminifers in the "Chalk-like unit".

TABLEAU 5.— Répartition des foraminifères planctoniques dans "l'unité crayeuse".

SAMPLES	Heterohelix globulosa	Heterohelicids	Globigerinelloidds	Globigerinelloides asper	Contusotruncana plummerae	Globotruncana arca	Globotruncana orientalis	Globigerinelloides messinae	Hedbergella holmdelensis	Hedbergella cf. holmdelensis	Globotruncana linneiana	Globotruncana marlei	Archaeoglobigerina sp.	Globotruncana rugosa	Globotruncanita cf. subspinosa	Rugoglobigerina rugosa	Globotruncana aegyptiaca	Archaeoglobigerina cretacea	Globotruncanita stuartiformis	Heterohelix labellosa	Pseudoguembelina costulata	Pseudoguembelina sp.	Globotruncana falsostuarti	Heterohelix semicostata	Globotruncanella pschadae	Rugoglobigerina macrocephala	Laeviheterohelix dentata	Rugotruncana subcircumnodifer	Laeviheterohelix pulchra	Abathomphalus intermedius	Globotruncanella minuta	Rugoglobigerina pennyi	Planoglobulina carseyi	PLANKTONIC FORAMINIFERA	BENTHIC FORAMINIFERA	Benthic foram. preservation	RADIOLARIANS	CALCISPHERES	Planktonic Foram ZONES	NANNOFOSSIL ZONES	AGE
MK411		F	F					1																								1	F	A	fr		A	G. gansseri	CC 24	MAASTRICHTIAN
MK410		R	VR																														R	A	fr	VR	A			
MK409		R	VR																														R	A	fr	VR	A			
MK408	2	R	R	2		1					1		2/cf																				R/F	A		VR	AA			
MK407	2	R	R								1													1				1					R/F	A			AA			
MK406	2	R	R								2		1																				F	A			AA			
MK405	2	F	F								2					2																	F	A			AA			
MK404	2	R		1												2																	F	A			AA			
MK403		F		1												1																1	R/F	A		VR	A			
MK402	1	F				1				3																							F	A			A			
MK401	1			1																													F	A			A			
MK400	1		3																														VR	A			A			
MK399	3			2	1			2		3	2																						VR	A			A			
MK398		R				1		2		2															2				1			1	F	A			AA			
MK397	2	R	R	3				2	1																			1	1		1		R	A			AA			
MK396	2	R		2							1		1			1									2				1				R	A			AA			
MK395	1			1					2	3	1					1											1/cf	1					R	A		VR	AA			
MK394				1				2			1		1			1		1							3		1						R	A		VR	AA			
MK393	1		R																						1	1							VR	A			AA			
MK392	1			3		3						1													2								VR	A			AA			
MK391	1			1																													VR	A		VR	AA	G. aegyptiaca		
MK390		R				1					1		1																				R	A		VR	AA			
MK389		R				1					1		1																				R	A		VR	A			
MK388		R											1																				R	A		VR	A			
MK387		R											1																				R	A		VR	A			
MK386		R											1																				R	A		VR	A			
MK385	2			1														1		1													F/C	C/A		VR	A	G. havanensis		
MK384	F			2		3					1		1			1/cf	2				2												F/C	C/A		VR	A			
MK383				F		3					3		1				1	1	4				1	2									C	C/A		R	A			
MK382	F			2				2			4/cf		2				2					2											F/C	C/A		R	C			
MK381		F				2		3				2																					F	C/A		R	C			
MK380	F					3																1											F	C/A		R	C			
MK379		F	,	F		4					3						2		3														F/C	C/A		R	C			
MK378	R/F	F/C	R/F	1				2				1	1				2			2	1	3											C	C/A		R	C/A			
MK377	F	C	F		1	3							2	1				1															C	C/A		R/F	C/A	R. calcarata	CC 22- 23	CAMPANIAN
MK376	F	C	F	1							3			2			1																C	C/A		R/F	C/A			
MK375	F	C	F	2								1	1		1/cf																		C	C/A		R/F	C/A			
MK374	F	F/C	F			1								2																			C	C/A		F	C/A			
MK373	F	C			1	3							2	1																			C	C/A		F	C/A			
MK372		C																															F/C	C/A		F	C/A	Globotruncana ventricosa		
MK371	F	C	F								2	1	2																				C	C/A		F	C/A			
MK370	F	C	F					1																									C	C/A		F	C/A			
MK369	F	C	F																														C	C/A		F	C/A			
MK368	F	C	F					2																									C	C/A		F	C/A			
MK367	F	C	F																														C	C/A		F	C/A			
MK366	F	C	F																														C	C/A		F	C/A			
MK365	F	C	F					1																									C	C/A		F	C/A			
MK364	F	C	F																														C	C/A		F	C/A			
MK363	F	C	F																														C	C/A		F	C/A			
MK362	F	C	F					1																									C	C/A		F	C/A			
MK361	F	C	F																														C	C/A		F	C/A			
MK360	F	C	F								1																						C	C/A		F	C/A			
MK359	F	C		F							1																						C	C/A		F	C/A			
MK358	F	C		F																													C	C/A		F	C			
MK357	F	C		F																													C	C/A		F	C			
MK356	F	C		F																													C	C/A		F	C			
MK355	F	C		F				2	1	2																							C	C/A		F	C			
MK354		C																															C	C/A		F	C			

Source : MNHN, Paris

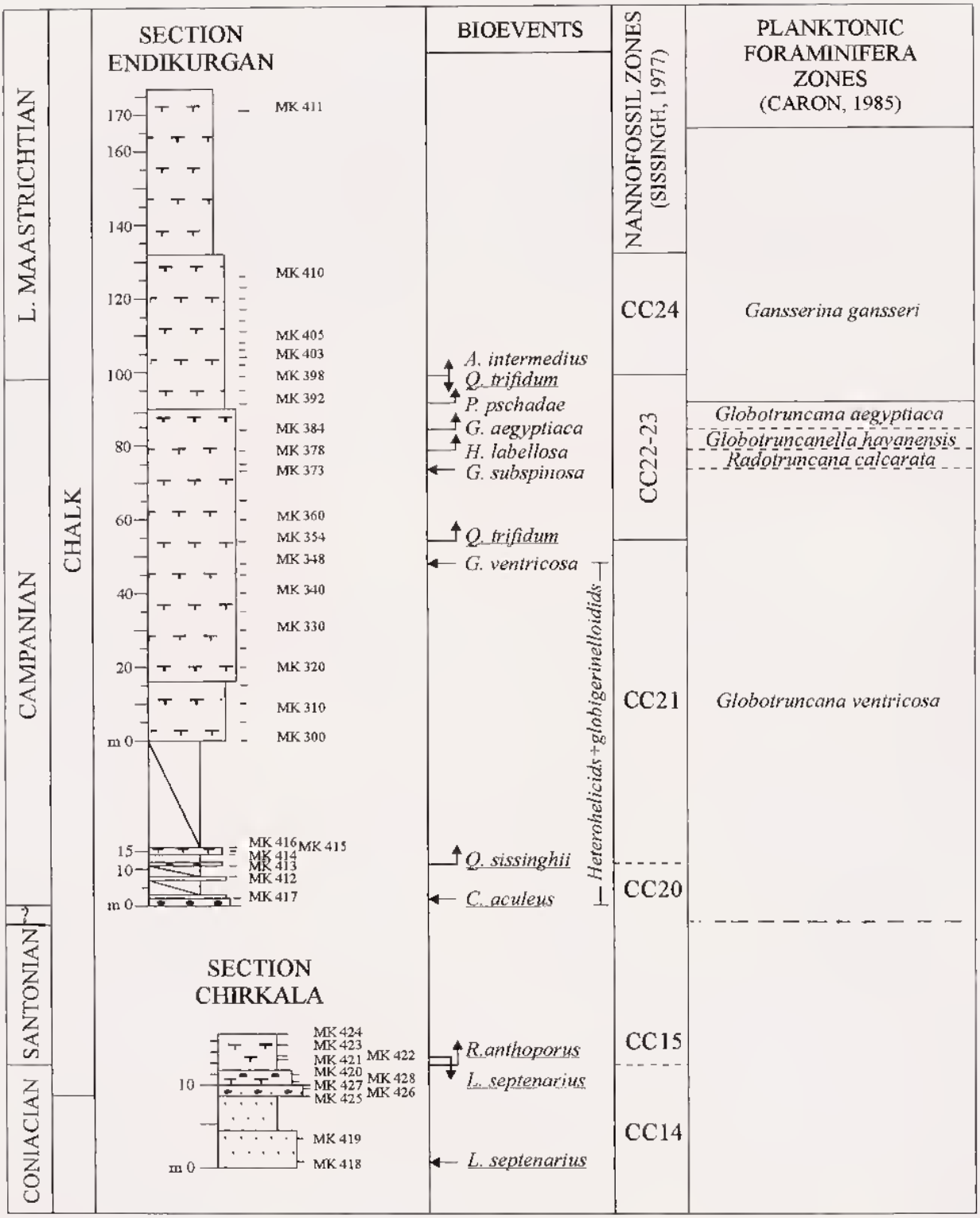

FIG. 12.— Upper Cretaceous sections measured on the northern side of Gorny Mangyshlak, with calcareous nannofossil and foraminiferal ranges.

FIG. 12.— Coupes levées dans le Crétacé supérieur de la partie nord du Gorny Mangyshlak, avec les répartitions des nannofossiles calcaires et foraminifères planctoniques.

Source : MNHN, Paris

sample MK 342, whereas *Quadrum trifidum* was found for the first time in sample MK 354. This taxon was consistently observed upward through sample MK 398, but not in the uppermost part of the section. Only a single specimen of *Quadrum trifidum* was identified tentatively in the top sample MK 411, due to extremely poor preservation.

Although never abundant, nannoconids (*Nannoconus multicadus*, *Nannoconus dauvillieri* and cross sections of narrow-canal forms) are present in the lower part of the section (samples MK 300 through 354), but are absent or extremely rare upwards. A few *Nannoconus* spp., *N. multicadus* and *N. dauvillieri* were observed in sample MK 378 which also contained a few specimens of *Thoracosphaera* sp.

The lower part of the section is assigned to the mid-Campanian CC 20-21 zones of SISSTNGH (1977). The first occurrence of *Quadrum trifidum* in sample MK 354 indicates the base of the CC 22 Zone (SISSTNGH, 1977). The continuous range of this taxon up to sample MK 398 indicates the CC 22 and 23 zones and therefore place the Campanian/Maastrichtian boundary very close to sample MK 398. Both *Eiffellithus eximius* and *Tranolithus phacelosus* are extremely rare and sporadic throughout the section and therefore are not considered as stratigraphic markers in this study.

FORAMINIFERS

A total of 117 samples from the Endikurgan section were investigated for planktonic foraminifers (Table 5). They were separated in three fractions corresponding to mesh sizes of >250 µm, >150 µm and >40 µm, respectively. Small-sized planktonic specimens dominate throughout the section. This is due to the constant presence of the generally small-sized heterohelicids and globigerinelloidids. Both fractions larger than 150 µm consist only of benthic foraminifers and are devoid of planktonic forms. Consequently, the normally large-sized (> 250 µm) planktonic taxa with ornamentation (keels, costellae, etc.) are represented only as small-sized or juvenile specimens. This fact made species identification extremely difficult. In addition, the few species identified are recorded very discontinuously. Therefore, age-diagnostic taxa are rare and their paucity resulted in generally poor biostratigraphic resolution.

The lower segment of the Endikurgan section yields a very poor planktonic foraminiferal assemblages consisting of rare specimens of *Heterohelix*, mainly not identifiable at the species level (see Table 6). Only single specimens of *Heterohelix globulosa* and *Globigerinelloides asper* could be identified with certainty in one out of three of the six samples. The washed residues of this segment yielded abundant, fairly well-preserved benthic foraminifers and abundant radiolarians.

In the lowermost part of the upper segment planktonic foraminifers increase slightly in abundance, always in association with abundant benthic foraminifers and radiolarians. The heterohelicids are the only planktonic component and *H. globulosa* is present constantly. No *Globigerinelloides* could be identified in the lowermost 6 samples (MK 300 to MK 305). In the upper three samples of this interval rare to few calcispheres are also recorded.

In the interval from MK 307 to MK 315, the washed residues contain few planktonic foraminifers mainly belonging to *Heterohelix* (rare *H. globulosa*), frequently associated with globigerinelloidids. Peculiar to this interval is the poor preservation of the abundant benthic foraminifers, which are commonly fragmented. Rare to few calcispheres and abundant radiolarians occur throughout the interval.

In the overlying interval (MK 316 to MK 347) planktonic foraminifers become common, even though the diversity remains very low. The planktonic faunas consist only of *Heterohelix* and *Globigerinelloides*, rarely identified at the species level. The increase in abundance of planktonic foraminifers coincides with a decrease in radiolarians from abundant to common. Benthic foraminifers are abundant and fairly well preserved throughout the interval, while calcispheres, still rare to few in the lower part of the interval, increase slightly in abundance in the upper part.

A major change is observed beginning with sample MK 348. In this sample, planktonic foraminifers become more diversified and rare keeled species such as *Globotruncana ventricosa*, *Contusotruncana plummerae* and *C. fornicata* appear, in addition to the still common *Heterohelix* and few *Globigerinelloides*. This increase in diversity among planktonic foraminifers coincides with a marked increase in abundance of calcispheres, paralleled by a decrease in abundance of radiolarians and benthic foraminifers.

Source : MNHN, Paris

Above this level, up to about sample MK 378, planktonic foraminifers tend to increase in diversity, although the distribution of single species is discontinuous. Calcispheres continue to increase in abundance, benthic foraminifers remain highly abundant, whereas only a few radiolarians remain.

All organic components from the remaining upper part of the section fluctuate in abundance, with intervals that are very rich in calcispheres associated with rare but diversified planktonic foraminifers alternating with intervals that contain slightly more common planktonic foraminifers and less abundant calcispheres. The group of planktonic foraminifers affected most drastically are the heterohelicids, which are rare overall, and occasionally confined to a single specimen of *H. globulosa*. Benthic foraminifers show very little changes in abundance throughout the interval, whereas radiolarians become progressively rare to absent.

Despite the very scattered record and distribution of planktonic foraminifers, three biozones could be reliably identified (ERBA *et al.*, 1995):

— the Globotruncanella havanensis Zone, based on the presence of *Heterohelix labellosa* in sample MK 378, whose first appearance, according to NEDERBRAGT (1990), almost coincides with the base of this zone;

— the Globotruncana aegyptiaca Zone, based on the presence of a single specimen of the nominal taxon in sample MK 384;

— the Gansserina gansseri Zone, based on the appearance of *Globotruncanella pschadae*, which, according to CARON (1985), is equated with the base of this zone. This occurrence in sample MK 392 is also supported by the evolutionary appearance of *Abathomphalus intermedius* slightly higher in sample MK 398. In the absence of further biostratigraphic events, the G. gansseri Zone is extended to the top of the Endikurgan section.

In addition, the occurrence of two specimens identified as *Globotruncanita subspinosa* in samples MK 373 and MK 375 suggests that the Radotruncana calcarata Zone might be represented from sample MK 373 to MK 377, below the G. havanensis Zone.

The remaining lower part of the section, including the lower segment, is remarkably poor in age-diagnostic planktonic taxa. Based on its lower stratigraphic position and especially on calcareous nannofossil data, this lower part is inferred to belong to the Globotruncana ventricosa Zone.

AGE

The biostratigraphy of planktonic foraminifers is in agreement with the calcareous nannofossil data. The correlation between calcareous nannofossil and planktonic foraminiferal zones is reported in Fig. 12 showing that the inferred R. calcarata Zone falls within the CC22-CC23 nannofossil zones, suggesting that its presence may be real. Finally, the position of the Campanian/Maastrichtian boundary, equated with the CC23/CC24 nannofossil zonal boundary, is further supported by the appearance of *A. intermedius* within the G. gansseri Zone.

On the basis of both calcareous nannofossil and planktonic foraminiferal data, we conclude that the Endikurgan section spans the interval from the mid Campanian to the lower Maastrichtian for a duration of about 10 m.y., and that sedimentation in this interval appears to be continuous.

ENVIRONMENT

The white chalk sedimentation indicates an open shelf environment under the wave base. The abundance of small-sized foraminifers with heterohelicids in the lower part indicates an area influenced strongly by upwelling. The frequency of short-duration gaps with short lateral extent and with cherty horizons, especially in the Maastrichtian part (NATDIN *et al.*, 1984), suggests that the bottom was extensively swept by currents.

CONCLUSION

Time available for field work was too short to produce a complete picture of the Mesozoic stratigraphy of the Gorny Mangyshlak. Our conclusions are innovative in the following points.

Source : MNHN, Paris

TRIASSIC

— The main features in a sequential scheme are reported in Fig. 13.

— The Tyururpa Group was extensively sampled, which resulted in the first finding of conodonts and foraminifers. In particular, the Dorikranites Beds may be assigned to the early Spathian on the basis of conodonts.

— Palynomorphs at the base of the Akmysh Formation may delimit the age of this unit to the Carnian. Consequently, the regional paraconformity at its base is positioned around the Ladinian/Carnian boundary.

— Most important is the palaeogeographic problem posed by the petrographic analysis of the Triassic sandstones of Mangyshlak. They consist of volcanic detritus, possibly derived from an active magmatic arc related to the northward subduction of the Palaeo-Tethys (SENGÖR *et al.*, 1988; BAUD *et al.*, 1991; DERCOURT *et al.*, 1993). Their petrographic signature and time trends, peculiar when compared to typical arc-derived suites, broadly compare with volcaniclastics found in modern strike-slip settings and with other Triassic clastic wedges also related to final consumption of the Palaeo-Tethys (e.g., GARZANTI, 1985). Alternatively, detrital modes may indicate erosion of an arc orogen and deposition in a retroarc foreland basin (MCBRIDE *et al.*, 1975; DICKINSON, 1985) or even provenance from a relict Palaeozoic arc terrane and accumulation in a "Chinese-type" collisional successor basin (GRAHAM *et al.*, 1993) (Fig. 13). Climate was probably semiarid with a humid season (e.g. HENDRIX *et al.*, 1992; GARZANTI *et al.*, 1995; MUTTI & WEISSERT, 1995), and became progressively subhumid in the Late Triassic, when coal was deposited in nearby areas (RUTTNER *et al.*, 1991; ZHIDOVINOV, 1994).

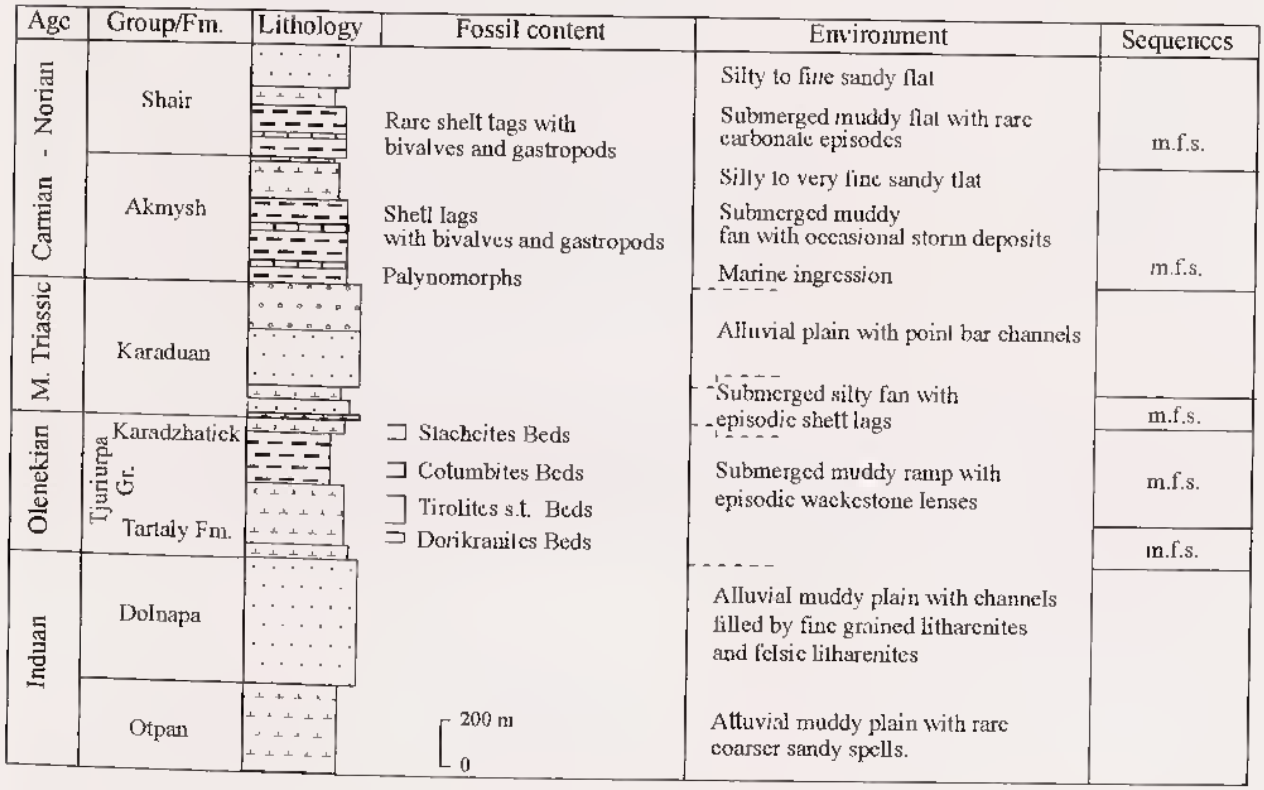

FIG. 13.— Main features of the Triassic formations in Karatauchik and West Karatau of Gorny Mangyshlak.

FIG. 13.— Principales caractéristiques des formations du Trias dans les coupes de Karatauchik et ouest Karatau, Gorny Mangyshlak.

Source : MNHN, Paris

JURASSIC

The analysis of the Jurassic succession brought to attention the need for a revision of its lower part, below the Callovian transgression. Sporomorphs and especially dinocysts indicate the possible presence of important pre-Callovian gaps and a very detailed analysis is needed to have a more accurate picture of the mostly continental to marginal successions of the Middle Jurassic.

CRETACEOUS

Results are sparse. The age refinement in the Lower Cretaceous was limited, because of the poor or mostly absent calcareous nannofossils. Additional data on the *Semenoviceras* horizon are discussed by CECCA (1997).

The first findings of calcareous nannofossils and a list of planktonic foraminifers for the "chalk-like unit" in the Coniacian-Maastrichtian interval are presented. Sedimentation rate slightly increased in the mid Campanian-Maastrichtian part, compared to the basal part, where frequent condensations occurred, like the one described by MARCINOWSKI *et al.* (1996) for the Cenomanian-Turonian interval.

Also for this part, new and intriguing is the hypothesis about of the provenance of Middle Jurassic and Lower Cretaceous sandstones. Despite the limited number of sufficiently coarse arenites available for counting, the Middle Jurassic and Lower Cretaceous sandstones of Mangyshlak display an almost identical petrographic composition. Detritus largely derives from volcanic rocks, with significant contribution from plutonic, hypoabissal, metasedimentary and sedimentary rocks. Detrital modes plot between the "Recycled Orogen" and "Dissected Magmatic Arc" provenance fields (Fig. 13; DICKINSON & SUCZEK, 1979; DICKINSON, 1985), suggesting a collisional successor basin setting (GRAHAM *et al.*, 1993). The pronounced volcanic character of these siliciclastics is not a function of contemporaneous arc volcanism, but rather resulted from the erosion of relict arc assemblages of Paleozoic to Triassic age. Detritus was derived from an orogenic belt including arc volcanics and volcaniclastics, uplifted by the latest Triassic collision between the Iranian Block and the southern active margin of the Turan Block. Volcanic rock fragments are still abundant (particularly in finer-grained sandstones), but less homogeneous than in the Triassic succession, with the occurrence of mafic (basalts) to felsic (rhyolites, rhyodacites) grain types. Low quartz content and the scarcity of sedimentary rock fragments indicate that most detritus was not derived from a thin-skinned foreland fold-thrust belt involving a thick passive margin sedimentary succession. Rather, occurrence of radiolarian chert and a few greenschist to chloritoschist lithics suggests contributions from Eo-Cimmerian to Neo-Cimmerian suture belts, as for the roughly coeval siliciclastics found in central Asia (GAETANI *et al.*, 1993). Granitoid detritus, as well as abundance of feldspar grains and low P/F ratio, document the erosion of basement rocks at the core of the orogen soon after the Eo-Cimmerian collision (GARZANTI *et al.*, 1996).

The overall conclusion concerning the petrographic analysis is that changes in detrital mineralogy are minor throughout the Mesozoic (Fig. 14). In particular, composition of Middle Jurassic and Lower Cretaceous units is virtually identical, indicating that if the Eo-Cimmerian orogenic event was surely significant, the Neo-Cimmerian collision probably simply rejuvenated sources of detritus already active in the Jurassic.

We may summarize the sedimentary and geodynamic evolution of the Mangyshlak in the following scheme (Table 6).

Source : MNHN, Paris

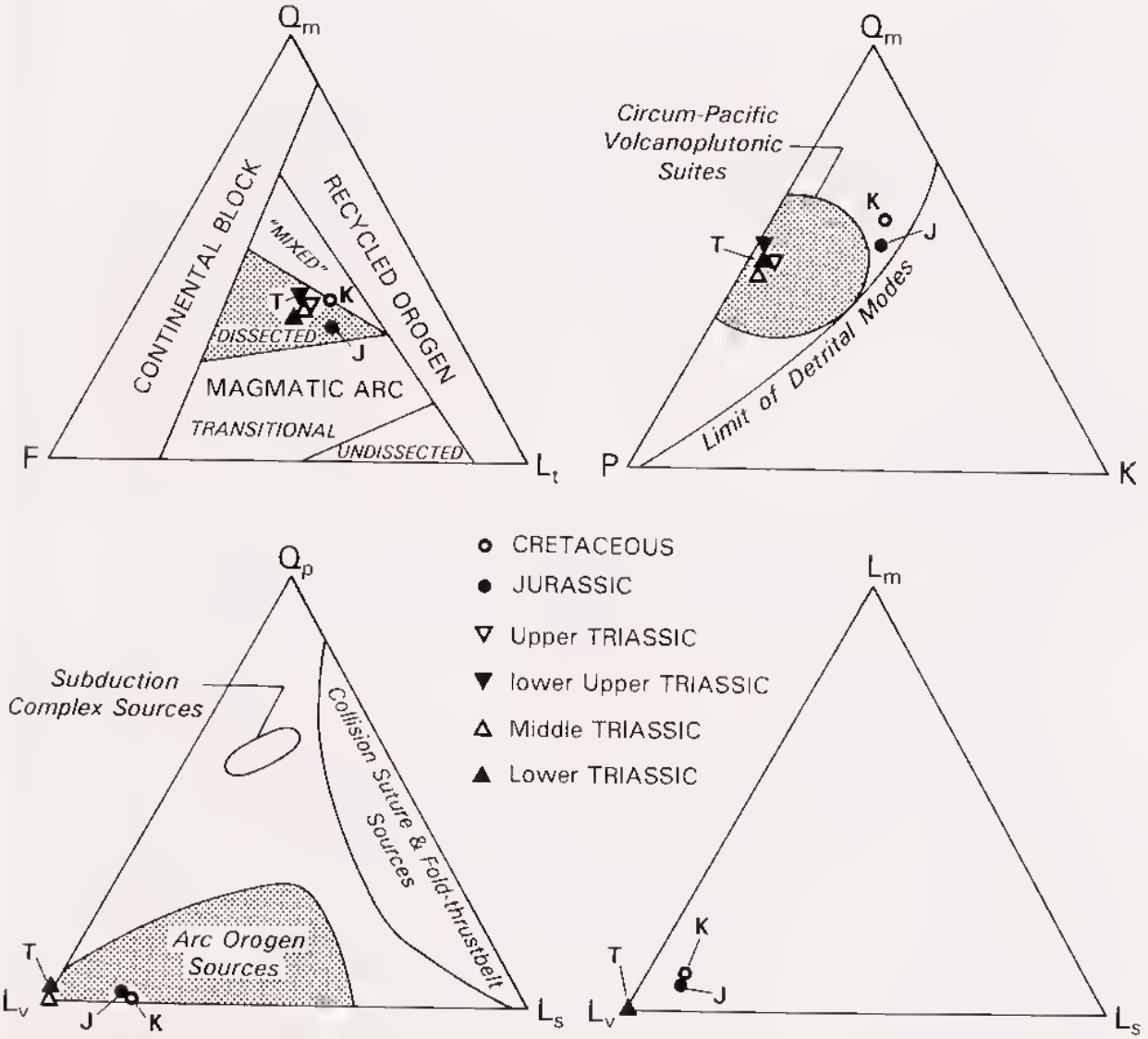

FIG. 14.— The Mesozoic sandstones of Mangyshlak are all dominated by volcaniclastic detritus, and they are virtually indistinguishable from Circum-Pacific volcanoplutonic suites with standard plots. A collisional successor basin origin is nevertheless indicated, at least for Jurassic and Cretaceous units (see text for discussion). T= Triassic (Lower Triassic samples include the Otpan, Dolnapa and Tyurupa Formations: Middle, lower Upper and Upper Triassic samples correspond with the Karaduan, Akmysh and Shair Formations respectively); J= Jurassic; K= Cretaceous. Q = quartz (Qm: monocrystalline; Qp: polycrystalline); F: feldspars (P: plagioclase; K: alkali feldspars, including chessboard albite); L: "aphanite" lithic grains (Lm: metamorphic; Lv: volcanic; Ls: sedimentary). Provenance fields after DICKINSON (1985).

FIG. 14.— Les grès mésozoïques du Mangyshlak sont tous dominés par des détritiques volcaniques et ne sont virtuellement pas différenciables des suites volcanoplutoniques circum-pacifiques avec des reports standards. Une origine de bassin en collision est néanmoins indiquée, au moins pour les unités du Jurassique et du Crétacé (voir texte pour la discussion). T : Trias (les échantillons du Trias inférieur incluent les formations de Otpan, Dolnapa et Tyurupa ; Trias moyen, Trias supérieur basal et Trias supérieur correspondent aux formations de Karaduan, Akmysh et Shair respectivement) ; J : Jurassique ; K : Crétacé ; Q : quartz (Qm : monocristallin ; Qp : polycristallin) ; F : feldspaths (P : plagioclase ; K : feldspath alcalins, incluant l'albite en échiquier) ; L : fragments de roches aphanitiques. (Lm : métamorphique ; Lv : volcanique ; Ls : sédimentaire). Zones de provenance d'après DICKINSON (1985).

Source : MNHN, Paris

TABLE 6.— Sedimentary and geodynamic evolution of the Mangyshlak.
TABLEAU 6.— Évolution sédimentaire et géodynamique du Mangyshlak.

AGES	ENVIRONMENT	GEODYNAMIC SETTING
Palaeocene - Coniacian	Outer shelf mostly feeded by planktonic rain	Stable continental shelf with low subsidence rate
Turonian - Aptian	Muddy outer submarine fan, with sandy spells and phosphatic condensation horizons	Continental shelf with fairly large fine terrigenous input and high subsidence, decreasing upwards
		Regional unconformity. End of the Neo-Cimmerian movements
Barremian - Berriasian	Shallow water terrigenous sequences with glauconitic horizons, ending with regional emersion in the Barremian	Continental shelf with low subsidence rate. Gentle epirogenic movements
		Regional unconformity linked to the Neo-Cimmerian events
Oxfordian - Callovian	Muddy outer shelf with non depositional surfaces, enriched in iron	Gentle sea-level rise in a low subsidence regime
Bathonian - Aalenian	Coastal plains and marshes with coal seams, locally ingressed by marginal sea	Low subsidence rates
		Major regional unconformity. Folding due to the propagation of the Eo-Cimmerian events. Evolute pedogenesis
Norian - Carnian	Terrigenous internal shelf with restricted ponds. Shelly tempestitic lags	Partially submerged fan in a back-arc basin setting.
		Regional paraconformity
Middle Triassic-Olenekian	Marine to alluvial volcaniclastic fan with several sequences. Deepest water in the Olenekian	Back-arc basin setting
Induan	Alluvial volcaniclastic fan	Back-arc basin setting
	? Upper Permian deposits ?	

Source : MNHN, Paris

ACKNOWLEDGMENTS

The authors are indebted for field help and assistance to N. LYBERIS and J.T. POLI (Paris), H. YOUSUFOKAEV, V.I. TROITSKY and Y. ZAHID (Tashkent). M. BALINI and V.A. GAVRILOVA worked out the Triassic ammonoids, V. J. VUKS the Triassic and Jurassic foraminifers, E. GARZANTI the sandstone petrography, A. NICORA the conodonts, E. ERBA the nannoplankton, E. CARIOU the Jurassic ammonites, F. CECCA the Cretaceous ammonites, I. PREMOLI SILVA and M. R. PETRIZZO the Cretaceous foraminifers, S. CIRILLI the palynomorphs and R. BUCEFALO PALLIANI the dinocysts. M. GAETANI assembled all these data and prepared the final version of the paper. Financial support by the Peri-Tethys Program and by the Italian CNR, grant No. 95/00390/05 to M. GAETANI.

REFERENCES

ANONYMOUS, 1973.— Stratigraphy of the USSR. *In*: L.D. KIPARISOVA, G.P. RADCHENKO & V.P. GORSKY (eds), *Triassic System, Scythian-Turanian Plate, Gorny Mangyshlak*. Nedra, Moscow: 186-207 (in Russian).

ASTAKHOVA, T.V., 1960.— Triassic system. New data on the Triassic stratigraphy of Mangyshlak. *Transactions All Union Scientific Research Geological Prospecting Oil Institute*, **29**: 146-163 (in Russian).

ASTAKHOVA, T.V., 1964.— New ammonites from the *Doricranites* horizons of Mangyshlak. *Dopovidi Akademia Nauk Ukrain. RSR*, **3**: 378-382 (in Russian).

AZBEL, A.YA., 1979.— About foraminiferal assemblages of the Upper Jurassic of Mangyshlak. *Voprosy Micropaleontologii*, **22**: 64-73.

AZBEL, A.YA. & HOFFMAN, E.A., 1982.— Mangyshlak. *In*: A.A. GRIGELIS (ed.), *Upper Jurassic Biostratigraphy of the USSR according to Foraminifera*. Vilnius, Mokslas: 61-68.

BAJARUNAS, M.V., 1936.— The age of the strata containing *Doricranites*. *Izvestiya Akademiy Nauk SSSR, Seriya Geologicheskaya*, **4**: 539-548 (in Russian).

BAUD, A. & STAMPFLI, G., 1989.— Tectonogenesis and evolution of a segment of the Cimmerides: the volcano-sedimentary Triassic of Aghdarband (Kopet-Dagh, north-east Iran). *In*: A.M.C. SENGÖR (ed.), *Tectonic Evolution of the Tethyan Region*. Kluwer, Deventer: 265-275.

BAUD, A., STAMPFLI, G. & STEEN, D., 1991.— The Triassic Aghdarband Group: volcanism and geological evolution. *In*: A.W. RUTTNER (ed.), The Triassic of Aghdarband (AqDarband), NE-Iran, and its pre-Triassic frame. *Abhandlungen Geologisches Bundesanstalt*, **38**: 125-137.

BRUGMAN, W. A., 1986.— Late Scythian and Middle Triassic palynostratigraphy in the Alpine realm. *Albertiana*, **5**: 19-20.

BUCEFALO-PALLIANI, R. & RIDING, J., in press.— The palynology of the Toarcian-Aalenian transition in the Wittnau borchole (Obemhein, Southwest Germany). *Newes Jahrbuch für Geologie und Paläontologie*.

CAMERON, K.L. & BLATT, H., 1971.— Durabilities of sand size schist and "volcanic" rock fragments during fluvial transport, Elk Creek, Black Hills, South Dakota. *Journal of Sedimentary Petrology*, **41**: 565-576.

CARON, M., 1985.— Cretaceous planktic foraminifera. *In*: H.M. BOLLI, J.B. SAUNDERS & K. PERCH-NIELSEN (eds), *Plankton Stratigraphy*. Cambridge University Press, Cambridge Earth-Sciences Series, Cambridge: 17-86.

CARROLL, A.R., GRAHAM, S.A., HENDRIX, M.S., YING, D. & ZHOU, D., 1995.— Late Paleozoic tectonic amalgamation of northwestern China: sedimentary record of the northern Tarim, northwestern Turpan, and southern Junggar Basins. *Geological Society of America Bulletin*, **107**: 571-594.

CECCA, F., 1997.— The Late Albian ammonoids from the Semenoviceras litschovi Zone from Mangyshlak (West Kazakhstan). *Rivista Italiana di Paleontologia Stratigrafia*, **103**: 323-342, 4 pl.

DAGYS, A. S., 1974.— *Triassic Brachiopods*. Nedra, Novosibisrk: 1-233 (in Russian).

DAVIES, D.K., VESSEL, R.K., MILES, R.C., FOLEY, M.G. & BONIS, S.B., 1979.— Fluvial transport and downstream sediment modification in an active volcanic region. *In*: A. MIALL (ed.), Fluvial sedimentology. *Memoirs of the Canadian Society of Petroleum Geologists*, **5**: 61-83.

DERCOURT, J., RICOU, L.E. & VRIELYNCK, B., 1993.— *Atlas Tethys Palaeoenvironmental Maps*. Gauthier-Villars, Paris: 1-309.

DICK, H.J.B. & BULLEN, T., 1984.— Chromian spinel as a petrogenetic indicator in abyssal and alpine-type peridotites and spatially associated lavas. *Contributions to Mineralogy and Petrology*, **86**: 54-76.

DICKINSON, W.R., 1970.— Interpreting detrital modes of graywacke and arkose. *Journal of Sedimentary Petrology*, **40**: 695-707.

Source : MNHN, Paris

DICKINSON, W.R., 1985.— Interpreting provenance relations from detrital modes of sandstones. *In*: G.G. ZUFFA (ed.), Provenance of arenites. *Reidel Publishing Company, Nato ASI Series, Dordrecht*, **148**: 333-361.

DICKINSON, W.R. & SUCZEK, C.A., 1979.— Plate tectonics and sandstone composition. *AAPG Bulletin*, **63**: 2164-2172.

DOBRUSHKINA, I.A., 1982.— Triassic floras of Eurasia. *Transactions Geological Institute, Academy of Sciences USSR*, **365**: 1-196 (in Russian).

EFIMOVA, N.A., 1991.— Triassic System. *In*: A.J. AZBEL & A.A. GRIGELIS(eds), *Practical manual on Microfauna of the USSR*, Vol. 5: *Mesozoic Foraminifers*. Nedra, Leningrad: 16-25 (in Russian).

ERBA, E., PREMOLI SILVA, I., WILSON, P.A., PRINCLE, M.S., SLITER, W.V., WATKINS, D.K., ARNAUD-VANNEAU, A., BRALOWER, T.I., BUDD, A.F., CAMOIN, G.F., MASSE, J.-P., MUTTERLOSE, J. & SAGER, W.V., 1995.— Synthesis of stratigraphies from shallow-water sequences at Sites 871 through 879 in the Western Pacific Ocean (Leg 144). *In*: J.A. HAGGERTY, I. PREMOLI-SILVA, F. RACK & M.K. MCNUTT (eds), *Proceedings Ocean Drilling Program, Scientific Results*, **144**. Ocean Drilling Program, College Station, Texas: 873-885.

FEINBERG, H., GUREVITCH, E.L., WESTPHAL, M., POZZI, J-P. & KHRAMOV, A.N., 1996.— Paleomagnetism of a Permian/Triassic sequence in Mangislak (Kazakhstan, CIS). *Comptes Rendus de l'Académie des Sciences, Paris*, **322**, IIa: 617-623.

FILATOFF, J., 1975.— Jurassic palynology of the Perth Basin, Western Australia. *Palaeontographica*, Abt. B, **154**: 1-113.

FISHER, M.J. 1979.— The Triassic palynofloral succession in the Canadian Arctic Archipelago. *American Association Stratigraphy Palynology, Contributions Series*, **5B**: 83-100.

FISHER, M.J. & DUNAY, R.E., 1984.— Palynology of the petrified forest member of the Chinle formation (Upper Triassic), Arizona, U.S.A. *Pollen et Spores*, **25 (2)**: 241-284.

GAETANI, M., JADOUL, F., ERBA, E. & GARZANTI, E., 1993.— Jurassic and Cretaceous orogenic events in the North Karakorum: age constraints from sedimentary rocks. *In*: P.J. TRELOAR & M.P. SEARLE (eds). Himalayan tectonics. *Special Publications- Geological Society of London*, **74**: 39-52.

GARZANTI, E., 1985.— The sandstone memory of the evolution of a Triassic volcanic arc in the Southern Alps, Italy. *Sedimentology*, **32**: 423-433.

GARZANTI, E., 1986.— Source rocks versus sedimentary control on the mineralogy of deltaic volcanic arenites (Upper Triassic, Northern Italy). *Journal of Sedimentary Petrology*, **56**: 267-275.

GARZANTI, E., CRITELLI, S. & INGERSOLL, R.V., 1996.— Paleogeographic and paleotectonic evolution of the Himalayan Range as reflected by detrital modes of Tertiary sandstones and modern sands (Indus transect, India and Pakistan). *Geological Society of America Bulletin*, **108**: 631-642.

GARZANTI, E., GNACCOLINI, M. & JADOUL, F., 1995.— Anatomy of a semiarid coastal system: the Upper Carnian of Lombardy. *Rivista Italiana di Paleontologia Stratigrafia*, **101**: 17-36.

GAVRILOVA, V.A., 1989.— On some Dimaritidae (Ammonoidea) from Mangyshlak. *Annual of the All-Union Paleontological Society*, **32**: 162-179, 2 pl. (in Russian).

GAVRILOVA, V.A., 1992.— Lower Triassic biostratigraphy of Mangyshlak by bivalve molluscs. *Izvestiya Akademiy Nauk SSSR, Seriya Geologicheskaya*: 151-157 (in Russian).

GAVRILOVA, V.A., 1995.— On some Early Triassic Pectinacea (Bivalvia) from Eastern Precaucasus and Mangyshlak. *Bulletin Moskovskovo Obsh. Ispyitatelei Prirodyi Otdeleunyi Geologiy*, **70/5**: 83-97 (in Russian).

GAVRILOVA, V.A. & KURUSHIN, N.I., 1986.— Early Triassic Bivalves from Mangyshlak. *Annual of the All-Union Paleontological Society*, **29**: 124-138 (in Russian).

GERGEN, L.D. & INGERSOLL, R.V., 1986.— Petrology and provenance of Deep Sea Drilling Project sand and sandstone from the North Pacific Ocean and the Bering Sea. *Sedimentary Geology*, **51**: 29-56.

GRAHAM, S.A., HENDRIX, M.S., WANG, L.B. & CARROLL, A.R., 1993.— Collisional successor basins of western China: impact of tectonic inheritance on sand composition. *Geological Society of America Bulletin*, **105**: 323:344.

GUY, D.J.E., 1971.— Palynological investigations in the Middle Jurassic of St. Wilhelmsfjäll boring, southern Sweden. *Publications Institutes of Mineralogy, Palaeontology and Quaternary Geology, Lund University*, **168**: 1-104.

GUY-OHLSON, D., 1989.— Spore and Pollen assemblage zonation of Swedish Bajocian and Bathonian sediments. *In*: D.J. BATTEN & M.C. KEEN (eds), *Northwest European Micropalaeontology and Palynology* Halstead Press, Chichester: 70-91.

HENDRIX, M.S., GRAHAM, S.A., AMORY, J.Y. & BADARCH, G., 1996.— Noyon Uul syncline, southern Mongolia: lower Mesozoic sedimentary record of the tectonic amalgamation of central Asia. *Geological Society of America Bulletin*, **108**: 1256-1274.

HENDRIX, M.S., GRAHAM, S.A., CARROLL, A.R., SOBEL, E.R., MCKNIGHT, C.L., SCHULEIN, B.J. & WANG, Z., 1992.— Sedimentary record and climatic implications of recurrent deformation in the Tian Shan: evidence from Mesozoic strata of the north Tarim, south Junggar, and Turpan basins, northwest China. *Geological Society of America Bulletin*, **104**: 53-79.

HERNGREEN, G.F.W. & DE BOER, K.F., 1974.— Palynology of Rhaetian, Liassic and Dogger strata in the eastern Netherlands. *Geologie en Mijnbouw*, **53**: 343-368.

HISADA, K. & ARAI, S., 1993.— Detrital chrome spinels in the Cretaceous Sanchu sandstone, central Japan: indicator of serpentinite protrusion into a fore-arc region. *Palaeogeography, Palaeoclimatology, Palaeoecology*, **105**: 95-109.

HOCHULI, P.A., COLIN, J.P. & VIGRAN, J.O., 1989.— Triassic biostratigraphy of the Barents Sea Area. *In*: J.D. COLLINSON (ed.), *Correlation in Hydrocarbon Exploration*. Graham & Trotman, London: 131-153.

Source : MNHN, Paris

HOELSTAD, T., 1985.— Palynology of the uppermost Lower to Middle Jurassic strata on Bornholm, Denmark. *Bulletin of the Geological Society of Denmark*, **34**: 111-132.

ILYINA, V. I., KUL'KOVA, I. A. & LEBEDEVAN, K., 1994.— Microphytofossils and detail *(sic)* stratigraphy of marine Mesozoic and Cenozoic of Siberia. *United Institute of Geology, Geophysics and Mineralogy Transaction*, **818**: 1-192 (in Russian).

INTERDEPARTIMENTAL STRATIGRAPHIC COMMITTEE, 1977.— *Interdepartimental scheme for the Mesozoic of Central Asia (Samarkand 1977)*. VSEGEI, Leningrad: 1-47 (in Russian).

KIRICHKOVA, A.I. & DOLYDENKO, M.P., 1996.— New data on the phytostratigraphy of the Jurassic of Kazakhstan. *Stratigraphy and Geological Correlations*. **4/5**: 35-52 (in Russian).

KIRICHKOVA, A.I., TIMOSHKINA, N.A. & MENSCHIKOVA, N.J., 1989.— Phytostratigraphy of the Jurassic stages in Mangyshlak. *Soviet Geology*, **1989/2**: 73-82 (in Russian).

KITTL, E., 1903.— Die Cephalopoden der Oberen Werfener Schichten von Muc in Dalmatien. *Abhandlungen Geologisches, Reichsanstalt*, **20**: 1-77, 11 pl.

KOPAEVICH, L.F., 1989.— Paleodepth determination on the base of analyses of planktonic foraminifera assemblages (according to materials from Upper Cretaceous of Transcaspian). *Vestnik Moskovskogo Gusudarstogo Universitety, Seryia Geologicheskaya*, **3**: 25-34.

KUMMEL, B., 1969.— Ammonoids of the Late Scythian. *Harvard Museum Comparative Zoology Bulletin*, **137/3**: 311-701, 71 pl.

LIPATOVA, V.V., 1984.— Draft of the Stratigraphic schemes for Triassic deposits of Mangyshlak and Ustyurt. *In*: *Stratigraphy and Paleontology of Triassic Deposits in Mangyshlak and Ustyurt, Collection of Papers*. VNIGNI, Moscow: 33-56 (in Russian).

LOZOWSKY, V.P., 1974.— Stratigraphy of Lower and Middle Triassic Deposits of Gornyi Mangyshlak. *Geology and Prospecting*, **1974/8**: 12-22 (in Russian).

LOZOWSKY, V.P., DOBRUSKINA, I.A., VINOGRADOVA, K.V., MIKHAILENKO, O.I. & IVANSHIN B.F., 1986.— Are there Upper Permian Deposits in Gorny Mangyshlak? *Izvestiya Vuzov, Geologiya i Razvedka*, **9**: 92-95 (in Russian).

LUND, J. J. & PEDERSEN, K.J., 1985.— Palynology of the marine Jurassic formations in the Vardeklift ravine, Jameson Land, East Greenland. *Bulletin of the Geological Society of Denmark*, **33**: 371-399.

LUPPOV, N.P., BOGDANOVA, T.N., LOBACHEVA, S.V., AKOPYAN, V.T., DZHALILOV, M.R., KOROTKOV, V.A., MYATLYUK, E.V. & PORETSKAYA, E.S., 1988.— *Berriasian of Mangyshlak*. Nauka, Leningrad: 1-204 (in Russian).

MARCINOWSKI, R., WALASZCZYK, I. & OLSZEWSKA-NEJBERT, D., 1996.— Stratigraphy and regional development of the mid-Cretaceous (Upper Albian through Coniacian) of the Mangyshlak Mountains, Western Kazakhstan. *Acta Geologica Polonica*, **46** (1-2): 1-60.

MARSAGLIA, K.M. & INGERSOLL, R.V., 1992.— Compositional trends in arc-related, deep-marine sand and sandstone: a reassessment of magmatic-arc provenance. *Geological Society of America Bulletin*, **104**: 1637-1649.

MATHISEN, M.E., 1984.— Diagenesis of Plio-Pleistocene nonmarine sandstones, Cagayan Basin, Philippines: early development of secondary porosity in volcanic sandstones. *In*: D.A. MCDONALD & R.C. SURDAM (eds), Clastic diagenesis. *American Association of Petroleum Geologists Memoir*, **37**: 177-193.

MCBRIDE, E.F., WEIDIE, A.E. & WOLLEBEN, J.A., 1975.— Deltaic and associated deposits of Difunta Group (Late Cretaceous to Paleocene), Parras and La Popa Basins, northeastern Mexico. *In*: M.L. BROUSSARD (ed.), *Deltas, Models for Exploration*. Houston Geological Society, Houston: 485-522.

MUROMCHEV, V.S., 1968.— The geological structure and the naftogenic potential of Mangyshlak. *Trudy VNIGRI*, n.s. **265**: 1-161 (in Russian).

MUTTI, M. & WEISSERT, H., 1995.— Triassic monsoonal climate and its signature in Ladinian-Carnian carbonate platforms (Southern Alps, Italy). *Journal of Sedimentary Research*, **B65**: 357-367.

NAIDIN, D.P., BENIAMOVSKY, V.N. & KOPAEVICH, L.F., 1984.— *Methods of Transgression and Regressions Study Exemplified by Late Cretaceous Basins of West Kazakhstan*. Moscow University Press, Moscow: 1-162 (in Russian).

NEDERBRAGT, A.J., 1990.— *Biostratigraphy and Paleoceanographic Potential of the Cretaceous Planktic Foraminifera Heterohelicidae*. Ph. D. Dissertation, Vrije Universiteit te Amsterdam, Amsterdam, Netherlands: 1-203.

NORRIS, M.S. & HALLAM, A., 1995.— Facies variation across the Middle-Upper Jurassic boundary in Western Europe and relationships to sea-level changes. *Palaeogeography, Palaeoclimatology, Palaeoecology*, **166**: 189-245.

ORCHARD, M., 1995.— Taxonomy and correlation of Lower Triassic (Spathian: segminate conodonts from Oman and revision of some species of *Neospathodus*) *Journal of Paleontology*, **69**: 110-122.

PACKER, B.M. & INGERSOLL, R.V., 1986.— Provenance and petrology of Deep Sea Drilling Project sands and sandstones from the Japan and Mariana forearc and backarc regions. *Sedimentary Geology, Amsterdam*, **51**: 5-28.

REPIN, Y.S. & RASHWAN, N., 1996.— Chronology and biochores of Callovian Ammonites from Mangyshlak. *Stratigraphy and Geological Correlations*, **4/5**: 53-66 (in Russian). English transl.: 467-479.

RIDING, J.B., 1984.— A palynological investigation of Toarcian and early Aalenian strata from the Blea Wyke area, Ravenscar, North Yorkshire. *Proceedings of the Yorkshire Geological Society*, **46/3**: 231-266.

RIDING, J.B. & THOMAS, J.E., 1992.— Dinoflagellate cysts of the Jurassic System. *In*: A.J. POWELL (ed.), A stratigraphic index of dinoflagellate cysts. *British Micropalaeontology Society Publication Series*: 7-97.

Source : MNHN, Paris

SCHUURMAN, W.M.L., 1977.— Aspects of Late Triassic palynology. 2: Palynology of the "Grès et Schiste à Avicula contorta" and "Argiles de Levallois" (Rhaetian) of north-eastern France and southern Luxemburg. *Review of Palaeobotany and Palynology*, **23**: 159-253.

SCHUURMAN, W.M.L., 1979.— Aspects of Late Triassic palynology. 3: Palynology of latest Triassic and earliest Jurassic deposits of the Northern Limestone Alps in Austria and southern Germany, with special reference to a palynological classification of the Rhaetian Stage in Europe. *Review of Palaeobotany and Palynology*, **27**: 33-75.

SELF, R.P., 1975.— Petrologic changes in fluvial sediments in the Rio Naulla drainage basin, Veracruz, Mexico. *Journal of Sedimentary Petrology*, **45**: 140-149.

SENGÖR, A.M.C., ALTINER, D., CIN, A., USTAEMER, T. & HSU K.J., 1988.— Origin and assembly of the Tethyside orogenic collage at the expense of Gondwana Land. *In*: M.G. AUDLEY-CHARLES & A. HALLAM (eds), Gondwana and Tethys. *Special Publications- Geological Society of America*, **37**: 119-181.

SHEVYREV, A.A., 1968.— Triassic ammonoids of southern USSR. *Transactions of Paleontological Institute, Academy of Sciences USSR*, **119**: 1-272. 21 pl (in Russian).

SHEVYREV, A.A., 1990.— *Ammonoids and Chronostratigraphy of the Triassic*. Nauka Leningrad: 1-179, 8 pl.

SHLEZINGER, A.YE., 1965.— Structural setting and description of the Mangyshlak dislocations. *Transactions of Geological Institute. Academy of Sciences USSR*, **132** (in Russian).

SILBERLING, N.J. & WALLACE, R.E, 1969.— Stratigraphy of the Star Peak Group (Triassic) and overlying rocks, Humboldt Range, Nevada. *US Geological Survey, Professional Papers*, **592**: 1-50.

SISSINGH, W., 1977.— Biostratigraphy of Cretaceous calcareous nannoplankton. *Geologie en Mijnbouw*, **56**: 37-65.

TIMOSHKINA, N.A. & MENSHIKOVA, N.J., 1985.— New data on the palynostratigraphy of the Jurassic stages in Mangyshlak. *Soviet Geology*, **1984/4**: 71-80 (in Russian).

TITOV, B.I., GAVRILOVA, V.A. & VINOGRADOVA, K.V., 1985.— On the significance of ammonoids for the study of the naflogenic Lower Triassic of the Southern Mangyshlak. *Annual of the All-Union Paleontological Society*, **26**: 70-77 (in Russian).

TOZER, E.T., 1972.—Triassic Ammonoids and Daonella from the Nakhlak Group, Anarak Region, Central Iran. *Geological Survey Iran*, **28**: 29-39, 10 pl.

TRALAU, H., 1968.— Botanical investigation into the fossil flora of Erikdal in Fyledalen, Scania. *Palaeobotanist, Abteilung B*, **62**: 195.

VAN DER EEM, J.G.L.A., 1983.— Aspects of Middle and Late Triassic palynology. 6: Palynological investigations in the Ladinian and lower Karnian of the western Dolomites, Italy. *Review of Palaeobotany and Palynology*, **39**: 189-300, 10 pl.

VINYUKOV, V.N., 1966.— On the presence of the Induan stage in the stratigraphical section of Mangyshlak. *Oil and Gas Geology*, **9**: 45-47 (in Russian).

VISSCHER, H. & BRUGMAN, W.A., 1981.— Ranges of selected palynomorphs in the Alpine Triassic of Europe. *Review of Palaeobotany and Palynology*, **34**: 115-128.

VISSCHER, H. & BRUGMAN, W.A., 1986.— The Permian and Triassic boundary in the Southern Alps: a palynological approach. *Memorie della Società Geologica Italiana*, **34**: 121-128, 3 pl.

VISSCHER, H. & KRYSTYN, L., 1978.— Aspects of Late Triassic palynology. 4: A palynological assemblage from ammonoid-controlled Late Karnian (Tuvalian) sediments of Sicily. *Review of Palaeobotany and Palynology*, **26**: 93-112.

VISSCHER, H., SCHUURMAN, W.M.L. & VAN ERVE, A.W., 1980.— *Aspects of a Palynological Characterization of Late Triassic and Early Jurassic "Standard" Units of Chronostratigraphical Classification in Europe: IV International Palynological Conference, Lucknow, 1976-1977*. Vol. 2. Birbal Sahni Institute. Lucknow: 281-287.

VOLKHEIMER, W. & QUATTROCCHIO, M. E., 1981.— Distribucion estratigrafica de los palinomorfos jurasicos y cretacicos en la faja andina y areas adjacentes de America del sur Austral con especial consideracion de la Cuenca Neuquina. *Cuencas sedimentarias del Jurasico y Cretacico de America del Sur*, **2**: 407-444.

VOLOZH, YU.A., ANTIPOV, M.P., LIPATOVA V.V., VOZNESENSKY, A.I., POLIANSKY, B.V. & SHLEZINGER, A.YE., submitted.— The seismostratigraphy of the Scythian and South-west Turanian Plates. *Geodiversitas*.

WARRINGTON, G., 1996.— Triassic spores and pollens. *In*: J. JANSONIUS & D.C. MCGREGOR (eds), Palynology: principles and applications. *American Association Stratigraphy Palynology Foundation*, **2**: 755-766.

ZHIDOVINOV, S.N., 1994.— Paleogeography and conditions of Triassic formations in the territory of the Pricaspian Region. *Stratigraphy and Geological Correlations*, **2/3**: 51-66 (in Russian).

Source : MNHN, Paris

Development and deformation of a Mesozoic basin adjacent to the Teisseyre-Tornquist Zone: The Holy Cross Mountains (Poland)

Juliette LAMARCHE [1], *Jolanta* SWIDROWSKA [2], *Françoise* BERGERAT [1], *Maciej* HAKENBERG [2], *Jean-Louis* MANSY [3], *Josef* WIECZOREK [4], *Ewa* STUPNICKA [5] & *Thierry* DUMONT [6]

[1] Département de Géotectonique, CNRS ESA 7072, Université Pierre et Marie Curie T25-26, E.1, case 129, 4 place Jussieu, F-75252 Paris Cedex 05, France

[2] Institute of Geological Sciences, Polish Academy of Sciences (PAN) Twarda 51/55, 00-818 Warszawa, Poland

[3] Laboratoire de sédimentologie et géodynamique, CNRS URA 719, Université Lille1 Cité Scientifique, F-59655 Villeneuve d'Ascq, France

[4] Geotermia Podhalanska, ul. Szmony 17a, 34500 Zakopane, Poland

[5] University of Warszawa, Department of Geology, Zwirki i Wigury 93, 02-089 Warszawa, Poland

[6] CNRS UPRES-A 5025, Université Joseph Fourier, rue Maurice Gignoux, F-38031 Grenoble Cedex, France

ABSTRACT

The NW-SE stricking Teisseyre-Tornquist Zone marks the contact between the Palaeozoic west European platform and the Precambrian east European craton. It developped during the Palaeozoic, and was repeatedly reactivated during the Mesozoic and Cenozoic times, under extensional (Polish Trough) and compressional (Polish Swell) tectonic regimes. The NW-SE trending Polish Swell is superimposed on the Teisseyre-Tornquist Zone. The Polish Swell crops out in the Holy Cross Mountains, where we investigated its structural evolution. From Late Permian to Late Cretaceous times, the tectonic regime was extensional, controlling the basin developement and synchronous filling. In the northern part of the Holy Cross Mountains, subsidence maps (Late Permian to Late Jurassic) retrace the extensional basin subsidence and emphasize the role of two main synsedimentary faults, the WNW-ESE trending Holy Cross fault, and the NW-SE trending Nowe Miasto-Ilza fault that parallels the Teisseyre Tornquist Zone. From Late Permian to Late Jurassic, the basin development occurred in three stages: a) Late Permian and Early Triassic, b) Early Jurassic, c) Late Jurassic. During the two first phases major activity along the basin bounding faults is recorded whith the main subsidence axis trending NW-SE. In this zone, a set of NW-SE trending faults gave

LAMARCHE, J., SWIDROWSKA, J., BERGERAT, F., HAKENBERG, M., MANSY, J. L., WIECZOREK, J., STUPNICKA, E. & DUMONT, T., 1998. — Development and deformation of a Mesozoic basin adjacent to the Teisseyre-Tornquist Zone: The Holy Cross Mountains (Poland). *In*: S. CRASQUIN-SOLEAU & E. BARRIER (eds), Peri-Tethys Memoir 4: epicratonic basins of Peri-Tethyan platforms, *Mém. Mus. natn. Hist. nat.*, **179** : 75-92, Paris ISBN : 2-85653-518-4.

Source : MNHN, Paris

rise to the development of horsts and grabens during the Middle and Late Triassic. Activity along the Holy Cross fault varies: important during the first stages, it decreases to become null during the Late Jurassic stage so that the subsidence appears homogenous. Sedimentary dykes, filled with Late Permian-Early Triassic sediments, suggest a N-S compressional and E-W extensional tectonic regime at that time. Laramide shortening (Latest Cretaceous and Palaeogene) gave rise to basin inversion. Palaeostress computation from fault data sets indicate NE-SW compression, perpendicular to the Teisseyre-Tornquist Zone. Micro-structures (conjugate strike-slip and reverse faults, stylolites, joints) are compatible with large-scale structures (uplifting of Holy Cross Mountains, NW-SE fold axes). Detailed structural analyses reveal a complex tectonic evolution. The folds are localised in a narrow zone along the SW border of the Holy Cross Mountains (NW-SE fold axes), attibuted to reactivation of Triassic NW-SE trending basement fault, and in the northwestern prolongation of the Holy Cross fault (Radomsko Elevation), where sinistral reactivation of the Holy Cross fault gave rise to the developpment of *en échelon* folds.

RÉSUMÉ

Mise en place et déformation d'un bassin sédimentaire adjacent à la Zone Teisseyre-Tornquist : les Montagnes Sainte Croix (Pologne).

La Zone Teisseyre-Tornquist, orientée NW-SE constitue le contact entre la plate-forme paléozoïque de l'Europe occidentale et la plate-forme précambrienne de l'Europe orientale. Initiée au Paléozoïque, elle fut réactivée au Mésozoïque et Cénozoïque, sous des régimes tectoniques extensif ("fossé polonais" ou *Polish Trough*) et compressif ("soulèvement polonais" ou *Polish Swell*). Le "soulèvement polonais" est superposé à la Zone Teisseyre-Tornquist et affleure dans les Montagnes Sainte Croix (*Holy Cross Mountains*) où nous avons réalisé une étude structurale sur le terrain. Le développement et le remplissage du bassin polonais résulte d'un régime tectonique extensif du Permien supérieur au Crétacé supérieur. Dans la partie nord des Montagnes Sainte Croix, des cartes de subsidence du Permien supérieur au Jurassique supérieur illustrent le développement du bassin, effectué en trois étapes : a) au Permien supérieur - Trias inférieur, b) au Jurassique inférieur et c) au Jurassique supérieur. Ces cartes révèlent l'activité synsédimentaire de deux failles: la faille Sainte Croix de direction WNW-ESE et la faille Nowe Miasto-Iiza de direction WNW-ESE, parallèle à la Zone Teisseyre-Tornquist. L'activité de la faille Sainte Croix est importante lors de la première étape puis décroît jusqu'à l'inactivité durant la troisième étape. Sur le terrain, les indicateurs de l'extension dans le bassin sont des filons sédimentaires à remplissage de Permien supérieur - Trias inférieur ouverts lors d'une extension E-W et compression N-S. Le bassin est ensuite inversé lors d'un racourcissement NE-SW déterminé par les calculs de paléo-contraintes, et d'âge laramien (Crétacé supérieur - Paléogène). Cette direction NE-SW indiquée par les micro-structures (failles inverses et décrochantes, stylolithes, joints) mesurées dans les roches mésozoïques, est cohérente avec les déformations à grande échelle du bassin (failles inverses et plis NW-SE). L'étude structurale de détail montre que les micro-structures sont antérieures au plissement à grande échelle. Dans la couverture mésozoïque, les plis sont localisés. Dans une zone étroite orientée NW-SE sur la bordure sud des Montagnes Sainte Croix, les plis d'axes NW-SE sont attribués à la réactivation d'une faille d'âge triasique dans le substratum paléozoïque. Dans le prolongement NW des Montagnes Sainte Croix (élévation de Radomsko), des plis en échelon, dans la couverture mésozoïque, sont attribués à la réactivation senestre de la faille Sainte Croix dans le substratum paléozoïque.

OVERVIEW

The Teisseyre-Tornquist Zone (TTZ) makes the boundary between the Precambrian east European platform (Russian Platform on Fig. 1) and the Phanerozoic west European platform which was affected by the Caledonian, Variscan and Alpine (Alps, Carpathians on Fig. 1) orogens. The Moho discontinuity is located at about 43-45 km below the east European Platform, deepens to 50-55 km below the TTZ and shallows to 30-35 km under the west European platform (GUTERCH *et al.*, 1986). The TTZ trends NW-SE, and extends from the Baltic Sea in the North (Poland) to the Black Sea in the South (Dobrogea in Romania) (Fig. 1). In its central part (Ukraine), the TTZ is concealed beneath the Carpathian nappes. The TTZ is revealed in Dobrogea, where Palaeozoic and Mesozoic rocks crop out. There, the Peceneaga-Camena fault is the main element of the TTZ, reactivated as a reverse fault during the Palaeogene (HIPPOLYTE *et al.*, 1996). In Poland, the TTZ is covered by the Late Permian - Mesozoic Polish sedimentary basin ("Polish Trough") which was inverted during the Palaeocene and now forms the so called "Polish Swell". This structure crops out in the Holy Cross Mountains where a nearly complete sequence of Palaeozoic and Mesozoic strata is exposed (Fig. 2).

The Polish Trough developed during the Mesozoic times, superimposed to the TTZ. Therefore this crustal discontinuity appears to have controlled the location and development of the Polish Trough. Subsequently, Laramide compressional intraplate tectonics were responsible for the inversion of the basin. Our objective was to gain a better understanding of the effect of the TTZ and other major ancient structures on the development and deformation of the Polish Trough.

Source : MNHN, Paris

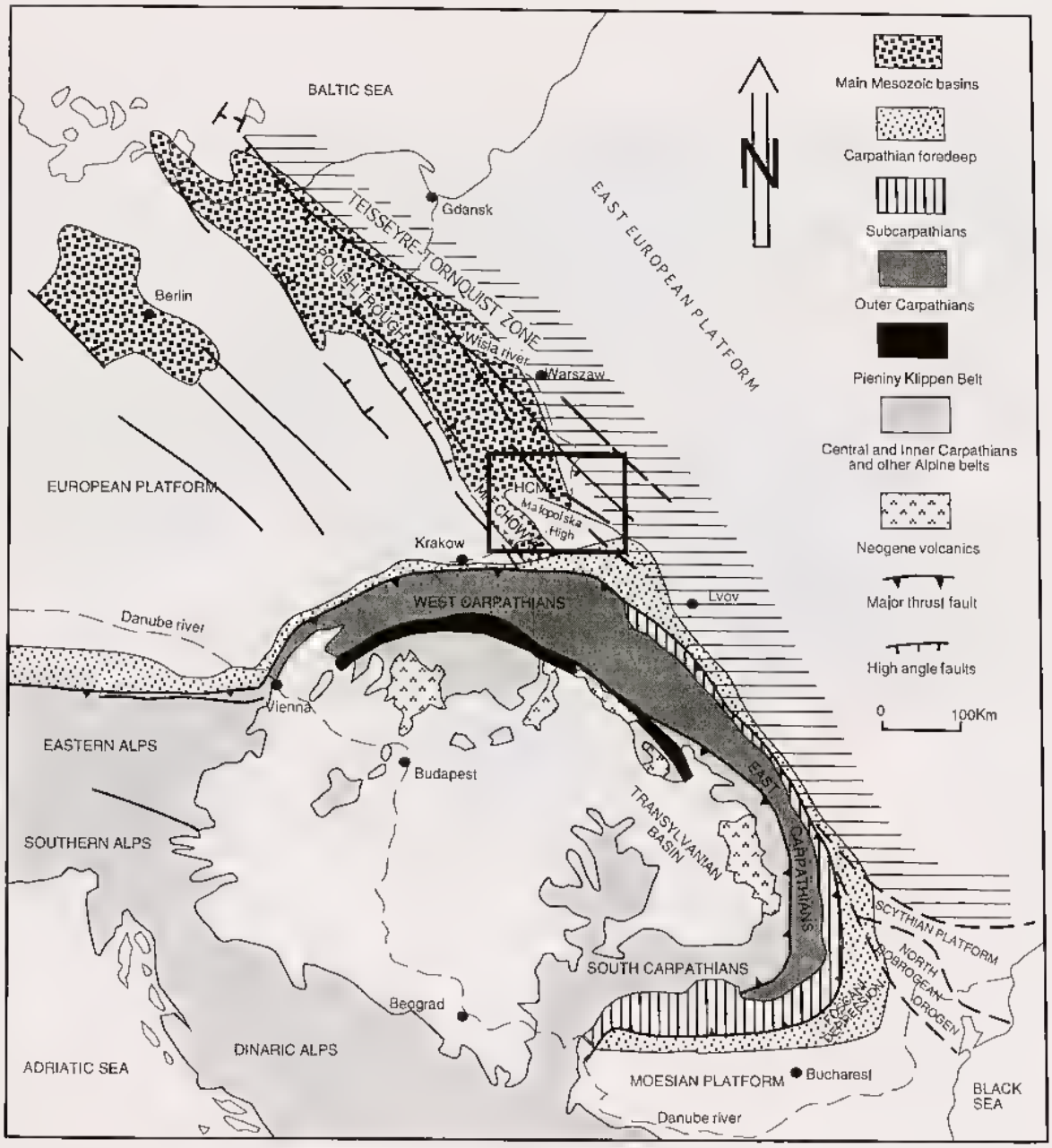

FIG. 1.— Main structural units of central Europe showing the Teisseyre-Tornquist Zone (modified after ROURE *et al.*, 1996; KOLAROWA & ROTH, 1977; KSIAZKIEWICZ *et al.*, 1977; ZIEGLER, 1987, 1990; POPRAWA & NEMCOK, 1988-1989; OSZCZYPKO & SLACZKA, 1989; ZYTKO *et al.*, 1989).

FIG. 1.— Principales unités structurales de l'Europe centrale montrant la Zone Teisseyre-Tornquist (modifié d'après ROURE et al., *1996 ; KOLAROWA & ROTH, 1977 ; KSIAZKIEWICZ* et al., *1977 ; ZIEGLER, 1987, 1990 ; POPRAWA & NEMCOK, 1988-1989 ; OSZCZYPKO & SLACZKA, 1989 ; ZYTKO* et al., *1989).*

Apart from the Dobrogea in Romania, the Holy Cross Mountains of southern Poland are the only place where the Permian and later structural and stratigraphic evolution of the TTZ can be studied in outcrops. In the Holy Cross Mountains, rocks ranging in age from Cambrian to Miocene are exposed. Sediments were almost continuous from Permian to Late Cretaceous, resting unconformably on deformed Palaeozoic series. After the Laramide event, the Holy Cross Mountains were partly covered by Miocene sediments. This exceptional area allows the acquisition of palaeostress indicators, in order to analyse the relationship between the Palaeozoic and the Meso-Cenozoic structures and the importance of

Source : MNHN, Paris

tectonic inheritance. As main tools we applied quantitative subsidence analyses and palaeostress reconstructions, in addition to classical structural work.

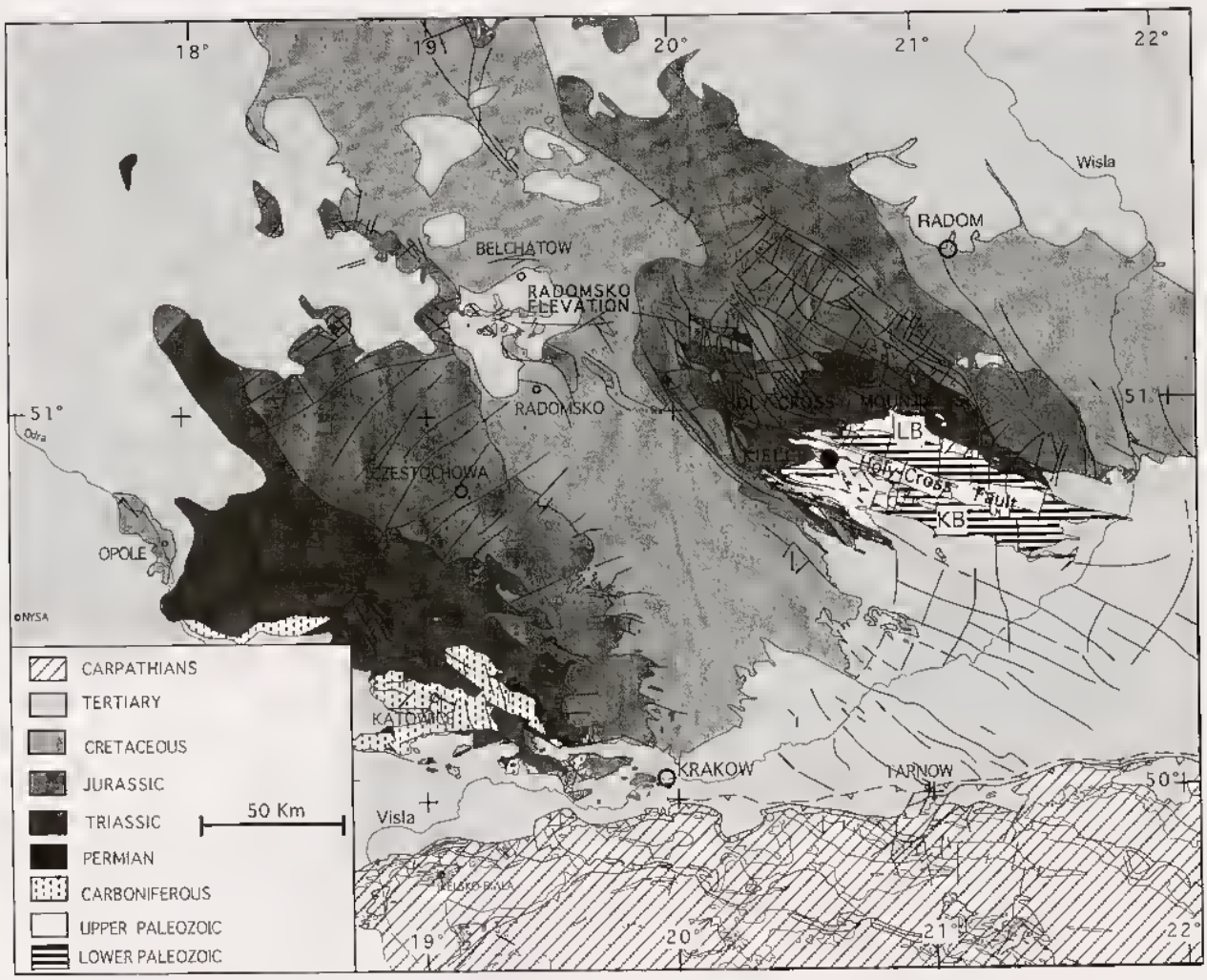

FIG. 2.— Geological map of southern Poland (modified from the geological map of Poland, scale 1:1 000 000, 1972). LB: Lysogory Block; KB: Kielce Block.

FIG. 2.— Carte géologique du sud de la Pologne (modifié d'après la carte géologique de la Pologne à l'échelle 1:1 000 000, 1972). LB : bloc de Lysogory ; KB : bloc de Kielce.

PALAEOZOIC BASEMENT OF THE HOLY CROSS MOUNTAINS

The Holy Cross Mountains are located in the foreland of the Variscan orogen of western Europe and adjacent to the southwestern margin of the Precambrian east European craton (POZARYSKI & KARNKOWSKI, 1992). The Palaeozoic part of the Holy Cross Mountains is composed of two blocks, the Kielce block and Lysogory block, which are separated by the WNW-ESE striking Holy Cross fault (Fig. 2), trending oblique to the TTZ (CZARNOCKI, 1957; GUTERCH *et al.*, 1976).

The Lysogory block to the North (LB on Fig. 2) has been interpreted as (1) an epicratonic element of the East European Platform (TOMCZYK, 1988; MIZERSKI, 1995); (2) a Caledonian terrain (Lysogory terrain, POZARYSKI & TOMCZYK, 1993); (3) the area of main Caledonian folding (DADLEZ *et al.*, 1994); (4) an area of Variscan foreland folding (CZARNOCKI, 1957). The Kielce block (KB on Fig. 2) to the

Source : MNHN, Paris

South is considered to form a part of the Malopolska Massif (Fig. 1) (TOMCZYK, 1988), belonging to the Cadomia, a collage of Variscan suspect terrane (BERTHELSEN, 1992).

The two blocks differing in their tectonic, stratigraphic and lithologic characters (MIZERSKI, 1988), were distant from each other during the Early Palaeozoic (STUPNICKA, 1992). They came close together during the Variscan times (LEWANDOWSKI, 1993). Palaeomagnetic data from Lysogory and Kielce blocks show their relative rotation with respect to each other and both with Baltica in a dextral wrench regime (60° anticlockwise rotation of the south Holy Cross Mountains, LEWANDOWSKI, 1993). The Malopolska Massif was probably a sliver of Baltica detached from Crimea - Dobrogea region and transfered along a dextral truncated margin of the Old Red Continent (LEWANDOWSKI, 1994). The Holy Cross fault might be a remnant fragment of the former truncated margin of Baltica (LEWANDOWSKI, 1993). The Variscan tectonics resulted in intensive folding with cleavage and affected both the Lysogory and Kielce blocks. The Permo-Carboniferous dextral wrench faulting known in western and central Europe (ZIEGLER, 1990) is not obvious in the Holy Cross Mountains and will be discussed later (cf. section: Micro-structural data). This polyphased deformation results in a complex Palaeozoic basement over which the Permo-Mesozoic rocks lie unconformably.

DEVELOPMENT OF THE HOLY CROSS PART OF THE POLISH TROUGH: THE PERMIAN TO CRETACEOUS TIMES

From Late Permian onward till the end of the Cretaceous, the Polish Trough sedimentary basin subsided on top of the TTZ. Its development is partly related to the intrusion of mantle material into the lower crust and its densification, and partly to crustal extension and thinning of the lithosphere (DADLEZ *et al.*, 1995). In an effort to reconstruct the evolution of the southern part of the Polish Trough, we constructed subsidence rate maps from boreholes back stripped data (Fig. 3) (HAKENBERG & SWIDROWSKA, 1997). The mapped area covered the northern part of the present Holy Cross Mountains and part of the Warszawa-Lublin Syncline. The studied period ranges from Late Permian to Late Jurassic times. The analysis of the Cretaceous period is in progress.

SUBSIDENCE AND FAULT PATTERN

Biostratigraphic data, facies patterns, depositional environments and sediment thickness were the basis for the reconstruction of palaeogeographic and palaeotectonic conditions controlling the basin development from the Late Permian to Late Jurassic. The Late Permian to Late Jurassic sediments, dominated by clastics, reached a thickness of 4.5 km, in the part of the basin that was addressed by our study.

Deep faults controlling the subsidence are associated with zones of great thickness gradients approximately paralleling the presumed basin margins. A comparison between facies and isopachs patterns was an additional factor in our analysis of the tectonic subsidence and the identification of synsedimentary faulting. The coincidence of lithofacies boundaries with zones of high subsidence rates was taken as a strong argument for synsedimentary faulting.

The basin subsidence history based on subsidence rates derived from preserved sediments accumulation, is presented on 7 maps (Fig. 3). The isolines values were obtained by dividing sediment thicknesses, corrected for effects of compaction, by the duration of respective time interval, using the ODIN & ODIN time scale (1990). The two main bounding faults, defining the margins of the Holy Cross segment of the Polish Trough, during Late Permian to Middle Jurassic times are the Nowe Miasto-Ilza fault and the Holy Cross fault (NMIF and HCF). The first one trends NW-SE, parallel to the Teisseyre-Tornquist Zone, whereas the second trends WNW-ESE. The HCF is a pre-Permian basement discontinuity; the Nowe Miasto-Ilza fault may have originated later (CZARNOCKI, 1957; KOTANSKI & MILACZEWSKI, 1977). In the Late Permian to the Late Jurassic basin evolution, 4 stages are recognized (HAKENBERG & SWIDROWSKA, 1997):

Source : MNHN, Paris

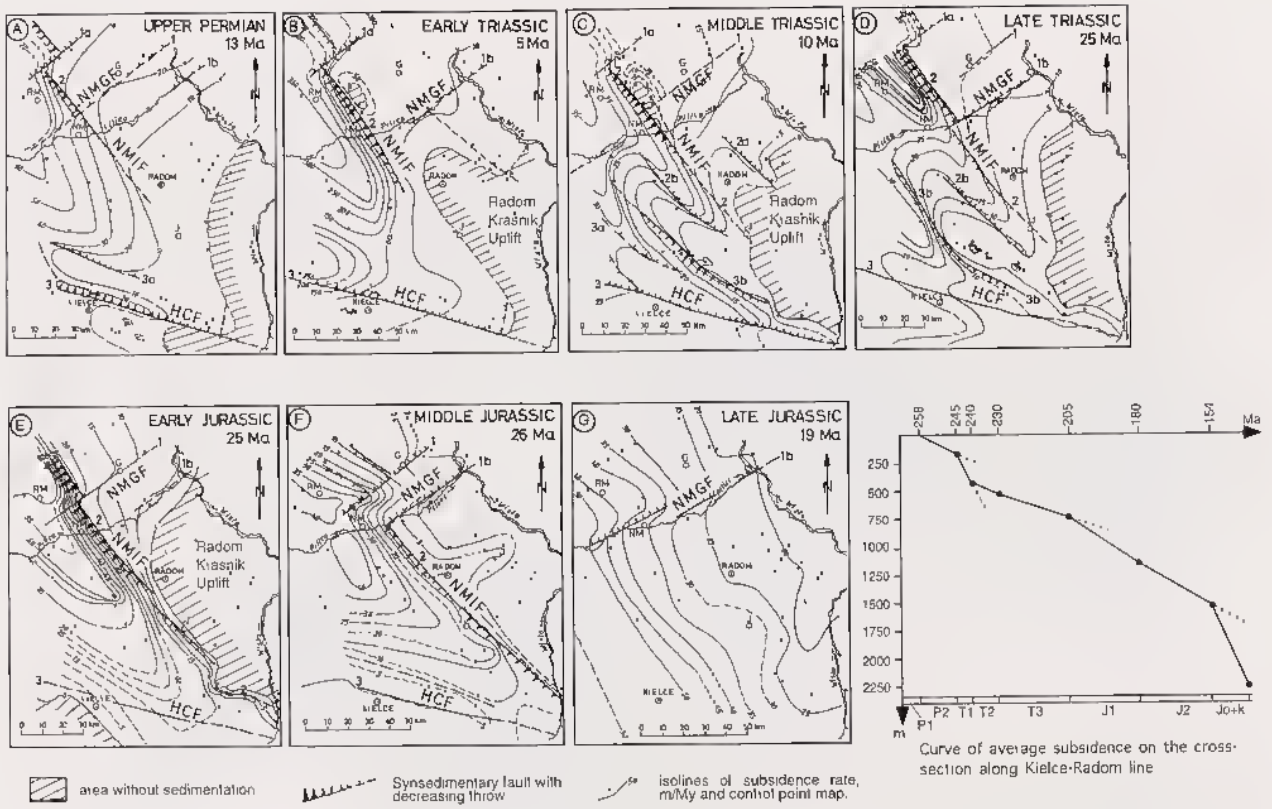

FIG. 3.— Maps of iso-subsidence lines for Late Permian to the Late Jurassic times (A to G) in the northern area of the Holy Cross Mountains and a part of the Warszawa-Lublin Syncline and curve of average subsidence on the Kielce-Radom cross section (after HAKENBERG & SWIDROWSKA, 1997). **1** - 1a - 1b: Nowe Miasto-Grojec fault zone; **2**: Nowe Miasto-Ilza fault (NMIF); **3**: Holy Cross fault (HCF), G: Grojec, NM: Nowe Miasto, RM: Rawa Mazowiecka, J: Ilza, P1: Early Permian, P2: Late Permian, T1: Early Triassic, T2: Middle Triassic, T3: Late Triassic, J1: Early Jurassic, J2: Middle Jurassic, Jo+k: Oxfordian and Kimmeridgian.

FIG. 3.— Cartes des courbes d'iso-subsidence du Permien supérieur au Jurassique supérieur (A à G) au nord des Montagnes Sainte Croix et dans une partie du synclinal Varsovie-Lublin ; et courbe de subsidence moyenne le long de la coupe Kielce-Radom (HAKENBERG & SWIDROWSKA, 1997). 1 - 1a - 1b : zone faillée de Nowe Miasto-Grojec ; 2 : faille Nowe Miasto-Ilza (NMIF) ; 3 : Faille Sainte Croix (HCF) ; G : Grojec ; NM : Nowe Miasto ; RM : Rawa Mazowiecka ; J : Ilza ; P1 : Permien inférieur, P2 : Permien supérieur, T1 : Trias inférieur, T2 : Trias moyen, T3 : Trias supérieur, J1 : Jurassique inférieur, J2 : Jurassic moyen, Jo+k : Oxfordien et Kimméridgien.

THE LATE PERMIAN AND EARLY TRIASSIC basin subsidence was closely controlled by the high activity along the basin border faults (Fig. 3 A-B). The asymmetry of the Zechstein basin fill reflects the geometry of two half grabens. In the south, a narrow half graben is located on the northern side of the HCF. To the NW, a second half graben with opposite polarity is controlled by activity along the NW-SE trending Nowe Miasto-Ilza fault. The two half grabens are limited by an accommodation zone transverse to the basin axis (Nowe Miasto-Grojec zone, n° 1, 1a,b in Fig. 3 A-B). This zone coincides with a decrease in evaporite content of the Zechstein succession toward the SE of the Pilica river line (MORAWSKA, 1992). The polarity of rifted basins often changes where a rift crosses preexisting dislocation zones (COLLETTA *et al.*, 1988; MILANI & DAVISON, 1988; ROSENDAHL *et al.*, 1992; RING, 1994); this appears to apply for the studied area in which there is evidence for Carboniferous activity along the Grojec fault (ZELICHOWSKI *et al.*, 1983). As main subsidence axes display a Z-shape, the established fault pattern ressembles that of a convergent accommodation zone (terminology after MORLEY *et al.*, 1990).

During the Early Triassic, the two main bounding faults formed an overlapping set. Two half grabens of opposite polarities, filled by lacustrine-continental sediments, dip away from each other (Fig. 3 B). At the same time, an interference accommodation zone developed (terminology after ROSENDAHL *et al.*,

Source : MNHN, Paris

1992), expressed in the central part of the basin by a ridge with relatively smal subsidence rates. When rifting was initiated, two opposite low-angle detachments may have developed simultaneously (BOSWORTH, 1985). Therefore it is possible that, at that time, a relative symmetry of the basin was maintained. The most important characteristic of the Early Triassic basin is a high subsidence rate (350 m/Ma).

During the *MIDDLE AND LATE TRIASSIC* the two bounding faults were still active (Fig. 3 C-D), although the subsidence rates decreased more than ten times. A few trough-parallel faults appeared inside the basin. They delineate two subsident domains and a central horst. An interference accommodation zone developed, limited by longitudinal faults (2b, 3a, b on Fig. 3 C,D). Such structures dominate where the extension is relatively weak (MOUSTAFA, 1996). Tilted fault blocks have been described in many extensional basins (COLLETTA *et al.*, 1988; YIELDING, 1990; WESTAWAY & KUSZNIR, 1993; ROBERTS & YIELDING, 1995). The uppermost part of the central horst, was eroded during the Late Triassic (Fig. 3 D). The erosional areas of Middle Triassic sediments does not coincide with those of Upper Triassic, suggesting two separate deformation phases during the Late Triassic (the early Cimmerian unconformities, ZIEGLER, 1990).

To the NW, in the prolongation of the central horst, a synsedimentary salt pillow grew inside the Rawa Mazowiecka basin segment, indicating extensional conditions also in the central part of the trough. Observed thickness changes in the NW are partly the result of Zeichtein salt displacements underlying the Lower Triassic sediments.

During the *EARLY-MIDDLE JURASSIC* subsidence patterns were more uniform (Fig. 3 E-F). Activity along the Holy Cross fault had almost ceased. By this time, the basin had assumed the geometry of a large half graben dipping towards the NE, due to a continued activity along the north-eastern Nowe Miasto - Ilza fault (NMIF) system. During the Early Jurassic the NMIF propagated southeastwards as a system of right-stepping *en échelon* faults (Fig. 3 E). During the Middle Jurassic this bounding fault zone evolved into rectilinear feature. The evolution of such an *en échelon* normal fault pattern consisting of straight faults concentrated within a single band, may characterize oblique rifting as proposed by TRON & BRUN (1991). Therefore, we suspect southeastward propagation of this fault, controlled by highly oblique sinistral NNE transtension. During the Early Jurassic, the surface extent of the basin had decreased. The basin flanks were uplifted; simultaneously the thickness gradients increased, though subsidence rate did not reach great values (a little more than 50 m/Ma) (Fig. 3 E).

Across the Nowe Miasto-Grojec fault zone (1 and 1b Fig. 3 E-F) depocenters are offset, the polarity of the half grabens switching during the Middle Jurassic. Such linking between basin segments of diferent polarity across transfer zone are already evident in the Late Permian map (Fig. 3 A), however with an opposite sense.

The *LATE JURASSIC* was an episode of overall subsidence that was not associated with high thickness gradients (Fig. 3 G). The basin expanded and downwarping of the basin floor was greater over the entire area. Isolines of subsidence rate trend NW-SE, parallel to the border of the East European Platform. The former stability characterizing the Southwest region had come to an end. However, there is no evidences for synsedimentary activity along the former basin bounding faults. Therefore the hypothesis of a Late Jurassic rifting phase in this area (KUTEK, 1994) cannot be validated. A Late Jurassic extensional episode was proposed also for the central and northwestern part of the Polish Trough by DADLEZ *et al.* (1995).

The decreasing of longitudinal asymmetry of the basin presumably resulted from the linking of the southeastward propagating described segment with a supposed new one, located in the south-east (present Carpathians) and developing northwestward.

The preliminary results on *CRETACEOUS* maps (HAKENBERG & SWIDROWSKA, *in prep.*) show that in the area of the Holy Cross segment of the Polish Trough, a period of accelerated subsidence is recorded during the Turonian and Coniacian. It occurred just before the first stage of tectonic inversion, Santonian in age. In the central and northwestern parts of the Polish Trough, a similar phase of subsidence acceleration occured during Cenomanian times (DADLEZ *et al.*, 1995) and is followed by the beginning of the tectonic inversion during the Turonian and Coniacian (JASKOWIAK-SCHOENEICHOWA & KRASSOWSKA, 1988).

Source : MNHN, Paris

MICRO-STRUCTURAL DATA

Micro-structural analyses provide information on the Late Permian-Early Triassic rifting period. In Devonian rocks, highly folded by Variscan tectonics, we observed numerous open fractures showing a complex history (Fig. 4). These fractures trend roughly N-S and cross-cut Variscan folds. Thus they obviously post-date Variscan folding. The lips of the open fractures are covered by calcite. The calcite fibers grow perpendicular to the lips, showing that the opening occurred perpendicularly to the fractures plans. This opening is attributed to an E-W extensional and N-S compressional strike-slip regime ($\sigma 1$ N-S, $\sigma 2$ vertical, $\sigma 3$ E-W). It can be related to the dextral wrench regime along the TTZ dated as Permo-Carboniferous and affecting western and central Europe. In the core of this calcite cover, occure red sandstones, dated as Late Permian-Early Triassic (LEWANDOWSKI, in preparation). This sediment contains clasts of the calcite fibers, and clasts of the Devonian host rock (limestone). This characterizes a second phase of fracture opening that was accompanied by sediment infilling during Late Permian-Early Triassic times. As such it is taken as evidence of the early rifting period. On the red standstones and the pieces of broken calcite and Devonian limestone contained in it, we observed superimposed strike-slip slickenside lineations. As they affect the Late Permian-Early Triassic sediments, this deformation occurred later. The dextral sense of slickensides on the N-S oriented fracture plane is compatible with a NE-SW trending major Laramide compression (see section: Tectonic inversion).

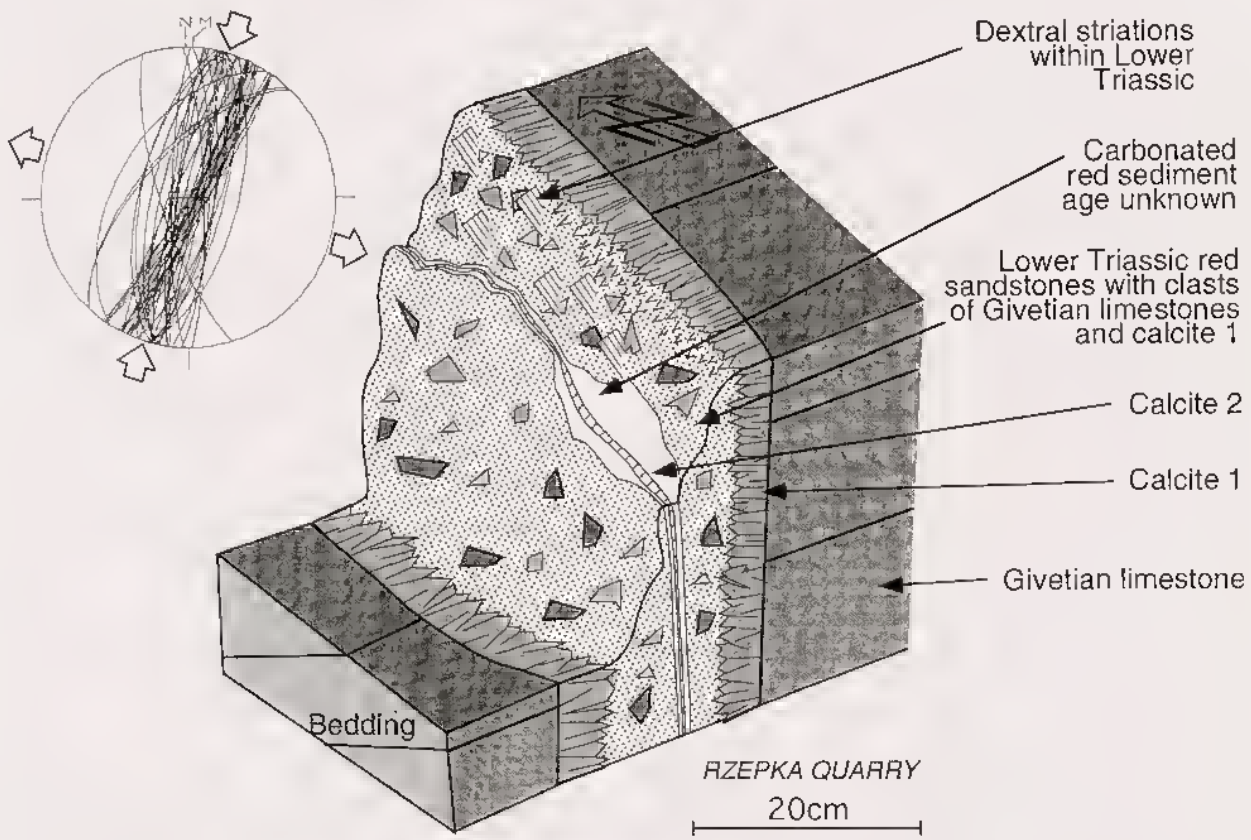

FIG. 4.— Example of sedimentary dyke in the Givetian limestones of Rzepka quarry (SW part of Holy Cross Mountains) showing a polyphased opening and the dextral reactivation; see explanations in text.

FIG. 4.— Exemple de filon sédimentaire dans les calcaires du Givétien de la carrière de Rzepka (Sud-Ouest des Montagnes Sainte Croix) montrant une ouverture polyphasée et une réactivation dextre ; cf explications dans le texte.

Source : MNHN, Paris

Excepted this illustration for first extensional stages during the Late Permian-Early Triassic, there are no obvious traces of the Mesozoic extension in terms of microtectonic structures. We investigated numerous sites in the Holy Cross Mountains, and did not find obvious normal faulting despite of the tectonic subsidence regime. The lack of extensional data may partly result from the age of the investigated rocks. Most of them were of Late Jurassic age. Rocks of other ages crop out in very few areas and their lithologies are not favorable for palaeostress investigations. However the Palaeozoic rocks in the core of the Holy Cross Mountains, do not provide evidence for normal faulting data. Thus it is likely that normal faults were localized in specific areas, not accessible todays. Thus the outcrops we investigated did not provide information about the Late Permian-Early Triassic and Early Jurassic stages of subsidence, characteristic for their important synsedimentary faulting. As third Late Jurassic subsidence stage was not accompanied with significant fault activity, this may explain the lack of corresponding micro-tectonic features. Nevertheless, we demonstrated from boreholes studies (section: Subsidence and fault pattern) the occurrence of some important synsedimentary activity along border faults (Nowe Miasto-Ilza fault, and Holy Cross fault, Fig. 3), specifically during the Triassic and Early Jurassic.

TECTONIC INVERSION

After the Late Permian to early Senonian subsidence period, the Polish Trough was affected by compressional deformations resulting in its inversion during the late Senonian and Palaeocene, and the uplift of the so called "Polish Swell". This inversion results in uplift of the Holy Cross Mountains, faulting of its Palaeozoic basement and folding of the Late Permian and Mesozoic sediments (Fig. 2). The Polish Swell trends NW-SE, strictly parallels and is superimposed on the Teisseyre-Tornquist Zone. Tectonic inversion being so obvious and well documented, we aim to determine the precise orientation and evolution of the stress pattern during the tectonic movements.

METHODS OF INVESTIGATION

In the field, we attempted to differenciate successive tectonic events and where possible, to establish their relative chronology and date them. Arguments for relative chronology between faulting and folding are the tilting of fault systems during subsequent stage of folding, or on the contrary, the primary position of faults cross-cutting through previously folded rocks. Successive events of faulting are deduced from the superposition of successive striae on the same fault plane or from the cross-cutting relationships between different sets of faults. On the other hand, compressional events were often accompanied by horizontal tectonic stylolites. The relative position of the stylolitic peaks compared to the bedding and the cross-cutting of sets of stylolites also constrain the sequence of tectonic events. Where available, sedimentary filling of open fractures may permit dating of activity along fractures. Sometimes, the overprinted deformation (slickensides) on the sedimentary fill of fractures can be used to date their reactivation.

The sequence of events being recognized in the field, we computed the orientation of palaeostress axis by the mean of fault-slip data inversion following the Angelier's method (ANGELIER, 1990). This method is based on the shear-stress relationships. The inversion of fault data consists of determining the reduced stress tensor knowing the direction and sense of slip on numerous faults of various orientations. The computation allows to determine the orientation of the main stress axes $\sigma 1$, $\sigma 2$ and $\sigma 3$, responsible for the faulting (ANGELIER, 1990). The sense of motion on individual fault is determined in the field: we measured the direction and plunge of the faults and the slickenside lineations.

AGE OF THE DEFORMATION

The large scale features of the Laramide deformation was due to the inversion of the Polish Trough (KUTEK & GLAZEK, 1972). In the Holy Cross Mountains surroundings, the youngest folded rocks are Maastrichtian in age. The folds are sealed by Palaeogene sediments (Fig. 2), dated as late Eocene in the axial part of the Middle Polish Swell. Most authors agree with a Maastrichtian and Palaeocene age of the

Source : MNHN, Paris

tectogenesis. On the geological maps of Poland (scale 1:200 000), the Palaeogene rests unconformably on Maastrichtian strata. Correspondingly the deformation is said to be "Laramide" *sensu lato*. However, in the Holy Cross Mountains, folds on the SW part are not covered by Palaeogene sediments. The nearest Cenozoic deposits resting unconformably on Cretaceous or older rocks, occur on the southern part of the Holy Cross Mountains. They are Miocene in age (Badenian). Thus in the area of the Holy Cross Mountains the age of the observed deformation is stratigraphically less well constrained. During this long gap a complex and polyphased deformation could occurred as discussed below.

TABLE 1.— Palaeostress results in investigated sites, from left to right: name of the site; coordinates; lithology; age of rock; stress regime : S = strike-slip faulting, R = reverse faulting, N = normal faulting; n: number of fault data; σ1, σ2, σ3: maximum, medium and minimum stress axes respectively; $\phi = (\sigma2-\sigma3)/(\sigma1-\sigma3)$ ratio of stress differences; RUP: estimator as refered to ANGELIER (1990); α: average angle between observed slip and computed shear; Q: quality estimator of the fault data (A = good, B = fair, C = poor). All angles are in degree.

TABLEAU 1.— Résultats des paléo-contraintes dans les sites étudiés, de gauche à droite : nom du site ; coordonnées ; lithologie ; âge de la roche ; régime de contraintes : S = décrochant, R = inverse, N = normal ; n : nombre de données de failles ; σ1, σ2, σ3 : contrainte respectivement maximale, intermédiaire et minimale ; $\phi = (\sigma2-\sigma3)/(\sigma1-\sigma3)$ rapport de forme ; RUP : estimateur de qualité (ANGELIER, 1990) ; α : angle moyen entre la strie observée et le cisaillement calculé ; Q : estimateur de qualité de la population de failles (A = bon, B = moyen, C = mauvais). Tous les angles sont en degrés.

Name	Lat. °	Long. °	lithology	age of rocks	Stress	n	σ1		σ2		σ3		ϕ	RUP	α	Q
					regime		trend	plunge	trend	plunge	trend	plunge				
Skarbka	50,36	21,33	limestones	U.Oxf. L.Kim	S	7	71	10	289	77	162	2	0,4	25	9	A
Ballow	50,36	21,33	limestones	M.Oxl.	S	6	44	34	223	56	314	1	0,7	38	9	A
					S	4	73	9	247	81	343	1	0,6	28	7	B
Ozarow	50,34	21,07	lime. marles	U.Kim Turo.	S	6	35	2	294	80	125	10	0,3	32	8	B
					S	12	70	2	224	88	340	1	0,4	22	5	A
Jaworznia	50,31	20,2	limestones	Devonian	S	5	225	4	315	6	101	83	0,3	25	6	B
Gniezdziska	50,31	20,03	limestones	M.Oxf.	S	8	215	16	101	55	314	30	0,2	35	8	B
					R	7	231	3	139	20	329	70	0,3	35	16	B
Zagnask	50,34	20,32	limestones	Devonian	S	10	221	6	124	51	316	38	0,3	35	10	A
					S	6	343	4	239	75	74	14	0,4	25	11	A
Malogoszcz	50,29	20,09	clays sandsl.	Kim. Alb.	S	15	235	14	7	69	141	15	0,4	38	8	A
Checiny	50,28	20,16	limestones	Frasnian	S	4	256	11	115	76	348	8	0,3	15	5	C
Oslowka	50,3	20,12	lime. clays	Frasnian	R	5	200	14	295	18	75	67	0,6	24	7	C
					S	4	237	16	61	74	328	1	0,4	52	9	C
Sobkow	50,25	20,16	limestones	Kim.	S	5	29	0	122	84	299	6	0,1	38	6	C
					S	5	237	9	119	71	330	17	0,4	41	12	A
					S	9	136	11	282	68	69	19	0,3	31	13	A
Wielzbica	50,25	20,16	limestones	M.U.Oxl.	S	7	77	4	306	84	167	5	0,7	12	5	B
Wolica	50,26	20,16	limestones	Oxl.	S	4	247	2	338	28	154	62	0,4	34	14	C
Starocheciny	50,27	20,17	limestones	Oxl.	S	16	13	29	153	55	273	19	0,3	40	11	A
Debska Wola	50,26	20,21	limestones	Oxl.	S	8	56	18	268	69	149	10	0,2	45	17	A
Wisniowka	50,33	20,32	quartzites	Cambrian	S	7	85	0	175	68	355	22	0,4	15	5	A
Czarnow	50,32	20,2	limestones	Frasnian	S	11	212	0	304	79	122	11	0,2	28	13	A
					S	4	167	11	310	76	75	8	0,5	17	6	B
Rzepka	50,28	20,16	dolomites	Givetian	S	13	252	38	71	52	162	0	0,7	30	10	A
Wietrznia	50,3	20,23	limestones	Frasnian	S	26	33	1	301	70	123	20	0,4	41	18	A
					S	11	155	2	289	88	65	2	0,3	43	19	B
Kadzielnia	50,3	20,22	reef lime.	Frasn. Fam.	S	8	18	24	191	66	287	3	0,3	44	17	B
					RS	6	357	22	98	26	232	55	0,3	39	13	B
Laskowa	50,33	20,21	dolomite	Givetian	S	6	212	9	343	76	120	10	0,5	29	5	B
					N	4	53	73	198	14	291	9	0,5	15	3	C
					S	8	100	5	213	78	9	11	0,4	26	12	A
					S	5	354	6	140	82	264	4	0,6	25	13	A
					S	12	332	3	240	25	68	65	0,1	41	16	A
Jazwica	50,28	20,2	lime. marl.	Frasn. Fam.	R	8	286	11	191	22	40	65	0,4	32	12	B
					S	19	265	5	15	76	174	13	0,2	33	16	A
					S	4	348	12	247	41	91	46	0,4	33	12	C
Joselka	50,3	20,3	lime. clays	Give. to Fam.	S	10	156	2	53	80	246	10	0,2	44	21	C
					S	11	279	3	187	22	17	68	0,1	26	9	B
					S	7	189	28	15	62	280	3	0,3	34	14	B
					N	4	105	81	3	2	273	9	0,5	13	2	B

Source : MNHN, Paris

MICRO-STRUCTURAL ANALYSIS AND PALAEOSTRESS RECONSTRUCTION

We collected microstructural data at 61 sites in the Holy Cross Mountains (active and old quarries and natural outcrops) including 55 in the Mesozoic formations. In 22 of them, data allowed us to compute palaeostresses.

The main Laramide direction of compression detected in the field and characterized in terms of palaeostress tensor is a NE-SW compression (Figs 5 and 6) (see also JAROSZEWSKI, 1972; SWIDROWSKA, 1980). We recognized this shortening over all the Holy Cross Mountains, in the Mesozoic rocks as well as in the Palaeozoic ones. At most sites it is characterized by conjugate strike-slip fault system (Fig. 7A). In scarce sites this compression is characterized by conjugate reverse faults (Fig. 7B). In sites where the bedding is steep, the faults system appear tilted as well as the strata. Therefore the faulting took place before the folding, while the bedding was flat. Stylolitic peaks trending about N050 further constrain the NE-SW direction of compression (Fig. 7C). The stylolitic peaks still parallel to the bedding planes in the steep limbs of the folds. This is illustrated in figure 7D where the stylolitic peak symbols are located on the bedding plane traces. This means that the stylolitic peaks formed horizontally when the bedding was flat, and were subsequently tilted during the folding of the strata.

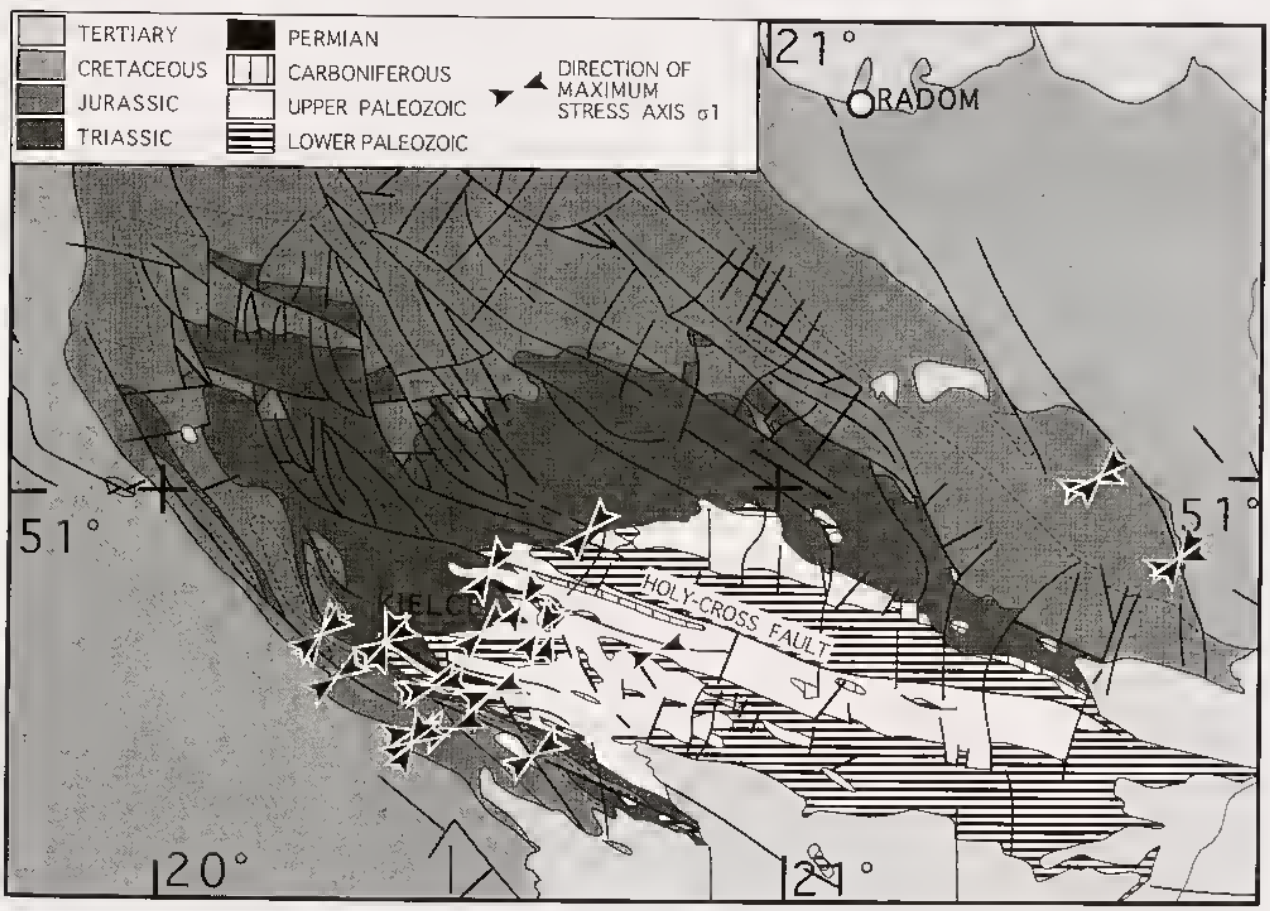

FIG. 5.— The Laramide palaeostress pattern in the Holy Cross Mountains. The NE-SW compression is marked by the convergent black arrows at each measured site.

FIG. 5.— Champ de contraintes laramien dans les Montagnes Sainte Croix. La compression NE-SW est figurée par les flèches convergentes noires localisées sur chaque site de mesures.

Source : MNHN, Paris

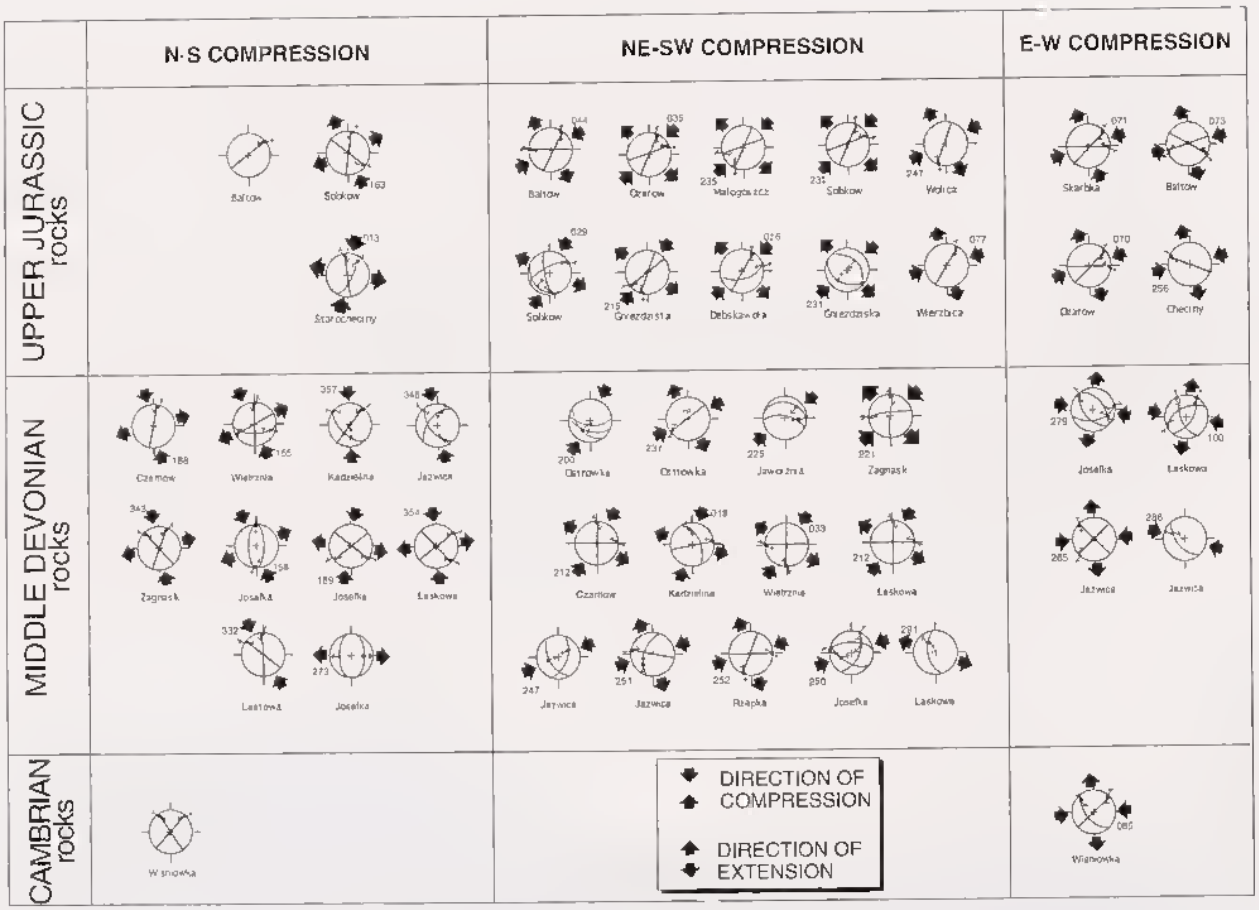

FIG. 6.— Schematic representation of post-Variscan brittle micro-structures and palaeostress computation in the Holy Cross Mountains (direction of compression and extension as black arrows; lower hemisphere Schmidt projection). The main Laramide event corresponds to the NE-SW compression of the central vertical column.

FIG. 6.— Représentation schématique des micro-structures cassantes post-varisques et paléo-état des contraintes dans les Montagnes Sainte Croix (flèches noires: directions de compression et d'extension ; hémisphère inférieur projection de Schmidt). L'événement laramien principal correspond à la compression NE-SW dans la colonne centrale.

In some Palaeozoic outcrops, we described N-S calcite veins with a sedimentary fill (cf. section: Micro-structural data). This fill, that was dated as Late Permian-Early Triassic, was affected by dextral movements (Fig. 4). The dextral motion on N-S fault planes is coherent with the NE-SW shortening and would be conjugated to a sinistral movement on nearly E-W faults. That means that in the basement, pre-existing N-S structures were reactivated whereas in the cover new conjugate strike-slip faults were formed.

Some sets of faults indicate other directions of compression. One direction is about N-S, marked by conjugate strike-slip faults. This direction is local and poorly constrained in Mezosoic formations. On the opposite, it is well determined in the Palaeozoic rocks (N-S compression in Middle Devonian rocks, Fig. 6). As corresponding faults cross-cut the Variscan folds, they are post-Variscan. The age of this event still uncertain. It could be related to the late Variscan N-S compression and E-W extension as postulated for the calcite veins openning (section: Micro-structural data), as well as to a step of deformation related to the Laramide tectonics.

An other direction of compression trends about E-W, and is characterized by conjugated strike-slip faults in Mezosoic rocks and further constrained by E-W stylolitic peaks. The E-W stylolites show sequencial relationships both with the N050 ones and with the bedding. In Wola Morawicka quarry (SW border of the Holy Cross Mountains), a bedding plane cleared over a large surface allowed the

Source : MNHN, Paris

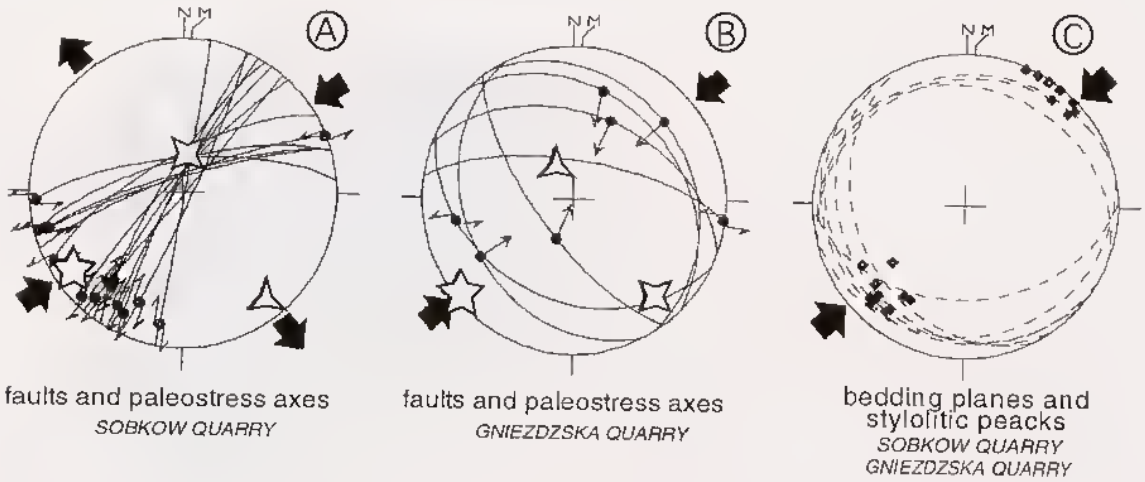

FIG. 7.— Example of typical Laramide structures in the Jurassic limestones in the Sobkow and Gniezdziska quarries. A, conjugate strike-slip faults and palaeostress computation (faults as thin lines ; palaeostress axes as five (σ1) four (σ2) and three (σ3) pointed stars; direction of compression and extension as black arrows; lower hemisphere Schmidt projection); B, conjugated reverse faults and palaeostress computation; C, relationship between stylolites and bedding planes.

FIG. 7.— Exemple de structure laramienne caractéristique dans les calcaires jurassiques des carrières de Sobkow et Gniezdziska. A, failles décrochantes conjuguées et calcul de paléo-contrainte : étoiles à cinq (σ1) quatre (σ2) et trois (σ3) branches, flèches noires : directions de compression et d'extension, hémisphère inférieur projection de Schmidt) ; B, failles inverses conjuguées et calcul de paléo-état de contraintes ; C, relation entre les stylolites et la stratification.

observation of two sets of stylolites (Fig. 8A and B). The first one is N050 characteristic for the NE-SW main Laramide shortening. The peaks were affected and partly dissolved by a second generation of stylolites trending N090 in average (N095 on the Fig. 8). They were formed during an E-W compressional event that occurred later than the NE-SW one (WARTOLOWSKA, 1972). N050 stylolitic peaks stand parallel to the bedding planes (Fig. 8D). As shown on the stereoscopic projection, the peaks symbols are located on the traces of the bedding. Thus the N050 stylolites occurred before the tilting of the bedding, that means before the folding deformation related to a NE-SW compression (see section: Large scale structures analysis). In this quarry orthogonal sets of joints developed without sequencial relationships (Fig. 8C and D). However, the E-W set is more homogeneous and less scatered directions than the N-S one. Moreover it is parallel to the E-W direction of compression deduced from the stylolites. Thus it may result from the E-W compression event. The joints stand perpendicular to the bedding. It is clear in the field as shown by the sketch C of figure 8, and on the stereographic projection on which the intersection of the two sets of joints correspond to the poles to the bedding (open dots). Thus the joints as well as the N050 stylolitic peaks are linked to deformation events which occurred before the folding.

LARGE SCALE STRUCTURES ANALYSIS

To the NW of the Holy Cross Mountains, the Radomsko elevation is related to *en échelon* folds (Fig. 2), dated as Laramide, like the folds in the Holy Cross Mountains. They affect Cretaceous rocks and are blanketed by the Miocene rocks. These folds display a WNW-ESE alignment, identical to the Holy Cross fault, and are isolated in the middle of a large NW-SE trending gentle syncline. Their "S" shape suggests sinistral shear, coherent with the NE-SW major Laramide compression (POZARYSKI, 1976). We carried out a detailed fault slip analysis on this area. The palaeostress computation show a single direction of compression trending NE-SW. We interprete the *en échelon* folds as resulting from the sinistral reactivation of the deep seated Holy Cross basement fault, synchronous with the NE-SW Laramide shortening characterized in the Holy Cross Mountains.

Source : MNHN, Paris

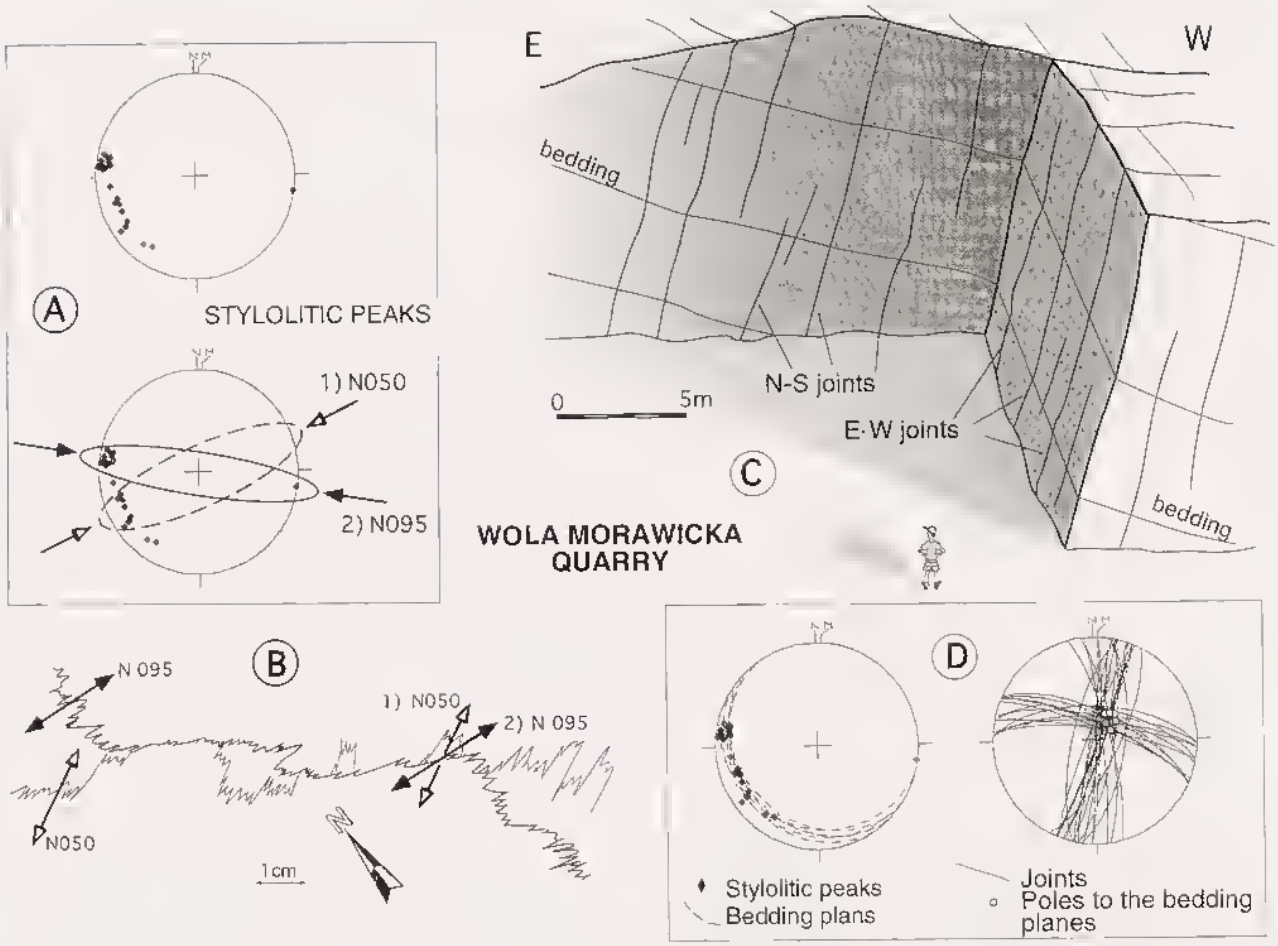

FIG. 8.— Sequencial relationship between stylolites, joints and tilting of bedding in Wola Morawicka quarry. A, stereoscopic projection of stylolitic peaks measured on a cleared bedding surface and chronology between the NE-SW (1) and the E-W (2) sets; B, sketch of the observed stylolite sequence on the bedding surface; C, sketch of the walls of the quarry showing the tilting of the joints and of the bedding planes; D, stereographic projection of joints, stylolitic peaks and bedding planes.

FIG. 8.— Relations chronologiques entre les stylolites, les joints et le basculement de la stratification dans la carrière de Wola Morawicka. A, projection stéréoscopique des pics stylolitiques mesurés sur une surface de stratification dégagée et chronologie relative entre les systèmes (1) NE-SW et (2) E-W ; B, Schéma des relations chronologiques entre stylolites observés sur une surface de stratification ; C, schéma des murs de la carrière montrant le basculement des joints et des plans de stratification ; D, projection stéréographique des joints, des pics stylolitiques et des plans de stratification.

In the SW part of the Holy Cross Mountains is located a narrow highly folded zone (Figs 2 and 5) with folds wave lenght of 1 to 2 km. The axis of this zone trending NW-SE is oblique to the Palaeozoic horst and parallel to the Teisseyre-Tornquist Zone. It forms the southwestern boundary of the uplifted area (STUPNICKA, 1971). As proposed for the *en échelon* folds in the Radomsko elevation, the narrow folded zone may result from the reactivation of a deep seated NW-SE striking basement fault during the Laramide shortening, localizing above it the deformation in the Mesozoic cover.

The NE-SW Laramide shortening, oblique to the WNW-ESE Holy Cross fault caused its sinistral reactivation (Radomsko Elevation) while the NW-SE striking basement fault was reactivated as a reverse fault (SW border of Holy Cross Mountains). As a result, two different geometries of fold developed in the Mesozoic cover above these deep seated large faults.

Source : MNHN, Paris

SYNTHESIS

BASIN OPENING

From the Late Permian to the Middle Jurassic the Polish Trough propagated progressively towards the SE by reactivation of the pre-existing crustal discontinuity of Holy Cross fault (during the early continental rifting phase, *i.e.* in the Late Permian and Early Triassic time). The southeastwards prolongation of the Nowe Miasto Ilza fault (Fig. 3), paralleling the Teisseyre-Tornquist Zone, occurred later, mainly during Early and Middle Jurassic time. The geometry of the basin fill indicates many similarities with features characteristic for rifting basins (COLLETTA *et al.*, 1988; MILANI & DAVISON, 1988; NELSON *et al.*, 1992; RING, 1994; ROSENDAHL *et al.*, 1992). These similarities are: (1) subsidence connected with a big activity of bounding faults; (2) domination of clastic sediments at the beginning of the basin opening, joined with (3) high subsidence rate (Fig. 3 A,B); (4) transverse asymetry of the trough (Fig. 3 A, B, E, F); (5) changes of basin polarities resulting in the Z-shape subsidence axis (Fig. 3 A, F); (6) activity of transfert fault zone; and (7) developement of the accomodation zone expressed by a ridge of relatively smaller subsidence in the central part of the basin (Fig. 3 A, C, D).

Three stages of high subsidence rate are recorded in the basin history; namely during the Late Permian and Early Triassic, the Early Jurassic and the Late Jurassic. The first two episodes were strictly connected with the tectonic activity along the major normal faults bounding the basin.

The southern part of the Polish Trough initiated during an early stage of intracontinental rifting devoid of volcanism, probably due to simple shear regime during Late Permian and Early Triassic times (lithospheric shear model of WERNICKE, 1981; ZIEGLER, 1990). In the field it is shown by an extensional regime with opening and sedimentary filling of pre-existing N-S veins.

During the Middle and Late Triassic, faulting was associated with lithospheric flexuring (HAKENBERG & SWIDROWSKA, 1997) reflecting a vertical trajectory of the maximal principal stress axis ($\sigma 1$). The Early and Middle Jurassic rocks of the basin was formed under sinistral NNE-SSW transtensional stres regime which developed along the Teisseyre-Tornquist Zone, acting as oblique slip fault. During the Late Jurassic, fault activity ceased and the basin entered apparently in the thermal sag stage.

BASIN INVERSION

The existence of different directions of compression and relative chronologies determined in the Mesozoic sites indicate that the Laramide deformation occurred gradually. The main compression trends NE-SW. It caused large scale structures involving previous micro-scale features. We saw that the first markers of the NE-SW compression were N050 trending horizontal stylolitic peaks. There is no available relative chronology between the stylolites and the faulting. But the conjugate strike-slip faulting and the NE-SW stylolites occurred both before the folding, when the bedding was still flat. An E-W set of stylolites indicates an E-W compression subsequent to the NE-SW one. This compressional phase was also marked by orthogonal sets of joints, also prior to the folding. Finally, with increasing deformation, the Holy Cross Mountains were uplifted and folded.

The main folding stage in the Mesozoic cover is related to the reactivation of the deep Palaeozoic structures. On the NW-SE fault, the perpendicular NE-SW trending Laramide shortening caused a reactivation as reverse fault. It is revealed by NW-SE folds in the cover of the Holy Cross Mountains, while on the oblique WNW-ESE Holy Cross fault, the Laramide shortening provocated a sinistral strike-slip reactivation, reavealed by the *en échelon* folds in the Radomsko elevation. The Laramide compression also reactivated smaller inherited structures: for instance the N-S sedimentary dykes originated from the Late Permian-Early Triassic rifting extensional period, were favorably oriented for reactivation as dextral strike-slip faults.

Source : MNHN, Paris

CONCLUSION

The Late Permian-Mesozoic Polish Trough basin developed over a complex basement. The analysis of the iso-subsidence curves in the Holy Cross Mountains area shows that the shape of the basin was characterized by two directions, related to (1) the inherited Palaeozoic faults of which the Holy Cross fault is a major one, and (2) the deep Teisseyre-Tornquist Zone resulting in the NW-SE faults as for instance Nowe Miasto-Ilza fault. Some of the synsedimentary normal faults active during the basin evolution were reactivated as reverse strike-slip faults during the Laramide inversion.

We pointed out variable subsidence rate from the Late Permian to the Late Jurassic characterized by three stages of higher subsidence rates : Late Permian-Early Triassic, Early Jurassic and Late Jurassic. The palaeostress computation revealed a N-S compression and an E-W extension that we associate to the early stage of rifting during the Late Permian-Early Triassic.

The Laramide inversion resulted from a NE-SW compression characterized by (1) uplifting of the Holy Cross Mountains, and (2) reverse reactivation of the NW-SE bounding faults and of the WNW-ESE basement fault and by folding in the Mesozoic cover. The NE-SW compression applied to the WNW-ESE Holy Cross fault resulted in the developpement of *en échelon* folds in the Mesozoic sedimentary cover and sinistral shear reactivation of the deep seated fault. The palaeostress pattern compuled from the minor faults analysis is coherent with the information provided by large scale folds. The detailed analysis of microstructural data made obvious a complex continous deformation, starting with joints, stylolites and faults development, all of them being subsequently tilted during the folding.

The field investigation, palaeostress computation and subsidence analysis from borehole data, were necessary to get a synthetic view and understanding for basin subsidence, inversion process and role played by crustal features responsible for deformation localization.

REFERENCES

ANGELIER, J., 1990.— Inversion of field data in fault tectonics to obtain the regional stress. III: A new rapid direct inversion method by analytical means. *Geophysical Journal International*, **103**: 363-376.

BERTHELSEN, A., 1992.— Mobile Europe. *In*: D. BLUNDEL, R. FREEMAN & ST. MULLER (eds), *Continent Revealed: the European Geotraverse*. Cambridge University Press, Cambridge: 11-32.

BOSWORTH, W., 1985.— Geometry of propagating continental rifts. *Nature*, **316**: 625-627.

COLLETTA, B., QUELLEC LA, P., LETOUZEY, J. & MORETTI, I., 1988.— Longitudinal evolution of the Suez rift structure (Egypt). *Tectonophysics*, **153**: 221-233.

CZARNOCKI, J., 1957.— Geology of the Lysa Gora Region (Swiety Krzyz Mountains). *Prace Panstwowego Instytutu Geologicznego*, **18**: 1-404.

DADLEZ, R., KOWALCZEWSKI, Z. & ZNOSKO, J., 1994.— Some key problems of pre-Permian tectonics of Poland. *Geological Quarterly*, **38** (2): 169-189.

DADLEZ, R., NARKIEWICZ, M., STEPHENSON, R.A., VISSER, M.T.M. & VAN WEES, J-D., 1995.— Tectonic evolution of the Mid-Polish Trough: modelling implications and significance for central European geology. *Tectonophysics*, **252**: 179-195.

GUTERCH, A., KOWALSKI, T.J., MATERZOK, R., PAJCHEL, J. & PERCHUC, E., 1976.— O glebokiej strukturze skorupy ziemskiej w rejonie Gor Swietokrzyskich. *In*: W. POZARYSKI & J. GLAZEK (eds), *Przewodnik 48 Zjazdu Polskiego Towarzystwa Geologicznego Starachowice, 24-26 Wrzesnia*. Instytut Geologiczn, Wydawnictwa Geologiczne,Warszawa: 52-58.

GUTERCH, A., GRAD, M., MATERZOK, R. & PERCHUC, E., 1986.— Deep structure of the Earth's crust in the contact zone of the Palaeozoic and Precambrian Platforms in Poland (Teisseyre-Tornquist zone). *Tectonophysics*, **128**: 251-279.

HAKENBERG, M. & SWIDROWSKA, J., 1997.— Propagation of the southeastern segment of the Polish Trough connected with bounding fault zones (from Permian to Late Jurassic). *Comptes Rendus de l'Académie des Sciences, Paris*, **324**: 1-11.

HIPPOLYTE, J.C., SANDULESCU, M., BADESCU, D. & BADESCU, N., 1996.— L'activité d'un segment de la ligne Tornquist-Teisseyre depuis le Jurassique supérieur: la faille de Peceneaga-Camena (Roumanie). *Comptes Rendus de l'Académie des Sciences, Paris*, **323**, IIa: 1043-1050.

JAROSZEWSKI, W., 1972.— Mesozoic structural criteria of tectonics of non-orogenic areas: an example from north-eastern Mesozoic margin of the Swietokrzyskie Mountains. *Studia Geologica Polonica*, **38**: 9-215.

Source : MNHN, Paris

JASKOWIAK-SCHOENEICHOWA, M. & KRASSOWSKA, A., 1988.— Paleothickness, lithofacies and paleotectonics of the epicontinental Upper Cretaceous in Poland. *Geological Quarterly*, **32** (1): 177-198.

KOLAROWA, M. & ROTH, Z., 1977.— Geology of the platform entering below the Carpathian foredeep and its Carpathian nappes in SE Moravia. *Bulletin of the Geological Survey Prag.*, **52-5**: 257-265.

KOTANSKI, Z. & MILACZEWSKI, L., 1977.— The paleotectonic development of the Zwolen anticlinal structure of Devonian age. *Biuletyn Instytut Geologiczny*, **303**: 53-89.

KSIAZKIEWICZ, M., OBERC, J. & POZARYSKI, W., 1977.— *Geology of Poland*. Vol. IV; *Tectonics*. Instytut Geologiczn, Wydawnictwa Geologiczne, Warsawa: 1-718.

KUTEK, J., 1994.— Jurassic tectonic events in south-eastern cratonic Poland. *Acta Geologica Polonica*, **44** (3-4): 167-221.

KUTEK, J. & GLAZEK, J., 1972.— The Holy Cross area, Central Poland, in the Alpine cycle. *Acta Geologica Polonica*, **22** (4): 603-653.

LEWANDOWSKI, M., 1993.— Paleomagnetism of Paleozoic rocks of the Holy Cross Mts (Central Poland) and the origin of the Variscan orogen. *Publications of the Institute of Geophysics Polish Academy of Sciences*, **A-23** (265): 1-85.

LEWANDOWSKI, M., 1994.— Paleomagnetic constraints for Variscan mobilism of the Upper Silesian and Malopolska Massifs, southern Poland. *Geological Quarterly*, **38** (2): 211-230.

LEWANDOWSKI, M., submitted.— Palaeomagnetic study of some fracture fills in the Holy Cross Mts (Central Poland). *Pure applied Geophysics*.

MILANI, E.J. & DAVISON, I., 1988.— Basement control and transfer tectonics in the Reoncavo-Tucano-Jatoba rift, Northeast Brazil. *Tectonophysics*, **153**: 221-233.

MIZERSKI, W., 1988.— Tectonic evolution of the Lysogory region, Holy Cross Mts. [sum]. *Przeglad Geologiczny*, **1**: 142-146.

MIZERSKI, W., 1995.— Geotectonic evolution of the Holy Cross Mts in Central Europe. *Biuletyn Panstwowego Instytuta Geologiczniego*, **372**: 1-47.

MORAWSKA, A., 1992.— Permian north of the Holy Cross Mts (Central Poland). *Przeglad Geologiczny*, **468** (4): 216-223.

MORLEY, C.K., NELSON, R.A., PATTON, T.L. & MUNN, S.G., 1990.— Transfer zones in the East African rift system and their relevance to hydrocarbon exploration in rifts. *AAPG Bulletin*, **74** (8): 1234-1253.

MOUSTAFA, A., 1996.— Internal structure and deformation of an accommodation zone in the northern part of the Suez rift. *Journal of Structural Geology*, **18** (1): 93-107.

NELSON, R.A., PATTON, T.L. & MORLEY, C.K., 1992.— Rift-segment interaction and its relation to hydrocarbon exploration in continental rift systems. *AAPG Bulletin*, **76** (8): 1153-1169.

ODIN, S.G. & ODIN, CH., 1990.— Échelle numérique des temps géologiques. *Géochronique*, **35**.

OSZCZYPKO, N. & SLACZKA, A., 1989.— The evolution of the Miocene basin in the Polish outer Carpathians and their foreland. *Geologica Carpathica*, **40**: 23-86.

POPRAWA, D. & NEMCOK, J., 1988-1989.— *Geological Atlas of the western outer Carpathians and their foreland (1:500 000)*. Panstwowy Instytut Geologiczny, Warszawa.

POZARYSKI, W.,1976.— Ogolna charakterystyka tektoniczna mesozoiku swietokrzyskiego. *In*: W. POZARYSKI & J. GLAZEK (eds), *Przewodnik 48 Zjazdu Polskiego Towarzystwa Geologicznego Starachowice, 24-26 Wrzesnia*. Instytut Geologiczn, Wydawnictwa Geologiczne,Warszawa: 7-13.

POZARYSKI, W. & KARNKOWSKI, P. (eds), 1992.— *Tectonic map of Poland during the Variscan Time*. Wydawnictwa Geologiczne, Warszawa.

POZARYSKI, W. & TOMCZYK, H., 1993.— Geological cross-section through SE Poland. *Przeglad Geologiczny*, **41** (10): 687-695.

RING, U., 1994.— Pre-existing structure and the evolution of the Cenozoic Malawi rift. *Tectonics*, **13** (2): 313-326.

ROBERTS, A. & YIELDING, G., 1995.— Continental Extensional Tectonics. *In*: P. HANCOCK (ed.), *Continental Deformations*. Pergamon Press, Oxford: 223-250.

ROSENDAHL, B.R., KILEMBE, E. & KACZMARICK, K., 1992.— Comparison of the Tanganica, Malawi, Rukwa and Turkana Rift zones from analyses of seismic reflection data. *Tectonophysics*, **213**: 235-256.

ROURE, F., KUSMIEREK, J., BESSEREAU, G., ROCA, E. & STRZETELSKI, W., 1996.— Initial thickness variation and basement-cover relationships. *In*: F. ROURE *et al.* (eds), *Geodynamic Evolution of Sedimentary Basins: Proceedings of the International Symposium held in Moscow, May 18-23, 1992*. Technip, Paris: 255-279.

STUPNICKA, E., 1971.— Tectonics of Mesozoic rocks in the southern border of the Holy Cross Mts. *Annales de la Société géologique de Pologne*, **40** (3-4): 393-409.

STUPNICKA, E., 1992.— The significance of the Variscan orogeny in the Swietokrzyskie Mountains (Mid Polish Uplands). *Geologische Rundschau*, **81** (2): 561-570.

SWIDROWSKA, J., 1980.— Tectonic stylolites as a tectogenetic index on the area of SW margin of the Holy Cross Mountains. *Przeglad Geologiczny*, **28** (3): 159-164.

TOMCZYK, H., 1988.— Tectonic movements between margin of East-European Platform and the Holy Cross Mts region in Paleozoic. *Przeglad Geologiczny*, (1): 9-17.

TRON, V. & BRUN, J.P., 1991.— Experiments on oblique rifting in brittle-ductile systems. *Tectonophysics*, **188**: 71-84.

Source : MNHN, Paris

WARTOLOWSKA, J., 1972.— An example of the processes of tectonic stylolitization. *Bulletin de l'Académie des Sciences, Série Sciences de la Terre*, **20** (3): 197-204.

WERNICKE, B., 1981.— Low angle normal faults in the Basin and Range province: nappe tectonics in an extending orogen. *Natures, Londres*. **291**: 645-648.

WESTAWAY, R. & KUSZNIR, N., 1993.— Fault and bed "rotation" during continental extension: block rotation or vertical shear?. *Journal of Structural Geology*, **15** (6): 753-770.

YIELDING, G., 1990.— Footwall uplift associated with Late Jurassic normal faulting in the northern North Sea. *Journal of the Geological Society, London*, **147**: 219-222.

ZELICHOWSKI, A.M., CHLEBOWSKI, R., GROTEK, I., KMIECIK, H., KOWALSKI, W. & WOSZCZYNSKA, S., 1983.— The Carboniferous deposition the fault zone of Grojec. *Biuletyn Instytut Geologiczny*, **44**: 57-115.

ZIEGLER, P.A., 1987.— Late Cretaceous and Cenozoic intraplate compressional deformation in the Alpine foreland-a geodynamic model. *Tectonophysics*, **163**: 277-284.

ZIEGLER, P.A., 1990.— *Geological Atlas of Western and Central Europe*. Shell Internationale Petroleum Maatschappij B.V., The Hague: 1-239.

ZYTKO, K., GUCIK, S., RYLKO, W., OSZCZYPKO, N., ZAJAC, R., GARLICKA, I., NEMCOK, J., ELIAS, M., MENCIK, E., DVORAK, J., STRANIK, Z., RAKUS, M. & MATEJOWSKA, O., 1989.— *Geological Map of the Western Outer Carpathians and their Foreland without Quaternary Formations (1:500 000)*. Panstwowy Instytut Geologiczny, Warszawa.

Source : MNHN, Paris

4

The Mid-Cretaceous events in eastern Europe: development and palaeogeographical significance

Evgenij J. BARABOSHKIN [1], *Ludmila F. KOPAEVICH* [1] & *Alexander G. OLFERIEV* [2]

[1] Department of Historical and Regional Geology, Geological Faculty, Moscow State University Vorobjovy Gory: 119899, Moscow, Russia

[2] PGO "Centrgeologia", Geosintez, Varshavskoe Shosse, 39A, 113105, Moscow, Russia

ABSTRACT

Biostratigraphy and regional peculiarities of the Mid-Cretaceous (Albian to Turonian) of the Russian Platform and its south framework are discribed in the paper. The similarity in the fossil content permits the application of the standard west European ammonite and inoceramid zonation and gives a possibility to recognize some of the wide - distributed bio-events (*Turrilites costatus, Praeactinocamax plenus* for example). The fauna assemblages support the idea that the studying area belongs to the eastern part of the European palaeobiogeographical area during the Mid-Cretaceous. At the same time, short-ternt boreal invasions were recognized for the early Albian due to the opening of submeridional seaways. Analysis of sedimentary successions and unconformities of the first order demonstrates eustatic and regional tectonic control of basins history. The sedimentary succession of the Russian Platform reflects the record of the second order sea-level changes. For the Hercynian frame, the tectonical overprint of the sea-level effect is typical. Various combinations of these factors and their consequences resulted in the general style of sedimentation (i.e. palaeogeography) and completeness of geological record. An observation of the main basin events (sedimentary, anoxic and volcanic) demonstrates that all of them did not appear simultaneously, but with a short time - shift.

RÉSUMÉ

Les événements du Crétacé moyen en Europe orientale : développement et signification paléogéographique.

La biostratigraphie et les particularités régionales du Crétacé moyen (Albien à Turonien) de la plate-forme russe et de sa bordure sud sont analysées dans cet article. La similitude du contenu fossile permet l'application de la zonation standard occidentale à ammonites et inocerames et donne la possibilité de reconnaître quelques bio-événements mondiaux (*Turrilites costatus, Praeactinocamax plenus* par exemple). Les assemblages fauniques confortent l'idée que la région étudiée appartient à

BARABOSHKIN, E. J., KOPAEVICH, L. F. & OLFERIEV, A. G., 1998. — The Mid-Cretaceous events in eastern Europe: development and palaeogeographical significance. *In:* S. CRASQUIN-SOLEAU & É. BARRIER (eds), Peri-Tethys Memoir 4: epicratonic basins of Peri-Tethyan platforms, *Mém. Mus. natn. Hist. nat.*, **179** : 93-110. Paris ISBN : 2-85653-518-4.

Source : MNHN, Paris

brèves ont été reconnues pour la base de l'Albien, dues à l'ouverture de zones marines méridionales. L'analyse des successions sédimentaires et des discordances de premier ordre démontrent le contrôle eustatique et tectonique régional de l'histoire du bassin. La série sédimentaire de la plate-forme russe enregistre des changements du niveau de la mer de second ordre. Pour la structure hercynienne, la surimposition tectonique de l'effet des changements du niveau de la mer est typique. Différentes combinaisons de ces facteurs et de leurs conséquences ont pour résultat le style général de la sédimentation (c'est à dire la paléogéographie) et complètent l'enregistrement géologique. L'observation des événements des principaux bassins (sédimentation, anoxie et volcanisme) démontrent que tous n'apparaissent pas simultanément mais avec un léger décalage.

INTRODUCTION

The investigation is a contribution to the "Peri-Tethys Program". It is a synthesis based on numerous previous publications and new data obtained by the authors. Earlier geological studies focused mainly on general stratigraphy and lithological aspects of the subject. Detailed stratigraphy and event analysis were out of interest. The first works on that topic were made for the Russian Platform (SASONOVA & SASONOV, 1967) and then for Mangyshlak and Turkmenia regions (SAVELIEV, 1971; NAIDIN *et al.*, 1984, 1995; TASHLIEV & TOVBINA, 1992). It was demonstrated that different events had different importance in the global sense. Recently comparable data were obtained for the Mid-Cretaceous interval of the Russian Platform and for the Crimean, northern Caucasus and Turkmenian sedimentary basins (Great Balkhan and Tuarkyr; Fig. 1). A preliminary event scale was published in BARABOSHKIN & KOPAEVICH (1996). Several groups of events are discussed in the paper: anoxic events, volcanic events and significant stratigraphical gaps.

FIG. 1.— Map of the position of mentioned localities: **1**, Aksu-Dere and Katcha - Bodrak Rivers sections, north-west Crimea; **2**, Kuma section, northern Caucasus; **3**, Baksan River section, northern Caucasus; **4**, Heu River section, northern Caucasus; **5**, Akusha section, northern Caucasus; **6**, Aksyirtau - Koksyirtau and Shetpe sections, Mangyshlak; **7**, Besokty section, Mangyshlak; **8**, Akkyr section, Tuarkyr; **9**, Kiariz section, The Great Balkhan; **10**, Vorona River section, Riasan - Saratov Trough, Russian Platform; **11**, Ulianovsk section, Simbirsk syneclise, Russian Platform; **12**, Paromonovo section near Moscow, Moscow Syneclise, Russian Platform; **13**, Eza River section near Vladimir, Moscow syneclise, Russian Platform; **14**, Borehole n° 426, Smolensk district, Moscow syneclise, Russian Platform; **15**, Borehole n° 453, Kursk district, Moscow syneclise, Russian Platform.

*FIG. 1.— Carte de localisation. **1**, coupes des rivières Aksu-Dere et Katcha-Bodrak, nord ouest de la Crimée ; **2**, coupe de Kuma, nord du Caucase ; **3**, coupe de la rivière Baksan, nord du Caucase ; **4**, coupe de la rivière Heu, nord du Caucase ; **5**, coupe d'Akusha, nord du Caucase ; **6**, coupes d'Aksyirtau-Koksyirtau et de Shetpe, Mangyshlak ; **7**, coupe de Besakty, Mangyshlak ; **8**, coupe d'Akkyr, Tuarkyr ; **9**, coupe de Kiariz, Grands Balkans ; **10**, coupe de la rivière Vorona, dépression de Riasan-Saratov, plate-forme russe ; **11**, coupe d'Ulianovsk, synclinal de Moscau, plate-forme russe ; **12**, coupe Paramonovo près de Moscou, synclinal de Moscou, plate-forme russe ; **13**, coupe de la rivière Eza près de Vladimir, synclinal de Moscou, plate-forme russe ; **14**, forage n°426, district de Smolensk, synclinal de Moscou, plate-forme russe ; **15**, forage n°453, district de Smolensk, synclinal de Mascou, plate-forme russe.*

Source : MNHN, Paris

BIOSTRATIGRAPHY AND GENERAL SEDIMENTOLOGY

Eastern Europe was a system of communicating epicratonic basins during the Mid-Cretaceous. Geologically the area of investigations belongs to the ancient Russian Platform, the Hercynian Scythian and Turan Platforms and to the Alpine mobile belt in particular (MILANOVSKY, 1987-1991). The only exclusion is the Peri-Caspian Basin that had its own geological history, which does not coincide with the history of the surrounding area. It was already demonstrated that tectonic activity of those regions was strongly different during Mid-Cretaceous time (NIKTSHIN *et al.*, 1998). The investigated Albian through Turonian interval is characterized by various basin events and the main sedimentary change (terrigenous to carbonate) around the Lower/Upper Cretaceous boundary.

ALBIAN

Albian biostratigraphy is based mainly on ammonites for all of the investigated area. All regions could be correlated by the zonation similarity (Fig. 2). It reflects, of course, general characteristics of water mass and climate.

STAGE	SUBSTAGE	BARABOSHKIN, 1996 and 1997, CRIMEA	BARABOSHKIN, in press, NORTH CAUCASUS	BARABOSHKIN, 1996 RUSSIAN PLATFORM	SAVELIEV, 1992, modified by BARABOSHKIN, 1996 and in this paper, MANGYSHLAK & PERICASPIAN	SAPOZHNIKOV, 1973, LUPPOV, 1981, BARABOSHKIN, this paper, GREAT BALKHAN
		ZONE, SUBZONE	ZONE, SUBZONE	ZONE, SUBZONE, BEDS	ZONE, SUBZONE	ZONE, SUBZONE
ALBIAN	UPPER	Stoliczkaia (S.) dispar: Mortoniceras (Durnovarites) perinflatum	Stoliczkaia (S.) dispar: Mortoniceras (Durnovarites) perinflatum	Stoliczkaia (S.) dispar: ?	Stoliczkaia (S.) dispar: Plentahaplites stadeei	Stoliczkaia (Stoliczkaia) dispar & Lepthoplites
		Mortoniceras (Mortoniceras) rostratum	Mortoniceras (Mortoniceras) rostratum	Callihoplites vraconensis	Callihoplites vraconensis	Mortoniceras (Mortoniceras) rostratum & Cantabrigites
		Mortoniceras (Mortoniceras) inflatum	Mortoniceras (Mortoniceras) inflatum	Mortoniceras (Mortoniceras) inflatum	Mortoniceras (Mortoniceras) inflatum	Mortoniceras (Mortoniceras) inflatum
		Hysteroceras varicosum	Hysteroceras varicosum	Semenovites (Semenovites) michalskii	Semenovites (Semenovites) michalskii	Semenovites (Semenovites) michalskii
		Hysteroceras orbignyi	Hysteroceras orbignyi	Semenovites (Semenovites) Semenovites (Planhoplites) pseudocarinatus	Semenovites (Semenovites) Semenovites (Planhoplites) pseudocarinatus	Hysteroceras orbignyi
		Dipoloceras (Dipoloceras) cristatum	Dipoloceras (Dipoloceras) cristatum	Semenovites (Semenovites) tamalakensis	Semenovites (Semenovites) tamalakensis	Dipoloceras (Dipoloceras) cristatum
	MIDDLE	?	Euhoplites lautus	Anahoplites asiticus	Anahoplites asiticus	Anahoplites asiticus
			?	?	Euhoplites lautus	Anahoplites daviesi
			Daghestanites daghestanensis	Hoplites (Lautihoplites) dentatiformis	Daghestanites daghestanensis	Daghestanites daghestanensis
		Anahoplites intermedius	Anahoplites intermedius	Dimorphoplites peetethydis	Anahoplites intermedius	Anahoplites intermedius
		?	Oxytropidoceras roissyanum	Hoplites (Lantihoplites) volgushensis	Haplites (Haplites) spathi	Hoplites (Hoplites) spathi
		Haplites (Haplites) spathi	Haplites (Hoplites) spathi	Haplites (Haplites) spathi		
		?	Lyelliceras (Lyelliceras) lyelli	Hoplites (Hoplites) benettianus	Lyelliceras (Lyelliceras) lyelli	Hoplites (Hoplites) benettianus
			Pseudosaynella (Isohapl.) eodeniata	Pseudosaynella (Isohapl.) eodeniata	Pseudosaynella (Isohapl.) eodeniata	Pseudosaynella (Isohapl.) eodeniata
	LOWER	Dauvilliericeras mammillatum	Dauvilliericeras mammillatum: ?	Dauvilliericeras mammillatum: Otohoplites raulinianus	Sonneratia (E.) sinzowi: Otohoplites raulinianus	Dauvilliericeras mammillatum
			Protohoplites (H.) puzosianus	Protohoplites (H.) puzosianus	Protohoplites (H.) puzosianus	
			?	Cleaniceras (C.) floridum	Sonneratia (E.) vaigni: Sonneratia (E.) caperata	
			Cleaniceras (C.) floridum		Sonneratia (E.) rotula	
			?	?	Sonneratia (E.) salida	
				Sonneratia (G.) perinflata	Sonneratia (G.) globulosa	
		?	Leymeriella (Neoleymeriella) regularis	Leymeriella (N.) regularis: ?	Leymeriella (N.) regularis: Beds with Leymeriella (Neoleymeriella)	Leymeriella (Neoleymeriella) regularis
				Beds with Anadesmoceras	Beds with Anadesmoceras	
		Leymeriella (Leymeriella) tardefurcata	Leymeriella (Leymeriella) tardefurcata	Leymeriella (L.) tardefurcata: ?	Leymeriella (L.) tardefurcata: Leymeriella (Leymeriella) acuticostata	Leymeriella (Leymeriella) tardefurcata
				Aconthoplites (Arcthoplites) jacobi	Aconthoplites (Arcthoplites) jacobi	
				?	Aconthoplites (Subarcl.) probus	

FIG. 2.— Biostratigraphic zonation of the Albian of Crimea, northern Caucasus, Russian Platform, Mangyshlak - Peri-Caspian and Great Balkhan area based on ammonites.

FIG. 2.— Zonation basée sur les ammonites pour l'Albien de Crimée, du nord Caucase, de la plate-forme russe, du Mangyshlak, de la région péri-Caspienne et des Grands Balkans.

Source : MNHN, Paris

The biostratigraphic scheme of Crimea - Northern Caucasus region is close to the "standard" zonation for mediterranean region (HOEDEMAEKER *et al.*, 1995; BARABOSHKIN, 1996). It is also very similar to the zonation of the historical Albian "stratotype" (DESTOMBES, 1979) and to the well-investigated zonation of European province (OWEN, 1996).

CRIMEA

The main peculiarity for Crimea is the great difference between the disposition of plains and mountains and completeness of ammonite successions (BARABOSHKIN, 1996, 1997). Marine sedimentation was more continuous in the plain Crimea than in the mountain Crimea and most of Albian ammonite zones are present there (LESCHUKH, 1992). Albian successions in the plain Crimea are presented mainly by coarse terrestrial facies, being more fine-grained towards the end of the Albian, especially in central Crimea. Terrigenous sedimentation changed into volcanic deposits in the middle Albian (LESCHUKH, 1992), due to the opening of the back-arc rift basin on the border of plain Crimea and Russian Platform (NIKISHIN *et al.*, 1998). Total thickness of Albian sediments varies from 250 to about 1000 m in the depressions of the plain Crimea.

Crimea was mountain region even during Albian time. Sedimentation started there only in the late Albian, in the beginning of *Hysteroceras orbignyi* Chron (YANIN & VISHNEVSKY, 1989; BARABOSHKIN, 1996, 1997) and after a widespread tectonic phase in the end of *Dipoloceras cristatum* Chron (OWEN, 1996). Generally, it coincides with the beginning of Albian transgression in many other regions. Because of the elevated primary position of mountain Crimea, its Albian sequences reflect sea-level falls and rises very sensitively. The basal parts of the terrigenous Albian succession are very coarse and typical for ingressive conditions (YANIN & VISHNEVSKY, 1989). They were replaced shortly by terrigenous-carbonate sedimentation in *Mortoniceras inflatum* Chron (YANIN & VISHNEVSKY, 1989; BARABOSHKIN, 1996, 1997). The latest Albian sequence in mountain Crimea is characterized by terrigenous deposition with thin tuff layers near the Albian/Cenomanian boundary. Total thickness of Albian succession reaches 80-100 m here.

NORTHERN CAUCASUS

Albian succession of northern Caucasus is represented mainly by clays with limestone/marl interbedding, sandy in the base (BARABOSHKIN, 1996). It contains many stratigraphic gaps marked by erosional surfaces, softgrounds and phosphorites. The most complete succession is the Akusha section (Fig. 2) in Daghestan (BARABOSHKIN *et al.*, 1997a). An important feature of Albian successions is the presence of series of strongly dysaerobic to anoxic events represented by "black shales" and the absence of a benthic fauna. Tuff layers are also present in the topmost part of the succession. They have exactly the same position as in the mountain Crimea. Albian sediments reach 100-120 m thick in depressions and are completely eroded in uplifts.

RUSSIAN PLATFORM

Albian deposits of the Russian Platform were observed by many investigators, and a general summary was published by SASONOVA & SASONOV (1967), BARABOSHKIN (1991, 1996) and BARABOSHKIN & MIKHAILOVA (1987). The distribution of Albian sediments is very irregular (BARABOSHKIN, 1996). Even in the depressions and syneclises different parts of the Albian are preserved in different places because of the numerous stratigraphical gaps and unconformities. For example, it was counted up to 30 morphologically expressed gaps (erosion surfaces, softgrounds, etc.) per 0.5 m of succession in some sections of Ryasan - Saratov Trough. This means that complete sections are absent here and that it is very difficult to build up a composite section. The lower Albian is represented by cross-bedded sands with phosphorites in the top. It is preserved in depressions of the central part of the Russian Platform as well as on top of the Voronezh anteclise. The basin was characterised by boreal water masses (with an *Arcthoplites* fauna) during early Albian time. The middle Albian is represented by an anomalously thin succession in comparison with lower and upper Albian

Source : MNHN, Paris

because of the numerous and polyphase gaps. It consists of quartz-glauconite sands rich in phosphorites, which were deposited in waters of moderate temperature (BARABOSHKIN, 1996). The transgressive upper Albian is built up fine-grained sands, silts and clays (as usual) under the influence of warm tethyan water masses (BARABOSHKIN, 1996). Originally upper Albian sediments were widely distributed all over the Russian Platform, hut they were eroded in many of regions during Cenomanian time. The former existence of upper Albian sediments was reconstructed owing to the presence of redeposited phosphatic pebbles in the base of Upper Cretaceous succession. The total thickness strongly varies, but commonly is 20-30 m.

MANGYSHLAK AND PERI-CASPIAN

Albian succession of Mangyshlak and Peri-Caspian is represented by shallow-water terrigenous sediments, mainly by silts and sands with sandstone carbonate concretions. The lower parts of the Albian succession are more fine-grained than the upper ones. Usually the coarsest parts of the section in Mangyshlak belong to the middle - basal upper Albian. They are represented by near-shore cross-bedded sandstones. In opposite, the coarsest interval of Albian successions is occurred in the uppermost Albian in Peri-Caspian. It consists of near-shore to continental cross-bedded sandstones, gravelstones with pebbles and plant remains. It has regional distribution and is not connected with salt diapirism. The most of the sections are incomplete (SAVELIEV, 1971), so we draw up a composite section. Stratigraphic gaps are different in morphology and extent of the stratigraphic hiatus. The most condensed intervals are marked by phosphatic nodules and phosphorite "plates". Very strong condensation is typical for the lower Albian as well as for the uppermost Albian in Mangyshlak, but the main hiatus is dated as the basal upper Albian (SAVELIEV, 1971). This is due to the fact that the base of the upper Albian coincides with the transgressive phase in this area. The upper Albian reflects the regressive phase, during which deltaic and continental facies prograded into the Peri-Caspian basin. This phase was initiated by the compression of the Hercynian Scythian-Turan Platform and upliftings in the South Urals. In the Aktubinsk area of the Peri-Caspian, volcanoclastic sediments are also known in the uppermost Albian (SASONOVA & SASONOV, 1967). The total thickness of Albian sediments reaches 300-400 m up to 1000 m in Mangyshlak and the Peri-Caspian.

GREAT BALKHAN

The Albian succession of the Great Balkhan is similar to that of the Mangyshlak is represented by sandstones, silts and clays. The lower Albian is represented by near-shore cross-bedded sandstones with small phosphorite pebbles, placed above erosional surfaces. Basin deepening is indicated by appearance of clays and silts with interbedded sands near the lower/middle Albian boundary. The basin became more shallow in the lower upper Albian, when cross-bedded phosphorite sandstones appear again. In particular, the succession is similar to the Peri-Caspian, but finally it is characterized by the strong deepening in the uppermost Albian and basal Cenomanian. The succession does not contain volcanoclastic material, nor anoxic levels in comparison with the other basins discussed in the paper. It reflects the shallower conditions of the basin and weak tectonic activity of the region. The total thickness is about 400 m.

CENOMANIAN

CRIMEA

The main peculiarity of the Crimea Cenomanian series is the carbonate composition of the succession: rhythmically - bedded marls and limestones. Marls can have different colours - from light-grey till completely black or dark-grey. The Cenomanian succession is very similar in plain and mountain Crimea except the thickness, which varies from 20-70 m in mountain Crimea up to 500 m in the plain Crimea (Tarkhankut Peninsula). Cenomanian sediments are completely eroded in the Simpheropol city region. The most complete sections consist of two sedimentary successions, which coincide with global cycles of sea-level-changes (KOPAEVICH, 1997). The first one consists of four

Source : MNHN, Paris

lithological units while the second contains three units (NAIDIN & ALEKSEEV, 1981). There is an erosional surface between these successions with the distinctive *Thalassinoides*-type burrows. The bed above is a glauconite marl with about 6-7 cm pebbles of limestones and sandstones of Taurik and Bodrak Formations (Triassic - Liassic). The surface coincides with the "mid-Cenomanian non-sequence", which has very wide distribution (see Fig. 4). The latest Cenomanian is well - marked by the appearance of the black (or dark) marly clays with silt-size quartz grains, glauconite, volcanoclasts, and a complete lack of calcite macro- and microfossil remains (see Fig. 4, Aksu-Dere section). In the other sections the boundary is usually represented by a submarine erosional surface or horizon with intraclasts and "Radiolarian sands". The lower sequence corresponds with the lower Cenomanian and the second one - with the middle and upper Cenomanian. The stratigraphical subdivision of the upper part of middle and upper Cenomanian is based on foraminiferal data only (Fig. 3).

Cenomanian biostratigraphy in Crimea is based mainly on ammonite and inoceramid assemblages (Fig. 3). The biostratigraphic scheme is very close to the "standard" zonation proposed by KENNEDY (1984). Only the uppermost part of the scheme differs since macrofauna is practically absent. The inoceramid scheme is identical to that of Central Europe (TRÖGER, 1989, 1996). The planktic foraminiferal zonation is also very similar to the European "standard" and the Mediterranean zonal scheme (ROBASZYNSKI & AMEDRO, 1980; ROBASZYNSKI *et al.* 1996).

RUSSIAN PLATFORM

Cenomanian deposits are irregularly distributed over the Russian Platform. Different parts of Cenomanian - lower Turonian succession are preserved in different areas due to the numerous stratigraphical gaps and unconformities. Normal marine sedimentation characterizes early Cenomanian time only. The middle and especially upper Cenomanian deposits are strongly condensed and represented by phosphorite horizons, phosphorite plates or are completely missing. This is the reason why the Cenomanian - Turonian composite profile is built up from different sections. The Cenomanian succession is represented only by terrigenous facies, mainly by quartz sand with small phosphorite nodules, fragments of black flints and with *Thalassinoides* burrows. Two phosphorite horizons exist: in the base and in the upper part of the Cenomanian (Fig. 4).

Characteristic fauna of the Cenomanian time is very poor: rare ammonites, remains of bivalves, shark teeth and benthic foraminifera. The first appearance of *Praeactinocamax plenus* marks the base of the upper Cenomanian. The benthic foraminiferal zonation is the same for this region and adjacent areas (VASSILENKO, 1961, AKIMETZ *et al.*, 1992, NAIDIN *et al.*, 1984) and similar to the west European shallow water sections in south England, north Germany, north France and Bohemian Massif (CARTER & HART, 1977; ROBASZYNSKI & AMEDRO, 1980; HRADECKA, 1996). There are several correlative bioevents: appearance of *Gavelinella cenomanica* near the Albian/Cenomanian boundary; appearance of *Lingulogavelinella globosa* at the lower/middle Cenomanian boundary and appearance of *Brotzenella berthelini* inside the terminal part of the Cenomanian succession. *Gavelinella cenomanica* is a very important Cenomanian marker. It represents the most conspicuous component of the Cenomanian assemblage in different geographical regions. First occurrences of this species were reported from upper Albian of France and south England, however, its maximal development falls into the Cenomanian. It also represents the index species of the Cenomanian foraminiferal assemblage not only for the Russian Platform, but also at the Mangyshlak and Peri-Caspian Basin (VASSILENKO, 1961; NAIDIN *et al.*, 1984), Poland and Germany, Bohemian Basin (HRADECKA, 1996). The distribution of this species in the Cenomanian series of Crimea coincides with the distribution of *Rotalipora appenninica*. The first *Lingulogavelinella globosa* appears in the middle part of the succession and indicates beginning of the middle Cenomanian. The upper part of Cenomanian is strongly condensed or is absent. It exists in a few complete sections only and contains poor foraminiferal assemblage, very similar to the one of the *Lingulogavelinella globosa* Zone, but younger, because *Brotzenella berthelini* developed here.

MANGYSHLAK

Cenomanian through middle Turonian exists in terrigenous facies whereas carbonates are present in the upper Turonian - Coniacian of the Mangyshlak. The middle Cenomanian - middle Turonian interval

Source : MNHN, Paris

STAGE	SUBSTAGE	ALEKSEEV, 1989 KOPAEVICH & WALASZCZYK, 1990 CRIMEA		ALEKSEEV et al., 1995 RUSSIAN PLATFORM		NAIDIN et al., 1984; MARCINOWSKI et al., 1996 MANGYSHLAK	
		MOLLUSCA ZONES	FORAMINIFERA ZONES	MOLLUSCA ZONES	FORAMINIFERA ZONES	MOLLUSCA ZONES	FORAMINIFERA ZONES
CON.	LOW.	*Cremnoceramus deformis* / *Cremnoceramus rotundatus*	*Marginatruncana renzi - coronata*	*Cremn. brogniarti* / *Cremn. rotundatus*	*Gavelinella kelleri*	*Cremn. brogniarti* / *Cremn. rotundatus*	*Reussella kelleri* - *Gavelinella praeinfrasantonica*
TURONIAN	UPPER	*Cremnoceramus waltersdorfensis*	*Marginotruncana marginata*	*Cremnoceramus waltersdorfensis*	*Gavelinella moniliformis*	*Mytiloides incertus*	*Ataxophragmium nautiloides*
		Inoceramus costellatus		*Inoceramus costellatus*		*Inoceramus costellatus*	
		Inoceramus lamarcki		*Inoceramus lamarcki*		*Inoceramus lamarcki*	*Gavelinella moniliformis*
		Inoceramus apicalis	*Marginotruncana pseudolinneiana*	*Inoceramus apicalis*		*Inoceramus apicalis*	
		Mytiloides hercynicus		*Mytiloides hercynicus*		*Mytiloides hercynicus*	
	LOWER	*Mytiloides labiatus*	*Helveto-globotruncana helvetica*	*Mytiloides labiatus*	*Gavelinella nana*	*Mytiloides labiatus*	*Globorotalites hangensis*
		Mytiloides mytiloides	*Whiteinella archeocretacea*	*Praeactinocamax plenus* / *triangulus*		*Mytiloides kossmati* / *Mytiloides hattini*	*Whiteinella archeocretacea*
CENOMANIAN	UP.		*Rotalipora cushmani*	*Praeactinocamax plenus plenus*	*Lingulogavelinella globosa*	*Praeactinocamax plenus*	*Brotzenella berthelini*
	MIDDLE			*Inoceramus pictus*		*Acanthoceras jukesbrownei*	*Lingulogavelinella globosa*
		Turrilites costatus		*Turrilites costatus*	*Gavelinella cenomanica*	*Turrilites costatus*	
	LOWER		*Rotalipora deecki*	*Shloenbachia varians*		*Mantelliceras dixoni*	*Gavelinella cenomanica*
		Mantelliceras mantelli	*Rotalipora appenninica*	*Mantelliceras mantelli*		*Mantelliceras mantelli*	

FIG. 3.— Biostratigraphic zonation of the Cenomanian - Turonian of Crimea, Russian Platform and Mangyshlak - Peri-Caspian area based on ammonites (for Cenomanian), inoceramids (for Turonian) and foraminifera.

FIG. 3.— Zonation par les ammonites (pour le Cénomanien), les inocéramidés (pour le Turonien) et les foraminifères du Cénomanien - Turonien de Crimée, de la plate-forme russe, du Mangyshlak et de la région péri-Caspienne.

Source : MNHN, Paris

is characterized by a very reduced sedimentation. Only the lower Cenomanian had "normal" sedimentary rates and a complete record being relatively thick in the most sections. The middle and upper Cenomanian are strongly condensed or missing. There are two phosphoritic horizons inside the Cenomanian: the first one is in the base of Cenomanian and the second one at the lower/middle Cenomanian boundary. The thickness of Cenomanian changes from 35 up to 50 m in the Mangyshlak.

The biostratigraphic division of the Cenomanian of this area based on ammonites and inoceramids. As for Crimea, the ammonite zonation based on the "standard" schemes, proposed by KENNEDY (1984). The inoceramid scheme is the same as in central Europe (TRÖGER, 1989, 1996). Planktic forams are very rare in Mangyshlak and were recognized in the restricted intervals of the sections. Benthic foraminiferas are very abundant, in the contrary, and have long stratigraphical ranges. The base of the Cenomanian is marked by the appearance of the ammonites *Neostlingoceras*, *Mantelliceras* and *Schloenbachia*. The beginning of the middle substage is characterized by the mass occurrence of *Turrilites costatus*. The upper Cenomanian is well developed in isolated sections (Aksyirtau - Koksyirtau) and nicely marked by *Praeactinocamax plenus* event. *Neocardioceras juddi* appears in the top of the Plenus Zone (MARCINOWSKI *et al.*, 1996).

The foraminiferal zonal scheme is based on distribution of benthic taxa and therefore is of limited value for correlation. Luckily, the same levels exist in the Mangyshlak as in the other regions described: (1) the appearance of *Gavelinella cenomanica* near the Albian/Cenomanian boundary; (2) the appearance of *Lingulogavelinella globosa* in the middle Cenomanian and (3) *Brotzenella berthelini* in the upper Cenomanian.

TURONIAN

CRIMEA

In Crimea the Turonian succession is represented only by carbonate sediments. The lower part of the succession consists of marls with flint intercalations at its top. A minute omission surface (1.4 m above the base) and an incipient hardground (2 m above the base) exist in this part. The upper part of the Turonian is built up of marly stylolitic limestones. The thickness of the lower part is 20 m and the thickness the upper part is about 18 m. This succession terminates by a mature hardground (NAIDIN, 1987) with distinctive *Thalassinoides*-type burrows and very hard cemented surface.

The marls and flinty marls belong from the base to the top Mytiloides mytiloides Zone (1), Mytiloides labiatus Zone (2) and Mytiloides hercynicus Zone (3) (KOPAEVICH & WALASZCZYK, 1990). These biostratigraphical subdivisions belong to the lower (1 and 2) and middle (3) Turonian. The lower part of succeeding Stylolitic Limestones represents the Inoceramus lamarcki and I. costellatus Zones of the middle Turonian and Cremnoceramus waltersdorfensis Zone of the upper Turonian (Fig. 4). The upper boundary of the Turonian is recognized by the appearance of *Cremnoceramus rotundatus,* which is assumed to correlate with the entry of *Forresteria petrocoriense* index ammonite of the lower Coniacian. Some events of planktic and benthic foraminifers can be followed from the Crimea to west European sections (e.g., ROBASZYNSKI & AMEDRO, 1980) inside Turonian. They are: (1) the common entrance of numerous *Whiteinella* species; (2) the appearance of *Helvetoglobotruncana helvetica* and *Globorotalites haugeusis* in the lower Turonian; (3) the first appearance of the of the genera *Marginotruncana* and *Gavelinella moniliformis* in the middle Turonian and (4) the appearance of "Grandes *Rosalines*" ex gr. *Marginotruncana coronatarenzi* with *Gavelinella* cf. *vombensis* (Brotzen) (= *G. praeinfrasantonica* (Mjatliuk) around the Turonian/Coniacian boundary (KOPAEVICH, 1996).

RUSSIAN PLATFORM

Turonian sections of the Russian Platform consist of white and light-grey coarse chalk with inoceramids fragments. Two thin layers (2-3 cm) of bentonite exist in the middle and the terminal part of the sections. The thickness of the sections is about 25 m. The upper boundary of the Turonian could be distinguished only by paleontological data.

Source : MNHN, Paris

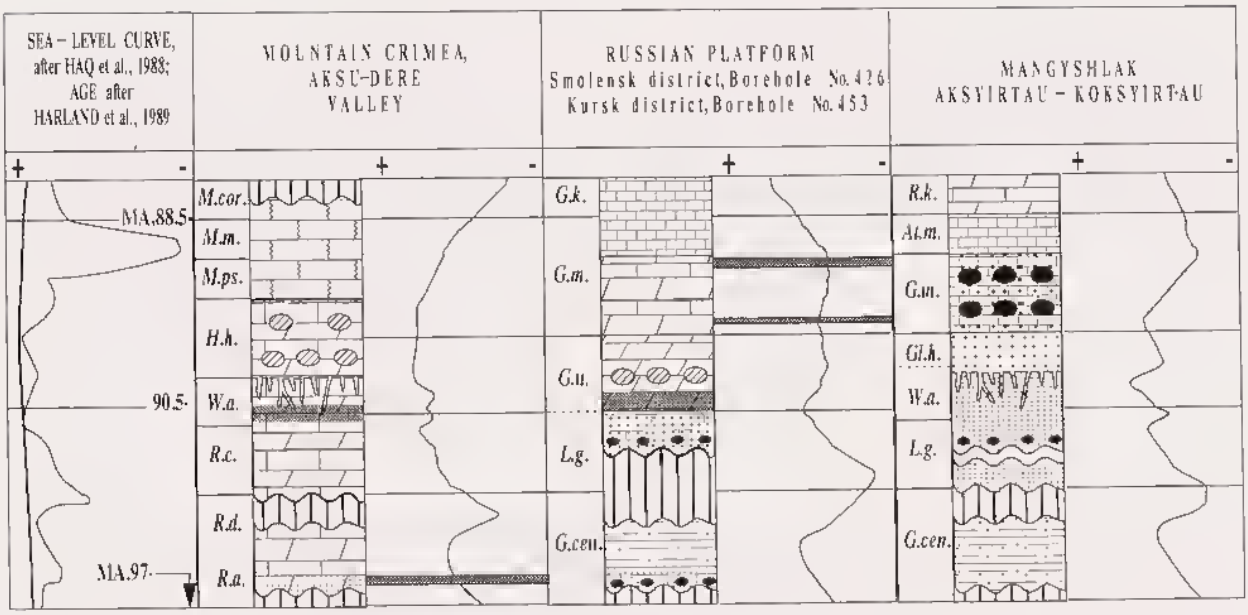

FIG. 4.— Relative sea-level changes, main unconformities and anoxic events for Cenomanian - Turonian of Crimea, Russian Platform and Mangyshlak - Peri-Caspian. Abbreviations in columns mean names of ammonite zones/subzones and horizons illustrated on fig. 3. Same legend as fig. 5.

FIG. 4.— Variations du niveau marin, principales discordances et événements anoxiques pour le Cénomanien - Turonien de Crimée, de la plate-forme russe, du Mangyshlak et de la région péri-Caspienne. Les abréviations dans les colonnes correspondent aux zones / sous-zones à ammonites et aux horizons de la fig. 3. Même légende que fig. 5.

The faunal assemblage is very rich in inoceramids, with zones very similar to the one of Crimea, west and central European regions (Fig. 3). The benthic foraminifera zonation includes the same levels as in Crimea and Mangyshlak. The lower Turonian contains *Gavelinella nana* zonal assemblage, but with high planktic foraminifera content in the base. This assemblage probably coincides with the Whiteinella archeocretacea Zone in Crimea. The abnormal consistence of planktic foraminifera exists near Turonian/Coniacian boundary as well as in the Crimea and Mangyshlak.

MANGYSHLAK

Turonian succession begins by a thin layer of black clays (0.2 m). A second horizon of black clays is placed higher, above 0.9 m of green limy clays and shows *Chondrites* structures. The black clays lie inside poorly cemented siltstones and sandstones. The total thickness is about 10 m.

The overlying lithological unit is built up of yellow-greenish soft marly quartz - glauconite sandstones. Two concretional horizons exist in the lower and middle parts of the succession, which are characterised by inoceramids. The thickness is 25 m.

The following carbonate succession begins with a horizon with numerous dark-brown phosphorite concretions in a sandy marl matrix. The thickness is 0.5 m. The phosphatic concretions are very rare higher in the succession. The numerous fauna, represented by ammonites, echinids and brachiopods, is phosphatized. The top of the succession is represented by coarse "spherical chalk" with hardground surfaces on the Turonian/Coniacian boundary.

Turonian biostratigraphy in Mangyshlak mainly based on inoceramid fauna. The inoceramid zonation is similar to the one of central and eastern Europe. It is more precise than the ammonite zonation for the whole stage. The inoceramid fauna is well represented for both condensed and non-condensed intervals (NAIDIN *et al.*, 1984; MARCINOWSKI *et al.*, 1996). The base of the Turonian is determined by the appearance of *Mytiloides hattini* and the lower Turonian inoceramid zonation

Source : MNHN, Paris

comprises three zones (Fig. 3). The lower/middle Turonian boundary is marked by *Mytiloides hercynicus*, and the base of the upper Turonian coincides with the first occurrence of *Inoceramus costellatus*. The Turonian/Coniacian boundary is determined by the appearance of *Cremnoceramus rotundatus*.

The foraminiferal zonation is as follows: the base of Turonian corresponds to the first planktic foraminiferal Zone - *Whiteinella archeocretacea* and with an anoxic episode; the appearance of *Globorotalites hangensis* is correlated with lower Turonian Mytiloides labiatus Zone; Gavelinella moniliformis Zone coexists with middle Turonian Mytiloides hercynicus - Inoceramus apicalis - Inoceramus lamarcki Zone and upper Turonian Ataxophragmium nautiloides with Inoceramus costellatus - Mytiloides incertus Zones; the Turonian/Coniacian boundary is determined here by the appearance of *Rennsella kelleri* and high content of planktonic species of *Marginotruncana* (Fig. 3).

MAIN BASIN EVENTS

ANOXIC EVENTS

Anoxic events were recognized only for the northern Caucasus area by analysis of total organic carbon content (TOC, made in Moscow State University), magnetic susceptibility ($\Delta\chi = \chi - \chi_t$, made in Palaeomagnetic laboratory of Saratov State University) and fauna palaeocoenoses. Several dysaerobic to anoxic events were recognized in the succession (BARABOSHKIN & KOPAEVICH, 1993).

The analogue of "Paquier Level" (HART *et al.*, 1996) is weakly developed near the base of regularis Zone (Fig. 5). It is characterized by absence of benthic fauna, development of *Chondrites*-beds and fine lamination in clays.

Dysaerobic conditions prevailed in the middle Albian time. This view is supported by the development of a *Actinoceramus (Byrostrina) - Nucula* bentbic bivalve assemblage and high dispersed pyrite content ($\Delta\chi$=60-70 units SI ; BARABOSHKIN *et al.*, 1997b). The level extends from the base of middle Albian up to roissyanum Zone with a maximum in spathi and roissyanum Zones.

For the upper Albian time three dysaerobic events were recognized.

The orbignyi - varicosum Zones are characterized by dysaerobic conditions, where the Actinoceramus *(Byrostrina)-Variamussium-Nucula* benthic bivalve palaeocoenoses changed into an *Ancellina* palaeocoenoses. The maximum of anoxic conditions in this level was reached in the *varicosum* Zone, where $\Delta\chi$ is maximal (=80-90 units SI).

Dysaerobic conditions started in the uppermost part of the inflatum Zone and reached their maximum in the middle of the rostratum Subzone, where $\Delta\chi$=60-80 units SI and TOC=5%. The level is probably the analogue of "Breistroffer Level" (BREHERET & DELAMETTE, 1989). This anoxic event was reflected in *Ancellina* benthic paleocoenosis reduction in the Albian succession of northern Caucasus. In some sections it could be recognized as fine-laminated interval (0.7-1 m) with rare belemnites.

The uppermost anoxic event found in the sections is in the perinflatum Subzone. This event was the shortest one, with $\Delta\chi$=60-70 units SI, about 2% TOC and the same *Ancellina* palaeocoenoses reduction. This event was interrupted locally by volcanic ash "rain".

The development of *Ancellina* paleocoenosis is a typical feature of the northern Caucasus Basin, indicating dysoxic conditions. In the Crimea and Mangyshlak - Great Balkhan areas, *Ancellina* are also present in the sections, but they do not produce great populations because of the quite good bottom oxygenation.

Upper Albian maximum sea-level rise coincides with the maximum of dysaerobic and anoxic conditions in a relatively shallow basin. The model of transgressive "black shales" (WIGNALL & MAYNARD, 1993) could explain the appearance of such conditions, characterized by the coexistence of "normal marine" nektonic and planktonic faunas with poor benthic assemblages.

Anoxic events are more easily recognizable in the Cenomanian time of the Crimea and northern Caucasus areas, due to their lithological peculiarities and high TOC content. The analogue of the "Bonarelli Level" was recognised near the Cenomanian/Turonian boundary. It is characterized by the

Source : MNHN, Paris

existence of organic-rich sediments ("black shales"), the development of *Chondrites* beds and by the absence of benthic fauna. Pre-Cenomanian sediments of these areas are characterised by low TOC content with an important terrestrial component. During the Cenomanian, TOC increased, culminating around the Cenomanian/Turonian boundary. Organic-rich sediments have progressively declined since the Turonian, being replaced by "normal" sediments (GAVRILOV & KOPAEVICH, 1996).

A dysaerobic event can be determined in the base of the lower Turonian in terrigenous facies of Mangyshlak. It is represented by "black clays" with *Chondrites* burrows, rare remains of inoceramid and ammonites. Above, sediments contain an exclusively planktonic foraminiferal assemblage. This is the only planktic zone for the whole Upper Cretaceous in Mangyshlak.

In the Russian Platform the Cenomanian/Turonian anoxic event is not represented in the sections. Only a positive $\delta^{13}C$ isotope shift helps to recognise dysaerobic conditions inside the Lower Turonian succession, coeval with the anoxic event in the other areas.

Thus, Cenomanian/Turonian organic-rich sediments occur in a wide range of different facies from planktic carbonate to terrigenous facies. It is easy to see that all dysaerobic and anoxic events coincide with short-term sea-level changes (Fig. 4) and that the duration of the interval depends from long-term sea-level change.

The same intervals of the Mid-Cretaceous are also characterised in the Atlantic and Mediterrenean regions (REYMENT & BENGTSON, 1986, KUHNT *et al.*, 1992).

VOLCANIC EVENTS

Several volcanic events were recognised in the Crimea - Peri-Caspian region. The most intensive intermediate volcanism developed in the plain Crimea during the rifting stage in this region (NIKISHIN *et al.*,1998). It started in middle Albian time and was most active during late Albian - early Cenomanian times (LESCHUKH, 1992), when volcanic tuffs spread also over the Mountain Crimea.

Tuff layers were recognized in the uppermost Albian (Durnovarites prinflatum Subzone), near the Albian - Cenomanian boundary in Heu River and Baksan River in northern Caucasus. The thickest tuff layer was found in the Akusha and in some other sections of Daghestan (GORBUNOVA, 1966). It is close to the area of intensive Albian - Cenomanian intermediate to basic volcanism in the south slope of the Great Caucasus. There is an evidence that some volcanism was developed in the north-west Caucasus in the late Aptian time (KORNEV, 1965) or, more likely, in the late Albian time. Unfortunately, palaeontological data are very poor and could only be obtained from borehole cores.

The unique evidence of the existence of a tuff layer in the Peri-Caspian (SASONOVA & SASONOV, 1967) is known in the uppermost Albian, near the Albian/Cenomanian boundary. In other sections, the tuff layer is not preserved due to erosion at the beginning of Cenomanian time. It seems that the volcanic ash source was the same as for the north-east Caucasus.

The maximum of the eustasy deduced from mountain Crimea and northern Caucasus series, correlate with the position of the tuffs (Fig. 5). This is quite understandable, because volcanic events were related to the rifting stage of Scythian Platform. For this reason, tuff layers do not exist on the Russian Platform. The latter lay on a rigid basement was not affected by the movements of the north tethyan margin. Hence, the appearance of tuffs in Peri-Caspian is occasional and was possibly due to aerial transport.

In contrast to the Scythian Platform, Mangyshlak - Great Balkhan region developed in a different way during the late Albian time (Fig. 5). The long-term sea-level fluctuation is opposite to that of the Crimea-Caucasus-Russian Platform region as well as to that of the North America continental margin (HAQ *et al.*, 1988). This means that the rifting phase was shifted compared to those areas or did not occur at all. Similar events were reported for western Europe (ZIMMERLE, 1989), where they are supposed have been connected with the Atlantic opening.

Volcanic events can be well recognized in Crimea - Northern Caucasus regions in the early Cenomanian. A bentonite layer exists in lower Cenomanian in the Crimea and northern Caucasus areas (ALEKSEEV, 1989). The volcanic ash sources were placed in the Small Caucasus volcanic arc, where

Source: MNHN, Paris

collision volcanism occurred during Late Cretaceous time. The next volcanic event took place during late Turonian on the Russian Platform (OLFERIEV data, unpublished). The sources of ashes were probably the same as during the Cenomanian. It is puzzling that these bentonite layers are absent in the southern area - Crimea and northern Caucasus.

Clay-rich beds, containing altered volcanic ashes (bentonites), are present in Turonian sediments of the Münster Basin and Lower Saxony region of northern Germany. Analyse of these beds demonstrate that it is possible to correlate individual bentonites and to use them as stratigraphical markers (WRAY *et al.*, 1996).

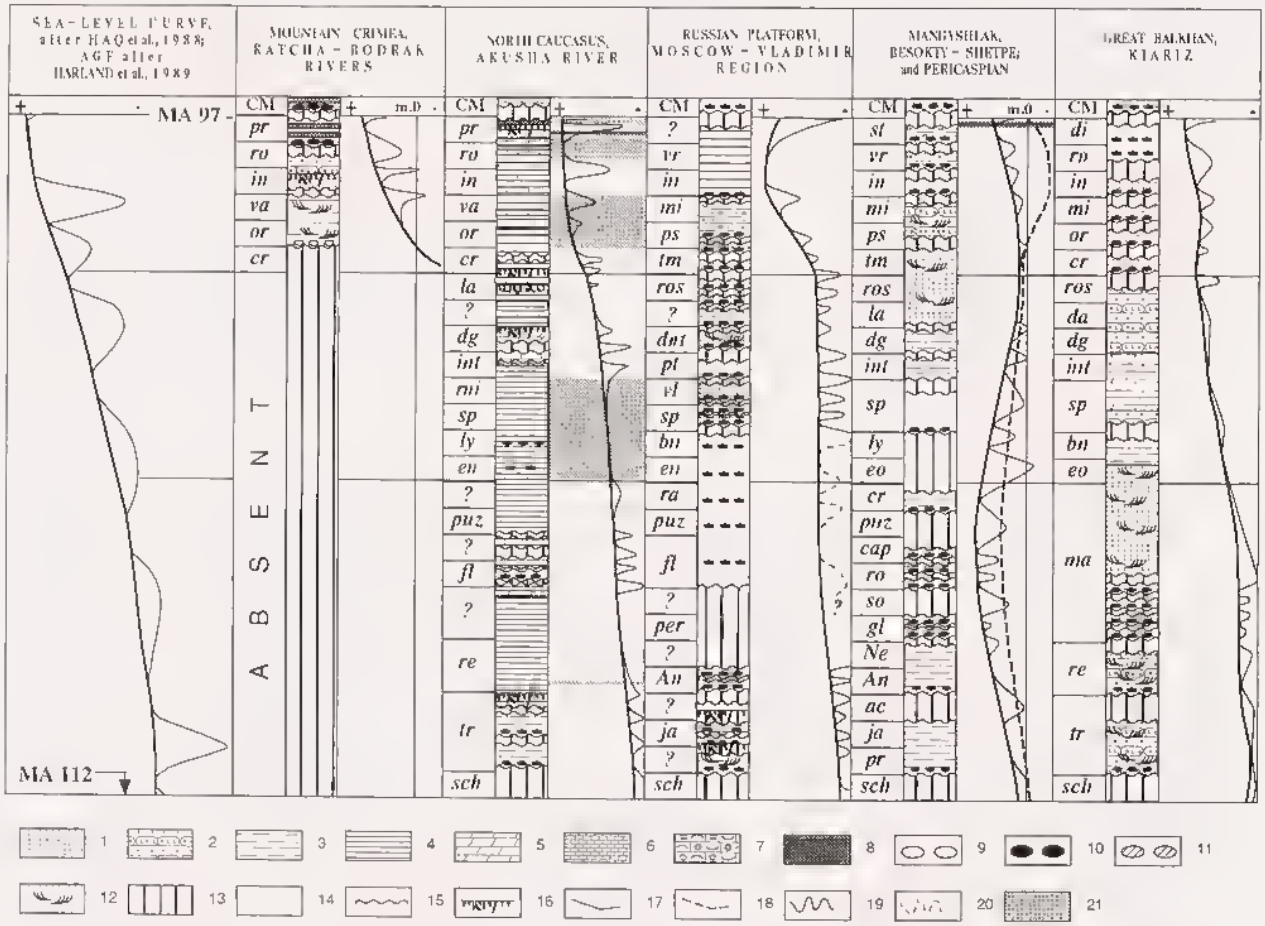

FIG. 5.— Relative sea-level changes, main unconformities, anoxic events and position of volcanoclastic levels in Albian of Crimea, northern Caucasus, Russian Platform, Mangyshlak - Peri-Caspian and Great Balkhan. Abbreviations in columns mean names of ammonite zones/subzones and horizons illustrated on fig. 2. **1**, sands, sandstones; **2**, soft sandstone / hard sandstone alternation; **3**, silts, siltstones; **4**, clays; **5**, marls; **6**, limestones; **7**, shelly oolitic limestones; **8**, tuff layers; **9**, pebbles, conglomerates; **10**, phosphorite pebbles and conglomerates; **11**, flint levels; **12**, cross - bedding; **13**, hiatuses; **14**, eroded intervals, that could be reconstructed from fossil record in the basal horizons; **15**, erosional surfaces; **16**, hard/sofigrounds; **17**, relative sea-level fluctuations of the 1th order; **18**, relative sea-level fluctuations of the 1th order for Peri-Caspian (only); **19**, relative sea-level long-term fluctuations; **20**, assumed relative sea-level short-term fluctuations for reconstructed intervals; **21**, anoxic and dysaerobic intervals.

FIG.5.— Fluctuations du niveau marin, principales discordances, événements anoxiques et position des niveaux volcanoclastiques dans l'Albien de Crimée, du nord Caucase, de la plate-forme russe, du Mangyshlak, de la région péri-Caspienne et des Grands Balkans. Les abréviations dans les colonnes correspondent aux zones / sous-zones à ammonites et aux horizons de la fig. 2. 1, sables, grès ; 2, alternances de grès meubles et indurés ; 3, limons, microgrès ; 4, argiles; 5, marnes ; 6, calcaires ; 7, calcaires oolithiques coquilliers ; 8, niveaux de tuff ; 9, galets, conglomérats ; 10, galets phosphatés et conglomérats ; 11, niveaux siliceux ; 12, stratifications entrecroisées ; 13, hiatus ; 14, intervalles érodés pouvant être reconstruits à partir des fossiles dans les niveaux basaux ; 15, surface d'érosion ; 16, surfaces durcies, surfaces meubles ; 17, fluctuations de 1er ordre du niveau marin ; 18, fluctuations de 1er ordre du niveau marin pour la région péri-Caspienne ; 19, variations à long terme du niveau marin ; 20, variations à court terme supposées du niveau marin pour les intervalles reconstruits ; 21, intervalles anoxiques ou disaérobiques.

Source : MNHN, Paris

STRATIGRAPHIC UNCONFORMITIES

Each of the studied sections reveals numerous stratigraphical gaps which differs in genesis and morphology. The most complete succession is in the northern Caucasus - Crimea area, and the most incomplete is in the Russian Platform.

We can divide stratigraphic gaps in several orders correspondingly to their significance and the area of their development. In this paper we discuss only stratigraphic unconformities of the first order (SU-I), which could he recognised for all of the mentioned regions. SU-I extents from one ammonite zone up to a substage or even more. They were recognized almost in every region at the following levels.

Aptian/Alhian boundary. Everywhere it is represented by a phosphorite conglomerate with reworked Aptian/Albian fauna above an erosional surface (BARABOSHKIN, 1996). Probably the time of non-deposition corresponds to the Proleymeriella schrammeni Zone of Europe. The presence of the Schrammeni Zone in northern Caucasus (MIKHAILOVA & SAVELIEV, 1989) was not supported by the new data. The lowermost Albian beds were recognised there in the Akusha section, where *Leymeriella* (*Leymeriella*) co-occurs with *Hypacanthoplites*. The hiatus corresponding to this SU-I varies from one zone (northern Caucasus sections) up to two zones (Russian Platform and Peri-Caspian sections).

Basal part of the middle Albian. Phosphorite levels in the Eodentata and Lyelli Zones marked short stops in sedimentation in the northern Caucasus. In the Mangyshlak - Peri-Caspian area and in the Russian Platform this SU-I was "erased" in the *Spathi* Chron. during the sea-level rise. This led to the strongest condensation of Albian sediments in the Moscow syneclize, with reworking of the lower-middle Alhian ammonite faunas in a single horizon (BARABOSHKIN, 1996). In the Great Balkhan region, this SU-I was not so significant, but the interval is marked by coarsening of sediments. It seems that this SU-I appeared due to the influx of tethyan waters rather than of boreal ones. It is supported by finds of tethyan ammonites *Lyelliceras* in northern Caucasus and Mangyshlak sections together with European ammonites *Hoplites*.

Basal part of upper Albian. An erosional SU-I unconformity is characteristic for the Dipoloceras cristatum Zone (= Semenovites tamalakensis Subzone of the Russian Platform - Mangyshlak).

An additional and stronger SU-I is recognised for the Hysteroceras orbignyi Zone. It was the time when the low mountainous relief of the Crimea began to be covered by sea (ingressive series). In the Transcaspian area, it is marked usually by cutting and eroding of the sediments below, in the Russian Platform - by the next stage of condensation.

The base of Mortoniceras inflatum Zone. This SU is recognized by the erosion in Mangyshlak - Great Balkhan area (up to Intermedius Zone of the middle Albian), by phosphorite condensation in the Russian Platform (including the whole lower - middle Albian in Ulianovsk section, Simbirsk Syneclise) and by erosion in mountain Crimea. In the northern Caucasus this SU is recognised by the relative coarsening of sections.

Base of Stoliczkaia dispar Zone. A SU-I is recognized by strong condensation in the Mangyshlak - Great Balkhan area, and strong erosion in the Russian Platform. In mountain Crimea this SU was reflected by erosion and deposition of conglomerate member (YANIN & VISHNEVSKY, 1989). Sections of the central northern Caucasus are also marked by an erosional surface and phosphorite - belemnite condensation (Kuma section). Even in Akusha section (the very complete one) sandy rocks were deposited during this SU (BARABOSHKIN *et al.*, 1997a).

Alhian/Cenomanian boundary. This SU exists everywhere, but has a very variable morphology. It is represented by erosional surface and phosphorite condensation in Crimea. In northern Caucasus three phenomena express that SU: (a) erosion, (b) non-deposition and soft-ground development, and (c) phosphorite condensation. Section-to-section those phenomena could be recognized in a 2-3 cm thick interval. In other cases the last phenomenon completely reworked the previous ones. In the Russian Platform and Peri-Caspian the boundary is marked by an erosional surface, and the hiatus is more important, as a rule. The boundary SU is represented by condensed phosphorite horizon in Mangyshlak and Great Balkhan area. The hiatus usually corresponds to one ammonite Zone, but in Tuarkyr (Akkyr

Source : MNHN, Paris

Mountains) it embraces the whole *Stoliczkaia dispar* Zone and the lower-middle Cenomanian. This SU occurs also in Europe (England, France, Germany), Tunisia, and other regions.

A mid-Cenomanian SU is well recognised all over the studied area, but very variable in morphology and the extent of the stratigraphical hiatus. In Crimea the SU is characterized by an erosional surface and a hiatus shorter then one foraminiferal zone. In the North Caucasus mid-Cenomanian SU practically exists in all sections, but the hiatus varies from a part of one zone up to the whole upper Cenomanian. The mid-Cenomanian SU is well represented in the Russian Platform, Peri-Caspian region and Mangyshlak basin, in the terrigenous facies. The phosphoritic horizon marks this SU and the hiatus changes from of part of one biostratigraphical zone to the all upper Cenomanian - lower Turonian interval.

Cenomanian/Turonian boundary. A horizon of condensation or a submarine erosional surface is sometimes situated at the Cenomanian/Turonian boundary. The duration of this hiatus corresponds to the lower part or the whole Whiteinella archeocretacea Zone in Crimea and northern Caucasus. This SU exist in the terrigenous facies of Mangyshlak, even in relatively complete sections. The appearance of stratigraphic gaps could be controlled by short-term sea-level changes (Fig. 4).

DISCUSSION

The combined appearance of different events makes possible to formulate hypotheses about the combined effect of different factors.

TECTONIC MOVEMENTS

Tectonic subsidence rate is the main factor that determines the completeness of the sedimentary record. This is well illustrated by comparison of northern Caucasus and mountain Crimea sections. Aptian/Albian folding movements led drainage of the mountain Crimea, whereas the upper Albian record in that part of the Crimea is much more complete. The rifting processes accelerated the subsidence in the late Albian even in the mountains region. At the same time, northern Caucasus successions were deposited in more stable conditions, far from the shore-line. This resulted in more complete record, but delayed filling of the depressions.

Another effect of tectonic movements is the opening/closing of sea-way connections between different basins (BARABOSHKIN, 1996). This led to the formation of numerous phosphorite levels in the Russian Platform - Mangyshlak area, especially during the early - middle Albian, when cool water penetrated from the Boreal Realm into the northern Tethys shelf area through a system of depressions on the Russian Platform. In other regions, phosphorite horizons are less frequent and are not so rich in phosphate. Local tectonic factors can also have a strong influence on the sedimentary conditions. Albian through Turonian transition was characterized by global warming (REYMENT & BENGTSON, 1986) and overall eustatic sea-level rise (HANCOCK & KAUFFMAN, 1979; HAQ *et al.*, 1988). In the Albian of the Peri-Caspian area, we have an opposite situation in terms of facies. According to us an activation of the Hercynian basement during the Austrian compressional stage led to an accelerated denudation in the south Urals (Mugodzhary) area and intensive deposition in the prograding delta system. This effect was not so strong in the Mangyshlak-Great Balkhan of the Turanian Platform (TASHLIEV & TOVBINA, 1992), because of the different tectonic position, and not so weak as for the northern Caucasus.

The Albian is characterized by an acceleration in tectonic activity. The Cenomanian-Turonian interval is thus be largely controlled by the original basin geometry and eustatic changes. The effects of local tectonics would be rather small though in some places the strata geometry has been influenced by synsedimentary tectonics. In the Russian Platform local tectonics had only a minor influence on the general composition of the studied successions, though the synsedimentary activity of the particular blocks leads to the SU appearance.

Source : MNHN, Paris

VOLCANIC EVENTS

Volcanic events are closely related with tectonic activity. They were initiated by the back-arc rifting stage in the Crimea region and collisional volcanism in the Small Caucasus region. Volcanic sedimentation strongly affected the depositional system, having the avalanche type in the volcanic area. It leads to the intensive water exchange. Probably this was the main reason for the absence of anoxic Albian sediments in the plain Crimea in opposite to the northern Caucasus.

SEA-LEVEL FLUCTUATIONS

Another important factor are long- and short-term sea-level fluctuations. All of the anoxic beds are located in the deepest parts of basins and their appearance was controlled by the first order sea-level changes. This is one of the main reasons, why the strongest anoxic conditions developed during upper Albian time in northern Caucasus: this was the time of a long-term eustatic rise. In other regions it was too shallow for anoxia development (mountain Crimea and Russian Platform) or the relative sea-level trend had an opposite direction. It could be possible when the rate of the tectonical uplift is higher than the rate of the eustasy. Short-term sea-level changes controlled the appearance of stratigraphic gaps in the successions.

Several recent publications deal with the sea-level curves during Aptian - Cenomanian times (ALEKSEEV *et al.*, 1996) and Bajocian - Santonian times for the Russian Platform (SAHAGIAN & JONES, 1993; SAHAGIAN *et al.*, 1996). The former authors are very close to our point while one of the latter publications has been criticized (NAIDIN & BARABOSHKIN, 1994).

CLIMATIC CHANGES

General climatic changes were reflected in the facial record. Almost everywhere in the studied area Albian - lower Cenomanian succession exists in terrigenous facies. Exclusively carbonate deposition took place there since the late Turonian time. An expansion of the warm climate and Tethyan water was the main cause of the depositional break: carbonate sedimentation starts in the early Cenomanian in Crimea, in the middle-late Cenomanian in the northern Caucasus. Carbonate sedimentation appears only in the late Turonian time in the central parts of the Russian Platform, Peri-Caspian and Mangyshlak basins.

The Cenomanian, lower and middle Turonian ammonite assemblages of Mangyshlak and the Peri-Caspian Basins are dominated by hoplitids, schloenbachiids and acanthoceratids of European type (MARCINOWSKI *et al.*, 1996). Heteromorph ammonites, puzosiids, phyllo- and lytoceratids were observed with European forms in the Crimea and northern Caucasus area. This suggests the existence here of deep offshore environments. Foraminiferal assemblages confirm that in Crimea and Caucasus the Cenomanian - Turonian succession contains a significant quantity of planktic foraminifera (about 50-75%). At the same time, Mangyshlak, Peri-Caspian and Russian Platform successions contain assemblages where benthic forms prevail (about 90%: KOPAEVICH, 1989).

Massively ornamented forms are noted within terrigenous facies of the lower and middle Turonian of Mangyshlak. The late Turonian change of the ecomorphic characteristics in ammonites reflects the relative deepening of the basin and the appearance of carbonate sediments (MARCINOWSKI *et al.*, 1996). In this interval the ratio planktic/benthic foraminifera increases also. Thus, the fluctuations of the ammonite and foraminifera assemblages can be described to some environmental conditions (bathymetry) rather than to climatic one.

Source : MNHN, Paris

CONCLUSION

Examination of different event data from the Russian Platform and adjacent areas to the south demonstrate that most of the events were occurred during brief time spans and furthermore did not appear simultaneously. The main causes originating the events were tectonics and sea-level fluctuations forced by climatic changes. Various combinations of these factors and their consequences resulted in the general style of sedimentation (i.e. palaeogeography) and completeness of geological record.

ACKNOWLEDGMENTS

Authors are grateful to Peri-Tethys Program (Grants N° 95/43 and 95-96/43), Programme IGCP 362, INTAS (Grant N° 94-1805) and RBSF foundation (Grants N°95-07-19015, 96-05-657339 and 97-05-567) for the financial support of the investigations.

REFERENCES

AKIMETZ, V.S., BENTAMOVSKY, V.N. & KOPAEVICH, L.F., 1992.— Cretaceous System. Upper Series. The Western part of the European area of the USSR and West Kazakhstan. *In*: B.S. SOKOLOV, A.J. ZIIAMOIDA & M.S. MESEZHNIKOV (eds). *Practical Manual on Microfauna of the USSR*. Vol. 5: *Mesozoic foraminifera*. Nedra Press, Leningrad: 161-191 (in Russian).

ALEKSEEV, A.S., 1989.— The Cretaceous. Upper Series. *In*: O.A. MAZAROVICH & V.S. MILEEV (eds), *Geology of the Kacha Uplifting of the Mountain Crimea. Mesozoic Stratigraphy*. Moscow University Press, Moscow: 123-157 (in Russian).

ALEKSEEV, A.S., OLFERIEV, A.G. & SCHIK, S.M., 1995.— *Explanatory note to the Unificated Stratigraphical Schemes of Upper Cretaceous of the East-European Platform*. MP Devon, Saint-Petersburg: 1-58 (in Russian).

ALEKSEEV, A.S., GORBACHIK, T.N., SMIRNOVA, S.B. & BRAGIN, N.J., 1996.— The age of Paramonovo formation (Albian of the Russian Platform) and the global transgressive-regressive Cretaceous cyclisity. *Stratigraphy and Geological Correlations*, **4** (4): 31-52 (in Russian).

BARABOSHKIN, E.J. & KOPAEVICH, L.F., 1993.— Albian/Cenomanian anoxic, volcanic and bioevents in the Northern Caucasus. *In*: *Global Boundary Events, Abstracts of Interdisciplinary Conference, Kielce, Poland, 27-29 September, 1993*. Polish Geological Institute, Warsaw: 6-7.

BARABOSHKIN, E.J. & KOPAEVICH, L.F., 1996.— Mid-Cretaceous event scale for Peri-Tethys area. *In*: *Peri-Tethys programme in Moscow, Moscow Workshop, January 16-17, 1996*. Moscow State University, Moscow: 5.

BARABOSHKIN, E.J., 1992.— The Lower Albian of Central parts of the Russian Platform. *In*: S.M. SHIK (ed.), *The Phanerozoic Stratigraphy of the Central Part of the East-European Platform*. Tzentrgeologia, Moscow: 20-36 (in Russian).

BARABOSHKIN, E.J., 1996.— Russian Platform as a controller of the Albian Tethyan/Boreal ammonite migration. *Geologica Carpathica*, **47** (5): 1-10.

BARABOSHKIN, E.J., 1997.— The new stratigraphic scheme of the Lower Cretaceous between Kacha and Bodrak River (South-Western Crimea). *Vestnik Moskovskogo Universiteta, serie 4, Geology*, **3**: 22-29 (in Russian).

BARABOSHKIN, E.J., GUZHIKOV, A.J. & EREMIN, V.N., 1997a.— Albian bio- and magnetostratigraphy in Akusha section (Daghestan). Article 1: Biostratigraphy. *Bulletin of Moscow Society of Naturalists, Geological Series*, **72** (1): 30-46 (in Russian).

BARABOSHKIN, E.J., GUZHIKOV, A.J. & EREMIN, V.N., 1997b.— Albian bio- and magnetostratigraphy in Akusha section (Daghestan). Article 2: Magnetostratigraphy. *Bulletin of Moscow Society of Naturalists, Geological Series*, **72** (3): 41-51 (in Russian).

BARABOSHKIN, E.J. & MIKHAILOVA, I.A., 1987.— Albian ammonites and stratigraphy of Northern Podmoskovie. Article 2: Stratigraphy. *Bulletin of Moscow Society of Naturalists. Geological Series*, **62** (6): 91-100 (in Russian).

BREHERET, J.-G. & DELAMETTE, M., 1989.— Correlation between Mid-Cretaceous Vocontian Black Shales and Helvetic Phosphorites in the Western External Alps. *In*: J. WIEDMANN (ed.), *Cretaceous of the Western Tethys: Proceeding 3rd International Cretaceous Symposium, Tübingen 1987*. E. Schweizerbart'sche Verlagsbuchandlung: 637-655.

CARTER, D.J.& HART, M.B., 1977.— Aspect of Mid-Cretaceous stratigraphical micropaleontology. *Bulletin of the British Museum of Natural History, Geology*, **29**: 1-85.

DESTOMBES, P., 1979.— Les ammonites de l'Albien inférieur et moyen dans le Stratotype de l'Albien: gisements, paléontologie, biozonation. *In*: P. RAT *et al.*, *Les Stratotypes français*. Vol. 5. Comité français de Stratigraphie. Paris: 51-194.

Source : MNHN, Paris

GAVRILOV, J.O. & KOPAEVICH, L.F., 1996.— On the geochemical, biochemical and biotic subsequences of the eustatic fluctuations. *Stratigraphy and Geological Correlations*, **4** (4): 3-14 (in Russian).

GORBUNOVA, L.I., 1966.— Volcanic rocks in the Cretaceous deposits of Daghestan. *Lithology and Mineral Resources, New York*: 229-232.

HANCOCK, J.M. & KAUFFMAN, E.G., 1979.— The great transgressions of the Late Cretaceous. *Journal of the Geological Society, London*, **136** (2): 175-186.

HAQ, B.W., HARDENBOL, J. & VAIL, P.R., 1988.— Mesozoic and Cenozoic chronostratigraphy and cycles of sea-level change. *In*: C.K. WILGUS, B.J. HASTINGS, H. POSAMMENTIER, J.C. VAN WAGONER, C.A.ROSS. & C.G.S.C. KENDALL (eds), Sea-level changes: an integrated approach. *Society of Economic Paleontologists and Mineralogists, Special Publication*, **42**: 71-108.

HARLAND, W.B., ARMSTRONG, R.L., COX, A.V., CRAIG, L.E., SMITH, A.G. & SMITH, D.G., 1989.— *A Geologic Time Scale*. Cambridge University Press, Cambridge: 1-236.

HART, M., AMEDRO, F., OWEN, H., AVRAM, E., BARABOSHKIN, E.J., BENGTSON, P., CZAZAR, G., DIAS-BRITO, D., ERBA, E., GALE, A.S., GOROG, A., KAUFFMAN, E.G., KOPAEVICH, L.F., KOTETISHVILI, E., LEEREVELD, H., MACHADO BRITO, I., MARTINEZ, R., MELINTE, M.C., MIKHAILOVA, I.A. & MUTTERLOSE J., 1996.— The Albian Stage and Substage boundaries: Proceedings of Second International Symposium on Cretaceous Stage Boundaries, Brussels, 8-16 September 1995. *Bulletin de l'Institut royal des Sciences naturelles de Belgique, Sciences de la Terre*, **66**-suppl.: 45-56.

HART, M.B. & TARLING, D.H., 1974.— Cenomanian palaeogeography of the North Atlantic and possible Mid-Cenomanian eustatic movements and their implications. *Palaeogeography, Palaeoclimatology, Palaeoecology*, **15** (2): 95-108.

HOEDEMAEKER, P.J., CECCA, F., AVRAM, E., COMPANY, M., DELANOY, G., ERBA, E., ETTACHFINI, M., FARAONI, P., KAKABADZE, M.V., LANDRA, G., MARINI, A., MEMMI, L., PALLINI, G., RAWSON, P.F., POPOLO, P., SANDOVAL, J., TAVERA, J.M. & VASICEK, Z., 1995.— Ammonite zonation for the Lower Cretaceous of the Mediterranean region; basis for the stratigraphic correlations within IGCP-project 262. *Memorie Descrittive della Carta Geologica d'Italia*, **LI**: 213-215.

HRADECKA, L., 1996.— *Gavelinella* Brotzen, 1942 and *Lingulogavelinella* Malapris, 1969 (*Foraminifera*) from the Bohemian Cretaceous Basin. *Sbornik geologickych Ved Paleontologie*, **33**: 79-96.

KENNEDY, W.J., 1984.— Ammonite faunas and "the standard zones" of the Cenomanian to Maastrichtian stages in their type areas, with some proposals for the definition of the stage boundaries by ammonites. *Bulletin of the Geological Society of Denmark*, **33** (1-2): 147-161.

KOPAEVICH, L.F., 1989.— Determination of paleodepth on the base of analysis of planktonic foraminiferal assemblages (on the data from the Upper Cretaceous of Transcaspian region). *Vestnik Moskovskoga Universiteta, Serie 4, Geology*, **3**: 25-34 (in Russian).

KOPAEVICH, L.F., 1996.— The Turonian strata in southwestern Crimea and Mangyshlak (foraminiferal biostratigraphy and palaeobiogeography). *In*: New developments in Cretaceous research topics, Jost Wiedmann Memorial Volume, Proceeding of the 4th International Cretaceous Symposium, Hamburg 1992. *Mitteilungen aus dem Geologisch-Palaeontologischen Institut der Universität Hamburg*, **77**: 203-211.

KOPAEVICH, L.F. & WALASZCZYK, I., 1990.— An integrated inoceramid-foraminiferal biostratigraphy of the Turonian and Coniacian strata in south-western Crimea, Soviet Union. *Acta Geologica Polonica*, **40** (1-2): 83-96.

KORNEV, G.P., 1965.— The Armavir volcanic horizon. *Trudy Krasnodarskogo Filiala Vsesoyuznogo Nauchno-Issledovatelskogo Instituta Nefti*, **16**: 382-410 (in Russian).

KUHNT, W., THUROW, J., WIEDMANN, J. & HERBIN, J.P., 1986.— Oceanic anoxic conditions around the Cenomanian/Turonian boundary and the response of the biota. *Mitteilungen aus dem Geologisch-Palaeontologischen Institut der Universität Hamburg*, **60**: 205-246.

LESCHUKH, R.J., 1992.— *Lower Cretaceous Western and Southern Ukraine*. Naukova Dumka, Kiev: 1-208 (in Ukrainian).

LUPPOV, N.P., 1981.— Stratigraphy of the Middle-Upper Albian of Transcaspia. *Soviet Geology*, **7**: 46-57 (in Russian).

MARCINOWSKI, R., 1980.— Cenomanian ammonites from German Democratic Republic, Poland, and the Soviet Union. *Acta Geologica Polonica*, **30** (3): 215-235.

MARCINOWSKI, R., WALASZCZYK, I. & OLSZEWSKA-NEJBERT, D., 1996.— Stratigraphy and regional development of the mid-Cretaceous (Upper Albian through Coniacian) of the Mangyshlak Mountains, Western Kazakhstan. *Acta Geologica Polonica*, **46** (1-2): 1-60.

MIKHAILOVA, I.A. & SAVELIEV, A.A., 1989.— The Albian stage. *In*: V.A. PROZOROVSKY (ed.), Zones of Cretaceous system in the USSR, Lower series. *Stratigraphical Committee of the USSR*, **20**: 141-217 (in Russian).

MILANOVSKY, E.E., 1987-1991.— *Geology of the USSR*. Part 1-3, MSU, Moscow, 1987: pt. 1, 1-416, pt. 2, 1-271; 1991: pt. 3, 1-272 (in Russian).

NAIDIN, D.P., 1987.— The "Hardgrounds" in epicontinental carbonate sections of Upper Cretaceous. *In*: E.E. MILANOVSKY & I.A. DOBRUSKINA (eds), *Historical Geology: Results and Perspectives*. Moscow University Press, Moscow: 242-262 (in Russian).

NAIDIN, D.P., ALEKSEEV A.S., 1981.— On the importance of the Ocean drilling data for interpretation of sedimentation and fauna mode in the Cenomanian of the Mountain Crimea. *In*: V.A. KRASSILOV (ed.), *Evolution of Organisms and Biostratigraphy of the Mid-Cretaceous*. Biological-Soil Institute, Vladivostok: 7-21 (in Russian).

Source : MNHN, Paris

NAIDIN, D.P. & BARABOSHKIN, E.J., 1994.— On the application of stratigraphic data for the Russian Platform to reconstruct the eustatic sea-level variations in the Jurassic and Cretaceous. *Bulletin of Moscow Society of Naturalists, Geological Series*, **69** (5): 118-127 (in Russian).

NAIDIN, D.P., BENIAMOVSKY, V.N. & KOPAEVICH, L.F., 1984.— *Methods of Transgressions and Regressions Study*. Moscow University Press, Moscow: 1-163 (in Russian).

NAIDIN, D.P., BENIAMOVSKY, V.N. & KOPAEVICH, L.F., 1995.— *Paleogeographical Determination of Stratigraphical Subdivisions*. Moscow University Press, Moscow: 1-136 (in Russian).

NIKISHIN, A.M., CLOETINGH, S., BOLOTOV, S.N., BARABOSHKIN, E.J., KOPAEVICH, L.F., NAZAREVICH, B.P., PANOV, D.I., BRUNET, M.-F., ERSHOV A.V., ILINA, V.V. & KOSOVA, S.S., 1998.— Scythian Platform: chronostratigraphy and polyphase stages of tectonic history. *In*: S. CRASQUIN, É. BARRIER (eds), Peri-Tethys Memoir 3: stratigraphy and evolution of Peri-Tethyan platforms. *Mémoires du Muséum national d'Histoire naturelle*, **177**: 151-162.

OWEN, H.G., 1996.— Boreal and Tethyan late Aptian to late Aptian ammonite zonation and palaeobiogeography. *In*: New developments in Cretaceous research topics, Josi Wiedmann Memorial Volume, Proceeding of the 4th International Cretaceous Symposium, Hamburg 1992. *Mitteilungen aus dem Geologisch-Palaeontologischen Institut der Universität Hamburg*, **77**: 461-481.

REYMENT, R.A. & BENGTSON, P. (eds), 1986.— Events of the Mid-Cretaceous. Final report on Results Obtained by IGCP Project No.58, 1974-1985. *Physics and Chemistry of the Earth*, **16**: 1-209.

ROBASZYNSKI, F., AMEDRO, F. (eds), 1980.— Synthèse biostratigraphique de l'Aptien au Santonien du Boulonnais à partir de sept groupes paléontologiques: Foraminifères, Nannoplankton, Dinoflagellés et Macrofaunes. *Revue de Micropaléontologie, Paris*, **22** (4): 195-321.

SAHAGIAN, D.L. & JONES, M., 1993.— Quantified Middle Jurassic to Paleocene eustatic variations based on Russian Platform stratigraphy: Stage level resolution. *Geological Society of America Bulletin*, **105** (8): 1109-1118.

SAHAGIAN, D.L., PINOUS, O., OLFERIEV, A. & ZAKHAROV, V., 1996.— Eustatic Curve for the Middle Jurassic-Cretaceous based on Russian platform and Siberian stratigraphy: zonal resolution. *AAPG Bulletin*, **80** (9): 1433-1458.

SAPOZHNIKOV, V.B., 1973.— *Stratigraphy of the Lower and Middle Albian of Southern and Western Turkmenia*. Avtoreferat dissertatzii kandidata geologo-mineraloguicheskikh nauk, Leningrad, USSR: 1-25 (in Russian).

SASONOVA, I.G. & SASONOV, N.T., 1967.— Paleogeography of the Russian Platform during Jurassic and Cretaceous period. *Trudy VNIGNI*, **62**: 1-260 (in Russian).

SAVELIEV, A.A., 1971.— On stratigraphical unconformities in the Lower Cretaceous of Mangyshlak. *Bulletin of Moscow Society of Naturalists, Geological Series*, **46** (2): 68-72 (in Russian).

SAVELIEV, A.A., 1992.— *Lower Albian Ammonites of the Mangyshlak, their Phylogeny and Importance for the Albian Zonal Stratigraphy of the South of USSR (Cleoniceras Mangyschlakense Superzone)*. Nedra Publication, Saint-Petersburg: 1-223 (in Russian).

TASHLIEV, M.S. & TOVBINA, S.Z., 1992.— *Cretaceous Paleogeography of Western Parts of Middle Asia*. Nedra Press, Saint-Petersburg: 1-324 (in Russian).

TRÖGER, K.-A., 1989.— Problems of Upper Cretaceous inoceramid biostratigraphy and paleobiogeography in Europe and Western Asia. *In*: J. WIEDMANN (ed.), *Cretaceous of the Western Tethys: Proceedings 3rd International Cretaceous Symposium, Tübingen 1987*. E. Schweizerbart'sche Verlagsbuchandlung: 911-930.

TRÖGER, K.-A., 1996.— Comparison of the Cenomanian through Middle Turonian faunas and facies between Central and Eastern Europe. *Acta Geologica Polonica*, **46** (1-2): 81-88.

VASSILENKO, V.P., 1961.— Foraminifers of the Upper Cretaceous of Mangyshlak. *Trudy VNIGRI*, **171**: 1-437 (in Russian).

WIGNALL, P.B. & MAYNARD, J.R., 1993.— The Sequence stratigraphy of transgressive Black Shales. *In*: B.J. KATZ & L. PRATT (eds), Source Rock in a sequence stratigraphic framework. *AAPG Studies in Geology*, **37**: 35-47 (in Russian).

WRAY, D.S., WOOD, C.J., ERNST, G. & KAPLAN, U., 1996.— Geochemical subdivision and correlation of clay-rich beds in Turonian sediments of northern Germany. *Terra Nova*, **8** (6): 603-610.

YANIN, B.T. & VISHNEVSKY, L.E., 1989.— The Cretaceous. Lower Series. *In*: O.A. MAZAROVICH & V.S. MILEEV (eds), *Geology of the Katcha Uplifting of the Mountain Crimea. Mesozoic Stratigraphy*. Moscow University Press, Moscow: 81-123 (in Russian).

ZIMMERLE, W., 1989.— Vestiges of volcanic activity in Cretaceous sediments of Europe. In: J. WIEDMANN (ed.), Cretaceous of the Western Tethys: Proceedings of the 3rd International Cretaceous Symposium, Tübingen 1987. E. Schweizerbart'sche Verlagsbuchandlung, Stuttgart: 951-987.

Source : MNHN, Paris

Evolution of the eastern Fore-Caucasus basin during the Cenozoic collision: burial history and flexural modelling

Andrei V. ERSHOV [1], *Marie-Françoise BRUNET* [2], *Anatoly M. NIKISHIN* [1], *Sergey N. BOLOTOV* [1], *Maxim V. KOROTAEV* [1] & *Svetlana S. KOSOVA* [3]

[1] Geological Faculty, Moscow State University, Vorobievy Gory, 119899 Moscow, Russia

[2] CNRS ESA 7072, Université Pierre et Marie-Curie, case 129, 4 place Jussieu, F-75252 Paris Cedex 05, France

[3] Central Geophysical Expedition, Moscow, Russia

ABSTRACT

The Late Cenozoic evolution of the eastern Fore-Caucasus molasse basin was controlled by the collisional history of the Caucasus segment of Alpine-Himalayan fold belt. There are two main stages of syncollisional evolution of the basin: (1) 34-15.8 Ma (Maikopian stage) - "soft" collision in the area of Lesser Caucasus, simultaneously with a rapid subsidence of a broad area which could be caused by flow in the mantle induced by a modification in the subduction regime (rotating down of the slab); and (2) 15.8-0 Ma - collisional climax, Great Caucasus orogenesis, accompanied by formation of the molasse basins. This paper presents the mean results of backstripping of 129 wells, a 2D burial history along a seismic section and a 2D flexural model for the eastern Fore-Caucasus molasse basin during the second stage of syncollisional evolution. During the first (Maikopian) stage, investigated basin underwent rapid long wavelength subsidence, nearly homogeneous in the investigated basin, slightly increasing to the south. Palaeowater depths were near 500-800 in the central part and reached 1200 m at the southern edge (estimation proposed with the technique of palaeobathymetric restoration from the shape of clinoforms accounting for the compaction of sediments and regional isostatic compensation). Two-dimensional restoration of the evolution shows the presence of a post-Maikopian uplift, visible by an important erosion in the north of the basin. Two-dimensional flexural modelling demonstrates that observed subsidence of this area at late Miocene - Quaternary time can be explained by an effect of the elastic flexural response of lithosphere, with EET near 60 km, to the loading in the area of Great Caucasus orogen.

ERSHOV, A. V., BRUNET, M.-F., NIKISHIN, A. M., BOLOTOV, S. N., KOROTAEV, M. V. & KOSOVA, S. S., 1998. — Evolution of the eastern Fore-Caucasus basin during the Cenozoic collision: burial history and flexural modelling. *In*: S. CRASQUIN-SOLEAU & É. BARRIER (eds), Peri-Tethys Memoir 4: epicratonic basins of Peri-Tethyan platforms. *Mém. Mus. natn. Hist. nat.*, **179** : 111-130, Paris ISBN : 2-85653-518-4.

Source : MNHN, Paris

RÉSUMÉ

Évolution du bassin du Pré-Caucase oriental durant la collision Cénozoïque: histoire de l'enfouissement et modélisation flexurale.

L'évolution fini-Cénozoïque du bassin molassique d'avant-pays du Caucase oriental a été contrôlée par l'histoire de la collision du segment caucasien de la chaîne Alpes-Himalaya. L'histoire syncollision du bassin comprend deux étapes: (1) 34-15.8 Ma (stade Maikopien) - début de la collision dans la zone du Petit Caucase, simultanément avec une subsidence rapide d'une large zone qui pourrait être due à des mouvements mantelliques induits par une modification du régime de subduction (rotation du " slab " vers le bas); (2) 15.8-0 Ma - climax de la collision, orogenèse du Grand Caucase, accompagnée de la formation de bassins molassiques. Ce papier présente les résultats moyennés du "backstripping" de 129 forages, une reconstitution 2D de l'histoire de l'enfouissement le long d'une section sismique et un modèle flexural 2D pour la portion orientale du bassin molassique d'avant-pays du Caucase pendant le second stade de l'évolution syncollision. Durant le premier stade (Maikopien), le bassin étudié a subi une subsidence rapide de grande longueur d'onde, assez homogène dans l'ensemble du bassin, et s'accroissant légèrement vers le sud. Les paléoprofondeurs étaient proches de 500-800 m dans la partie centrale et atteignaient 1200 m dans la partie méridionale (estimation proposée en utilisant la technique de reconstitution paléobathymétrique à partir de la forme des " clinoformes " tenant compte de la compaction des sédiments et de la compensation isostatique régionale). La reconstitution en deux dimensions de l'évolution met en évidence la présence d'un soulèvement post-Maikopien visible par une érosion importante au nord du bassin. La modélisation flexurale bi-dimensionnelle montre que la subsidence observée dans cette région au Miocène supérieur - Quaternaire peut être expliquée par un effet de réponse flexurale élastique de la lithosphère à la surcharge de l'orogène du Grand Caucase, l'épaisseur élastique équivalente étant proche de 60 km.

INTRODUCTION

The Caucasus region is a part of the Alpine-Himalayan orogenic belt, located between the Black Sea and the Caspian Sea. Tectonically, it can be subdivided into: the Great Caucasus orogen, the western (Indol-Kuban) and eastern (Terek-Caspian) Fore-Caucasus molasse basins (to the north of Great Caucasus), which are separated by the basement uplift (the Stavropol High), and, finally, the western (Rioni) and the eastern (Kura) Trans-Caucasus molasse basins (to the south of Great Caucasus) (Fig. 1).

The area of the eastern Fore-Caucasus molasse basin is well studied. It is a productive oil province with many wells and seismic sections. Extensive literature describes the geology of this region, mainly in Russian. The stages of geological history and the reconstruction of palaeogeography and palaeotectonics are presented briefly in NIKISHIN *et al.* (1998a-b).

In contrast to the geological studies, only a few numerical geodynamical models have been made. ARTEMIEV & BALAVADZE (1973) presented an analysis of isostatic anomalies of the Caucasus region. RUPPEL & MCNUTT (1990) analyzed gravity anomalies in the framework of the model of elastic flexure and reconstructed the flexural rigidity of the lithosphere. MIKHAILOV (1993) made a 2D kinematical restoration and palaeotectonical analysis for the evolution of the Terek-Caspian trough. BOLOTOV (1996) calculated 129 subsidence curves for wells located in the eastern Caucasus molasse basin.

In this paper we present 1D and 2D burial history models of the eastern Fore-Caucasus molasse basin. The results of the kinematic restoration form the basis for flexural modelling.

GEOLOGICAL DATA

This region has for a long time been the object for oil production. Existing data (network of seismic sections, more than thousand wells, heat flow data and gravity data) provide a good basis for modelling. Our kinematic restoration of burial history of the basin was made on the basis of one seismic section and more than one hundred wells, which were averaged to produce a statistically mean burial history for the whole basin.

Source : MNHN, Paris

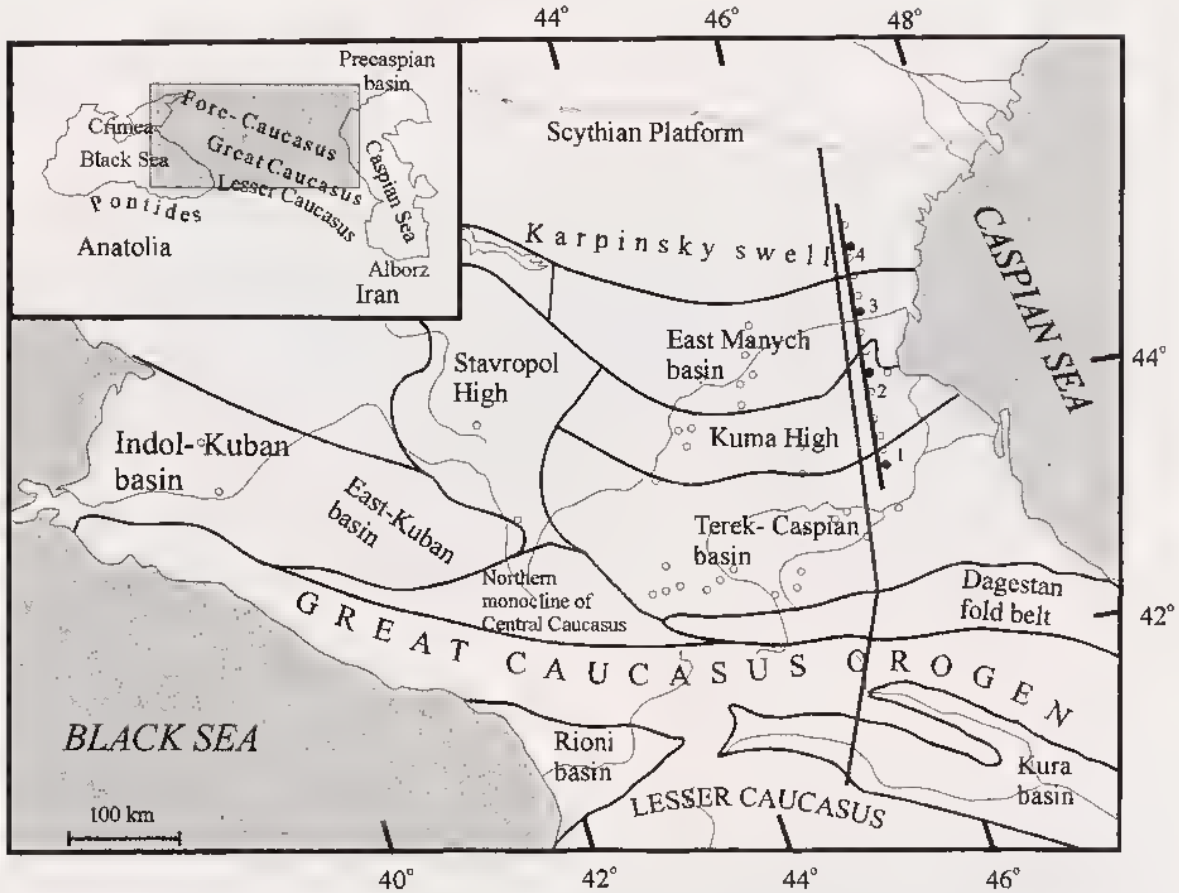

FIG. 1.— Schematic map of investigated area, backstripped wells, seismic section (black line) and synthetic section (grey line). The location of backstripped wells is shown by the open circles (one circle may represent a set of wells in its area). The closed circles show location of wells presented on the figure 5: 1, Zapadno-Aksaiskaya-3, 2, Tarumovskaya, 3, Vostochno-Ozernaya, 4, Profilnaya-8.

FIG. 1.— Carte schématique de la zone d'étude : forages, section sismique (ligne noire) et section synthétique (ligne en grisé). La localisation des forages étudiés par la méthode de backstripping est indiquée par des cercles (un cercle peut représenter un ensemble de forages). Les cercles pleins montrent la localisation des forages présentés sur la figure 5 : 1, Zapadno-Aksaiskaya-3, 2, Tarumovskaya, 3, Vostochno-Ozernaya, 4, Profilnaya-8.

CRUSTAL STRUCTURE

The eastern Fore-Caucasus basin is the eastern part of the Scythian Platform which is situated between the Russian Platform and the Great Caucasus, the Crimean and the Carpathian orogens. The basement of the Scythian Platform is Hercynian in age (LETAVIN, 1980). The main source of information about crustal structure of the region is the deep seismic sounding section Volgograd-Nakhichevan, crossing the eastern part of Caucasus orogen and molasse basins, which was used to produce a crustal section of the investigated region (Fig. 2). The location of this synthetic section (grey line on Fig. 1) is close to the location of the modelled seismic line (black line on Fig. 1) in the northern Fore-Caucasus basin. Geophysical processing of this crustal section was done by KRASNOPEVTSEVA (1984). Unfortunately we do not have new high resolution deep seismic data in this region, details of crustal structure under the Great Caucasus orogen and in the Trans-Caucasus areas are not discriminated. Upper part of the section is constructed on the basis of geological data resulting from field observations in orogenic area, and from seismic and well data in the basins.

We can characterize four layers in the section of the Scythian Platform on the basis of seismic data: (1) Jurassic-Quaternary sediments; (2) Palaeozoic (Hercynian) basement with Triassic inclusions

Source : MNHN, Paris

(seismic velocities 5.3-5.8 km/sec); (3) Precambrian folded rocks with seismic velocities 6.0-6.6 km/sec and (4) lower crust with seismic velocities 6.8-7.2 km/sec. The crust below the Scythian platform is about 40 km in thickness and it thins below the Terek-Caspian basin to about 30 km.

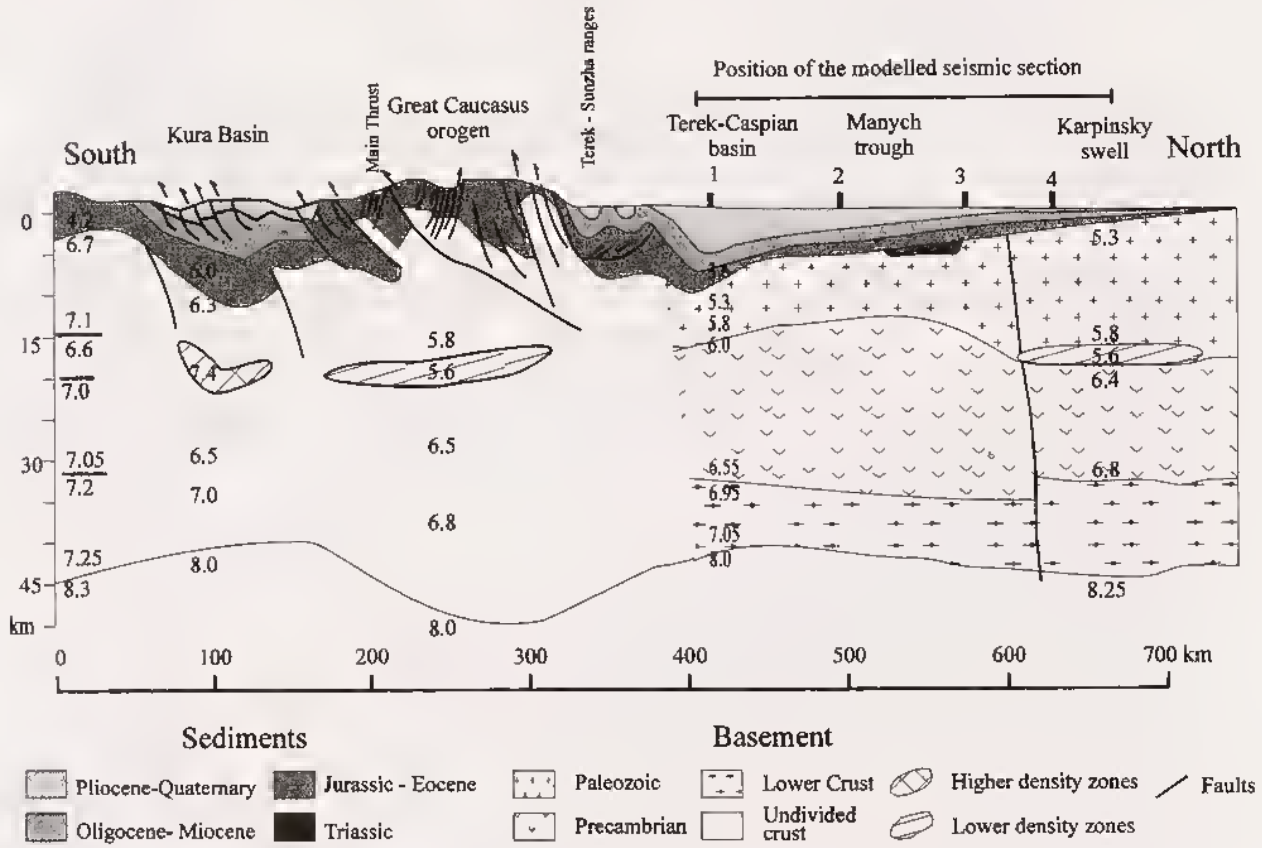

FIG. 2.— Crustal scale synthetic section through the eastern Caucasus and adjacent sedimentary basins. Position of the synthetic section is shown on the figure 1 (grey line). The section is drawn on the basis of deep seismic section Volgograd-Nakhichevan (based on the interpretation of KRASNOPEVTSEVA, 1984). Upper part is constructed on the basis of field geological data in orogen areas, and of seismic and well data in basins areas.

FIG. 2.— Section crustale synthétique à travers le Caucase oriental et les bassins sédimentaires adjacents. La position de la section synthétique est indiquée sur la figure 1 (ligne grisée). La section a été construite sur la base de la section de sismique profonde Volgograd-Nakhichevan (basée sur l'interprétation de KRASNOPEVTSEVA, 1984). La partie supérieure est construite sur la base des données géologiques de terrain dans les zones orogéniques et des données de sismique et de forages dans les zones de bassins.

Palaeozoic rocks are penetrated by the wells in the areas of the Karpinsky swell and the Kuma High (LETAVIN, 1980); this layer thins towards the Great Caucasus. To the north, the bottom of this layer is correlated with the bottom of Palaeozoic sediments (or with top of crystalline basement) on the Russian Platform (KRASNOPEVTSEVA, 1984). On the deep seismic section Stepnoe-Bakuriani (KRASNOPEVTSEVA, 1984, just to the west of our section, not presented here) it is possible to trace the third seismic layer to the surface, where Precambrian crystalline, metamorphic schists, gneisses and Hercynian granitic intrusions are outcropped.

SEDIMENTARY DATA

As a basis for the modelling we have chosen a seismic section traversing the main tectonic units of the eastern Fore-Caucasus molasse basin: the Karpinsky swell, the east-Manych basin, the Kuma High,

Source : MNHN, Paris

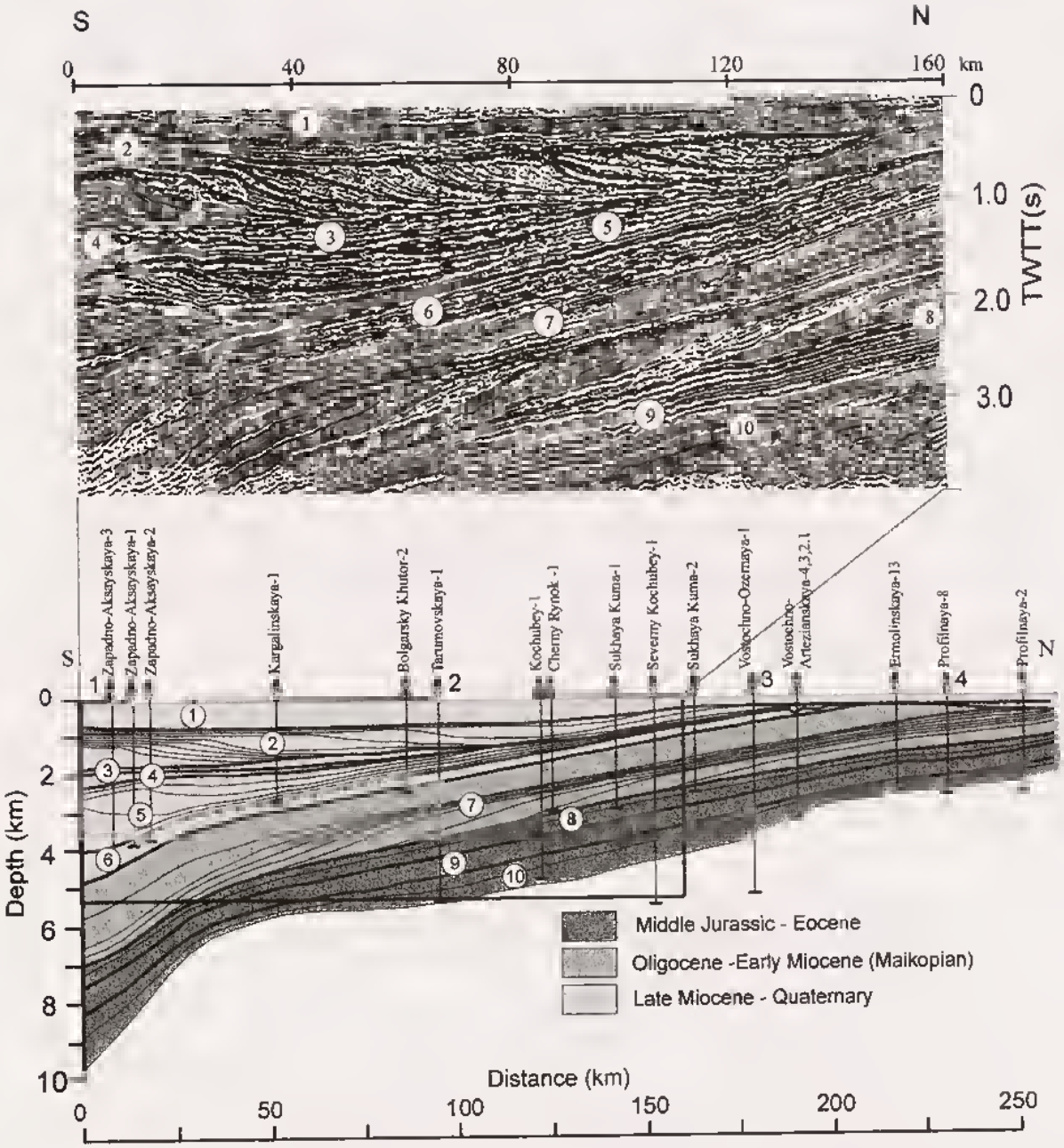

FIG. 3.— Geological section constructed on the basis of regional seismic section V (black line on Fig. 1) and well data (exaggeration 1:10); fragment of the seismic section (horizontal scale in kilometers, vertical scale seconds two-way travel time); numbers 1-4 near the wells denote wells presented on the Fig. 5. The numbers on the sections correspond to units: **1**, Quaternary; **2**, Akchagylian; **3**, Pontian; **4**, Meotian; **5**, Sarmatian; **6**, Chokrakian-Karaganian; **7**, Maikopian; **8**, Palaeocene-Eocene; **9**, Cretaceous; **10**, Jurassic.

FIG. 3.— Coupe géologique construite d'après la section sismique régionale V (ligne noire Fig. 1) et les données de forages (exagération 1 :10) ; fragment de la section sismique (échelle horizontale en kilomètres, échelle verticale en secondes temps double) ; les chiffres 1-4 situés à côté des forages indiquent les forages présentés dans la figure 5. Les chiffres sur les sections correspondent aux unités : 1, Quaternaire ; 2, Akchagylien ; 3, Pontien ; 4, Méotien ; 5, Sarmatien ; 6, Chokrakien-Karaganien ; 7, Maikopien ; 8, Paléocène-Eocène ; 9, Crétacé ; 10, Jurassique.

Source : MNHN, Paris

the Terek-Caspian hasin (Fig. 1). A geological section based on seismic data and a portion of the seismic section are presented on figure 3. We have used the seismostratigraphical interpretation of eastern Caucasus seismic sections made hy KUNTN *et al.* (1990). The section contains three complexes with clinoforms: one each in the lower-middle Maikopian (unit 7), the Sarmatian (5) and the Akchagylian (2) sedimentary complexes. Buried erosional relief is present in the northern part of the section. A detailed seismostratigraphical interpretation of this seismic section, representative of the basin subsidence history, was used to produce a 2D burial history of the basin. Wells situated along the profile were used to validate geological interpretation of the seismic line.

It is difficult to correlate the regional stratigraphic units with the global time scale for the late Eocene - Quaternary time, because a common time scale does not exist for the northern intercontinental basins of Tethys during the Middle-Late Cenozoic time. The use of palaeomagnetic data is problematic because of lack of some parts of section (in the stratigraphical sense), due to numerous erosional events.

For an absolute dating of Maikopian units (Oligocene-early Miocene), we have used the biostratigraphical scale based on the micropalaeontological zonation correlated with mediterranean time scale (POPOV *et al.*, 1993). The early Maikopian part of section is composed by the clinoform bodies. To define time span of deposition of each clinoform, we use the calculations based on the analysis of the total 3D volume of each clinoform (reconstructed from seismic network) and the hypothesis that the rate of clastic material input was constant through time (KUNTN *et al.*, 1990). For late Miocene-Quaternary (13.7-0.5 Ma), the radiometric dating of CHUMAKOV (CHUMAKOV *et al.*, 1992; CHUMAKOV, 1993) was used. It is based on the analysis of ^{235}U fission tracks in volcanic glass from tuffs.

These datations as well as seismic and well data were used to construct a chronostratigraphical chart (Fig. 4) of the basin. The seismic section was used to show general architecture of the basin. Wells situated along seismic line gave informations on the lithological composition and stratigraphy of the basin. It is also shown a comparison of regional units with time scales of HARLAND *et al.* (1989) and ODTN (1994). Scale of ODIN (1994) was used in the modelling. These scales are close for Middle and Late Cenozoic times. In general, lithological composition of the Oligocene-Quaternary sediments is represented by two distinct complexes. The lower complex (Maikopian-Tarkhanian) is composed hy thin clastic sediments (clays and siltstones with rare sandstone lenses). The upper one (Chokrakian - Quaternary) contains mainly limestones, sandstones, marls, siltstones and conglomerates. The Meotian-Pontian part of the section contains numerous unconformities corresponding to hiatuses and erosional events in the basin history during which a part of sediments was removed on the northern side of the section.

SUBSIDENCE EVOLUTION OF THE FORE-CAUCASUS BASINS ON THE BASIS OF BURIAL HISTORY RESTORATION

METHOD

A standard backstripping technique (STECKLER & WATTS, 1978) was used to restore 1D burial histories. The compaction correction was made according to the porosity-depth dependencies, which were calculated using published porosity data for western Caucasus basin (AVCHYAN & OZERSKAYA, 1985). We have supposed an exponential compaction law for five standard lithological types (clay, siltstone, sandstone, limestone and marl) and used least-square fit to obtain statistically averaged compaction dependencies. Obtained parameters of exponential porosity-depth relationships are presented in Table 1.

TABLE 1.— Parameters in exponential porosity-depth dependencies for basic lithotypes, obtained by the least-square fitting of measured porosities in the western Caucasus basins (data from AVCHYAN & OZERSKAYA, 1985); $f=f_0 e^{-z/c}$; f, porosity at depth z; f_0, surface porosity; c, scale factor.

TABLE 1.— Paramètres de dépendance exponentielle de la porosité avec la profondeur pour les lithologies de base, obtenus par un ajustement (méthode des moindres carrés) aux porosités mesurées dans les bassins situés dans la partie occidentale du Caucase (d'après les données de AVCHYAN & OZERSKAYA, 1985); $f=f_0 e^{-z/c}$, f, porosité à la profondeur z, f_0, porosité de surface, c, facteur d'échelle.

Lithotype	Surface Porosity (%)	Scale Factor (km)
Clay	32	3.9
Sandstone	24	6.4
Marl	22	3.6
Limestone	21	2.6
Siltstone	27	4.7

Source : MNHN, Paris

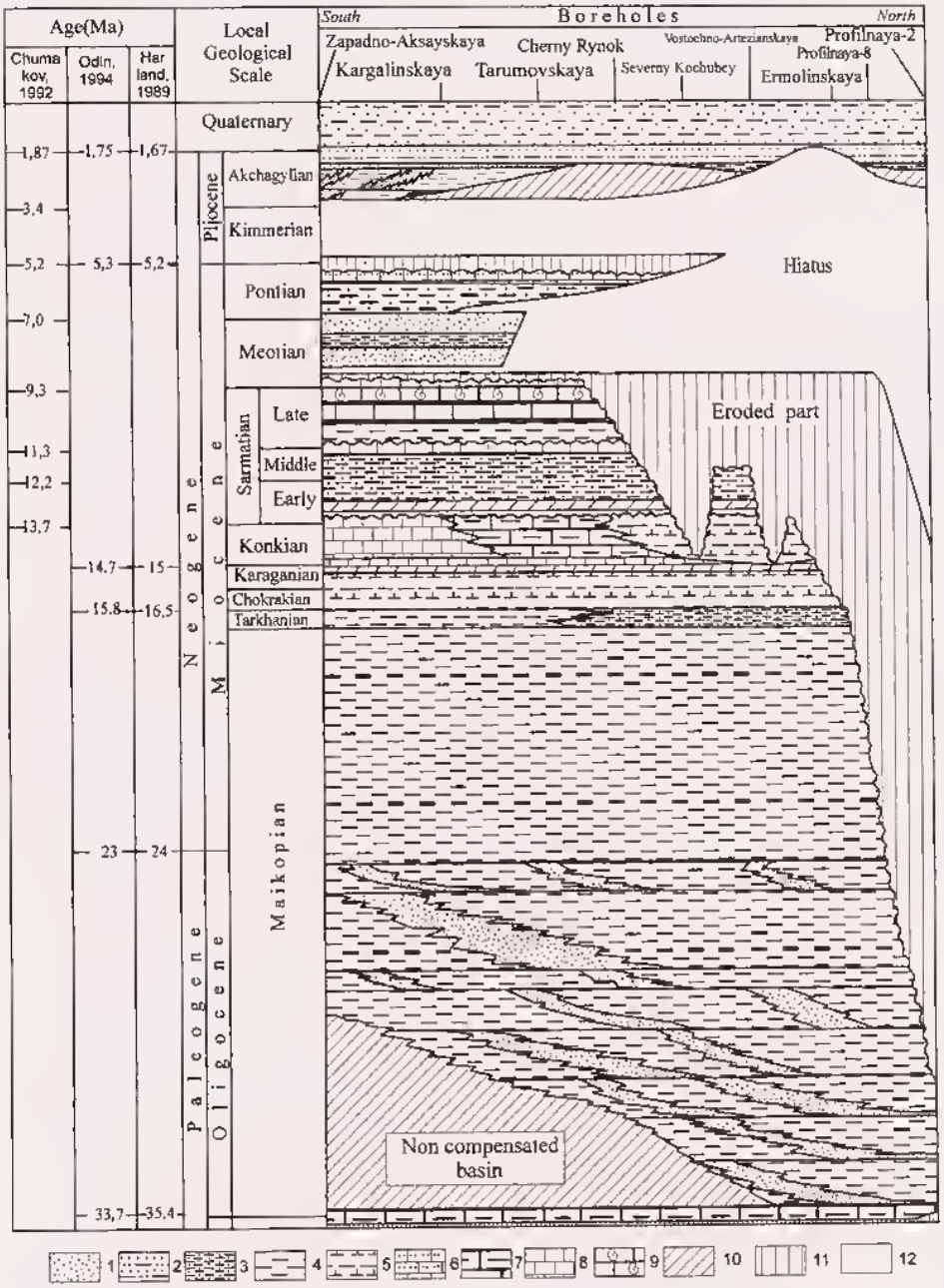

FIG. 4.— Chronostratigraphical chart along seismic section (black line, Fig. 1), time scales of HARLAND *et al.* (1989) and ODIN (1994), datations of CHUMAKOV *et al.* (1992). Legend: **1**, sandstones; **2**, clayey-sandstones; **3**, siltstones; **4**, clays; **5**, clayey siltstones and limestones; **6**, sandy limestones; **7**, clayey limestones; **8**, limestones; **9**, organogenic detritic limestones; **10**, underwater hiatus due to uncompensated sedimentation; **11**, eroded rocks; **12**, hiatus.

FIG. 4.— Charte chronostratigraphique le long de la section sismique étudiée (position ligne noire, Fig. 1), échelles des temps de HARLAND et al. *(1989) et* ODIN *(1994), datations de* CHUMAKOV et al. *(1992). Légende : 1, grès ; 2, grès argileux ; 3, silts ; 4, argiles ; 5, silts et calcaires argileux ; 6, calcaires sableux ; 7, calcaires argileux ; 8, calcaires ; 9, calcaires organogénes détritiques ; 10, hiatus sub-aquatique dû à une sédimentation non compensée ; 11, roches érodées ; 12, hiatus.*

Source : MNHN, Paris

Subsidence curve of one well is often reflecting local tectonic or sedimentation conditions and often may not be a good representative of whole region. We use data and results after the work of BOLOTOV (1996) who calculated subsidence curves on 129 wells in the Fore Caucasus basin. From these data, we have computed an average subsidence curve of the basin. Whole time interval was subdivided into subintervals so that any boundary present in any well was present also in the average curve. For each time span, in this subdivision, the rates of tectonic subsidence and basement subsidence were averaged only for the wells really penetrating this interval of the section. After that the tectonic subsidence and basement subsidence were found by an integration of corresponding rates.

Palaeobathymetric and sea level corrections are not performed on the 1D tectonic subsidence curves due to poor knowledge of absolute values of sea level variation and palaeobathymetry. Knowing also that there were 3 main periods of clinoformal sedimentation, during the Maikopian, the Sarmatian and the Akchagylian, sedimentary thicknesses and palaeobathymetries might be very different from one point to another one and rapidly changing with time. Consequently the changes in tectonic subsidence rates (Figs 5, 6) are the results of a combination of tectonics and conditions of sedimentation. We have restored palaeobathymetries for clinoformal stages in 2D case when it was possible.

To make 2D reconstructions, the section was subdivided into a set of pseudowells and 1D reconstructions were made for each pseudowell, then the section is reconstituted through time with sediments decompacted and palaeowater depths. The main difficulty is the estimation of the palaeobathymetry/palaeotopography. An estimation can be attempted for the clinoformal stages (Maikopian, Sarmatian, Akchagylian) as geometrical shape of clinoforms is correlated with palaeobathymetry. A special algorithm was used to reconstruct palaeobathymetry from the shape of clinoforms allowing to take into account correction for the compaction and regional isostasy.

The clinoform has two parts: shelf and slope. The shelf part is near the sea level during deposition. The problem is to restore palaeobathymetry of the clinoform slope and of the bottom of the deep-water non-compensated basin, not covered by sediments. During its deposition, a clinoform fills the accomodation space created by the subsidence before and during deposition and also by the variation of sea level. We cannot discriminate a general subsidence from a sea level variation and later we will say subsidence, meaning subsidence or sea level variation or their combination. If we can discriminate the subsidence which was existing before from the subsidence during deposition, then we will be able to restore palaeobathymetry. Subsidence appeared during clinoform deposition contains tectonic component and component due to loading of clinoform itself. For the simplicity, as a first order approximation, we suppose that tectonic component of subsidence during deposition is constant or proportional to the total thickness of whole layer composed by the clinoforms, along the horizontal axis. In this case we can define it from the thickness of the shelf part of following clinoform which is overlapped by shelf parts of preceding one, because bathymetry of shelf part is known.

Let us suppose that the bathymetry of the layer deposited after a considered clinoform is known. Then we can restore the bathymetry during the deposition of clinoform by subtraction of thickness of above layer from its bathymetry and adding tectonic and isostatic components of subsidence during deposition of the clinoform. Starting from the layer with known bathymetry (it may be layer of the end of clinoformal stage when all the basin is filled by the sediments) we can subsequently restore palaeobathymetry for each clinoform backstripping them step by step and performing corresponding corrections for the compaction, subsidence/sea level variation during the deposition of the clinoform and isostasy. We have performed such procedure for the Maikopian and the Akchagylian stages, using regional isostatic corrections (EET: 60 km).

On the modelled section some layers in the northern part are partly removed due to erosion. The thicknesses of eroded parts of these layers were restored by the interpolation of thickness of remaining parts. The interpolation was performed for the Maikopian, the Chokrakian and the Sarmatian layers.

RESULTS

The burial histories of four selected wells along the studied section are presented on figure 5. The location of these wells is shown on figure 1 and on the section on figures 2 and 3. A statistically averaged burial history of the basin is presented on figure 6, after the work of BOLOTOV (1996) on the

Source : MNHN, Paris

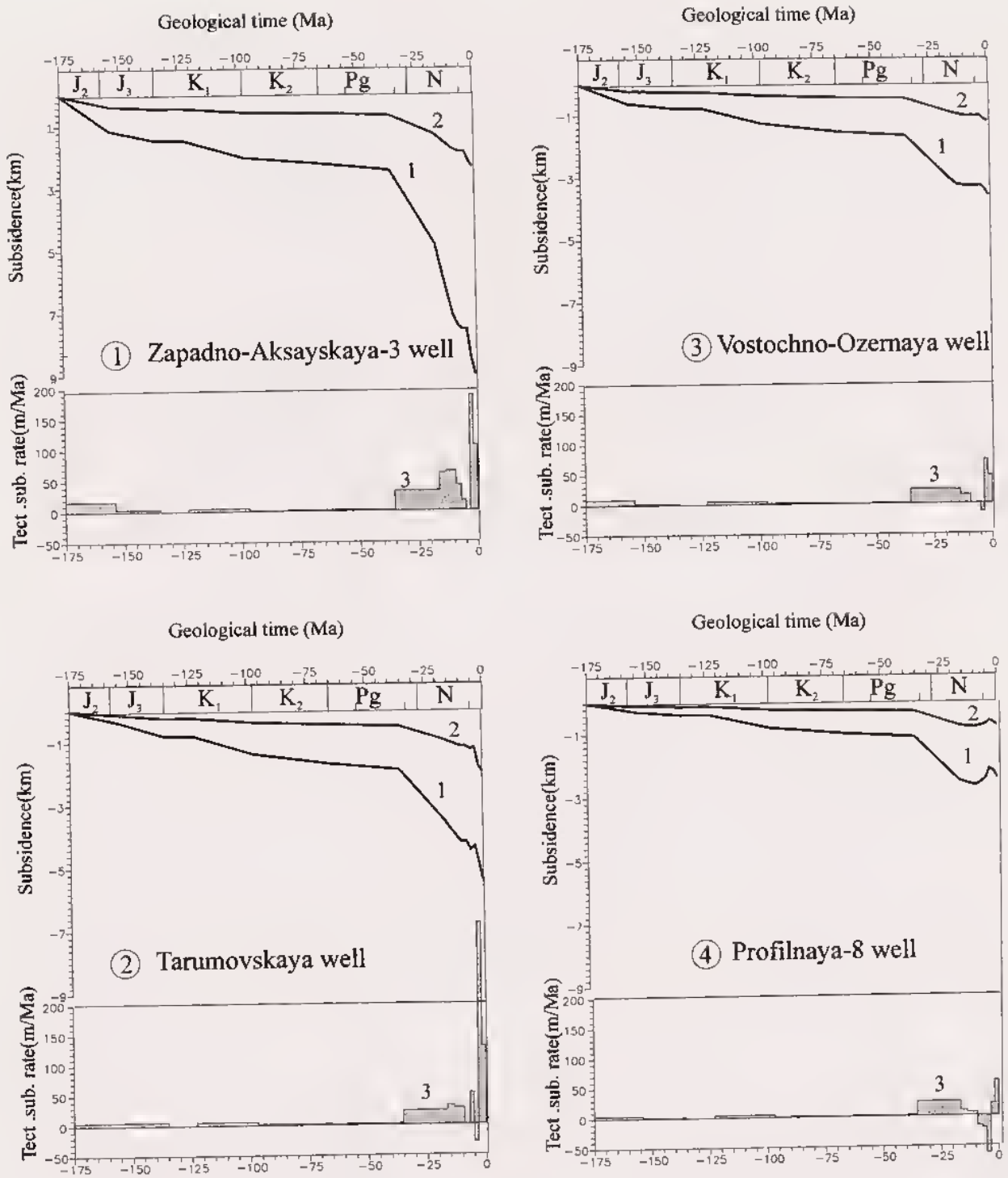

FIG. 5.— Burial history (basement subsidence [curve 1], tectonic subsidence (air-loaded, ρ_m=3.3 g/cm^3) [2] and rate of tectonic subsidence [3]) for 4 selected wells near the seismic section studied in eastern Fore-Caucasus basin: **1** Zapadno-Aksaiskaya-3, **2** Tarumovskaya, **3** Vostochno-Ozernaya, **4** Profilnaya-8. Location of wells is shown on the figure 1 by the closed circles with numbers and on the figure 3. Lower part of Zapadno-Aksaiskaya well is synthetic, constructed on the basis of seismic section.

FIG. 5.— Histoire de l'enfouissement (subsidence du socle [courbe 1], subsidence tectonique (à l'air libre, ρ_m=3.3 g/cm^3) [2] et taux de subsidence tectonique [3]) pour 4 forages proches de la section sismique dans le bassin oriental du Pré-Caucase : 1 Zapadno-Aksaiskaya-3, 2 Tarumovskaya, 3 Vostochno-Ozernaya, 4 Profilnaya-8. La position des forages est montrée sur la figure 1 par les cercles pleins numérotés et sur la figure 3. La partie inférieure du forage Zapadno-Aksaiskaya est synthétique, construite d'après la section sismique.

Source : MNHN, Paris

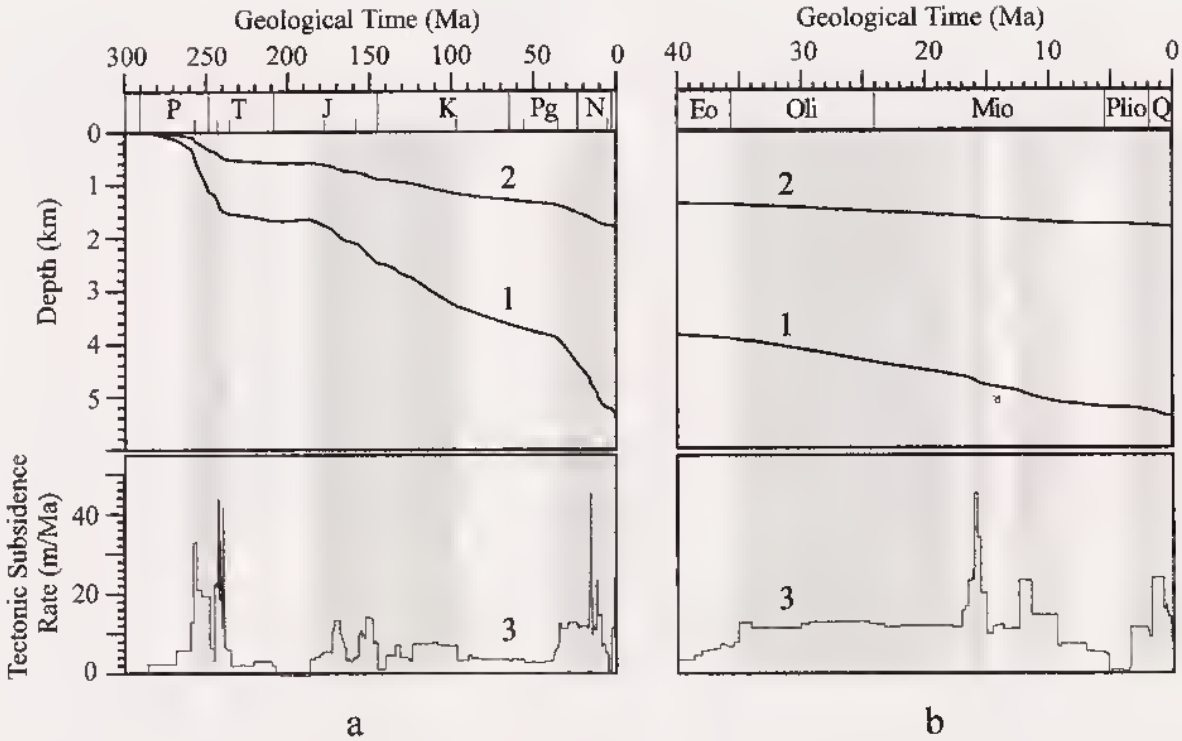

FIG. 6.— Burial history (basement subsidence and rate of tectonic subsidence) averaged for 129 wells (after BOLOTOV, 1996) in the eastern Fore-Caucasus basin (location of wells is shown on figure 1). **a)** for Permian-Quaternary time interval, **b)** more detailed for end of Eocene-Quaternary interval (time scale of HARLAND *et al.* (1989)). The grey areas indicate periods of increased subsidence rate discussed in the text.

FIG. 6.— Histoire de l'enfouissement (subsidence du socle et taux de subsidence tectonique), moyennée pour 129 forages (d'après BOLOTOV, 1996) dans le bassin oriental du Pré-Caucase (la position des forages est montrée sur la figure 1). a) pour l'intervalle de temps Permien-Quaternaire, b) avec plus de détails pour l'intervalle de temps fin de l'Eocène-Quaternaire (échelle des temps de HARLAND et al. *(1989). Les zones en grisé indiquent les périodes d'augmentation du taux de subsidence discutées dans le texte.*

subsidence curves of 129 wells, using the time scale of HARLAND *et al.* (1989). Subsidence curves for Permian-Quaternary time interval are shown on figure 6a ; figure 6b presents a portion of the figure 6a for the end of Eocene-Quaternary interval. Chronostratigraphical chart (Fig. 4) and two-dimensional (Fig. 7) along the seismic section (black line, Fig. 1) illustrate the 2D late Palaeogene - Neogene burial history of the basin. As our main subject is Late Cenozoic history of the basin we will describe previous stages only briefly.

The Mesozoic history of the basin started with Triassic riftogenesis and subsidence of the whole basin during postcollisional relaxation of Late Palaeozoic Scythian orogen (NIKISHIN *et al.*, 1998b). The Triassic history is not well known because the most part of Triassic sediments was removed during orogeny in Late Triassic - Earliest Jurassic and only some remnants of deformed Triassic sediments are preserved. Next major subsidence event occurred during the Middle - Upper Jurassic (Figs 5, 6) as a result of rifting with maximum of extension located in the area to the south, which led to formation of the Great Caucasus basin (NIKISHIN *et al.*, 1998a-b). During the remaining of Cretaceous and Palaeocene-Eocene, investigated region was a part of the shelf basin of the East European Platform opening into the deep-water Great Caucasus basin (SCHERBA, 1993). A decrease of the subsidence is observed at this time (Figs 5, 6). Such quiet and decreasing subsidence is characteristic for the postrift basins and we speculate that this subsidence was caused by the thermal cooling of lithosphere.

At the end of Eocene, sediments were deposited in shallow water environment (KORONOVSKY *et al.*, 1987). The Eocene/Oligocene boundary is pointed by a fall of the eustatic sea level which caused a separation of the northern part of Tethys named Paratethys (BALDI, 1980). At the same time, in the eastern part of Paratethys, a specific deep water Maikopian basin was formed. Subsidence of the basin

Source : MNHN, Paris

was nearly homogeneous with a slight tilting towards the south (Fig. 7A-D). Water depth estimations are ranging from 500 to 1000 m, on the basis of palaeontological criteria (SCHERBA, 1993). Our estimations based on the shape of clinoforms (as it is described above) give values 500-800 m in the central part of the modelled section and up to 1200 m in its southern part (Fig. 7A-B). During the early and middle Maikopian time, the basin was filled by clinoforms prograding from the north-east (Fig. 7A-B) and later the basin continued to subside (Fig. 7 C). In the early Miocene, after filling of the basin by sediments, the palaeowater depths were not deep in the investigated area. From a total amount of near 2 km of the Maikopian subsidence, approximately 1.3 km is induced by loading of sediments and 0.7 km is of tectonic origin.

On the basis of analysis of subsidence curves and 2D restoration, we can separate two main stages in the Oligocene-Quaternary evolution of the basin: an Oligocene-early Miocene (34-15.8 Ma) (Maikopian) stage and a late Miocene-Quaternary (15.8-0) (orogenic) stage. The latter stage began with a short Chokrakian-Karaganian (15.8-15 Ma) event of rapid subsidence (Figs 5, 6). Another event of high subsidence rates took place in the middle-late Sarmatian (12.2-9.3 Ma) (Figs 5, 6). It was coeval with significant changes in the palaeogeography, when the eastern segment of the Great Caucasus orogen was exposed palaeogeographically as a continental area, fans of conglomerates and reefs were formed on the periphery of the orogen (KORONOVSKY *et al.*, 1987). In plane configuration of the basin was changed (NEVESSKAYA *et al.*, 1984), shape of the basin became asymmetrical with deepening towards the orogen (Fig. 7 D-E).

The Meotian-Pontian-Kimmerian time is characterized by alternating periods of opening and closing of the eastern Paratethys and associated variations of sea level (NEVESSKAYA *et al.*, 1984). During most of this time the basin was in continental conditions and periods of sedimentation were interlaced with erosional periods (Fig. 4). Thicknesses of Meotian-Pontian sediments are small (Figs 3, 7 F), they are composed mainly by clastic material (Fig. 4) which was transported by slope sliding from the Great Caucasus orogen. The most significant fall of sea level occurred in the middle-late Pontian (6.5-5.6 Ma) and led to separation of the Palaeo-Caspian sea from the Palaeo-Black sea (NEVESSKAYA *et al.*, 1984). This event is correlated with the Messinian event in the Mediterranean sea (CHUMAKOV, 1993). Kimmerian (5.2-3.4) sediments are absent everywhere in the basin (Fig. 4).

Small thicknesses of the Meotian-Pontian sediments can be explained either by the small subsidence at this time or by the small input of clastic material from the Caucasus. The Meotian and Pontian sediments have a shape similar to clinoform, but as sedimentation occurred in continental conditions by slope sliding, its upper part is not necessarily horizontal and may be inclined. Even if we suppose that inclination is small (basing on the small rate of sedimentation) we can restore palaeotopography only at the southern part of the section as its northern part is eroded. The only possible thing is to restore Pre-Akchagylian topography. The rapid rise of sea level in the Akchagylian (3.4-1.8 Ma) led to the clinoformal sedimentation, when clinoforms filled the accommodation space created before (Fig. 7 G-H). We can suppose different ways of subsidence before Akchagylian: either the accomodation space filled by the Akchagylian clinoform was created just before the Akchagylian as a result of abrupt tectonic processes or it was formed continuously during the Meotian-Pontian-Kimmerian due to gradually increased loading of Caucasus. Data do not allow to discriminate between these two hypotheses.

To the north of the molasse basin a peripheral bulge uplifted and this uplift led to the erosion of the northern part of the section (Figs 4, 7 F-G). We cannot discriminate the time of beginning of uplift as related part of the section is removed. It is possible only to say that it began not in Maikopian but probably after Chokrakian, as thicknesses of these layers are constant on the most part of the section and not decreasing gradually but sharply truncated by the erosional boundary. The amplitude of the erosion in the northernmost part of the section is more than 1 km and the erosion had lasted some time to be able to remove such large amount of sediments, therefore uplift began at least several million of years before the Akchagylian when sediments covered the erosional palaeorelief (Fig. 7 H). Such logical argumentation allows us to put beginning of uplift into Sarmatian-Pontian interval of time.

In the Quaternary the whole basin, including its northern flank, has subsided and was covered by sediments (Fig. 7 I). The Late Quaternary is characterized by a fall of sea level and now the basin is in a continental environment.

Source : MNHN, Paris

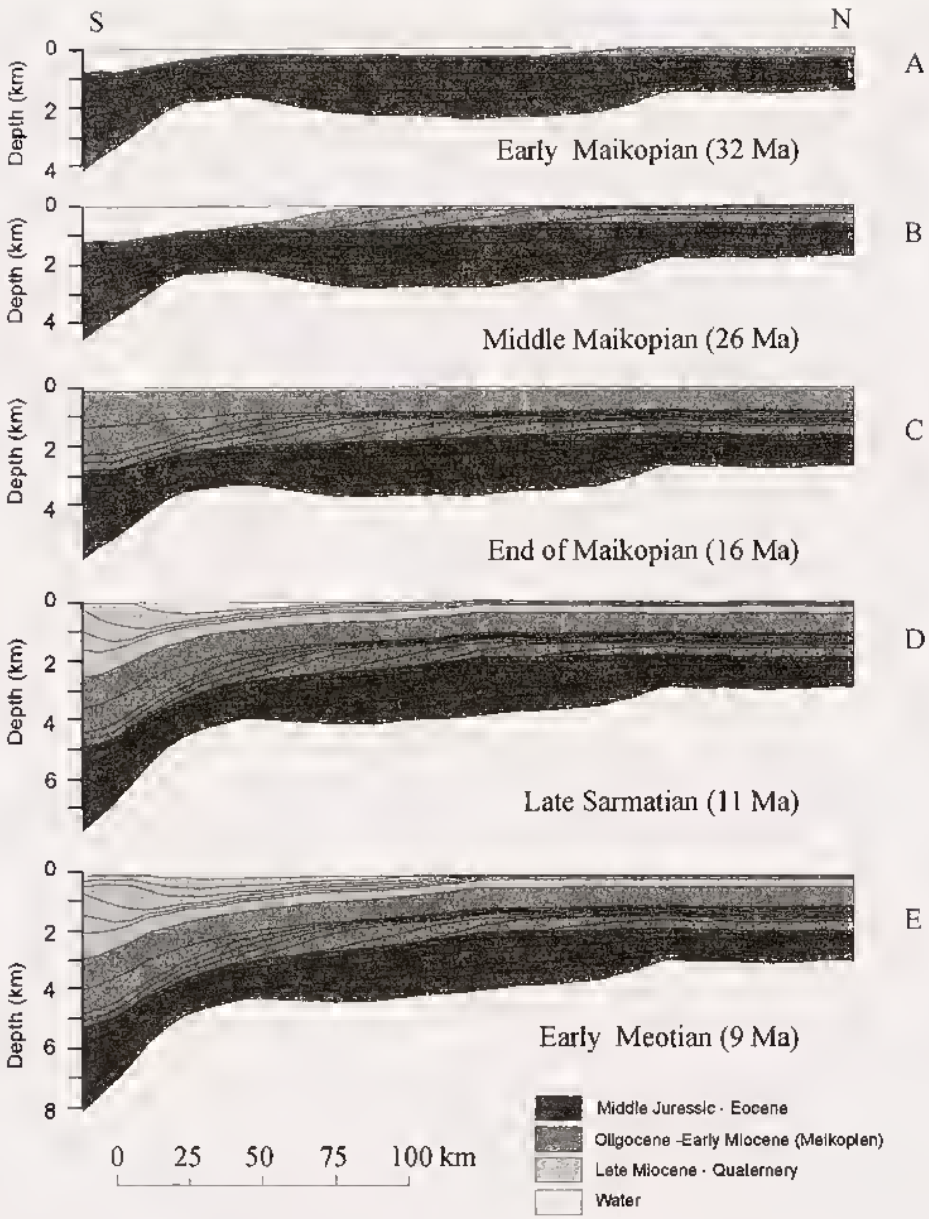

FIG. 7.— 2D burial history restoration along the section (black line, Fig. 1) shown on figure 3. The chronostratigraphical chart along the section is shown on figure 4; selected time slices for Oligocene-Quaternary (34-0 Ma).

FIG. 7.— Reconstitution de l'histoire de l'enfouissement en 2D le long de la section (ligne noire, Fig. 1) présentée sur la figure 3. La charte chronostratigraphique le long de la section est montrée sur la figure 4 ; étapes sélectionnées dans l'intervalle de temps Oligocène-Quaternaire (34-0 Ma).

GEODYNAMICAL MODEL

Late Cenozoic geodynamics of the Fore-Caucasus basin is a part of collisional dynamics of a more general region. The collisional history of the Caucasus region is not well constrained by data yet and several different interpretations exist (e.g. KORONOVSKY *et al.*, 1987; BELOV & SATIAN, 1989; DERCOURT *et al.*, 1993; ZONENSHAIN *et al.*, 1990). Here we follow the recently published interpretation of NIKISHIN *et al.* (1998a-b). A scheme, illustrating the collisional history of Caucasus and giving the geodynamic context of the area through time, is presented on the figure 8.

Source : MNHN, Paris

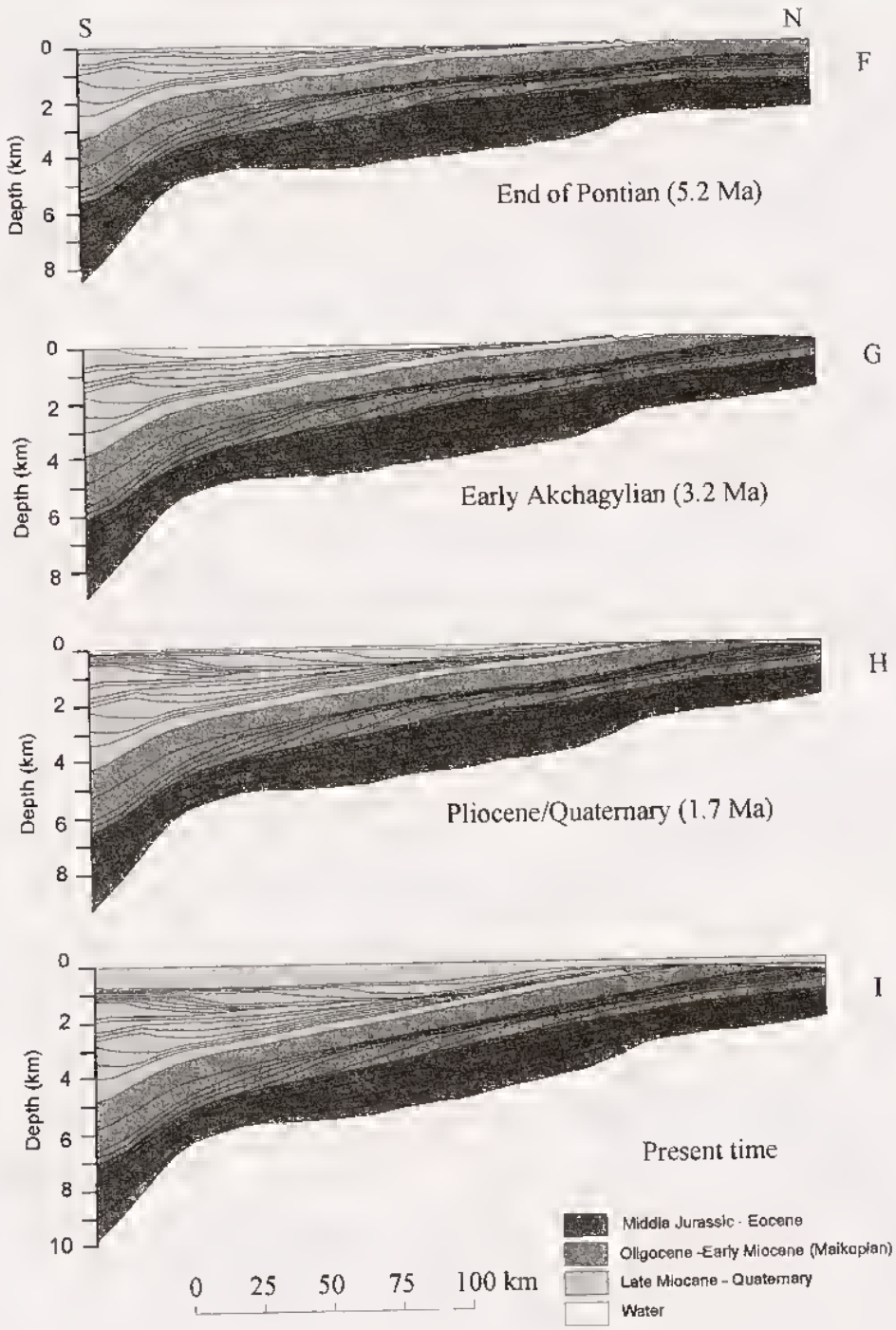

The Great Caucasus polyphase orogeny started at the Eocene/Oligocene boundary. In the Eocene (pre-collisional time) a deep water basin (similar to Black Sea and south Caspian basins) was situated in the place of recent Great Caucasus orogen (SCHERBA, 1993; ZONENSHAIN *et al.*, 1990). All these basins were deep-water back-arc basins with oceanic or very thinned continental crust. The subduction zone was situated to the south of Pontides-Transcaucasus-Alborz belt (ZONENSHAIN *et al.*, 1990; DERCOURT *et al.*, 1993). At the Eocene/Oligocene boundary the north-dipping subduction was changed into collision of the Tauride-Anatolide and Iranian terranes with the Pontides-Transcaucasus-Alborz area (Fig. 8) (SENGOR & KIDD, 1979; ZONENSHAIN *et al.*, 1990; NIKISHIN *et al.*, 1998a). It led to uplift of the

Source : MNHN, Paris

Transcaucasus region, thrusting along the northern margin of the Great Caucasus trough (MILANOVSKY, 1968), and subsidence (Maikopian subsidence) of a broad area including Black Sea, south Caspian Sea, Fore-Caucasus basin and Great Caucasus trough (SCHERBA, 1993; POPOV *et al.*, 1993). The central segment of the Great Caucasus orogen began to grow from this time (NESMEYANOV, 1992). It means that a zone of underthrusting in the area of recent southern slope of Great Caucasus orogen was formed also probably at the same time due to a blockage of the subduction to the south by collision. Thrusts formed at earliest Oligocene were observed in the field by SHARAFUTDINOV (1991) in the Dagestan (see Fig. 1 for location) to the north of Great Caucasus, but they were not active during the remaining of Maikopian.

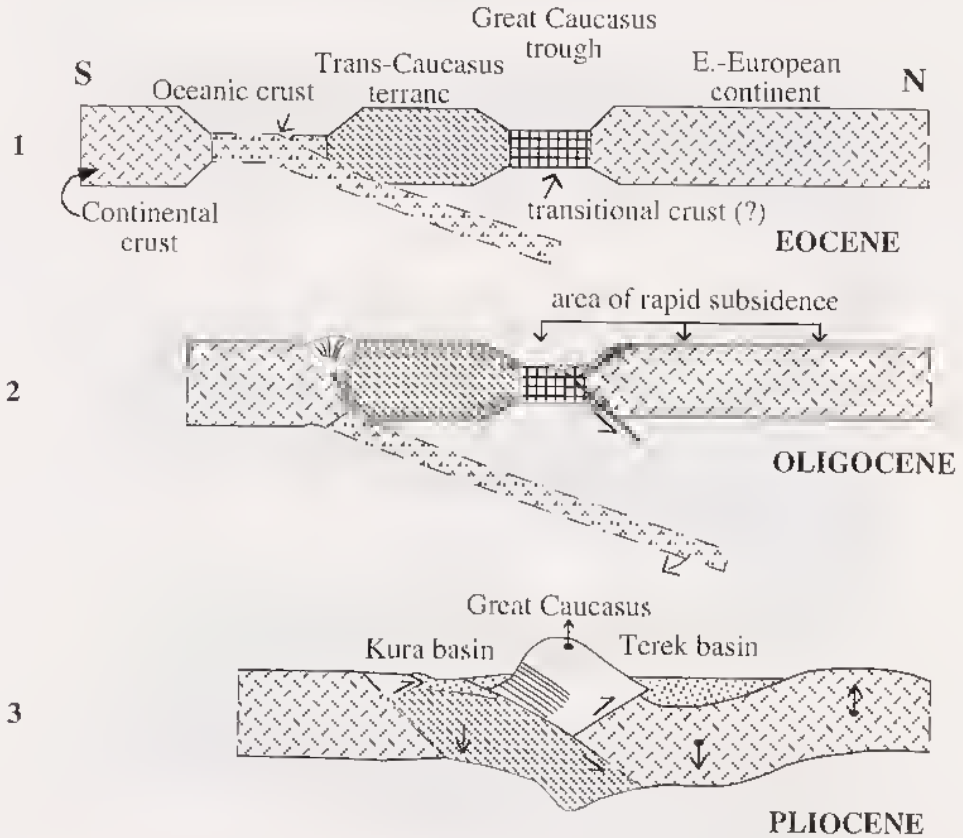

FIG. 8.— Schematic illustration of geodynamical evolution of eastern part of Caucasus and adjacent areas (modified after ERSHOV *et al.*, 1996). Three main stages are shown: **1**, pre-collisional Eocene configuration; **2**, Maikopian stage, soft collision in the Trans-Caucasus area, rapid subsidence of a broad region; **3**, orogenic stage, Great Caucasus orogeny, molasse basins formation.

FIG. 8.— Illustration schématique de l'évolution géodynamique du Caucase oriental et des régions adjacentes (modifié d'après ERSHOV et al., *1996). Trois stades principaux sont présentés : 1, configuration anté-collision Eocène ; 2, stade Maikopien, collision faible dans la région de Trans-Caucasie, subsidence rapide d'une large région ; 3, stade orogénique, orogenèse du Grand Caucase, formation des bassins molassiques.*

The Maikopian subsidence is too long in wavelength to be explained by a flexural response to orogenic loading. This broad platform subsidence can be driven by loading from a deep source, probably by flow in the mantle induced by subduction. The proposition of the subsidence of continental lithosphere above a subduction zone has been made and modelled by MITROVICA *et al.* (1989) and GURNIS (1992, 1993). In their model, oceanic lithosphere subducting under a continent acts as a load inducing the subsidence of a large area in the continent above (scale of 500-1000 km, width increasing with the shallowing of the slab dip). The model has been used to explain a broad subsidence shown by deep palaeowater depth in the Late Tertiary development of the Taranaki basin, New Zealand (HOLT & STERN, 1994), which, as in the Caucasus, precedes the evolution of a more restricted flexural foreland

Source : MNHN, Paris

basin. In this model, the subsidence is associated with the beginning of subduction; termination of subduction leads to an uplift of the area. In our case, the subsidence is contemporaneous with termination of subduction and new zone of underthrusting only began to form when deep water basin already existed in the broad area. We suggest that Maikopian subsidence was induced by a rotation down of the slab after the termination of "southern" subduction. This led to a dragging "of mantle wedge above the slab downward, resulting in a depression at the surface" as it was discussed by HSUI *et al.* (1990). This process is suggested to induce 1 km excess subsidence in back-arc basins and we have similar amplitude of Maikopian subsidence taking into account loading of sediments. On the other hand this process is transient in nature. Influence of the rotating down slab will he decreasing with time and after some period such "dynamically supported" subsidence has to be changed into uplift. This post-Maikopian uplift can be attributed as a cause of excess uplift of the bulge on the north of the basin, which has led to more than 1 km of erosion. But on most of the territory of the basin the effect of this uplift is masked by subsidence of the next stage induced by the processes of the next stage of collisional history.

A collision between the Arabia and the " Europe " took place in the middle Miocene-Quaternary (SENGOR & YILMAZ, 1981) further to the south in the Zagros area. This continent-continent collision has led to orogeny in the Caucasus-Crimea region and molasse basins formation. Since 3.4 Ma, a drastic change in the vertical movements regime occurred in the general area. The Peri-Caspian basin underwent uplifting in the Miocene which was dramatically changed by rapid subsidence up to 600 meters during the last 3.4 Ma (ZHIDOVINOV *et al.*, 1995). The eastern Black Sea hasin had a decrease of the subsidence rate 17-3.4 Ma ago changed by rapid subsidence till the recent time (ROBINSON *et al.*, 1996). In the south Caspian Sea, the onset of rapid sedimentation and tectonic subsidence began during early Pliocene at around 5 Ma and the tectonic subsidence reached a very high rate during the mid-Pliocene (BRUNET *et al.*, 1997).

As it is clearly seen on the 2D restorations (Fig. 7), the Maikopian basin (34-15.8) differs from Chokrakian-Quaternary basin (15.8-0 Ma). The shape of Maikopian basin is flattened with slight dipping to the south, the characteristic wavelength is larger than the size of the section. On the other side the geometry of the molasse basin (Chokrakian-Quaternary) has a characteristic asymmetrical shape with flexural deepening to the orogen. This shape is typical for flexural foreland basins formed due to elastic flexure of lithosphere in response to orogen loading. Such hasins were recognized broadly across Alpine-Himalayan orogenic belt (e.g. KARNER & WATTS, 1983; LYON-CAEN & MOLNAR, 1983; BRUNET, 1986; LILLIE *et al.*, 1994) and for the Caucasus such model was supposed by RUPPEL & MCNUTT (1990).

Some alternative models of Caucasus foredeep have been presented in the literature. ARTYUSHKOV (1993) suggested a basalt-eclogite phase transition in the lower crust as a cause of the Caucasus foredeep origination. He emphasized the deficiency of the Great Caucasus topographical loading and the diachronism in the appearance of topographic elevation of orogen (since middle Sarmatian) and molasse basin subsidence (since Maikopian). Indeed, insufficiency of topographic loading itself was recognized by many researchers for different orogens (e.g. KARNER & WATTS, 1983) and additional loading factors were proposed as subsurface loading or bending momentum of the slab (KARNER & WATTS, 1983, BRUNET, 1986; SHEFFELS & MCNUTT, 1986). Phase transitions may be a part of subsurface loading, new in ARTYUSHKOV's model is the fact that phase transition acts as subsurface loading also in the basin area. The physical properties of basalt-eclogite phase transition is poorly studied and existing information shows that in dry conditions the P-T conditions in the lower crust are insufficient for it; the arguments about input of the fluids are only speculative and do not allow quantitative test at this time. The contradiction of diachronism between topographic elevation and basin subsidence disappears if we discriminate Maikopian subsidence and later foreland-type subsidence as induced by different causes. Other model of Fore-Caucasus foredeep basin was proposed by MIKHAILOV *et al.* (1997). The origination and the evolution of the foredeep is connected with small scale viscous convection in the crust and upper mantle. This model was proposed recently but not fully puhlished and now we have not enough informations to discuss it.

We will not model the Maikopian subsidence as its characteristic length is larger than the investigated region and we need to include data on a larger area which is not subject of the present paper. In this paper, we will model in the flexural mode, only the second part of the basin evolution with the formation of molasse basin near the orogen. We use the dynamic model of the Fore-Caucasus basin

Source : MNHN, Paris

evolution during the last 16 Ma based on the proposition that the main control is elastic response of basin lithosphere to the loading in the area of Great Caucasus orogen.

FLEXURAL MODEL OF LATE MIOCENE-QUATERNARY STAGE

Model of foreland basin origination due to flexural response of lithosphere to loading was proposed by JORDAN (1981) and BEAUMONT (1981) and was widely used in the 80'th (e.g. KARNER & WATTS, 1983; ROYDEN & KARNER, 1984; LYON-CAEN & MOLNAR, 1983, 1985, 1989; LYON-CAEN *et al.*, 1985; BRUNET, 1986; SHEFFELS & MCNUTT, 1986). RUPPEL & MCNUTT (1990) made such modelling for the Caucasus orogen. These works were based mainly on the gravity and topography data and often these constraints were insufficient (e.g. LYON-CAEN & MOLNAR, 1989). In our case, we have an additional constraint coming from 2D restoration of burial history. It is the shape of the basin and as we know its evolution in time we can apply flexural model through time. The deep structure of the Caucasus orogen is complex and poorly known and, in turn, structure of basin lithosphere is more simple and relatively well known. Our approach allowing to avoid the indefinities related to complexity of orogen deep structure is to divide the whole system of orogen and adjacent sedimentary basins into two parts: a basin and a orogen - and to consider the interplay between these parts (Fig. 9) (ERSHOV, 1997). The geometry of flexural basin depends mainly on three factors: loading of orogen, intraplate stress and elastic properties of lithosphere. The knowledge of the basin geometry allows us to estimate the orogen loading force. Knowledge of the basin shape through time (reconstituted from the 2D kinematical restoration, Fig. 7) allows us to obtain loading history through time.

The model is based on the numerical solution of standard equation of elastic flexure:

$$(D\,w'')''+(P\,w')'+\rho_{ast}gw=q_{sed}$$

where $D(x)$ – flexural rigidity, P – intraplate stress, $w(x)$ – vertical deflection of lithosphere, $q_{sed}=\rho(z)\,g\,dz$ – loading of sediments and water, $\rho_{ast}gw$ – buoyancy force. The effective elastic thickness is expressed through the flexural rigidity:

$$D=E\,T_e^3/12(1-\nu^2),$$

where E - Young modulus, ν- Poisson coefficient.

The difference from the standard model is the considered area (basins area only) (Fig. 9) and, correspondingly, the boundary conditions. The boundary conditions on the right corner were a deflection $w(x_1)$, derived from backstripped section, and zero bending moment ($D(x_1)w''(x_1)=0$). The boundary conditions on the left corner were a deflection $w(x_0)$ and a bending momentum $D(x_0)\,w''(x_0)$, which both were varied to obtain the best fit with observed shape of the basin. By changing intraplate stress, flexural rigidity (EET), left corner deflection and bending momentum values, we have matched the shape of the basin for each time slice.

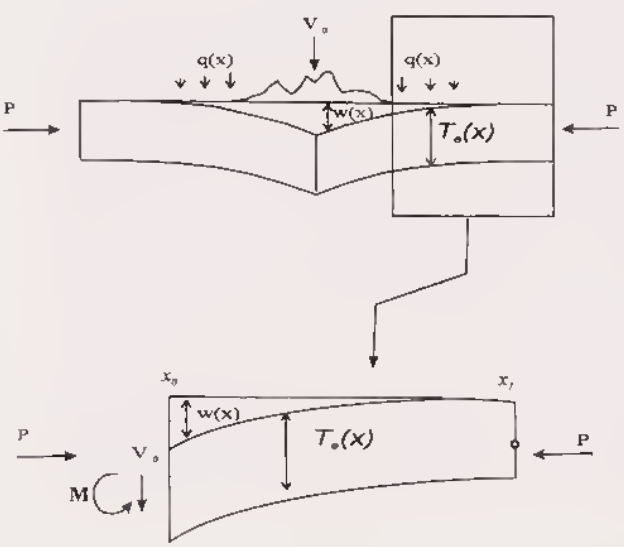

FIG. 9.— Configuration and boundary condition of the flexural model. Only basin lithosphere is considered in flexural modelling. Observed deflection (w) and zero bending moment are used as right-corner boundary conditions; loading force and bending moment as left-corner boundary conditions. The values of EET (T_e), intraplate stress P, left-corner bending moment M and loading force V_0 were varied to fit observed geometry of the basin at each time span.

FIG. 9.— Configuration et conditions aux limites du modèle flexural. La lithosphère du bassin est seule considérée dans le modèle en flexion. La déflexion observée (w) et le moment fléchissant ont sont utilisés comme conditions aux limites à droite du modèle tandis que la force de surcharge et le moment fléchissant sont utilisés comme conditions aux limites à gauche du modèle. Les valeurs de l'épaisseur élastique équivalente EET (T_e), de la contrainte intraplaque P, du moment fléchissant à gauche M et de la force de surcharge V_0 ont été variées pour ajuster la géométrie du bassin observée à chaque étape.

Source : MNHN, Paris

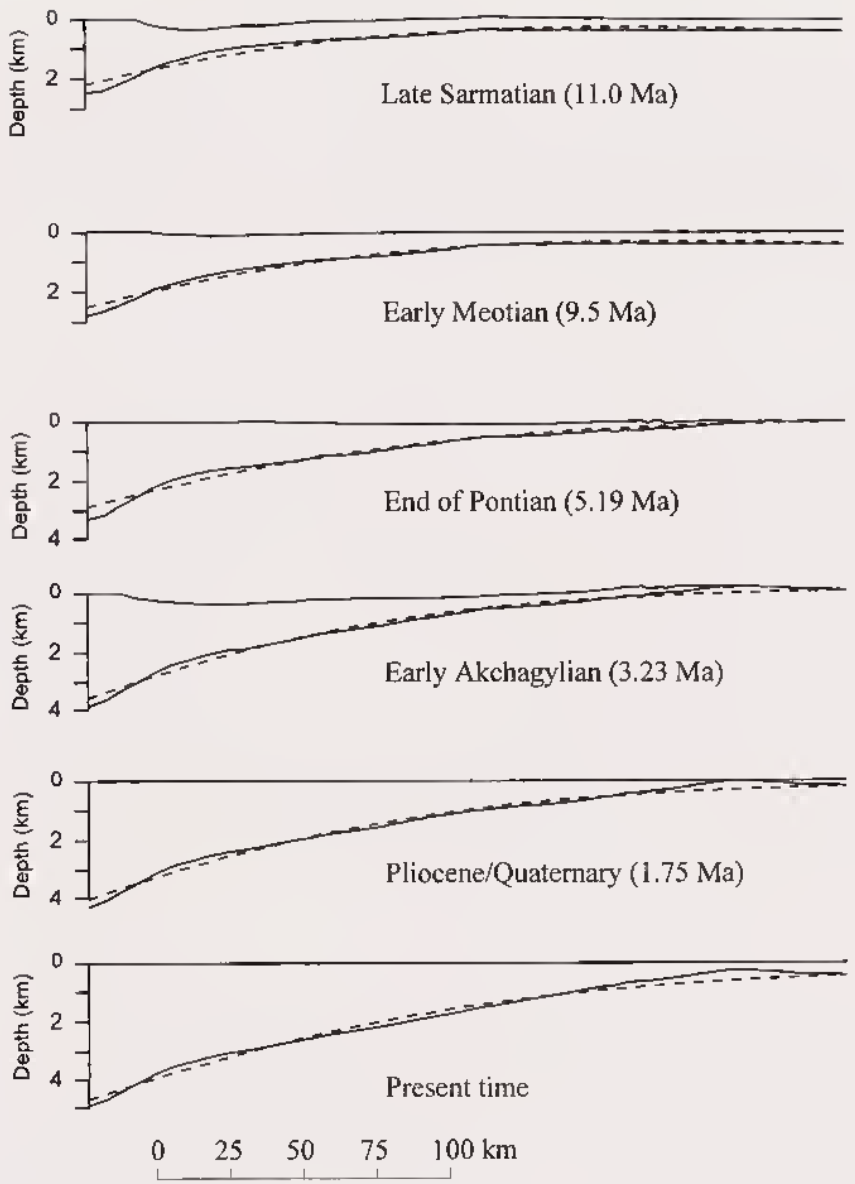

FIG. 10.— Set of diagrams, illustrating the agreement between backstripped section and profile obtained from the flexural modelling. The dashed line represents the top of Maikopian from the flexural modelling, the solid line - the top of Maikopian from the backstripped section (Fig. 7). The time slices are the same as on the picture 7 from the late Sarmatian.

FIG. 10.— Ensemble de diagrammes illustrant le bon accord entre les coupes résultant du "backstripping" et celles obtenues par le modèle flexural. La ligne en pointillés correspond au toit du Maikopien déduit du modèle flexural, la ligne continue correspond au toit du Maikopien sur la section après "backstripping" (Fig. 7). Les tranches de temps sont les mêmes que sur la figure 7 à partir du Sarmatien supérieur.

As a result, we have time slices of modelled best-fitted flexural shapes of the basin. We have chosen as reference boundary top of Maikopian which is bottom of the foreland-stage basin. The results of the flexural modelling for selected time slices are presented on figure 10. The solid line represents the reference boundary (top of Maikopian) from kinematical restoration of the profile (Fig. 7). The dashed line represents the modelled position of this boundary from flexural dynamic modelling. The results show the good agreement between backstripped and flexurally modelled basin geometry.

Source : MNHN, Paris

The fitted level of intraplate stress is far from critical value and its influence on basin shape has a second order effect. The variation of EET value with time used to obtain the best fit was not large and all the values were near 60 km. These results are in general agreement with those of RUPPEL & MCNUTT (1990) for the central and eastern parts of Caucasus. where they have found a 40 km thick elastic plate.

To go further in the modelling of this area, we need now to take into account the rheological structure of the lithosphere and the gravity anomalies for a model of a section crossing the Caucasus and using the constraints, even poorly known of the southern basin. Other sections in the central and western part of the Caucasus will be modelled to compare the difference of behaviour of the basins and lithosphere along the Caucasus orogen, through a different history of the basins evolution.

CONCLUSION

The collisional history of Caucasus area started at the Eocene/Oligocene boundary when north-dipping subduction was changed by collision in the Transcaucasus area with Tauride-Anatolide terranes. It led to the uplifting of the Transcaucasus region, compressional tectonics in the northern areas and subsidence of broad area including the Fore-Caucasus and Caucasus, the Black Sea and the south Caspian Sea. On the basis of restored burial history we can separate two main stages of syncollision molasse basin formation: (1) 34-15.8 Ma ago (Maikopian stage) - early collision, with rapid subsidence of a broad area; (2) 15.8-0 Ma ago - collisional climax, contemporaneous with a rapid subsidence of molasse basins, upthrusting of the Great Caucasus to the south, and a local retrothrusting to the north.

The Maikopian subsidence has a too large wavelength to be explained by the elastic flexure of lithosphere. The cause for Maikopian subsidence of a broad area could be related with the change in subduction system, when slab rotated down after the termination of subduction in the Transcaucasus area and induced large scale flow in the mantle causing the subsidence of the continental crust above. Such subsidence is "dynamically supported" and after some time subsidence has to be changed into uplift.

The mean palaeowater depths during the early Maikopian estimated on the basis of shape of clinoforms were near 500-800 m in the middle part and up to 1200 m in the southern part of the basin. These estimated values are in general agreement with palaeontological data.

Two-dimensional flexural modelling of eastern Fore-Caucasus molasse basin demonstrates that the observed subsidence of this area during late Miocene - Quaternary time can be explained by the effect of loading of Great Caucasus orogen. The EET lies near 60 km on the basis of flexural modelling.

On the northern edge of the basin the peripheral bulge uplifted at least during last 5 Ma and probably since Sarmatian. The time of beginning of uplift is difficult to establish as northern part of the section is eroded now. The amplitude of erosion is more than 1 km in the northernmost part of investigated area. The cause of it may lie in a broad uplift inherited from Maikopian subsidence. An asymmetrical foreland-type subsidence due to the loading of orogen surpassed the effect of post-Maikopian uplift in the areas adjacent to Great Caucasus orogen.

ACKNOWLEDGMENTS

This work was funded by Peri-Tethys Program (funds n° 95/66, 95-96/66, 95/44 and 95-96/44). The international programmes Europrobe, INTAS, IGCP-369, and Lithosphere supported our communications and discussions. We thank A. S. ALEKSEEV, S. CLOETINGH, J. DERCOURT, V. E. KHAIN, N. V. KORONOVSKY, E. E. MILANOVSKY, B. P. NAZAREVICH, D. I. PANOV, Yu PODLADCHIKOV, P. ZIEGLER for fruitfull discussions, J. GRANATH, R. STEPHENSON and an anonymous reviewer for their constructive remarks on a first version of the paper.

Source : MNHN, Paris

REFERENCES

ARTEMIEV, M.E. & BALAVADZE, B.K., 1973.— Isostasy of the Caucasus. *Geotectonics*, **6**: 20-32 (in Russian).

ARTYUSHKOV, E.B., 1993.— *Physical Tectonics*. Nauka, Moscow: 1-456 (in Russian).

AVCHYAN, G.M. & OZERSKAYA, M.L. (eds), 1985.— *Petrophysical characteristics of sedimentary cover of oil and gas bearing provinces of USSR*. Nedra, Moscow: 1-192 (in Russian).

BALDI, T., 1980.— The early history of Paratethys. *Földt közlöny*, **110** (3,4): 456-471.

BEAUMONT, C., 1981.— Foreland basins. *Geophysical Journal of the Royal Astronomical Society*, **65**: 291-329.

BELOV, A.A. & SATIAN, M.A. (eds), 1989.— *Geodynamics of the Caucasus*. Nauka, Moscow: 1-215 (in Russian).

BOLOTOV, S.N., 1996.— *Mesozoic-Cenozoic History of Scythian Platform and Numerical Characteristics of Basic Stages of Evolution on the Basis of Computer Modelling*. Ph. D. Thesis, Lomonosov Moscow State University, Geological Faculty, Moscow, USSR: 1-195 (in Russian).

BRUNET, M.-F., 1986.— The influence of the Pyrenees evolution on adjacent basins. *Tectonophysics*, **129**: 343-354.

BRUNET, M.-F., REBETSKY, Y.L. & NIKITINA, Y.S., 1997.— First steps of modelling in the South Caspian Sea. *Peri-Tethys Program Annual Meeting, Rabat*: 25-26.

CHUMAKOV, I.S., BYZOVA, S.L. & GANZEI, S.S., 1992.— *Radiometric Scale for Late Cenozoic of Eastern Paratethys*. Nedra, Moscow: 1-124 (in Russian).

CHUMAKOV, I.S., 1993.— Radiometric scale for Late Cenozoic of Paratethys. *Priroda*, **12**: 68-75 (in Russian).

DERCOURT, J., RICOU, L.E. & VRIELYNCK, B. (eds), 1993.— *Atlas Tethys, Paleoenvironmental Maps*. Gauthier-Villars, Paris: 1-307, 14 maps, 1 pl.

ERSHOV, A.V., 1997.— *The Modelling of Evolution of Sedimentary Basins and Deformation of Lithosphere (on the Examples of the Basins of East-European and Scythian Platforms)*. Ph. D. Thesis, Lomonosov Moscow State University, Geological Faculty, Moscow, USSR: 1-295 (in Russian).

ERSHOV, A.V., BRUNET, M.-F., BOLOTOV, S.N. & NIKISHIN, A.M., 1996.— Numerical modelling of the fore- and trans-Caucasus-Crimea molasse basins. *In*: *Proceedings of the 30th International Geological Congress, 4-14 august 1996, Beijing, China*. Geological Publishing House, Beijing: 1-176.

GURNIS, M., 1992.— Rapid continental subsidence following the initiation and evolution of subduction. *Science*, **255**: 1556-1558.

GURNIS, M., 1993.— Depressed continental hypsometry behind oceanic trenches: a clue to subduction controls on sea-level change. *Geology*, **21**: 29-32.

HARLAND, W.B., ARMSTRONG, R.L., COX, A.V., CRAIG, L.E., SMITH, A.G. & SMITH, D.G., 1989.— *A Geologic Time Scale*. Cambridge University Press, Cambridge: 1-263, 1 pl.

HOLT, W.E. & STERN, T.A., 1994.— Subduction, platform subsidence, and foreland thrust loading: the Late Tertiary development of Taranaki Basin, New Zealand. *Tectonics*, **13**: 1068-1092.

HSUI, A.T., TANG X.-M. & TOKSÖZ, M.N., 1990.— On the dip angle of subducting plates. *Tectonophysics*, **179**: 163-175.

JORDAN, T.E., 1981.— Thrust loads and foreland basin evolution, western United States. *AAPG Bulletin*, **65**: 2506-2520.

KARNER, G.D. & WATTS, A.B., 1983.— Gravity anomalies and flexure of the lithosphere at mountain ranges. *Journal of Geophysical Research*, **88**: 449-477.

KORONOVSKY, N.V., KOZHEVNIKOV, A.V., PANOV, D.I., VISHNEVSKY, L.E., GUSCHIN, A.I., NIKITIN, M.YU., VORONINA, A.A., STAFEEV, A.N., PANINA, L.V., KOPAEVICH, L.F., STOR, M.A. & BELYAKOV, G.A., 1987.— History of geological development and formation of structure of central part of Terek-Caspian foreland. *In*: E.E. MILANOVSKY & N.V. KORONOVSKY (eds), *Geology and Mineral Resources of Great Caucasus*. Nauka, Moscow: 147-174 (in Russian).

KRASNOPEVTSEVA, G.V., 1984.— *Deep Structure of Caucasus Seismoactive Region*. Nauka, Moscow: 1-107 (in Russian).

KUNIN, N.YA., KOSOVA, S.S. & BLOKHINA, G.YU., 1990.— The subdivision of Cenozoic deposits of Eastern Fore-Caucasus. *Izvestiya Akademiy Nauk SSSR, Seriya Geologicheskaya*: 71-81 (in Russian).

LETAVIN, I.A., 1980.— *Basement of the Young Platform of the Southern Part of the USSR*. Nauka, Moscow: 1-153 (in Russian).

LILLIE, R.J., BIELIK, M., BABUSKA, V. & PLOMEROVA, J., 1994.— Gravity modelling of the lithosphere in the Eastern Alpine-Western Carpathian-Pannonian Basin region. *Tectonophysics*, **231**: 215-235.

LYON-CAEN, H. & MOLNAR, P., 1983.— Constraints on the structure of the Himalaya from an analysis of gravity anomalies and a flexural model of the lithosphere. *Journal of Geophysical Research*, **88**: 8171-8192.

LYON-CAEN, H. & MOLNAR, P., 1985.— Gravity anomalies, flexure of the Indian plate and the structure, support and evolution of the Himalaya and Ganga Basin. *Tectonics*, **4**: 513-538.

LYON-CAEN, H. & MOLNAR, P., 1989.— Constraints on the deep structure and dynamic processes beneath the Alps and adjacent regions from an analysis of gravity anomalies. *Geophysical Journal International*, **99**: 19-32.

LYON-CAEN, H., MOLNAR, P. & SUAREZ, G., 1985.— Gravity anomalies and flexure of the Brazilian shield beneath the Bolivian Andes. *Earth and Planetary Sciences Letters*, **75**: 81-92.

Source : MNHN, Paris

MIKHAILOV, V.O., 1993.— Crustal control on the Terek-Caspian trough evolution: constraints based on a new paleotectonic analysis method. *Tectonophysics*, **238**: 21-32.

MIKHAILOV, V.O., POLINO, R., TIMOSHKINA, E.P. & PANINA, L.V., 1997.— North Caucasus foredeep: subsidence history and model of formation. *Terra Nova Abstracts, European Union of Geosciences 9, Strasbourg*: 138.

MILANOVSKY, E.E., 1968.— *Neotectonics of the Caucasus*. Nedra, Moscow: 1-482 (in Russian).

MITROVICA, J.X., BEAUMONT, C. & JARVIS, G.T., 1989.— Tilting of continental interiors by the dynamical effects of subduction. *Tectonics*, **8**: 1079-1094.

NESMEYANOV, S.A., 1992.— *Neostructural Subdivision of the North-West Caucasus*. Nedra, Moscow: 1-255 (in Russian).

NEVESSKAYA, L.A., VORONINA, A.A., GONCHAROVA, I.A., ILINA L.B., PARAMONOVA, N.P., POPOV, S.V., CHEPALYGA, A.L. & BABAK, E.B., 1984.— The history of Paratethys. *In*: *Proceedings of the 27th International Geological Congress, Paleooceanology*, Vol. 3. Nauka, Moscow: 91-101 (in Russian).

NIKISHIN, A.M., CLOETINGH, S., BOLOTOV, S.N., BARABOSHKIN, E.YU., KOPAEVICH, L.F., NAZAREVICH, B.P., PANOV, D.I., BRUNET, M.-F., LINA, V.V., KOSOVA, S.S. & STEPHENSON, R.A., 1998a.— Scythian Platform: chronostratigraphy and polyphase stages of tectonic history. *In*: S. CRASQUIN-SOLEAU & É. BARRIER (eds), Peri-Tethys Memoir 3: stratigraphy and evolution of Peri-Tethyan platforms. *Mémoires du Muséum national d'Histoire naturelle*, **177**: 151-162.

NIKISHIN, A.M., CLOETINGH, S., BRUNET, M.-F., STEPHENSON, R.A., BOLOTOV, S.N. & ERSHOV, A.V. 1998b.— Scythian Platform, Caucasus and Black Sea region: Mesozoic-Cenozoic tectonic history and dynamics. *In*: S. CRASQUIN-SOLEAU & É. BARRIER (eds), Peri-Tethys Memoir 3: stratigraphy and evolution of Peri-Tethyan platforms. *Mémoires du Muséum national d'Histoire naturelle*, **177**: 163-176.

ODIN, G.S., 1994.— Geological Time Scale 1994. *Comptes Rendus de l'Académie des Sciences, Paris*, **318**, II: 59-71.

POPOV, S.V., AKHMETIEV, M.A., ZAPOROZHETS, N.I., VORONINA, A.A. & STOLYAROV, A.S., 1993.— History of Eastern Paratethys in Late Eocene-Early Miocene. *Stratigrapfiya i Geologicheskaya Korrelyatsiya*, **1**, (6): 10-39 (in Russian).

ROBINSON, A.G., RUDAT, J.H., BANKS, C.J. & WILES, R.L.F., 1996.— Petroleum geology of the Black Sea. *Marine and Petroleum Geology, London*, **13**: 195-223.

ROYDEN, L.H. & KARNER, G.D., 1984.— Flexure of the lithosphere beneath Apennine and Carpathian foredeep basins: evidence for an insufficient topographic load. *AAPG Bulletin*, **68**: 704-712.

RUPPEL, C. & MCNUTT, M., 1990.— Regional compensation of the Great Caucasus mountains based on an analysis of Bouguer gravity data. *Earth and Planetary Sciences Letters*, **98**: 360-378.

SCHERBA, L.G., 1993.—*Stages and Phases of Cenozoic Development of Alpine Fold Belt*. Nauka, Moscow: 1-231 (in Russian).

SENGOR, A.M.C. & KIDD, W.S.F., 1979.— Post collisional tectonics of the Turkish-Iranian plateau and a comparison with Tibet. *Tectonophysics*, **55**: 361-376.

SENGOR, A.M.C. & YILMAZ, Y., 1981.— Tethyan evolution of Turkey: a plate tectonic approach. *Tectonophysics*, **75**: 181-241.

SHARAFUTDINOV, V.F., 1991.— *Geological Structure and Formation of Paleogene Olistostromes on the North-Eastern Caucasus*. Ph. D. Thesis, Lomonosov Moscow State University, Moscow, USSR: 1-250 (In Russian).

SHEFFELS, B. & MCNUTT, M., 1986.— Role of subsurface loads and regional compensation in the isostatic balance of the Ranges, California: evidence for intracontinental subduction. *Journal of Geophysical Research*, **91**: 6419-6431.

STECKLER, M.S. & WATTS, A.B., 1978.— Subsidence of the atlantic-type continental margin off New-York. *Earth and Planetary Sciences Letters*, **41**: 1-13.

ZHIDOVINOV, N.A., FEDKOVICH, Z.N. & KOVALENKO, N.D., 1995.— New data on the stratigraphy of the Upper Pliocene and Eo-Pleistocene of the Lower Volga region and northern Pre-Caspian. *Stratigraphia i Geologicheskaya Korrelyatsiya*, **3** (1): 73-81 (in Russian).

ZONENSHAIN, L.P., KUZMIN, M.I. & NATAPOV, L.M., 1990.— *Geology of the USSR: a Plate Tectonic Synthesis*. American Geophysical Union, Geodynamic Series, Washington DC, serie 21: 1-242.

Source : MNHN, Paris

Stratigraphic analysis of the Upper Jurassic (Oxfordian-Kimmeridgian) Antalo limestone in the Mekele outlier (Tigrai, Northern Ethiopia): preliminary data

Luca MARTIRE, *Pierangelo* CLARI & *Giulio* PAVIA

Dipartimento di Scienze della Terra, via Accademia delle Scienze 5, 10123 Torino, Italy

ABSTRACT

The Antalo limestone is an Upper Jurassic formation mainly consisting of interbedded limestones and marls, and is comprised between two arenaceous, continental formations, the Adigrat sandstone and the Amba Aradam formation. The Antalo limestone has been studied in its type-area, the Mekele outlier. Two stratigraphic sections have been measured and correlated. Four units have been distinguished in the Antalo limestone on the basis of gross lithological features. From bottom to top: a) calcareous-marly unit A (170 m). Massive stromatoporoid- and coral-rich limestones at the base, and cross-bedded oolitic grainstones, in the upper half, are interbedded with a poorly exposed succession of marls; b) arenaceous unit B (115 m). Herringbone cross-bedded coarse-grained brown sandstones grade upwards into prevailing marls with thin-bedded sandstones with parallel and low-angle oblique laminae; c) calcareous unit C (180 m). After a poorly exposed marly unit, a thick succession of micritic grey to light brown limestones follows with subordinate marly interlayers. The only ammonites to date found in the Antalo limestone of the Mekele outlier come from these layers; and d) marly calcareous unit D (280 m). It consists of alternating marls and limestones. Noteworthy is the presence of oolitic grainstones and of stromatoporoid floatstones in the lower part of the member, and of whitish micritic limestones in the upper part. At the top, the Antalo limestone formation grades into the overlying marls of the Agula Shales. Stromatoporoids and benthic foraminifer assemblages show that units A and B are referable to the Oxfordian whereas the units C and D to the Kimmeridgian. Ammonites found in unit C confirm this picture. Although the geometry of sedimentary bodies is tabular, some slight lateral changes in thickness and facies have been recognized. The overall depositional setting was probably represented by a low-gradient ramp basically controlled by storm processes and gently dipping to the East.

RÉSUMÉ

Analyse stratigraphique du calcaire Antalo dans la région de Mekele (Tigrai, nord de l'Éthiopie) (Jurassique supérieur, Oxfordien - Kimméridgien) : données préliminaires.

Le calcaire Antalo est une formation du Jurassique supérieur, composée essentiellement d'alternance de calcaires et de marnes et est encadré de deux formations arénacées continentales, les grès d'Adigrat et la formation de Amba Aradam. Le calcaire Antalo a été étudié dans sa région type, dans les environs de Mekele. Deux coupes stratigraphiques ont été levées et

MARTIRE, L., CLARI, P., & PAVIA, G., 1998. —Stratigraphic analysis of the Upper Jurassic (Oxfordian-Kimmeridgian) Antalo limestone in the Mekele outlier (Tigrai, Northern Ethiopia): preliminary data. *In*: S. CRASQUIN-SOLEAU & É. BARRIER (eds). Peri-Tethys Memoir 4, epicratonic basins of Peri-Tethyan platforms, *Mém. Mus. natn. Hist. nat.*, **179** : 131-144. Paris ISBN : 2-85653-518-4.

Source : MNHN, Paris

corrélées. Quatre unités ont été distinguées dans le calcaire Antalo sur la base de caractères lithologiques généraux. De la base au sommet : a) une unité calcaro-marneuse A (170 m) ; calcaires massifs riches en stromatoporidés et coraux à la base et des calcaires oolithiques à stratifications entrecroisées dans la partie supérieure, intercalés avec des marnes affleurant mal ; b) une unité arénacée B (115 m) ; grès bruns grossiers à stratifications entrecroisées en chevrons passant graduellement vers le haut à des marnes dominantes avec des grès en petits bancs avec des lamines parallèles ou faiblement obliques ; c) une unité calcaire C (180 m). Après une unité marneuse affleurant mal, on rencontre une épaisse succession de calcaires micritique gris à marron clair avec des interlits marneux. Les seules ammonites trouvées dans le calcaire Antalo de la bordure Mekele proviennent de ces niveaux ; d) une unité de calcaires marneux D (280 m). Elle est formée d'une alternance de marnes et de calcaires. À noter la présence de grainstones oolithiques et de floatstones à stromatoporidés dans la partie basale et de calcaires blanchâtres dans la partie supérieure. Au sommet la formation du calcaire Antalo passe graduellement aux marnes de la formation Agula. Les assemblages de stromatoporidés et de foraminifères montrent que les unités A et B peuvent être rattachées à l'Oxfordien et les unités C et D au Kimméridgien. Les ammonites découvertes dans l'unité C confirment ce schéma. Bien que la géométrie des corps sédimentaires soit tabulaire, quelques légers changements latéraux d'épaisseur et de faciès ont été reconnus. Le milieu général de dépôts était probablement représenté par une rampe de gradient faible, fondamentalement contrôlée par des processus de tempêtes et plongement vers l'Est.

INTRODUCTION

The Antalo limestone consists of a package of shallow marine limestone-marl alternations about 700 metres thick referable to the Late Jurassic. The type-area of the Antalo limestone, defined by BLANFORD (1870), is the Mekele outlier, in northeastern Ethiopia, where it crops out over an area of about 7000 km^2 (Fig. 1). Here, this succession of marine sedimentary rocks is comprised between continental, terrigenous sediments. The older ones are represented by the Adigrat sandstone in turn unconformably overlying the Upper Paleozoic Karroo complex. The boundary between the Adigrat sandstone and the Antalo limestone is considered conformable and transitional. The upper continental formation (Amba Aradam formation) consists of conglomerates and sandstones. An erosional angular unconformity separates the Antalo limestone from the Amba Aradam formation which, in the westernmost parts of the Mekele outlier, directly rests upon the Adigrat sandstone. Because of the extreme scarcity of fossils, direct dating of both Adigrat and Amba Aradam formations has never been possible. The Adigrat formation has been considered of Permo-Triassic age, after paleobotanical studies (BEAUCHAMP & LEMOIGNE, 1974), or Triassic?-Bathonian on the basis of the supposed transitional boundary to the Callovian-Kimmeridgian Antalo limestone (MERLA & MINUCCI, 1938; MERLA *et al.*, 1979). The Amba Aradam, instead, is totally devoid of fossils. It can therefore only be dated in a very general way, being bracketed between the Upper Jurassic Agula Shales and the Eocene volcanics. It is however generally referred to the (Early) Cretaceous.

Many references to the Antalo limestone from different parts of the Horn of Africa may be found in literature (e.g. MERLA & MINUCCI, 1938; DAINELLI, 1943; ARKIN *et al.*, 1971; BEYTH, 1972; FICCARELLI *et al.*, 1975; MERLA *et al.*, 1979; TURI *et al.*, 1980; RUSSO *et al.*, 1994; BOSELLINI *et al.*, 1995; SAGRI *et al.*, 1998). The most detailed description of the stratigraphic succession of the Mekele outlier is due to the work of BEYTH (1972) who compiled the explanatory notes of the Mekele sheet n° 37-11 of the Geological Map of Ethiopia (ARKIN *et al.*, 1971). Five members were distinguished within the Antalo limestone and four broad facies identified on the basis of sediment composition, texture and association: the spatial arrangement of these facies, according to the author, points to a progressive eastward deepening from nearshore to deeper marine basin. Moreover, the upper part of the Antalo limestone, mainly represented by marls and scarcely exposed, was separated in a new lithostratigraphic unit named Agula shale (BEYTH, 1972). It was still considered of Jurassic age and, because of the presence of gypsum lenses, attributed to a marginal marine environment.

Fossils with precise biostratigraphic resolution, such as ammonites, are generally lacking in the Antalo limestone of the Mekele outlier and therefore its age is not well constrained. However, on the basis of quite rich mollusc and brachiopod associations, it has been referred to the Late Jurassic (Oxfordian - Kimmeridgian: MERLA & MINUCCI, 1938; DAINELLI, 1943; MERLA *et al.*, 1979).

A recent attempt of revision of the Antalo limestone in the Mekele outlier in terms of sequence stratigraphy has been made by BOSELLINI *et al.* (1995). Four units have been distinguished on the basis of gross lithologic characters: basal member; subtidal member; stromatoporoid-oolitic member; marly member. These units, together with the overlying Agula shale, are interpreted as a single 2nd order transgressive-regressive cycle named Mekele Sequence (BOSELLINI *et al.*, 1995).

Source : MNHN, Paris

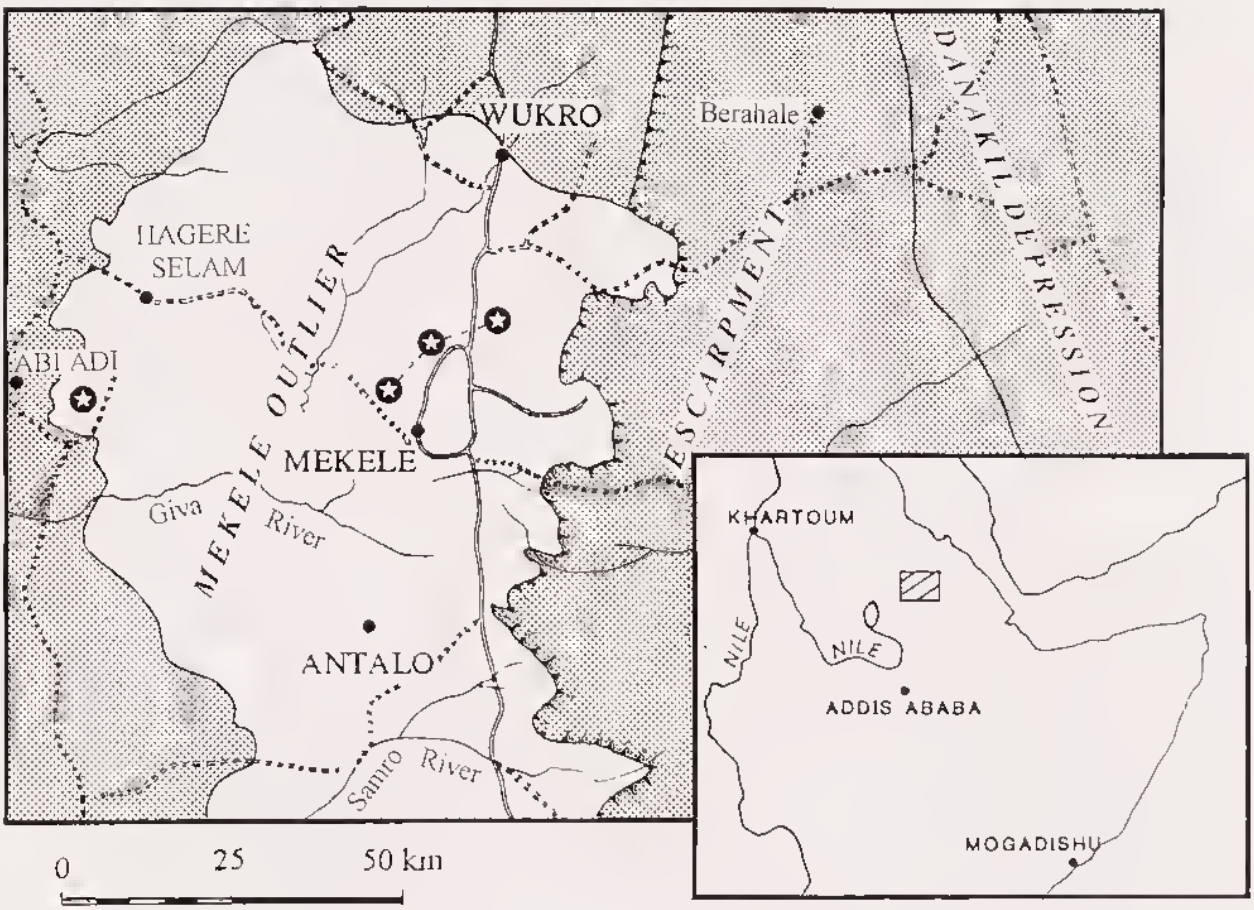

FIG. 1.— Geographic map of the Mekele outlier and location of the two measured stratigraphic sections (white stars).

FIG. 1.— Carte géographique de la région de Mekele et localisation des deux coupes levées (étoiles blanches).

Marine, mainly carbonate, deposits of comparable facies and stratigraphic position, still defined Antalo limestone, are known from other regions of eastern Africa: Blue Nile Basin: RUSSO *et al.* (1994); east central Ethiopia: FICCARELLI *et al.* (1975), TURI *et al.* (1980); Danakil Alps: SAGRI *et al.* (1998). In all these cases, however, the base of the formation seems to be older, Callovian or even Bathonian on the basis mainly of benthic foraminifera associations (e.g. *Pfenderina* gr. *trochoidea*) or ammonites (*Peltoceras* sp.) and nannofossils (SAGRI *et al.*, 1998).

Detailed studies are still needed for defining variations in lithology, facies and paleobiological communities, identifying discontinuities and cyclic patterns, and eventually tracing depositional sequences across the Mekele outlier. In this paper, the results of a first field trip will be presented. Two stratigraphic sections have been measured and sampled both for sedimentologic and biostratigraphic purposes. In spite of the preliminary character of the analysis, some new and interesting data have been obtained regarding both the age and the sedimentary evolution of the Antalo limestone in the Mekele outlier.

REGIONAL GEOLOGIC FRAMEWORK

The Mesozoic stratigraphic succession present in the Mekele outlier reflects the tectonic evolution of the Horn of Africa which is essentially the result of the breakup of the Gondwana supercontinent with opening of the Indian Ocean as recently summarized by BOSELLINI (1992). This crustal extension was preceded, in Late Paleozoic times, by a rifting phase that gave rise to a series of faulted basins mainly

Source : MNHN, Paris

oriented NE-SW. These basins were basically filled with continental sediments of the well known Karroo complex and are best represented in Somalia, Madagascar and India. This rift system was inundated by the sea, likely coming from the paleo-Tethyan margin sited to the North East (Oman, Pakistan, North India), at the beginning of the Jurassic (Pliensbachian or even before: Hamanlei sequence of BOSELLINI, 1992). On the contrary, to the the North e.g. in North Somalia, Ethiopia and Arabia, the deeply incised Karroo topography was replaced by a flat landscape of alluvial plains. Here the first marine deposits are therefore represented by the much younger Callovian, or even Oxfordian, to Kimmeridgian Antalo limestone (Uarandab sequence of BOSELLINI, 1992). The Late Jurassic transgression is obviously due to sea-floor spreading between Africa and the Madagascar-India-Seychelles block that began in Callovian-early Oxfordian time. This marine episode, however, was short-lived because an Early Cretaceous tectonic event, interpreted as a distal intraplate effect of the South Atlantic opening, caused an upwarping of the whole Horn of Africa. This resulted in emersion of most of the Ethiopian and northern Somalia territory and in the deposition of alluvial conglomerates and sandstones of the Amba Aradam formation.

THE ANTALO LIMESTONE IN THE MEKELE OUTLIER

The study has been carried out in the north-western part of the Mekele outlier geographically comprised between Mekele, Hagere Selam and Wukro (Fig. 1). Several localities have been visited during a first campaign (january 1996) and two stratigraphic successions have been measured and sampled: one is in the western sector, close to the small village of Agbe, between Hagere Selam and Abi Adi, where only the lower part of the formation is present because of a deeply incising erosional unconformity which is directly overlain by the continental sediments of the Amba Aradam formation (Cretaceous) (Fig. 2). The other section was measured few kilometres north of Mekele along the road to Wukro, where the middle and upper parts are present (Fig. 2). This section was already described by BOSELLINI *et al.* (1995). It has been measured and sampled in greater detail with both petrographic-sedimentologic and biostratigraphic purposes. The physical correlation between the Agbe and Mekele sections is possible because of the presence of an arenaceous unit overlain by micritic limestones and marls where the only ammonite moulds hitherto found have been collected. This correlation has been confirmed by microfacies analysis, foraminifers and ammonite biostratigraphy (Fig. 2).

A collection of about 100 rock samples from limestones and sandstones for petrographic analysis of thin sections and peels, and of 50 samples from marls for micropaleontological purposes (calcareous nannofossil analysis) has been made.

LITHOSTRATIGRAPHY

The Antalo limestone may be subdivided in four main lithostratigraphic units to be provisionally considered as informal members. This subdivision has no sedimentological/ paleoenvironmental connotation or even less sequence stratigraphic meaning: it is just based on gross lithologic differences and on morphology of weathering profiles with the main aim of enabling identification of the lithosomes for mapping purposes. Furthermore, each unit is not homogeneous internally but consists of a succession of several packages of beds with even marked lithologic and facies differences from one another. In the following description all these lithostratigraphic units will be treated with some detail in order to give a clear, albeit synthetic, picture of the Antalo limestone stratigraphy and to pose the basis for an interpretation of the sedimentary evolution of the basin.

From bottom to top the succession of the four units is (Fig. 2):

— Calcareous-marly unit A (about 170 m). The boundary with the underlying sandstones of the Adigrat formation is rather sharp: the colour changes from white or red to yellow ochre, burrows and marine fossils appear (bivalves and brachiopods), and the carbonate component of the rock, mainly represented by bioclasts, becomes abruptly important. Quartz grains, however, are very abundant at the base and remain still common in the first metres of the Antalo limestone. This unit is here described for the first time because it is not exposed in the Mekele section studied by BOSELLINI *et al.* (1995). The calcareous-marly unit may be further subdivided into three subunits:

Source : MNHN, Paris

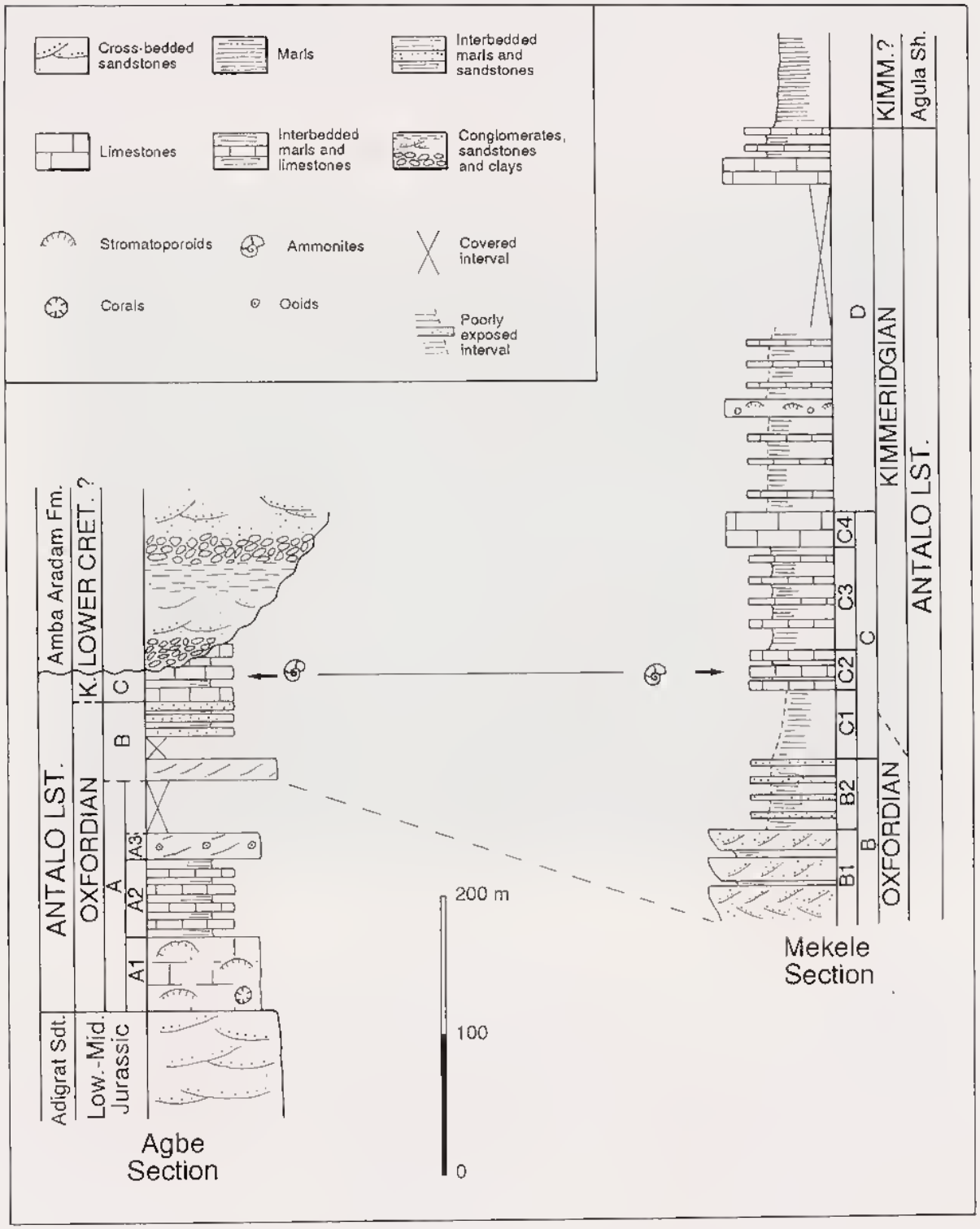

FIG. 2.— Simplified stratigraphic columns of the Mekele and Agbe sections.

FIG. 2.— Colonnes stratigraphiques simplifiées des coupes de Mekele et Agbe.

Source : MNHN, Paris

A1 (55 m) - Stromatoporoid- and coral-rich floatstones to rudstones are interbedded with grainstones to wackestones. Stromatoporoids and corals are found mainly in life position (Fig. 3). The grainstones are usually well sorted and contain skeletal grains (benthic foraminifers, debris of crinoids, ostreid bivalves) which are commonly coated by thin oolitic cortices or show a micritized rim; intraclasts and small oncoids are also present. In the wackestones, instead, the grains are represented by sponge spicules and rhaxes, gastropods and small fragments of stromatoporoids. In the middle part of this subunit, a clearly recognizable interval, 4-5 metres thick, consists of limestones with light grey to yellow chert nodules. In thin section they appear to consist of packstones with abundant reniform sponge rhaxes. This subunit is characterized by the presence of several discontinuities: omission surfaces (*sensu* BROMLEY, 1975, 1996) identified by firm ground burrows and the reddening of the surface; a hard ground, underlined by borings, encrustation by oysters, serpulids and iron oxides, which marks the top of the subunit A1 (Fig. 4).

FIG. 3.— Antalo limestone, subunit A1: globose stromatoporoids encrusted by corals. Agbe section.

FIG. 3.— Calcaire Antalo, sous-unité A1 : stromatoporidés globuleux incrustés par des coraux. Coupe de Agbe.

A2 (55 m) - This subunit is mainly made up of poorly exposed yellowish marl-limestone alternations. Brachiopods and pholadomiid bivalves, in life position, are common in the marls. Limestone beds, from 10 to 80 cm thick, consist of a variety of lithologies, from bioclastic rudstones or grainstones with stromatoporoid and echinoderm fragments, to oolitic grainstones and subordinated bioclastic wackestones. Some limestone layers show basal erosional features (burrow casts) and/or parallel to low angle laminae. Hard grounds, highlighted by bivalve borings and oyster encrustations, are occasionally present at the top of wackestone beds.

A3 (18 m) - Cross-bedded oolitic grainstones with locally abundant siliciclastic sand fraction. Many quartz grains make up the nuclei of ooids. Bivalve-rich, coquinoid beds are common especially in the lower part. Rare bimodality in the dip of oblique laminae suggest a possible tidal influence. Thin beds of dasyclad-rich wackestones are also present (Fig. 5). In the upper 8 metres, overlying a burrowed and reddened horizon (hard ground), the facies changes again to alternations of medium beds of bioclastic-ooidal grainstones still showing low angle laminae with mottled locally nodular bioclastic marls. A

Source : MNHN, Paris

covered 40 m-thick interval, likely consisting of fine grained marly sediments, separates the A3 subunit from the overlying arenaceous unit.

— Arenaceous unit B. In the Agbe sector only 14 metres of cross-bedded, often burrowed, tobacco sandstones crop out; they are interbedded with coquinoid packstones rich in ostreid valves. Higher up the section continues with about 50 metres of limestone-marl alternations in which scattered sandstone layers still occur. The arenaceous unit is instead best developed in the Mekele section (Fig. 6). Here two subunits are recognizable.

FIG. 4.— Antalo limestone, subunit A1: hard ground bored and encrusted by Fe oxides and ostreids at the top of the subunit. Agbe section.

FIG. 4.— Calcaire Antalo, sous-unité A1 : surface durcie creusée et encroutée par des oxydes de fer et ostréidés au sommet de la sous-unité. Coupe de Agbe.

B1 (65 m) - Upward thickening and coarsening cycles evolving from marly siltstones or sandstones to cross-bedded coarse-grained brown sandstones. Coquinoid sandy limestones are frequent. A tidal influence on deposition of coarse sandstones is documented by herringbone structures. At the base, black-coloured, phosphatic ooid grainstones are present.

B2 (49 m) - This portion of succession is mainly represented by marls and therefore is poorly exposed. Scattered thin to medium layers of fine sandstones with variable amounts of ostreid disarticulated shells however are recognizable along gentle slopes. These beds are characterized by parallel or low angle laminae and by erosional bases which show casts of *Rhyzocoralliun* or *Thalassinoides* burrows.

— Calcareous unit C (180 m). The lower part (subunit C1) is represented by a mainly marly unit (about 50 m), poorly exposed but clearly distinguishable from the underlying marls because of the lighter colour and the absence of sandstone layers (Fig. 6). A thick succession of micritic grey to light brown limestones follows with subordinate marly interlayers (subunit C2: about 30 m). At the very base, stromatoporoid and coral fragments together with sponge spicules and rhaxes, benthic foraminifers (*Everticyclammina*, *Alveosepta*) and oncoids occur. Higher up in the section, *Zoophycos* are common,

Source : MNHN, Paris

brachiopods and Pholadomiid bivalves are frequently found in life position. Some ammonite moulds have also been found in these layers. The third subunit C3 (75 metres) is characterized by limestone-marl alternations. Most limestone beds display typical features of storm layers: grain-supported textures (peloidal grainstones to coquinoid rudstones), erosional bases with burrow casts (*Rhyzocorallium, Planolites, Thalassinoides*), parallel to low angle laminae (Fig. 7). Both thinning and thickening upward cycles occur: the former consists of thin to very thin beds, whereas the latter end with medium to thick beds showing omission surfaces or even reddened and bored hard grounds. The paleontological content is similar to that of the lower subunit, except for the absence of ammonites and the greater abundance of benthic foraminifers. At the top of the unit C, marly interlayers disappear and purely micritic limestones give rise to a cliff 25 metres high (subunit C4, Fig. 6). Mudstones and wackestones are the prevailing textures; they are organized in thick beds quite regularly bounded by omission surfaces. No meaningful change in palaeobiological assemblages has been recognized.

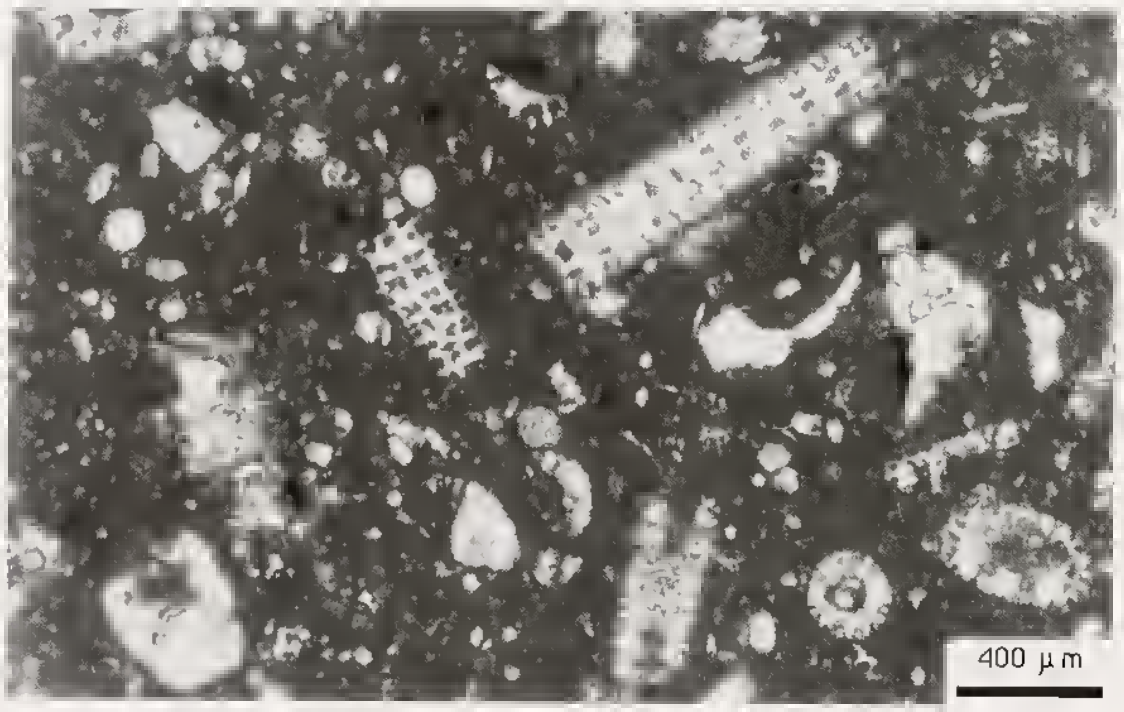

FIG. 5.— Antalo limestone, subunit A3: dasyclad-rich *(Trinocladus perplexus?)* wackestones interbedded with cross-bedded grainstones. Agbe section.

FIG. 5.— Calcaire Antalo, sous-unité A3 : wackestones riches en dasycladales (Trinocladus perplexus?) *intercalés avec des grainstones à stratifications entrecroisées. Coupe de Agbe.*

— Marly-calcareous unit D (280 m). On the whole this unit is poorly exposed because marls prevail over limestones especially in the upper part. Some prominent calcareous intervals however are recognizable which are potentially precious in facies analysis and lateral lithostratigraphic correlation. Over about 70 metres of poorly exposed marl-limestone alternations showing an increase of bioclastic packstones towards the top, the first of these calcareous intervals crops out. It is represented by a 10 metres thick set of beds of cross-bedded oolitic-bioclastic grainstones. Nerineid gastropods over 10 cm long are abundant and often display iso-orientation. Under the microscope, the presence of a debris of dasyclad algae is noteworthy. In the top 2 metres, the texture changes to wackestones and packstones; stromatoporoids, both in fragments and entire in life position, dominate the paleobiological assemblage. The second calcareous interval is located at 240 metres from the base of unit D. It consists of whitish micritic limestones about 20 metres thick. Bedding surfaces are plane parallel and beds range from thin

Source : MNHN, Paris

to medium. Both fossils and sedimentary structures are missing (Fig. 8). A hard ground, overlain by a thin lag of lithoclasts of the same micritic limestones, separates this interval from the following alternations of marls and bioclastic, current laminated limestones probably corresponding to storm layers. Worth mentioning are scattered thin beds occurring in the lower part of a 100 metres thick covered interval directly underlying the micritic limestones. These beds consist of spiculitic cherty limestones showing parallel and small scale cross laminations.

FIG. 6 .— Antalo limestone: the tract of section from subunits B1 to C4 is observable in the lower part of the Mekele section. The subunits B1 and C4 are particularly well exposed and recognizable in the weathering profile. Note the sharp change of colour between units B and C (large arrow).

FIG. 6.— Calcaire Antalo : l'ensemble de la coupe pour les unités B1 à C4 est observable dans la partie inférieure de la coupe de Mekele. Les sous-unités B1 et C4 sont particulièrement bien exposées et reconnaissables dans la coupe érodée. À noter le changement de couleur entre les unités B et C (flèche large).

In the studied area, the uppermost Antalo limestone is very poorly exposed. Therefore, the boundary with the overlying Agula Shale, defined by BEYTH (1972) probably on the basis of photogeological interpretations, cannot be recognized, as already observed by BOSELLINI *et al.* (1995).

The diagenetic features of the Antalo limestone have also been investigated and some selected samples have been studied also by means of cathodoluminescence (CL) observations. Some interesting, though preliminary, results have been obtained. They concern dissolution features present within ooid-bearing facies both in the subunit A3 and in the unit D. In the subunit A3 cm-wide, irregularly shaped dissolution vugs cut through grains and previous cements. In the other case, dissolution affected only nerineid shells. Cement stratigraphy, revealed by CL analyses, demonstrate that generation and filling of biomoldic cavities took place after the complete lithification of the surrounding sediment. In both cases dissolution was likely related to flushing of meteoric waters.

Source : MNHN, Paris

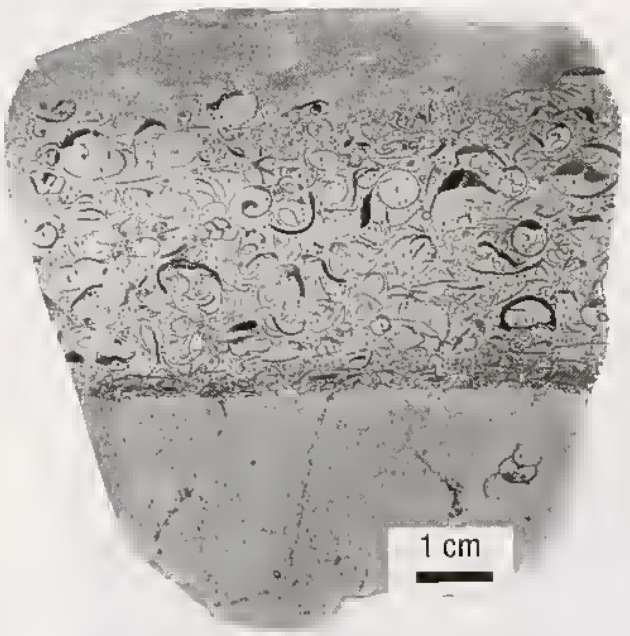

FIG. 7.— Antalo limestone, subunit C3: one of the frequent shell-rich storm layers. Note the sharp basal boundary. Mekele section.

FIG. 7.— Calcaire Antalo, sous-unité C3 : un des fréquents niveaux de tempêtes riches en coquilles. À noter le contact basal brutal. Coupe de Mekele.

BIOSTRATIGRAPHY

Biostratigraphic data concerning the Antalo limestone in the Mekele outlier are scattered. They are based essentially on foraminifers and stromatoporoids and allow to confirm an overall Oxfordian-Kimmeridgian age. The first significant micropalaeontological assemblage occurs about 30 metres over the base of the Antalo limestone, within the stromatoporoid-rich subunit A1. It is represented by *Kurnubia palastinienis* Henson, *Nautiloculina oolithica* Mohler and *Pseudocyclammina* sp. and points to the Oxfordian (e.g. SIMMONS & AL-THOUR, 1994) (Fig. 9a). This assemblage is replaced by a one dominated by taxa like *Alveosepta powersi* (Redmond) and *Everticyclammina virguliana* (Koechlin) characteristic of the early Kimmeridgian (Fig. 9b) (e.g. SIMMONS & AL-THOUR, 1994). This change occurs in the calcareous unit C about 20 metres above the top of the arenaceous unit B in the Agbe section. The data based on foraminifers seem to be confirmed by preliminary studies of stromatoporoids (A. RUSSO, pers. comm.). Taxa recognized in the same subunit A1 include *Shuqraia zuffardi* (Wells), *Dehornella harrarensis* (Wells), *D. crustans* Hudson and *Actinostromarianina praesalesensis* Zuffardi Comerci. According to TOLAND (1994), this assemblage may be referred to the Oxfordian because of the absence of the genus *Burgundia*. On the contrary, the stromatoporoid-rich layers occurring in the marly-calcareous unit D, is characterized by *Dehornella harrarensis* (Wells), ?*Promillepora pervinquieri* Dehorne, *Burgundia ramosa* Pfender, *B. trinorchii* Dehorne, *Actostroma danesini* Hudson, *Actinostromarianina lecompti* Hudson, which point to a Kimmeridgian age (TOLAND, 1994). Nannofossil assemblages have been also studied but, owing to the poor preservation state, they do not contribute to the refinement of the biostratigraphic framework (LOZAR, pers. comm.).

Ammonites have been found in the lower part of the calcareous unit C in both sections. At Agbe, at the top of the section, few metres below the boundary with the Amba Aradam formation, ammonites referable to *Ataxioceras (Parataxioceras)* gr. *polyplocum* (Reinecke) have been collected (Fig. 9c, d). In the other section (Mekele) the assemblage is richer although only two taxa have been found: *Ptychophylloceras* sp. (juv. specimens) and *Ataxioceras* (A.) gr. *discoidale* Schneid (Fig. 9e). These assemblages are not comparable to the ones described by SAGRI *et al.* (1998) in the Danakil Alps which are dominated by Mayaitids and indicative of the middle Oxfordian. The Mekele ammonites instead bear more elements of similarity with forms reported by VENZO (1959) from the Harar region and may be referred to the early Kimmeridgian.

DISCUSSION

The available data are not sufficient to propose a well-grounded paleoenvironmental and sedimentologic interpretation of the Antalo limestone in the Mekele outlier. The two measured sections are about 40 km apart and their stratigraphic overlap is minimum (Fig. 2). Moreover, the percentage of covered intervals is more than 40% at Agbe and in the lower part of the Mekele section, and exceeds 60% in the upper part. Facies analysis, although biased by the just exposed factors, has led to the recognition of some diagnostic facies or facies associations: cross-bedded oolitic grainstones associated to minor dasyclad-bearing wackestones, herringbone cross-bedded sandstones with ostreid-rich layers, stromatoporoid- and coral-bearing rudstones to floatstones, bioclastic or peloidal storm layers with erosional bases interbedded with marls, thin bedded micritic limestones and marls characterized by

Source : MNHN, Paris

pelagic biota (ammonites, nannofossils). These facies point to an overall carbonate ramp system episodically affected by a high siliciclastic input as already suggested by previous authors for the Antalo limestone in the same area (BOSELLINI *et al.*, 1995) or in other regions (SAGRI *et al.*, 1998). The vertical organization of these facies, ranging from inner ramp oolitic shoals or sandy estuarine systems to outer ramp or basin muddy sediments deposited below storm wave base level, reveals several relative sea-level changes. The complex pattern of these changes still bears some points of uncertainty because of

FIG. 8.— Antalo limestone, unit D: detail of the evenly bedded, barren micritic limestones present at the top of the unit. Mekele section.

FIG. 8.— Calcaire Antalo, unité D : détail de calcaires micritiques, régulièrement stratifiés, azoïques, présents au sommet de l'unité. Coupe de Mekele.

the presence of enigmatic facies such as the scarcely fossiliferous, homogeneous micritic limestones (subunit C4 and top of unit D) whose paleoenvironmental interpretation is douhtful. They could be interpreted either as deposits of a restricted inner ramp or as (hemi)pelagic basinal or outer ramp deposits. In fact the former interpretation has been applied to similar and coeval facies of the Antalo limestone by SAGRI *et al.* (1998). The absence of both biota and sedimentary structures distinctive of a lagoonal setting together with the presence of calcareous nannofossil remains, revealed by SEM observations, suggest a more likely basinal origin.

For the same reasons above exposed, a clear picture of lateral facies and thickness variations of sedimentary hodies cannot be reconstructed as well. However, reconaissance field work in the northwestern part of the Mekele outlier has evidenced some slight but significant changes. The thickness of the whole formation increases from west to east and, more in particular, the basal calcareous-marly unit A shows the following trends from west to east: a) massive coral- and stromatoporoid-bearing beds decrease in thickness and fossil content, and are separated by increasingly thicker marly layers; b) the oolitic unit (subunit A3), thick-bedded and characterized by large-scale cross bedding in the Agbe section, grades into a succession of thin bedded calcarenites with hummocky cross-stratification and

Source : MNHN, Paris

FIG. 9.— **a**, *Kurnubia palastiniensis* Henson and *Nautiloculina* sp. Agbe section, subunit A1; **b**, *Alveosepta powersi* (Redmond), Mekele section, subunit C3; **c**, **d**, *Ataxioceras* (A.) gr. *discoidale* Schneid. Agbe section, unit C, (1.65x); **e**, *Ataxioceras* (*Parataxioceras*) gr. *polyplocum* (Reinecke). Mekele section, subunit C2, (1.4 x).

*FIG. 9.— **a**,* Kurnubia palastiniensis *Henson et* Nautiloculina *sp. Coupe de Agbe, sous-unité A1 ; **b**,* Alveosepta powersi *(Redmond), Coupe de Mekele, sous-unité C3 ; **c**, **d**,* Ataxioceras *(A.) gr.* discoidale *Schneid. Coupe de Agbe, unité C - x1,65 ; **e**,* Ataxioceras (Parataxioceras) *gr.* polyplocum *(Reinecke). Coupe de Mekele, sous-unité C2 - x1,4.*

Source : MNHN, Paris

wave ripple lamination in the surroundings of Wukro. In addition to this, the arenaceous unit B, clearly recognizable in the morphology in the Mekele section, seems to disappear west of Wukro. This picture is congruent with an eastward trend of thickening and deepening of the Antalo limestone as suggested by BOSELLINI *et al.* (1995) and SAGRI *et al.* (1998) in the Shekat region and Danakil Alps respectively.

A so far underestimated feature of the Antalo limestone is the common presence of discontinuity surfaces which are widespread in every member except for the arenaceous one. They range from omission surfaces, evidenced by firm-ground burrows, to hard grounds, documented by borings, Fe-oxide coatings and/or bioencrustation by ostreids (Fig. 4). These surfaces, which underline hiatuses of variable extent and correspond to significant changes in the environmental parameters controlling deposition, may be a great aid in lateral correlations. They should be considered as potential tools for subdividing the formation in physical stratigraphic units (allostratigraphic units) correlatable across facies. Moreover, once the more laterally persistent surfaces are recognized, they will enable chronostratigraphic correlations with deeper parts of the basin more detailed than biostratigraphy can allow in a formation where ammonites are very scarce, nannofossils poorly preserved and benthic foraminifers poorly resolutive.

CONCLUSION

The preliminary results of this study may be summarized as follows:

— refinement of the lithostratigraphy of the Antalo limestone, which consists of more than 150 metres of limestones and marls underlying the well recognizable arenaceous member, previously held as the base of the formation (BOSELLINI *et al.*, 1995);

— recognition that the arenaceous unit is separated from the Adigrat sandstones by about 150 m of limestones, poses the question of the causes of this terrigenous input of sediments: a climatically driven increase in continental run-off or a tectonic-related rejuvenation of the inland are the more probable candidates. Moreover, the sequence stratigraphic interpretation of the Mekele sequence (BOSELLINI *et al.*, 1995) needs to be revised in the light of these new data;

— confirmation of the Oxfordian - Kimmeridgian age of the Antalo limestone based on benthic foraminifer and stromatoporoid assemblages. Ammonites, newly found in the middle part of the formation, allow to refer the lower part of the calcareous unit C to the early Kimmeridgian in accord to the other biostratigraphic data;

— paleoenvironmental interpretation: stratigraphic and sedimentologic analyses suggest that the overall depositional setting was represented by a low-gradient ramp basically controlled by storm processes. Relative sea-level changes are considered to be the main factor in causing the sharp superposition of outer ramp (micritic limestones, marls with thin tempestites) and inner ramp (oolitic grainstones, coral-stromatoporoid rudstones) facies;

— recognition of slight lateral changes in thickness and facies in an east-west direction revealing a possible eastward deepening of the ramp, in accord with palaeogeographic reconstructions proposed by other authors (BOSELLINI *et al.*, 1995; SAGRI *et al.*, 1998);

— recognition of several discontinuity surfaces, which are potential tools for subdividing the Mekele sequence (BOSELLINI *et al.*, 1995) in groups of cycles, or parasequences, and for correlation with deeper parts of the basin to be studied in the future.

ACKNOWLEDGMENTS

We wish to thank Dr. Solomon TADESSE and Dr. Getaneh ASSEFA (Addis Ababa) for introducing us into Ethiopian geology and stratigraphy, and for their kind collaboration in organizing the field work. C. NERI (Ferrara) and A. RUSSO (Modena) are gratefully acknowledged for their help in field and laboratory analyses, and F. ATROPS (Lyon) for useful advices about Kimmeridgian ammonites. Many

Source : MNHN, Paris

thanks to A. PAGANI, N. COLANERO and G. BALBI of the Italian Cooperation for logistic facilities during our stay at Mekele. Financial support by Peritethys programme, funds n° 94-65, 95-78 and 95/96-78.

REFERENCES

ARKIN, Y., BEYTH, M., DOW, D.B., LEVITTE, D., TEMESGEN HAILE & TSEGAYE HAILU, 1971.— Geological map of Mekele, sheet area ND-37-11, Tigre Province, scale 1:250.000. *Ethiopia Geological Survey*.

BEAUCHAMPS, J. & LEMOIGNE, Y., 1974.— Prèsence d'un bassin de subsidence en Éthiopie centrale et essai de reconstruction palèogèographique de l'Èthiopie durant le Jurassic. *Bulletin de la Société géologique de France, Paris*, (7), **16**: 563-569.

BEYTH, M., 1972.— Paleozoic-Mesozoic sedimentary basin of Mekele outlier, northern Ethiopia. *The American Association of Petroleum Geologists Bulletin*, **56**: 2426-2439.

BLANFORD, W.T., 1870.—*Observations on the Geology and the Zoology of Abyssinia during the Progress of British Expedition to that Country in 1867-1868*. McMillan, London: 1-487.

BOSELLINI, A., 1992.— The continental margins of Somalia. Structural evolution and sequence stratigraphy. *American of Association Petroleum Geologists. Memoir*, **53**: 185-205.

BOSELLINI, A., RUSSO, A. & GETANEH ASSEFA, 1995.— Il Calcare di Antalo nella regione di Makallé (Tigrai, Etiopia settentrionale). *Atti della Accademia Nazionale dei Lincei, Rendiconti Fisiche*, serie 9, **6**: 253-267.

BROMLEY, R.G., 1975.—Trace fossils at omission surfaces. *In*: R.W. FREY (ed.), *The Study of Trace Fossils*. Springer-Verlag, New York: 399-428

BROMLEY, R.G., 1996.— *Trace fossils: Biology, Taphonomy and Applications*. Chapman & Hall, London: 1-361.

DAINELLI, G., 1943.— *Geologia dell'Africa orientale italiana*. Reale Accademia d'Italia, Roma: 4 vol.

FICCARELLI, G., PIRINI-RADDRIZZANI, C. & TURI, A., 1975.— Analyses of the microfacies of Antalo Limestone in the Dire Dawa area, Ethiopia. *Società Geologica Italiana, Bollettino*, **94**: 759-770.

MERLA, G. & MINUCCI, E., 1938.—*Missione geologica nel Tigrai*. Reale Accademia d'Italia, Roma: 1-336.

MERLA, A., ABBATE, E., AZZAROLI, A., BRUNI, P., CANUTI, P., FAZZUOLI, M., SAGRI, M. & TACCONI, P., 1979.— *A Geological Map of Ethiopia and Somalia*. CNR, Firenze: 1-95.

RUSSO, A., GETANEH ASSEFA & BALAMWAL ATNAFU, 1994.— Sedimentary evolution of the Abbay River (Blue Nile) Basin, Ethiopia. *Neues Jahrbuch für Geologie und Palaeontologie, Monatshefte*, **5**: 291-308.

SAGRI, M., ABBATE, E., AZZAROLI, A., BALESTRIERI, M.L., BENVENUTI, M., BRUNI, P., FAZZUOLI, M., FICCARELLI G., MARCUCCI, M., PAPINI, M., PAVIA, G., REALE, V., ROOK, L. & TECLE, T.M., 1998.— New data on the Jurassic and Neogene sedimentation in the Danakil Horst and Northern Afar Depression, Eritrea. *In:* S. CRASQUIN-SOLEAU & E. BARRIER (eds), Peri Tethys Memoir 3: stratigraphy and evolution of Peri-Tethyan platforms. *Mémoires du Muséum national d'Histoire naturelle*, **177**: 193-214.

SIMMONS, M.D. & AL-THOUR, K., 1994.— Micropaleontological biozonation of the Amran Series (Jurassic) in the Sana'a region, Yemen Republic. *In*: M.D. SIMMONS (ed.), *Micropaleontology and Hydrocarbon Exploration in the Middle East*. Chapman & Hall, London: 43-79.

TOLAND, C., 1994.— Late Mesozoic stromatoporoids: their use as stratigraphic tools and palaeoenvironmental indicators. *In*: M.D. SIMMONS (ed.), *Micropaleontology and Hydrocarbon Exploration in the Middle East*. Chapman & Hall, London: 113-119.

TURI, A., BIGI, L. & PIRINI-RADDRIZZANI, C., 1980.— Microfacies of the Antalo Limestone (Middle to Upper Jurassic) in some sections of east-central Ethiopia. *Società Geologica Italiana, Bollettino*, **99**: 437-454.

VENZO, S., 1959.— Cefalopodi neogiurassici degli Altipiani Hararini. *Acradenia Nazionale dei Lincei*, **4**: 103-197.

Source : MNHN, Paris

7

Stratigraphic and palaeogeographic survey of the Lower and Middle Jurassic along a north-south transect in western Algeria

Serge ELMI [1], *Yves ALMÉRAS* [1], *M'Hamed AMEUR* [2], *Jean-Paul BASSOULLET* [3], *Mohamed BOUTAKIOUT* [4] *Miloud BENHAMOU* [2], *Abbés MAROK* [2], *Larbi MEKAHLI* [2], *Abderrahmane MEKKAOUI* [5] & *René MOUTERDE* [6]

[1] UFR des Sciences de la Terre, Université Claude Bernard, UMR 55-65 CNRS
27-43, boulevard du 11 Novembre, F-69622 Villeurbanne Cedex, France

[2] Institut des Sciences de la Terre (IGMO), Équipe de Recherche 3101-05-03-92, Université d'Oran,
B.P. 1524 El M'daouer, DZ-31000 Oran, Algérie

[3] CNRS, UPRES EA 2250 Laboratoire de Géobiologie, Biochronologie et Paléontologie humaine
Université de Poitiers, 40, avenue du Recteur Pineau, F-86022 Poitiers, France

[4] Institut des Sciences de la Terre, Faculté des Sciences, Université Mohamed V
Avenue Ibn Batouta, MA-Rabat, Maroc

[5] Établissement de Recherche et d'Exploitation Minières, Centre de Béchar, Algérie

[6] Centre International d'Études du Lias, Université catholique,
25, rue du Plat, F-69288 Lyon Cedex 02, France

ABSTRACT

A general review of the available data on the Lower and Middle Jurassic of western Algeria is briefly summarized here. The Tlemcen Domain is characterized by: a) late development of the initial carbonate platform (late Sinemurian to early Pliensbachian); b) a late transgression or a late deepening on the more prominent shoals (late Pliensbachian to early Bathonian); c) limited geographic expansion of the middle carbonate platform (Aalenian-early Bajocian); d) strong deepening during the late Bajocian and the early Bathonian leading to the submerging of the major part of the shoals with the exception of some

ELMI, S., ALMÉRAS, Y., AMEUR, M., BASSOULLET, J. P., BOUTAKIOUT, M., BENHAMOU, M., MAROK, A., MEKAHLI, L., MEKKAOUI, A. & MOUTERDE, R., 1998. — Stratigraphic and palaeogeographic survey of the Lower and Middle Jurassic along a north-south transect in western Algeria. *In*: S. CRASQUIN-SOLEAU & É. BARRIER (eds), Peri-Tethys Memoir 4: epicratonic basins of Peri-Tethyan platforms, *Mém. Mus. natn. Hist. nat.*, **179** : 145-211. Paris ISBN : 2-85653-518-4.

Source : MNHN, Paris

seamounts within the Traras Mountains; e) influxes of siliciclastic turbidites within the marly sedimentation during the Callovian and the early Oxfordian. The most important feature of the High Plains is the renewal of the sabkha regime during the Toarcian, in relation to tectonic reorganisation of the palaeogeographic pattern. The major feature of the Atlas domain (Ksour Mountains) is, by comparison with the Tlemcen domain, the early development of the initial carbonate platform, probably as early as the Rhaetian-Hettangian in the most subsiding subbasin (Aïn Ouarka, Chemarikh). The lower Hettangian age has been proved by the first known occurrence of an Hettangian ammonite, in the south of the Rif-Tell (*Caloceras* sp.). The Sinemurian is well dated by rich ammonite faunas. The subsiding umbilics became hemipelagic during the Sinemurian with radiolarian limestones. Regional peak deepenings happenned during the late Pliensbachian, the early Toarcian and the late Bajocian. The return to a platform environment began diachronously during the late Bajocian and the early Bathonian. The Figuig (eastern Morocco) Atlas sustained a rapid and strong subsidence and deepening during the late Sinemurian in the Figuig Umbilic. Sedimentary and structural features suggest the importance of local tectonic control. The transition to the Saharian Craton is documented in the Southern Grouz (Koudiat el Haïddoura) where newly collected brachiopods indicate late Pliensbachian (Domerian) and late Bajocian relative sea level rises. All these data are coherent with the model of aborted rifts or aulacogens developed along the Saharian Atlas and along the Tlemcen domain. But the evolution of these two longitudinal furrows has been diachronous. The present study clearly indicates that regional tectonic events overprint the global signal and that an eustatic sea-level chart must be the result of comparisons between different plates as tectonically uncoupled as possible. A new ammonite species (*Hammatoceras roubanense* n. sp. Elmi) from the middle Toarcian is described.

RÉSUMÉ

Étude stratigraphique et paléogéographique du Jurassique inférieur et moyen le long d'un transect nord-sud en Algérie occidentale.

Un exposé succint des faciès et des données biostratigraphiques sur le Jurassique inférieur et moyen de l'Ouest algérien conduit à une reconstruction paléogéographique et paléodynamique d'une transversale, longue de 700 km, depuis la Méditerranée et la Chaîne alpine jusqu'au Craton saharien. Le domaine tlemcenien se distingue par : a) installation tardive de la plate-forme carbonatée initiale (Sinémurien supérieur- Pliensbachien inférieur = Carixien) ; b) enfouissement tradif des hauts-fonds les plus saillants (du Pliensbachien supérieur-Domérien au Bathonien inférieur et même au Callovien inférieur dans la région des Traras ; c) extension géographique limitée de la plate-forme carbonatée médiane sur les bords de sillons ou d'ombilics en cours d'approfondissement par suite d'un découplage tectoniquement contrôlé (Aalénien-Bajocien inférieur) ; d) fort approfondissement pendant le Bajocien supérieur et le Bathonien inférieur ; e) arrivée de turbidites silicoclastiques au cours du Callovien et de l'Oxfordien inférieur. La profondeur maximale est atteinte à l'Oxfordien terminal. Elle est suivie d'une inversion rapide illustrée par la progradation des grès prodeltaïques de l'Oxfordien supérieur-Kimméridgien inférieur. Les Hautes Plaines sont caractérisées par la réapparition des faciès confinés, et même des sebkhas, pendant le Toarcien. Il s'agit, là encore, d'une preuve de l'intensité de la différenciation tectonique au début de cet étage puisque, dans les régions contiguës, un approfondissement notable se déroule contemporainement, illustré par des phénomènes de resédimentation en masse (turbidites calcaires). La principale caractéristique des Monts des Ksour (domaine atlasique) consiste dans le développement précoce de la plate-forme carbonatée initiale, probablement dès le Rhétien et le début de l'Hettangien dans l'axe des futurs sillons (Aïn Ouarka, Chemarikh). La présence d'une ammonite de l'Hettangien inférieur est établie, pour la première fois dans le Maghreb au Sud de la Chaîne alpine (Rif et Tell). Il s'agit probablement d'un *Caloceras* sp. Les ombilics deviennent hémipélagiques pendant le Sinémurien avec des calcaires à radiolaires. Après cette période de différenciation, des approfondissements importants se développent pendant le Toarcien inférieur et le Bajocien supérieur. Ces phénomènes sont largement contrôlés par la tectonique locale. Le cycle sédimentaire s'inverse ensuite avec le retour diachrone à un environnement de plate-forme proximale (de la fin du Bajocien supérieur à la fin du Bathonien inférieur). Dans l'Atlas de Figuig (Maroc oriental à l'extrémité occidentale des Monts des Ksour), la subsidence et l'approfondissement deviennent dominants pendant le Sinémurien supérieur. Les contrôles paléotectoniques provoquent la différenciation de l'ombilic de Figuig où les brèches de pente, la resédimentation de matériaux transportés depuis les bordures et les phénomènes de glissement sont spectaculaires. La transition au Craton saharien intervient brutalement; ainsi il y a passage en quelques kilomètres depuis les séries de sillon (Grouz marocain) à celles de la bordure saharienne (Grouz algérien : Koudiat el Haïddoura). Dans ces dernières, la découverte de gisements de brachiopodes permet de reconnaître les épisodes de haut niveau marin du Domérien et du Bajocien supérieur. Une nouvelle espèce d'ammonite du Toarcien moyen (*Hammatoceras roubanense* sp. nov. Elmi) est décrite.

INTRODUCTION

PRELIMINARY REMARKS

Our previous publications have set the framework for precise correlations at the regional scale, especially along transects situated westward and eastward of the Algeria-Morocco border (BASSOULLET, 1966, 1968, 1971; ELMI, 1971a, b; 1978, 1981a, 1983, 1987, 1996a, 1997; MEKAHLI *et al.*, 1994). Many

Source : MNHN, Paris

data are presented in several unpublished Ph-D and Master thesis (BASSOULLET, 1973; GUARDIA, 1975; DOUIHASNI, 1976; AMEUR, 1978, 1988; BENHAMOU, 1983; MEKAHLI, 1988, 1995; AÏT OUALI, 1991; MAROK, 1995, 1996; OUALI-MEHADJI, 1995; TLILI, 1995). A rapid survey has been also made by CISZAK (1993) using data available in the litterature. KAZI-TANI'S thesis (1986) is also a general review of second hand data. Some lithostratigraphic synthesis have tried to give a simple chart for a large part of Western Maghreb (FEDAN, 1989; KAZI-TANI, 1986; AÏT-OUALI, 1991) but the units are often diachronous and/or sedimentologically heterogenous and they suppose that the correlations are better established than they really are. Only a brief summary of some important results can be given here. Tables 1 and 2 summarize the chronostratigraphic and biostratigraphic units used for this report. They will not be discussed here. The general location of the Jurassic outcrops is given on figures 1 and 26.

The present paper has been written under the direction of Serge ELMI. The authors of the different parts are: Serge ELMI (Introduction; The Rhar Roubane and Tlemcen Mountains; Main palaeogeographical and palaeostructural events; Palaeontological remarks); Serge ELMI, M'Ahmed AMEUR & Miloud BENHAMOU (The Traras Mountains); Abbés MAROK, Serge ELMI & Larbi MEKAHLI (Oran High Plains, The Sidi el Abed Mountains); Larbi MEKAHLI, Serge ELMI, Jean-Paul BASSOULLET, Yves ALMÉRAS & René MOUTERDE (The Ksour Mountains and the Atlas Domain); Serge ELMI & Mohamed BOUTAKIOUT (Figuig Subbasin or Umbilic); Abderrahmane MEKKAOUI, Serge ELMI, Miloud BENHAMOU & Larbi MEKAHLI (The transition to the Sahara).

The Jurassic of north west Maghreb can be divided conveniently into three formal lithostratigraphic "Groups" (AUGIER, 1967; GUARDIA, 1975) which are diachronous as they are related to the tectono-sedimentary history of the area as well as to more general controls (Tethyan and Atlantic dynamics and global eustacy). These groups are named here in the north-west corner of Algeria:

— the Lower Carbonate Group or Traras Group (Lower Jurassic to Bathonian);

— the Middle Sandy-Argillaceous Group or Selib Group (Callovian to lower Kimmeridgian);

— the Upper Carbonate Group or Tlemcen Group (Kimmeridgian-Tithonian).

In the Atlas of Morocco and western Algeria, the Upper Carbonate Group is replaced by deltaic sediments (Ksour Sandstones Group, for instance). Sequential divisions will be used with care because they are often interpretative and controversial. The present sequential language is too much linked to a sedimentologic model which does not take into account the actual physiography of the sedimentary areas.

The charts of the formations (Tables 3 and 4) are relatively detailed in order to reflect the structural and palaeogeographical complexity of the area and to avoid simplified and erroneous correlations. They reflect also the diversified pattern of the facies in a region during a period of intensive taphrogenetic differentiation. Formations will be briefly defined when necessary. The tentative division of the Lower Jurassic in four formations (L1 to L4) by AÏT OUALI (1991) is based on sequential hypothesis. Their chronologic correlations are rarely proved. They are roughly comparable to the "tectono-stratigraphical episodes" of ELMI (1996b).

Lists of fossils will be given only if they are necessary for the correlations or when they have been newly established. Some ammonites will be figured because of their stratigraphic or palaeontologic importance.

Concerning the spelling of the transcriptions of arabic names, we have adopted the common use as given on recent maps or as established by national rules. Thus we shall write "Djebel" for Algerian localities and "Jebel" for Moroccan ones.

PALAEOGEOGRAPHIC UNITS BETWEEN THE MEDITERRANEAN (TRARAS MOUNTAINS) AND THE SAHARA

From north to south, the major structural zones can be defined on their palaeogeographic and structural features, illustrated on a palaeogeographic map for the Toarcian (Fig. 1; see also Fig. 26). North Africa is classically divided in two major structural domains, north of the Saharian craton.

Source : MNHN, Paris

TABLE 1.— Chronostratigraphic and biostratigraphic units used in NW Maghreb (Lower Jurassic = Lias) and explanation of the abbreviations used on the figures. Remarks on the zonal divisions. 10: identification of the Jamesoni Zone is not easy in NW Maghreb; 11: the local Demonense Zone (ELMI 1987) is approximately comparable to the European Ibex Zone but its lower limit is probably older since *Tropidoceras* appears at the end of the Jamesoni Zone in Europe; 13-15: classic Tethyan equivalents of, respectively, the Stokesi, Margaritatus and Spinatum Zones; 20-23: cf. ELMI *et al.* (1993, 1997).

TABLEAU 1.— Divisions chronostratigraphiques et biostratigraphiques utilisées dans le NW du Maghreb (Jurassique inférieur = Lias). Les symboles et abréviations sont ceux utilisés sur les figures. Remarques sur les divisions. 10 : l'identification de la zone à Jamesoni n'est pas facile dans le NW du Maghreb ; 11 : la zone à Demonense locale (ELMI, 1987) est approximativement comparable à la zone à Ibex européenne, mais sa limite inférieure est probablement plus ancienne car Tropidoceras *apparaît à la fin de la zone à Jamesoni en Europe ; 13-15 : équivalents téthysiens classiques, respectivement, des zones à Stokesi, Margaritatus et Spinatum ; 20-23 : cf. ELMI* et al. *(1993, 1997).*

STAGES (and SUBSTAGES)		Ammonites Zones South Tethyan Domain		Regional Markers
AALENIAN (Lower) L Aa MIDDLE JURASSIC		24 OPALINUM	Op	
LOWER JURASSIC		23 AALENSIS	Al	
		22 MENEGHINII	Me	
TOARCIAN To	UPPER UTo	21 SPECIOSUM	Sp	
		20 BONARELLII	Bo	
	MIDDLE MTo	19 GRADATA	Gr	Alticarinata Gradata
		18 BIFRONS	Bi	Bifrons Sublevisoni
	LOWER LTo	17 LEVISONI	Le	
		16 POLYMORPHUM	Po	Mirabile Horizon
PLIENSBACHIAN Pl	UPPER = DOMERIAN Do	15 EMACIATUM	Em	
		14 ALGOVIANUM	Ag	
		13 CELEBRATUM	Ce	Celebratum Subzone Portisi Subzone
	LOWER = CARIXIAN Cx	12 DAVOEI	Da	
		11 "DEMONENSE"	De	
		10 (JAMESONI)	Ja	appearance of *Tropidoceras*
SINEMURIAN Si	UPPER U Si	9 RARICOSTATUM	Ra	
		8 OXYNOTUM	Ox	
		7 OBTUSUM	Ob	Margarita "Horizon"
	LOWER L Si	6 TURNERI	Tu	Rejectum Interval
		5 SEMICOSTATUM	Se	
		4 BUCKLANDI	Bu	
HETTANGIAN He	UPPER MIDDLE LOWER	3 ANGULATA	An	
		2 LIASICUS	Li	
		1 PLANORBIS	Pl	

— The Rif-Tell domain, part of the Alpine Chain of North Africa (Maghrebids), related to the opening of the central Atlantic since the Bathonian-Callovian. Before, it appears to belong to the Tethyan Domain. North of the transect, it includes a composite Oran Basin (GUARDIA, 1975). It overthrusts the Alpine foreland.

Source : MNHN, Paris

TABLE 2.— Chronostratigraphic and biostratigraphic units of NW Maghreb (Middle Jurassic = Dogger) and explanations of the abbreviations used on the figures. Remarks. 41: the range of the Retrocostatum Zone is here considered as extended to all the Upper Bathonian because *Clydoniceras* appears as early as the lower Bathonian and because the Discus Zone is always poorly documented in the Tethyan realm and no reliable equivalent is defined; 44 and 46: local indexes for, respectively, the Anceps and Athleta Zones (ELMI, 1971a); they are used here because the correlations are not definitively established. The uppermost Callovian (Lamberti Zone) is not documented in the studied area.

TABLEAU 2.— Tableau des divisions chronostratigraphiques et biostratigraphiques utilisées dans le NW du Maghreb (Jurassique moyen = Dogger). Les symboles et abréviations sont ceux utilisés sur les figures. Remarques. 41 : la répartition de la zone à Retrocostatum est ici considérée comme s'étendant sur tout le Bathonien supérieur car Clydoniceras *apparaît dès le Bathonien inférieur et parce que la zone à Discus est toujours très mal connue dans le domaine téthysien et il n'existe pas d'équivalents clairement définis ; 44 et 46 : index locaux pour, respectivement, les zones à Anceps et Athleta (ELMI, 1971a) ; ils sont utilisés ici car les corrélations ne sont pas définitivement fixées. Le Callovien terminal (zone à Lamberti) n'est pas connu dans la zone étudiée.*

STAGES (and SUBSTAGES) UPPER JURASSIC		Ammonites Zones South Tethyan Domain		Regional Markers
MIDDLE JURASSIC		?		
CALLOVIAN Ca	UPPER UCa	46 TREZEENSE	Tz	
	MIDDLE MCa	45 CORONATUM 44 ARKELLI	Co Ar	
	LOWER LCa	43 GRACILIS 42 BULLATUS	Gl Bs	
BATHONIAN Bt	UPPER UBt	41 RETROCOSTATUM	Re	
	MIDDLE MBt	40 BREMERI 39 MORRISI 38 SUBCONTRACTUS 37 PROGRACILIS	Br Mo Sc Pg	
	LOWER LBt	36 AURIGERUS 35 ZIGZAG	Au Zi	← Oraniceras Or
BAJOCIAN Bj	UPPER U Bj	34 PARKINSONI 33 GARANTIANA 32 NIORTENSE	Pa Ga Ni	← main level with Ermoceras
	LOWER LBj	31 HUMPHRIESIANUM 30 PROPINQUANS 29 LAEVIUSCULA 28 DISCITES	Hu Pr Le Di	← Sauzei ↕ Haplopleuroceras
AALENIAN Aa	UPPER UAa	27 CONCAVUM	Cc	
	MIDDLE M Aa	26 BRADFORDENSIS 25 MURCHISONAE	Bd Mu	
	LOWER L Aa	24 OPALINUM	Op	

— The Berberids extend south of the Alpine overthrust. They are composed of three great structural and palaeogeographic units: the Tlemcen domain, the High Plains and the Atlas (Ksour) domain. To the south, extends the Sahara Platform or Craton. The Lower and Middle Jurassic successions are given on tables 3 and 4.

Source : MNHN, Paris

TABLE 3.— Major formal lithostratigraphic units, successions, facies and environments along the NW-SE transect Traras-Saharian Atlas - Part 1: Lower Jurassic.

TABLEAU 3.— Principales unités lithostratigraphiques (formations) et leurs faciès et environements le long de la transversale NW-SE Traras-Atlas saharien, 1ère partie : Jurassique inférieur.

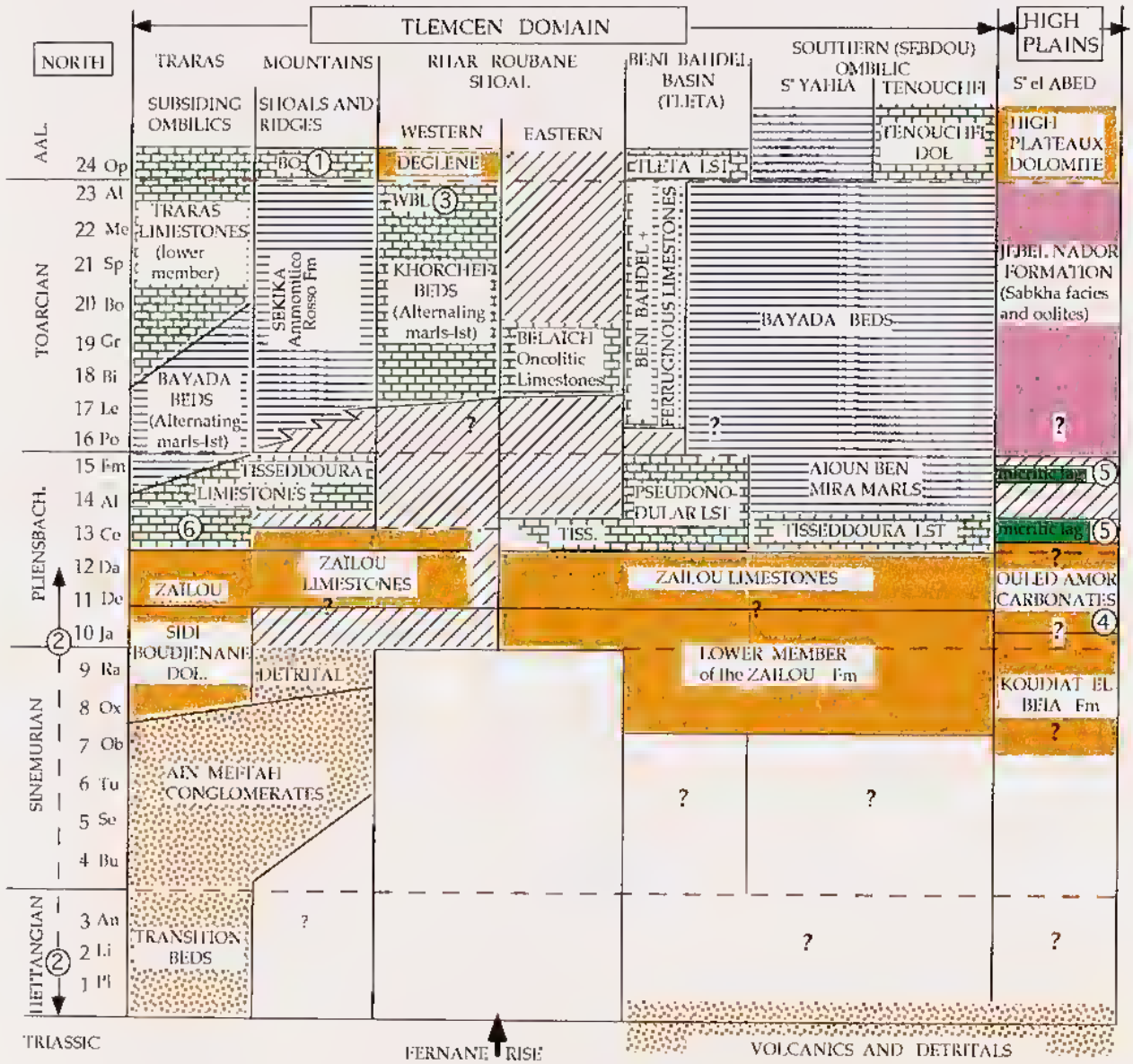

① Beni Ouarsous oncolitic and stromatolitic condensed ferruginous bed (TRARAS)
② No ammonites in the Tlemcen and the High Plains
③ WBL : wavy bedded limestones of the Upper Toarcian
④ Several cherty levels with *Hesperithyris* terebratulids
⑤ Rare ammonites
⑥ Including the *Beni Seria beds*
A-G : "members" of the *Aïn Ouarka Fm.*

Source : MNHN, Paris

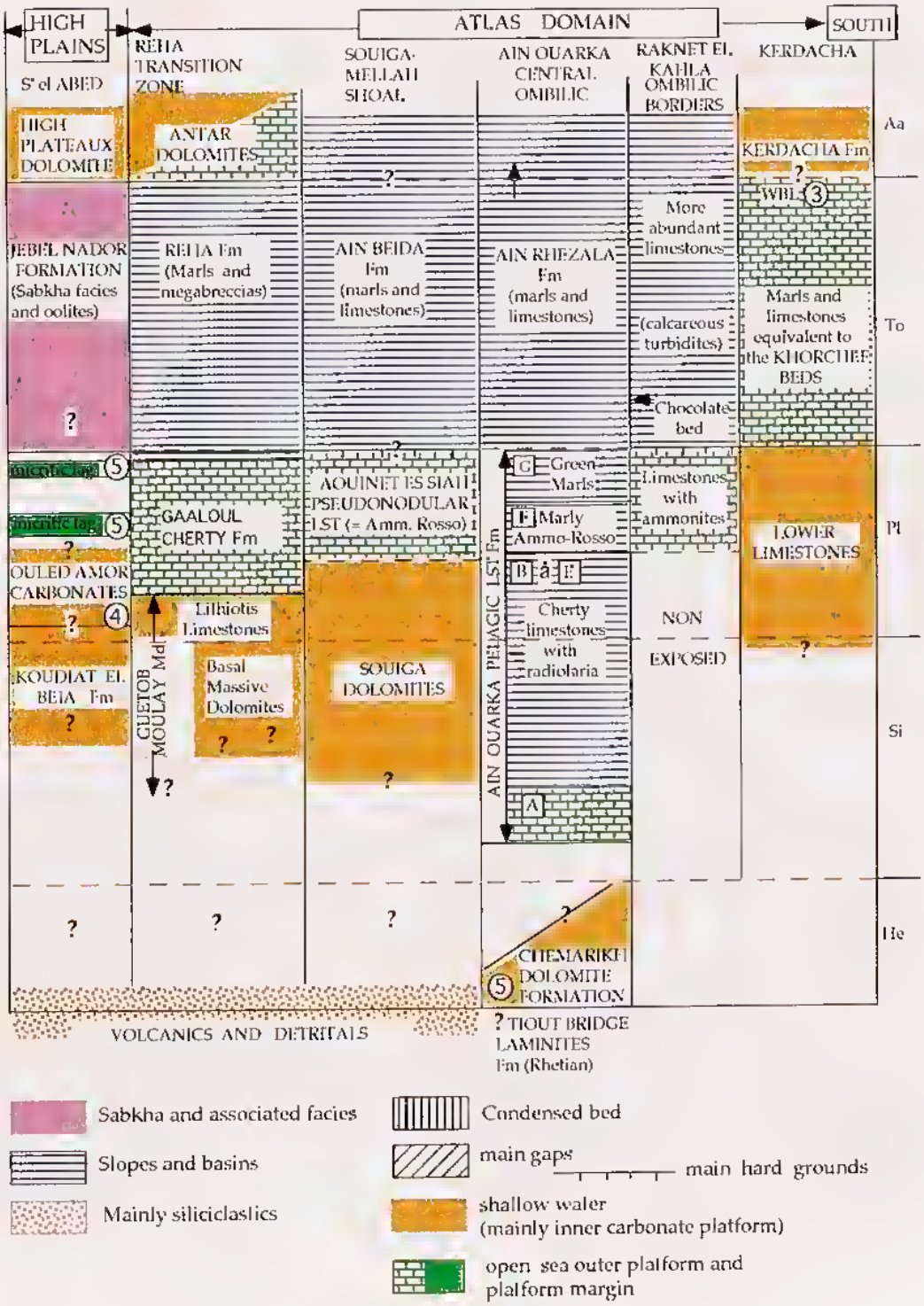

Source : MNHN, Paris

TABLE 4.— Major formal lithostratigraphic units, successions, facies and environments along the NW-SE transect Traras-Saharian Atlas - Part 2: Middle Jurassic.

TABLEAU 4.— Principales unités lithostratigraphiques (formations) et leurs faciès et environnements le long de la transversale NW-SE Traras-Atlas saharien. 2ème partie : Jurassique moyen.

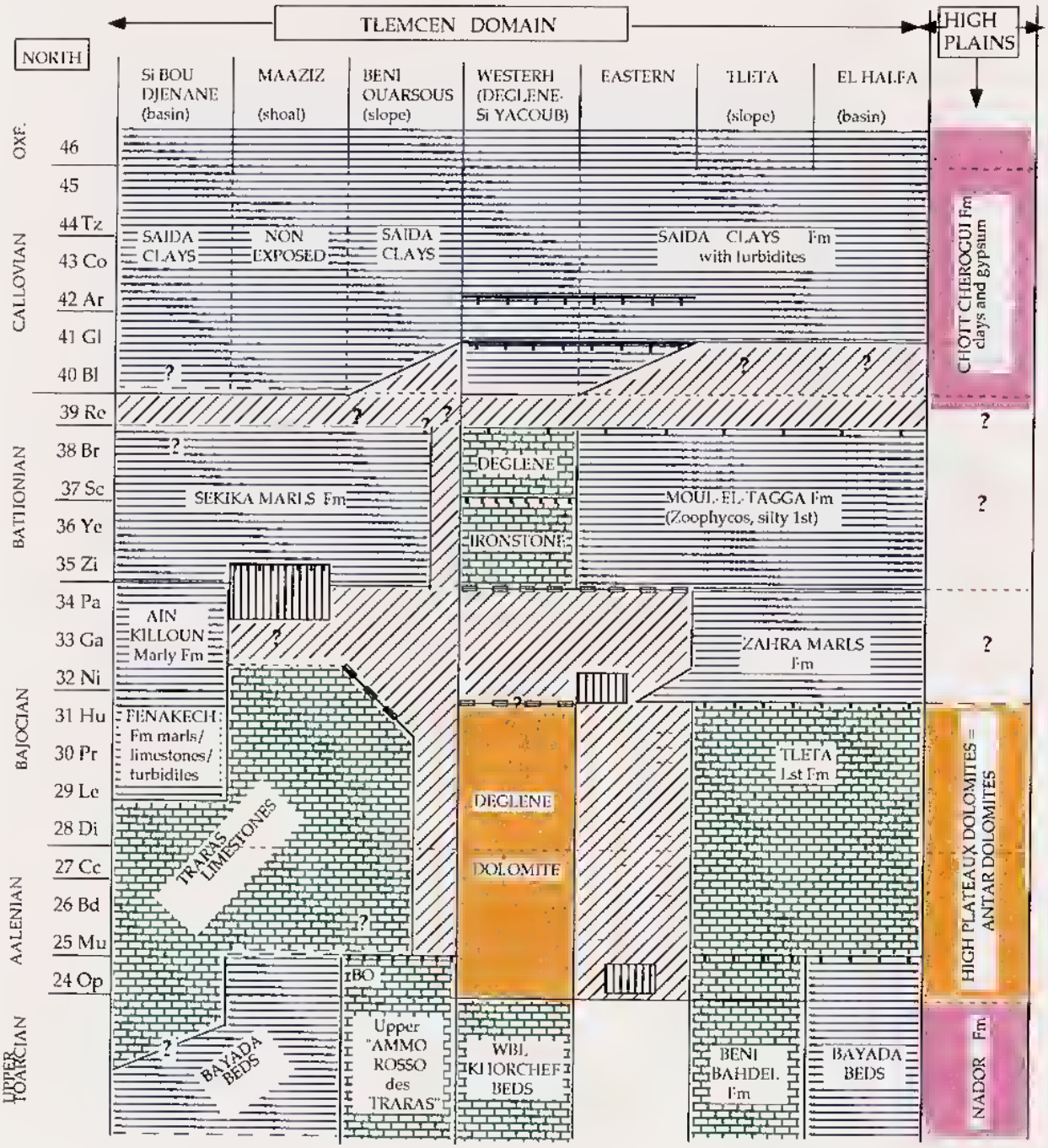

Source : MNHN, Paris

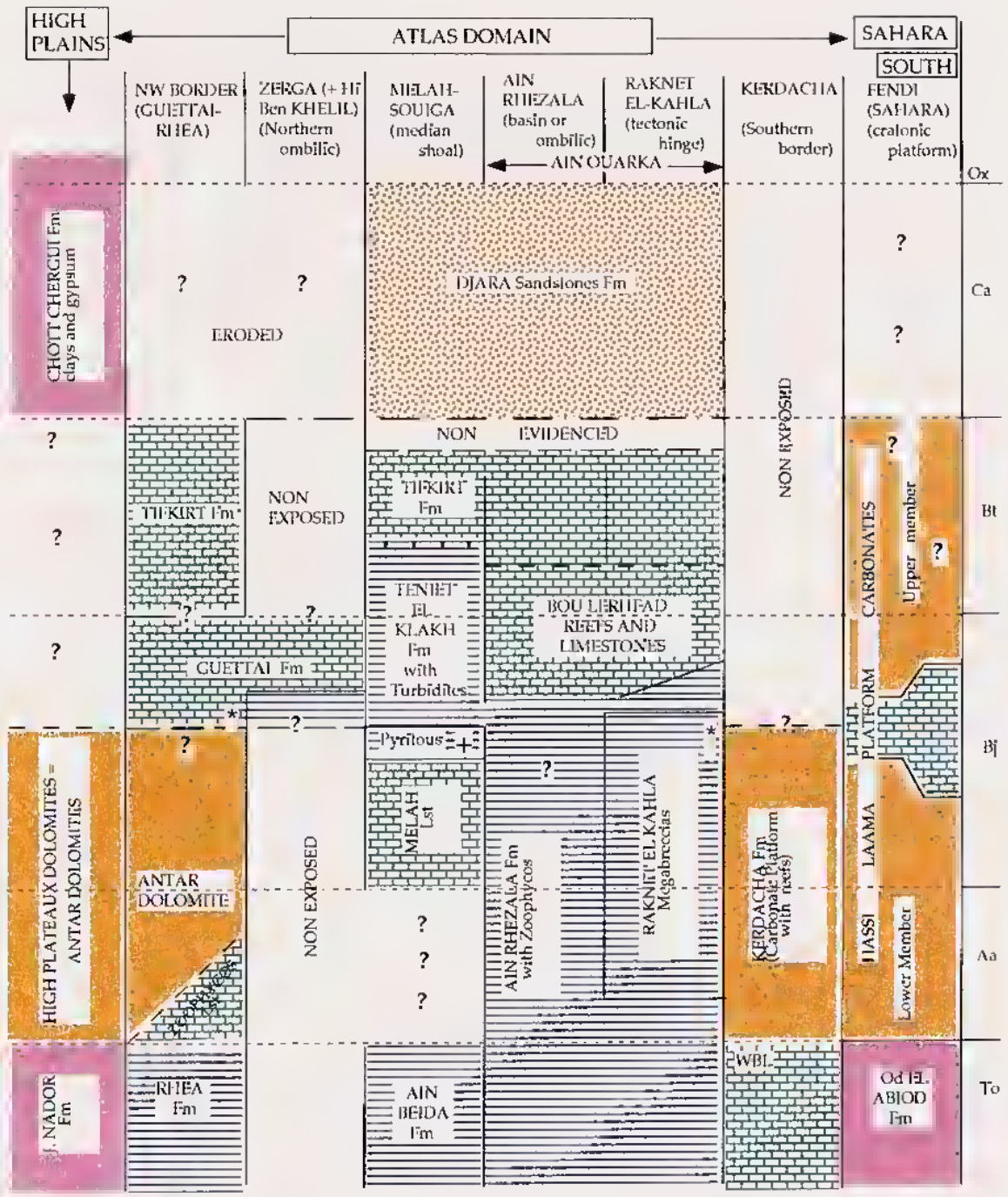

Source : MNHN, Paris

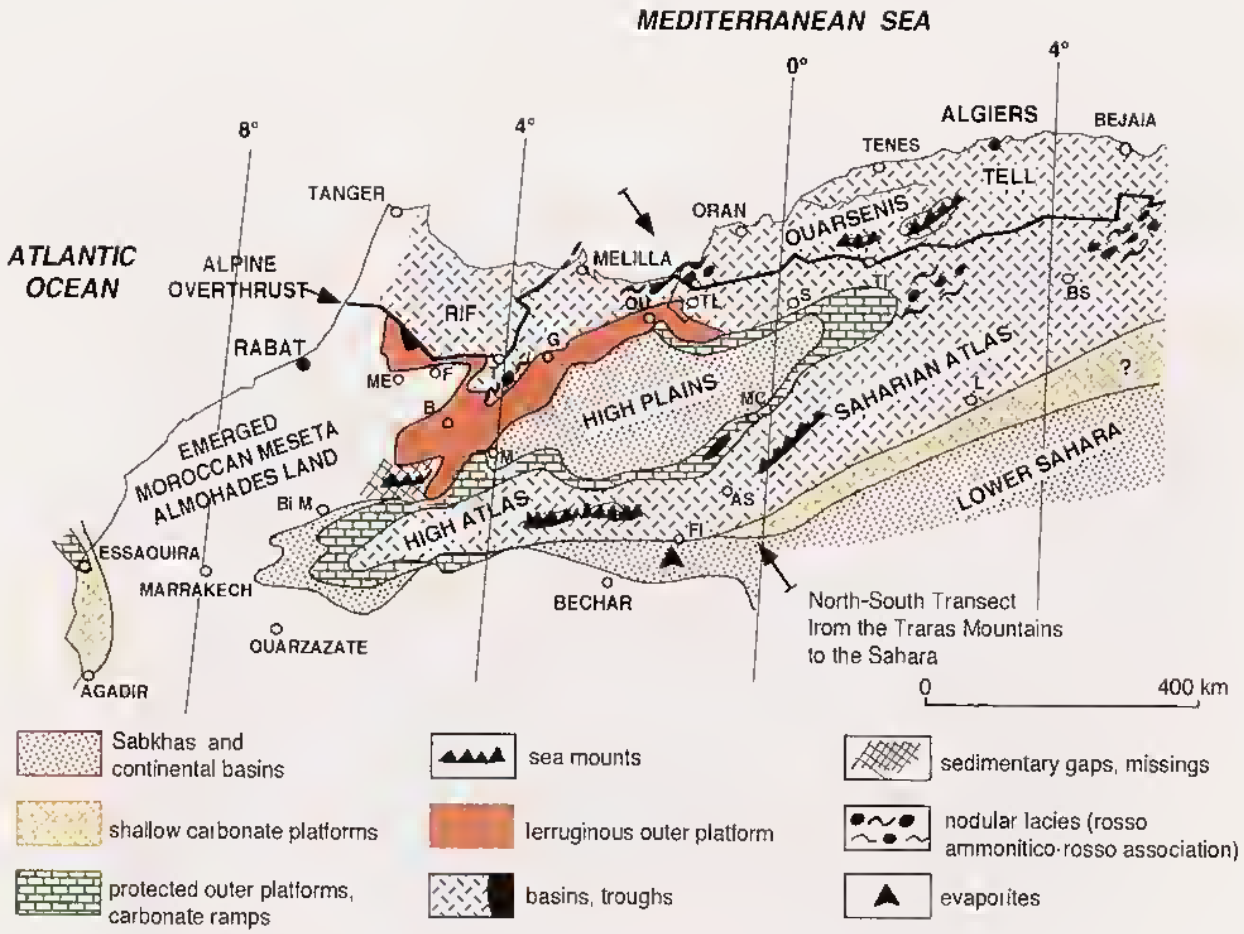

FIG. 1.— Palaeogeographical map of the North-Western Maghreb during the Toarcian. Localities: AS, Aïn Sefra; B, Boulemane; BIM, Béni-Mellal; BS, Bou Saada; F, Fés; Fi, Figuig; G, Guereif; L, Laghouat; M, Midelt; MC, Mécheria; ME, Meknès; OU, Oujda; S, Saïda; T, Taza; Ti, Tiaret; Tl, Tlemcen.

FIG. 1.— Carte paléogéographique du Nord Ouest maghrébin pendant le Toarcien. Localités : AS, Aïn Sefra ; B, Boulemane ; BIM, Béni-Mellal ; BS, Bou Saada ; F, Fés ; Fi, Figuig ; G, Guercif ; L, Laghouat ; M, Midelt ; MC, Mécheria ; ME, Meknès ; OU, Oujda ; S, Saïda ; T, Taza ; Ti, Tiaret ; Tl, Tlemcen.

THE TLEMCEN DOMAIN

The Tlemcen Domain (Fig. 2) shows the following main stratigraphic features:

— late development of the initial carbonate platform (late Sinemurian to early Pliensbachian);

— during the late Pliensbachian and the Toarcian: archipelago of isolated platforms (sometimes emergent) and intervening troughs;

— late transgression on the shoals;

— limited extension of the Middle Jurassic carbonate platform (Aalenian-early Bajocian);

— deep outer platform and basin sedimentation during the late Bajocian-Bathonian;

— siliciclastic turbidites during the Callovo-Oxfordian;

— prodeltaic and deltaic sedimentation during the late Oxfordian-early Kimmeridgian;

— late Jurassic shallow carbonate platform.

Source : MNHN, Paris

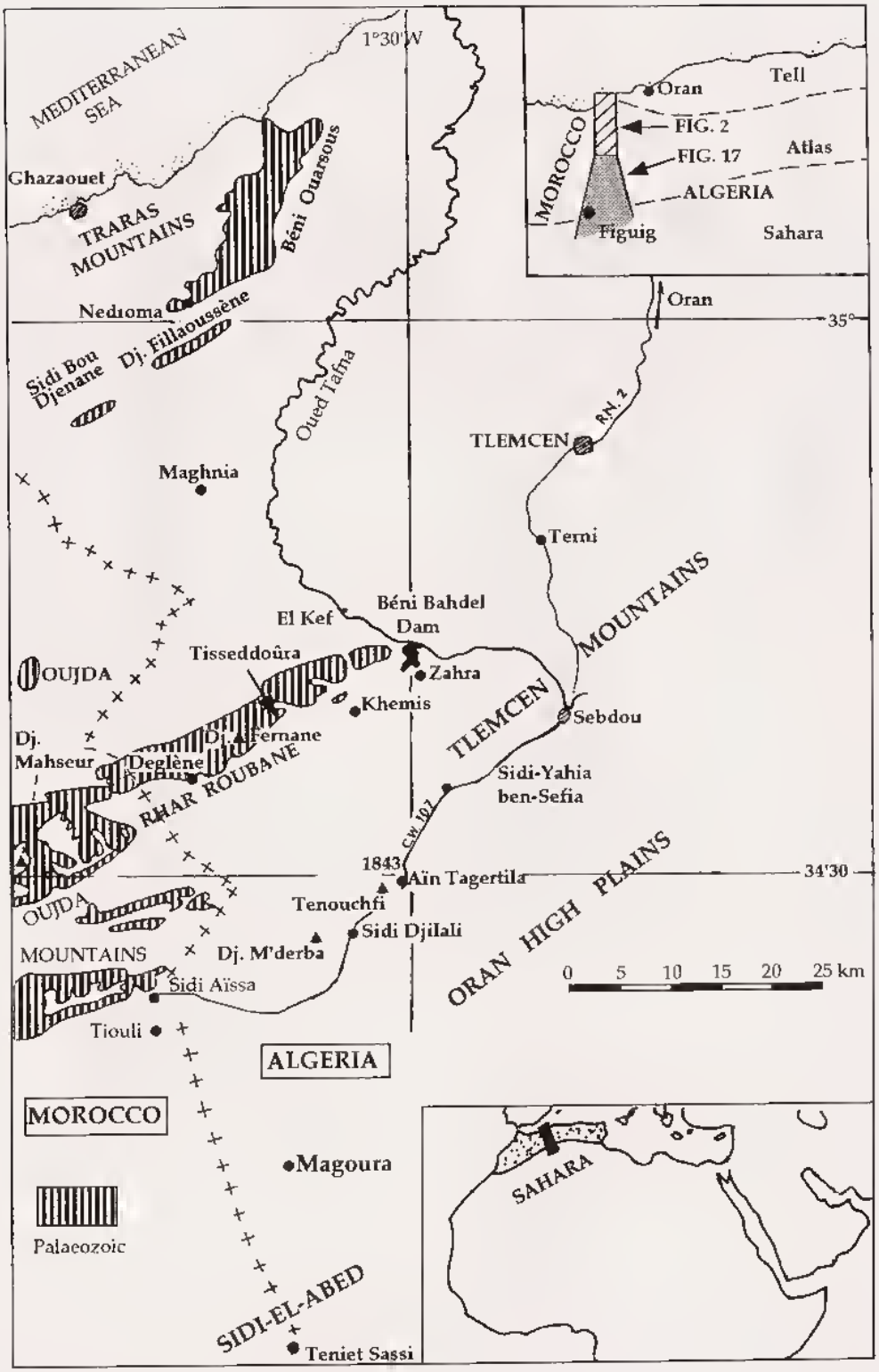

FIG. 2.— Map of the northern part of the studied transect (Tlemcen Domain and Oran High Plains).

FIG. 2.— Carte de la partie septentrionale du transect étudié (Domaine tlemcénien et Hautes Plaines oranaises).

Source : MNHN, Paris

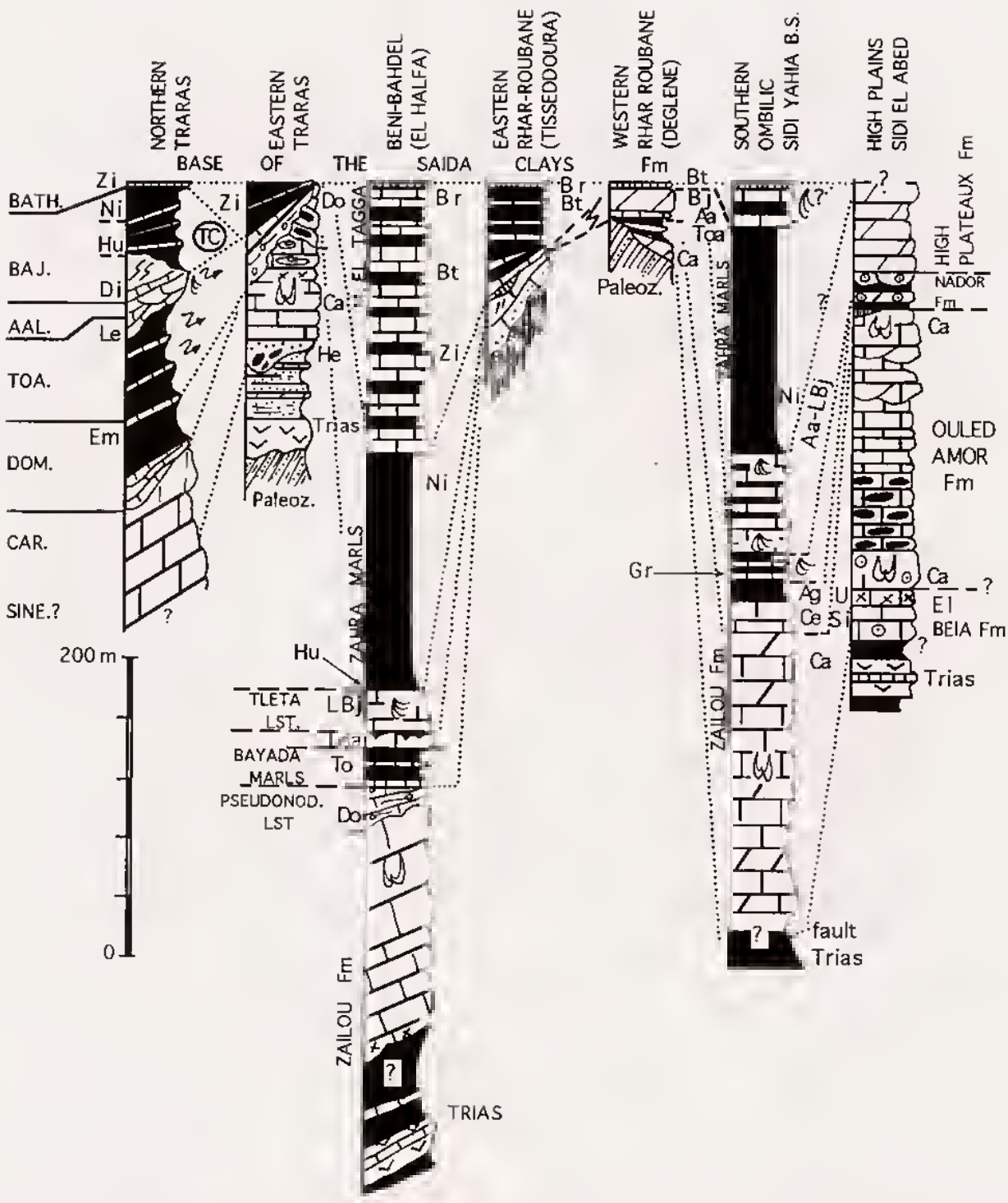

FIG. 3.— Comparisons of the stratigraphic profiles in different sectors of the Tlemcen Domain and of the Oran High Plains. Each log is a synthesis of several measured field sections.

FIG. 3.— Comparaison des séries stratigraphiques dans les différents secteurs du domaine tlemcénien et des Hautes Plaines oranaises. Chaque colonne est la synthèse de plusieurs coupes.

Source : MNHN, Paris

The southern border of this area is hidden by the Cenozoic conglomerates (Eocene High Plateaux Conglomerates; see BENSALAH *et al.*, 1987). It outcrops only in the Tiouli area, south of Oujda (Morocco). Several palaeogeographic units became distinct inside the Tlemcen domain, mainly during Liassic to Bathonian times. They will be briefly defined from north to south and their lithostratigraphic columnar sections are compared on Fig. 3.

THE TRARAS MOUNTAINS

These mountains, including the Djebel Fillaoussène, are part of the northern margin of the Tlemcen Domain. They are the equivalent of the Moroccan Béni Snassène Mountains and are geographically limited to the south by one of the main depressions of the western Maghreb, ranging from Guercif to the Mleta Plain (south of Oran). From the Early Jurassic to the Bathonian, the Traras are composed of several small subsiding basins in a network of stable shoals and ridges (GUARDIA, 1975; ELMI 1978, 1981b; AMEUR, 1978, 1988; BENHAMOU, 1983). Two kinds of composite lithologic successions are given here: one for the thick series of the subsiding umbilics, the other for the thin and incomplete series of the shoals or transition zones (Figs 4-5). The geometry of the main units is controlled by three tectonic trends: N020°, N040°-050° and N110°-150°. The relative movements of the faults changed during time and strong modifications occurred at the beginning of the Domerian, during the early Toarcian and throughout the Aalenian-early Bajocian, causing the episodes of differentiation and mosaic stages of development (for a more complete definition: see BENSHILI & ELMI, 1994; ELMI, 1996b).

The Jurassic transgression is often marked by spectacular breccias and conglomerates at the base of the Zaïlou Formation (Carixian) (Fig. 6a). In the Béni Mishel, this conglomerate consists in granitic blocks deposited in coarsely quartzose limestones at the foot of littoral cliffs (Djerf el Kebir Member, Fig. 9a, b).

Tectonic unconformities are well documented:

— between the Zaïlou Limestones Formation (shallow platform carbonates mainly of Carixian age with the famous "calcaires à grands lamellibranches" facies (large pelecypods); AMEUR, 1978; BENHAMOU, 1986a) and the Tisseddoûra Formation (cherty limestones with Domerian brachiopods);

— at the end of the Domerian and during the Toarcian, unconformities are spectacular between the Tisseddoûra Formation and the ferruginous crusts related to the Sekika ammonitico rosso (ELMI, 1981b; see Figs. 1, 2 and Fig. 6b to e), in the Djebel es Sekika sector (Béni Ouarsous; BENHAMOU, 1986b);

— in the lower Toarcian basinal facies (Bayada Formation), tectonic instability is illustrated by mass sliding (Fig. 9d) and by turbidites;

— between the top of the ammonitico rosso (topmost Toarcian to lower Aalenian) and the Humphriesianum Zone in the Djebel Gorine (BENHAMOU, 1983) (Fig. 9c).

The general instability led to the widespread development of reworked megabreccias, slumps and turbidites (AMEUR & ELMI, 1981), especially during the early Toarcian and the early Bajocian (calciturbidites of the Fenakech Marls Formation). Local tectonics are documented until the Callovian: the Saïda Clays Formation rests locally directly on the Zaïlou Limestones in the Sekika-Gorine region (GENTIL, 1908; GUARDIA, 1975) where they include megabreccias reworking Liassic and Palaeozoic pebbles (ELMI & BENEST, 1978) (Fig. 6f).

Two main associations of facies can be distinguished in the Toarcian of the small basins of the northern Tlemcen Domain, in a zone which is transitional to the Alpine Tell. They belong to two formations: the marl-dominated Bayada Formation (alternating marls and micritic limestones) and the predominantly nodular Sekika ammonitico rosso Formation.

Bayada Formation: basinal environment; alternating marls and limestones in thin decimetric beds, more marly at the base; colour grey or greenish, sometimes pink. The marls are silty and strongly bioturbated, with poor microfauna. The ammonite fauna consists of small individuals owing to the restricted conditions developed in these small basins (umbilics).

Source : MNHN, Paris

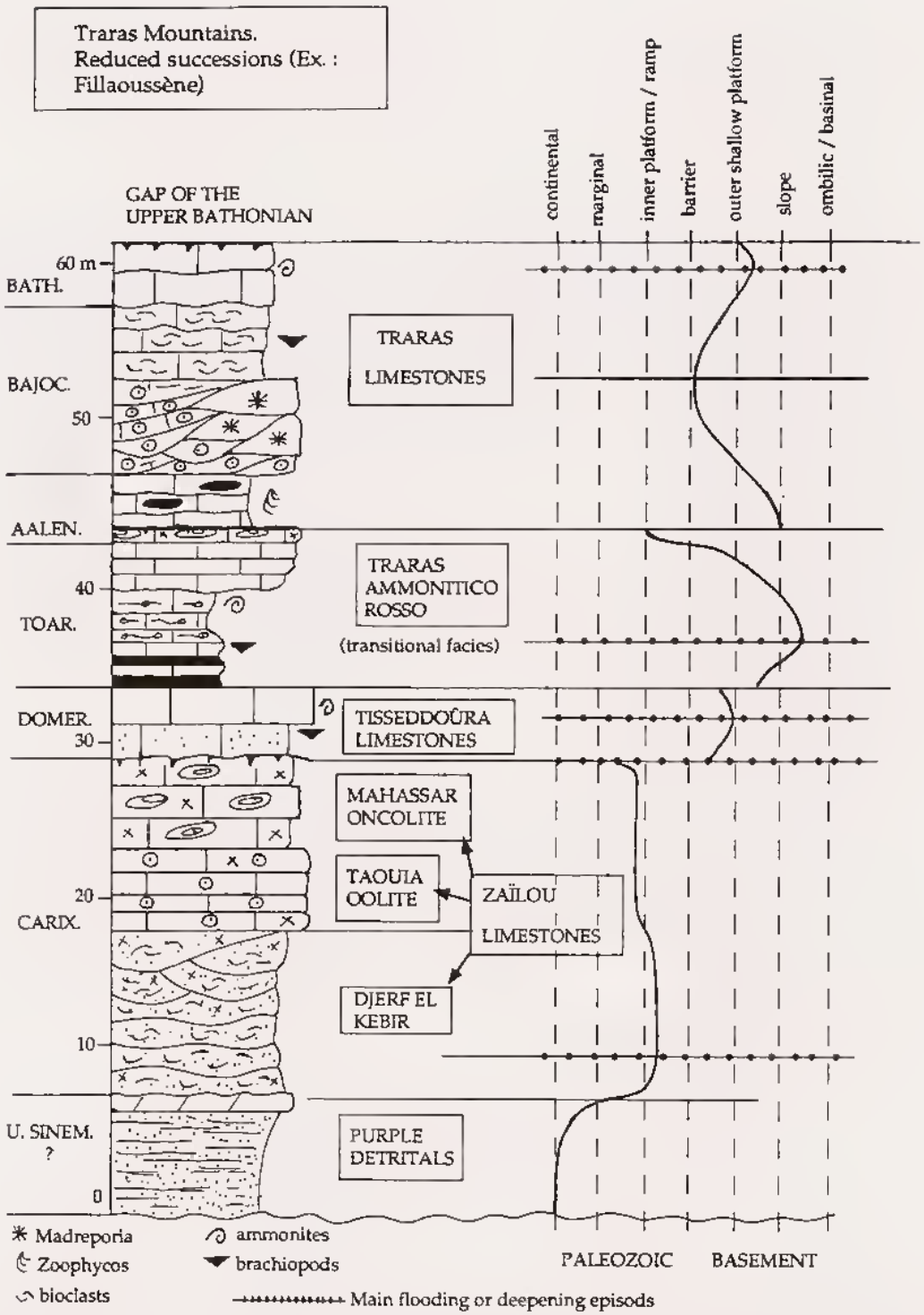

FIG. 4.— Synthetic profile of the reduced Middle and Upper Jurassic series of the Central and Eastern Traras Mountains, especially in the Fillaoussène Range (Mahassar, Aïn Tolba) and in the Béni Mishel. This succession sustains abrupt lateral variations.

FIG. 4.— Succession synthétique du Jurassique inférieur et moyen dans les séries réduites des Traras orientaux et centraux en particulier dans les régions du Fillaoussène (Mahassar, Aïn Tolba) et des Béni Mishel. Cette série montre des variations latérales abruptes.

Source : MNHN, Paris

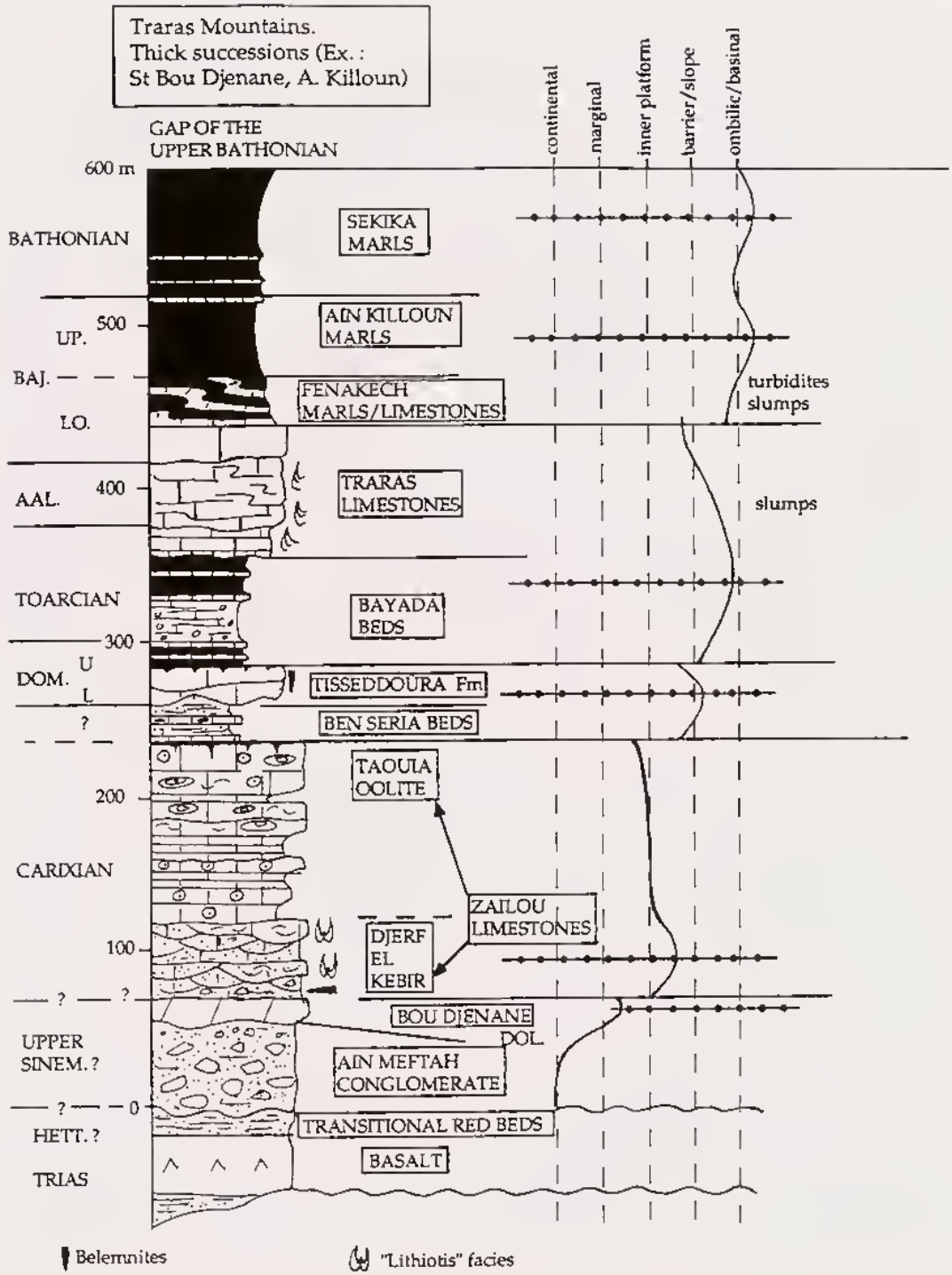

FIG. 5.— Synthetic profile of the Lower and Middle Jurassic (up to the Bathonian) thick succession of the Western Traras Mountains (Sidi Bou Djenane, Aïn Killoun). This succession is everywhere affected by sedimentary and tectonic instability (erosion, gravity flows, turbidites).

FIG. 5.— Succession synthétique du Jurassique inférieur et moyen (jusqu'au Bathonien) dans les séries dilatées des Traras occidentaux (Sidi Bou Djenane, Aïn Killoun). Les variations latérales sont rapides et spectaculaires en raison de l'instabilité sédimentaire et tectonique (érosion, flux gravitaires, turbidites).

Source : MNHN, Paris

Sekika ammonitico rosso Formation (previously known as Traras ammonitico rosso: we change the name here in order to avoid confusion with the Traras Limestones Formation of the Aalenian-Bajocian and to match international usage): largely marly in the lower part (Fig. 6b), with thin centimetric calcareous beds and residual nodules, changing upwards to bioturbated and subnodular limestones. On the shoals (Figs 7-8), the formation is capped by oncolitic and ferruginous limestones dated to the Opalinum Zone (Béni Ouarsous oncolitic bed: BENHAMOU, 1983).

FIG. 6.— Details of some Jurassic outcrops of the Eastern Traras Mountains (Beni Mishel and Beni Ouarsous, Algeria, Tlemcen Wilaya).

a, Transgression of the basal Zaïlou Limestones Formation (lower Pliensbachian = Carixian) on red beds of possible Triassic-Hettangian age. Heterometric and heterogeneous conglomerate reworking Palaeozoic (quartzites, schists) and lower Liassic (tidal carbonates) pebbles at the base of shallow platform carbonates. Road C.W. 213 at the foot of Djebel Anina Boudjelil near Djebel es Sekika and Souk el Arba. Coll. ELMI, 73A12.

b, Sekika ammonitico rosso Formation. The lower part (nodular alternating grey marls and limestones; basal Sublevisoni Subzone) is not exposed here. The outcrop shows the red median part (middle Toarcian, Sublevisoni Subzone) which is marly dominated. The calcareous beds become more frequent upward and they present a pseudonodular aspect due to an intense bioturbation. (See Fig. 9c). Oued el Merzouf on the south east side of Djebel Gorine. Coll. ELMI, 83DZ637.

c, "Neptunian" dyke open through Carixian Zaïlou Carbonates and filled by Toarcian pink micrite. It is interpreted as an extensional marker (see also: Figs 7 and 8). Souk el Arba near es Sekika Djebel. Coll. ELMI, 73A17.

d, **e**, Ferruginous and probably stromatolitic red crust (probable middle Toarcian) coating a palaeorelief in "marches d'escalier" (steps) dug out in the cherty limestones of the upper Pliensbachian (Domerian Tisseddoûra Formation). The grey blocks on the surface are cherts of the Tisseddoûra Formation, exhumed by the pre-Toarcian erosion, and Palaezoic quartzite pebbles. Between the crust and the Domerian limestones, there remain traces of nodular grey limestones with rare ammonites *(Hildaites)* of the lower Toarcian (Levisoni Zone). These remain traces are preserved on horizontal and vertical surfaces. These data document the occurrence of a second erosional phase which had taken place at the end of the Levisoni Zone after a first covering of the palaeorelief. Laterally, the succession rapidly becomes complete: Sekika ammonitico rosso Formation, similar to that illustrated on Fig. 6b, developed in less than 500 m. Change to the basinal Bayada Marls Formation occurs in less than 2 km. Same locality as Fig. 6c; the two outcrops are ten meters distant. Coll. ELMI, 73A22-23.

f, Heterometric and heterogeneous conglomerate near the base of the Saïda Clays Formation (lower Callovian - Palaeozoic quartzites, Liassic or perhaps Bajocian limestone pebbles). Track from Souk el Arba village to Djebel es Sekika. Coll. ELMI, 73A33.

FIG. 6.— Détails de quelques affleurements jurassiques des Monts de Traras orientaux (Béni Mishel et Béni Ouarsous, Algérie, Wilaya de Tlemcen).

a, Transgression de la base de la Formation des Calcaires compacts de Zaïlou (Pliensbachien inférieur = Carixien) sur des couches rouges d'âge probablement triasico-hettangien. Le conglomérat de base des carbonates de plate-forme peu profonde comprend des éléments hétérométriques et hétérogènes remaniés aussi bien du Paléozoïque (quartzites, schistes) que du Lias inférieur (carbonates tidaux). Route C.W. 213 ; Souk el Arba, au pied du Djebel Anina Boudjelil près du Djebel es Sekika et Souk el Arba. Coll. ELMI, 73A12.

b, Formation de l'ammonitico rosso du Sekika. La partie inférieure (alternance de calcaires et marnes grises noduleux ; base de la sous-zone à Sublevisoni) n'affleure pas. L'affleurement expose la partie rouge médiane de la formation où les marnes sont abondantes (Toarcien moyen, sous-zone à Sublevisoni). Les bancs calcaires deviennent plus épais et plus rapprochés vers le haut (Fig. 9c) où ils prennent un aspect pseudonoduleux. La bioturbation est importante sur toute l'épaisseur. Oued el Merzouf, flanc Sud Est du Djebel Gorine. Coll. ELMI, 83DZ637.

c, Fissure ("dyke neptunien") ouverte dans les Calcaires de Zaïlou (Carixien). Elle est comblée par des micrites roses du Toarcien. Ceci est interprété comme un marqueur d'extension (voir aussi : Figs 7 et 8). Souk el Arba près du Djebel es Sekika. Coll. ELMI, 73A17.

d, e, Croûte ferrugineuse d'origine vraisemblablement stromatolithique, d'âge probablement toarcien moyen. Elle fossilise un paléorelief en marches d'escalier creusées dans les calcaires à silex du Pliensbachien supérieur (Formation domérienne du Tisseddoûra). Les blocs gris visibles sur les surfaces horizontales des bancs sont des silex de la Formation du Tisseddoûra, dégagés par l'érosion anté-toarcienne et des fragments de quartzites paléozoïques. Des lambeaux de calcaires micritiques noduleux gris sont conservés entre la croûte et les calcaires du Domérien ; ils ont livré de rares Hildaites *du Toarcien inférieur (zone à Levisoni). Ces lambeaux sont préservés sur les surfaces verticales et horizontales. Le colmatage du paléorelief s'est donc fait en deux phases avant et après la zone à Levisoni. La succession toarcienne se complète rapidement sur les flancs de la paléostructure de Souk el Arba. Les assises de la formation de l'ammonitico rosso du Sekika, similaires à celles illustrées sur la Fig. 6b, se développent en moins de 500 m et le passage au faciès bassin (Formation de Bayada) intervient en moins de 2 km. Localité : voir fig. 6c. Les deux affleurements sont distants de 10 mètres. Coll. ELMI, 73A22-23.*

f, Conglomérat hétérométrique et hétérogène près de la base de la formation des Argiles de Saïda (Callovien inférieur - quartzites paléozoïques, galets de calcaires liasiques ou peut être bajociens). Sentier entre Souk et Arba et le Djebel Sekika. Coll. ELMI, 73A33.

Source : MNHN, Paris

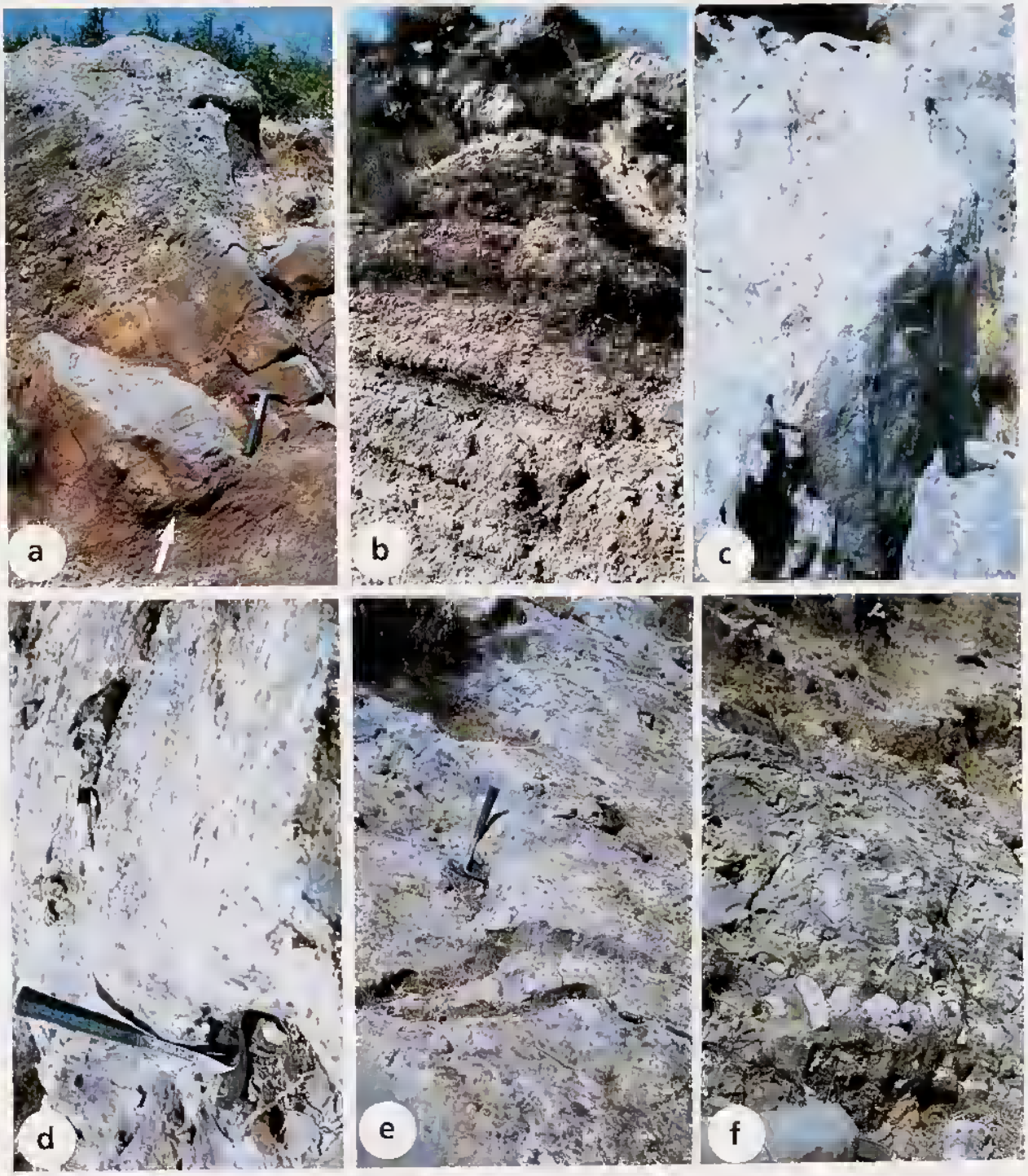

Source : MNHN, Paris

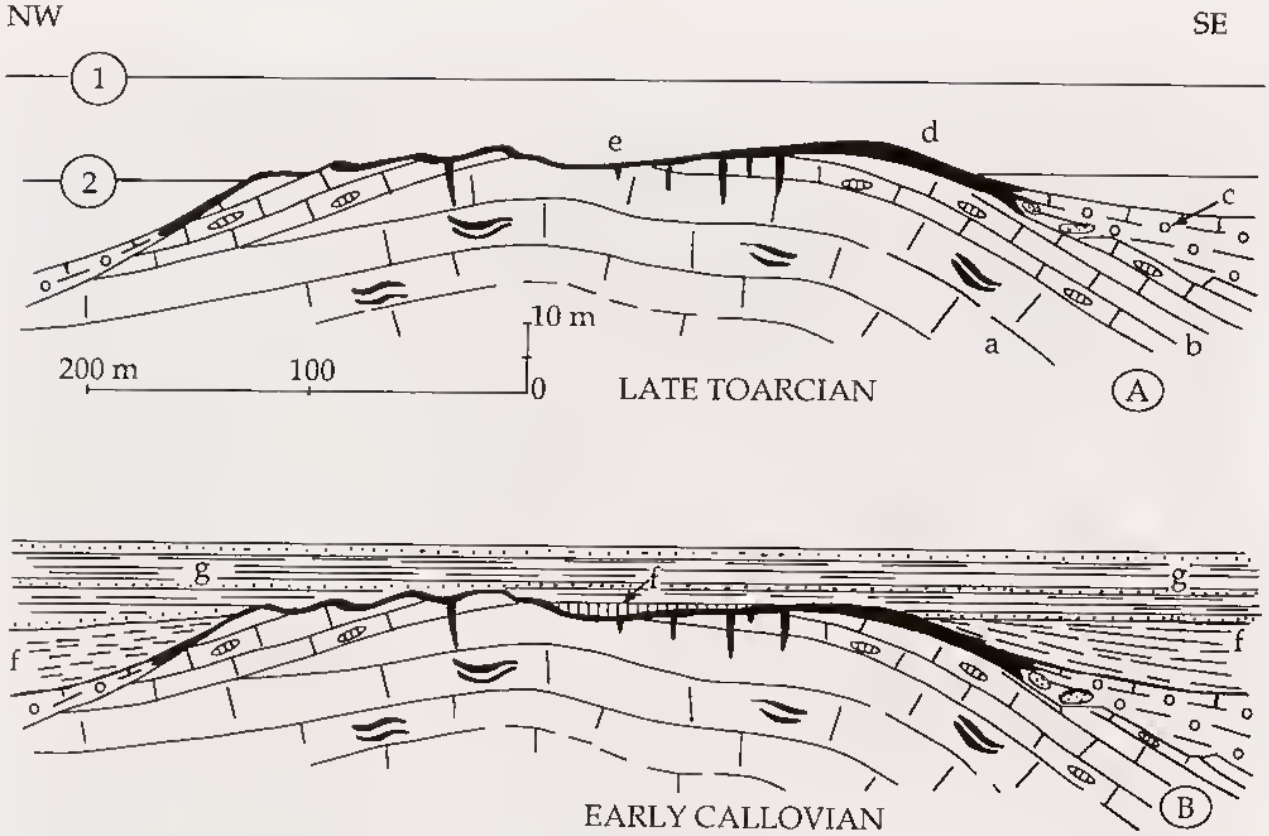

FIG. 7.— Transverse profiles through the Souk el Arba palaeostructure (Béni Ouarsous near Djebel es Sekika in the Traras Mountains). The palaeorelief was differentiated progressively from the end of the Toarcian (A) and it remained prominent until the Bathonian (B). The submerging of the structure began during the early Bathonian but was terminated only during the Callovian. Dips, unconformities and erosion figures have been drawn in the field. 1, relative sea level during the maximum flooding (Sublevisoni Subzone of the middle Toarcian); 2, relative sea level at the beginning and at the end of the Toarcian and during the early Aalenian; a, "Lithiotis" limestones of the top of the Zaïlou Formation (early Pliensbachian = Carixian); b, cherty limestones of the Tisseddoûra Formation (late Pliensbachian, early to middle Domerian); c,d,e, ammonitico rosso of Sekika Formation; c, nodular limestones with reworked pebbles; d, breccias; e, fissures ("neptunian dykes") and stromatolitic crusts; f, Sekika Marls Formation (early Bathonian), beginning by a condensed bed yielding *Prohecticoceras* sp. A and B (ELMI, 1971b) on top of the anticline; g, Saïda Clays Formation (Callovian) (from ELMI, 1981b; fig. 9).

FIG. 7.— Coupes transversales de la paléostructure de Souk el Arba (Djebel es Sekika, Béni Ouarsous, Monts des Traras). Le paléorelief s'est différencié progressivement depuis la fin du Toarcien (A) et est demeuré proéminent jusqu'au Bathonien (B). L'ennoyage progressif de la structure débute au Bathonien inférieur mais ne sera terminé que durant le Callovien. Pendages, discordances et figures d'érosion ont été tracés par observation directe sur le terrain. 1, niveau marin relatif lors du maximum de la transgression toarcienne (sous-zone à Sublevisoni du Toarcien moyen) ; 2, niveau marin relatif au début et à la fin du Toarcien et pendant l'Aalénien inférieur ; a, calcaires à "Lithiotis" de la Formation de Zaïlou (Pliensbachien inférieur = Carixien) ; b, calcaires à silex de la Formation du Tisseddoûra Pliensbachien supérieur, (Domérien inférieur-moyen); c,d,e, ammonitico rosso du Sekika ; c, calcaires noduleux contenant des éléments remaniés ; d, brèches ; e, fentes ("dykes neptuniens") et croûtes stromatolithiques ; f, Marnes du Sekika (Bathonien inférieur) débutant par un niveau condensé livrant Prohecticoceras *sp. A et B (ELMI, 1971b) ; g, Argiles de Saïda (Callovien) (d'après ELMI, 1981b : fig. 9).*

The isopach map of the Toarcian deposits shows spectacular variations in their thickness (Fig. 10) allowing recognition of several basins, ten kilometers long: Aïn Killoun (Mellala), Béni Ouarsous, Béni Mishel and Boudjenane. On the bottom of these basins, the microfauna and the dwarfed ammonite and brachiopod faunas indicate that the environment became progressively restricted. They give a good model of the "umbilic" (or umbilicus stage; see BOUTAKIOUT & ELMI, 1996; ELMI, 1996b). An umbilic shows deepening because sedimentation does not keep pace with subsidence. It follows the rifting phase and requires active tectonic control. It represents a juvenile stage in the development of the basin, resulting in a distinct partitioning of the sea-bottom. In the areas studied, the anoxic or hypoxic early

Source : MNHN, Paris

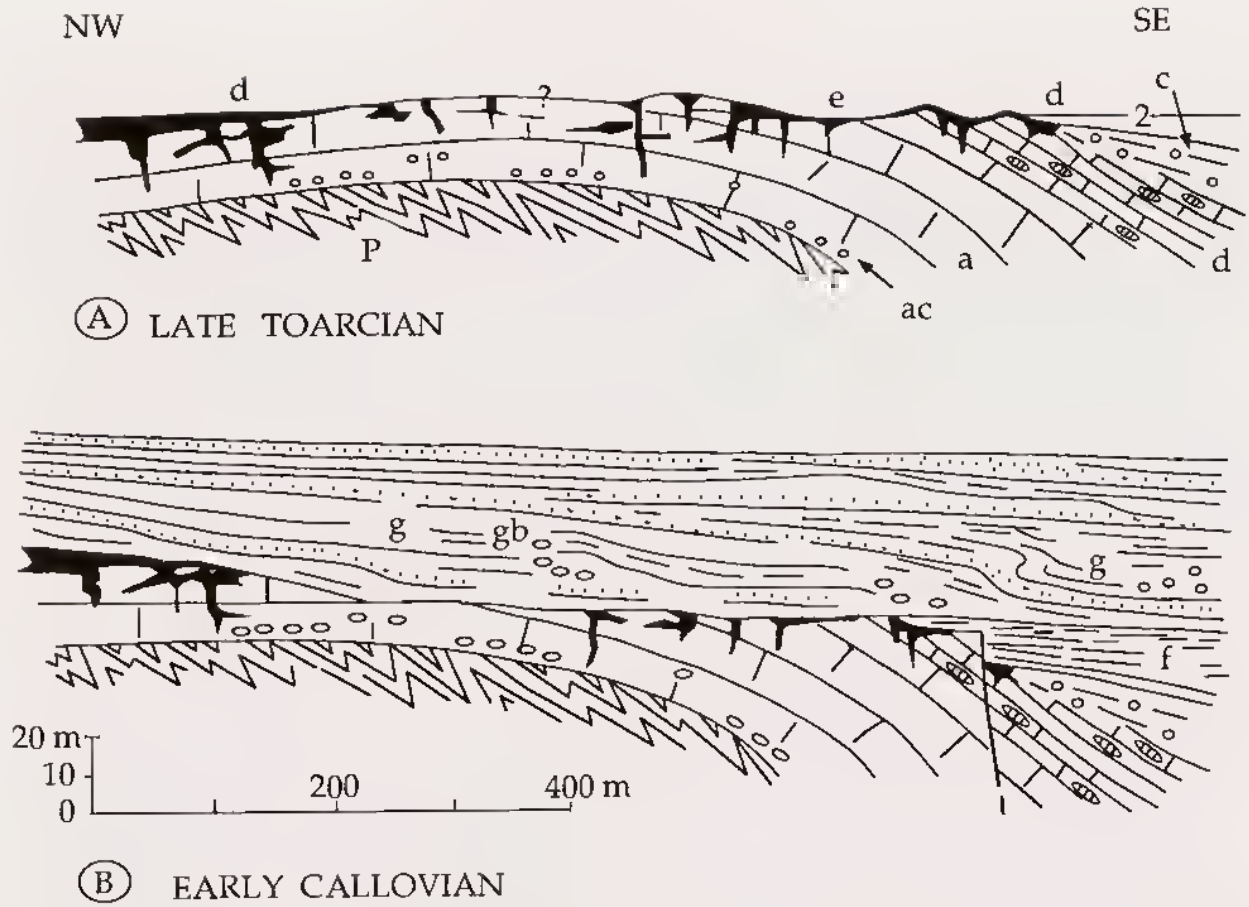

FIG. 8.— Submergence of the palaeorelief on the axis of the Souk el Arba structure during the Toarcian and the early Aalenian. See Fig. 7. Other symbols: gb, cherty and quartzose limestones (Domerian); c,e, calcareous ammonitico rosso capped by ferruginous oncolites and crusts with *Leioceras* sp. (Béni Ouarsous Oncolitic Beds; BENHAMOU, 1983). During the early Aalenian the top of the structure was emergent (tidalites, mud-cracks, vadose diagenesis) and the tilting to the nearby basin was rapid (from ELMI, 1981b: fig. 11).

FIG. 8.— Évolution des dépôts sur l'axe de la paléostructure de Souk el Arba pendant le Toarcien et le début de l'Aalénien. Pour les symboles: voir Fig. 7. En plus : gb, calcaires à grains de quartz et à silex (Domérien) ; c,e, ammonitico rosso calcaire se terminant par le "niveau à oncolithes ferrugineux des Béni Ouarsous" (BENHAMOU, 1983) à ammonites (Leioceras sp.) et à surfaces encroûtées. Durant l'Aalénien inférieur, l'axe de la paléostructure fut alors soumis à des émersions temporaires comme en témoignent des mud cracks et des tidalites à figures de dessiccation. Le passage au bassin a dû être rapide le long d'une pente nettement marquée (d'après ELMI, 1981b : fig. 11).

Toarcian event is widespread, but the preservation of organic matter is limited by the physiography of the basins.

These observations and the resulting maps can be used as models of the dynamics of the umbilics as well as of the hinge zones between other kinds of troughs and their margins. The telescoping of the isopachs gives good evidence of tectonically controlled steep slopes. They demonstrate also the existence of such small basins which are good traps for organisms as well as for organic matter. They can be easily compared with structural pattern known elsewhere during the rifting stages, especially in the Apennines (ELMI & AMEUR, 1987), during the Early Jurassic, and in the North Sea during the Late Jurassic.

The tectonic instability continued in the Traras all along the Bajocian (frequent gaps, calciturbidites in the Fenakech Formation, slumping and sliding in the Traras Limestones Formation, heterogenous conglomerate at the base of the Saïda Clays Formation (Fig. 6f) (ELMI & BENEST, 1978; AMEUR, 1988). The marly sedimentation appeared during the early Bajocian in the western subsiding subbasins (Fig. 5; Fenakech Formation with alternating marls and marly limestones) followed by the Ain Killoun Marls

Source : MNHN, Paris

Formation (upper Bajocian) and the lower Bathonian Sekika Marls Formation. After a gap of the upper Bathonian, sedimentation resumed with the onlapping of the marl-dominated Saïda Clays Formation. This partly turbiditic formation sealed the previous palaeoreliefs and shoals. It can rest on the lower Bathonian (centres of the umbilics) or on older formations ranging from the Bajocian to the Carixian (in the Sekika - Gorine - Sidi Sefiane area; GENTIL, 1908; GUARDIA, 1975; ELMI, 1981b; BENHAMOU, 1983; AMEUR, 1988).

FIG. 9.— Lower and Middle Jurassic of the Traras Mountains and the Jurassic transgression on the Rhar Roubane horst (Algeria, Tlemcen Wilaya).

a, **b**. Djerf el Kebir Conglomerates (lower member of the Zaïlou Formation). Metric blocks of hercynian granite sedimented in disorder in a marly and quartzose limestone containing rare belemnites (probable early Pliensbachian = Carixian). They have been accumulated at the toe of a cliff and concealed during the Pliensbachian transgression. Upwards, they are organized in a thinning up and shallowing up sequence passing to the Taouia Oolite Member. Beni Mishel basin. Djerf el Kebir near Zaïlou. Coll. ELMI, 76CA7A and 83DZ609.

c. Angular discordance of the *Stephanoceras* beds (Traras Limestones) (Humphriesianum Zone) on the erosion surface of the Sekika ammonitico rosso, capped by the Béni Ouarsous Oncolitic Beds. Lower Aalenian Opalinum Zone. Oued el Merzouf near Djebel Gorine. Coll. ELMI, 82DZ337.

d, Slumping in the Traras Limestones Formation. The transported material consists of synsedimentary marly limestones and marls belonging to the same environment. The slumps are sealed by a discordant decimetric bed (black arrow). Lower Toarcian (Levisoni Zone). Sidi Boudjenane Basin (or Umbilic). Chabet Sof Ahmed, SW Traras. Coll. ELMI, 85DZ89.

e, Discordance, transgression and onlap of the Bajocian Déglène Dolomites (1) on the Upper Palaeozoic (2). The vertical ancient cliff (3) consists of Dinantian dolomites (see Fig. 12). The palaeorelief is submerged during the lower Bathonian by the Moul el Tâgga Formation (4). In the background: Palaeozoic hills (Devonian-Dinantian, sandstones and argilites) of the Djebel Fernane. Elevation point 1222, "Fernane Pass" (LUCAS, 1942). Ras Afour gate, East of Sidi Yacoub, Rhar Roubane Mountains. Coll. ELMI, 93DZ642.

f. Discordance and transgression of the Liassic beds on the irregularly eroded Palaeozoic rocks (Silurian?-Devonian). Residual palaeoreliefs (Palaeozoic quartzites) are concealed by the Zaïlou Limestones Formation (Carixian) which are only preserved on the bottom of the gullies (1). The top of the cliff corresponds to the bioclastic limestones with *Protogrammoceras celebratum* (d'Orbigny) of the Tisseddoûra Formation (type section, lower Domerian) (cf. ELMI, 1977a, 1983) (2) and to the Belaïch Beds (type-section Toarcian) (see Fig. 13a). The upper parts of the palaeorelief are concealed by the onlap of Moul-el-Tâgga Formation which is locally uncomformable. Note the strong reduction of the cliff at the track way. Djorf Tisseddoûra Cliff, along the old track from Kef to Sidi Djillali, eastern Rhar Roubane horst near Khemis of the Beni Snouss. Coll. ELMI, 84DZ805.

FIG. 9.— Jurassique inférieur et moyen des Monts des Traras et transgression jurassique sur le horst de Rhar Roubane (Algérie, Wilaya de Tlemcen).

a, b, Conglomérats des Djerf el Kebir (membre inférieur de la Formation de Zaïlou). Blocs métriques de granite hercynien sédimentés en désordre dans un calcaire argilo-quartzeux contenant de rares bélemnites (probablement du Pliensbachien inférieur = Carixien). Il s'agit de la fossilisation d'un éboulis formé au pied d'une falaise lors de la transgression pliensbachienne. Les assises superposées s'organisent en une séquence qui enregistre à la fois l'affinement des sédiments et la diminution de la profondeur (Membre des Calcaires oolithiques de Taouia). Bassin des Béni Mishel. Djerf el Kebir près de Zaïlou, Algérie. Coll. ELMI, 76CA7A and 83DZ609.

c, Discordance angulaire des couches à Stephanoceras *(Calcaires des Traras) (Zone à Humphriesianum) sur la partie supérieure érodée des niveaux oncolithiques des Béni Ouarsous (zone à Opalinum, Aalénien inférieur) qui terminent l'ammonitico rosso du Sekika. Oued el Merzouf près du Djebel Gorine. Coll. ELMI, 82DZ337.*

d, Glissements dans la Formation des "Calcaires des Traras". Ils mettent en jeu des blocs de calcaires argileux et de marnes appartenant au même environement. La cicatrisation est réalisée par un banc de calcaire micritique (flèche noire). Toarcien inférieur (zone à Levisoni). Chabet Sof Ahmed. Bassin (ombilic) de Sidi Boudjenane, Traras SW. Coll. ELMI, 85DZ89.

e, Transgression et discordance de la Dolomie de Déglène du Bajocien (1) sur le Paléozoïque supérieur (2) (cf. Fig. 12) où la dolomie dinantienne forme un écueil (3) qui ne fut enfoui que lors du Bathonien inférieur (Formation de Moul el Tâgga, 4). A l'arrière plan : collines paléozoïques (grès et argilites du Dévono-Dinantien) du Djebel Fernane. Point coté 1222, connu sous le nom de "Col du Fernane" (LUCAS, 1942). Barrière du Ras Afour, à l'Est de Sidi Yacoub, Monts de Rhar Roubane. Coll. ELMI, 93DZ642.

f, Transgression et discordance des assises liasiques sur les formations paléozoïques érodées (Silurо?- Dévonien). Les quartzites paléozoïques constituent des reliefs résidnels qui sont cicatrisés par le dépôt des Calcaires de Zaïlou du Carixien. Ces derniers sont seulement préservés dans le fond des dépressions (1). La partie supérieure de la falaise calcaire correspond à des calcaires bioclastiques à Protogrammoceras celebratum *(d'Orbigny) du Domérien inférieur (coupe-type de la Formation des Calcaires du Tisseddoûra ; cf. ELMI, 1977a, 1983). Les "Calcaires oncolithiques du Belaïch", affleurent au sommet de la falaise (coupe-type, Toarcien) (voir Fig. 13a). Les points les plus hauts du paléorelief sont cicatrisés par la disposition en débordement (onlap) de la Formation du Moul-el-Tâgga (2) qui est localement discordante. Noter la forte réduction de la falaise au niveau où passe la piste. Falaise du Djorf Tisseddoûra, le long de l'ancienne piste du Kef à Sidi Djillali. Horst oriental de Rhar Roubane près du Khemis des Béni Snouss. Coll. ELMI, 84DZ805.*

Source : MNHN, Paris

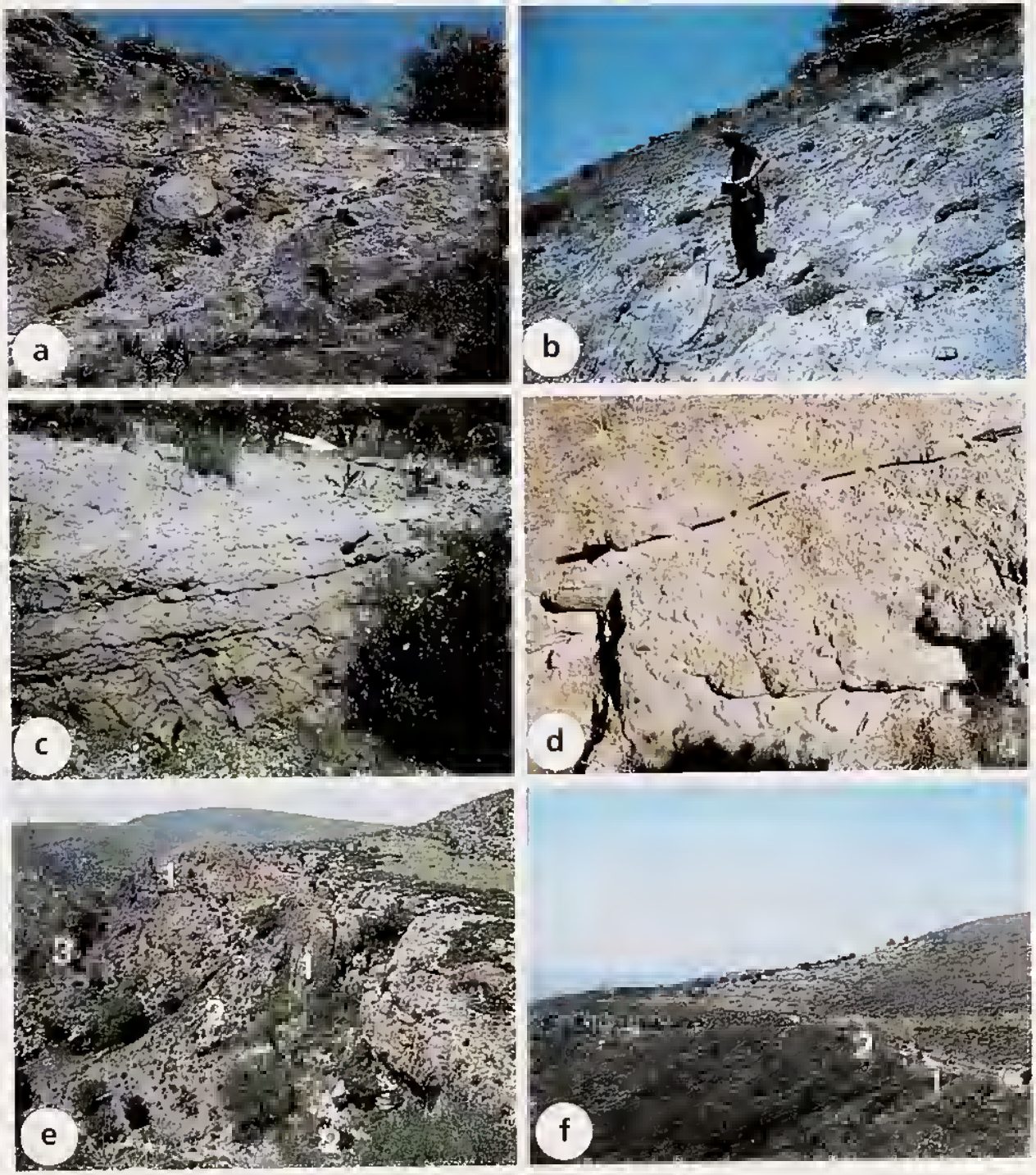

Source: MNHN, Paris

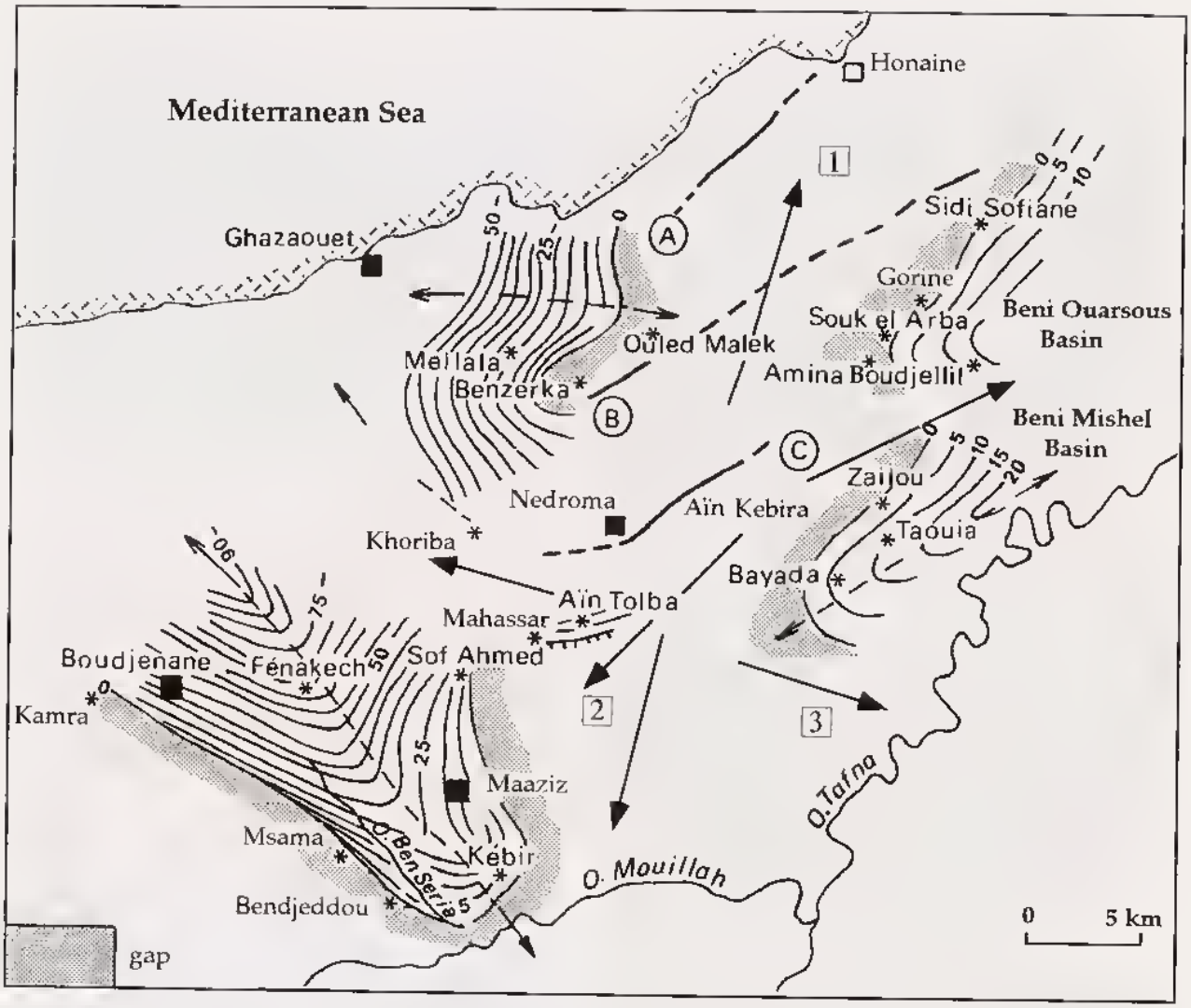

FIG. 10.— Isopach map of the Toarcian illustrating the umbilics differentiated within the Traras Mountains. Small basins (Béni Ouarsous, Béni Mishel, Aïn Killoun-Mellala, Boudjenane) rapidly subsiding and deepening have not been balanced by the sedimentation rate during the early Toarcian and are good examples of the "umbilic concept". The broken lines indicate the main trend of the umbilics. The resistant shoals are oriented along three main directions (solid lines): SSW-NNE (**1**, Honaine shoal); SW-NE (**2**, Fillaoussène-Nedroma shoal); WNW-ESE (**3**, Aïn Tolba shoal). **A**, Cap Noé fault; **B**, Dahr ed Diss fault; **C**, Nedroma fault (nomenclature of the faults from GUARDIA, 1975 and AMEUR, 1988).

*FIG. 10.— Carte des isopaques du Toarcien illustrant les ombilics (Monts de Traras). Ces petits bassins (Béni Ouarsous, Béni Mishel, Aïn Killoun-Mellala, Boudjenane) ont subi, pendant le Toarcien inférieur, un enfoncement et un approfondissement rapides qui ne furent pas compensés par la sédimentation. Ils fournissent un bon exemple de la notion d'ombilic. Les tiretés indiquent la direction d'allongement de ces ombilics. Les seuils (axes) résistants se répartissent selon trois directions (lignes continues) : SSW-NNE (1, axe de Honaine) ; SW-NE (2, axe Fillaoussène-Nedroma) ; NNW-ESE (3, axe d'Aïn Tolba) ; **A**, faille du Cap Noé ; **B**, faille de Dahr ed Diss ; **C**, faille de Nedroma (nomenclature des failles d'après GUARDIA, 1975 et AMEUR, 1988).*

Source : MNHN, Paris

THE RHAR ROUBANE AND TLEMCEN MOUNTAINS

They are also divided into several palaeogeographic units, defined by the structural pattern and marked by important and well documented Jurassic movements. Westward, the Rhar Roubane Mountains extend to the Moroccan border, and are limited to the east by the Tafna fault (lineament). Their median part consists of a Palaeozoic horst bounded by Upper Jurassic plateaux, and covered by thin Lower Jurassic transgressive beds. The different sectors will be briefly described from north to south in order to summarize the previous published data (LUCAS, 1942, 1952, 1966; AUGIER, 1967; ELMI, 1997).

THE SUBSIDING NORTH MARGIN

Oujda Trough, adapted from LUCAS (1942, 1952) ("vasière Oujda-Sebdou"). This trough or umbilic may be the prolongation of the subsiding Zekkara Zone of east Morocco (northern Oujda Mountains), but the Lower and Middle Jurassic does not outcrop in Algeria.

THE AXIAL RHAR ROUBANE SHOAL

It is divided into two parts by a major transverse palaeorelief (Fernane Shoal along the Béni Bou Saïd Fault; LUCAS, 1942; ELMI, 1973a).

The West Déglène Sector

In this area, the lower Pliensbachian (Carixian; Zaïlou Limestones) consists of shallow carbonates resting on the Palaeozoic basement and it can be locally missing. The Toarcian is made of shallow ramp carbonates and marls (Khorchef Beds) with rare ammonites (*Hildoceras*; Sublevisoni Subzone, Bifrons Zone) and small-sized brachiopods (*Soaresirhynchia bouchardi* (Davidson) and *Homoeorhynchia tifritensis* (Dubar)). These two levels are respectively correlated with the Levisoni and the Bifrons ammonite Zones. At the top of the Khorchef beds, wavy-bedded limestones (WB on Tables 3 and 4) are attributed to the upper Toarcian by comparison with well dated areas such as the Saïda Mountains (ELMI *et al.*, 1985). Upward, the shallowing of the environment continued during the deposition of the Déglène Dolomite. Near its base, rare brachiopods (*Stroudithyris pisolithica* (Buckman) and *S. fredericiromani* (Roché)) document the Aalenian (MEKAHLI *et al.*, 1993) but the major part of the formation is made of oolitic grainstones and of tidalites with desiccation markers (ELMI & ATMÉRAS, 1985; MEKAHLI, 1988).

The upper Bajocian is probably missing and the overlying Déglène Oolitic Ironstone rests unconformably on the weathered top of the Dolomites (N.B.: these dolomites have been worked as lead-zinc ore at Déglène and in the well known El Abed and Touissit-Bou Beker Mines along the western edge of the Rhar Roubane Mountains). The Déglène Oolitic Ironstone (MEKHALI *et al.*, 1994) is an ammonite rich level, thickening to the east (from 2 to 50 m in 4 km between Déglène and Fernane-Sidi Yacoub; LUCAS, 1942). It ranges from the lower Bathonian (Zigzag Zone) to the top of the middle Bathonian *sensu gallico* (Bremeri Zone). The most significant marker of the early Bathonian (Zigzag Zone and, possibly, beginning of the Aurigerus Zone) is *Oraniceras hauyaneuse* Flamand. One specimen from Jorf Henndia between Sidi Mohammed and Sidi Jabeur along the Oued Mellah (Oujda Mountains, Morocco), coming from the same formation, is figured here (Fig. 11b) because it shows clearly the carina-like shape of the ventral edge as in the types which come from the Ksour El Harchaia locality (FLAMAND, 1911: Pl. VII, Figs 10-13). This feature indicates a strong difference with the classic parkinsonid *Gonolkites*.

The upper Bathonian (Retrocostatum Zone) is missing as it is usual in all the Tlemcen Domain (ELMI 1971a, 1973b).

The Callovian begins with another oolitic and ferruginous decimetric bed yielding some *Kheraiceras bullatum* (d'Orbigny) and several specimens of the subgenus *Macrocephalites*. It is overlain by the thick

Source: MNHN, Paris

beds of the Saïda Clays Formation (rhythmic turbiditic sandstones, marls and ferruginous limestones) well dated from the Gracilis Zone in their lower part (LUCAS, 1942; ELMI, 1971a, b) and ranging into the lower Oxfordian at their top during the maximum deepening stage which was followed by a rapid shallowing (ELMI & BENEST, 1978).

The tectonic control is well documented near the Fernane Pass (Elevation Point 1222; Figs 9e and 12) where the shallow marine Déglène Dolomite onlaps the Palaeozoic palaeoreliefs. This formation has been faulted, probably during the late Bajocian and the fault scarp has been levelled and sealed by the the lower Bathonian (Moul el Tâgga Silty Limestones Formation) well dated by newly collected faunas (numbers indicating the place of the faunas are spotted on Fig. 12: n° 32: *Parkinsonia (Gonolkites) convergens* Buckman, *Morphoceras (Ebrayiceras?) parvum* Buckman, *Planisphinctes* sp., *Nannolytoceras tripartitum* (Raspail), *Holcophylloceras* sp. at the top of the fault; n° 33, at the top of the down-faulted block: *P. (G.)* cf. *convergens* (Buckman) associated with brachiopods -*Burmirhynchia terminierae* Rousselle and *Capillirhynchia ardescica* (Rollier)- and bivalves commonly known from the more neritic environment of the Ksour Mountains, such as *Ctenostreon palati* Flamand, indicating the proximity of shallow seamounts; n° 36, in the beds sealing the faulted stucture: *Procerites subprocerus* Buckman, *Asphinctites* cf. *polysphinctus* Dietl, *"Morphoceras"* aff. *pingue* De Grossouvre (inner whorls very involute and smooth body-chamber), *Siemiradzkia aurigera* (Oppel) *in* Sturani, *Oxycerites yeovilensis* (Rollier), *Holcophylloceras* sp.; this fauna is difficult to correlate (top Zigzag or lower Tenuiplicatus Zones).

The variability of the Morphoceratids seems to be different from that of their european equivalents. For this reason, we figure here an atypical specimen of *"Morphoceras" parvum* from bed 32 (Fig. 11a).

FIG. 11.— Jurassic ammonites of the Rhar Roubane (Tlemcen W., Algeria), Oujda (Eastern Morocco) and Ksour Mountains (Naâma W., Algeria). All figures = x 1.

a, *Morphoceras parvum* Buckman. Lower Bathonian. Moul el Tâgga Formation. Bed 32. Height 1222 near Sidi Yacoub, Fernane Pass (Rhar Roubane Mountains). Coll. ELMI, Univ. Lyon, n° 299668.

b, *Oraniceras hamyanense* Flamand. Lower Bathonian Déglène Oolitic Ironstone. Jorf el Henndia near Sidi Mohammed (Oued Melah, Sidi Jabeur, Oujda Mountains). Specimen showing the carina-like ventral area. Coll. ELMI, Univ. Lyon, n° 299667.

c, *Hammatoceras roubanense* Elmi nov. sp. Holotype. Middle Toarcian Gradata Zone. Alticarinata Subzone. Belaïch Oncolitic Limestones ("banc carié"). Djorf Tisseddoûra, Sidi Yahia ou Djabert, Khemis des Béni Snouss, Rhar Roubane Mountains. Coll. ELMI, Univ. Lyon, n° 299800.

d, *Hammatoceras roubanense* Elmi nov. sp. Paratype. Same locality and bed. Coll. ELMI, Univ. Lyon, n° 299801.

e, *Psiloceras (Caloceras)* sp. Lower Hettangian. Chemarikh Dolomite Formation. NW slope of Djebel Chemarikh, Aïn Ouarka near Aïn Sefra (Ksour Mountains). Coll. MEKAHLI, Univ. Lyon, n° 299671.

f, *Pleuroceras* cf. *solare* (Phillips). Upper Pliensbachian (Domerian), lower Emaciatum Zone. Calcareous equivalent of the topmost Aïn Ouarka Formation (member G). Raknet el Kahla, 2 km NE of Aïn Ouarka near Aïn Sefra (Ksour Mountains). Coll. MEKAHLI, Univ. Lyon, n° 299669.

FIG. 11.— Ammonites jurassiques des Monts de Rhar Roubane (W. de Tlemcen, Algérie), d'Oujda (Maroc oriental) et des Ksour (W. de Naâma, Algérie). Toutes figures = x 1.

a, Morphoceras parvum *Buckman. Bathonien inférieur. Calcaires microgréseux de Moul el Tâgga. Banc 32. Côte 1222, col du Fernane près de Sidi Yacoub (Monts de Rhar Roubane). Coll. ELMI, Univ. Lyon, n° 299668.*

b, Oraniceras hamyanense *Flamand. Bathonien inférieur. Oolithe ferrugineuse de Déglène. Jorf el Henndia près de Sidi Mohammed de l'Oued Melah près de Sidi Jabeur. Monts d'Oujda. Exemplaire montrant bien l'aspect caréné de l'aire ventrale. Coll. ELMI, Univ. Lyon, n° 299667.*

c, Hammatoceras roubanense *Elmi nov. sp.. Holotype. Toarcien moyen. Zone à Gradata. Sous-zone à Alticarinata. Calcaires oncolithiques du Belaïch (banc carié). Djorf Tisseddoûra, Sidi Yahia ou Djabert, Khemis des Béni Snouss, Monts de Rhar Roubane. Coll. ELMI, Univ. Lyon, n° 299800.*

d, Hammatoceras roubanense *Elmi nov. sp. Paratype. Mêmes localité et niveau. Coll. ELMI, Univ. Lyon, n° 299801.*

e, Psiloceras (Caloceras) *sp. Hettangien inférieur. Dolomie du Chemarikh. Flanc W du Djebel Chemarikh, Aïn Ouarka près d'Aïn Sefra (Monts des Ksour). Coll. MEKAHLI, Univ. Lyon, n° 299671.*

f, Pleuroceras *cf.* solare *(Phillips). Pliensbachien supérieur (Domérien), partie inférieure de la zone à Emaciatum. Équivalent calcaire de la partie terminale de la Formation d'Aïn Ouarka (membre G). Raknet el Kahla, à environ 2 km au NE du village d'Aïn Ouarka près d'Aïn Sefra (Monts des Ksour). Coll. MEKAHLI, Univ. Lyon, n° 299669.*

Source : MNHN, Paris

Source : MNHN, Paris

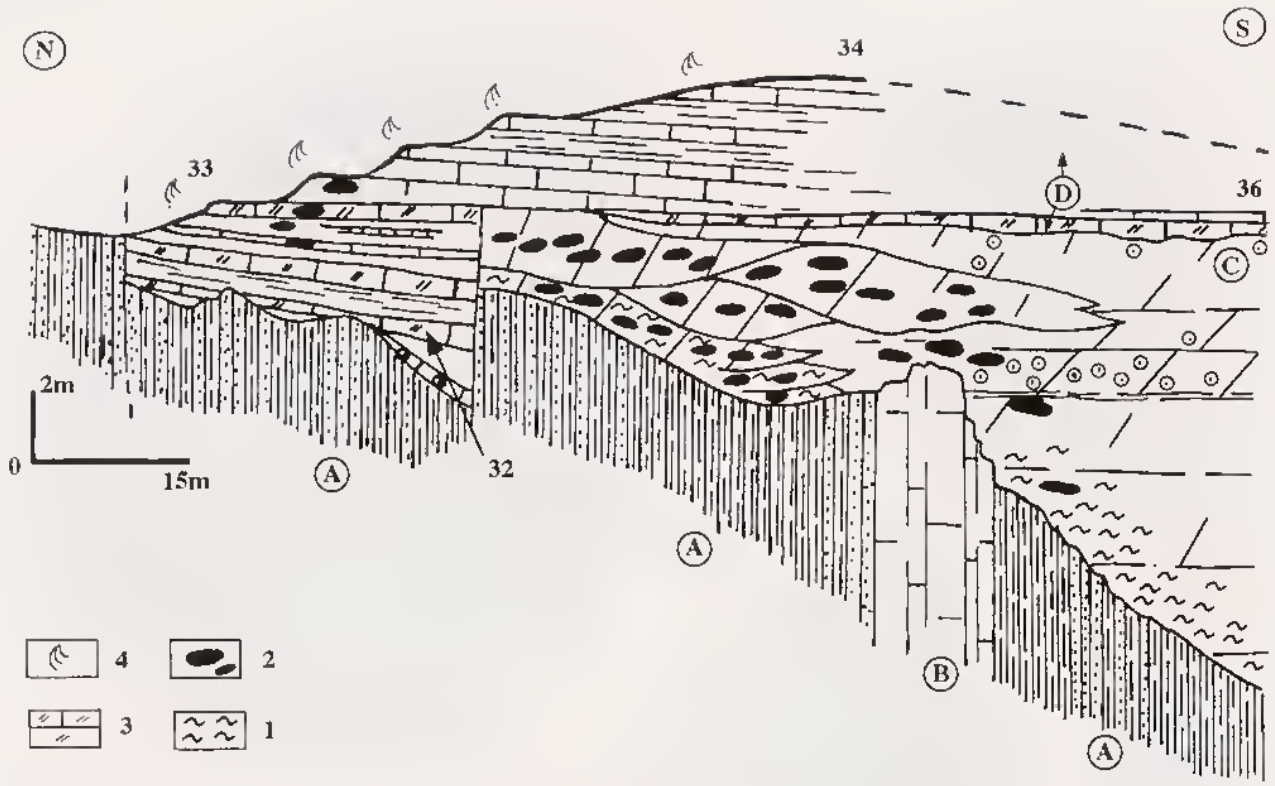

FIG. 12.— Semi-diagrammatic view of the Fernane Pass (height 1222) illustrating the onlap of the Bajocian and Bathonian beds on the Palaeozoic basement. Western Déglène Sector of the Rhar Roubane axial shoal, near its limit with the eastern Tisseddoûra Sector.

A, Schists and quartzites, probably of the Devonian-Dinantian, dipping vertically. They are strongly weathered and rubefacted on several meters; **B**, Dinantian dolomite; **C**, Déglène Dolomite; Aalenian - lower Bajocian. The dolomites (oodolosparites) result from the crystallisation of oolitic grainstones and packstones; with channelized debris flows reworking pebbles made of palaeozoic quartzites. The lower part is pink - purplish-blue, due to the washing of Palaeozoic palaeosoils (n° 1). Pression-solution features are common (vadose diagenesis). Birdeyes, algal laminations, oncolites and desiccation breccias become frequent slightly toward the South (between Sidi Yacoub and elevation 1222). Mass flows of big carbonate and quartzite pebbles indicate the importance of the topographic slopes (gravity-flows). **D**, Moul-el-Tâgga Silty Limestones (early Bathonian) represented here by thinning-up alternances of argillaceous limestones, more or less bioclastic and rich in quartz-silts in decimetric beds ("microgrès" of LUCAS, 1942), and of laminated marls. *Zoophycos* are frequent. Conglomeratic beds with quartzite blocks (up to 50 cm) are present to the south of the fault which is sealed by the fossiliferous Bathonian bed n° 36 and the associated bioclastic limestone. N° 32 to 36: fossiliferous beds. N° 32 is a crinoid-bioclastic grainstone. See Fig. 9e. 1, transgressive beds of the Déglène Dolomite colored in purple and pink by washing of the palaeosurfaces and "palaeosols"; 2, reworked palaeozoic blocks (quartzites and schists); 3, bioclastic limestones interbeded in the Moul el Tâgga Formation; 4, *Zoophycos*.

FIG. 12.— Vue schématique du panorama de la côte 1222 du Col du Fernane. Horst occidental de Rhar Roubane (bordure orientale du secteur de Déglène). Le débordement ("onlap") des assises du Bajocien-Bathonien sur le paléorelief paléozoïque est particulièrement bien exposé.

A, Schistes et quartzites, rapportés au Dévono-Dinantien. Pendage subvertical. Surface altérée et rubéfiée sur plusieurs mètres d'épaisseur. B, Dolomie dinantienne. C, "Formation de la Dolomie de Déglène" ; Aalénien-Bajocien inférieur. Les dolomies (oodolosparites) sont dérivées de grainstones et de packstones oolithiques. Elles présentent des chenaux dans lesquels sont disséminés des blocs décimétriques de quartzites paléozoïques. La partie inférieure est colorée en rose-violacé par suite du lessivage des paléosols développés à la surface du Paléozoïque (n° 1). Elles présentent des traces de diagenèse vadose et des ciments en ménisque; latéralement (vers le Sud entre Sidi Yacoub et la côte 1222), elles montrent des structures fenestrées (birdeyes), des oncolithes et des laminations algaires passant à des brèches de dessiccation. L'influence des pentes est marquée par des éboulis gravitaires (grands galets de carbonate et de quartzite). D, formation des "Calcaires microgréseux du Moul el Tâgga" ; Bathonien inférieur. Calcaires argileux, finement bioclastiques, plus ou moins chargés en silts ("microgrès" de LUCAS, 1942), alternant avec des marnes feuilletées. Zoophycos *abondants. N° 32 à 36 : niveaux fossilifères. L'ensemble s'organise en lithoclines stratodécroissantes. Des passées de conglomérats à blocs de quartzite atteignant 50 cm se développent au Sud de la faille qui est cicatrisée par le niveau fossilifère n° 36 et le calcaire bioclastique qui lui est associé. Le niveau n° 32 est un calcaire bioclastique (grainstone). Le dispositif transgressif est illustré sur la photographie de la Fig. 9e. 1, niveaux transgressifs de la Dolomie de Déglène, colorés en rose-violacé par lessivage des paléosols. 2, blocs de quartzites et parfois de schistes paléozoïques ; 3, calcaires bioclastiques intercalés dans la Formation de Moul el Tâgga ; 4,* Zoophycos.

Source : MNHN, Paris

The Tisseddoûra sector

In the East (eastern horst or Tisseddoûra sector; Figs 9f, 13a), environmental evolution was different until the Bathonian. Open sea conditions began during the early Domerian with the bioclastic Tisseddoûra Limestones containing some *Protogrammoceras celebratum* (d'Orbigny), *P. isseli* Fucini (involute type) and *Fuciniceras* sp. These followed an initial flooding indicated by the tidal Carixian Zaïlou Limestones preserved only in the lower parts of the palaeoreliefs. The rates of subsidence and of sedimentation were very slow (LUCAS, 1942; ELMI, 1977a, 1983).

Above, the Belaïch oncolitic Beds are highly condensed. The middle Toarcian is reduced to thin and lenticular limestones rich in ammonites, some of these having been figured (ELMI, 1977b; ELMI & BENSHILI, 1987; ELMI & RULLEAU, 1996). The most important level is a micrite with bioclasts and mineralized oncolites containing beautifully preserved and large sized ammonites of the Gradata Zone, such as the last *Hildoceras (H. snowssi* Elmi, 1977b: Pl. 4, Fig. 3, refigured *in* ELMI *et al.*, 1997, Fig. 2). *Fuciceras erbaense* (Hauer) (ELMI & RULLEAU, 1996: Pl. 9, Fig. 2) and *F. evolutum* (Merla) (ELMI & BENSHILI, 1987: Fig. 4), giant *Osperlioceras* and the first true *Haugmatoceras*, represented by the new species *H. roubanense* Elmi described below. The upper Toarcian is probably missing and the Aalenian is only known by centimetric lags with Graphoceratids.

The Niortense Zone is also lenticular and two decimetric levels have been recognized (4 and 5 on Fig. 15). Bed n° 4 (0 to 0.20 m) fills a channel furrowed in the Toarcian limestones; this is a micritic limestone containing ferruginous oolites and fragments of a nearby algal mat which has been encrusted by iron and eroded. The top of bed 4 is truncated by an erosion surface, cutting, in peculiar, the ammonites. The latter indicate probably the Polygyralis Subzone with *Strenoceras subfurcatum* (Schlotheim), *Leptosphinctes (L.) perspicuus* (Parona), *L. (L.) davidsoni* (Buckman), *L. (Cleistosphinctes) cleistus* Buckm., *Cadomites deslongchampsi* (Defrance), *Sphaeroceras brongniarti* (Sowerby), *Oppelia pouyanuei* (Flamand), *Oecotraustes* cf. *westermanni* Sapunov, *Holcophylloceras zignodianum* (d'Orbigny) and *Lytoceras endesianum* (d'Orb.). Bed 5 (0 to 0.30 m) is a lenticular representative of the Zahra Marls (laminated marly limestone). Newly recognized, it has yielded several *Spiroceras orbignyi* (Baugier & Sauzé) indicating the upper part of the Niortense Zone (upper Polygyralis and Baculata Subzones).

The Moul el Tâgga Silty Limestones Formation is transgressive and tectonically discordant and has been defined in this sector (ELMI, 1997) (Figs 14, 15). The mean thickness is of 50 m. At the base, the formation onlaps the tilted surface of the Belaïch Oncolitic Beds (Fig. 9f). The Moul el Tâgga Formation is characterized by the vertical stacking of several thinning and fining upwards rhythmic sequences of alternating marls and marly limestones, often silty and bearing abundant *Zoophycos*. In the upper part, the sequences end with limestones containing disseminated chamositic oolites reworked from the nearby seamounts (LUCAS, 1942; ELMI & BENEST, 1978). The age of the major part of the formation is early Bathonian as proved by scattered collections (*Morphoceras, Oraniceras*). Rare and poorly preserved *Bullatimorphites* could indicate the middle Bathonian. The top is marked by a major unconformity dated of the Bremeri Zone by comparison with Déglène.

The sedimentation resumed more or less rapidly during the early Callovian (Bullatus to early Gracilis Zones) with the beginning of the sedimentation of the Saïda Clays (up to 300 m thick). The top of the Gracilis Zone is well characterized on all the Rhar Roubane Horst by the *H. (Hecticoceras) boginense* Petitclerc assemblage (ELMI, 1971a. ELMI & BENEST, 1978): *H. (H.) boginense, H. (H.) posterius* Zeiss, *Collotia discus* (Bourquin) and *Dolikephalites gracilis* (Spath). Laterally (Béni Yabir), this assemblage includes also: *Indosphinctes* gr. *patina* (Neumayr), *R. (Rehmannia)* spp., *Hecticoceras (Chanasia) michalskii* (Lewinski), *Prohecticoceras (Zieteniceras) pseudolunula* Elmi. The Phylloceratids are abundant (up to 30% of the assemblage) with the genera *Phylloceras* and *Holcophylloceras*. *Ptychophylloceras* seems missing. The middle Callovian (Arkelli Zone) is well documented by numerous and varied *Lunuloceras*. The last dated level of the Saïda Clays Formation belongs to the early Oxfordian (*Parawedekindia* spp.). It is a thick marly bed (15 m) and it coincids with an inversion from a deepening-transgressive evolution to a shallowing-regressive episode. Upward, several breccias mark the beginning of the relative sea-level fall. This area, from Djebel Selib (near from

Source : MNHN, Paris

FIG. 13.— Details of some Jurassic outcrops of Western Algeria.

a, Reduced Toarcian-Bajocian beds on top of the Tisseddoûra Cliff illustrated on Fig. 9f. 1: decimetric marly level with *Hildoceras sublevisoni* Fucini (Sublevisoni Subzone, Bifrons Zone). 2: *Hildoceras snoussi* Elmi bed (Gemma Subzone, Gradata Zone). 3: *Hammatoceras roubanense* Elmi nov. sp. bed (Alticarinatus Subzone, Gradata Zone). 1-3 = Belaïch oncolitic Beds. 4: lenticular bed of the upper Bajocian (basal Niortense Zone). It is a micrite containing dispersed ferruginous black and green oolites washed from a nearby seamount and reworked red snuff-boxes resulting from the erosion of a ferruginous algal mat. At the top, it is truncated by an erosion surface which cut the ammonites and the snuff-boxes. 5: base of the Moul el Tâgga Formation. Locality: see Fig. 9f. Coll. ELMI, 73B29.

b, Megalodontids limestones (large lamellibranch facies) of the Zaïlou Formation. Lower Pliensbachian (Carixian). El Menzâl, road C.W. 106 between Khemis (Béni Snouss) and El Fahs. East Rhar Roubane Mountains (Tlemcen W.). Coll. ELMI, 93DZ610.

c, Contact between the top of the Pseudonodular limestones (2-13) and the base of the Béni Bahdel Ferruginous Limestones (2-14). Embankment of the road C.W. 46 along the Koudiat el Halfa Hill, Béni Bahdel. Coll. ELMI, 73B11. Bed 2-13 is dated of the Solare Subzone of the upper Domerian Emaciatum Zone. Vertically embedded *Pleuroceras solare* (Phillips) (1) and abundant belemnites. Rich microfauna: *Involutina liassica* Jones, *Lenticulina* sp., *Ophtalmidium* sp. (= *"Vidalina martana"*), Nodosariids, Epistominiids, Hexactinellids, Ophiurids, algae. Bioeroded surface. The rounded "block" (2) on the right is not a reworked pebble but an irregularity of the surface. The whole is capped by a laminated ferruginous crust. This probable algal mat indicates a shallowing that occurred between the Domerian and the Toarcian. It results from a tectonic decoupling between the shoals and the umbilics. Bed 2-14 is dated to the Levisoni Zone by several *Hildaites*. It marks the resumption of the sedimentation after a gap ranging from the Elisa Subzone (topmost Domerian) to the Polymorphum Zone (lowermost Toarcian). It can be interpreted as a sedimentologic "first flooding" and as a condensed bed in sequence-stratigraphy nomenclature (the actual maximum of deepening occurred later during the Sublevisoni Zone marls (local maximum "flooding").

d, e, Algal mat coating the bioeroded surface of the Béni Bahdel ferruginous Limestones (lower Aalenian). The surface corresponds probably to the washing of a soft ground and to its superficial lithification. Boring bivalves settled afterwards (clear perforations on fig. 13e) they can be deformed by compaction. The algal mat coated the irregular surfaces, during a shallowing episode followed by a relative sea level rise. Lower to upper Aalenian ammonites and belemnites are embedded in the micritic infilling preserved in the dips of the irregular surface. The Tleta Limestones are missing in this area. The surface is sealed by the *Bositra* marls (Zahra Marls Formation) (1) of the upper Bajocian (Niortense Zone). Gully at the foot of the southern wall of the Béni Bahdel Dam (Tlemcen W.). Coll. ELMI, 81DZ133 and 104.

f, Bou Lehrfad Reefs at the base of the Tifkirt Formation. The general shape of the reefs explains the arabian name of the mountain (lefrad = thigh or mutton-leg). On the right (North East) (1): Reef R3 (in ALMÉRAS *et al*, 1994). Reef R2 is situated at the foot of the slope on the left (2). Strong dipping to the NW. On the foreground, the Alfa steppe hides the marls and sandstones of the Teniet el Klakh Formation. Upper Bajocian, Niortense Zone. Djebel Bou Lerfahd and Aïn Rhezala depression near Aïn Ouarka, Saharian Atlas (Naâma Wilaya). Coll. ELMI, 93DZ819.

FIG. 13.— Détails de quelques affleurements jurassiques de l'Ouest algérien.

a, Niveaux réduits du Toarcien-Bajocien exposés au sommet de la falaise du Tisseddoûra (cf. Fig. 9f). 1 : niveau marneux décimétrique à Hildoceras sublevisoni *Fucini (sous-zone à Sublevisoni, zone à Bifrons). 2 : banc à* Hildoceras snoussi *Elmi (sous-zone à Gemma, zone à Gradata). 3 : banc à* Hammatoceras roubanense *Elmi nov. sp. (sous-zone à Alticarinatus, zone à Gradata). 1-3 :* Calcaires oncolithiques du Belaïch. *4 : banc lenticulaire du Bajocien supérieur (début de la zone à Niortense). C'est une micrite à oolithes ferrugineuses noires et vertes, dispersées depuis les hauts-fonds voisins: elle contient des fragments décimétriques rouges remaniés à partir d'une croûte oncolithique ferrugineuse. La surface d'érosion qui tronque ce niveau recoupe les ammonites et les fragments stromatolithiques. 5 : base de la Formation de Moul el Tâgga. Localité : voir Fig. 9f. Coll. ELMI, 73B29.*

b, Calcaires à "grands lamellibranches" avec des Megalodontidés. Formation des Calcaires compacts de Zaïlou (Pliensbachien inférieur = Carixien). El Menzâl, route C.W. 106 entre le Khemis des Béni Snouss et El Fahs. Partie orientale des Monts de Rhar Roubane (W. de Tlemcen). Coll. ELMI, 93DZ610.

c, Contact des Calcaires pseudonoduleux (2-13) et des Calcaires ferrugineux des Béni Bahdel (2-14). Talus de la route C.W. 46, en bordure de la Koudiat el Halfa, Béni Bahdel. Coll. ELMI, 73B11. Banc 2-13 ; sous-zone à Solare, zone à Emaciatum. Domérien supérieur. Pleuroceras solare *(Phillips) en position verticale (1) et nombreuses bélemnites. Riche microfaune :* Involutina liassica *Jones,* Lenticulina *sp.,* Ophtalmidium *sp. (=* "Vidalina martana"*), Nodosariidés, Epistominiidés, Hexactinellidés, Ophiuridés, algues. La surface supérieure du banc est bioérodée : le "bloc" arrondi (2) n'est pas un galet mais une apophyse des irrégularités de la surface. L'ensemble est recouvert par une croûte ferrugineuse laminée. Il s'agit vraisemblablement d'un tapis algaire indiquant une diminution de la profondeur entre le Domérien et le Toarcien. Ces observations confirment l'existence d'un découplage tectonique entre les seuils et les hauts-fonds d'une part, et les ombilics et les bassins d'autre part. Banc 2-14 : Zone à Levisoni (plusieurs* Hildaites*). Il marque la reprise de sédimentation après une lacune qui s'étend depuis la sous-zone à Elisa (fin du Domérien) jusqu'à la zone à Polymorphum. Ce banc peut être considéré comme indiquant une "inondation initiale" au sens sédimentologique et comme un "niveau condensé" en terminologie séquentielle : l'approfondissement réel intervient plus tard avec les marnes de la sous-zone à Sublevisoni qui indiquent un maximum local d'inondation.*

d, e. Surface supérieure des Calcaires ferrugineux des Béni Bahdel (Aalénien inférieur). Il s'agit d'une surface bioérodée revêtue par un tapis algaire qui suit les irrégularités du relief après que ce dernier a été perforé par des bivalves (perforations nettes sur la Fig. 13e) consécutivement à sa lithification. La baisse du niveau marin relatif ainsi enregistrée a été suivie par un

Source : MNHN, Paris

approfondissement. Des calcaires micritiques remplissent les creux de la surface et ils contiennent des ammonites et des bélemnites, parfois déformées par la compaction différentielle (Aalénien moyen et supérieur). Les Calcaires du Tleta sont absents et la surface est recouverte par les marnes à Bositra *du Bajocien supérieur (Marnes de Zahra) (1) ; zone à Niortense. Ravin au pied de la partie méridionale du barrage des Béni Bahdel (W. de Tlemcen). Coll.* ELMI, *81DZ133 et 104.*

f, Les récifs du Djebel Bou Lehrfad à la base de la Formation du Tifkirt. Leur forme générale est à l'origine du nom de la localité (lefrad = gigot). À droite (NE) (1) : récif R3 (in ALMÉRAS et al., *1994). Le récif R2 (2) se trouve au pied des reliefs à gauche (SW). L'ensemble présente un fort pendage vers le NW. Au premier plan, la steppe d'Alfa s'étend sur les marnes et les grès de la Formation du Teniet el Klakh. Bajocien supérieur, zone à Niortense. Djebel Bou Lerfahd et dépression d'Aïn Rhezala près d'Aïn Ouarka, Atlas saharien (Wilaya de Naâma). Coll.* ELMI, *93DZ819*

Source : MNHN, Paris

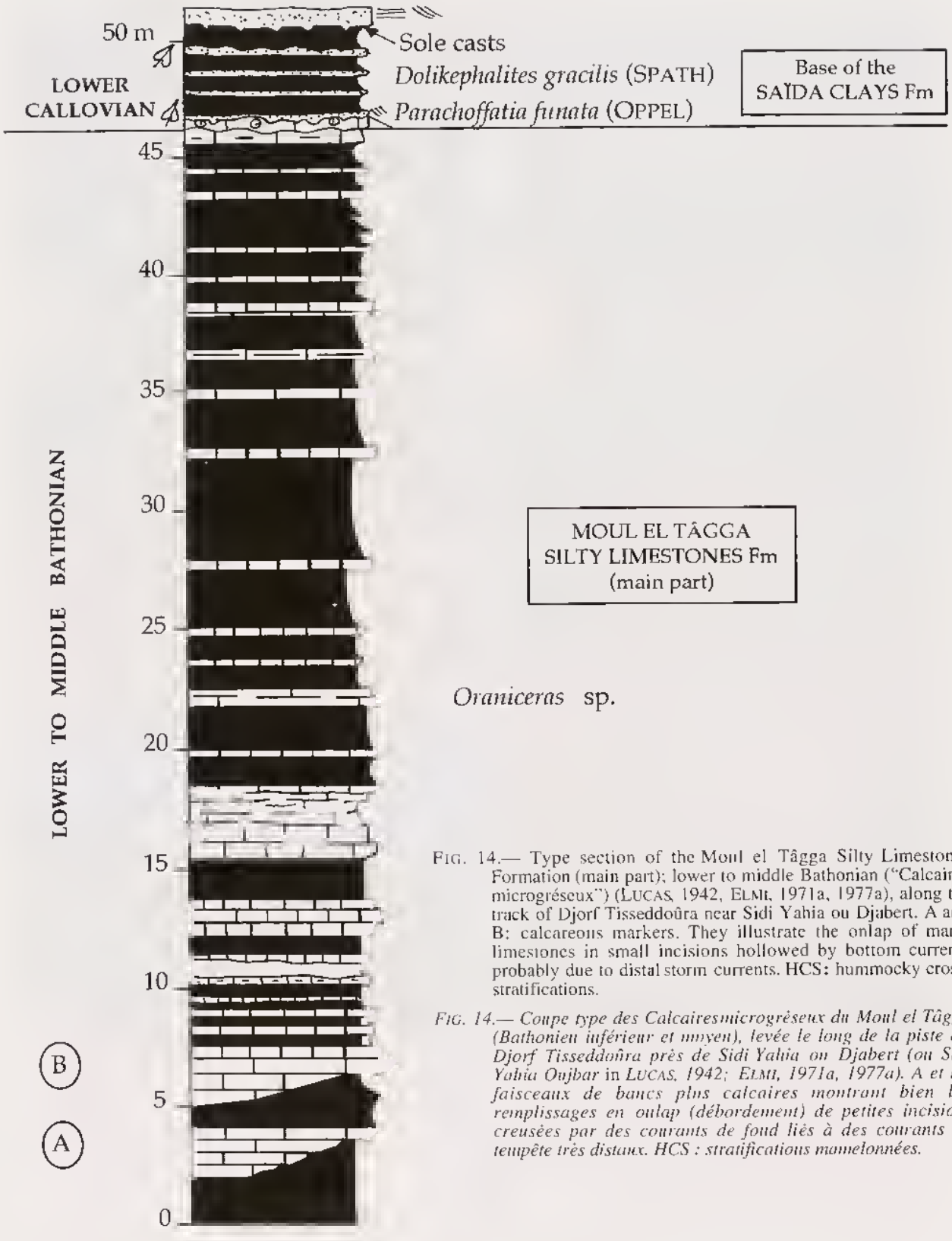

FIG. 14.— Type section of the Moul el Tâgga Silty Limestones Formation (main part); lower to middle Bathonian ("Calcaires microgréseux") (LUCAS, 1942, ELMI, 1971a, 1977a), along the track of Djorf Tisseddoûra near Sidi Yahia ou Djabert. A and B: calcareous markers. They illustrate the onlap of marly limestones in small incisions hollowed by bottom currents probably due to distal storm currents. HCS: hummocky cross-stratifications.

FIG. 14.— Coupe type des Calcaires microgréseux du Moul el Tâgga (Bathonien inférieur et moyen), levée le long de la piste du Djorf Tisseddoûra près de Sidi Yahia ou Djabert (ou Sidi Yahia Oujbar in *LUCAS, 1942; ELMI, 1971a, 1977a). A et B : faisceaux de bancs plus calcaires montrant bien les remplissages en onlap (débordement) de petites incisions creusées par des courants de fond liés à des courants de tempête très distaux. HCS : stratifications mamelonnées.*

Source : MNHN, Paris

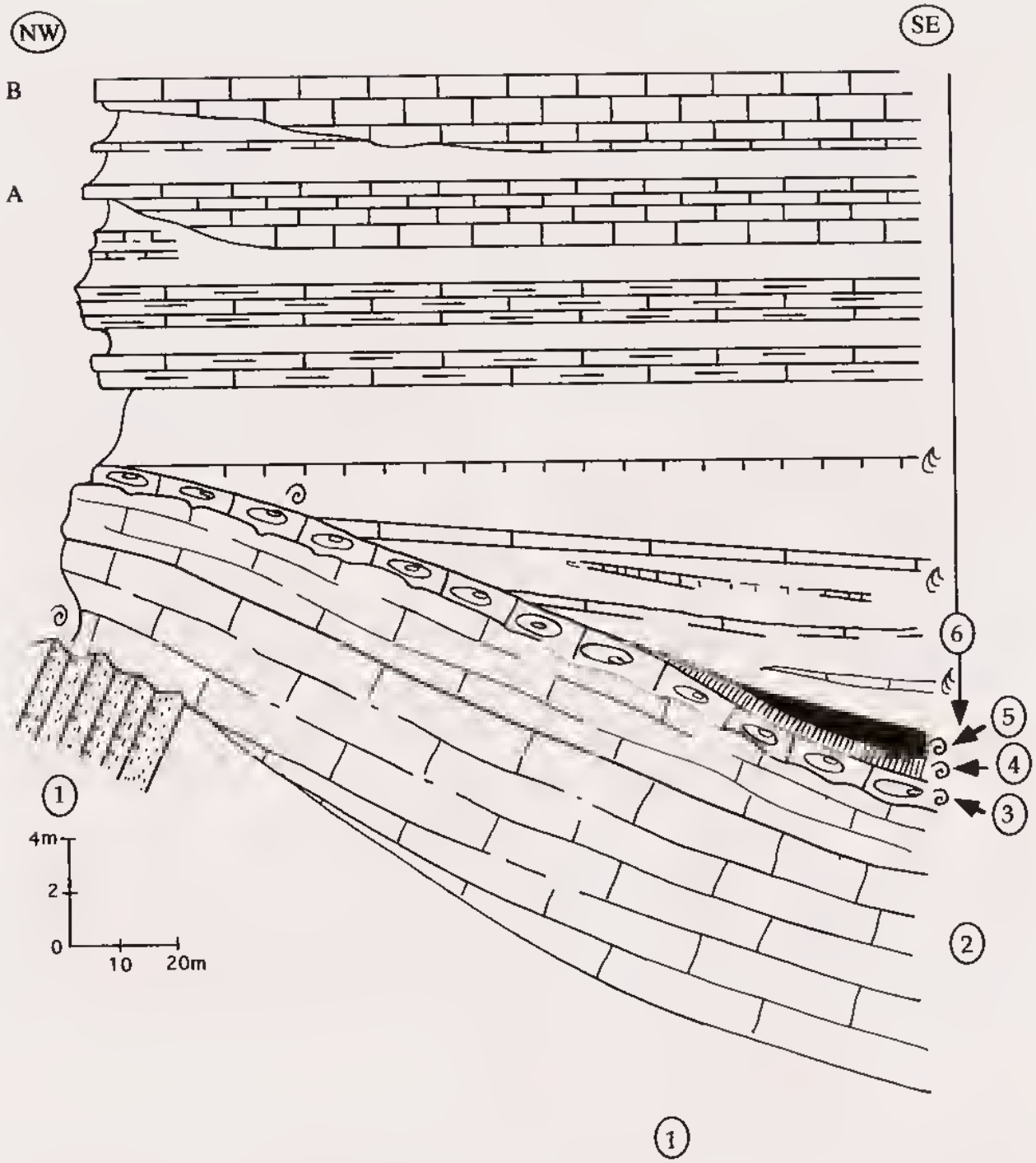

FIG. 15.— The progressive onlaps of the middle Lias to lower Bathonian on the palaeorelief of Djorf Tisseddoûra. **1**, Palaeozoic basement (rubefied schists and quartzites); **2**, Tisseddoûra Formation (lower Domerian, Celebratum Zone); **3**, Toarcian Belaïch Oncolitic beds; **4**, **5**, upper Bajocian (Niortense Zone); Moul el Tâgga Formation (lower Bathonien) thin marly bed (5) overlying the eroded surface of 4. A and B: same calcareous markers that on Fig. 14; **6**, Moul el Tâgga Formation (lower Bathonian).

FIG. 15.— Ennoyage et débordement progressifs du paléorelief du Djorf Tisseddoûra du Lias moyen jusqu'au Bathonien inférieur ; 1, Socle paléozoïque (schistes rubéfiés et quartzites) ; 2, Formation du Tisseddoûra (Domérien inférieur, zone à Celebratum) ; 3, Calcaires oncolithiques du Belaïch ; 4, 5, Bajocien supérieur (zone à Niortense) avec un mince liseré marneux (5) reposant sur la surface erodée de 4. A et B : niveaux calcaires, repères voir fig. 14 ; 6, Formation du Moul el Tâgga (Bathonien inférieur).

Source: MNHN, Paris

Tisseddoûra) to Déglène can be choosen as a reference -area for the Selib Group or Middle Sandy-Argillaceous Group.

THE BÉNI BAHDEL SUBBASIN

To the east of Rhar Roubane, is another complex but small unit developed along the Tafna N030° fault. It includes a transitional zone to the Rhar Roubane shoal with a moderately deep and narrow area (Koudiat el Halfa Zone) and a deeper area (Tleta Zone).

Above shallow carbonates, attributed to the upper Sinemurian (?) to Carixian Zaïlou Limestones, with Megalodontids Limestones (Fig. 13b), there occur outer platform (Tisseddoûra Limestones) and slope (Pseudonodular Limestones) deposits of the Domerian (ATROPS *et al.*, 1970; ELMI *et al.*, 1974). The Pliensbachian-Toarcian boundary is marked by an unconformity emphasized by ferruginous crusts (Fig. 13c). In the subsiding area (Tleta), at the top of palaeofaults, the Toarcian consists of a pelagic alternance of marls and limestones, attributed to the Bayada Formation. Brachiopods and ammonites have been recently found in these poorly fossiliferous beds. Together with the LUCAS data (1942), they allow recognition of the Levisoni (*Hildaites* sp.) and Bifrons Zones (*Frechiella* sp., *Porpoceras* sp.). In the neritic profiles (Koudiat el Halfa), the Toarcian is represented by the bioclastic Béni Bahdel Limestones in which the Levisoni, Bifrons, Gradata (?), Meneghinii Zones have been proved. The ferruginous beds of the Levisoni Zone rest directly on the belemnite bed of the lower Emaciatum Zone (*Pleuroceras solare* (Phil.); the eroded surface is underlined by a ferruginous crust which encompasses some breccia-like blocks). They are in fact due to bioerosion.

The lower part of the Tleta Limestones (with *Zoophycos)* is dated of the lower Aalenian (Opalinum Zone) under a hard ground with *Tmetoceras scissum* (Benecke). Several spectacular condensed levels capped by algal crusts are developed throughout the Aalenian and the lower Bajocian of the Béni Bahdel subbasin (particularity near the southern wall of the Béni Bahdel Dam; Fig. 13d-e). The lower Bajocian is often missing. When they exist, the Tleta Limestones end with a condensed level rich in stephanoceratids collected and figured by ATROPS (1974): *Emileia polyschides* (Waagen), *E. catamorpha* Buckman, *Stephanoceras* (*St.*) *humphriesianum* (Sowerby), *St. (St.) densicostatum* Atrops, *St. (Skirroceras) freycineti* (Bayle), *St. (Sk.) tlemceni* Atrops, *St. (Sk.)* cf. *skolex* (Buckman) (condensed Propinquans and basal Humphriesianum Zones).

The main lithostratigraphic feature is the occurrence of thick upper Bajocian *Bositra* bearing marls. They have yielded a rich pyritic ammonite fauna which has given a reference for the biostratigraphic succession of the Niortense Zone (Zahra Marls Formation). Four local associations have been defined in the Niortense (= Subfurcatum) Zone (adapted from ELMI, 1969, 1971a):

— *Teloceras* and *Caumontisphinctes* association: nucleus of *Sphaeroceras*, *Normannites* and *Teloceras* are associated with *Caumontisphinctes aplous* Buckman, *Oppelia pouyannei* Flamand, *Oecotraustes* cf. *westermanni* Stephanov, *Strigoceras* cf. *paronai* Trauth; this horizon can be correlated with the Banksi Subzone (Aplous horizon).

— *Spiroceras orbignyi* Baugier & Sauzé and *Oppelia pouyannei* Flamand; disappearance of *Teloceras* and *Normannites*; persistance of rare *Sphaeroceras*.

— *Oppelia pouyannei* Flamand and *Cadomites deslongchamspi* Defrance association. Rare *Caumontisphinctes (C.) polygyralis* Buckman. The second and third associations can together be compared with the Polygyralis and Baculata Subzones. These marls (more than 150 m) reduce dramatically to the highly condensed oncolitic beds of the Eastern Rhar Roubane (Tisseddoûra) in 4-5 kilometers (LUCAS, 1942, 1952). This change occurs across a major palaeofault sealed only during the early Bathonian by the Moul el Tâgga Formation as already described by LUCAS (1942).

The lower part of the Moul el Tâgga Formation contains abundant *Zoophycos* and some crushed or pyritic ammonites: *Nannolytoceras tripartitum* (Raspail), *Lytoceras adeloides* (Kudernacht), *Partschiceras* gr. *viator* (d'Orbigny), *Morphoceras (Ebrayiceras?) parvum* Wetzel, *M. (E.)* cf. *sulcatum* (Hehl) and nuclei of Parkinsonids.

Source : MNHN, Paris

THE SOUTHERN MARGIN

A southern margin ("vasière de Sebdou", adapted from LUCAS 1942, better named Tenouchfi Zone or Umbilic) ranging from the Tenouchfi Massif to the west to Sidi Yahia ben Sefia to the east, sustained a rapid subsidence rate. The shallow water Zaïlou Limestones are thick, with Megalodontids beds in their upper part and a rich microfauna described by BASSOULLET & BENEST (1976). Deep platform conditions appeared during the early Domerian with cherty limestones (Tisseddoûra Formation) changing abruptly to the Aïoun ben Mira Marls (ATROPS *et al.*, 1970) containing a rich pyritic fauna of the Algovianum Zone; *Pleuroceras* occurs in the upper Domerian documenting the displacement of these north west european ammonites along moderately deep platform along the Sahara craton and along the palaeoreliefs and seamounts (LUCAS, 1942). The Toarcian consists of alternating marls and limestones which are marly dominated at the base and become progressively more calcareous upwards. These beds are attributed to the basinal Bayada Formation. The lower metres have yielded a rich pyritic fauna of the lower Polymorphum Zone with *Eodactylites* spp. and *Paltarpites* gr. *paltus* Buckman-*madagascariensis* (Lemoine). In the Tenouchfi Umbilic, *Zoophycos* are common from the middle Toarcian (Gradata Zone) up to the Bathonian (ELMI & BENEST, 1969). In the Gradata Zone, *Merlaites* gr. *alticarinatus* (Merla) is associated with *Hammatoceras ronbanense* Elmi nov. sp. (= *H.* nov. sp., ELMI & BENEST, 1969; ELMI *et al.*, 1974: Pl. 5, Fig. 1).

During the Aalenian and early Bajocian, the eastern and southern borders of the Tenouchfi Umbilic sustained strong carbonate allodapic inputs with, in the same time, a deepening of the trough. The upper Bajocian is represented by thick marls (Zahra Marls Formation), containing abundant pyritic ammonites (Niortense Zone, Polygyralis and Baculata Subzones): *Strenoceras* gr. *subfurcatum* (Zieten), *Cannontisphinctes (Infraparkinsonia)* sp., *Leptosphinctes* cf. *perspicuus* (Parona), *Cadomites* gr. *deslongchampsi* (d'Orbigny), *Strigoceras truellei* (d'Orbigny), *Oppelia ponyanuei* Flamand, *Oecotranstes* cf. *westermanni* Stephanov, *Spiroceras* spp. associated with rare specimens of the isolated coral *Montlivaltia*.

The areas of thick sedimentation surrounding the Rhar Roubane have been grouped into a so-called "vasière Oujda-Sebdou" by LUCAS (1942, 1952) who also used the name "pretellian zone or facies" (see also CISZACK, 1993). This latter name is inappropriate because it can be confused with the structural and tectonic regional nomenclature (GUARDIA, 1975).

The southern border of the Rhar Roubane is hidden by Recent deposits. The transition to the High Plains can be documented slightly to the west in Morocco (southern Oujda Mountains around Tiouli). It can be presumed that this transition is marked by a fringe of oolitic barriers, which provided the reworked material known in the basin (Tenouchfi Dolomite), along the border of the High Plains Platform (BENEST *et al.*, 1978; MAROK, 1996). The Tenouchfi Dolomite is a *Zoophycos* hemipelagic formation; its dolomitization is mainly due to a subsequent tectonically provoked recrystallization; its age is probably comparable to the Aalenian-lower Bathonian "Dalle des Hauts Plateaux" (High Plateaux Dolomite) deposited in a tidal environment. It may also be correlated with the Déglène Dolomite which is limited to the top and to the edge of small seamounts. But, whatever the precise and local environment, this spreading of the carbonate production is under the control of global events which are well known also north of the Tethys, especially on the french platform from the Lyon promontory to the Paris Basin (ROUSSELLE & DROMART, 1996).

THE ORAN HIGH PLAINS: THE SIDI EL ABED MOUNTAINS

The Oran High Plains (or Oran Meseta, or High Plateaux) are a large subtabular steppe (covered with "alfa" or esparto = *Stipa tenacissima*) with a mean elevation of 1000 m, dominated by higher mountains to the north as well as to the south. The use of the expression Oran Meseta is here discarded because it has often been misused (FLINCH, 1996: Fig. 1, for instance), and because this region does not correspond to a true meseta: rare outcrops of the Palaeozoic basement, occurrence of several subsiding basins or furrows, inversion to general subsidence during the Cenozoic (for a more complete discussion, see MAROK, 1996).

The High Plains reach a width between 150 and 200 km. The Sidi el Abed Mountains are the only prominent relief where the Lias-Bajocian beds outcrop. Geophysical data (MAROK, 1996) suggest that

Source : MNHN, Paris

the Sidi el Abed was a relatively subsiding WSW-ENE area, limited by basement faults and inverted during the Atlas Orogeny.

The sedimentary and dynamic evolution from the Lias to the Bajocian (more recent Jurassic beds are eroded) will be summarized briefly in order to indicate the new results which are of importance for stratigraphic correlations and for palaeogeography (Fig. 16). This is the first revision of this key frontier

---

FIG. 16.— Tentative correlations between the Lower Jurassic successions of the Oran High Plains and the Moroccan High Plateaux and comparison with the Southern Border of the Figuig Atlas Domain (Algerian Southern Grouz). The horizontal marker line has been drawn with the appearance of the mottled facies (shallow-water to sabkha deposits) of the Toarcian (lower part of Jebel Nador Formation).

NW High Plateaux, Jebel Nador Sector, South of Debdou. From MEDIONI (1971).

NE High Plateaux, Béni Yala, near Guefaït; from DUBAR (1947) *in* MEDIONI (1971). No recent measured field profile has been made. Thicknesses are indicative and evaluated by comparison with Sidi el Abed.

Oran High Plains, Sidi el Abed Moutains; simplified from MAROK (1996) and from unpublished field observations by ELMI. The log is a composite drawing based on field observations in the following areas, from base to top. Koudiat el Beia (KB): 1, oolitic limestones with three brachiopods beds; 2, cherty limestones; 3, bird eyes limestones. Chebiket en Nmer, Oulad Amor Formation (OA): 1, bioclastic and oolitic limestones with large bivalves ("*Lithiotis*", *Cochlearites*, etc.); 2, cherty limestones with *Gervilleioperna* and brachiopods beds (100, 122, 125, 166, 178); 3, oolitic and oncolitic limestones; 4, black dolomites with frequent channels; 5, *Cochlearites* and Megalodontids limestones beginning with a breccia containing Palaeozoic and Liassic quartzite pebbles. Brachiopod bed at the top. Teniet Sassi: Jebel Nador Formation (JN) and boundary with the overlying High Plateaux Dolomites.

Southern Grouz, Koudiat el Haïddoura and Hassi Diab, composite log, new data by MEKKAOUI, unpublished.

Key to the symbols. Formations. KB, Koudiat el Beia; OA, Oulad Amor; JN, Jebel Nador; HP, High Plateaux and High Plains; BS, Ben Seriane; KH, Koudiat el Haïddoura; OM, Oued Mennat; OAB, Oued el Abiod; HL, Hassi Laâma (Southern Grouz).

Facies. 1, limestones; 2, bioclastic limestones; 3, emersion markers; 4, oolitic limestones (packstones, grainstones); 5, oncolitic limestones; 6, cherty limestones; 7, dolomites; 8, marls ; 9, basalts, dolerites; 10, coarse conglomerates; 11, channels; 12, foresets and oblique stratifications; 13, horizontal laminations; 14, algal mats.

Fossils. a, ammonites; b, brachiopods; c, *Lithiotis* and *Cochlearites*; d, Megalodontids; e, *Perna* s.l.; f, other bivalves; g, corals; h, *Orbitopsella*; i, other foraminiferas; j, reefs and build-ups.

FIG. 16.— Essai de corrélations des séries stratigraphiques du Jurassique inférieur des Hautes Plaines oranaises, des Hauts Plateaux marocains et de la bordure méridionale de l'Atlas de Figuig (partie algérienne du Djebel Grouz). Les corrélations ont été graphiquement calées sur l'apparition des faciès argileux bariolés du Toarcien (base de la Formation du Jebel Nador).

NW des Hauts Plateaux, Jebel Nador au Sud de Debdou. D'après MEDIONI (1971).

NE des Hauts Plateaux, Béni Yala, près de Guefaït. D'après DUBAR (1947) in MEDIONI (1971). En l'absence de levés récents, les épaisseurs sont estimées d'après celles du Sidi el Abed.

Hautes Plaines oranaises, Monts du Sidi el Abed; simplifié d'après MAROK (1996) et des observations inédites de ELMI. La colonne stratigraphique est un résumé synthétique des levés réalisés dans les secteurs suivants (de la base au sommet). Koudiat el Beia (KB) : 1, calcaires oolithiques avec trois niveaux fossilifères à brachiopodes ; 2, calcaires à silex ; 3, calcaires à structures fenestrées. Chebiket en Nmer. Formation des Oulad Amor (OA) : 1, calcaires bioclastiques et oolithiques à grands bivalves ("Lithiotis", Cochlearites, etc.) ; 2, calcaires à silex avec des bancs à Gervilleioperna *et à brachiopodes (100, 122, 125, 166, 178) : 3, calcaires oolithiques et oncolithiques ; 4, dolomites noires avec chenaux fréquents ; 5, calcaires à* Cochlearites *et Megalodontidés commençant par une brèche à galets de quartzites paléozoïques et de calcaires liasiques ; ils se terminent par un banc à brachiopodes. Teniet Sassi : Formation du Jebel Nador (JN) et passage aux Dolomies des Hauts Plateaux.*

Grouz méridional, colonne stratigraphique synthétique de la Koudiat el Haïddoura et de Hassi Diab d'après des levés inédits de MEKKAOUI.

Légende des symboles. Formations. KB, Koudiat el Beia ; OA, Oulad Amor ; JN, Jebel Nador ; HP, High Plateaux and High Plains ; BS, Ben Seriane ; KH, Koudiat el Haïdoura ; OM, Oued Mennat ; OAB, Oued el Abiod ; HL, Hassi Laâma (Grouz méridional).

Faciès. 1, calcaires; 2, calcaires bioclastiques; 3, indices d'émersion; 4, calcaires oolithiques (packstones, grainstones); 5, calcaires oncolithiques; 6, calcaires à silex; 7, dolomies; 8, marnes; 9, basaltes, dolérites; 10, conglomérats grossiers; 11, chenaux; 12, stratifications obliques; 13, laminations horizontales; 14, tapis algaires.

Fossils. a, ammonites ; b, brachiopodes ; c, Lithiotis *et* Cochlearites *; d, Megalodontidés ; e,* Perna *s.l. ; f, autres bivalves ; g, coraux ; h,* Orbitopsella *; i, autres foraminifères ; j, récifs et biocostructions.*

Source : MNHN, Paris

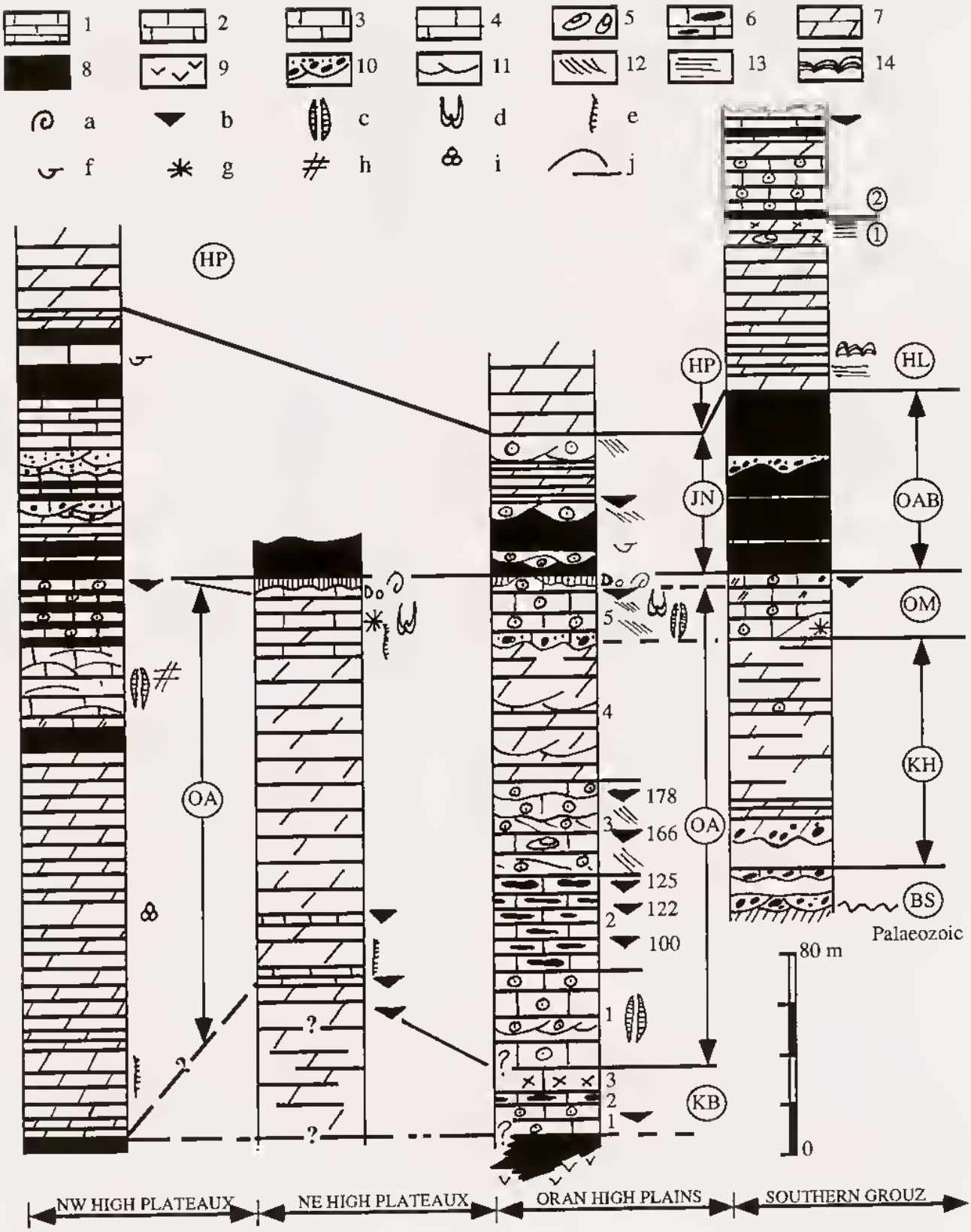

Source: MNHN, Paris

region since the basic works of LUCAS (1942, 1952). The lithostratigraphic nomenclature has been adapted from that of the Moroccan High Plateaux (south of Debdou and Tendrara area; MEDIONI, 1971: NEHNAHI, 1996) and has been also compared with the north east part of this region (Béni Yala near Guefaït, DUBAR, 1947) and with the Atlas-Sahara transition zone, where the successions are very similar (documented by Mekkaoui -new data, see below- along the Algerian southern side of Djebel Grouz).

The oldest Mesozoic beds are clays with gypsum and evaporites, associated with two basaltic (dolerite) flows, separated by thin (few meters) laminated tidal carbonates, which outcrop along faults. These rocks are classically attributed to the Triassic but their upper part may range into the Hettangian. An ostracofauna has been recently described in the lower part of the upper red beds, overlying the last basalt flow (CRASQUIN-SOLEAU *et al.*, 1997) in the near Oujda Mountains.

During the late Sinemurian and the Carixian, carbonate sedimentation developed: inner platform or shallow ramp with brief incursion of the open sea (outer platform) indicated by several brachiopods beds. The lower formation (Koudiat el Beïa Formation; *ca* 25 m) contains a middle cherty level which has yielded *"Rhynchonella" moghrabiensis* (Dubar) and *Tamaromenia arethusa* (Di Stefano) of the upper Sinemurian. Upwards, the Ouled Amor Formation (200 m) is the local representative of the "faciès à grands lamellibranches" (*Lithiotis, Cochlearites, Protodiceras, Opisoma*). A succession of five members has been recorded: 1- lower *Lithiotis* oolitic limestones; 2- cherty limestones with brachiopods collected in three successive levels; 3- oolitic and oncolitic limestones with another brachiopods level; 4- dolomites; 5- finally, *Protodiceras* limestones. These beds have been wrongly attributed to the Toarcian. In fact, the brachiopods can be referred to the lower Pliensbachian. In beds 100-125 (member 2: Fig. 16) occur: *Antacothyris* nov. sp. A, *Hesperithyris ternieri* (Dubar) and its var. *minor* (so-called "térébratules multiplissées"), *Lobothyris subpunctata* (Davidson), *Parathyridina mediterranea* (Canavari) and *Gibbirhynchia curviceps* (Quenstedt). In beds 166 and 178 (member 3: Fig. 16) occur *Hesperithyris* sp. and *H. ternieri* (Dubar). In member 5, small *"Protodiceras"* sp. are associated to *Zeilleria sestii* (Fucini) and *Antacothyris* nov. sp. A. The faunas are linked to repeated deepening episodes (flooding surfaces). Member 5 is overlain by lenticular micritic beds which have yielded very rare Domerian ammonites (*Protogrammoceras celebratum* (Fucini), *Amalthens* sp.) indicating a marked deepening of the sea. These micrites are included in the top of the Oulad Amor Formation, as in the Moroccan High Plateaux (Béni Yala; DUBAR, 1947 *in* MEDIONI, 1971).

The most important stratigraphic feature of the High Plains is the presence of very shallow marine to sabkha facies of the Toarcian (Jebel Nador Formation; 50 m) which extend to the first folds of the Ksour Mountains (Djebel Hafid and Antar). The palaeogeographic limits do not coincide with the geographic and tectonic boundaries. Eastwards, the Jebel Nador Formation has been recorded from the Skouna well, situated on the shore of the Chott ech Chergui (Skouna Clays and Gypsum Formation) (AUGIER, 1967; LUCAS, personal comm.).

Carbonate platform conditions reappear above with the High Plateaux Dolomites (= "Dalle des Hauts Plateaux") consisting of more or less massive dolomites with intercalations of channelized oosparites (total thickness unknown; exposed: *ca* 50 m).

THE KSOUR MOUNTAINS AND THE ATLAS DOMAIN

The Ksour Mountains are part of the folded Saharian Atlas; long and tight anticlines offer good exposures of the Jurassic (BASSOULET, 1973; MEKAHLI, 1995, 1998). It must be stressed that the folded range is larger than the Atlas Jurassic trough. The main stratigraphic characteristics are:

— early installation of the initial carbonate platform, probably as early as the early Hettangian (inside the Chemarikh Dolomites) or, even, the Rhaetian (Tiout Bridge Formation, BASSOULLET, 1971, 1973); at the top, some episodic deepening can be documented by poorly preserved Hettangian (and possibly lowermost Sinemurian) brachiopods and ammonites indicative of the first "maximum floodings" (or, more accurately, main deepenings);

— early deepening with pelagic facies appearing during the early Sinemurian (Semicostatum Zone); in the southern Aïn Ouarka umbilic, BASSOULLET (1973) has shown evidence that the radiolarias occurred as early as this age (lower member of the Aïn Ouarka Pelagic Limestones); in the westernly

Source : MNHN, Paris

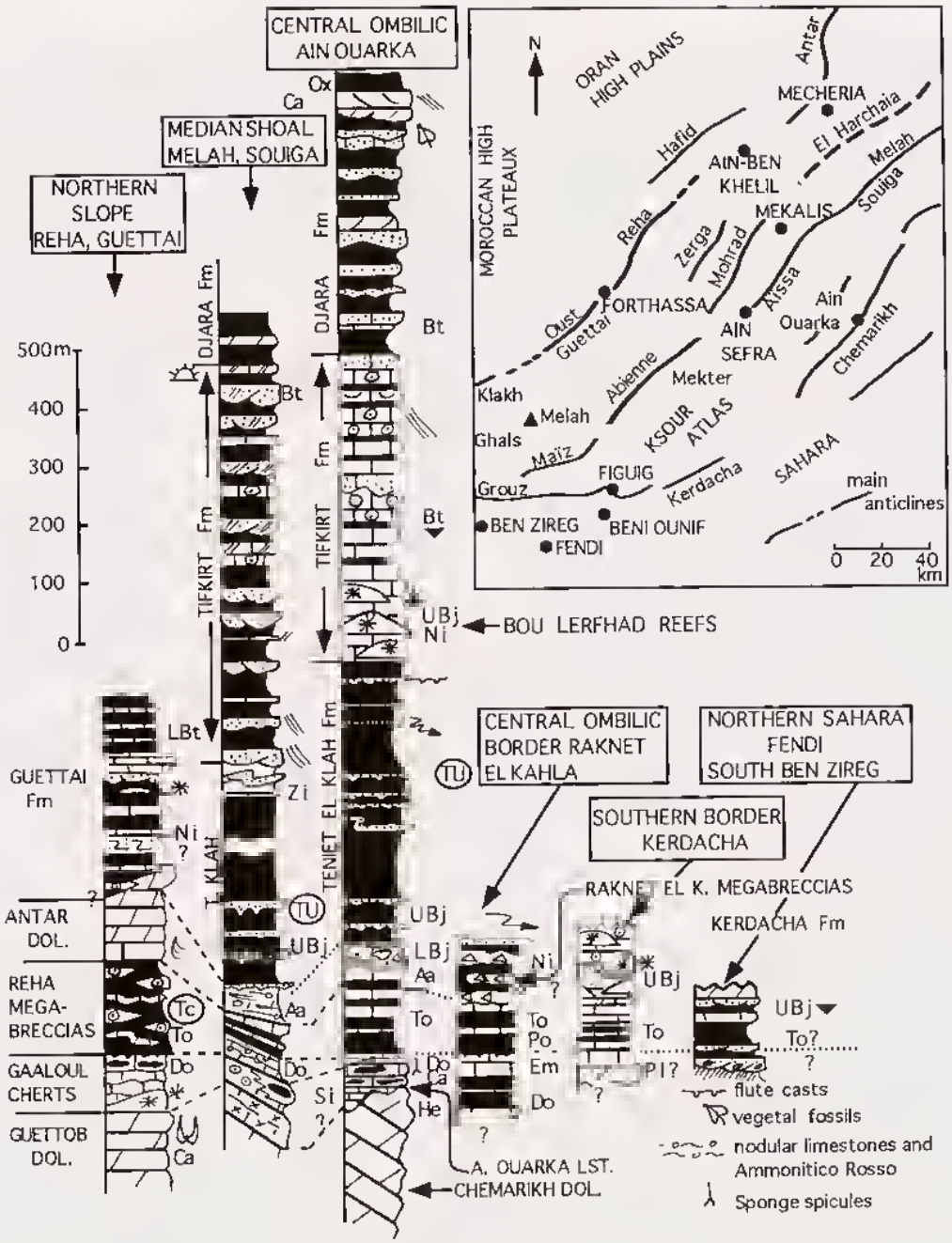

FIG. 17.— Comparison of the stratigraphic profiles through the Saharian Atlas (Ksour Mountains) from the Northeastern marginal folds to the Sahara (South of Ben Zireg, between Bechar and Figuig). Each log is a synthesis of several measured sections. For abbreviations of stages and zones: see tables 1 and 2. For the facies and fossils symbols: see fig. 16; TU, quartzose turbidites; TC, calciturbidites. Remark: the Raknet el Kahla is situated 2 km to the North East from the village of Aïn Ouarka.

FIG. 17.— Comparaison des séries stratigraphiques le long d'un transect dans les Monts des Ksour depuis les plis marginaux du NE jusqu'au Sahara (Coupe de Ben Zireg-Sud entre Béchar et Figuig). Chaque profil est la synthèse de plusieurs coupes. Abréviations des étages et des zones : voir tableaux 1 et 2. Explication des symboles pour les faciès et les fossiles voir fig. 16 ; TU, turbidites quartzeuses ; TC, calciturbidites. Remarque : la Raknet el Kahla se situe à 2 km au NE du village d'Aïn Ouarka.

Source: MNHN, Paris

Figuig umbilic. radiolarias seem to appear slightly later at the beginning of the late Sinemurian (ELMI, 1996c);

— basinal facies ranging up to the beginning of the late Bajocian, when quartzose turbidites were interbedded within basinal marls (Teniet el Klakh Formation);

— quartzose sedimentation became progressively dominant during the late Bajocian; the return to carbonate platform conditions was diachronous and emphasized by the development of build-up reefs at the lower part of theTifkirt Formation while arabian ammonites arrived in the adjacent platforms. This basin to platform inversion occurred during the middle part of the Niortense Zone (Bou Lerfahd near Aïn Ouarka; Djebel Sfissifa; Djebel Guettaï, for instance) with the exception of the Median Shoal (Souiga-Melah) and of the neighbouring El Harchaïa anticline where siliciclastic turbidites and/or calciturbidites persisted until the end of the early Bathonian.

— no carbonate platform during the Late Jurassic; the area is invaded by the deltaic and prodeltaic sediments of the Ksour Sandstones Group (BASSOULLET, 1973; DELFAUD, 1975; ELMI, 1978).

From the North to the South, the Ksour are composed of several zones characterized by their different sedimentary and geodynamic history as documented by the comparison of the synthetic profiles summarized on Fig. 17.

FIG. 18.— Jurassic outcrops of the Atlas Domain of South West Algeria and South East Morocco.

a, Marly ammonitico rosso. Local facies of the Melah Formation. Aalenian-lower Bajocian. Aïn Beida, Eastern slope of Djebel el Melah (Naâma W.). Coll. ELMI, 89DZ158.

b. Lower surface of a turbiditic sandstone bed, bearing flute casts and ammonites (*Leptosphinctes* sp.). Base of the Teniet el Klakh Formation (Niortense Zone, upper Bajocian). Same locality as Fig. 18a. Coll. ELMI, 89DZ165.

c. Onlap of the lower Sinemurian Aïn Ouarka Formation (decimetric beds) on the truncated massive strata of the Chemarikh Dolomites Formation (Hettangian). NW slope of Djebel Chemarikh, Aïn Ouarka (Naâma W.). Coll. ELMI 75D24.

d, Raknet el Kahla Megabreccia (brèche n° 5). Vertical dip. Heterometric blocks of platform carbonates are reworked into marls of the same facies than the Teniet el Klakh Formation. One *Ermoceras* has been collected in these reworked elements. The block in the foreground measures more than 1 m. These features illustrate sedimentation occurring at the toe of a scarp. Raknet el Kahla, North East of Aïn Ouarka (Naâma W.). Coll. ELMI, 93DZ799.

e, Megabreccia in the Jebel Haïmeur Blue Cherty Limestones Formation. Pliensbachian. Jebel Haïmeur, North of Figuig (Morocco). Coll. ELMI, 95MA1359.

f, Transgression of the Jurassic on the Saharian Palaeozoic Platform. The lower carbonates can be attributed to the Pliensbachian. The scarp in the background has given a brachiopods fauna dating the upper Bajocian transgression over the Northern Margin of the Western Sahara. Near Meksem Nedjoua, between Fendi and Ben Zireg (Algeria, Bechar W.). Coll. ELMI 83DZ757.

FIG. 18.— Affleurements jurassiques du domaine atlasique d'Algérie du SW et du Maroc du SE.

a, Ammonitico rosso marneux, développé localement dans la Formation du Melah. Aalénien et Bajocien inférieur. Aïn Beida sur la retombée orientale du Djebel Melah. Coll. ELMI, 89DZ158.

b. Flute casts sur la semelle du banc de grès marquant la base de la Formation du Teniet el Klakh. Les turbidites emballent des ammonites (Leptosphinctes *sp.) de la zone à Niortense (Bajocien supérieur). Localité: voir Fig. 18a. Coll. ELMI, 89DZ165*

c, Disposition transgressive des bancs décimétriques de la Formation d'Aïn Ouarka (Sinémurien inférieur) sur les bancs massifs et tronqués par l'érosion de la Formation des Dolomies du Chemarikh (Hettangien). Flanc NW du Djebel Chemarikh, Aïn Ouarka (W. de Naâma). Coll. ELMI, 75D24.

d, Mégabrèche de la Raknet el Kahla (brèche n° 5). Pendage vertical. Des blocs hétérométriques, présentant un faciès de carbonate de plate-forme, sont remaniés dans les marnes et des calcaires argileux de même faciès que ceux de la Formation du Teniet el Klakh. Un Ermoceras *a été récolté dans un des blocs remaniés. Le bloc situé à l'arrière plan mesure plus d'un mètre ; il s'agit d'une sédimentation de pied de pente ou d'escarpement. Raknet el Kahla au NE d'Aïn Ouarka (W. de Naâma). Coll. ELMI, 93DZ799.*

e, Mégabrèche de la Formation des Calcaires bleus à silex du Jebel Haïmeur. Pliensbachien. Flanc SE du Jebel Haïmeur au Nord de Figuig (Maroc). Coll. ELMI, 95MA1359.

f, Transgression jurassique sur la plate-forme saharienne paléozoïque. Les carbonates inférieurs peuvent être attribués au Pliensbachien. Une faune de brachiopodes du Bajocien supérieur a été récoltée sur les reliefs situés à l'arrière plan. Elle date la transgression du Bajocien supérieur sur la marge septentrionale du Sahara occidental. Près de Meksem Nedjoua, entre Fendi et Ben Zireg (Algérie, W. de Béchar). Coll. ELMI 83DZ757.

Source : MNHN, Paris

Source: MNHN, Paris

THE NORTH EAST BORDER

This border, with the Hafid and Antar anticlines, belongs to the palaeogeographic domain of the High Plains (see above). The basal Guettob Moulay Mohamed Carbonates (exposed *ca* 30 m) may be equivalent to the Koudiat el Beia Formation (Sinemurian?). Above, BASSOULLET (1968, 1973) has recorded *Orbitopsella dubari* Hottinger, *Planisepta compressa* (Hottinger) *sensu* SEPTFONTAINE 1984, 1985, quoted as *Labyrinthina recoarensis* (Cati) and abundant *Palaeodasycladus mediterraneus* Pia from the Oulad Amor Formation (35 to 85 m). These can be attributed to the lower Pliensbachian (Carixian) by comparison with similar beds (especially in the Middle Atlas) and by the occurrence of *Hesperithyris reynerii* (Catullo) var. *sinuosa* or *minor* Dubar. The Jebel Nador Formation is represented by thick purple marls, bioclastic limestones and dolomites (60 to 120m). The Middle Jurassic shallow carbonates (Antar Dolomites Formation) and the overlying sandstones are not accurately dated.

THE NORTHERN TRANSITIONAL SLOPE

The Ksour Mountains are limited to the north-west by a trend of anticlines bordering directly the High Plains (Djebel Guettaï, Reha, Guetob Moulay Mohammed). The Lower Jurassic outcrops especially at the top of the Djebel Reha.

It consists of three formations. At the base, the Guetob Moulay Mohamed Carbonates Formation has a thickness of more than 150 m. It begins by a massive Dolomites Member changing upwards onto a Lithiotis Limestones Member, rich in thick shelled bivalves, randomly disposed and containing corals at several levels. They are overlain by the Gaaloul Cherty Formation (95-100 m and 95 m). It consists of grey cherty limestones in decimetric beds separated by thin marls. The surface of the beds are locally covered by varied bioclasts and oolites. These beds document an outer platform environment. Their top is a rubefied hard ground bearing belemnites rostrums, indicating a condensed episode. The age range from the Carixian (*Tropidoceras* sp., in the lower part) to the late Domerian (with *Emaciaticeras* sp. and *Tauromeniceras*) at the top. The main part is dated of the middle Domerian (*Reynesoceras* gr. *inditeuse* (Meneghini), *Prodactylioceras* sp., *Arieticeras* sp.).

Above, the Reha Formation (150 m) is a thick cyclic sequence:

— alternance marls-limestones beginning at the top of the Domerian (*Tauromeniceras* sp.) and ranging onto the early Toarcian (*Paltarpites* sp. and *Dactylioceras (Eodactylites)* gr. *mirabile* Fucini, indicate the lower Mirabile Subzone of the Polymorphum Zone; higher, *Dactylioceras (Orthodactylites)* sp. marks probably the top of the same zone);

— marls bearing a pyritic ammonite fauna of the Bifrons Zone; the Gradata Zone is badly documented at the top by loose ammonites: *Pseudogrammoceras subregale* Pinna and "*Podagrosites*" gr. *aratum* (Buckman) associated with *Alocolytoceras dorcadis* (Meneghini). These marls have been accumulated along a slope, indicating the presence of a narrow oolitic barrier limiting the Atlas open sea from the High Plains sabkha (CORNET *et al.*, 1953; BASSOULLET, 1973; MEKAHLI, 1995). Toarcian marls containing dwarf or miniature ammonites indicate a tendancy to the isolation of the area in a relatively deep marine environment.

This general instability can be compared to similar conditions which are known during the early-middle Toarcian along the northern ridges of the Moroccan Central High Atlas (Talghemt Pass) or along the faults limiting the Figuig Atlas and the Western (Higher) Sahara. This marked Toarcian deepening led to the differenciation of umbilics along the bordering faults. The return to a platform setting was rapid with the deposition of *Zoophycos* limestones, passing vertically and laterally to shallow carbonates (Antar Dolomites Formation). During the late Bajocian, oolitic bodies and reefs prograded from the SW and the west (Guettaï Formation) over alternating marls and neritic limestones yielding the now classical *Ermoceras* fauna (ARKELL & LUCAS, 1953; DU DRESNAY, 1964b; ALMÉRAS *et al.*, 1994; ENAY, 1996).

Source : MNHN, Paris

THE AÏN BEN KHELIL SUBBASIN

This is known from wells (see KAZI-TANI, 1986; AÏT-OUALI, 1991; AÏT-OUALI & DELFAUD, 1995) and Toarcian outcrops (Ras el Guenatis). The Toarcian facies (alternating marls and micritic limestones) seems to indicate that the sea bottom was then less deep than at the top of the Reha slope. This is consistent with the data given by the ammonites *(Furloceras* of the Gradata Zone which have been previously misidentified as Boulceiceratids; AÏT-OUALI, 1991) which have a "normal" size. The area was not invaded by the Bajocian reefs and the deposition of siliciclastic turbidites continued until the early Bathonian, particularily in the famed locality of El Harchaïa (FLAMAND, 1911) where the alternating sandstones-marls is rhythmically interrupted by allodapic oolites and by bioclastic limestones (ELMI & ALMÉRAS, 1985), rich in ammonites, brachiopods and bivalves. It is the type locality of *Oraniceras hamyanense* Flamand (see also Fig. 11b). The abundance of *Ctenostreon* (= *Lima*) *palati* Flamand is noteworthy (BASSOULLET, 1973). These beds can be considered as a marginal facies of the Teniet el Klakh Formation.

THE MELAH -SOUIGA (OR MEKALIS) MEDIAN SHOAL

The initial platform carbonates (Souiga Dolomites Formation) indicate a tidal to intertidal dominated environment. However, their upper part is more calcareous and it yields a rich rhynchonellids fauna, similar to that of the Ouarsenis where it has been collected below *Tropidoceras* (BENHAMOU, 1996). It is associated with *Zeilleria hierlazica* (Oppel) which appeared only during the Sinemurian. Above, calcareous red nodular or pseudonodular (bioturbated) limestones occur (calcareous ammonitico rosso) at the base of the Domerian Aouinet es Siah Formation. The upper part of the formation consists of cherty limestones. The Toarcian is represented by the marl-dominated lower part of the Aïn Beida Formation overlain by the Aalenian *Zoophycos* limestones (Djebel Souiga) passing into a marly ammonitico rosso (Melah) (Fig. 18a).

The dynamic role of this region seems to have changed during the Aalenian-Bathonian: there are no Bajocian carbonate platform nor reef. Distal turbidites occurred during the early Bathonian; they are associated with slumps and brachiopods-rich limestones (top of the Teniet el Klakh Formation which is younger than in the Guettaï (to the north) and in the Aïn Ouarka (to the south) areas). In the Aïn Beida section of Djebel Melah, the Teniet el Klah Formation begins with a turbiditic bed showing flute-casts and containing rare ammonites *(Leptosphinctes)* of the upper Bajocian (Fig. 18h). Channelized sandstones have appeared after the early Bathonian (BENHAMOU & ELMI, unpublished). Note that the limit between the Teniet el Klakh Formation and the Tifkirt Formation is now placed under the first channelized sandstones instead of being defined on biostratigraphic data (BASSOULLET, 1973; ELMI, 1978). The type locality of these two formations is situated across the pass separating the Djebel Souiga and the Djebel Tifkirt.

THE AÏN OUARKA SUBBASIN OR CENTRAL UMBLIC

This was the most strongly subsiding area of the Ksour where the thickness of the sedimentary accumulation depended largely on pull apart dynamics up to the late Bajocian (BASSOULLET, 1973; MEKAHLI, 1995, 1998; MEKAHLI & ELMI, 1997). The Jurassic succession begins with the initial platform carbonates of the Chemarikh Dolomites Formation documenting a shallow protected subtidal environment, with indication of a reef-barrier (AÏT-OUALI, 1991). Near the top, some brachiopods including *Zeilleria perforata* (Piette) (= *Terebratula psilonoti* Quenstedt) indicate the first open sea influences. They occur under the first occurrence of an ammonite (MEKAHLI, 1995). It is a poorly preserved but significant specimen belonging probably to the subgenus *Caloceras* (Fig. 11c) and suggesting that a seaway has been temporarily open through the eastern Atlas Ranges. It also indicates that the first important Jurassic deepening took place as early as the early Hettangian.

Source: MNHN, Paris

The Chemarikh Dolomites were tilted and eroded before the onlap of the following Aïn Ouarka Pelagic Limestones. These limestones consist of pelagic micrites bearing radiolarias and *Diotis*. Their deposition began during the early Sinemurian. On the north west side of Djebel Chemarikh, this relatively thick unit (120 to 160 m) shows a succession of seven members (A to G) (Table 3).

Member A

Deep platform limestones onlapping the truncated Chemarikh Dolomites. They consist in micrites with silty quartz, scarce bioclasts and foraminifera, including Nodosariids and *Involutina liassica* Jones (BASSOULLET, 1973: 147, 431-433), an association commonly found in basinal or slope facies. The composition of the ammonite fauna, discovered by BASSOULLET (1966, 1973) indicates that it may be correlated with the Semicostatum Zone. This has been completed by recent field sampling: *Arnioceras geometricum* (Oppel), *A. miserabile* Fucini, *A.* cf. *speciosum* Fucini, *A.* cf. *flavum* Buckman. This fauna may range into the Turneri Zone and globally it can be compared with the Rejectum interval, defined by DOMMERGUES *et al.* (1994) in the Central Apennines and EL HARTRI *et al.* (1996: Fig. 15) in the High Atlas of Béni Mellal. The Chemarikh data (Central Aïn Ouarka Umbilic on Fig. 17) allow a better definition of the biostratigraphic range of this interval (or "horizon"). It does not range up into the upper Sinemurian since it is overlain by *Asteroceras* -bearing limestones.

Member B

Wavy bedded, grumelous and bioturbated limestones, irregularily coloured pink (1-3 m, disappearing toward the north east, near the crest of the palaeorelief; KAZI-TANI, 1986; AÏT-OUALI, 1991). It has yielded a rich fauna of the Obtusum Zone with large and well preserved *Asteroceras* which are figured here because of their exceptional interest, not only for the Maghreb but for all the Tethyan realm. They bear a strong affinity with the lombardian fauna illustrated by PARONA (1896): *Asteroceras stellare* (Sowerby) *in* PARONA (Fig. 21a), *A.* cf. and aff. *confusum* Spath (Figs 19b, 20), *A. meridionale* Dommergues, Meister & Mettraux (Fig. 21b, c), *A. varians* Parona, *A. margarita* Parona (which can be slightly younger than the rest of the fauna) (Fig. 22a), *Arnioceras* cf. *arnouldi* (DUMORTIER). *Epophioceras* sp. (cf. *E.* sp. *in* DOMMERGUES *et al.*, 1994: Pl. 3, Fig. 1) comes from the nearby locality of M'zimer on the South East edge of the Djebel Chemarikh. The *Asteroceras* beds are overlain by 5 m of suhlithographic limestones containing *Gleviceras* gr. *doris* (Reynès) (Fig. 22b) (Oxynotum Zone). They may rest directly on the truncated Chemarik Dolomites (Fig. 18c).

Member C

Radiolarias rich cherty limestones. Ammonites become rare but several levels of the Raricostatum Zone are present:

— a lower level with *Plesechioceras* cf. *delicatum* (Buckman) (Fig. 22c) and badly preserved Oxynoticeratids;

— a level with Schlotheimiids: *Angulaticeras* gr. *dumortieri* (Fucini);

— an upper level with *Paltechioceras* nov. sp. (showing a relatively narrow umbilicus for the genus and straight ribbing; it is close to *P. boehmi in* PALLINI (1986: pl.1, fig. 2) *non* Hug).

Member D

Wavy bedded limestones and marls. The upper part is a coquina with thin-shelled bivalves (*"Diotis" jamis* Meneghini; BASSOULLET, 1973: Pl. 5, Fig. 2). Small ammonites: *Galaticeras* cf. *aegoceroides* (Gemmellaro) of the Carixian.

Member E

The marls become progressively frequent. The Demonense Zone (Carixian) is documented by the appearance of *Tropidoceras calliplocum* (Gemmellaro). The late Carixian (corresponding to the Davoei Zone) is known near the top where the *Protogrammoceras* appears with *P.* gr. *dilectum-psendodilectum* (Fucini) and *P.* gr. *volubile-pantanelli* (Fucini).

Source : MNHN, Paris

FIG. 19.— Jurassic ammonites of the Rhar Roubane and Ksour Mountains (respectively Tlemcen and Naâma Wilayate, Algeria).

a, *Hammatoceras roubaneuse* Elmi nov.sp. Topotype. Same locality and bed as Fig.11c-d. Coll. Elmi, Univ. Lyon, n° 299802 ; x 1.

b, *Asteroceras* aff. *confusum* Spath. Upper Sinemurian, Obtusum Zone. *Asteroceras* beds, member B of the Aïn Ouarka Formation. NW slope of Djebel Chemarikh, Aïn Ouarka near Aïn Sefra, Ksour Mountains. Coll. ELMI, Univ. Lyon, n° 299661 ; x 0.6.

FIG. 19.— Ammonites jurassiques des Monts de Rhar Roubane et des Ksour (respectivement Wilayate de Tlemcen et de Naâma, Algérie).

a, Hammatoceras roubanense *Elmi nov. sp. Topotype. Même localité et niveau que sur la Fig. 11c-d. Coll. ELMI, Univ. Lyon, n° 299802 ; x 1.*

b, Asteroceras *aff.* confusum *Spath. Sinémurien supérieur, zone à Obtusum. Bancs à* Asteroceras, *membre B de la Formation d'Aïn Ouarka. Flanc NW du Djebel Chemarikh, Aïn Ouarka près d'Aïn Sefra, Monts des Ksour. Coll. ELMI, Univ. Lyon, n° 299661 ; x 0.6.*

Source: MNHN, Paris

FIG. 20.— *Asteroceras* cf. *confusum* Spath. Upper Sinemurian, Obtusum Zone. *Asteroceras* beds, member B of the Aïn Ouarka Formation. Locality: see Fig. 19b. Coll. ELMI, Univ. Lyon, n° 299662; x 0.6.

FIG. 20.— Asteroceras *cf.* confusum *Spath. Sinémurien supérieur, zone à Obtusum. Bancs à* Asteroceras, *membre B de la Formation d'Aïn Ouarka. Localité : voir Fig. 19b. Coll. ELMI, Univ. Lyon, n° 299662 ; x 0.6.*

Source : MNHN, Paris

FIG. 21.— Sinemurian ammonites of the NW slope of Djebel Chemarikh, Aïn Ouarka near Aïn Sefra (Ksour Mountain, Algeria).

a, *Asteroceras stellare* (Sowerby) *in* Parona. Locality and bed: see Fig. 19b. Coll. ELMI, Univ. Lyon, n° 299664.

b, *Asteroceras* aff. *meridionale* Dommergues *et al.* Locality and bed: see Fig. 19b. Coll. MEKAHLI, Univ. Lyon, n° 299666.

c, *Asteroceras* aff. *meridionale* Dommergues *et al.* Locality and bed: see Fig. 19b. Coll. MEKAHLI, Univ. Lyon, n° 299665; x 0.6.

FIG. 21.— Ammonites sinémuriennes du flanc NW du Djebel Chemarikh, Aïn Ouarka près de Aïn Sefra (Monts des Ksour, Algérie).

a, Asteroceras stellare *(Sowerby)* in *Parona. Localité et niveau : voir Fig. 19b. Coll. ELMI, Univ. Lyon, n° 299664.*

b, Asteroceras *aff.* meridionale *Dommergues* et al. *Localité et niveau : voir Fig. 19b. Coll. MEKAHLI, Univ. Lyon, n° 299666.*

c, Asteroceras *aff.* meridionale *Dommergues* et al. *Localité et niveau : voir Fig. 19b. Coll. MEKAHLI, Univ. Lyon, n° 299665 ; x 0.6.*

Source : MNHN, Paris

Member F

Ammonitico rosso (micritic pink limestones in decimetric beds separated by thin marly layers). It contains a rich fauna of the Celebratum and Algovianum Zones with abundant large macroconch *Reynesoceras* (including *Aveyroniceras*).

Member G

Green marls and limestones, stacked into a upward stratodecreasing sequence. They begin in the Algovianum Zone and the top is dated to the Emaciatum Zone. One specimen of *Pleuroceras solare* (Phillips) has been collected. This is the first occurrence of this northern ammonite known at the toe of the Saharian margin (Fig. 11f). To the north-east (Raknet el Kahla), the facies changes to micritic limestones containing several levels rich in *Tauromeniceras* (Elisa Subzone).

Upward, the Aïn Rhezala Formation is a thick marl-dominated unit, changing to micritic limestones at the top. All the Toarcian zones have been evidenced. The lower Gemma Subzone of the Gradata zone is particularily fossiliferous. The succession of the first *Pseudogrammoceras* is well illustrated. *P. subregale* Pinna and *P. pinnai* Rivas are abundant in the Alticarinatus Subzone (upper Gradata Zone). On the other hand, the micritic limestones of the Aalenian and of the lower Bajocian, interrupted by some inputs of reworked material (oolites and lenticular breccias) (Raknet el Kahla Megabreccias), have yielded only a few ammonites: *Leioceras (Cypholioceras)* cf. *comptum* (Reinecke) (Opalinum Zone, Bifidatum = Comptum Subzone), *Staufenia (=Ancolioceras) opalinoides* (Mayer) (Murchisonae Zone, Haugi = Opalinoides Subzone), *Ludwigella* cf. *arcitenens* (Buckman) and *Euaptetoceras* sp. (Concavum Zone). Calciturbidites, slumping and megabreccias become frequent.

Siliciclastic turbidites were widespread at the beginning of the Niortense Zone (upper Bajocian) and the first sandstones mark the beginning of the Teniet el Klakh Formation which documents a particularity high subsideuce ratio (thickness up to 300 m for the lower part of the zone). A rapid and clear shallowing occurred at the end of this zone, preceeding the progradation of the Bou Lerfahd Reefs and Limestones within the neritic limestones, marls and sandstones of the Tifkirt Formation which begins, here, at the top of the Niortense Zone and ranges up to the early Bathonian. This evolution suggests a tectouic interruption of the basinal conditions leading to progradation of the carbonate and siliciclastic platforms (final or senile homogeneization stage). This dynamic inversion from a general deepening to a shallowing regime is interrupted by oscillatory parasequences. This inversion seems due to a major tectonic event (ELMI, 1978) with change from the umbilic (extension) stage to the depocenter (sag) stage; after this event the sedimentatiou rate kept pace with subsidence even when this latter was enhanced by more global controls (eustacy).

Tectonically controlled slopes arc evident from the existence of the Raknet el Kahla Megabreccias which have been deposited diachronously from the early Aalenian to the early Niortense Zone. They are transitional to the Saharian border but some are transverse to the general trend. Thus a south-western

---

FIG. 22.— Sinemurian ammonites of the NW slope of Djebel Chemarikh (continued).

a, *Asteroceras margarita* Parona. Upper Sinemurian, Obtusum Zone. Top of the *Asteroceras* beds. Aïn Ouarka Formation (Member B). Locality: see Fig.19b. Coll. ELMI, Univ. Lyon, n° 299663.

b, *Gleviceras* gr. *doris* (Reynés). Upper Sinemurian, Oxynotum Zone. Aïn Ouarka Formation, member B, above the *Asteroceras* beds. Locality: see Fig. 19b. Coll. MEKAHLI, Univ. Lyon, n° 299803.

c, *Plesechioceras* cf. *delicatum* (Buckman). Upper Sinemurian, lower Raricostatum Zone. Member C, Aïn Ouarka Formation. Locality: see Fig. 19b. Coll. BASSOULLET, Univ. Poitiers; x 1.

FIG. 22.— Ammonites sinémuriennes du flanc NW du Djebel Chemarikh (suite).

a, Asteroceras margarita *Parona. Sinémurien supérieur, zone à Obtusum. Sommet des bancs à* Asteroceras. *Formation d'Aïn Ouarka (Membre B). Localité: voir Fig. 19b. Coll. ELMI, Univ. Lyon, n° 299663.*

b, Gleviceras *gr.* doris *(Reynés). Sinémurien supérieur, zone à Oxynotum. Formation d'Aïn Ouarka, membre B au-dessus des bancs à* Asteroceras. *Localité : voir Fig.19b. Coll. MEKAHLI, Univ. Lyon, n° 299803.*

c, Plesechioceras *cf.* delicatum *(Buckman). Sinémurien supérieur, partie inférieure de la zone à Raricostatum. Formation d'Aïn Ouarka, membre C. Localité: voir Fig. 19b. Coll. BASSOULLET, Univ. Poitiers ; x 1.*

Source : MNHN, Paris

Source: MNHN, Paris

sector (Chemarikh), with thicker, deeper and more argillaceous deposits, can be separated from an north-eastern one (Raknet el Kahla) where megabreccias are more frequent and thicker (some blocks exceed 1 m) (Fig. 18d). These megabreccias appear here late as the underlying alternating marls and limestones (Aïn Rhezala Formation) range from the early Toarcian (*Eodactylites)* to the end of the early Bajocian [*Emileia* cf. *brocchi* (Sowerby), *Otoites* cf. *sauzei* (d'Orbigny)]. The lower Toarcian is noteworthy by the presence of a "niveau chocolat" (brown coloured) which is a thin calciturbidite. Similar and coeval beds are known in the Middle Atlas (COLO, 1962) and in the Lusitanian Basin of Portugal (MOUTERDE *et al.*, 1979; WRIGHT & WILSON, 1982; DUARTE, 1994, 1996). The breccias contain limestones (with bioclasts, corals and brachiopods) reworked from the adjacent platforms and, also, resedimented "arabic ammonites" (*Ermoceras)* known to have been restricted to the epineritic shallow platform surrounding the northern Gondwanian Margin.

In conclusion, these data and the progradation of the Bajocian Bou Lerfahd Reefs allow us to interpret that a polygonal tilted block was differentiated along the Djebel Chemarikh in the median part of the Aïn Ouarka Subbasin. It was rising from the SW to the NE and supporting evidence can be found from the sedimentary perturbations shown by the Liassic formations. This block was limited by steep slopes. The present Aïn Ouarka N90 fault and Triassic outcrop underline the northern limit of this palaeostructure.

THE SOUTHERN BORDER (KERDACHA)

To the south of the Aïn Ouarka umbilic, there are no outcrop of the Saharian Jurassic. The transition is known only to the west in the Djebel Kerdacha where the Liassic to Bajocian deposits show evidence of shallow platform conditions. However a ditinct deepening occurred probably during the late Pliensbachian (sponge-spicules) and the Toarcian. The Toarcian history of the Kerdacha evokes that of the coeval ramps known in the Western Rhar Rouhane (Khorchef Beds) and in the Saïda Mountains (Keskess Beds) (ELMI *et al.*, 1985). Southward, a subsiding basin extended onto the Lower Sahara but the environment remained always margino-littoral and sabkhaïc (see BUSSON, 1967).

THE FIGUIG ATLAS

The stratigraphy and the palaeogeographic evolution of this area located along the frontier have not been studied during the last 20 years. An extensive study of so large a region exceeds the scope of this paper. A partial revision and new observations have been made to complete the data necessary to a good representation of the Atlas - Sahara transition in one of the very rare regions where it is well exposed.

The Figuig-Bou Arfa region has previously been united with the more eastern Ksour Mountains (Saharian Atlas) (ROCH, 1950) or to the so-called Eastern High Atlas (DU DRESNAY, 1964a; EL KOCHRI *et al.*, 1997). It is, however, really different in its physiographic, structural and stratigraphic features. The general trend of the Atlas range changes from W-E (to the west) to SW-NE (to the east). The longitudinal W-E trend is also disrupted by transverse north-south trends, resulting in a network of narrow ridges limiting small subsiding umbilics, from 10 to 15 km wide.

This structural pattern is partly inherited from the Trias-Jurassic divergent palaeostresses and palaeomotions which have led to a rift stage (DU DRESNAY, 1975; EL KOCHRI *et al.*, 1997) probably complicated by a detachment fault along the Saharian border as supposed in the Central High Atlas (WARME, 1988; WARME *et al.*, 1988). The steepness of the transition from the Atlas trough to the Saharian platform is well documented between the Southern (Algerian) Djebel Grouz and the slopes and umbilics situated a few kilometers to the north along the political border. The extensional palaeostresses shifted obliquely to the trough from WNW-ESE to NNW-SSE / N-S. It is well documented by abrupt sedimentary and environmental changes.

The present description will deal only with the southern area corresponding to the Figuig Umbilic (ROCH, 1950) which presents a situation similar to those of Béni-Bassia (south of Bou Dahar to the west) and Aïn Ouarka (north east). The major palaeogeographic events and stratigraphic data have been established by DU DRESNAY (1956, 1957a, b, 1958, 1964a). The Figuig umbilic is limited by the Maïz

Source : MNHN, Paris

ridge to the north. To the south, the transition to the Saharian Platform is exposed in the Algerian part of the Djebel Grouz.

FIGUIG SUBBASIN OR UMBILIC

We present a preliminary revision of the previous data on the Jebel Haïmeur (ROCH, 1950; DU DRESNAY, 1963; 1964a; 1966: p. 18, fig. 73; 1988b) (Fig. 23).

Lower Dolomites

They are comparable to the Chemarikh Dolomites Formation of the Saharian Atlas. Thickness: more than 100 m. Rare limestones containing silicified gastropods (Hettangian-lowermost Sinemurian). DU DRESNAY & DUBAR (1963) have cited a fauna coming from limestones preserved from the dolomitization. The ammonite genus *Arnioceras* documents the lower Sinemurian.

"Calcaires bleus du Jebel Haïmeur" Formation (= Jebel Haïmeur Blue Cherty Limestones Formation)

They were informally named by ROCH, 1950; cropping out to 75 m. They begin with onlapping grey micrites rich in radiolarias, sponge-spicules and silt-sized quartz grains. Interbedded greenish marls contain silts and ferruginous and carbonate particles but no microfauna. This indicates a main deepening episode which can be compared to a maximum flooding surface in the sequence stratigraphy nomenclature (Fig. 23). In the canyon situated at the south of the television relay station, the onlapping beds have yielded a pyritic condensed fauna at 2.50 m above their contact with the dolomites. Rare representants of the Obtusum Zone (*"Vermiceras" rothpletzi in* FUCINI, with a whorl section similar to that of *Epophioceras*) are asociated with abundant *Paltechioceras* indicating the higher part of the Raricostatum Zone. DU DRESNAY & DUBAR (1963) have already established the occurrence of *Paltechioceras tardecrescens* (Hauer) in the first beds of the limestones (DU DRESNAY's outcrop 1968). They yield a probably condensed *Plesechioceras* fauna (transgressive interval; stratodecreasing parasequence). Their association indicates probably the presence of the Obtusum zone. These levels are younger than the *Arnioceras* beds of the Ksour Mountains. In consequence, the main deepening (from platform to slope-basin) occurred later in the Figuig umbilic than in the relatively close Aïn Ouarka area. Slightly North of Figuig, we have recently discovered the *Asteroceras* beds (*A. stellare, A.* aff. *confusum)* at the base of the Jebel Haïmeur Formation outcropping on the eastern pericline of Jebel Maïz (near Sidi el Hadj Bahous). They are limited from the underlying Lower Dolomites by lenticular (0 to 1 m) biomicritic and oolitic limestones, yielding badly preserved Schlotheimiids and *Arnioceras.*

Cherty limestones and greyish (base) to greenish (top) marls occur above. The main part consists of three parasequences of alternating marls and cherty limestones, becoming progressively carbonate-dominated (cherty limestones). To the west, the presence of the lowermost Pliensbachian has been supposed by DU DRESNAY & DUBAR (1963; DU DRESNAY's outcrop 2474). We have not been able to find these levels in the eastern part of the Jebel Haïmeur. Microfacies: clayey micrites with abundant radiolarias and sponge-spicules, rare silt-size quartz grains. The marls are strongly bioturbated and contain abundant calcareous and ferruginous particles but no foraminifera. In the uppermost 2 meters, the cherty limestones are interbedded with intrabiomicrite (wackestones-packstones) containing abundant reworked allodapic, badly sorted bioclasts (crinoid ossicles, echinoid radioles, brachiopods) and oolites. Spicules-bearing intraclasts are abundant ("tuberoids"). Radiolarias remain present in the micritic parts. These facies are coherent with an environment situated at the toe of more or less steep slopes. They are related to the deepening of numerous Tethyan basins during the late Sinemurian (Maghreb; Lusitanian Basin of Portugal).

Several microbreccias, conglomerates and megabreccias are spectacular, especially at the approximate position of the limit between the Carixian and the Domerian, as indicated by the occurrence of reworked *Plauisepta compressa* (Hottinger). They are composed of Liassic carbonate pebbles (centimetric to decimetric) embedded in oomicrites. Oolites as well as transported exotic corals are often abundant in a micritic matrix. The main megabreccia (Fig. 18e) can reach a thickness of 4 m. These features illustrate a "mass flow" resedimentation.

Source : MNHN, Paris

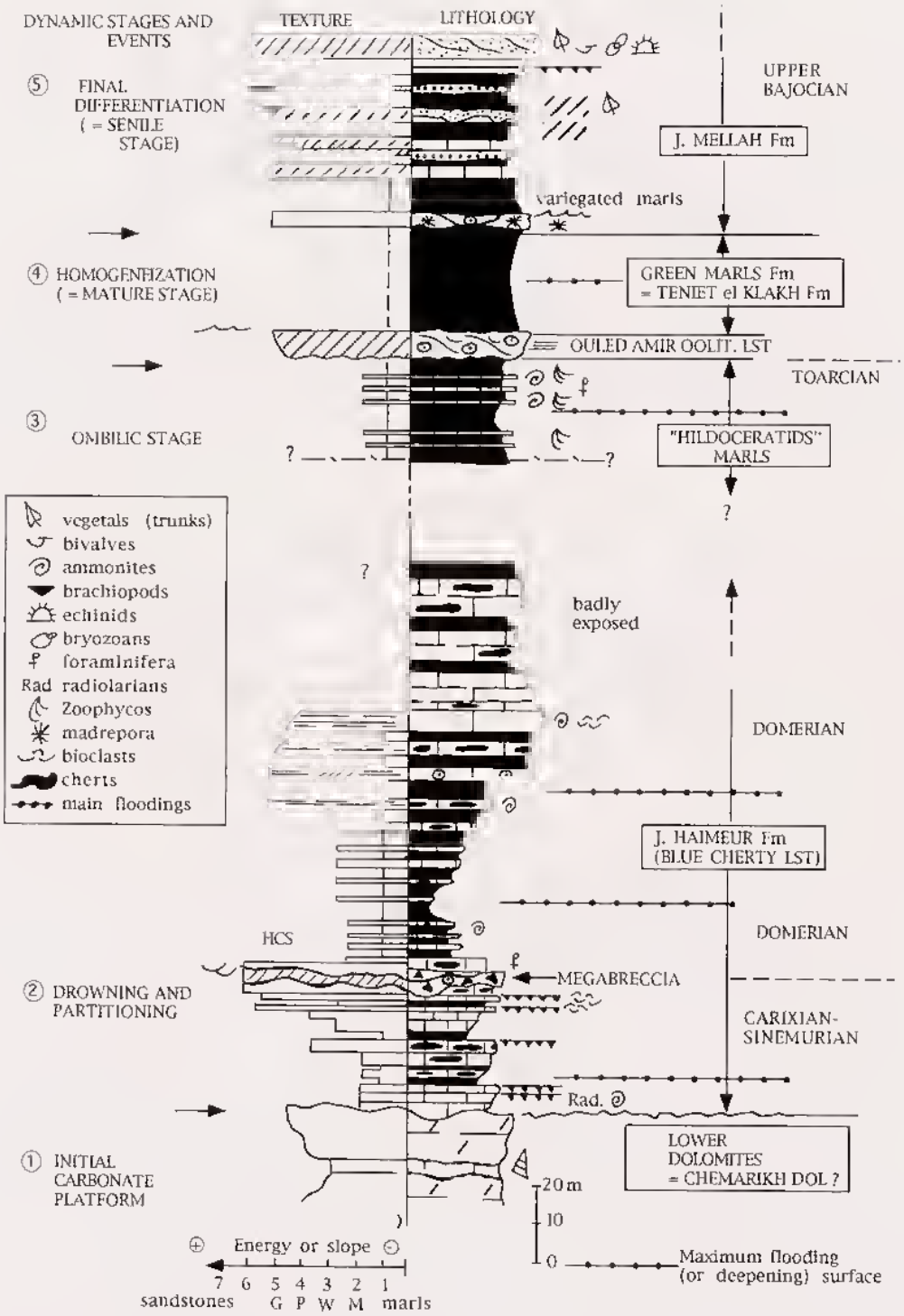

FIG. 23. — Log of the Jurassic of the Figuig umbilic, between Jebel el Haïmeur, Teniel Oulad Amir and El Haitama.

FIG. 23.— Coloune stratigraphique du Jurassique de l'ombilic de Figuig entre le Jebel el Haïmeur, le col de Teniet Oulad Amir et les reliefs d'El Haïtama.

Source : MNHN, Paris

Above, the cherty limestones continue. They are made of elementary thickening-upward sequences of marls and micrites. Cherts are abundant and correspond to the silicification of ancient burrows which may be anastomosed in black layers. Two maximum deepening episodes (so called "maximum flooding surfaces") are indicated by metric levels of greenish marls during the early Domerian with two poorly fossiliferous ammonite levels, the first with *Prodactylioceras* sp., the second with *Protogrammoceras celebratum* (d'Orbigny). Frequent reworked material (bioclasts, oolites) indicate the vicinity of slopes (turbidites, distal tempestites). The environment was unfavourable to benthic microfauna; rare individuals of *Lenticulina* and *Dentalina* have only been recorded. The upper thick greenish marls have yielded foraminiferas indicating a deep platform to basinal environment: *Ammodiscus siliceus* (Terquem), *Lenticulina sublaevis* (Franke) (mg *Saracenaria*), *Lenticulina* sp., *Marginula prima* (d'Orbigny), *Lingulina tenera* (Bornemann), *Dentalina terquemi* (d'Orbigny), *D. obscura* (Terquem).

The last cherty limestones are dated as middle Domerian (Algovianum Zone) by *Arieticeras* sp. They are composed of marly and micritic thickening-up sequences interrupted by bioclastic and ooïdal laminated beds (badly sorted packstones to grainstones with some neogenetic bipyramidal quartz) indicating the proximity of the toe of the slope near the transition to the Sahara Platform.

The upper part of the Jebel Haïmeur Formation is composed of similar cherty limestones with more or less thick marly levels.

Near the northern border of the Figuig umbilic (Mrit-Khouabi outcrops), the Pliensbachian beds become nodular (similar to a marly rosso ammonitico) and disturbed by spectacular slumps (Fig. 24a-b); megabreccias and oolitic allodapic deposits are frequent as described by DU DRESNAY. Some ammonites have been collected. Near the base, *Platypleuroceras* gr. *brevispina* (Sowerby) indicates the Jamesoni Zone. Under the main slump, *Tropidoceras* sp., *Reynesocoeloceras* sp. and Polymorphitids (Demonense Zone) have been collected; several *Protogramiuoceras* sp. and *"Fuciniceras"* sp. indicate the upper Celebratum zone in the ammonitico rosso outcropping on the left side of the river, at the south of the figured outcrop. Palaeocurrent measurements have been made in the prograding redeposited oolitic and bioclastic beds. They indicate that the transport has been multidirectional both from the south and, mainly, from the north (from the nearby Maïz Ridge). The slumps indicate a more general palaeoslope to the NW.

"Marnes à Hildoceratidés" (DU DRESNAY, 1964a, 1975b) (20-25m).

Greenish marls with several decimetric beds of bioclastic limestones. The lower part contains ammonites of the middle Toarcian (Bifrons Zone: *Hildoceras sublevisoni* Fuc., *H. bifrons* (Brug.), *H. angustisiphonatum* Prinz, *H.* gr. *semipolitum* (Buck.); Gradatum Zone: *Crassiceras gradata* (Merla), *Colliuites* sp.), especially on the southern size of the Jebel Maïz (near Aïn Mirid) where red nodular beds (marly rosso-ammonitico) occur. Near the top: more frequent calcareous beds with *Zoophycos* and *Chondrites;* foraminifers are relatively diversified in the upper part (Aalensis Zone): *Lenticulina muensteri* (Roemer), *L. subalata,* (Reuss), *L. d'orbignyi* (Roemer) (mg *Astacolus*), *L. deslongchampsi* (Terquem) (mg *Falsopalmula*), *Dentalina nodigera* (Terquem & Berthelin), *Ammobaculites* sp. The Hidoceratids Marls are onlapping on the underlying beds, especially to the west (Abou el Kehal, for instance; DU DRESNAY, personal communication).

"Ouled Amir oolitic Limestones" (="crêtes du Dogger", DU DRESNAY, 1964a) (5-10m).

The size of the oolites is well sorted (inframillimetric) but their shapes are irregular. They are not contiguous despite the sparitic nature of the matrix. The structure is mainly fibro-radial and the size and nature of the nuclei are varied. The general structure suggests that the oolites have been transported from a nearby southern or south-eastern barrier. The Ouled Amir Formation represents the local facies of the Dalle des Hauts Plateaux and Oued Lâma Formations but in a similar palaeotopographic position to the Tenouchfi Dolomites. The arrival of these prograding oolitic bodies indicates a shallowing which occurred earlier than in the Aïn Ouarka Basin, where, coevally, breccias accumulated at the feet of the bordering slopes.

Green marls (*Posidoniomya ornati* Marls of DU DRESNAY, 1964a).

Outcrops of these are limited and scattered along the Oued el Hallouf Valley and at the North of the Zenaga oasis. They can be tentatively compared to the lower Bajocian Talsiunt Marls of the eastern

Source : MNHN, Paris

High Atlas or to the greenish marls of the turbiditic Teniet el Klakh Formation of the Ksour (base of the upper Bajocian).

"Jebel Mellah Formation" (DU DRESNAY, 1964a).

Shallow platform sequences of marls, bioclastic and oolitic limestones, laminated grainstones and laminated sandstones. The foresets of the sandstones indicate a transport to the NW and to the WNW. This observation is of prime importance as it indicates that the sand body prograded at first to the NW and that the material has been transported to the NE only in a second phase. This must be compared with the data obtained from the Bajocian of the Northern Ksour (near the frontier; Djebel Guettaï, Forthassa; see OUALI-MEHADJI, 1995). The quartzose arrivals began probably in the upper Bajocian but they were mainly Bathonian with the echinid *Bothriopneustes galhanseni* Lambert fauna (DU DRESNAY, 1964a). These deposits indicate that the basin had reached a "senile stage" or flexuration stage; subsidence remained strong but it was compensed by sedimentation (depocenter stage) with a large ratio of shallow water siliciclastics.

FIG. 24.— Slidings and slumpings in the Pliensbachian beds in the middle part of the Figuig umbilic. The pictures are orientated from the SSE (right) to the NNW (left). Between the two main passages of the road through the Oued Mrit (Morocco, Figuig Province). Coll. ELMI, 96MA 3-1 et 7. **a**, Detail of the SSE corner of the outcrop; **b**, General view.

*FIG. 24.— Glissements et slumpings des couches pliensbachiennes dans la partie médiane de l'ombilic de Figuig. Orientation SSE-NWW de la droite à la gauche. Entre les deux grands radiers de la route (Oued Mrit) (Maroc, Province de Figuig). Coll. ELMI, 96MA 3-1 et 7. **a**, Détail de la partie SSE de l'affleurement ; **b**, Vue d'ensemble.*

Source : MNHN, Paris

The Figuig succession is important because it has been accumulated in a highly mobile basin (deepening umbilic until the Toarcian) which recorded the same main Atlasic events as in the west and in the east but the location is nearer to the slopes transitional to the platform which provided a large amount of reworked material. The north-western direction of the palaeocurrents and slope deposits underlines the importance of the transverse, N160 to N030, structures. It suggests that the area has sustained conjugate stresses which may have been caused by transtensional movements. The final change to a subsiding but shallowing platform (depocenter stage) occurred earlier than in the adjacent areas. All these features suggest strong local tectonic control. It is here interpreted that these conditions occurred in a kind of pull-apart structure located on the area where the general trend of the Atlas changes.

THE TRANSITION TO THE SAHARA (KOUDIAT EL HAÏDDOURA AND GUENNAFID CLIFFS ALONG THE SOUTHERN GROUZ ATLAS MOUNTAINS)

Measured sections have been surveyed along the frontier (MEKKAOUI, BENHAMOU, MEKAHLI, unpublished, new data) in the southern (Algerian) side of the Jebel Grouz between Mourhal (=Moughel) and Koudiat el Haïddoura (Fig. 17). They are briefly described here because the discovery of several brachiopods studied by ALMÉRAS, indicates close similarities with the High Plateaux of eastern Morocco and with the Oran High Plains.

The Mesozoic deposits begin with the Ben Serhane Conglomerate (thickness: 6 to 65 m) which is transgressive and discordant on the Visean or the Precambrian. It can be tentatively attributed to the lower Liassic (Hettangian-Sinemurian) or even to the Triassic. It extends southward to Fendi where it has been attributed to the so-called "Permo-Trias" on geological maps without conclusive evidence.

The Koudiat el Haïddoura Formation (mean thickness: 120 m) is the local facies of the "calcaires à grands lamellibranches" (*Protodiceras*, *Cochlearites*,....). The formation begins with micritic limestones interrupted by a synsedimentary dolomitic breccia. Upward the usual facies of shallow carbonate platform are well developed: oolitic limestones, birds eyes, laminites (stromatolitic?). The age of these beds has long been questionned. It is here presumed to be early Pliensbachian; regionally, their upward limit cannot exceed the earliest Domerian (base of the Celebratum Zone). This is consistent with the new data collected in the Oran High Plains (see above).

The late Pliensbachian (Domerian) is represented by the bioclastic limestones of the Oued Mennat Formation (25 m) which are dated here for the first time by brachiopods (*Liospiriferina praerostrata* (Flamand) and *Zeilleria sarthacensis* (d'Orbigny)). Some small corals build-ups occur. Oolites and oncolites appear in the upper part of the formation, which is capped by a hard-ground.

The overlying Oued el Abiod Formation (50 m) begins with red silty or sandy clays, changing upward to stromatolitic laminated dolomites and to evaporitic (gypsum) marls. This formation can be attributed to the Toarcian and it is equivalent to the Jebel Nador Formation of the Moroccan High Plateaux and the Algerian Sidi el Abed. These new correlations are of great geodynamic value because they indicate that the southern borders of the Atlasic furrows sustained a relative uplift during the Toarcian while a major deepening occurred coevally in the basins and in the umbilics.

The overlying limestones and dolomites (30 m) (Hassi Laâma Formation) have yielded some brachiopods (*Burmirhynchia termierae* Rousselle dated as Humphriesianum to Niortense Zones). These beds can be compared with the "Dalle des Hauts Plateaux" (Aalenian-early Bajocian). The limestones are bioclastic and oolitic.

Southward, the Toarcian evaporitic beds are known south of the Ben Zireg Shoal in the Fendi area where the Dogger carbonates have recorded a marked deepening and flooding episode. Jurassic rocks disappear rapidly to the south, on the Sahara Platform (Figs 17, 18f).

Source : MNHN, Paris

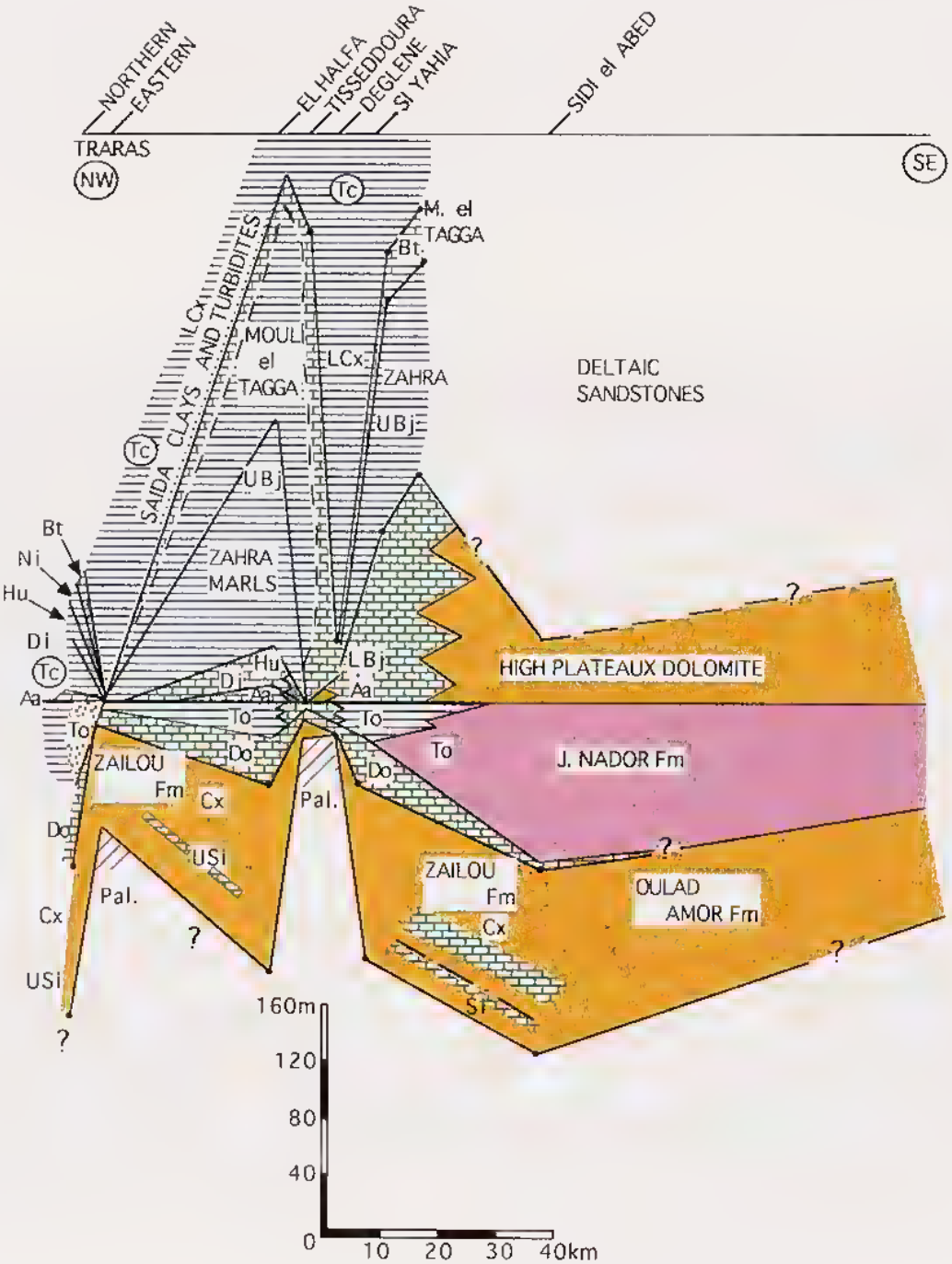

Source : MNHN, Paris

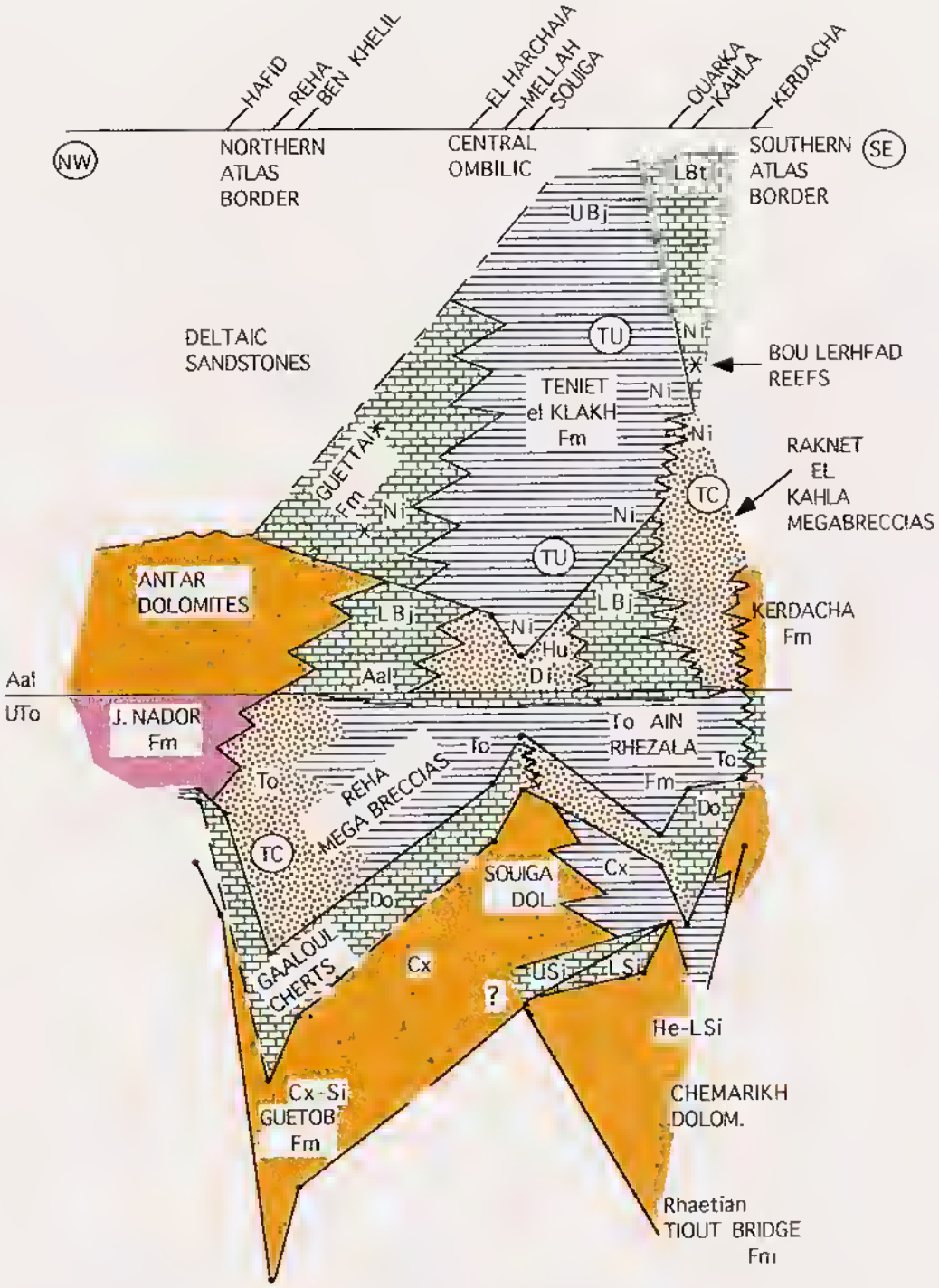

FIG. 25.— Changes in facies and in thicknesses of the Lower and Middle Jurassic deposits along a North-South transect from the Mediterrancan (Traras Mountains) to the Sahara. Key for colours and symbols: see Tables 3 and 4. TU: siliciclastic turbidites; TC: calciturbidites.

FIG. 25.— Variations des faciès et des épaisseurs des dépôts du Jurassique inférieur et moyen le long d'un transect Nord-Sud de la Méditerranée (Monts des Traras) au Sahara. Explication des couleurs et des figurés : voir Tableaux 3 et 4. TU : turbidites silicoclastiques. TC : calciturbidites.

Source : MNHN, Paris

THE MAIN PALAEOGEOGRAPHIC AND PALAEOSTRUCTURAL EVENTS

CHRONOLOGY AND EVENT STRATIGRAPHY

A general diagram of the variations in thicknesses and facies is given on Fig. 25 along a NW-SE transect from the Traras, near the Mediterranean Sea, to the Sahara margin, along the Algerian side of the border.

In western Algeria, the Jurassic history of the Alpine Foreland can be summarized as a great sedimentary (transgressive-regressive) cycle from the early partitioning between shoals and basins differentiated along the Northern Gondwana margin until the final extension of the late carbonate platform and of the atlasic delta. The succession of the different stages has been clearly described and accurately dated.

The early development of the initial carbonate platform occurs from the Rhaetian to the early Hettangian in the future troughs. The first arrival of rare ammonites happened during the late Planorbis Zone in the most subsident area. This is the first occurrence of an ammonite in the Atlasic NW Maghreb. Several citations of Hettangian ammonites in the old papers have not been confirmed in the Atlas Domain. This discovery suggests that a seaway was temporarily open to the NE through the Eastern Atlas Ranges. It also indicates that the first important Jurassic opening took place as early as the early Hettangian and that it was linked with the westward progression of the Tethys. As Hettangian ammonites are known in the Rif (GRIFFON & MOUTERDE, 1964) and in the Kabylia (MOUTERDE *et al.*, 1998), it may be supposed that there were two main seaways opening from the east to the west. The southern one has been stopped by the Tamlelt shoal which limits the eastern High Atlas from the Figuig Atlas.

As the Chemarikh Dolomites are eroded before the Semicostatum Zone deepening (early Sinemurian), it seems that a major relative sea level fall occurred at the end of the Hettangian or at the beginning of the Sinemurian.

Several levels yield poorly preserved brachiopods which may indicate short and badly documented sea-level rises during the rest of the Hettangian.

The pre-Semicostatum unconformity resulted probably from several and telescoped changes in relative sea level, some of them related to local tectonic stresses.

During the Semicostatum and Turneri Zones (early Sinemurian), a deepening-transgressive episode occurred in the differentiating Atlasic umbilics. The deepening continued during the late Sinemurian in the subsiding axes (furrows and umbilics), associated with poorly dated local transgressions. In the intermediate zones between troughs and platforms, the initial carbonates are capped by brachiopods-bearing limestones indicating a late Sinemurian event, which is, until now badly dated. These late Sinemurian events are better documented in the Moroccan High Atlas by the widespread occurrence of the *Plesechioceras* fauna (DU DRESNAY & DUBAR, 1963; see also DUBAR, 1962).

A major transgression occurred during the earliest Pliensbachian (early Carixian-Demonense event) as the result of a regionaly enhanced general sea level-rise. Ammonites arrived in previously flooded regions coevally with the transgression of shallow carbonate platforms on continent or sabkhas. During this deepening-flooding episode, the marker facies of thick shelled bivalves limestones (so called "*Lithiotis* and Megalodontids limestones" or "calcaires à grands lamellibranches") was at its climax. This fauna is well known in the Maghreb where it has been cited for the first time by DUBAR (1932). It has been attributed to the Domerian (DUBAR, 1948) and the majority of the following authors have considered that it would be marker of this "substage". However, in the Bou Dahar, some of these bioaccumulations are interbedded in middle Carixian limestones. A fragment of *Tropidoceras* has been sampled in this situation near Ksar Moghal (east part of Bou Dahar, AMHOUD *et al.*, 1997). In the same area (Kheneg-Grou), DUBAR & MOUTERDE (1978, locality 15) have quoted the occurrence of *T.* cf.

Source : MNHN, Paris

calliplocum (Gemmellaro) in pink limestones deposited at the foot of the eastern slope of the reef (DU DRESNAY, pers. comm.). These beds range from the Ibex zone up to the early Domerian (Celebratum zone). Slightly North of Kheneg Grou, DUBAR & MOUTERDE (1978, locality 18) have also quoted a rich fauna of the Ibex Zone in similar pink limestones which are transitional to the basin and equivalent to the Megalodontids limestones.

Renewed deepening occurred near the end of the early Domerian (final Celebratum Subzone of the Celebratum Zone).

During the Elisa Subzone (latest Domerian) and Polymorphum Zone (earliest Toarcian) telescoped, opposed or enhanced local and global events led to an exaggeration of the differences between shoals, slopes and basins. The result was a large range of reduced to thick beds and a wide distribution of slope deposits and fissures (Sekika; Bou Dahar, DUBAR, 1950).

A peak of deepening occurred during the end of the early Toarcian and the beginning of the middle Toarcian (Levisoni Zone and, mainly, Sublevisoni Subzone; see legend of Fig. 13c) but it did not coincid everywhere with real transgression because of local tectonic uplift. The bottom of the umbilics was deepening in the meantime whereas the borders remained stable or, even, emergent. Subsequently, shallowing-up and filling-up sequences followed. The Gemma Subzone event occurred as a condensed bed indicating a relative deepening. A clear regressive trend appeared near the end of the Toarcian (pre-Meneghinii unconformity). It is documented by the inversion to carbonate dominated sediment production.

Condensed beds were frequent during the Opalinum Zone (early Aalenian). They document both a global transgressive regime and a global change in sediment production. Hard-grounds, erosion surfaces, rapid vertical changes from shallow stromatolitic beds (Fig. 13d-e) to relatively deep ammonites-rich, ferruginous or phosphatic layers and to *Zoophycos* hemipelagic limestones are spectacular, especially in the Tlemcen Domain and along the borders of the Atlas.

This highly perturbed regime continued until the end of the early Bajocian. The consequences differ greatly from an area to an another. The climax of these perturbations appears to have happened through the Aalenian-Bajocian boundary, but continued until the late Bajocian in some areas (Rhar Roubane horst for instance) or even later (to the end of the Bathonian on the shoals of the Traras Mountains). In the basins of Western Algeria, a strong deepening occurred at the beginning of the late Bajocian (Niortense Zone) with the accumulation of thick marls (Zahra Marls Formation) in the Tlemcen Domain. These are interbedded with siliciclastic turbidites in the Ksour (Teniet el Klakh Formation). In the deep and narrow umbilics of the Traras, the deepening happened earlier (early Bajocian), with calcareous turbidites (Fenakech Formation) and marls (Aïn Killoun Formation) . During the late Bajocian, the Saharian Atlas (Ksour) sustained a decoupling between the shallowing borders (progradation of the reef) and the still deepening umbilics. In the meantime, the Moroccan Atlas had reached their "senile" stage with shallowing depocentres succeeding the deepening umbilics (Jebel Mellah Formation of the Figuig Atlas, for instance). In the High and Middle Atlas, these events are diachronous by comparison with the Ksour. A peak deepening is obvious during the Humphriesianum Zone, following a Sauzei Zone unconformity indicated by condensation, erosion and reworking (BENSHILI, 1989; FEDAN, 1989; SADKI, 1996).

Transgression and deepening resumed in the north during the early Bathonian: hemipelagic marls and limestones, often silty, accumulated in the basins (Moul el Tâgga Formation of Rhar Roubane; Sekika Marls of the Traras) changing laterally to ferruginous oolitic limestones (Déglène Oolitic Ironstone) or to condensed beds.

The middle Bathonian was a time of general shallowing illustrated either by thick neritic accumulations interbedded with prograding sandstones (Tifkirt Formation) of the Ksour, or by ferruginous limestones (top of the Déglène Oolitic Ironstone).

A general sedimentary gap of the upper Bathonian is well documented in the Tlemcen Domain (ELMI, 1971a, b). Sedimentation resumed diachronously during the early Callovian (Bullatus and Gracilis Zones). The numerous shallowing turbiditic sequences of the Saïda Clays Formation are, however, stacked in a general deepening evolution leading to the last deepening peak which took place during the early Oxfordian (*Parawedekindia* level). After, sea-depth diminished abruptly and the Tlemcen area was invaded by the prograding cross-bedded and channelizing sandstones of the

Source : MNHN, Paris

Boumedine Sandstones Formation ranging from the Oxfordian to the lower Kimmeridgian (BENEST, 1985).

PALAEOSTRUCTURAL AND DYNAMIC EVOLUTION (Fig. 26)

At the end of Triassic times, and probably at the beginning of the Hettangian. North Africa was occupied by lands and by large sabkhas, extending far south to the Lower Sahara. Magmatic events occurred, related to the first abortive rifting which is known all around the future Central Atlantic. The palaeostructural evolution was largely controlled by a tectonic network inherited from the Variscan events, as stated by DU DRESNAY (1963, 1975, 1988a) who compared the High Atlas during the Early Jurassic to the present day Red Sea.

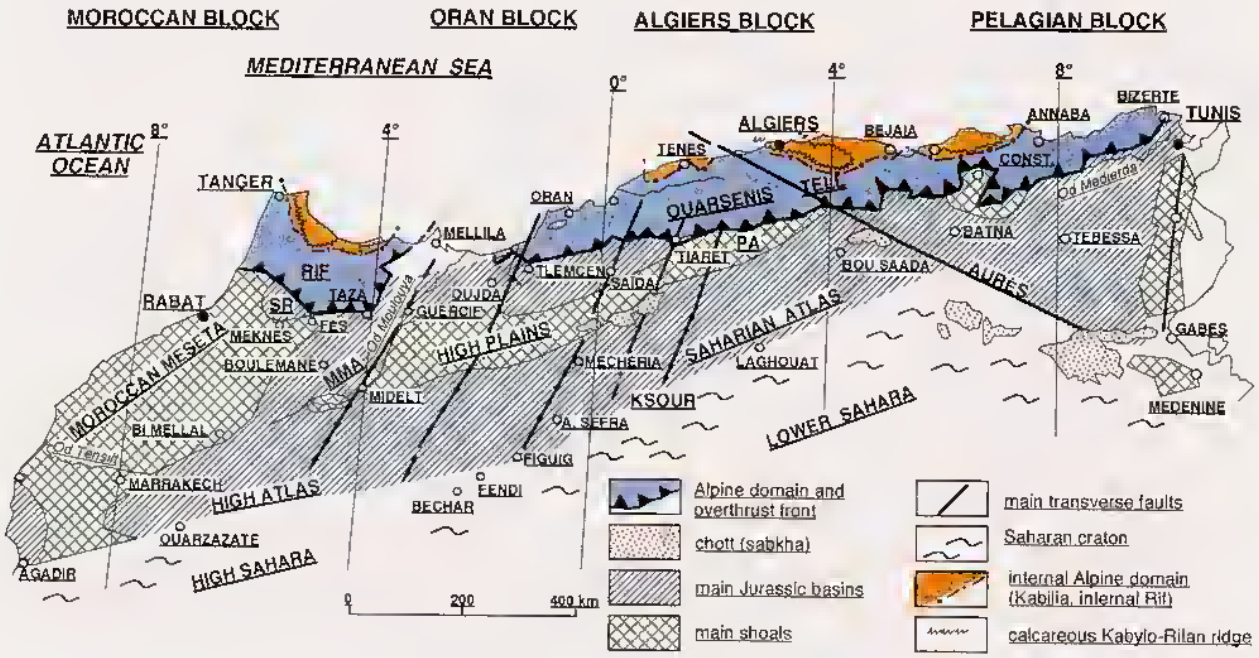

FIG. 26.— Generat sketch of the major structural units of Northwestern Maghreb. Abbreviations: SR= Sudrifan ridges; MMA= Middle Atlas; PA= Preatlasic sector, East of Tiaret; CONST= Constantine.

FIG. 26.— Schéma des principales unités structurales du nord-ouest du Maghreb. Abréviations : SR = Rides sudrifaines ; MMA = Moyen Atlas ; PA = domaine préatlasique à l'Est de Tiaret ; CONST = Constantine.

During the Hettangian-earliest Sinemurian the future Atlas troughs were flooded by a shallow marine transgressiou. This is the first expansion of the initial carbonate platform. Rare ammonites occur at the top of the lower Hettangian (Johnstoni Subzone of the Planorbis Zone) in the Saharian Atlas, indicating that an open seaway existed briefly to the ENE, probably through the Tunisian trough. The Oran High Plains, and the Tlemcen Domain were covered by large sabkhas, inherited from the Trias and changing through time into more or less isolated lagoons.

Near the end of the early Sinemurian (Semicostatum Zone), the weakest parts of the Atlas troughs began subsidence and deepening. This is especially well documented in the Figuig Eastern High Atlas and in the Saharian Atlas (Chemarikh) where Semicostatum Zone micrites of the Aïn Ouarka Formation onlap the eroded carbonates of the Chemarikh Dolomite (Fig. 18c). This extensional regime continued during the late Sinemurian, resulting in a clear differentiation between relatively deep basins (hemipelagic to pelagic), slopes and shoals within the Atlas Domain. Radiolarias may be frequent in the Aïn Ouarka and Jebel Haïmeur Formations. The Atlas Domain was divided into numerous small and

Source : MNHN, Paris

often rhombic basins, whose differentiation depended on extensional and transtensional tectonic stresses (beginning of the mosaic stage). This is the local expression of the Mc Kenzie's rift stage.

A general sea-level-rise at the end of the Sinemurian and during the early Carixian (pre-Demonense) resulted in a transgression of regional scale and in the establishment of the initial carbonate platform in previously emergent or sabkha areas (Oran High Plains, margins of the Atlas troughs, some intra-Tellian shoals such as the Ouarsenis). In the Atlas umbilics (Aïn Ouarka, Figuig), pelagic sedimentation continued and coarse synsedimentary breccias were deposited at the toe of the scarps (Figuig). Thus, a strong dynamic and environmental decoupling is evident between the Atlas domain and the northern sectors. The beginning of the mosaic episode is often marked by the development of megabreccias and ammonitico rosso facies along the margins (Figuig and Ksour Mountains) where slumping, reworking and calcareous turbidites are widespread (Central High Atlas; Figuig; see also DU DRESNAY, 1988a). Reefs (bioaccumulations and bioconstructions) are widespread along the furrows borders in Morocco (DUBAR, 1962; DU DRESNAY, 1977, 1988b). They are less spectacular in western Algeria. During the early Domerian (Celebratum Zone), partitioning reached the northern areas (Tlemcen and Tell Domains). Coevally a large transgression occurred. Even the High Plains were locally invaded by the open sea (Sidi el Abed, Béni Yala).

These episodes can be related to a detachment fault dynamic as stated in the High Atlas (WARME *et al.*, 1988). The main detachment may be situated in the evaporitic levels of the Triassic since BELLHACENE *et al.*, (1997) stated that the main South Atlas fault zone does not affect the Palaeozoic (see also VIALLY *et al*, 1994).

During the Toarcian, the mosaic episode extended and resulted in a divided pattern of subsiding and deepening umbilics separated by a structurally controlled network of shoals and ridges. A first deepening peak occurred during the early Toarcian but the uplift of some large blocks (Oran High Plains, Tleta "zone" of the Béni-Bahdel (Fig. 13c); southern Saharian borders of the Atlas) indicates that tectonic controls had become stronger. Sabkhas isolated by oolitic barriers developed on the High Plains and on the Lower Sahara. Elsewhere, thick marly sediments accumulated in the umbilics and narrow furrows. The slopes were characterized by mass-flows, calcareous turbidites and ammonitico rosso. Siliciclastic turbidites are known in the Traras (Polymorphum Zone of Mellala near Aïn Killoun; unpublished). This tectonically controlled event is now recognized all around the High Atlas. Thus, a new interpretation (SOUHEL, 1996) of the succession of the Béni Mellal borders and shoals (western end of the Central High Atlas) indicates a similar evolution with strong local tectonic control. The turbiditic Toarcian episodes (BRECHÜBLER, 1984) of the Moroccan central High Atlas (Talghemt; Levisoni to Gradata Zones) have been restudied (BOUTAKIOUT & ELMI, data unpublished) and correlated with the slope deposits of the Saharian Atlas (Hassi Beu Khelil Umbilic). All these reworked deposits are located in a comparable structural and palaeogeographical setting at the toe of the slopes bordering the High Plains, High Plateaux and High Moulouya shoals and ridges. Differential movement between the subsiding umbilics and their rising borders is striking and highly significative of local tectonic controls. The Traras Mountains give a good model for this (Mellala and Sidi Boudjenane; see part "The Tlemcen Domain", Fig. 10).

Some of the largest shoals or shallow outer platforms developed neritic conditions, similar to those in NW Europe (borders of the French Massif Central) with the deposition of oolitic or bioclastic ironstones (ferruginous platforms; Middle Atlas, Western Rhar Roubane, some shoals of the Tunisian Ridge).

Synsedimentary compression has been locally documented in peculiar in the Traras Mountain where a gentle folding of the Pliensbachian limestones has been described. It occurred before the erosion of the palaeorelief and the filling of the extensional fissures during the Toarcian (Figs 7 and 8; ELMI, 1979; ELMI, 1981b). This episode can be compared with the coeval events recognized in the central High Atlas (STUDER & DU DRESNAY, 1980). These data have been interpreted as a dynamic change from transtension to transpression (FAVRE *et al.*, 1991). However, these compressions are scarce and they may have been provoked by the antagonistic movements of the Atlas Tethys to the south and of the Maghrebian Tethys to the north (ELMI, 1978). More locally, they can depend on the blockage of some of the small rhombic subbasins dividing the NW Maghreb. Similar data have been described by DUBAR (1950) in the Jebel Bou Dahar (eastern High Atlas) where fissures opened in Megalodontids limestones (Carixian to, perhaps, lowermost Domerian but no upper Domerian as it has been often stated) are filled by pink micrites containing rich brachiopod faunas and some ammonites and ranging from the middle

Source : MNHN, Paris

Toarcian (Bifrons zone) to the lower Aalenian (Opalinum zone) (see also the map in AGARD & DU DRESNAY, 1965). The Toarcian uplift observed on the borders of the main western Algerian basins can be compared with the thermal shouldering supposed by FAVRE *et al.* (1991) on the Atlantic border of Morocco.

Aalenian and early Bajocian times were marked by tectonic and sedimentary instabilities which were, at that time, general over all the NW Maghreb. The contrast between shoals (often islands), slopes and deepening basins reached its climax. Along the northern Sahara, on the Moroccan Meseta and on the Oran High Plains, carbonate platforms and sabkhas began to develop again. Marls accumulated in the troughs, interrupted by gravity-flows transporting neritic material from adjacent platforms. Breccias were frequent at the toe of the steepest scarps and pass laterally into calcareous or, even, quartzose turbidites, indicating that some uplifted blocks have been eroded down to the basement, or at least to Triassic-Lowermost Jurassic siliciclastics to provide a source. *Zoophycos* limestones or marls-limestones interbeds were widespread along the less marked slopes, emphasizing the transitions to the basins (Middle Atlas, Tlemcen Domain). Incomplete, thin, neritic and often ferruginous sequences capped the more prominent shoals. More generally, sedimentation was carbonate dominated from the late Toarcian (Meneghinii Zone) up to the lower Bajocian (Sauzei to Humphriesianum Zones, depending on the local conditions).

In the Atlas Domains, a second peak of deepening was diachronous: end of the early Bajocian or beginning of the late Bajocian and is indicated by thick marls and turbidites. The final homogeneization (or sag) stage was attained in the Atlas with the spectacular development of the intermediate carbonate-platform. Coral build-ups were widespread in the High, Middle and Saharian Atlas. Deep basins disappeared in the south and the west of the NW Maghreb. Quartzose sediments began to spread to the North from the western High Sahara (Bechar).

Thus, the Aalenian-early Bajocian was a carbonate dominated interval between two periods of great extent of the marly sedimentation. The first, presaged during the Domerian, was widespread during the early to middle Toarcian; it seems to have been a global event often associated with anoxic conditions (BASSOULLET & BAUDIN, 1994). The inversion of the dynamic evolution began more or less early during the middle Toarcian with the appearance of oxidized ferruginous beds. The end of the carbonate period seems to be partly controlled by local and/or regional factors. In the Tlemcen Mountains, it happened during the late Bajocian and is coeval with the first input of siliciclastics in the Atlas Domain. The change of the dominant sediment production appears to have been controlled by an inversion of the palaeotectonic stresses. This change was initiated in the south (Atlas) and has progressed to the north during the Bathonian and the Callovian (ELMI, 1978, 1981a).

In the Tlemcen Domain, thick marls accumulated, but shoals and horsts often remained prominent during the late Bajocian. These high areas began to be flooded and onlapped during the early Bathonian (final or "senile" homogeneization stage). During Bajocian-Bathonian, extensional tectonics were important and breccias are known everywhere. Redeposition of shallow-water sediments into deeper trough is frequent (for instance: Raknet el Kahla Megabreccias in the Ksour Mountains). A rejuvenation of the Saharian border gives the source of siliciclastics deposited in the Ksour turbidites. These events are also reminiscent of those occurring in the Hebrides Basin of the northwestern corner of Europe with the beginning of the Bearreraig Sandstone which indicates strong basin subsidence associated with hinterland rejuvenation (MORTON, 1989, 1990). This is a classic lithosphere extension "following mantle-driven thermal doming" as it has been established in the North Sea (UNDERHILL & PARTINGTON, 1993).

In the north Tlemcen and Tell-Rif Domains, a new deepening peak occurred late during the Callovian-early Oxfordian. Clays and quartzose turbidites were widespread in these areas (Saïda Clays Formation). These data illustrate the decoupling between the northern deepening furrows and the uplifted Southern regions (High Plains, Ksour).

However, the final differentiation stage, on a Maghrebian scale, is only reached during the middle or late Oxfordian:

— acceleration of subsidence and deepening of the future Alpine Domains, where radiolarites extend from the upper Bajocian to the lower Tithonian (Tell, Rif; recent data *in* OLIVIER *et al.*, 1996);

Source : MNHN, Paris

— extension of a large delta from Morocco into the eastern Saharian Atlas (AUGIER, 1967; DELFAUD, 1975; BENEST, 1985);

— from the Kimmeridgian onwards, the northern fringe of the delta became part of the late Jurassic Carbonate Platform, extending from the High Plains to the Tlemcen and Preatlasic Domains (BENEST, 1985).

All these data are coherent with the model of aborted rifts or aulacogens (DU DRESNAY, 1975; 1988b) developed along the Saharian Atlas and along the Tlemcenian Domain. But the evolution of these two longitudinal furrows has been diachronous (ELMI, 1978; 1996b). The present study clearly indicates that regional tectonic events overprint the global signal and that an eustatic sea-level chart must be the result of comparisons between "different plates as tectonically uncoupled as possible" (UNDERHILL & PARTINGTON, 1993).

PALAEONTOLOGICAL REMARKS

Hammatoceras roubanense Elmi sp. nov.

Figs 11, c-d; 19, a

1969. *Hammatoceras* nov. sp., ELMI & BENEST p. 295.
1974. *Hammatoceras* nov. sp. 1, ELMI, ATROPS & MANGOLD, pl.5. fig.1.

ETYMOLOGY.— From the Rhar Roubane Mountains in Western Algeria.

TYPE LOCALITY.— Djorf Tisseddoûra. North west of the Beni Snouss Khemis village.

TYPE LEVEL.— Bed 4 Ti 4 (ELMI, 1983: p. 405, fig. 3), Belaïch Oncolitic Limestones (see Table 3); Alticarinata Subzone, Gradata Zone, middle Toarcian.

TYPE MATERIAL.— Holotype (299 800), paratype (299 801) and figured topotype (299 802). Collection Elmi. UFR Sciences de la Terre, Claude Bernard Lyon 1.

DIAGNOSIS.— Hammatoceratids with prominent periumbilical tubercules (except the first whorls) remaining strong until the beginning of the body chamber; gently curved inner part of the secondary ribs; subogival ventral area without shouldering; relatively involute coiling.

DESCRIPTION.— All the specimens coming from Tisseddoûra are well preserved internal casts. They have been broken before their burial (Fig. 11c). The inner whorls are often calcitic.

The holotype is a moderately involute and slightly compressed ammonite. The involution line is approximately situated at middle height of the flank. The umbilical wall is vertical or subvertical and moderately elevated all along the growth. The umbilical edge is gently curved between the tubercules. The ventral area is regularily ogival and bears a neat carina. The overall shape of the section remains constant during the observable stages of growth of all the collected specimens.

The ornamentation consists in prominent periumbilical tubercules divided in ribs. The number of ribs per tubercule changes few during the growth. In consequence, they appeared to be more spaced in the outer whorls. The tubercules are always prominent and even spinous in the inner nucleus. The ribs (secondary ribbing) are monotonous but slightly flexuous on the ventral half of the whorl, and ventrally projected. The ribs appear generally by pair issued from a large tubercule. A triplicate division is less common. The transition from the tubercules to the ribs is progressive.

The paratype illustrates some complementary features of the ontogenic evolution of the ornamentation. Untill a diameter of D=18 mm, the dorsal (inner) ornamentation consists only in short primary ribs divided in 2 or 3 secondaries. Between D=18 mm and D=25 mm, the primaries become stronger and more prominent. After, they change into spinous tubercules.

Source : MNHN, Paris

MATERIAL.— Seven well preserved specimens from Djorf Tisseddoûra. Several from Sidi Yahia ben Sefia (west of Sebdou), from the *Zoophycos* bearing Bayada Formation. The species is also widespread in the Oujda Mountains (east Morocco) and in the Lusitanian Basin (Portugal).

MEASUREMENTS.— The dimensions given for the specimens are as follows: D. (diameter). Wh. (whorl height). (Wh/D). Wb. (whorl breadth). (Wb/D). Ud. (diameter of umbilicus). (Ud/D).

Holotype (2990800): preserved diameter: c.125 mm.

D. 85;	Wh. 30.5 (0.35);	Wb. 22 (0.26);	Ud. 31 (0.36)
80.5;	29 (0.36);	21 (0.26);	29 (0.36)
77.5;	28.5 (0.36);	21.5 (0.27);	27 (0.34)

PHYLETIC REMARKS.— *H. roubanense* is the oldest known species belonging to the true *Hammatoceras* lineage. It presents strong ressemblances with *H. speciosum* Janensch and *H. insigne* (Zieten) which are more recent and separated by an interval corresponding to the Bonarellii Zone (=Thouarsense Zone of NW Europe). The differences between the two homoemorphs *H. roubanense* and *H. speciosum* are the shape of the ventral section (ogival on *roubanense;* quadratic and shouldered on *speciosum*) and the ribbing style (more straight on *speciosum).* The peculiar feature of *roubanense* have not been observed in the large population of the Lyon area that we have studied.

ACKNOWLEDGEMENTS

This paper is a summary of the results obtained through the realization of several programs and collaborations. It has been finalized in the scope of Peri-Tethys Programme Projects 95/96-38 and 42. Personal grants have been obtained from the following supports: the franco-algerian programs 90MDU-157 and 96MDU-359, the Geological Survey of Morocco, the "Entreprise nationale de l'Industrie minière" (Algeria), the french "Centre national de la Recherche scientifique" UMR-5565.

Thanks to Noël PODEVIGNE (photographs of ammonites), Delphine FOUGEROUSE (drawings and text processing). Nicol MORTON (Birkbeck College, University of London) has carefully corrected this paper which has been greatly improved by his large knowledge of the Jurassic stratigraphy. Renaud DU DRESNAY (Rabat) has read this paper and given very valuable informations on the moroccan outcrops and bibliographic indications. Jacques THIERRY (Université de Bourgogne, Dijon) have been an helpfull referee and we have appreciated the constructive remarks of an other reviewer. Thanks also to Sylvie CRASQUIN-SOLEAU for her editorial work.

This paper is dedicated to the memory of the late M'HAMED and RABIA (Oran, Algeria).

REFERENCES

AGARD, J. & DU DRESNAY, R., 1965.— La région minéralisée du jbel Bou-Dahar, près de Béni-Tajjite (Haut-Atlas oriental): étude géologique et métallogénique. Colloque gîtes stratiformes. *Notes et Mémoires du Service géologique du Maroc, Rabat,* **181**: 135-152, 6 fig., 1 carte.

AHMOUD, H., BOUTAKIOUT, M., ELMI, S. & BENSHILI K., 1997.— Les foraminifères du Domérien-Bajocien basal du synclinal de Sebbab Sghrir (Jbel Bou-Dahar, Haut-Atlas oriental, Maroc). *In:* B. PEYBERNES & J.P. VILA (eds), *Les marges téthysiennes d'Afrique du Nord.* Société géologique de France, Paris: 38.

AÏT OUALI R., 1991.— *Le rifting des Monts des Ksour au Lias. Organisation du bassin, diagenèse des assises carbonatées. Place dans les ouvertures mésozoïques au Maghreb.* Thèse Doctoral d'État, Université d'Alger, Alger, Algérie: 1-298, 147 fig.

AÏT OUALI, R. & DELFAUD, J., 1995.— Les modalités d'ouverture du bassin des Ksour au Lias dans le cadre du "rifting jurassique" au Maghreb. *Comptes Rendus de l'Académie des Sciences, Paris,* **320,** IIa: 773-778, 4 fig.

Source : MNHN, Paris

ALMÉRAS, Y., ELMI, S., MEKAHLI, L., OUALI-MEHADJI, A.E.K., SADKI, D. & TLILI, M. 1994.— Biostratigraphie des brachiopodes du Jurassique moyen dans le domaine atlasique (Maroc, Algérie). Contraintes environnementales et relations avec l'évolution verticale des peuplements d'ammonites. *Servizio Geologico Nazionale, Miscellana, Roma*, **5**: 219-242, 8 fig., 3 pl.

AMEUR, M., 1978.— *Étude stratigraphique et sédimentologique du Jurassique inférieur et moyen de la partie orientale de la chaîne du Fillaoussène.* Thèse 3ème cycle, Université d'Oran, Oran, Algérie: 1-192, 16 fig. 10 pl.

AMEUR, M., 1988.— *Histoire d'une plate-forme carbonatée de la marge sud téthysienne: l'autochtone des Traras (Algérie occidentale) du Trias supérieur jusqu'au Bathonien moyen.* Thèse Doctorat d'État, Université de Lyon, Lyon, France: 1-548, 188 fig., 24 pl.

AMEUR, M. & ELMI, S., 1981.— Relations spatio-temporelles entre "Ammonitico Rosso", calcaires à "Zoophycos" et récifs coralliens dans le Toarcien et la base du Jurassique moyen (Monts des Traras, Djebel Fillaoussène, Algérie NW). *In*: A. FARINACCI & S. ELMI (eds), *Rosso Ammonitico Symposium Proceedings, 1980.* Tecnoscienza, Roma: 9-25, 3 fig., 1 pl.

ARKELL, W.J. & LUCAS G., 1953.— Découverte récente du genre *Eruoceras* Douvillé dans l'Atlas saharien occidental. Conséquences stratigraphiques et paléogéographiques. *Comptes Rendus de l'Académie des Sciences, Paris*, **236**: 2257-2259.

ATROPS, F., 1974.— Le Bajocien inférieur et moyen des Beni Bahdel au Sud-Ouest de Tlemcen (Ouest algérien). *Géologie méditerranéenne, Marseille*, **1** (2): 75-88, 2 text.-fig, 3 pl.

ATROPS, F., DUBEL, C., ELMI S. & REVERT J., 1970.— La limite Domérien-Toarcien et l'apparition de la sédimentation marneuse dans le Lias des Monts de Rhar-Roubane (Ouest algérien). *Bulletin de la Société d'Histoire naturelle de l'Afrique du Nord, Alger*, **61** (3-4): 9-18.

AUGIER. C., 1967.— Quelques éléments essentiels de la couverture sédimentaire des Hauts Plateaux. *Service de la Carte géologique de l'Algérie, Alger*, N.S., **34**: 47-80. 8 fig., pl. 1-6.

BASSOULLET, J.P., 1966.— Présence de Lotharingien daté par Ammonites dans l'Atlas Saharien sud-oranais (Algérie). *Comptes Rendus de la Société géologique de France, Paris*, **4**: 157-158.

BASSOULLET, J.P., 1968.— Le Lias du Djebel Hafid, sur la bordure nord-ouest de l'Atlas saharien occidental (Algérie). *Comptes Rendus de la Société géologique de France, Paris*, **2**: 45-46.

BASSOULLET, J.P., 1971.— Découverte d'empreintes de pas de reptiles dans l'Infralias de la région d'Aïn Sefra (Atlas saharien, Algérie). *Comptes Rendus de la Société géologique de France, Paris*, **7**: 358-359, 1 fig.

BASSOULLET, J.P., 1973.— *Contribution à l'étude stratigraphique du Mésozoïque de l'Atlas saharien occidental (Algérie).* Thèse Doctorat d'État, Université de Paris VI, Paris, France: 1-497, 50 fig., texte-pl. A-I et h.t. 1-3. 32 pl.

BASSOULLET, J.-P. & BAUDIN, F., 1994.— Le Toarcien inférieur: une période de crise dans les bassins et sur les plates-formes carbonatées de l'Europe du Nord-Ouest et de la Téthys. *Geobios, Lyon*, M.S. **17**: 645-654.

BASSOULLET, J.P. & BENEST, M., 1976.— Microfaciès, structures sédimentaires et phénomènes diagénétiques précoces des dépots carbonatés inter et supracotidaux du Lias de Sidi Yahia Ben Sefia. *Bulletin du Service géologique de l'Algérie, Alger*, **45**: 35-63.

BELLHACENE, A., BRACENE, R., BEKKOUCHE, D., DJELLIT, H., DERDER M.E.M., YELLES CHAOUCHE, A.K. & AÏT OUALI R., 1997.— The South Atlasic accident geometry and the associated structures in the SW of the Saharan Atlas. *Peri-Tethys Program Annual Meeting, Rabat*: 14.

BENEST, M., 1985.— Évolution de la plate-forme de l'Ouest algérien et du Nord-Est marocain au cours du Jurassique supérieur et au début du Crétacé: stratigraphie, milieux de dépôt et dynamique sédimentaire. *Documents des Laboratoires de Géologie de Lyon*, **95**: 1-581.

BENEST, M., DUBEL, C. & ELMI, S., 1978.— Modalités de l'apparition de la sédimentation carbonatée de plate-forme interne sur la frange méridionale du domaine tlemcénien pendant l'Aalénien et le Bajocien: les "Dolomies du Tenouchfi" (Algérie nord-occidentale). *Documents des Laboratoires de Géologie de Lyon*, H.S., **4**: 29-69, 10 fig., 6 pl.

BENHAMOU, M., 1983.— *Stratigraphie et milieux de dépôt du Jurassique inférieur et moyen des Beni-Ouarsous et des Beni-Khallad (Massif des Traras, Oranie W).* Thèse 3ème cycle, Université d'Oran, Oran, Algérie: 1-168, 56 fig., 8 pl.

BENHAMOU, M., 1986a.— Les "Calcaires compacts de Zaïlou" (Massif des Traras, Oranie W). Implications paléogéographiques. *6ème Séminaire national des Sciences de la Terre, Alger*: 31.

BENHAMOU, M., 1986b.— L'"ammonitico rosso" des Traras (Massif des Traras, Oranie W). Exemples de reliefs résiduels. *6ème Séminaire national des Sciences de la Terre, Alger*: 32.

BENHAMOU, M., 1996.— *Évolution tectonique et eustatique d'un bassin de la Téthys maghrébine: l'Ouarsenis (Algérie) pendant le Jurassique inférieur et moyen.* Thèse Doctorat d'État, Université d'Oran, Oran, Algérie: 1-430. 139 fig., 28 pl.

BENSALAH, M., BENEST, M., GAOUAR, A., TRUC, G. & MOREL, J.L., 1987.— Découverte de l'Éocène continental à Bulimes dans les Hautes Plaines oranaises (Algérie): conséquences paléogéographiques et structurales. *Comptes Rendus de l'Académie des Sciences, Paris*, **1**, II: 304, 35-38, 1 fig.

BENSHILI, K., 1989.— Lias-Dogger du Moyen Atlas plissé (Maroc). Sédimentologie, biostratigraphie et évolution paléogéographique. *Documents des Laboratoires de Géologie de Lyon*, **106**: 1-285, 96 fig., 24 pl.

BENSHILI, K. & ELMI, S., 1994.— Enregistrement biostratigraphique et séquentiel des événements toarciens-bajociens dans le Moyen Atlas plissé (Maroc). *Servizio Geologico Nazionale, Miscellana, Roma*, **5**: 277-284, 3 fig., 1 pl.

Source : MNHN, Paris

BOUTAKIOUT, M. & ELMI, S., 1996.— Tectonic and eustatic controls during the Lower and Middle Jurassic of the South Rif Ridge (Morocco) and their importance for the foraminifera-communities. *GeoResearch Forum, Zürich*, **1-2**: 237-248.

BRECHBÜLER, Y.A., 1984.— *Étude structurale et géologique du Haut-Atlas calcaire entre le Jebel Ayachi et Rich (Maroc).* Thèse, Université de Neuchâtel, Neuchâtel, Suisse: 1-128, 56 fig.

BUSSON, G., 1967.— Le Mésozoïque saharien. 1ère partie: extrême-sud tunisien. *Publications du Centre de Recherches sur les zones arides. Géologie, Centre National de la Recherche Scientifique, Paris*, **8**: 1-194, 18 fig., 3 pl.

CISZAK, R., 1993.— Évolution géodynamique de la chaîne tellienne en Oranie (Algérie occidentale) pendant le Paléozoïque et le Mésozoïque. *Strata, Toulouse*, série 2, **20**: 1-513, 107 fig., 17 pl.

COLO, G., 1962.— Contribution à l'étude du Jurassique du Moyen-Atlas septentrional. *Notes et Mémoires du Service géologique du Maroc, Rabat*, **139**: 1-226, 28 fig.

CORNET, A., GALMIER, D. & LUCAS, G., 1953.— Sur l'âge liasique de la riche faune à Polypiers, dite "sénonienne", de Raha Zerga (région d'Aïn Sefra, Atlas Saharien occidental). *Comptes Rendus de l'Académie des Sciences, Paris*, **4**: (237): 345-347.

CRASQUIN-SOLEAU, S., RAKUS M., OUJIDI, M., COUREL, L., ET TOUHAMI, M., & BENAOUISS, N., 1997.— Découverte d'une faune d'ostracodes dans le Trias des monts d'Oujda (Maroc): relations paléogéographiques entre les plates-formes nord et sud de la Téthys. *Comptes Rendus de l'Académie des Sciences, Paris*, **324**: 111-118, 4 fig.

DELFAUD, J., 1975.— Les grès des Ksour (Algérie). Un delta de plate-forme stable. *9ème Congrès international de Sédimentologie, Nice.* Université de Nice: International Association of Sedimentologists, Nice thème 5, **1**: 159-162, 6 fig.

DOMMERGUES, J. L., FERRETTI, A. & MEISTER, C. 1994.— Les faunes d'ammonites du Sinémurien de l'Apennin Central (Marches et Toscane, Italie). *Bollettino della Società Paleontologica Italiana, Modena*, **33** (1): 13-42, 10 fig., 4 pl.

DOUTHASNI, M., 1976.— *Étude géologique de la région d'Aïn Ouarka-Boussemghoun (partie centrale des Monts des Ksour). Analyse structurale.* Thèse 3ème cycle, Université d'Oran, Oran, Algérie: 1-272, 52 fig., 5 pl.

DUARTE, L.V., 1994.— La sédimentation cyclique marne-calcaire dans le Toarcien du basin lusitanien. *Geobios, Lyon*, M.S. **17**: 663-669, 6 fig.

DUARTE, L.V., 1996.— *O Toarciano da Bacia Lusitanica. Estratigrafia e evolução sedimentogenética.* Ph. D. Thesis, Universidade de Coimbra, Coimbra, Portugal: 1-349.

DUBAR, G., 1932.— Faunes liasiques du Moyen Atlas marocain. *Annales de la Société géologique du Nord, Lille*, **57**: 181-182.

DUBAR, G., 1947.— Rapport provisoire sur la couverture secondaire à l'ouest du bassin houiller de Djerada. *Archives Charbonnages nord-africains*. Rabat, inédit. *In*: MEDIONI, R., 1971.— Les formations liasiques des Oulad-Amor et du jbel Nador (Hauts Plateaux du Maroc oriental) et leurs relations avec les séries liasiques voisines. *Notes et Mémoires du Service géologique du Maroc, Rabat*, **31** (237): 17-27, 6 fig.

DUBAR, G., 1948.— La faune domérienne du djebel Bou-Dahar près de Béni-Tadjit. *Notes et Mémoires du Service géologique du Maroc, Rabat*. **68**: 1-247, 30 pl.

DUBAR, G., 1950.— Sur des faunes de brachiopodes du Lias supérieur dans les fentes du Domérien supérieur au djebel Bou-Dahar (Haut-Atlas marocain). *Annales de la Société géologique du Nord, Lille*, **70**: 205-213, 5 fig.

DUBAR, G., 1962.— Notes sur la paléogéographie du Lias marocain (domaine atlasique). Livre à la mémoire du Professeur Paul Fallot, *Société Géologique de France*, **1**: 525-544.

DUBAR, G. & MOUTERDE, R., 1978.— Les formations à ammonites du Lias moyen dans le Haut Atlas de Midelt et du Tadla. *Notes et Mémoires du Service géologique du Maroc, Rabat*, **274**: 1-112, 11 fig., 6 pl.

DU DRESNAY, R., 1956.— Contribution à l'étude de la série détritique jurassique-crétacé dans le Haut-Atlas oriental. *Notes et Mémoires du Service géologique du Maroc, Rabat*, 14, **133**: 9-32, 9 fig.

DU DRESNAY, R., 1957a.— Le Lias inférieur du Haut Atlas marocain oriental. *Comptes Rendus de l'Académie des Sciences, Paris*, **245**: 2341-2343.

DU DRESNAY, R., 1957b.— Le Lias supérieur du Haut Atlas marocain oriental. *Comptes Rendus de l'Académie des Sciences, Paris*, **245**: 2517-2520.

DU DRESNAY, R., 1958.— La transgression du Lias supérieur dans le Haut-Atlas marocain oriental. *Comptes Rendus de l'Académie des Sciences, Paris*, **246**: 556-558.

DU DRESNAY, R., 1963.— Les discontinuités de sédimentation pendant le Jurassique, dans la partie orientale du domaine atlasique marocain, leurs conséquences stratigraphiques et leurs relations avec l'orogenèse atlasique. Colloque du Jurassique, 1962. *Comptes Rendus et Mémoires de l'Institut grand ducal, Luxembourg*: 899-912.

DU DRESNAY, R., 1964a.— Carte géologique du Haut Atlas oriental au 1/200 000, feuilles Bou-Arfa, Iche, Talzaza et Figuig. *Notes et Mémoires du Service géologique du Maroc, Rabat*, **158**.

DU DRESNAY, R., 1964b.— Les découvertes, dans le Dogger du Maroc, de faunes d'Ammonites de la province arabique à "*Ermoceras*": historique, localisations et répartition paléogéographique. *Comptes Rendus de l'Académie des Sciences, Paris*, **259**: 4754-4757, 1 fig.

DU DRESNAY, R., 1966.— Observations stratigraphiques au sujet des gisements de Gastéropodes liasiques du Causse moyen-atlasique et du Haut Atlas oriental, étudiés par R. Bourrouilh. *Notes et Mémoires du Service géologique, Rabat*, **196**: 5-22, 15 fig.

Source : MNHN, Paris

DU DRESNAY, R., 1975.— Influence de l'héritage structural tardi-hercynien et de la tectonique contemporaine sur la sédimentation jurassique, dans le sillon marin du Haut-Atlas, Maroc. *9ème Congrès International de Sédimentologie, Nice*. Université de Nice; International Association of Sedimentologists, Nice: 103-108, 2 fig.

DU DRESNAY, R., 1977.— Le milieu récifal fossile du Jurassique inférieur (Lias) dans le domaine des Chaînes atlasiques du Maroc. Second symposium international sur les coraux et récifs coralliens fossiles (1975). *Mémoires du Bureau des Recherches géologiques et minières, Paris*, **89**: 296-312, 8 fig., 4 pl.

DU DRESNAY, R. & DUBAR, G., 1963.— Découverte de Rhynchonellines liasiques associées à des Ammonites dans le Haut Atlas oriental marocain. *Comptes Rendus de l'Académie des Sciences, Paris*, **256**: 3721-3723.

DU DRESNAY, R., 1988a.— Recent data on the geology of the Middle Atlas (Morocco). *Lectures and Notes in Earth-Sciences* **15**: 293-320, 2 fig.

DU DRESNAY, R., 1988b.— Jurassic development of the region of the Atlas Mountains of Morocco: chronology, sedimentation and structural significance. *Geological Society of Lybia papers*, Tripoli, **4**: 77-99.

EL HARIRI, K., DOMMERGUES, J.L., MEISTER, C., SOUHEL, A. & CHAFIKI, D., 1996.— Les ammonites du Lias inférieur et moyen du Haut Atlas central de Béni Mellal (Maroc), taxonomie et biostratigraphie à haute résolution. *Geobios, Lyon*, **29-5**: 537-576, 15 fig.

EL KOCHRI, A., CHOROWICZ, J. & ALEM, E.M., 1997.— The Central and Eastern High Atlas: a Jurassic trough opening obliquely. *Peri-Tethys Program Annual Meeting, Rabat*: 35.

ELMI, S., 1969.— Les influences mésogéennes dans le Jurassique moyen du Sud-Est de la France. Comparaison avec l'Ouest algérien. *Annales de l'Institut géologique, Publication Hungarici, Budapest*, **54** (2): 471-481, 1 fig., 3 tables.

ELMI, S., 1971a.— Les zones d'ammonites dans la série Bajocien supérieur-Callovien de l'Oranie (Ouest algérien). *Bulletin de la Société géologique de France, Paris*, (7), **13**: 8-37, 1 fig.

ELMI, S., 1971b.— Les faunes à *Prohecticaceras (Oppeliidae, Ammonitina)* du Bathonien inférieur et moyen des confins algéro-marocains. *Geobios, Lyon*, **4** (4): 243-264, 2 fig., pl. 19-20.

ELMI, S., 1973a.— Décrochements et mouvements atlasiques dans la région frontalière algéro-marocaine (Monts de Rhar Roubane). *Comptes Rendus de l'Académie des Sciences, Paris*, **276**: 1521-1524, 1 fig.

ELMI, S., 1973b.— La lacune du Bathonien supérieur dans l'Oued Tazouggart (Maroc oriental): intérêt paléogéographique. *Comptes Rendus de l'Académie des Sciences, Paris*, **276**: 901-903.

ELMI, S., 1977a.— La sédimentation carbonatée en bordure du horst de Rhar Roubane (Algérie occidentale) pendant le Carixien. *Bulletin de la Société géologique de France, Paris*, (7), **19**: 355-365, 12 fig.

ELMI, S., 1977b.— Différences chronologiques dans l'évolution morphologique des dimorphes d'une même lignée (ammonoïdes jurassiques). Colloque "Polymorphisme chez les Mollusques", Dijon 1975. *Haliotis*, **6**: 71-95, 5 fig., 4 pl.

ELMI, S., 1978.— Polarité tectono-sédimentaire pendant l'effritement des marges septentrionales du bâti africain au cours du Mésozoïque (Maghreb). *Annales de la Société géologique du Nord, Lille*, **97**: 315-323, 3 fig.

ELMI, S. 1979.— *Tectonique synsédimentaire, émersions temporaires et sédimentation de type Ammonitico-Rosso: l'exemple du Lias du Djebel-es-Sekika (Monts des Traras, Algérie occidentale): 7ème Réunion annuelle des Sciences de la Terre, Lyon*. Société géologique de France, Paris: 1-179, 1 fig.

ELMI, S., 1981a.— Comparaison entre l'évolution jurassique de l'Apennin et de la marge nord-africaine. *Memorie della Società Geologica Italiana, Modena*, **21**: 33-40, 1 fig.

ELMI, S., 1981b.— Sédimentation rythmique et organisation séquentielle dans les ammonitico-rosso et les faciès associés du Jurassique de la Méditerranée occidentale. Interprétation des grumeaux et des nodules. *In*: A. FARINACCI & S. ELMI, *Rosso-Ammonitico Symposium Proceedings, 1980*. Tecnoscienza, Roma: 251-299, 14 fig., 5 pl.

ELMI, S., 1983.— L'évolution des Monts de Rhar Roubane (Algérie occidentale) au début du Jurassique. *In*: Livre jubilaire Gabriel Lucas: Géologie sédimentaire. *Mémoires de l'Université de Dijon*, **7**: 401-412, 7 text. fig.

ELMI, S., 1987.— Corrélations biostratigraphiques et mégaséquentielles dans le Jurassique inférieur et moyen d'Oranie. Comparaisons avec les régions voisines. *Revue de la Faculté des Sciences de Marrakech*, M.S. **2**: 225-247, 1 fig., 2 pl.

ELMI, S., 1996a.— Summary of the main paleogeographic and dynamic events in North-West Maghreb during the Early and Middle Jurassic. *Peri-Tethys Program Annual Meeting, Amsterdam*: 19-20.

ELMI, S., 1996b.— Stratigraphic correlation of the main Jurassic events in the Western Mediterranean Tethys (Western Algeria and Eastern Morocco). *GeoResearch Forum, Zürich*, **1-2**: 343-358, 8 fig.

ELMI, S., 1996c.— Comparative evolution of Jurassic Basins of Northern Morocco and Western Algeria. Report on the project 95-38, *Peri-Tethys Program Annual Meeting, Amsterdam*: 1-13, 6 fig. unpublished.

ELMI, S., 1997.— L'histoire jurassique de Rhar Roubane (Algérie occidentale) ou l'œuvre de Gabriel Lucas à l'épreuve du temps. *In*: Carbonates-intertropicaux, *Mémoires de la Société géologique de France, Paris*, **169**: 17-24, 3 fig.

ELMI, S., ALMÉRAS, Y., AMEUR, M. & BENHAMOU, M., 1985.— Précisions biostratigraphiques et paléoécologiques sur le Lias des environs de Tiffrit (Saïda, Algérie occidentale). *Cahiers de l'Institut catholique, Lyon*, **14**: 15-41, 3 fig., pl. 1-4.

ELMI, S. & ALMÉRAS, Y., 1985.— Physiography, palaeotectonics and palaeoenvironments as controls of changes in ammonite and brachiopod communities (an example from the Early and Middle Jurassic of western Algeria). *Palaeogeography, Palaeoclimatology, Palaeoecology, Amsterdam*, **47**: 347-360, 2 text. fig.

ELMI, S. & AMEUR, A., 1987.— Quelques environnements des faciès noduleux mésogéens. *Geologia Romana, Roma*, **23**: 13-22, 11 fig.

Source : MNHN, Paris

ELMI, S., ATROPS, F. & MANGOLD, CH., 1974.— Les zones d'ammonites du Domérien-Callovien de l'Algérie occidentale. 1ère partie: Domérien-Toarcien. *Documents des Laboratoires de Géologie de Lyon*, **61**: 183, 17 fig., 5 pl.

ELMI, S. & BENEST, M., 1969.— Précisions stratigraphiques sur le Jurassique inférieur et moyen de la partie méridionale des Monts de Tlemcen (Algérie). *Comptes Rendus de la Société géologique de France, Paris*, **8**: 295-296, 1 fig.

ELMI, S. & BENEST, M., 1978.— Les "Argiles de Saïda", faciès flyschoïde du Callovo-Oxfordien du sillon tlemcénien (Ouest algérien): stratonomie, environnement, interprétation et évolution paléogéographique. *Documents des Laboratoires de Géologie de Lyon*, **H.S. 4**: 203-261, 14 fig., 9 pl.

ELMI, S. & BENSHILI, K., 1987.— Relations entre la structuration tectonique, la composition des peuplements et l'évolution: exemple du Toarcien du Moyen-Atlas méridional (Maroc). *Bollettino della Società Paleontologica Italiana, Modena*, **26** (1-2): 47-62, 6 texte-fig., 2 pl.

ELMI, S., GABILLY, J., MOUTERDE, R., RULLEAU, L. & ROCHA, R.B. 1993.— L'étage toarcien de l'Europe et de la Téthys: division et corrélations. *Geobios, Lyon*, M.S. **17**: 149-159, 2 fig..

ELMI, S. & RULLEAU, L., 1996.— Données nouvelles sur la répartition des Phymatoceratinae (Ammonitina, Toarcien). Exemples de convergences et d'évolution itérative. *Hantkeniana, Budapest*, **1**: 83-96.

ELMI, S., RULLEAU, L., GABILLY, J. & MOUTERDE, R., 1997.— Étage Toarcien. *In*: É. CARIOU & P. HANTZPERGUE, Biostratigraphie du Jurassique ouest-européen et méditerranéen. Zonations parallèles et distribution des invertébrés et microfossiles. *Elf Aquitaine Édition, Pau, Mémoire*, **17**: 26-42, fig. 1-4, table 4, pl. 9-11.

ENAY, R., 1996.— Dimorphisme dans le genre *Ermoceras* DOUVILLE, 1916 Stephanoceratidae, Bajocien supérieur)et implication nomenclaturale. *Comptes Rendus de l'Académie des Sciences, Paris*, **232**: 791-798, 11 fig.

FAVRE P., STAMPFLI G. & WILDI W., 1991.— Jurassic sedimentary record and tectonic evolution of the northwestern corner of Africa. *Palaeogeography, Palaeoclimatology, Palaeoecology, Amsterdam*, **87**: 53-73, 14 fig.

FEDAN, B., 1989.— Évolution géodynamique d'un bassin intraplaque sur décrochements: le Moyen-Atlas (Maroc) durant le Méso-Cénozoïque. *Travaux de l'Institut des Sciences de Rabat, Série Géologie et Géographie Physique*, **18**: 1-142, 94 fig.

FLAMAND, G.B.M., 1911.— *Recherches géologiques et géographiques sur le Haut Pays de l'Oranie et sur le Sahara (Algérie et Territoires du Sud)*. Thèse, Université de Lyon, Lyon, France, **47**: 1-1001, 16 pl., 2 cartes, 152 + 5 fig.

FLINCH, J.F. 1996.— Accretion and extensional collapse of the external Western Rif (Northern Morocco). *In*: P.A. ZIEGLER. & F. HORWATH (eds), Peri-Tethys Memoir 2: Structure and Prospects of Alpine Basins and Forelands. *Mémoires du Muséum national d'Histoire naturelle, Paris*, **170**: 61-85, 11 fig., 2 encl.

GENTIL, L., 1908.— *Esquisse stratigraphique et pétrographique du bassin de la Tafna (Algérie)*. Thèse, Université d'Alger, Alger, Algérie, published by Jourdan: 1-536, 121 fig., 5 pl.

GRIFFON, J.C. & MOUTERDE R., 1964.— Découverte de faunes hettangiennes au Sud de Tétouan (Rif septentrional Maroc). *Comptes Rendus de la Société géologique de France, Paris*, **2**: 61.

GUARDIA, P., 1975.— *Géodynamique de la marge alpine du continent africain d'après l'étude de l'Oranie nord-occidentale*. Thèse Doctorat d'État, Université de Nice, Nice, France: 1-286, 141 fig.

KAZI-TANI, N., 1986.— *Évolution géodynamique de la bordure Nord-Africaine: le domaine intraplaque Nord-Algérien. Approche mégaséquentielle*. Vol. 1. Thèse Doctorat d'État, Université de Pau, Pau, France: 1-871, 347 fig.

LUCAS, G., 1942.— Description géologique et pétrographique des Monts de Ghar Rouban et du Sidi el Abed. *Bulletin du Service géologique de l'Algérie, Alger*, (2), **16**: 1-539, 131 fig., 34 pl.

LUCAS, G., 1952.— Bordure des Hautes Plaines dans l'Algérie occidentale. XIX[ème] Congrès géologique international, Alger. *Monographies régionales d'Algérie*, (1) **21**: 14.

LUCAS, G., 1966.— Fonds durcis, lacunes sous-marines, séries condensées et ondes marines séismiques ou "Tsunami". *Comptes Rendus de l'Académie des Sciences, Paris*, **262**: 2141-2144.

MAROK, A., 1994.— *Exemple de sédimentation carbonatée de plate-forme: Lias-début du Dogger. Stratigraphie, sédimentologie et interprétations géodynamiques (Monts de Sidi El Abed, hautes plaines oranaises, Algérie occidentale)*. Diplôme de Magistère, Université d'Oran, Oran, Algérie: 1-204, 88 fig, 11 pl.

MAROK, A., 1996.— Stratigraphie, sédimentologie et interprétations géodynamiques du Lias-début du Dogger: exemple de sédimentation carbonatée de plate-forme en Oranie (Monts de Sidi el Abed, Hautes Plaines, Algérie occidentale). *Documents des Laboratoires de Géologie de Lyon*, **141**: 1-199, 89 fig., 10 pl.

MEDIONI, R., 1971.— Les formations liasiques des Oulad-Amor et du jbel Nador (Hauts Plateaux du Maroc oriental) et leurs relations avec les séries liasiques voisines. *Notes et Mémoires du Service géologique du Maroc, Rabat*, **31** (237): 17-27, 6 fig.

MEKAHLI, L., 1988.— *Le Jurassique inférieur et moyen de la partie occidentale du horst de Rhar-Roubane (Tlemcen, Algérie occidentale): stratigraphie, sédimentologie et cadre dynamique*. Diplôme de Magistère, Université d'Oran, Oran, Algérie: 1-246, 102 fig., 7 pl.

MEKAHLI, L., 1995.— *Hettangien-Bajocien supérieur des Monts des Ksour: biostratigraphie, sédimentologie, évolution paléogéographique et stratigraphie séquentielle*. Thèse Doctorat d'État, Université d'Oran, Oran, Algérie: 1-358, 67 fig., 49 pl.

MEKAHLI, L., 1998.— Hettangien-Bajocien inférieur des Monts des Ksour (Algérie). *Documents des Laboratoires de Géologie de Lyon*, **147**: 1-319, 67 fig, 49 pl.

Source : MNHN, Paris

MEKAHLI, L., ALMÉRAS, Y. & ELMI S., 1993.— Mise en évidence de l'Aalénien dans la "Dolomie de Deglène" (Monts de Rhar Roubane, Algérie occidentale) et comparaison avec ses équivalents latéraux ("Dolomie du Tenouchfi", "Dalle des Hauts-Plateaux"). *Comptes Rendus de l'Académie des Sciences, Paris*, **316**, II: 1-10, 3 fig.

MEKAHLI, L. & ELMI S., 1997.— Hiérarchisation et datation des discontinuités stratigraphiques du Jurassique inférieur et moyen dans les Monts des Ksour (Atlas saharien, Algérie) et l'enregistrement des événements sédimentaires, tectoniques et eustatiques. *Peri-Tethys Program Annual Meeting, Rabat*: 61-62.

MEKAHLI, L., ELMI, S. & ALMÉRAS, Y., 1994.— L'Oolithe ferrugineuse de Deglène (Bathonien inférieur, Monts de Rhar-Roubane, Algérie occidentale): biotope à brachiopodes situé sur les escarpements d'un bassin. *Séminaire national des Sciences de la Terre, Tlemcen*: 92-93.

MORTON, N., 1989.— Jurassic sequence stratigraphy in the Hebrides Basin, NW Scotland. *Marine and Petroleum Geology, London*, **6**: 243-260, 9 fig.

MORTON, N., 1990.— Tectonic and eustatic controls of Jurassic genetic sequences in the Hebrides basin, NW Scotland. *Bulletin de la Société géologique de France, Paris*, série 8, **6** (6): 1001-1010, 3 fig., 1 table

MOUTERDE, R., CATTANEO, G. & GELARD, J.P., 1997.— Nouvelles données paléontologiques sur le Lias du Djurdjura (Grande Kabylie, Algérie). *In*: B. PEYBERNES & J.P. VILA (eds), *Les marges téthysiennes d'Afrique du Nord*. Société géologique de France, Paris: 55.

MOUTERDE, R., ROCHA, R.B., RUGET, C. & TINTANT, H., 1979.— Faciès, biostratigraphie et paléogéographie du Jurassique portugais. *Ciências da Terra (U.N.L.), Lisboa*, **5**: 29-52, 20 fig.

NEHNAIH, L., 1996.— *Dynamique sédimentaire et diagenèse dans les séries du Lias supérieur-Dogger inférieur des Hauts-Plateaux septentrionaux et de la région de Taourirt (Maroc Nord-Oriental)*. Thèse 3ème cycle, Université de Rabat, Rabat, Maroc: 1-193, 67 fig., 3 tables

OLIVIER, P., DURAND-DELGA, M., MANIVIT, H., FEINBERG, H. & PEYBERNES, B., 1996.— Le substratum jurassique des flyschs maurétaniens de l'ouest de Maghrébides: l'unité de Ouareg (région de Targuist, Rif, Maroc). *Bulletin de la Société géologique de France, Paris*, **167** (5): 609-616, 5 fig.

OUALI-MEHADJI, A.E.K., 1995.— *Brachiopodes des Monts des Ksour (Bajocien supérieur, Bathonien inférieur) (Atlas saharien occidental, Algérie)*. Diplôme de Magistère, Université d'Oran, Oran, Algérie: 1-220, 90 fig., 15 tables, 2 pl.

PALLINI, G., 1986.— L'orizzonte a *Paltechioceras* del Lotharingiano superiore nella "Corniola" del Monte Catria, Appennino Marchigiano. *Comitato tentennio Raffaele Piccinini, Pesaro*, **1**: 119-120.

PARONA, C.F., 1896.— Contribuzione alla conoscenza delle Ammoniti liasiche di Lombardia. Parte I: Ammoniti del Lias inferiore del Saltrio. *Mémoire de la Société paléontologique suisse, Genève*, **23**: 1-15, 8 pl.

ROCH, E., 1950.— Histoire stratigraphique du Maroc. *Notes et Mémoires du Service géologique du Maroc, Rabat*, **80**: 1-435, 77 fig., 22 pl.

ROUSSELLE, B. & DROMART, G., 1996.— Partitions stratigraphiques des environnements et produits carbonatés dans l'Aalénien du Sud-Est de la France. *Bulletin de la Société géologique de France, Paris*, **167**, (3): 399-408.

SADKI, D., 1996.— Le Haut Atlas central (Maroc). Stratigraphie et paléontologie du Lias supérieur et du Dogger inférieur. Dynamique du bassin et des peuplements. *Documents des Laboratoires de Géologie de Lyon*, **142**: 1-245, 50 fig., 10 pl.

SEPTFONTAINE, M., 1984.— Biozonation (à l'aide des Foraminifères imperforés) de la plate-forme interne carbonatée liasique du Haut Atlas (Maroc). *Revue de Micropaléontologie, Paris*, **27**, 3: 209-229, 4 text. fig., 2 pl.

SEPTFONTAINE, M., 1985.— Les Foraminifères imperforés des milieux de plate-forme au Mésozoïque: détermination pratique, interprétation phylogénétique et utilisation biostratigraphique. *Revue de Micropaléontologie, Paris*, **23**, (3/4): 169-203.

SOUHEL, A., 1996.— Le Mésozoïque dans le Haut-Atlas de Béni-Mellal (Maroc). Stratigraphie, sédimentologie et évolution géodynamique. *Strata, Toulouse*, série 2 (mémoires), **27**: 1-249, 125 fig., 5 tables, 6 pl.

STUDER, M.A. & DU DRESNAY, R., 1980.— Déformations synsédimentaires en compression pendant le Lias supérieur et le Dogger, au Tizi n'Irhil (Haut Atlas central de Midelt, Maroc). *Bulletin de la Société géologique de France, Paris*, 7, **22** (3): 391-397, 7 fig.

TLILI, M., 1995.— *Le phénomène récifal du Bajocien de la bordure méridionale de l'Atlas saharien occidental (secteur d'Aïn Ouarka)*. Diplôme de Magistère, Université d'Oran, Oran, Algérie: 1-154, 48 fig., 10 pl.

UNDERHILL, J.R. & PARTINGTON, M.A., 1993.— Jurassic thermal doming and deflation in the North Sea: implications of the sequence stratigraphic evidence. *In*: J.R. PARKER (ed.), *Petroleum Geology of Northwestern Europe: Proceedings of the 4th Conference*. The Geological Society, London: 337-345, 5 fig.

VIALLY, R., LETOUZEY, J., BÉNARD, F., HADDADI, N., DESFORGES, G., ASKRI, H. & BOUDJEMA, A., 1994.— Basin inversion along the North African margin. The Saharan Atlas (Algeria). *In*: F. ROURE (ed.), *Peri-Tethyan Platforms: Proceeding of the IFP Peri-Tethys Research Conference held in Arles, France, March 23, 1993*. Technip, Paris: 79-118, 28 fig.

WARME, J.E., 1988.— Jurassic carbonate facies of the Central and Eastern High Atlas rift, Morocco. The Atlas system of Morocco, Studies on its geodynamic evolution. *Lectures and Notes in Earth-Sciences*, **15**: 169-200.

WARME, J.E., CREVELLO, P.D., HAZLETT, B.A., ATMANE, F. & BEN BOUZIANE, M., 1988.— *Evolution of the Jurassic High Atlas Rift, Morocco: transtension, structural and eustatic controls on carbonate facies, tectonic inversion*. Association of American of Petroleum Geologists, Mediterranean Basins Conference, Tulsa, field trip 9: I-1-4; II-1-8; III-1-8; IV-1-16; V-1-24, VI-1-6; VII-1-29: VIII-1-12; IX-1-44; X-1-42; XI-1-20.

WRIGHT, V.P. & WILSON, R.C.L., 1982.— *The Toarcian-Aalenian in Peniche, Portugal, A Field Guide with Sedimentological Logs*. The Open University, Department of Earth-Sciences, London: 1-16.

Source : MNHN, Paris

Source : MNHN, Paris

8

The Jurassic of the southern Levant. Biostratigraphy, palaeogeography and cyclic events

Francis HIRSCH [1], *Jean-Paul* BASSOULLET [2], *Élie* CARIOU [2], *Brian* CONWAY [1], *Howard R.* FELDMAN [3], *Lydia* GROSSOWICZ [1], *Avraham* HONIGSTEIN [1], *Ellis F.* OWEN [4] & *Amnon* ROSENFELD [1]

[1] Geological Survey of Israel, Malchei Yisraelstreet 30, 95501 Jerusalem, Israel

[2] Laboratoire de Géobiologie, Biochronologie et Paléontologie Humaine, Université de Poitiers, 40, avenue du Recteur Pineau, F-86022 Poitiers Cedex, France

[3] American Museum of Natural History, Department of Invertebrate Paleontology, Central Park, New York 10024, USA

[4] Natural History Museum, Cromwell Rd., London SW7 5BD, U.K.

ABSTRACT

During the Jurassic, the Levant was part of the Gondwanian Tethys platform-shelf. The palaeotectonic setting of the Levant consisted in relative lows and highs, controlled by differential rates of subsidence: the shallow Negev high in southern Israel (900-2000 m), the Maghara basin in northern Sinai (3000 m), the central Israel Judean embayment (3000 m), extending to south Antilebanon (Hermon), the northern platform of Galilee (1500-2000 m), extending to Lebanon and northern Syria. Clastics are the result of the wearing down of the Arabian Massif in the South and South East. Yet, thickening of the early Oxfordian shales in the offshore wells, points to derivation from some landmass in the West, now hidden below the Mediterranean. The Gevar'Am trough, alongside the present Levant-coast, formed during the Tithonian. Volcanics mark the beginning and end of the Jurassic (Asher at 197 my and Tayasir from 140 my onward). The stratigraphic sequence consists at its base of lateritic palaeosols (Mishhor formation). Marine deposition set in during Pliensbachian times. In the North, monotonous platform carbonates (Haifa formation) are interrupted by the Oxfordian volcanics of Devorah. To the South, the fluviatile clastic intervals of the Toarcian - Aalenian (Inmar formation) and Bathonian (Sherif formation) characterize the Negev facies. Shales (Karmon formation) straddle the Bathonian - Callovian limit. A middle - late Callovian hiatus occurs in the Coastal plain. The deposition of Oxfordian shales (Majdal Shams formation) is restricted to the basins of North Sinai, central Israel to south Antilebanon (Judean embayement). Late Jurassic bioherms and reefs (Nir'Am formation) form a belt along the coastal plain area. In the Kimmeridgian, oolitic facies, shales and occasional sands recur (Nahar Sa'ar formation). The Tayasir volcanics and Gevar'Am turbidites cover a truncation surface.

HIRSCH, F., BASSOULLET, J. P., CARIOU, É., CONWAY, B., FELDMAN, H. R., GROSSOWICZ, L., HONIGSTEIN, A., OWEN, E. F. & ROSENFELD, A., 1998. — The Jurassic of the southern Levant. Biostratigraphy, palaeogeography and cyclic events. *In* : S. CRASQUIN-SOLEAU & É. BARRIER (eds), Peri-Tethys Memoir 4: epicratonic basins of Peri-Tethyan platforms, *Mém. Mus. natn. Hist. nat.*, **179** : 213-235. Paris ISBN : 2-85653-518-4.

Source : MNHN, Paris

RÉSUMÉ

Le Jurassique du sud Levant. Biostratigraphie, paléogéographie et cycles sédimentaires.

Durant le Jurassique, la région du Levant faisait partie de la plate-forme nord gondwanienne de la Téthys. La subsidence varie selon les régions considérées. On distingue dans le Sud d'Israël, le haut fond du Negev (900 - 2000 m) ; dans le Sinaï le bassin de Maghara (3000 m) ; au centre d'Israël le bassin de la baie de Judée (3000 m), prolongé jusqu'à l'Antiliban (Hermon) ; la plate-forme septentrionale de la Galilée (1500 - 2000 m) qui s'étend au Liban et au Nord de la Syrie. L'essentiel des apports clastiques provient de l'érosion du Massif arabe au Sud et au Sud-Est. Cependant, l'épaississement des shales oxfordiens dans les sondages offshore traduisent vraisemblablement l'existence d'une terre émergée située en Méditerranée. Au Tithonien, la fosse de Gevar'Am s'individualise parallèlement à la côte actuelle du Levant. Le début et la fin du Jurassique sont marqués par des épisodes volcaniques (Asher à 194 Ma et Tayasir à partir de 140 Ma). La succession lithologique est la suivante. Succédant à des dépôts latéritiques (formation de Mishhor), à la base du Jurassique, le régime marin s'établit au Pliensbachien. Au Nord, se déposent des calcaires monotones de plates-formes (formation de Haifa), interrompus à l'Oxfordien par l'épisode volcanique de Devorah. Vers le sud, des grès fluviatiles s'intercalent dans les intervalles Toarcien-Aalénien (formation de Inmar) et Bathonien (formation de Sherif). La limite Bathonien-Callovien est marquée par le dépôt de shales (formation de Karmon). Dans la plaine côtière, on constate une lacune du Callovien moyen et supérieur. Les shales oxfordiens (formation de Majdal Shams) se sont déposés dans les bassins de Maghara, du centre d'Israël et dans la partie méridionale de l'Antiliban (baie de Judée). Au Jurassique supérieur, la formation corallienne de Nir'Am s'étire le long de la plaine côtière. Au Kimméridgien, des faciès oolitiques, des shales et parfois des sables caractérisent la formation de Nahar Sa'ar. L'épisode volcanique de Tayasir, et les turbidites de Gevar'Am, d'âge tithonien, reposent sur une troncature d'érosion.

INTRODUCTION

Since the monograph on the Jurassic of Israel and adjacent countries (PICARD & HIRSCH, 1987; HIRSCH & PICARD, 1988), contributions have been added, in the field of palaeontology and biostratigraphy: palynomorphs (CONWAY, 1990), brachiopods (FELDMAN, 1987 ; FELDMAN *et al.*, 1991), ostracods (ROSENFELD *et al.*, 1987a, 1987b, 1988, 1991), ammonites (CARIOU, this paper), foraminifera and algae (BASSOULLET & GROSSOWICZ, this paper). In the more general field of palaeogeography, interpretation of seismic profiles in the east Mediterranean Levantine basin and the drilling activity offshore the Sinai coast (HIRSCH *et al.*, 1995) have shed new light on the existence of a thick sedimentary succession, including the Jurassic.

The biostratigraphy of the Jurassic in the Levant often exhibits an endemic character, related to that of the southern Tethys shelf. The Jurassic succession of the Levant is well known from the boreholes in Israel and from the outcrops of Gebel Maghara (Sinai, Egypt), Makhtesh Ramon, Hamakhtesh Hagadol (Negev, Israel) and Mt. Hermon (Antilebanon). The Jurassic facies of the Levant shares its particularities with African, Apulian and Arabian shelf-platforms. Boreholes supply a good insight in the development of the Jurassic in the Levant, linking the over 2000 m of late Liassic to Kimmeridgian strata of Sinai, similar to the Negev series, to the 2500 m of Middle to Upper Jurassic strata of Mount Hermon, which give a good insight of the succession hurried under central Israel. The Jurassic of Lebanon ressembles the succession of northern Israel. The Lower and Middle Jurassic series in Makhtesh Ramon (central Negev) provides the stratotypes of the Mishhor, Ardon and Inmar formations. The Middle - Upper Jurassic part of the Zohar formation and the late Callovian Matmor formation are exposed in Hamakhtesh Hagadol (northern Negev). The latter represents a unique facies of the late Callovian in the Middle East. The almost complete Middle to Upper Jurassic of Mount Hermon (Antilebanon) exposes the Hermon, Majdal Shams and Nahar Sa'ar formations. The latter, also exposed in eastern Samaria, is unconformably covered by the Tayasir volcanics.

The following sections were selected in the present study: the northern Israel Devorah borehole (I), the Hermon exposure and the southern coastal plain Helez-Deep borehole (II); the northern Negev Kurnub borehole and Hamakhtesh Hagadol exposure and western Negev Qeren borehole (III) and the northern Sinai Hallal borhole and Maghara exposure (Figs 1 and 2). In the stratigraphic subdivision of Israel, the Jurassic is comprised within the Arad group. The present review attempts to reduce the number of formations to units, well defined in exposed stratotypes, though in a few cases subsurface units, exposed nowhere, had to be retained (marked by *):

Mishhor, Asher*, Ardon, Inmar, Qeren, Haifa*, Daya*, Sherif*, Hermon, Zohar, Matmor, Niram*, Majdal Shams, Nahar Sa'ar and Gevar'Am*.

Source : MNHN, Paris

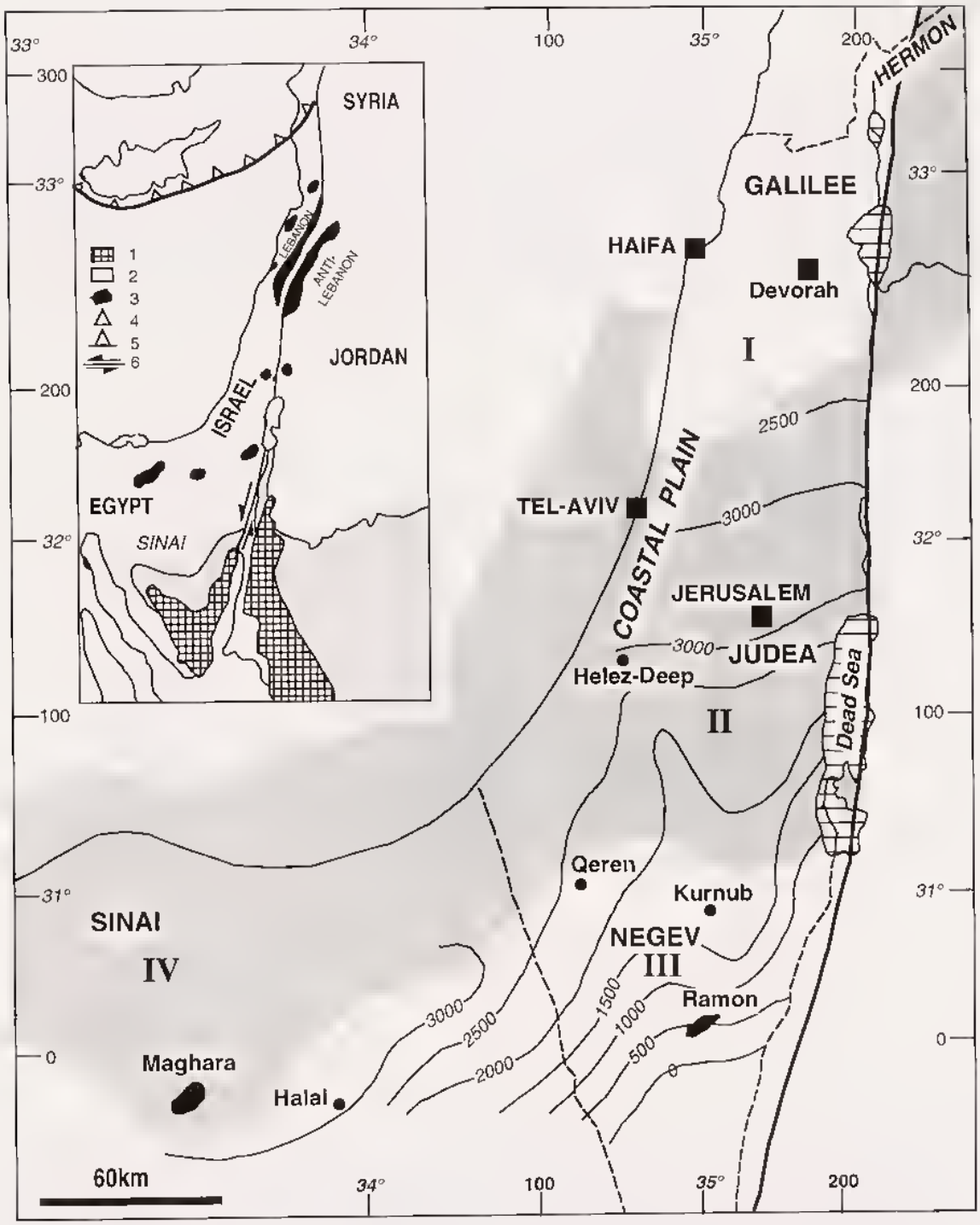

FIG. 1.— Location map and reference map to the Levantine countries. **1**, Precambrian; **2**, Palaeozoic- Triassic; **3**, Jurassic; **4**, Mount Hermon; **5**, Alpine thrust-front; **6**, Neogene sinistral transform. (I) Galilee High; (II) Judean embayement; (III) Negev High: (IV) Sinai Deep, with extension of lower Oxfordian Majdal Shams shales (shaded area) and total Jurassic isopachs.

*FIG. 1.— Carte de situation et de référence de la région levantine. **1**, Précambrien ; 2, Paléozoïque-Trias ; 3, Jurassique ; 4, Mont Hermon ; 5, chevauchement alpin ; 6, transformante sénestre Néogène. (I) Haut fond de Galilée ; (II) Baie de Judée ; (III) Haut fond du Negev ; (IV) Bassin du Sinaï ; Isopaques du Jurassique ; (en grisé) les shales oxfordiens de Majdal Shams.*

Source : MNHN, Paris

STRATIGRAPHIC OVERVIEW

LIASSIC

The Mishhor formation (GOLDBERG, 1969) consists of a bauxitic-lateritic palaeosoil and flint clays, resting on an eroded Triassic landsurface. Its average thickness does not surpass 50 m. In the North of the country it is replaced by the Asher volcanics. In the northern Sinai (Egypt) borehole of Gebel Halal, 500 m of red marls, some dolomites and sands of Norian (*Granuloperculatipollis rudis* Van Erve, 1977) through early Liassic (*Araucariasites australis* Van Erve, 1977) underley the typical Mishhor pisolites and red clays. Normally the Mishhor formation overlies a karstic surface leaching the Carnian Mohilla or Noro-Rhaetian Shefayim formation Ga'ash borehole).

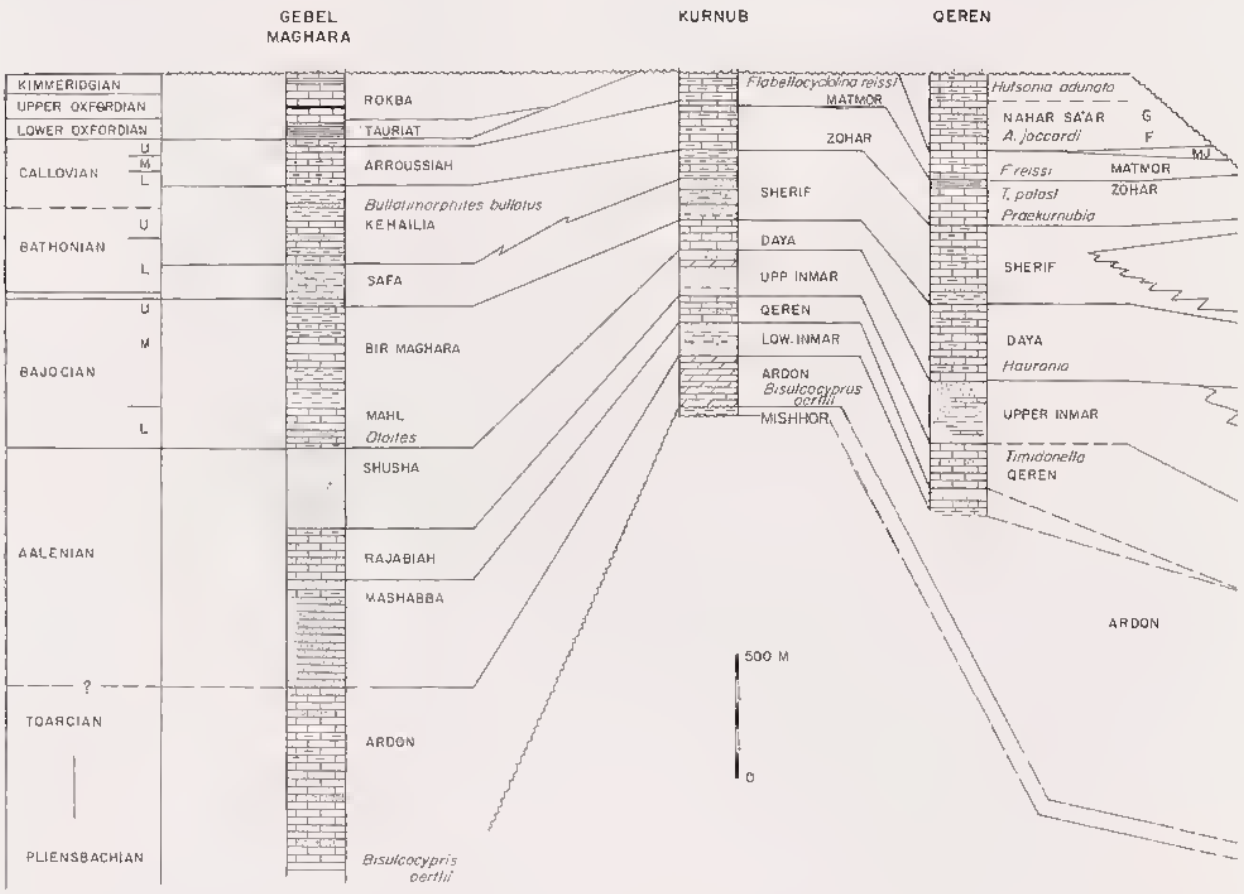

FIG. 2.— Stratigraphic sections. (I) Galilee High Devorah: the Liassic Asher volcanics are covered by the Middle Jurassic carbonatic Haifa formation, the volcanic Devorah tuffs, interstratified within the Oxfordian, followed by the Oxfordian - Kimmeridgan Nahar Sa'ar formation. (II) Judean embayment Helez - Hermon: in the Helez borehole, the Liassic Mishhor laterites are followed by Pliensbachian -Toarcian carbonates (Ardon). In the Ramallah borehole Aalenian carbonates (Qeren) directly overlie the Mishhor laterites. Middle Jurassic is primarely represented by carbonates of Haifa - Hermon type. The lower Oxfordian is characterized by the development of the Oxfordian Majdal Shams shales, which extend to the NW Negev and Sinai (Egypt). (III) Negev High (Kurnub- Qeren): The Negev section is characterized by numerous clastics in the Kurnub borehole, becoming more carbonatic toward the Qeren borehole. The Liassic consists of the Mishhor and Ardon formations. The Aalenian Inmar formation is split by the Qeren carbonates. The Middle Jurassic is diversified, comprising the Daya, Sherif, Zohar and Matmor formations. The Upper Jurassic is truncated in Kurnub, its development being well represented at Qeren by the Nahar Sa'ar formation. (IV) Maghara Deep: Gebel Maghara exposure and Halal borehole: In the more clastic succession of the Maghara Deep, the Negev units are still well represented, thought the total thickness has more than doubled. A-G : palynozones (after CONWAY, 1990).

Source : MNHN, Paris

The Asher volcanics in northern Israel (Atlit, Haifa, Asher and Devora) consist of basalt, agglomerates and tuffs (with few thin dolomite and shale interbeds), of 200-180 Ma (LANG & STEINITZ, 1989). The unusual thick basalt with enclaves of ?Triassic and Jurassic limestones and shales in Atlit suggests a Late Triassic-early Liassic Graben-like trough over 4000 m deep.

The Ardon formation (NEVO, 1963) overlies the Mishhor formation. At Ramon, up to 50 m of marly sandstones, sandy shales and sandy dolomites with algal mats and small molluscs represent a proximal nearshore facies. To the north and west the formation develops into hundreds of meters of shallow carbonates with evaporites. In the lowest section of the Ardon formation the foraminifer *Orbitopsella primaeva* (Henson), a Pliensbachian taxon occurs. The upper section of the Ardon formation is assumed to be mostly Toarcian. In the Hallal borehole (Sinai, Egypt) the Ardon formation reaches a thickness of almost 800 m.

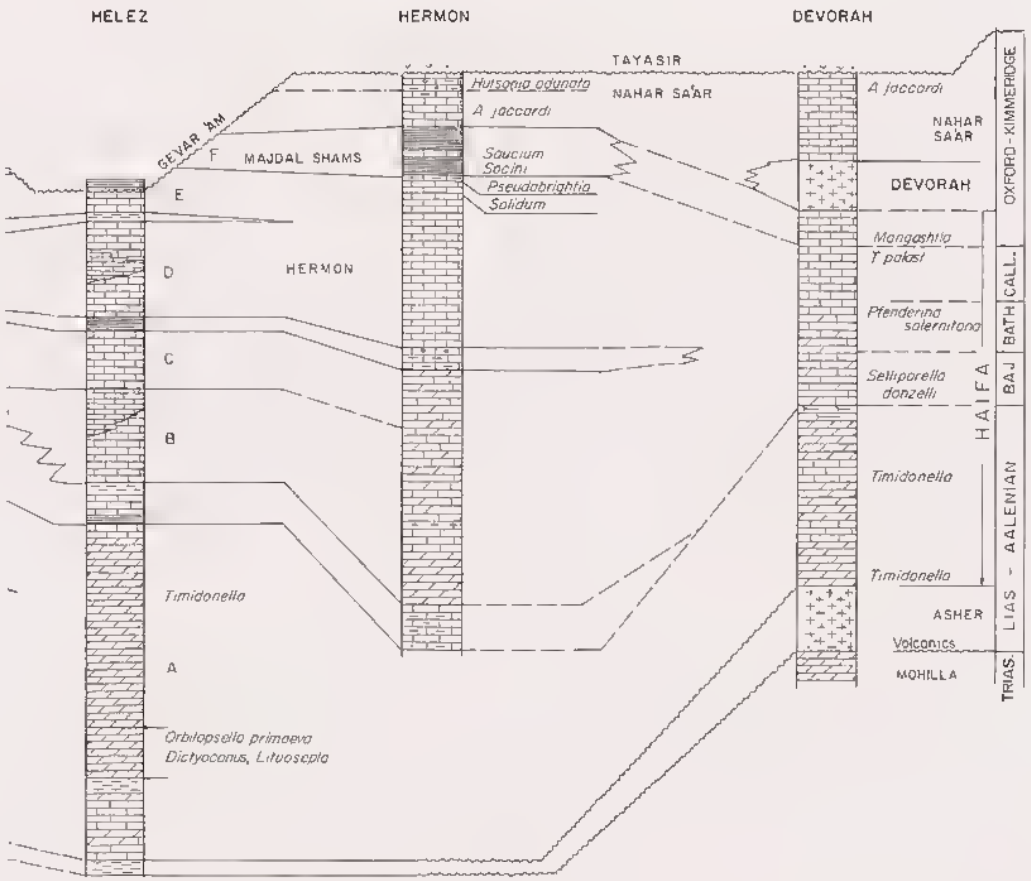

FIG. 2.— Coupes stratigraphiques. (I) Plate-forme de Galilée : les roches volcaniques de Asher sont recouvertes par la formation carbonatée de Haifa, les tufs volcaniques de Devorah interstratifiés à l'Oxfordien et la formation oxfordo-kimmeridgienne de Nahar Sa'ar. (II) La Baie de Judée de Helez à Hermon : dans le forage de Helez, les latérites liasiques de Mishhor sont suivies des carbonates du Pliensbachien-Toarcien (Ardon). Dans le forage de Ramallah, les carbonates de l'Aalénien (Qeren) reposent directement sur les latérites du Mishhor. Le Jurassique moyen est représenté par les carbonates du type Haifa - Hermon. L'Oxfordien se caractérise par le développement des marnes oxfordiennes de Majdal Shams, qui s'étendent au nord-ouest du Negnev et au Sinaï (Égypte). (III) Haut-fond du Negnev (Kurnub-Qeren) : la coupe du Negnev se distingue par son abondance en roches clastiques dans le sondage de Kurnub, devenant plus carbonaté en direction de Qeren. A l'Aalénien, les carbonates de Qeren s'imbriquent dans la formation de Inmar. Le Jurassique moyen est diversifié et comprend les formations de Dayn, Sherif, Zohar et Matmor. Le Jurassique supérieur est tronqué à Kurnub tandis que dans le sondage de Qeren la formation de Nahar Sa'ar est bien développée. (IV) Bassin de Maghara : dans la coupe du Gebel Maghara et du sondage de Hallal (Sinaï), les unités du Negnev sont représentées, tandis que leur épaisseur totale est doublée. A-G : palynozones (d'après CONWAY, 1990).

Source : MNHN, Paris

MIDDLE JURASSIC

From the northern coastal plain (Ga'ash) to the north (Carmel, Galilee and Lebanon) over 1000 m of dolomicrites, occasionaly anhydritic, build up an undifferenciated Aalenian to Oxfordian succession of the Haifa formation (DERIN, 1974). The Aalenian interval of the Haifa formation is characterized by the foraminifer *Timidonella* sp. The Bajocian interval contains *Haurania* and the Bathonian interval *Paleopfenderina salernitana* Sartoni & Crescenti. The Callovian is represented by a lower interval characterized by an assemblage of *Kilianina* sp., and an upper interval with *Trocholina palasteniensis* Henson, 1948. The uppermost part of the uniform sedimentary regime of the Haifa formation comprises micrites yielding the algae *Pseudoclypeina* and the foraminifer *Levantinella egyptiensis* (FOURCADE *et al.*, 1983) (ex *Manghastia*) of questionable late Callovian - early Oxfordian age.

AALENIAN

The Inmar formation (NEVO, 1963), consisting of cross-bedded sandstones, interbedded with kaolinitic clays, coally flint- clays and alunite horizons (GOLDBERY, 1982) was compared by LORCH (1967) with the Aalenian Yorkshire lower estuarine beds. A thin marine intercallation at Ramon yields Toarcian brachiopods (PARNES, 1980) and separates further North and West the Inmar clastics into a lower and upper part. This marine intercallation, known as the Qeren formation (GOLDBERG, 1964), consists of carbonates that in the boreholes west of Ramon, interwedge the fluvio aeolian -deltaic Inmar clastics, replacing gradually the clastic lower part of the Inmar formation until it merges with the underlying Ardon carbonates. These pelbiomicrites, oosparites and dolomicrites yield the Aalenian - lower Bajocian foraminifer *Timidonella* sp. (Bassoullet) accompanied in the oolitic shoals at Helez by *Dictyoconus cayeuxi* (Lucas) of the same age. At Maghara, an ammonite fragment was attributed to *Grammoceras* or *Sonninia*, confering a Toarcian-Aalenian age to the Qeren formation (ARKELL, 1956). In the Negev boreholes (Qeren, Makhtesh Qatan, Kurnub, Daya, Barbur, Boqer, Rekhme) and Sinai (Halal) the upper part of the Inmar formation consists of sandstones and shales. The Inmar formation passes from predominantly continental in Ramon to shallow marine to the west and north, consisting of shaly marls (Rosh Pinna) with ostracods and calcareous nannoplancton (MOSHKOVITZ & EHRLICH, 1976). Further west and north the Inmar facies wedges entirely out, replaced by the carbonate facies of the Haifa formation.

BAJOCIAN

Nearly 100 m of marine cross-bedded sands with ripple marks, ferruginous oolitic dolomites and plantiferous shales yield late middle and late Bajocian ammonites at Ramon (PARNES, 1981). The arenaceous facies of the central Negev develops into the foremostly carbonatic facies of the Daya formation (ELIEZRI *in* COATES *et al.*, 1963) of the Negev boreholes, which is defined by the foraminifer *Haurania*. It reaches in the Hermon section over 900 m of carbonates with volcanic intercalations.

In central Israel, the coastal plain and Judea, oosparites (Sederot facies) and micrites replcted with poriferan spiculae (Barnea facies) may reach up to 400 m. Differing from the latter, the marly 500 m of the Mahl and Bir Maghara formations (AL FAR, 1966) in North Sinai, yield a plantiferous clastic succession of shaly limestone, shales, shaly sandstone and coal streaks, followed by massive oo-oncolitic coralline limestones, interstratified by thick marls and shales, rich in ammonoids (DOUVILLE, 1916; ARKELL, 1952, 1956; PARNES, 1981), topped by black shales, from which the ammonite *Thambites planus* Arkell 1956 was determined (PARNES, 1981).

On the Syrian side of the Hermon, the 170 m medium - to fine-bedded oolitic organo-clastic, ochreous-stained limestone (J2bt) yield brachiopods and bivalves (RAZVALYAEV, 1966). These "calcaires ocres" (VAUTRIN, 1934) may correspond to a shaly horizon, interwedgind the oosparites and spiculites of the Sederot and Barnea facies, close to the Bajocian-Bathonian boundary in the southern coastal plain, around Helez (DERIN, 1974).

Source : MNHN, Paris

Bathonian

In most of the Negev boreholes, the Sherif formation (Eltezrt *in* Coates *et al.*, 1963) consists of alternating sandstone, shale, pelmicritic and some sparitic limestone. The more shaly upper part of the Sherif formation corresponds in the coastal plain and northenmost Negev to shales, rich in calcareous nannoplancton, ostracods and foraminifers of late Bathonian - early Callovian age. The lower part of the Sherif formation consists at Gebel Maghara of cross-bedded hematitic stained sandstones alternating with limonitic shales with abundant plant remains and several coal-seams (Safa formation). The upper part of the Sherif formation encompasses thin oolitic limestone with frequent shale and occasional thin sandstone beds (Kehailia formation). The ammonite *Micromphalites pustuliferus* (Douv.) in its lower part belongs to the early Bathonian. The shaley-carbonatic upper part yields *Bullatimorphites bullatus* (d'Orb.), indicating the upper Bathonian or lower Callovian.

The bright bluish-grey limestones and dolomites of the Hermon formation (Dubertret, 1960) with corals and brachiopods, that attain 700 m, are for Razvalyaev (1966) and Kutznetsova & Dobrova (1995) entirely of Callovian age (J2Cl). For Dertn (*in* Goldberg, 1969), the lower 600 m of the Hermon formation is equivalent to the Bathonian interval of the subsurface Haifa formation.

Callovian

The alternating limestone, marl and shale series that was identified in the northern Negev boreholes as the Zohar formation (Coates *et al.*, 1963) belongs entirely to the Callovian. The upper half of the Zohar formation is well exposed at Hamakhtesh Hagadol (Kurnub). It consists in its lower part of stromatoporoid and coral limestone, shale and sandstone, marl and limestone, placed in the middle Callovian coronatum Zone (Gill & Tintant, 1975; Gill *et al.*, 1985). Its upper part of alternating marl, limestone and shale, is placed in the late Callovian athleta Zone (Gtll & Tintant, 1975 and Lewy, 1983). The section at Hamakhtesh Hagadol, above the Zohar formation, consists of the alternating limestone and marl of the Matmor formation (Goldberg, 1963; emend. Hirsch & Roded, 1996). Its lower part yields ammonites of the late Callovian athleta Zone (Gill & Tintant, 1975; Lewy, 1983), with a bivalve and gastropod fauna still similar to that found in the Zohar formation. The upper part of the Matmor formation consists of an oolite near base, alternating yellow shales, white reefoidal and lagunar limestones. In its fauna of large bivalves and gastropods, the genera *Purpuroidea* and *Eunerinea* (Htrsch, 1979) show affinities with European Oxfordian taxa. The ammonite *Peltoceras solidum* Spath still belongs into the late Callovian athleta Zone, whereas *Psendobrightia* sp. puts the uppermost interval to the late Callovian lamberti Zone. This interval also yields the foraminifera *Flabellocyclolina reissi* Hottinger and *Kurnubia* gr. *palastiniensis* Henson. The Matmor formation occurs in the boreholes of the NW Negev and NE Sinai, among which Hallal (Sinai) and Qeren (Negev).

The upper 100 m of the Hermon formation also consist of massive limestone and yield foraminifera of Callovian age. Along the S-E slopes of Mount Hermon, the uppermost part of the Hermon formation consists of alternating limestone and marl beds that yield abundant late Callovian belemnites, bivalves and ammonites. Only a reduced, truncated Callovian interval is found in the coastal plain of Israel.

Upper Jurasstc

A reefoidal facies of biolithites of stromatoporoidea, corals, porifers and bryozoans occurs under the coastal plain around Caesarea and in the Kokhav field is identified as the Nir Am formation (Dertn, 1974). In the Beer Yaakov, Gerar, Kfar Darom, Nirim, and Kissufim wells it overlies thin Majdal Shams shales. The position of the Nir Am formation, between Hermon and Gevar Am formations confers probably a mostly Oxfordian age to this formation, that reaches a thickness of 400 m in the Carmel borehole.

Source : MNHN, Paris

LOWER - MIDDLE OXFORDIAN

The Majdal Shams formation (SALTZMAN *et al.*, 1968) (200 m) consists of fossiliferous shales at base, platy limestones and silicasites at top. The shales, with limonitic concretions, are interbedded by marls and occasional thin limestone or dolomitic beds. The basal beds are extremely rich in small pyritized ammonites, identified since NOETLING (1887) as the early Oxfordian Brightia socini zone, put by ARKELL (1956) to the "Mariae" Zone. In his monography, HAAS (1955) studied 7600 ammonites from Majdal Shams, the exact level of which, within the 43 m thick lower marls, was retrieved by the bed by bed collection reported by RAZVALYAEV (1966). The nuculide bivalve infaunal mobile detritus feeders confirm the statement of HAAS that the paramount darkish shale facies with pyritic dwarf forms intimate to less aerated depositional environment - remarkably also occurring in the Renggeri Zone with equal lithofacies in Switzerland, England and southern Russia. Vautrin's overlying "Lusitanian" consist of argillaceous marls and yellow limestone intercalated by marls holding fossils that ARKELL (1956) puts to the Transversarium Zone. RAZVALYAEV (1966) puts the upper pelitomorphic limestones and alternating dark marls "most probably to the Bimammatum Zone". The shale interval of the Majdal Shams formation is present in the Israeli subsurface and in the nearly 70 m Tauriat shale of Gebel Maghara (Sinai, Egypt). Thin bedded dark platy limestones with marl interbeds and a "tripoli"-like yellow silicatic ledge of spiculitic limestone close the succession of the Majadal Shams formation in the Hermon section. The dark highly pyritic shale with nodules and pyritised fossils, interbedded with few limestones or dolomites (GOLDBERG & FRIEDMAN, 1974) that overlie the Zohar carbonates in the Zohar-Kidod gas-field and in the coastal plain Helez-Kokhav oil-field, was termed "Kidod" by COATES *et al.* (1963), a term largely followed by exploration geologists. The unequivocal early Oxfordian age (Mariae Zone) of these shales on the base of ammonite-biostratigraphic data (LEWY, 1983; RAZVALYAEV, 1966) in the exposures of Gebel Maghara (Sinai, Egypt) and Majdal Shams (Mt. Hermon) was emphasized by PICARD & HIRSCH (1987) and HIRSCH (1996). These shales are absent in the area of Hamakhtesh Hagadol and boreholes of Qeren, Rehkme, Boqer and Gebel Hallal.

In many coastal plain wells, early Oxfordian shales rest directly on the thin calcarenite of the lower Zohar formation (Callovian), showing karstification (GOLDBERG & BOGOSH, 1978; BUCHBINDER, 1981).

The Majdal Shams formation reaches over 200 m in Central Israel (from the Helez Area eastwards to Judea and Jordan Valley). In most of the Northern Negev and Northern Sinai, it is reduced to an average of 100 m. In the offshore borehole of Delta-1, NW of Caesarea, a 200 m serie is still present, comprising a carbonitic upper and shaley lower section. The 80 m lower section consists foremostly of black and green shales rich in dinoflagellates, spores and coccolithes (MOSHKOVITZ & EHRLICH, 1980; COUSMINER & CONWAY, 1990), of early Oxfordian age. Fragments of volcanics and of bio-intrasparites were interpreted by FRIEDMAN *et al.* (1971) as cobbles or pebbles deriving from the shelf edge and transported by turbitity currents into the depositional area of mudstone called "Delta facies".

No trace of Oxfordian has been left in the larger and deep erosionfunnel around the Helez wells (Barnea, Gevar Am, Helez, Talme Yafe).

UPPER OXFORDIAN - KIMMERIDGIAN

The uppermost part of the Hermon section exposes along its SE flank the succession, totalizing up to 180 m. of the Nahar Sa'ar formation (SALZTMAN *et al.*, 1968). The echinoid limestone at base consists of ca. 40 m of massive limestones, yielding abundant spines as well as a few complete specimens of the echinoid *Balanocidaris glandifera* Muenster, for which a late Oxfordian - early Kimmeridgian age is attributed by the foraminifer *Alveosepta jaccardi* (Schrodt, 1894) (DERIN, 1974). Follow 140 m of well bedded yellow oolites, fossiliferous marls, with a massive limestone and more shale in its upper part at Wadi E Shatr, yielding the indicative ostracod *Hutsonia adunata* Bischoff, 1990 (ROSENFELD & HONIGSTEIN, this paper). RAZVALYAEV (1966) reports from dark-grey limestone and clayey limestone the brachiopods *Septaliphoria jordanica* (Noetling), *Somalirhynchia africana* Weir, and *S. somalica* Daque.

Source : MNHN, Paris

The lower subdivision correlates with 90 m of massive limestone rich in echinoid radioles in Lebanon, the flinty limestone, interstratified with yellow marls at Gebel Rokba at Gebel Maghara (Sinai, Egypt). The upper subdivision is equivalent to a much thicker succession in Lebanon (DUBERTRET, 1975). There the 80 m of brown to yellow oolitic limestones and marls of the "couches jaunes inférieures" or "couches d'Azour", still with *Alveosepta jaccardi* (Schrodt, 1894), represent a lower unit. Interwedged at this level, occurs the 180 m thick Bhannes volcanic complex, consisting of basaltic sheets and weathered pillows, volcanic tuffs interfingered by lignitiferous and marls alternating with thin limestones. Follows the middle unit of the limestone ledge of the "falaise de Bikfaya" and the upper unit of the "couches jaunes supérieures" or "couches de Salima" in which BISCHOFF (1964) mentions *Berriasella richteri* (Opp.), an upper Tithonian form for ARKELL (1956). The subsurface succession of the Nahar Sa'ar formation is subdivided in the lower massive limestone of the Beersheba formation (COATES *et al.*, 1963), followed by the oolite, shale and sand succession of the Haluza formation (COATES *et al.*, 1963). The foraminifer *Alveosepta jaccardi* (Schrodt, 1894) confers a late Oxfordian - early Kimmeridgian age to the lower 2 thirds of this section. In the Devora borehole of Galilee interformational volcanics occur. A younger unit, consisting of the upper massive carbonate ledge, the so-called Haifa Bay formation (DERIN, 1974), apparently equivalent to the Lebanon "falaise de Bikfaya", was identified in the northernmost Israel boreholes (Haifa Bay, Hazon, Hula). This ledge is, thought reduced in thickness, also found in the NW Negev boreholes (Qeren, Haluza), consisting of carbonates associated with *Campbeliella striata* Carozzi and *Alveosepta jaccardi personata* Tobler, 1928, confering a Kimmeridgian age to this part of the formation. Such an age can now also be attributed on the base of the ostracod *Hutsonia adunata* Bischoff, 1990, found in Lebanon in the Salima Formation and topmost part of the Nahl Sa'ar formation at Ein Qinia (Hermon).

TITHONIAN

Generally regarded as a Lower Cretaceous unit (Beriassian - Hauterivian), the gray dark sandy shales Gevar Am formation (DERIN & REISS, 1966), in borehole Negba-1 (from a core) yielded ammonites of Late Jurassic (Tithonian) affinity (RAAB, 1962). This assumption is strenghtened by the finding by MOSHKOVITZ & EHRLICH (1980) of *Conusphaera mexicana* Trejo, 1969 in the Gevar Am formation of offshore well Delta-1. Recently DE HAAN (1997) found Late Jurassic palynofloras in the Gevar Am shales of a number of wells of the coastal plain.

BIOSTRATIGRAPHY

The biostratigraphy of the Jurassic of Israel has been reviewed by PICARD & HIRSCH (1987). It is originally based on ammonites (PARNES, 1981; LEWY, 1983; GILL *et al.*, 1985), calcareous nannoplankton (MOSHKOVITZ & EHRLICH, 1976), foraminifers, algae and ostracods (MAYNC, 1966; DERIN, 1974), bivalvia and gastropods (HIRSCH, 1979), and palynomorphs (pollen, spores, dinocysts and acritarchs) (CONWAY, 1990). In the present paper, substantial additions are presented on ammonites, palynomorphs, ostracods, brachiopods and foraminifers.

AMMONITES

The zonal subdivision proposed by PARNES (1981) was revised by ENAY & MANGOLD (1994). The Jurassic of Israel and of the Hermon (south Antilebanon) belong palaeogeographically to the Arabian platform (HIRSCH, 1976; DERCOURT *et al.*, 1993).

PROVINCIALISM

Ecologic constraints particular to such a large and shallow area as the Arabian Platform, gave ammonites a markable endemic inprint (GILL *et al.*, 1985; ENAY *et al.*, 1987). This provincialism is the cause of difficulties in the establishment of a precise stratigraphic correlation with european reference sequences.

Source : MNHN, Paris

The proposed biostratigraphy uses species of the arabian bioma (ENAY & MANGOLD, 1994) at the level of sub-zones. The establishment of a stratigraphic correlation with the european standard is based on taxa common to both provinces. These are in general rather rare, or even absent, due to ecological or sedimentary (hiatus) reasons. Such conditions prevail generally in the Jurassic of Israel and the Hermon, with the exception of the transgressive pyritic ammonite bearing marls of the lower Oxfordian. This short timespan of very relative opening of the Arabian platform edge to the pelagic Tethys- platforms cased the comming in of Mediterrancan Tethyan taxa, enabling stratigraphic correlation with Europe. However, even during the lower Oxfordian, the confinement of the ammonite- population remained strong, characterised by the dominance of Hecticoceratinae, with forms specific to the region. As a result, a sample of 340 specimens from the basal level of the marls. was composed of 96 % Hecticoceratinae, 1% Aspidoceratinae, 1% Perisphinctinae and less than 1% Phylloceratinae. Due to this provincialism the proposed correlations (Table 1) remains necesseraly approximative.

BIOSTRATIGRAPHY

The zonal subdivision for the Hermon, Negev and northern Sinai proposed by PARNES (1981), LEWY (1983) and GILL *et al.* (1985), is now revised on the base of the subdivision for Arabia proposed by ENAY & MANGOLD (1994).

The late Bajocian age of *Thambites planus* Arkell, 1956 and the early Bathonian age of *Micromphalites* were proposed by ENAY & MANGOLD (1994) and differ from PARNES's original assumption. The presence of genuine middle Callovian (Coronatum zone) and late Callovian (Athleta and Lamberti Zones) is now clearly established at Hamakhtesh Hagadol. The Lamberti Zone is also well represented at Majdal Shams, encompassing numerous ammonites.

New biostratigraphic results were obtained in the Callovian and Oxfordian stages.

LATE CALLOVIAN.— Athleta Zone:

May be subdivided into two subzones, using indo-malagachy and/or arabian rather than the submediterranean index-species (GILL *et al.*, 1985):

— Pachycymnoceras sp. Subzone: The association comprises *Kurnubiella compressa* Gill, Thierry & Tintant, *Peltoceras* sp. juv., *Collotia* sp. and *Reineckeia nodosa* Till. *Pachycymnoceras* sp. reaches with its living chamber a diameter of 190 mm. This relatively involute form belongs into the group of *Pachycymnoceras kuerense* Mang., which together with other species characterize the Trezcense Subzone in Algeria (MANGOLD, 1988). It differs from the Algerian species by a larger number of undivided ribs, becoming strong toward growth- end (10 on the last half whorl). This fauna is found between subunits 33 et 41 of the Hamaktesh Hagadol section of GOLDBERG (1963).

— Solidum Subzone: The Indian species *Peltoceras solidum* Spath was selected as index-species by ENAY & MANGOLD (1994) for Arabia. In Arabia, it occurs in the upper part (T3) of the Tuwaiq Limestone formation. An almost complete specimen was collected by LEWY in subunit 48 (GOLDBERG, 1963) at Hamaktesh Hagadol. The species is frequent toward the top of the Hermon Limestone.

"Lamberti" Zone:

— Pseudobrightia sp. horizon

The equivalent of the Lamberti Zone in the southern Antilbanon section of Majdal Shams is found at the top of the Hermon formation. A thin horizon (0.30 m thick) of condensed platy marly limestone with phosphatic grains is rich in ammonites, mostly flattened calcareous molds of Hecticoceratinae: *Pseudobrightia* sp., *Hecticoceras (Putealiceras) intermedium* (Spath), *H. (Kheraites) ferrugineus* (Spath), *H. (Brightia)* aff. *salvadorii* (P. & B.), *H. (Putealiceras) donvillei* (Jean.), *Pachycymnoceras levantineuse* Lewy. *Pseudobrightia s. st.* individualises itself at the base of the Lamberti Zone in Europe (CARIOU, 1984). The association found at the Hermon is of the same age, corresponding *pro parte* to the Poculum Subzone of the submediterranean province (CARIOU, 1973; CARIOU *et al.*, 1985). The specimen of *Pseudobrightia* (coll. F. HIRSCH) in the scree of subunit 74 (GOLDBERG, 1963), top of Matmor formation, at Hamaktesh Hagadol, is figurated as *Brightia* sp. (LEWY, 1983, Pl. 1, Figs 17-18). Consequently the top of the Matmor formation is still late Callovian and not early Oxfordian as assumed

Source : MNHN, Paris

before. It is interesting to note that the end-Callovian condensed outer platform limestones at Mt. Hermon express clearly a transgressive system tract, like the deposits of the same age in western Europe (RIOULT *et al.*, 1991).

LOWER OXFORDIAN.— The lower Oxfordian at the Hermon is represented by tens of m of marl with small pyritised ammonites (Majdal Shams formation). This facies ressembles the "*Creniceras renggeri* marls" of the Jura Range, with which it shares several species (ENAY, 1966), among which *Creniceras renggeri* (Opp.). The Hermon fauna, first described by NOETLING (1887) and globaly attributed to the Socini Zone, was described in greater detail by HAAS (1955), who correctly interprets the Socini Zone as the southern Tethys equivalent of the Mariae Zone. RAZVALYAEV (1966) gave a precise stratigraphic ammonite species distribution. FREBOLD (1928) has proposed a subdivision into 2 zones: the Hecticoceras socini Zone at the base and the Oecotraustes scaphitoides Zone at top. The outcrop conditions do not permit the continuous bed by bed collection. Two levels have delivered hundreds of *in sitn* pyritised ammonites, one 2.50 m thick, at the very base of the sequence, the other, less abundant, ca 40 m higher. The two assemblages are clearly distinct:

— Socini horizon: abundant *Hecticoceras socini* (Noet.), associated with *H. kantzschi* (Noet. *in* Haas), *H. separandum* Haas, *H. solare* Haas, *H. schumacheri* (Noet.), *H. chatillonense* de Lor., *H.* cf. *gnthei* (Noet.), *H. coelatum* Coquand, *Taramelliceras* cf. *langi* (de Lor.), *Enaspidoceras snbbabeannm* (Sintzow), *E. douvillei* (Collot), *E. subcostatum* (*in* Haas, non Spath), *Perisphinctes bernensis* de Lor., *Mirosphinctes* aff. *robyi* (de Lor.), *Sowerbyceras helios* (Noet.).

— Socium horizon: the very characteristic *Hecticoceras socinm* Haas is associated with *H. syriacum* Haas, *H. bonarelli* de Lor., *H. kantzschi* (Noet.), *Creniceras renggeri* (Op.), *Enaspidoceras* sp., *Properisphinctes* sp., *Mirosphinctes* sp.

Correlation of both horizons with Europe can be made on the base of comparison with figurated european forms, the stratigraphic distribution of which in the fold of the Mariae Zone is precisely known (SCHIRARDIN, 1958; GYGI, 1990; VIDIER *et al.*, 1993; FORTWENGLER *et al.*, in press).

TABLE 1.— Ammonite levels in the Levantine series and their probable equivalences with submediterranean Europe zonal scheme. The units with asterisk are new.

TABLEAU 1.— Niveaux à ammonites des séries du Levant et leurs équivalences probables avec le schéma de zonation d'Europe sub-méditerranéenne. Les unités avec un astérisque sont nouvelles.

EUROPE (SUBMEDITERRANEAN PROVINCE)				LEVANT
STAGE	SUBSTAGE	ZONES	SUBZONES	(characteristic ammonites)
TITHONIAN				*? Virgatosphinctes*
OXFORDIAN	MIDDLE	Plicatilis		*Enaspidoceras* gr. *peramatum*
		Cordatum		*? Peltoceratoides*
	LOWER	Mariae	Praecordatum	*Hecticoceras socinm**
			Scarburgense	*Hecticoceras socini*
CALLOVIAN	UPPER	Lamberti	Lamberti	
			Poculum	*Pseudobrightia* sp.*
		Athleta	Collotiformis	*Peltoceras solidum*
			Trezeense	*Pachyerymnoceras* sp.*
	MIDDLE	Coronatum		*Kurumbiella ogivalis*
EARLY CALLOVIAN - LATE BATHONIAN ?				*Bullatimorphites* cf. *bullatus*
BATHONIAN	LOWER	Zigzag		*Micromphalites*
BAJOCIAN	UPPER	Parkinsoni		*Thambites planus*
		Garantiana		*Ermoceras mogharense*
		Niortense		*Ermoceras rimcinanm*
		Laeviuscula		*Dorsetensia* *Otoites*

Source : MNHN, Paris

The Socini horizon is equivalent to the Scarburgense Subzone. The Socium horizon would represent the top of the Scarburgense Subzone and the Praecordatum Subzone.

PALYNOMORPHS

The zonation was established on the base of the first appearance of the Jurassic palynomorphs in Israel and their correlation with their occurence in other parts of the world.

?LATE PLIENSBACHIAN TO MIDDLE BAJOCIAN APPLANOPSIS TURBATUS ZONE.— Terrestrial palynomorphs belong to a floristic province extending across north Africa, Arabia and into Iran and Afghanistan. Boreal floras are dominated by coniferalean disaccate pollen, whereas, northern Gondwanean floras are subtropical, characterized by non-disaccate coniferalean pollen (*Corollina*, *Applanopsis*); as well as, Filiciales *incertae sedis* and Bennettitalean floral elements (LORCH, 1967; CONWAY, 1990), disaccate pollen are absent to rare. Poor floristic diversity and limited evolution (at least until late Oxfordian times) indicates strong climatic restrictions in the Levant province.

Strata from the Mishhor, Ardon, Inmar and Qeren formations, although some are marginally marine, contain dinocysts of the *Applanopsis turbatus* Zone (including *Nannoceratopsis pellucida* Deflandre, 1938 and *Dapsilidinium? deflandrei* (Valensi, 1947)) that correlate well with coeval boreal suites.

LATE BAJOCIAN KORYSTOCYSTA KETTONENSE ZONE (LATE BAJOCIAN) DICHADOGONYAULAX SELLWOODII ZONE (LATEST BAJOCIAN).— In Israel, Mid-Jurassic assemblages from shallow shelf depocentres indicate normal marine salinities, they are dominated by proximate dinocysts with epitractal archeopyles (*Dichadogonyaulax* and *Korystocysta*), together with small proximate cysts with apical archeopyles (*Ellipsoidictyum*, *Sentusidinium*). These elements typify Tethyan warm water faunas elsewhere. Despite this close affinity and not withstanding their limited diversity the assemblages correlate well with boreal assemblages. Differences on the species level are probably due to ecological factors. In the Negev, strata from the upper part of the Inmar and Daya formations contain the taxa defining this Zone. In northern and central Israel it defines a portion of the Haifa formation.

BATHONIAN: ENERGLYNIA ACCOLARIS ZONE.— There is a continuity of ecological conditions in the Levant. No major evolutional changes occur, ctenidodinoid elements remain dominant, as in Europe, and are reinforced by the entry of *Energlynia*. The skolochorate cyst *Systematophora* appears, whose achme is younger.

Low diversity characterizes Bathonian assemblages of Israel, similar assemblages occur in contemporaneous intervals from NE Spain, Portugal and in NE Libya (SARGEANT, 1976; FENTON *et al.*, 1980; THUSU & VIGRAN, 1985). Although boreal assemblages appear more diverse, provincialism is difficult to define, many taxa are widespread, even with global distribution. This zone defines the Sherif formation and coeval portions of the Haifa and Hermon formations.

CALLOVIAN: POLYSTEPHANEPHORUS CALATHUS ZONE.— In Israel; low diversity again characterizes Callovian assemblages, and elsewhere in the Tethyan realm. The most distinct change in warm neritic Late Jurassic dinocyst assemblages is the acme of skolochorate cysts (*Adnatosphaeridium*, *Compositosphaeridium*, *Emmetrocysta*, *Polystephanephorus*, *Surculosphaeridium* and *Systematophora*). There is a decline of ctenidodinoid elements and small proximate cysts with apical archeopyles (*Ellipsoidictyum*, *Sentusidinium*). Large gonyaulacoid cysts with precinglar archeoyples are scarce. The Zone defines the Zohar and Matmor formations as well as the corresponding interval of the Haifa formation.

OXFORDIAN: MILLIOUDODINIUM NUCIFORMIS ZONE (EARLY TO MIDDLE OXFORDIAN) AND EPIPLOSPHAERA RETICULOSPINOSA ZONE (MIDDLE TO LATE OXFORDIAN).— In Israel, Oxfordian assemblages indicate normal marine salinities and continue to be characterized by skolochorate cysts morphologically related to *Systematophora*, which are more numerous in the Tethyan realm. Cavate dinocysts are rarer than in boreal assemblages. These features indicate some degree of isolationism or provincialism, although, there are broad similarities with western Neotethyan suites in Europe, differences being largely at species level. There is a dramatic entry of large gonyaulacoid dinocysts (*Hystrichogonyaulax*, *Milliondodinium*) that rise to dominate Oxfordian assemblages of Israel. These

Source : MNHN, Paris

zones define the Majdal Shams and Nahar Sa'ar formations. The lower zone also defines an age-equivalent interval of the Haifa formation.

OSTRACODS

The data on Jurassic Ostracods that were described from Gebel Maghara (Sinai, Egypt), Makhtesh Ramon, Hamakhtesh Hagadol (Negev) and Majdal Shams (Hermon), are summarized herein (ROSENFELD *et al.*, 1987a, 1987b, 1988, 1991 and in press).

LOWER-MIDDLE LIASSIC BISULCOCYPRIS OERTLII ASSEMBLAGE ZONE.— At Makhtesh Ramon (south Israel) shales at the base of the Ardon formation yield the non-marine ostracods *Bisulcocypris oertlii* Gerry, *Fabanella ramonensis* Rosenfeld & Honigstein and *Laevicythere* sp. In drillings, the marine *Ektyphocythere* cf. *vitilis* (Apotolescu, Magne & Malmoustier) may set in, but not in the same layers as the nonmarine taxa, pointing to alternating environments of fresh-brackish water and shallow sea. The nonmarine fauna is endemic at the specific level, whereas the marine form shows european affinity.

TOARCIAN-AALENIAN EKTYPHOCYTHERE BUCKI ASSEMBLAGE ZONE.— At Gebel Maghara (Sinai, Egypt) the clastic upper Inmar formation yields frequent *Cytherella ? toarcensis* (Bizon), rare to common *Ektyphocythere bucki* (Bizon), *Isobythocypris ovalis* (Bate & Coleman) and *Praeschuleridea inmarensis* Rosenfeld & Gerry and *Kinkelina kadeshensis* Rosenfeld & Gerry. The environment of deposition was warm shallow marine. The assemblage shows affinities with european forms.

BAJOCIAN GLYPTOGATOCYTHERE MAGHARAENSIS ASSEMBLAGE ZONE.— In the shales, that alternate with the carbonates of the Daya formation at Gebel Maghara, the frequent *Glyptogatocythere magharaensis* Rosenfeld & Gerry and the common to rare *Cytherella bashai* Rosenfeld & Gerry, *Monoceratina striata* Triebel & Bartenstein, *Rutlandella transversiplicata* Bate & Coleman and *Ektyphocythere zerqaensis* Basha are characteristic and restricted to this assemblage zone, whereas *Glyptocythere hunicnsis* Basha and *Bairdia* aff. B Jones proceed higher. The environment of deposition was warm shallow marine, though *Monoceratina* indicates somewhat deepening of the facies. The assemblage still shows affinities with european forms, though more taxa and the dominant taxon are endemic (Israel, Jordan).

BATHONIAN PROGONOCYTHERE HONIGSTEINI - FASTIGATOCYTHERE BAKERI ASSEMBLAGE ZONE.— In the Sherif formation at Gebel Maghara, this assemblage zone is dominated by *Progonocythere honigsteini* Rosenfeld & Gerry, *Fastigatocythere bakeri* (Basha), *Praeschuleridea hornei* Rosenfeld & Gerry, and *Zerqacythere subiehensis* Basha. Further occur for the first time: *Glyptogatocythere malzi* Basha, *Ektyphocythere shulamitae* Rosenfeld & Gerry, *E. aardaensis* Basha and *Terquemula goldbergi* Rosenfeld & Gerry. The environment of deposition was warm shallow marine and faunal affinity remains dominantly provincial (Israel, Jordan).

CALLOVIAN EKTYPHOCYTHERE ZOHARENSIS ASSEMBLAGE ZONE.— In the rather rare shale intercalations of the Zohar formation at Gebel Maghara *Ektyphocythere zoharensis* Rosenfeld & Gerry and *Terquemula gublerae* (Bizon) are found. Throughout the Zohar and lower Matmor formations at Hamakhtesh Hagadol (Negev, Israel) an assemblage is found that comprises *E. zoharensis* Rosenfeld & Gerry, *Bairdia* aff. *hilda* Jones, *Afrocytheridea faveolata* Bate, *Progonocythere* aff. *parastilla* Whatley and *Micropneumatocythere laevireticulata* Rosenfeld & Honigstein. In the upper part of the Matmor formation, the assemblage of *E. zoharensis* Rosenfeld & Gerry has a different composition. Here, along with the taxa of the assemblage found below, now also appear *Exophthalmocythere? kidodensis* Rosenfeld & Gerry, *Mandelstamia hirschi* Rosenfeld & Honigstein, *Cytherella index* Oertli and *Oligocythereis* aff. *fullonica* (Jones & Sherborn). The environment of deposition of the Zohar and Matmor formations is shallow warm marine and the faunal affinity is widely endemic (Israel, Saudi Arabia).

EARLY OXFORDIAN EXOPHTHALMOCYTHERE? KIDODENSIS ASSEMBLAGE ZONE.— The Tauriat shales (Majdal Shams formation) at Gebel Maghara yield *Exophthalmocythere? kidodensis* Rosenfeld & Gerry, *Progonocythere* aff. *parastilla* Whatley and *Terquemula gublerae* (Bizon). At the Hermon, the

Source : MNHN, Paris

Majdal Shams formation yields an abundant assemblage, comprising next to *E.? kidodeusis* Rosenfeld & Gerry and *T. gublerae* (Bizon), also *T.* cf. *martini* (Bizon), *Cytherella* cf. *umbilica* Bate, *Monoceratina stimulea* (Schwager) and *M.* cf. sp. B Bate, as well as *Cytherelloidea atlantolevantina* Rosenfeld & Honigstein, *Eucytherura oxfordiana* Rosenfeld & Honigstein, *Acrocythere dubertreti* Rosenfeld & Honigstein, *Howerocythere hermoneusis* Rosenfeld & Honigstein and *Oligocythereis irregularis* Rosenfeld & Honigstein. The environment of deposition of the Majdal Shams formation at the Hermon is definitely of deeper water with euxinic bottom conditions. The faunal affinity of ostracods remains endemic, notwithstanding a slight relation to western Europe, the Tethyan oceanic barrier held this province apart from its boreal eurasiatic counterpart north of the Tethys.

LATE OXFORDIAN - KIMMERIDGIAN HUTSONIA ADUNATA ASSEMBLAGE ZONE.— In the Nahar Sa'ar formation at Ein Quniya (Hermon) as well as in boreholes (Qeren, Haluza, Boqer, Kohal, Beersheva and Hazon) an assemblage identical to the one described from the couches d'Aazour and calcaires de Salima of Lebanon occurs (BISCHOFF, 1990). There stratigraphically important representatives of the genera *Schuleridea* and *Hutsonia* have a range from late Oxfordian - Kimmeridgian and possibly Tithonian.

BRACHIOPODS

Brachiopods of the region have been described by DOUVILLE (1916), MUIR-WOOD (*in* HUDSON, 1958), FELDMAN (1987) and by FELDMAN *et al.* (1982, 1991).

The affinity of these faunas is generally endemic to the Ethiopian province, the geographical distribution of which is wide, including a Gondwanian shelf crescent from east to north Africa (Somalia, Kenya, Tanzania, Arabia, the Levant, Egypt, Tunisia and the Maghreb). Middle to Upper Jurassic brachiopods described from Saudi Arabia, Israel, Egypt and Tunisia, while containing many genera and species common to all four subregions, also contain elements that are characteristic of the area of origin, an observation also made for bivalves, e.g. *Eligmus* (HIRSCH, 1979).

The Ethiopian province is suspected to have been invaded in the Early Jurassic from the north (Europe) and thereupon isolated for the remainder of the Jurassic, developing special morphological features which distinguish them from their original stock, a phenomenon also common in Callovian nerineids. Though Jurassic brachiopods from Cutch (India) were broadly correlated with lower Bathonian to Oxfordian faunas of Europe (KITCHIN, 1900; SPATH, 1927-1933; ARKELL, 1956), it is suggested that a number of genera and species from Israel, Saudi Arabia and Cutch are very closely related. The rhynchonellid *Pycnoria* described by COOPER (1989) from the upper Bathonian - Callovian of Saudi Arabia is almost certainly congeneric with *Rhynchonella fornix* Kitchin, 1900 and *R. nobilis* Kitchin of Cutch. The genus *Schizoria* described by COOPER (1989) from the upper Bajocian of Saudi Arabia appears to be represented by *R. assymetrica* Kitchin and the specimens of *Globirhynchia crassa* Cooper from late Bajocian beds, are similar to specimens described as *R. versabilis* Kitchin. Among Terebratulida, species of *Kutchithyris*, encountered in Israel and Saudi Arabia, are very similar in external morphology to those of Cutch. The works of WEIR (1925, 1929) and MUIR-WOOD (1925) give the impression of a rhynchonellid-dominated fauna of comparatively little diversity in the middle Upper Jurassic of Somalia. A similar impression is obtained from Tunisia (DUBAR, 1967), leading to the conclusion of a closer faunal and ecological relationship of these areas than actually exist. Likewise, Bathonian to Oxfordian beds in south Israel draw a closer comparison with the Somalian fauna than with the Saudi Arabia fauna monographed by COOPER (1989). Yet, a number of terebratulid species that occur in both South Arabia and Israel have not been recognized from Somalia and Tunisia. Rhynchonellida common to all four areas include unibiquitous *Somalirhynchia* and *Daghanirhynchia*, but the genera *Amydropthychus*, *Couarosia*, *Echysoria*, *Coloptoria*, *Eurysites*, *Lirellarina*, *Nastoria* and *Strongyloria* of COOPER (1989) do not occur in southern Israel, Somalia or Tunisia. However the genus *Pycnoria* occurs in Bathonian to Callovian beds in Gebel El-Maghara (FELDMAN, 1987) and Saudi Arabia (COOPER, 1989) and may also occur with forms such as *Schizoria* from the Bajocian, *Burmirhynchia* Bajocian - Callovian and *Globirhynchia* in both Gebel El-Maghara (Sinai, Egypt) as well as Cutch (India).

Source : MNHN, Paris

FORAMINIFERA

The extensive studies of MAYNC (1966), DERIN & REISS (1966), DERIN & GERRY (1972) and DERIN (1974) have laid the base to a comprehensive microfacies distribution, mainly based on foraminifera and algae. Jurassic foraminifera, in need of a revision in the field of taxonomy and biostratigraphy, were given special attention in the Peri-Tethys project. Lately, KUZNETSOVA & DOBROVA (1995) and KUZNETSOVA *et al.* (1996) have added information on Jurassic foraminifera from Syria.

LIASSIC.— From the few outcrops of the Ardon formation in Maktesh Ramon (Negev), the exact age of the marine Jurassic basal transgression in that part of the Levant is still uncertain. The formation only yielded *Glomospira* sp. with alga *Thaumatoporella parvovesiculifera* Raineri, in restricted lagoonal facies, taxons without chronostratigraphical value.

A revision of the subsurface Liassic confirmed the presence of *Orbitopsella primaeva* (Hottinger) in the lowest portion of the Ardon formation in boreholes of the coastal plain (DERIN, 1974), indicating a Pliensbachian age for the Liassic transgression. Forms previously identified as *Orbitopsella* aff. *praecursor* (Gümbel) and considered as indicative of the "Orbitopsella praecursor Zone" (Pliensbachian) are referable to *Timidonella* sp. In the same interval occur *Gutnicella* gr. *cayeuxi* (Lucas), *Spiraloconulus* cf. *percomigi* (Allemann & Schroeder) and at the top, *Limognella* sp. All these forms are elsewhere known in the Tethys from Aaleno-Bajocian time span.

MIDDLE JURASSIC.— To the Bajocian are related *Amijiella amiji* (Henson) and dasyclad *Selliporella donzellii* Sartoni & Crescenti, and to the Bathonian *Paleopfenderina salernitana* Sartoni & Crescenti.

However, the precedently quoted *Meyendorffina bathonica* Aurouze & Bizon and *Orbitammina elliptica* (d'Archiac), well known late Bathonian markers in western Europe, are actually a new species of flattened *Kilianina*. Its range is to be placed in early and / or middle Callovian and it is often associated with *Praekurnubia* and small primitive *Kurnubia (K.) variabilis* Redmond. The presence of *Satorina apuliensis* Fourcade & Chorowicz was not confirmed. In the Coronatum Zone (middle Callovian) *Praekurnubia crusei* Redmond and small *Kurnubia (K. variabilis* Redmond, *K. braukaupi* Redmond) are widespread. At Hamaktesh Hagadol, the larger *Kurnubia (K. palastiniensis* (Henson), *K.* cf. *wellingsi* (Henson)), together with small species, *Flabellocycloling reissi* Hottinger and *Steinekella* cf. *steinekei* Redmond appear. *F. reissi* seems only present in the upper Callovian.

LATE JURASSIC.— Lower Oxfordian can be characterized by "*Mangashtia*" *egyptiensis* Fourcade *et al.* (DERIN, 1974). The widespread *Alveosepta jaccardi* biozone is well represented (upper Oxfordian-Kimmeridgian). At the top of the range zone of this taxon *Anchispirocyclina praelusitanica* Mayne also occurs (MAYNC, 1966). Algae include *Pseudoclypeina* and *Clypeina jurassica* Favre.

PALAEOGEOGRAPHY

For a correct understanding of the Jurassic palaeogeographic setting of Israel prior to the infra-cretaceous truncation, one has to move the Golan - Jordan side about 100 km back to the south. In the south, the Negev High consists of the Avdat and Massada-Jordan "blocks", separated by the Kurnub "basin" (GOLDBERG & FRIEDMAN, 1974). Plunging toward the NW, the "nose" of the Negev High separates the depotcenters of the North Sinai (Maghara-Halal) from the Central Israel trough (Helez-Ramallah- Hermon) of the Judean embayment (HIRSCH, 1985). To the North, the overall thinner Jurassic column represents the Galilee High that extends to the adjacent Lebanon and northern Antilebanon (HIRSCH, 1985).

LOWER JURASSIC (Fig. 3).— Major uplift took place at the Rhaetian - Liassic boundary, resulting in denudation, karst and truncation processes. In northern Israel, a transversal trough was filled by pre-Toarcian Asher volcanics, the wearing down of which produced the materials found in the laterites of the Mishhor formation, covering most of Israel and adjacent areas (PICARD & HIRSCH, 1987).

Source : MNHN, Paris

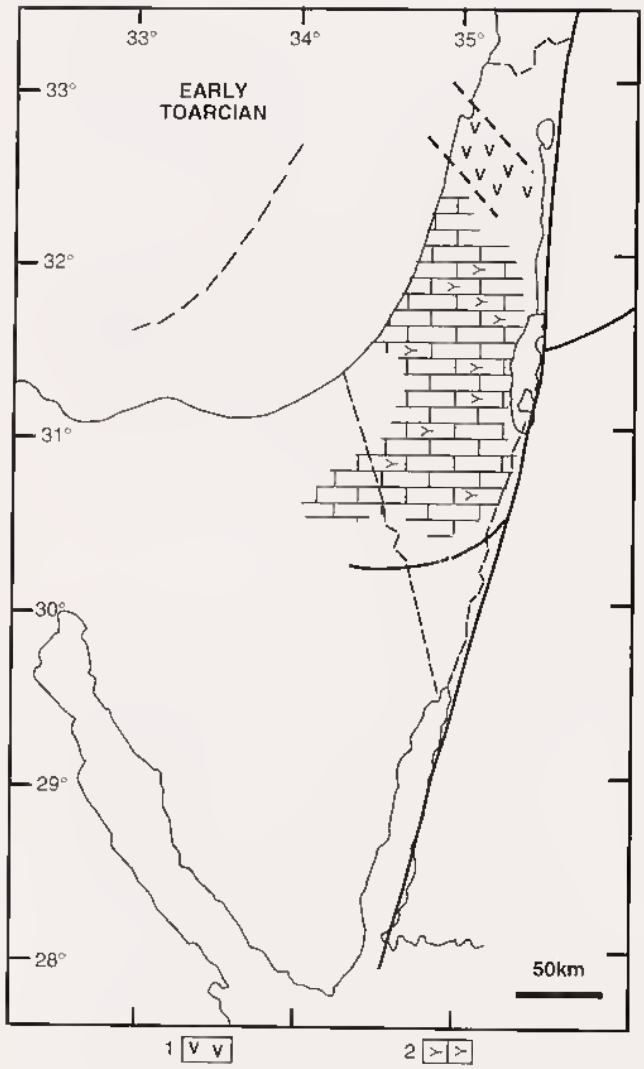

FIG. 3.— Early Toarcian facies map. The early Toarcian is represented by an interval within the huge mass of platform carbonates with evaporitic layers that build up the Ardon formation. Its existence toward Lebanon is not clear and the interval may onlap directly the Asher Basalts (VV) in the northern part of Israel. It is estimated to consist on the slope toward the Judean embayment of over 200 m, thickening towards the central axe of the embayment to the order of 500 m. **1**, basalts (193-194); **2**, carbonates and evaporites.

FIG. 3.— Carte des faciès au Toarcien inférieur. Le Toarcien inférieur représenté par un intervalle dans la masse immense des carbonates de plate-forme et évaporites qui constituent la formation de Ardon. Son extension vers le Liban n'est pas claire, intervalle pouvant couvrir les basaltes de Asher (VV) dans le nord d'Israël. En bordure de la baie de Judée l'intervalle peut atteindre 200 m et s'épaissit vers l'axe du bassin (de l'ordre de 500 m). 1, basaltes (193-194) ; 2, carbonates et évaporites.

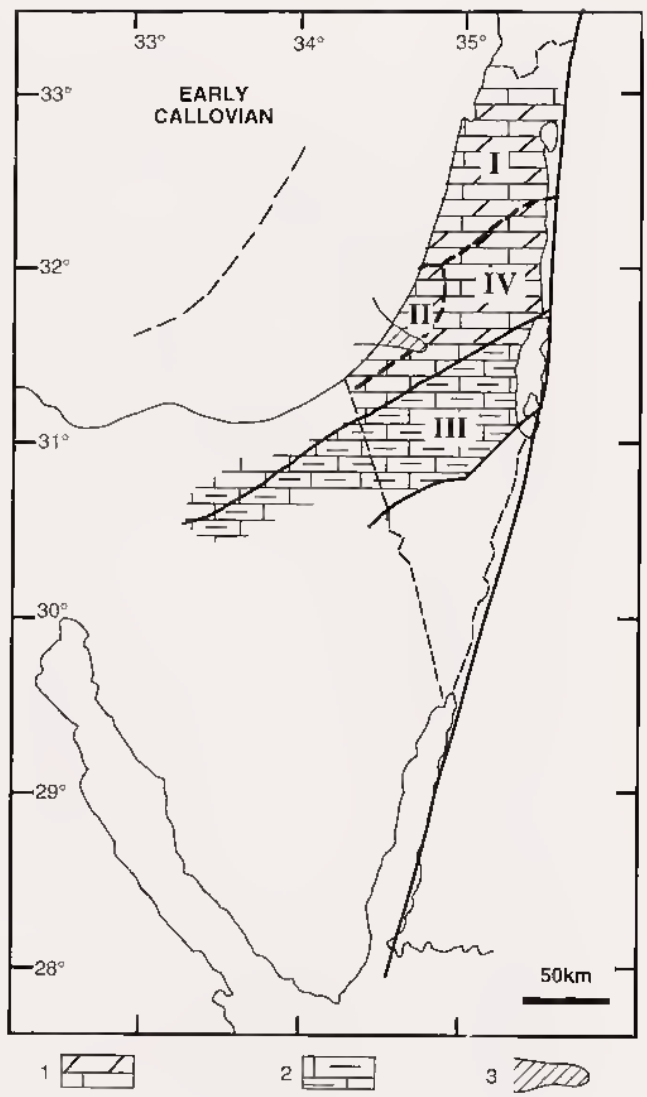

FIG. 4.— Early Callovian facies map. This ca. 100 m thick interval subdivides in tectono-sedimentary zones: I. calcarenites (Haifa); II. calcarenites (Brur) of the "unstable zone" , truncated by a karstic event; III. shales (Upper Sherif-Karmon), calcarenites and marls (lower Zohar); IV. massive calcarenites (Hermon). **1**, carbonates; **2**, limestones and marls; **3**, eroded.

FIG. 4.— Carte des faciès du Callovien inférieur. L'intervalle d'environ 100 m d'épaisseur se subdivise en zones tectono-sédimentaires : I, calcarénites (Haifa) ; II, les calcarénites (Brur) de la 'zone instable' sont tronquées par un événement karstique ; III, shales (Sherif supérieur-Karmon), calcarénites et marnes (Zohar) ; IV, calcarénites massives (Hermon). 1, carbonates ; 2, calcaires et marnes ; 3, érodé.

Source : MNHN, Paris

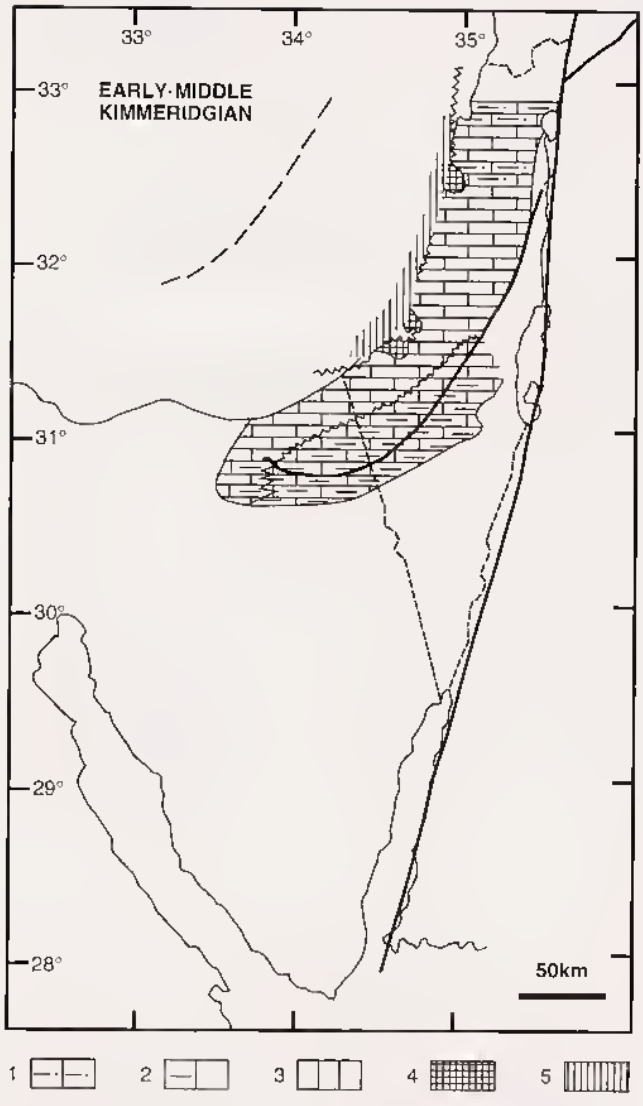

FIG. 5.— Early-middle Kimmeridgian facies map: consists of reefs, oolites, shales and sands (Nahar Sa'ar). Eroded by the infra-Cretaceous uplift along the present Levant coast and in the SE Negev. **1**, oolithes; **2**, marls; **3**, limestones; **4**, reef; **5**, eroded.

*FIG. 5.— Carte des faciès du Kimméridgien inférieur et moyen : se compose de récifs, oolites, shales et sables (Nahar Sa'ar). Tronqué lors du soulèvement infra-Crétacé le long de la côte actuelle du Levant et dans le Negev du SE. **1**, oolithe ; **2**, marnes ; **3**, calcaires ; **4**, récif ; **5**, érodé.*

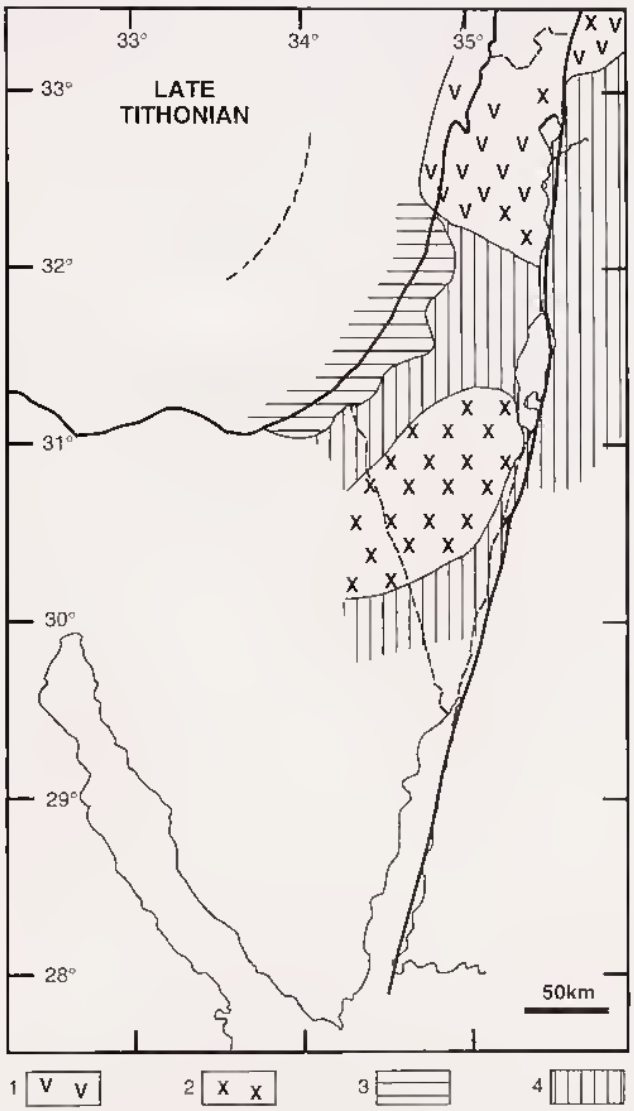

FIG. 6. — Late Tithonian facies map. This interval belongs virtually to the infra-Cretaceous tectono-environmental phase. It is marked by wide denudation, Tithonian -Hauterivian volcanics (Tayasir) and turbidites (Gevar 'Am canyon). **1**, alkalin basalts (140-115); **2**, basic intrusion; **3**, shales; **4**, eroded.

*FIG. 6.— Carte des faciès du Tithonien supérieur. Cet intervalle appartient virtuellement à la phase tectono-environnementale infra-Crétacé. Il est marqué par une dénudation étendue, un volcanisme tithonique - hautérivien (Tayasir) et par des turbidites (Canyon de Gevar' Am). **1**, basaltes alcalins ; **2**, intrusions basiques ; **3**, shales ; **4**, érodé.*

Source : MNHN, Paris

During the middle - late Liassic transgressions, true marine platform carbonate regime developped fast in the depocenters of north Sinai and of the Judean embayment. Clastics, the result of the wearing down of the Arabian massif to the South and South East, and intersparsed oolites and evaporites mark the proximal sides of the basins. Shales replace the sandstones of the upper Inmar formation and the carbonate bodies of Ardon and Qeren merge toward the distal part of the basin. In northern Israel, Lebanon and north Antilebanon platform all clastics have vanished and carbonates persist without interruption from the Liassic to the Upper Jurassic (Haifa formation).

MIDDLE JURASSIC (Fig. 4).— From the northern Israel (Haifa formation) to the central Israel and Israel coastal plain and Hermon (Hermon formation), calcarenites are interwedged in micrites.

In southern Israel (Negev) the interplay of continental (Arabian massif) arenaceous with littoral- tidal shales and carbonates characterize the Zohar formation. The micrites are interbedded with shale and a few thin sandstones of subordonate non fluviatile origin.

Contrasting with the apparent continuous platform sedimentation regime of north Israel, the emersion of part of the coastal plain belt, witnessed by karst phenomena in several boreholes (BUCHBINDER *et al.*, 1984), caused erosion and truncation of the Callovian carbonates. This infra-Oxfordian unconformity (POX) resulted in the filling of a karstic landscape by the transgressive early Oxfordian Majdal Shams shales.

LATE JURASSIC.— The Oxfordian palaeogeography is well delimited by the distribution of the lower - middle Oxfordian shale-facies (Majdal Shams). Absent from the northern High of Galilee (I) and southern High of the Negev (III), the shales reach 200 m thickness along the axis of the Judean embayement (II) and less than 100 m in the Sinai deep (IV). Volcanic tuffs occur in northern Israel (Devorah). In northern and central Israel, including the NW Negev, the lower Kimmeridgian (Fig. 5) is developped in the shallow marine facies of oolites, marls and shales of the Nahar Sa'ar formation.

A different palaeogeography is initiated by the Tithonian (Fig. 6) regional uplift, generating the Infra-Cretaceous unconformity. In the wells drilled into the canyons of the "Helez erosion embayment" nearly all Callovian and Upper Jurassic formations are missing, as they were removed by submarine Tithonian - Hauterivian chanelling of the turbiditic Gevar Am shale. Subareal truncation reached down to the Dogger in the Central Negev and to Triassic- Palaeozoic levels in the southern Negev.

TECTONO-EUSTATIC CYCLIC EVENTS

Several transgressive systems tracks or highstands were individualized, characterized by condensed facies and ferruginous oolites. Ammonites enable precise dating at Bajocian, early Bathonian, early late Bathonian, middle - late Callovian and latest Callovian-lower Oxfordian intervals. Their relatively good synchronism with system tracts of same signification in Europe shows the importance of tectono-eustatism as factor of sedimentary control, including 3rd order scale phenomena in the sense of HAQ *et al.* (1988). At longer term, the Jurassic transgression is here neatly expressed, by a sedimentary drift to a more and more marine pole, up to the Oxfordian. During this retrogradation, abundant and thick sandy intercalations up to the Bathonian, become scarcer and thin in younger levels until their disappearance. From the Kimmeridgian onwards, the sedimentary dynamic is inversed with typically prograding shallow bioclastic and corallian limestone deposits, as in Europe.

Lowstand system tracts are documented by the regressive intervals of formations: Inmar (late Toarcian ? - Aalenian), Safa (early Bathonian), Karmon (late Bathonian) and Nahar Sa'ar (late Oxfordian).

Highstand system tracts are found primeraly in the more proximal Negev-Sinai area: top Ardon (Toarcian), top Qeren (Aalenian), top Daya (Bajocian), middle Sherif (early late Bathonian), intra-Zohar (early late Callovian) and top Matmor (late Callovian). Such conditions occur over the entire region at top of the lower member of the Nahar Sa'ar formation (late Oxfordian).

The late Callovian - early Oxfordian highstand system tracts, in the more distal Hermon area, shows evidence for connection with the pelagic western Neo-Tethys.

Source : MNHN, Paris

The regional Jurassic cyclic evolution versus global events in the levantine portion of Gondwana (Fig. 7), starts with post-Triassic period of karst, the result of the early Liassic regional emersion of HAQ *et al.* (1988) long term sea level-drop upper Absaroka B (UAB 1-2), filled with Mishhor laterites. ?Pliensbachian-Toarcian Ardon evaporites with shallow lagoon and reefoid carbonates, alternating with deltaic and paralic lower Inmar sands, express the long term rise with minor short term oscillations, characterizing the end of UAB. Aalenian upper Inmar (Rosh Pinna) clastics abruptly set in with the onset of lower Zuni-A -1 sea-level drop and subsequent rise, reaching a significant highstand in the Bajocian Daya transgression (*Laeviuscula -Otoites)* and following characteristic *Ermoceras* and *Eligmus* assemblages, ending in *Parkinsoni - Thambites* lowstand, persisting into the early Bathonian. The early Bathonian lower Sherif / Safa sands and paralic coals seem to be either delineating a regression, which in terms of HAQ *et al.* (1988) global cycles is contradictory. This tectono-eustatic event appears to be characteristic of the entire Levantine - Arabian platform, witnessing a local epirogenetic pulse (S) (HIRSCH, 1987, 1988).

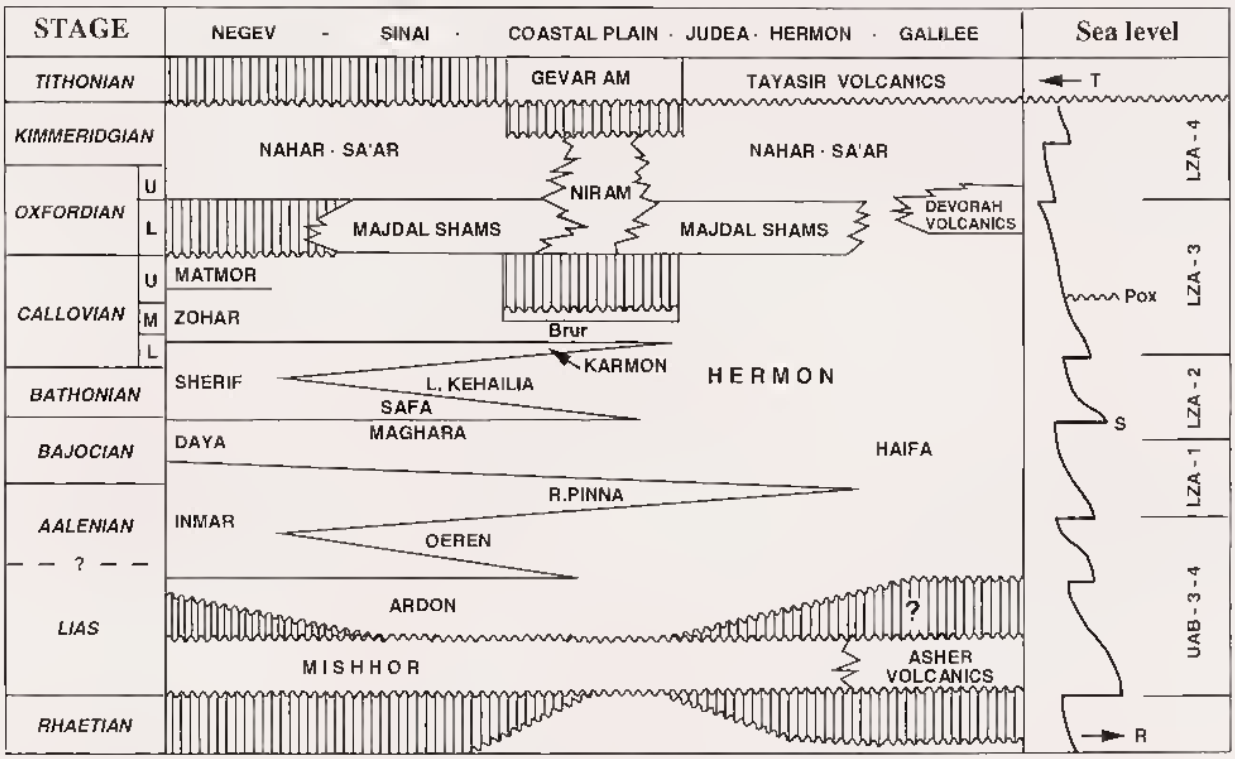

FIG. 7.— Schematic diagram of Jurassic formations with tectono-eustatic curve. Hiatus (vertical lines), unconformities (undulated), lateral facies-change (zigzag lines), mainly clastic facies (dots), shales (horizontal lines), mostly carbonatic (white). Tectono-eustatic curve and second order supercycles (HAQ *et al.*, 1988).

FIG. 7.— Diagramme schématique des formations jurassiques et courbe tectono-eustatique. Hiatus (lignes verticales), discontinuités (ondulée), variations latérales de faciès (ligne en zigzag), faciès clastique dominant (points), shales (lignes horizontales), prédominance carbonatée (blanc). Courbe tectono-eustatique et supercycles de second ordre d'après HAQ et al.*(1988).*

Follows the LZA-2.2 initial Bathonian phase of drowning (lower Kehailia) with ammonites (*Micromphalites*) in Israel and Arabia and the late Bathonian - early Callovian rise (LZA-3) with *Bullatimorphites* (upper Kehailia). According to the chart of HAQ *et al.* (1988), the late Bathonian is a lowstand, followed by an overall transgressive early Callovian.

The middle and upper Callovian reach a regional high, inundating most of the Arabian platform with typical "Zohar/ Matmor" type carbonates, that yield Nerineacea, foraminifers (*Kurnubia*- lineage), brachiopods and abundant bivalves (*Eligmus*), mostly related to Ethiopean - Somalian taxa.

Source : MNHN, Paris

The emersion along the coastal plain of Israel, causing karst-phenomena (BUCHBINDER *et al.*, 1984) and the hiatus of a significant part of the Callovian (PICARD & HIRSCH, 1987) is, in the present authors interpretation, apparently the result of pre-Oxfordian (POX) epirogenic movements.

The early Oxfordian (Mariae Zone) Majdal Shams shale-onlap covered the foregoing hiatus in the Judean embayment, extending from Maghara (Sinai) to the Hermon, possibly interfingering lateraly with the Galilee carbonatic type facies.

The late Oxfordian - Kimmeridgian shallowing and progressive regression (*Alveosepta jaccardi*) occured in contrast to the global trend of a general sea level rise (LZA-4), generating the emersion of the Syrian (Mardin) promontory, the development of thick evaporites in Central Arabia and the deposition of sands and shales from the Negev to north Egypt. Such progressive regression may occur in contrast of the global trend of a general sea level rise, and conform with the general evolution found in Europe. A generalized sea level rise, resulting in the extension of marine facies, may rapidly fill the available space, that due to tenfold sediment- production (biogenic in the present case), produces a shallow platform, until a regressive facies is reached as the filling up is progressing.

Epirogenic movements obscured the Late Jurassic global regression by juxtaposing "Tithonian" grahen-fillings with emersions, continental deposits and basaltic flows.

Changing ecological and tectono- environmental conditions in the middle eastern Levantine Jurassic are echoed by the composition of floral and faunal assemblages, endemism and cosmopolitism. Palaegeographical and environmental evolution to a wide extent match the cycles of HAQ *et al.* (1988), although it suggests that Levantine "African-Arabian-Apulian" sea level anomalies, due to "noises" generated by the Proto-Atlantic opening and southern Neo-Tethys rifting, perturbing the global sea level record.

ACKNOWLEDGMENTS

We express our thanks to R. ENAY (Lyon) for reading an early draft of the manuscript. We are indebted to J. THIERRY (Dijon) and M. MOUTY (Damascus) for reviewing the paper. We very much appreciated their constructive remarks, which contributed to the improvement of the paper. We thank P. GROSSMAN for drafting of the figures.

Part of the research was performed in the frame of the Peri-Tethys Program. Partial funding was provided to H-R FELDMAN by the National Geographic Society, grants 4739-92 and 5666-96.

REFERENCES

AL FAR, D.M., 1966.— Geology and coal deposits of Gabal El Maghara (N. Sinai). *Egypt, Geological Survey, Paper*, **37**: 1-59.

ARKELL, W.J., 1956.— *Jurassic Geology of the World*. Olivier and Boyd, London: 1-808.

ARKELL, W., 1952.— Jurassic Ammonites from Jebel Tuwaiq, Central Arabia. *Philosophical Transactions of the Royal Society of London*, Ser. B, **236**: 241-314.

BISCHOFF, G., 1964.— Die Gattung Cytherelloidea im Oberen Jura und in der Unterkreide. *Senckenbergiana Lethaea*, **45**:1-27.

BISCHOFF, G., 1990.— The Genus *Hutsonia* in the Late Jurassic. *Senckenbergiana Lethaea*, **70**: 397-429.

BUCHBINDER, L .G., 1981.— Dolomitization, porosity development and late mineralization in the Jurassic Zohar (Brur Calcarenite) and Sederot Formations in Ashdod-Gan Yavne. *Israel Journal of Earth-Sciences*, **30**: 64-80.

BUCHBINDER, L. G, MAGARITZ, M. & GOLDBERG, M., 1984.— Stable isotope study of karstic related dolomitization: Jurassic rocks from the Coastal Plain, Israel. *Journal of Sedimentary Petrolology*, **54**: 236-256.

CARIOU, É., 1973.— Ammonites of the Callovian and Oxfordian. *In*: A.HALLAM (ed.), *Atlas of Palaeobiogeography*. Elsevier, Amsterdam: 287-295.

CARIOU, É., 1984.— Biostratigraphic subdivisions of the Callovian stage in the Subtethyan province of ammonites, correlations with the Subboreal zonal scheme. *In*: O. MICHELSEN & A. ZEISS (eds), International Symposium on Jurassic Stratigraphy, Erlangen. *Geological Survey of Denmark*, 2: 315-326.

CARIOU, É., CONTINI, D., DOMMERGUES, J.L., ENAY, R., GEYSSANT, J., MANGOLD, CH. & THIERRY, J., 1985.— Biogéographie des ammonites et évolution structurale de la Téthys au cours du Jurassique. *Bulletin de la Société géologique de France, Paris*, 1, **5**: 679-697.

Source : MNHN, Paris

COATES, J., GOTTESMAN, E., JACOBS, M. & ROSENBERG, E., 1963.— Gas discoveries in the western Dead Sea Region. *Sixth World Petroleum Congress, Francfort*, **1**: 21-36.

CONWAY, B.H., 1990. Paleozoic-Mesozoic Palynology of Israel. II: Palynostratigraphy of the Jurassic Succession in the Subsurface of Israel. *Israel Geological Survey, Bulletin*, **82**: 1-39, 18 pls.

COOPER, G.A., 1989.— Jurassic brachiopods of Saudi Arabia. *Smithsonian Contributions to Paleobiology*, **65**: 1-213.

COUSMINER, H.L. & CONWAY, B., 1981.— Initial results and potential of Israeli palynology program. *Israel Geological Survey, Current Research*, 1980: 57-61.

DERCOURT, J., RICOU, L.E. & VRIELYNCK, B. (eds), 1993.— *Atlas Tethys Palaeoenvironmental Maps*. Gauthier-Villars, Paris: 1-307.

DERIN, B., 1974.— *The Jurassic of Central and Northern Israel*. Ph. D. Thesis, Hebrew University, Jerusalem, Israel: 1-70 (in Hebrew, English summary).

DERIN, B. & REISS, Z., 1966.— *Jurassic Microfacies of Israel*. Israel Institut of Petroleum. Special Publication, Tel Aviv: 1-43.

DERIN, B. & GERRY, E., 1972.— *Jurassic Biostratigraphy and Environments of Deposition in Israel. 5th African Micropaleontological Colloquium, Addis Abeba*. Israel Institut of Petroleum, Micropaleontological laboratory, Tel Aviv, report 2/12: 1-20.

DOUVILLE, H., 1916.— Les terrains secondaires dans le Massif du Moghara à l'est de l'Isthme de Suez d'après les explorations de M. Couyat Barthoux. *Mémoires de l'Académie des Sciences, Paris, Paléontologie*, **54** (2): 1-184.

DUBAR, G, 1967.— Brachiopodes Jurassiques du Sahara Tunisien. *Annales de Paléontologie, Paris*, **53**: 1-71.

DUBERTRET, L., 1960.— *Feuille Hermon, Notice explicative*. République Libanaise, Ministère des Travaux Publics, Beyrouth: 1-46.

DUBERTRET, L., 1975.— Introduction à la carte géologique à 1/50 000 du Liban. *Notes et Mémoires sur le Moyen-Orient*, **13**: 345-403.

ENAY, R., 1966.— L'Oxfordien dans la moitié sud du Jura français: étude stratigraphique. *Nouvelles Archives du Muséum d'Histoire naturelle de Lyon*, **1**, (8): 1-323.

ENAY, R., LENDRE, Y.-M., MANGOLD, CH., MANIVIT, J. & VASLET, D., 1987.— Le Jurassique d'Arabie Saoudite centrale: nouvelles données sur la lithostratigraphie, les paléoenvironnements, les faunes d'ammonites, les âges et les corrélations. *Geobios, Lyon*, M.S. **9**: 13-65.

ENAY, R. & MANGOLD, Ch., 1994.— Première zonation par ammonites du Jurassique d'Arabie Saoudite, une référence pour la province arabique. *In*: É. CARIOU & P. HANTZPERGUE (eds): 3rd International Symposium on Jurassic Stratigraphy, Poitiers 1991. *Geobios, Lyon*, M.S.: 161-174.

FELDMAN, H.R., HIRSCH, F. & OWEN, E., 1982.— *A Comparison of Jurassic and Devonian Brachiopod Communities: Trophic Structure, Diversity, Substrate Relations and Niche Replacement. Third North American Paleontological Convention, Proceeding*. Vol. I. B. Business and Economic Services. Montreal: 169-174.

FELDMAN, H.R., 1987.— A new species of the Jurassic (Callovian) Brachiopod *Septirynchia* from Northern Sinai. *Journal of Paleontology*, **61**, 6: 1156-1172.

FELDMAN, H.R., OWEN, E. & HIRSCH, F., 1991.— Brachiopods from the Jurassic of Gebel El-Maghara, Northern Sinai. *American Museum Novitates*, **3006**: 1-28.

FENTON, J.P.G., NEVES, R. & PIEL, K.M., 1980.— Dinoflagellate cysts and acrytarchs from upper Bajocian to Middle Bathonian strata of central and southern England. *Palaeontology, Londres*, **23**: 151-170.

FOURCADE, E., ARAFA, A.A. & SIGAL, J., 1983.— Description of a new species of foraminifera in the Malm of the Middle East: *Mangashtia? egyptiensis* n.sp. *Revue de Micropaléontologie, Paris*, **27**: 21-29.

FORTWENGLER, D., MARCHAND, D. & BONNOT A., in press.— Ammonites et limite Callovien-Oxfordien dans les "Terres noires" du Diois (bassin du Sud-Est, France). *Geobios*.

FREBOLD, H. VON, 1928.— Die stratigraphische Stellung der Grenzschichten des syrischen Callovien und Oxford. *Zentralblatt für Mineralogie, Geologie und Paläontologie*. Abt. B, **3**: 183-201.

FRIEDMAN, G., BARZEL, A. & DERIN, B., 1971.— Paleoenvironments of the Jurassic in the central coastal belt of northern and central Israel and their significance in the search for petroleum reservoirs. *Israel Geological Survey, Report*, OD/1/71: 1-26.

GILL, G.A. & TINTANT, H., 1975.— Les Ammonites Calloviennes du sud d'Israël. Stratigraphie et relations paléogeographiques. *Comptes Rendus de la Société géologique de France, Paris*, **4**: 103-106.

GILL, G.A., THIERRY J. & TINTANT H., 1985.— Ammonites calloviennes du Sud d'Israël: systématique, biostratigraphie et paléobiogéographie. *Geobios, Lyon*, **18**, (6): 705-751.

GOLDBERG, M., 1963.— Reference Section of Jurassic Sequence in Hamakhtesh Hagadol (Kurnub Anticline). Detailed binocularsample description, including field observations. Unpublished Internal Report, Oil Division. *Israel Geological Survey*: 1-50.

GOLDBERG, M., 1964.— Problems in the Jurassic stratigraphy of Southern Israel. *Israel Journal of Earth-Sciences*, **13**: 169-171.

GOLDBERG, M.,1969.— The Jurassic of Majdal Shams area, Mt Hermon. Measured and sampled by M. Goldberg, M. Brown, M. Raab, B. Derin. *In*: Remarks on the Jurassic lithostratigraphy of Mt. Hermon. *Israel, Geological Society, the Golan Heights meeting proceedings, Jerusalem*: 7-8.

Source : MNHN, Paris

GOLDBERG, M. & BOGOSH, R., 1978.— Dolomitization and hydrothermal mineralization in the Brur Calcarenite (Jurassic), southern coastal plain. *Israel Journal of Earth-Sciences*, **27**: 36-41.

GOLDBERG, M. & FRIEDMAN, G., 1974.— Paleoenvironments and palcogeographic evolution of the Jurassic system in southern Israel. *Israel Geological Survey, Bulletin*, **61**: 1-44.

GOLDBERY, R., 1982.— Paleosols of the Lower Jurassic Mishhor and Ardon Formations ("Latcritc Derivative Facies"), Makhtesh Ramon, Israel. *Sedimentology*, **29**: 669-690.

GYGI, R., 1990.— The Oxfordian ammonite succession near Liesberg B.E. and Pery BE, northern Switzerland. *Eclogae geologicae Helvetiae*, **83**, (1): 177-199.

HAAN, P.J. DE, 1997.— *Early Cretaceaous Palynomorphs from the Southern Coastal Plain of Israel and a study of the Fern Family Schizaeaceae*. Ph. D. Thesis, University of California, USA: 1-277.

HAAS, O., 1955.— Revision of the Jurassic ammonitc fauna of Mount Hermon, Syria. *Bulletin of the American Museum of Natural History*, **108**: 1-210.

HAQ, B., HARDENBOL, J. & VAIL, P., 1988.— Mesozoic and Cenozoic chronostratigraphy and cycles of sea-level change. *SEPM Special Publication*, **42**: 71-108.

HIRSCH, F., 1976.— Sur l'origine des particularismes de la faune du Trias et du Jurassique de la plate-forme africano-arabe. *Bulletin de la Société géologique de France, Paris*, part 7, vol. **18**, **2**: 543-552.

HIRSCH, F., 1979.— Jurassic bivalves and gastropods from northern Sinai and southern Israel. *Israel Journal of Earth-Sciences*, **28** (4): 128-163.

HIRSCH, F., 1985.— The Arabian sub-plate during the Mesozoic. *In*: the geological evolution of the eastern Mediterranean. *Special Publication- Geological Society of London*, **17**: 217-223.

HIRSCH, F., 1987.— The Gondwanian Triassic and Jurassic Tethys shelf: Sephardic and Ethiopian faunal realms. *Shallow Tethys 2, Balkema*: 215-232.

HIRSCH, F., 1988.— Jurassic biofacies versus sea level changes in the Middle eastern Levant (Ethiopian province). *2nd International Symposium Jurassic Stratigraphy, Lisbonne*: 963-981.

HIRSCH, F., 1996.— Geology of the Southeastern slopes of Mount Hermon. *Israel Geological Survey, Current Research*, **10**: 22-27.

HIRSCH, F. & PICARD, L., 1988.— The Jurassic facies in the Levant. *Journal of Petroleum Geology*, **11** (3): 277-308.

HIRSCH, F., FLEXER, A., ROSENFELD, A. & YELLIN-DROR, A., 1995.— Palinspastic and crustal setting of the eastern Mediterranean. *Journal of Petroleum Geology*, **18** (2): 149-170.

HIRSCH, F. & RODED, R., 1996.— The Jurassic stratigraphical nomenclature in Hamakhtesh Hagadol. *Israel Geological Survey, Current Research*, **10**: 10-14.

HUDSON, R.G.S., 1958.— The Upper Jurassic faunas of Southern Israel. *Geological Magazine*, **95**: 415-425.

KITCHIN, F.L., 1900.— *Jurassic Fauna of Cutch*. pt. 1: The Brachiopoda, ser. 9, **3**:1-87, pl. 1-15. *Paleontologia Indica*.

KUZNETSOVA, K.I., GRIGELIS, A.A., ADJAMIAN, J., JARMAKANI, E. & HALLAQ, L., 1996.— *Zonal Stratigraphy and Foraminifera of the Tethyan Jurassic (Eastern Mediterranean)*. Gordon and Breach, Amsterdam: 1-256.

KUZNETSOVA, K.I. & DOBROVA, M.R., 1995.— Endemic and cosmopolitan assemblages of Foraminifers and Ostracods from the Middle Jurassic basins of Syria. *Stratigraphy and Geological Correlations*, **3** (2): 134-146.

LANG, B. & STEINITZ, G., 1989.— K-Ar dating of Mesozoic magmatic rocks in Israel: A review. *Israel Journal of Earth-Sciences*, **38** (2-4): 89-104.

LEWY, Z., 1983.— Upper Callovian ammonites and Middle Jurassic geological history of the Middle East. *Israel Geological Survey, Bulletin*, **76**: 1-56.

LORCH, J., 1967.— A Jurassic flora of Makhtesh Ramon, Israel. *Israel Journal of Botany*, **16**: 177-188

MANGOLD, CH., 1988.— Les *Pachyerymnoceras* (Pachyceratidés, Périsphinctacés, ammonites) du Callovien moyen et supérieur de la région de Saida (Algérie occidentale). Origine phylétique et biogéographie des Pachyceratidés. *Geobios. Lyon*, **21** (5): 567-609.

MAYNC, W., 1966.— Microbiostratigraphy of the Jurassic of Israel. *Israel Geological Survey, Bulletin*, **40**; *The Institute for Petroleum Research and Geophysics Report*, **1007**: 1-56.

MOSHKOVITZ, S. & EHRLICH, A., 1976.— *Schizosphaerella punctulata* Deflandre et Dangeard and *Crepidolithus crassus* (Deflandre, Noel), Upper Liassic calcareous nannofossils from Israel and Northern Sinai. *Israel Journal of Earth-Sciences*, **25**: 51-57.

MOSHKOVITZ, S. & EHRLICH, A., 1980.— Late Jurassic calcareous nannofossils in Israel's offshore and onland areas. *Israel Geological Survey, Current Research*: 65-72.

MUIR-WOOD, M., 1925.—Jurassic Brachiopods from the Jordan Valley. *Annals and Magazine of Natural History, Londres*, **15**: 181-192.

NEVO, A., 1963.— The Jurassic strata of Makhtesh Ramon. *Israel Geological Society, Summary of Lectures, Makhtesh Ramon Symposium*: 11-12.

NOETLING, F., 1887.— *Der Jura am Hermon*. E. Schweizerbart'sche Verlagsbuchhandlung, Stuttgart: 1-46.

PARNES, A., 1980.— Lower Jurassic (Liassic) Invertebrates from Makhtesh Ramon (Negev, Southern Israel). *Israel Journal of Earth-Sciences*, **29**: 107-113.

Source : MNHN, Paris

PARNES, A., 1981. Biostratigraphy of the Mahmal Formation (Middle and Upper Bajocian) in Makhtesh Ramon (Negev, Southern Israel). *Israel Geological Survey, Bulletin*, **74**: 1-55.

PICARD, L. & HIRSCH, F., 1987.— *The Jurassic Stratigraphy in Israel and the Adjecent Countries*. The Israel Academy of Sciences and Humanities, Jerusalem: 1-106.

RAAB, M., 1962.— Jurassic-Early Cretaceous Ammonites from the Southern Coastal Plain, Israel. *Israel Geological Survey, Bulletin*, **34**: 24-30.

RAZVALYAEV, A.V., 1966.— *Explanatory Notes to the Geological Map of Syria, 1: 200 000*. Syrian Arab Report of the Ministry of Industry, Department of Geological and Mineral Research, Damacus: 1-122.

RIOULT, M., DUGUE, O., JAN DU CHENE, R., PONSOT, C., FILY, G., MORON, J.M. & VAIL, P.R., 1991.— Outcrop sequence stratigraphy on the Anglo-Paris basin, Middle to Upper Jurassic (Normandy, Maine, Dorset). *Bulletin des Centres de Recherches Exploration-Production Elf Aquitaine*, **1**: 101-194.

ROSENFELD, A., GERRY, E. & HONIGSTEIN, A., 1987a.— Jurassic Ostracodes from Gebel Maghara, Sinai, Egypt. *Revista Española de Micropaleontologia*, **19**: 251-280.

ROSENFELD, A., OERTLI, H., HONIGSTEIN, A. & GERRY, E., 1987b.— Oxfordian Ostracodes from the Kidod Formation of the Majdal Shams Area, Mount Hermon, Golan Heights. *Bulletin des Centres de Recherches Exploration-Production Elf Aquitaine*, **11**: 2:233-248.

ROSENFELD, A., HONIGSTEIN, A., GERRY, E., OERTLI, H. & FLEXER, A., 1988.— Early Jurassic Ostracodes from the Ardon Formation in Israel and Sinai. *Israel Geological Survey, Current Research*, **6**: 50-56.

ROSENFELD, A. & HONIGSTEIN, A., 1991.— Callovian-Oxfordian Ostracodes from the Hamakhtesh Hagadol Section, Southern Israel. *Revista Española de Micropaleontologia*, **23** (3): 133-148.

ROSENFELD, A. *et al.*, in press.— Personal communication. *Revista Española de Micropaleontologia*.

SALTZMAN, U., BARTOV, Y., GOTTLIB, G., MAGHARITZ, M. & MIMRAN, Y., 1968.— Composite columnar section of sequences exposed at the SE flank of Mt. Hermon. *In*: U. SALTZMAN (ed.), *The Geology of the Southern Hermon Slopes: Internal Report*. TAHAL, Tel Aviv: 1-46.

SARGEANT, W.A.S., 1976.— Dinoflagellate cysts and acritarchs from the Great Oolite Limestone (middle Jurassic: Bathonian) of Lincolnshire, England. *Geobios, Lyon*, **9**: 4-45.

SCHIRARDIN, J., 1958.— Les ammonites de l'Oxfordien du Jura alsacien de la région de Ferrette ; *Bulletin du Service de la Carte géologique d'Alsace et de Lorraine*, **11** (1): 1-50.

SPATH, L.F., 1927-1933.— Revision of the Jurassic Cephalopod fauna of Kachh (Cutch). *Palaeontologia Indica*, **9** (2): 1-945.

THUSU, B. & VIGRAN, O.S., 1985.— Middle-Late Jurassic (Late Bajocian-Tithonian) Palynomorphs. Palynostratigraphy of north-east Libya. *Journal of Micropaleontology*, **4**: 113-120.

VAUTRIN, H., 1934.— Contribution à l'étude de la série jurassique dans la chaîne de l'Anti-Liban et plus particulièrement dans l'Hermon (Syrie). *Comptes Rendus de l'Académie des Sciences, Paris*, **198**: 1438-1440.

VIDIER, J.P., MARCHAND, D., BONNOT, A. & FORTWENGLER, D., 1993.— The Callovian and Oxfordian of the Boulonnais area in northern France: new biostratigraphic data. *Acta Geologica Polonica*, **43** (3-4): 169-182.

WEIR, J., 1925.— Brachiopoda, Lamellibrachiata, Gastropoda and Belemnites. *In*: B.K.N. WYLLIE & W.R. SMELLIE (eds), *The Collection of Fossils and Rocks from Somaliland*. Glasgow University, Geological Department Hunterian Museum, 1 (6): 79-110.

WEIR, J., 1929.— Jurassic Fossils from Jubaland, East Africa. Collected by V.G. Glenday. *Glasgow University, Geological Department Hunterian Museum*, **3**: 1-63.

Source : MNHN, Paris

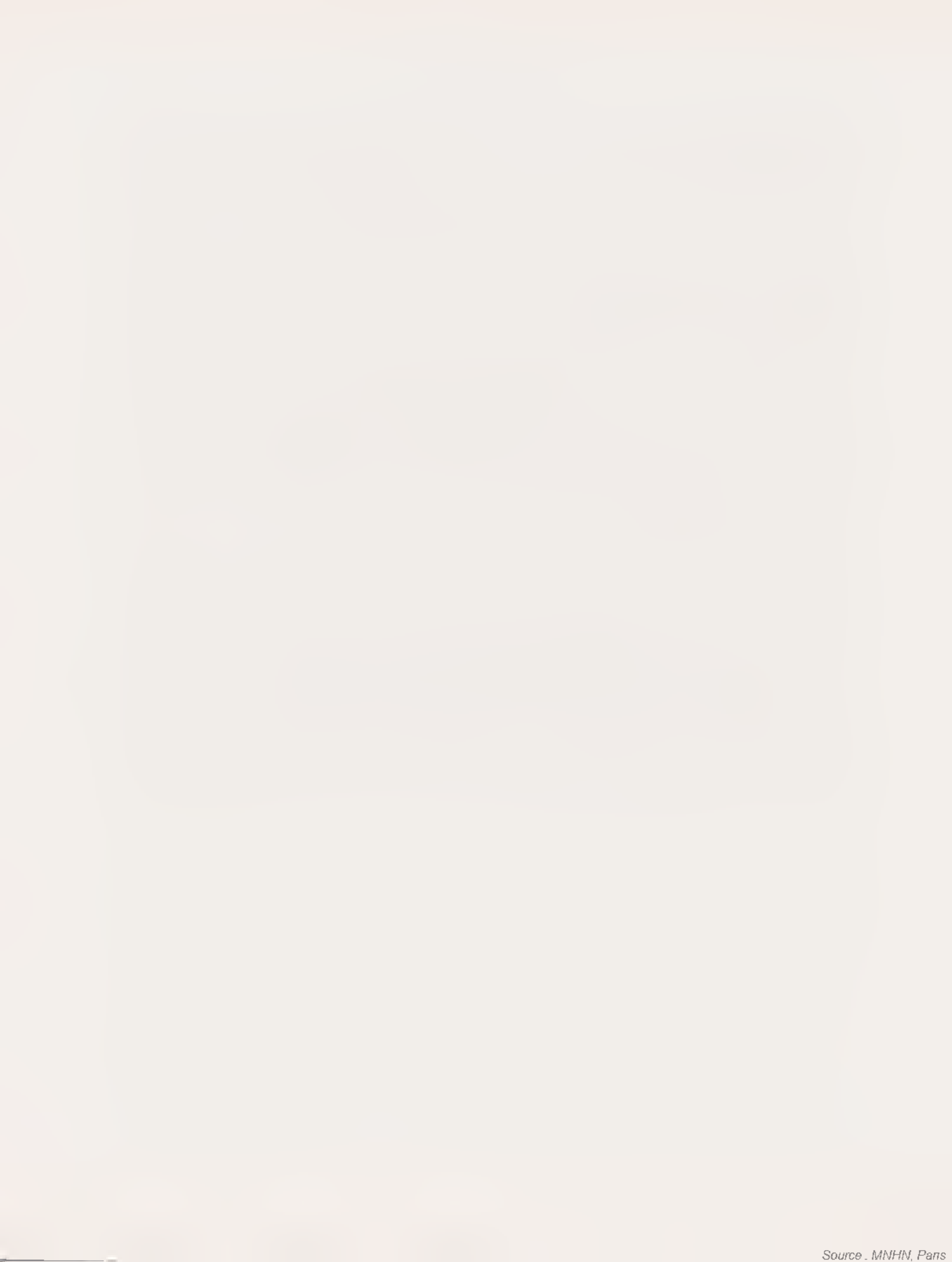

Source : MNHN, Paris

The central High-Atlas (Morocco). Litho- and chrono-stratigraphic correlations during Jurassic times between Tinjdad and Tounfite. Origin of subsidence

André POISSON [1], *Majid HADRI* [2], *Ahmed MILHI* [2]
Myriam JULIEN [1] & *Jean ANDRIEUX* [1]

[1] Université Paris-Sud, Orsay Terre, CNRS LP 1748, Bat. 504, F-91405 Orsay Cedex, France

[2] Ministère de l'Énergie et des Mines, Division Géologie, Département Géologie Générale, Rabat Agdal, Maroc

ABSTRACT

At the NW margin of the African craton the High-Atlas belt results from compressional tectonic events which took place during Tertiary times. The high elevation (which could reach 4160 m), and thrust faults resulted from these events. The initial extensional basins are part of the transfer zone between Atlantic Ocean and the eastern Mediterranean Neotethys which are opening during Early Mesozoic times. Coming from the east, the first marine flooding occured in early Liassic times and it suddenly covered all the High-Atlas domain. Shallow marine carbonates were deposited as the area was subsiding after an initial rifting phase, characterized by magmatism (Late Trias-earliest Lias). The Liassic epoch can be subdivided into two periods: early to middle Lias with strong subsidence (syn-rift) and late Lias with renewed subsidence. Extensional tectonic activity persisted while the whole basin continued to subside: the initial platform was broken so that during Liassic and early Dogger residual platforms and basins coexisted. In the central High-Atlas a wide platform persisted to the south while in the middle and northern parts narrow remnant-platforms separated elongated basins. A model of tilted blocks could explain the persistance of relatively shallow areas which represent the crests of the tilted blocks. Platforms remained shallow marine while basins became deeper, especially during the Toarcian and early Bajocian times. At the end of the Bajocian the sea began to retreat and deposits were characterized by shallow marine terrigenous detritics and carbonates. However, high rate of subsidence persisted, exactly compensated by sedimentary supply. Two curves of subsidence history are given as preliminary curves for the southernmost platform and the adjacent basin. They point out the two main stages of evolution with two maxima of subsidence (early-middle Lias and Toarcian to early Bajocian).

POISSON, A., HADRI, M., MILHI, A., JULIEN, M. & ANDRIEUX, J., 1998. — The central High-Atlas (Morocco). Litho- and chrono-stratigraphic correlations during Jurassic times between Tinjdad and Tounfite. Origin of subsidence. *In:* S. CRASQUIN-SOLEAU & É. BARRIER (eds), Peri-Tethys Memoir 4: epicratonic basins of Peri-Tethyan platforms, *Mém. Mus. natn. Hist. nat.*, **179** : 237-256. Paris ISBN : 2-85653-518-4.

Source : MNHN, Paris

RÉSUMÉ

Le Haut-Atlas central (Maroc). Corrélations litho- et chrono-stratigraphiques pendant le Jurassique entre Tinjdad et Tounfite. Origine de la subsidence.

À la marge NW du craton africain, la chaîne du Haut-Atlas est le résultat d'événements tectoniques compressifs qui se sont produits pendant le Tertiaire. Cette tectonique est responsable de la haute élévation de la chaîne (elle peut atteindre 4160 m), ainsi que des structures chevauchantes. Les bassins extensifs initiaux, qui se sont ouverts au début du Mésozoïque, font partie de la zone de transfert entre l'Océan Atlantique et la Neotethys de Méditerranée orientale. Venant de l'est la première invasion marine s'est produite au Lias inférieur et a recouvert très rapidement tout le domaine du Haut-Atlas. Après la phase de rifting initial caractérisée par du magmatisme (fin Trias-début Lias), la région reste subsidente et est recouverte de dépôts carbonatés marins peu profonds. Deux périodes peuvent être distinguées pendant le Lias : une période syn-rift avec forte subsidence au Lias inférieur et moyen, et une période qui commence au Lias supérieur avec une reprise de la subsidence. La tectonique en extension accompagne la subsidence et la plate-forme initiale est fracturée de telle sorte que pendant le Lias et le début du Dogger des plates-formes résiduelles et des bassins coexistent. Dans le Haut-Atlas central, une vaste plate-forme persiste au sud alors que dans le centre et au nord ce sont des plates-formes résiduelles étroites qui séparent des bassins allongés. Un modèle en blocs basculés peut rendre compte de la persistance de zones hautes qui peuvent représenter la crête des blocs basculés. Pendant le Toarcien et jusqu'au Bajocien inférieur, les plates-formes persistent pendant que les bassins adjacents deviennent plus profonds. À la fin du Bajocien, la mer commence à régresser et les dépôts deviennent peu profonds, terrigènes et carbonatés. Cependant la subsidence reste forte tout juste compensée par la sédimentation. Deux courbes de subsidence, encore préliminaires, sont données à titre d'exemples pour la plate-forme sud et le bassin adjacent situé juste au nord de cette plate-forme. Ces courbes mettent en évidence les deux stades d'évolution avec les deux maxima de subsidence (Lias inférieur et moyen, et Toarcien à Bajocien inférieur).

INTRODUCTION

The High-Atlas represents the NW part of the Peri-Tethyan epicratonic domain in Africa. This domain is an intracontinental fold belt which evolved from subsiding basins (since Triassic times), at the boundary between the stable Saharan platform and the Moroccan hercynian belt (Figs 1 and 2). The tectonic inversion responsible of the orogenic system is mainly Tertiary in age (along its northern and southern flanks, Cenozoic sequences are involved in the fold and thrust belt). The elevation of the belt reaches 4160 m to the west and 3750 m to the east and the amount of shortening is variable. It is maximum along the north and south margins where it could attain 50% in the Mesozoic formations (between Tinjdad and Aït Hani, HADRI, 1993) (Fig. 2). Within the belt itself it is moderate (5 to 10%). The main prominent tectonic lines are presently thrust faults, responsible for the thickening and elevation of the belt. Along the northern and southern margins the thrusts are generally very low angle thrust faults which could represent the flat of ramps which are suspected to have been derived from normal faults. As a result the restauration of transverse sections at the time of the initial rifting is not so easy and is highly dependant on the model which is considered. All the models insist on the role played by the inherited hercynian structural directions on the Triassic rifting. The Late Hercynian faults, a northeastward prolongation of the Tizi n'Test fault zone, have a NE-SW strike. They have been reactivated during this initial rifting and lava flows and red thick terrigenous deposits accumulated in fault-controlled graben. LAVILLE'S model (1981), points out the role of strike slip faults in the initiation of the depot centers as pull apart basins, while other models favoured another style of deformation mainly extensional (WARME, 1988). Extension-transtension is probably a good explanation.

The investigated area is located in the central High-Atlas between Tinerhir, Tounfite, Rich and Tinjdad (Fig. 1). Previous works have provided good data (BERNASCONI, 1983; FADIL, 1987; STUDER 1987; MILHI, 1992; HADRI, 1993). In this area the High-Atlas attains its maximum width and is sited on a Palaeozoic basement which has been folded and faulted during Hercynian times. Coming from the NE, from the Mediterranean Neotethys, the initial transgression occured in early Liassic times and, as a result, the flooded area acquired its general appearance of a NE-SW elongated gutter. This morphology was preserved all along Jurassic times (CHOUBERT & FAURE-MURET, 1962; DUBAR, 1962). The first marine deposits consisted of shallow marine carbonates, but, as early as the late Sinemurian (Lotharingian), more deep sediments appeared in the central part of the basin, not everywhere but in elongated small troughs separated by narrow platforms which remained the site of shallow carbonate deposits with coral reefs (DU DRESNAY, 1977). These narrow platforms have been interpreted either as

Source : MNHN, Paris

anticlines or as tilted blocs, depending on the models, and their origin remains under discussion. A large variety of facies resulted from such contrasted morphologies.

This paper is an attemp to reconstruct the palaeoenvironments of the Central High Atlas during Jurassic times along a N-S geotraverse from the Moulouya high to the North to the African craton to the South. This area is representative of the various types of palaeoenvironments which can be found all along the belt and could be used for further correlations at the scale of the entire High Atlas. In this area a transition between the platform carbonates and the deepest basinal facies can be observed. So we are able to present an emended review of the classical formations previously described. We hope our attempt will help to clarify rather confuse nomenclature. We shall discuss the question of the origin of the subsidence. This contribution concerns a part of the investigations which are going to be extended to the entire Morocco.

FIG. 1.— Location of the studied area and of the NW-SE cross section of figure 2.

FIG. 1.— Carte de localisation de la région étudiée et de la coupe de la figure 2.

THE CENTRAL HIGH-ATLAS. A N-S TRANSECT BETWEEN MOULOUYA HIGH AND ANTI-ATLAS BELT (Fig. 1)

LITHOSTRATIGRAPHY AND BIOSTRATIGRAPHY

We have focused at first on lithostratigraphy and chronology in order to constrain palaeogeography and palaeoenvironments. As a result of eustatic sea level fluctuations, and local tectonic events, Liassic and Dogger times can be subdivided into 3 periods, each of them being characterized by different palaeoenvironments and facies: initial marine flooding (Hettangian-Sinemurian), formation and deepening of basins in the northern half part of the initial platform (Lotharingian-Bajocian), and retreat of the sea and emergence (Bajocian-Bathonian).

Source : MNHN, Paris

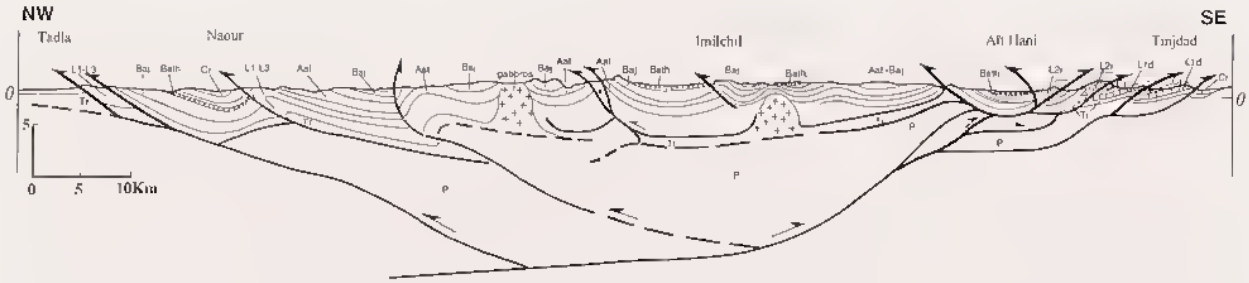

FIG. 2.— General NW-SE cross section of the central High-Atlas. This section crosses the central High-Atlas from the Marrakech-Tadla plain to the NW to the Ouarzazate basin to the SE, and it represents a tentative interpretation of the deep structures below the High-Atlas belt. It is only based on surface data (FADIL, 1987; HADRI, 1993, reinterpreted and recent field data), but it takes into acount another section located to the west (ERRARHAOUI, 1998), and which is more documented, especially for the Palaeozoic. The gabbroic boddies are a specificity of this section. Their roots have not been interpreted. They have been affected by the atlasic tectonic, and they probably have been translated from their primitive emplacement. Their origin and their mode of emplacement are hardly discussed (wrench faults or diapirs?). The rate of shortening is very important to the SE extremity of the section. It seems less important in the central part of the belt where it cannot be precisely estimated. It became again obviously more important to the NW. Cr: Cretaceous; Bath: Bathonian; Baj: Bajocian; Aal: Aalenian; L1-3: early to late Lias; L2r: middle Lias with coral reefs; L1d: Sinemurian, dolomitic; Tr: Trias; P: Palaeozoic.

FIG. 2.— Coupe générale NW-SE du Haut-Atlas central. Cette coupe traverse le Haut-Atlas depuis la dépression de Marrakech-Tadla au NW jusqu'au bassin de Ouarzazate au SE. Elle présente une interprétation de la structure profonde sous le Haut-Atlas d'après les données de surface (FADIL, 1987 ; HADRI, 1993), réinterprétées d'après des données de terrain récentes. Le Paléozoïque affleure peu et sa structure est interprétée d'après une coupe mieux documentée située plus à l'ouest (ERRARHAOUI, 1998). Les corps gabbroïques sont une spécificité de cette coupe. Leurs racines n'ont pas été interprétées. Ils ont été affectés par la tectonique atlasique et ils ont probablement été déplacés par rapport à leur position primitive. Leur origine et mode de mise en place sont très discutés (failles décrochantes ou diapirs ?). Le taux de raccourcissement est très important à l'extrémité SE de la coupe. Il semble moins important dans la partie centrale mais il ne peut pas y être estimé avec précision. Il redevient plus important au NW. Cr : Crétacé ; Bath: Bathonien ; Baj : Bajocien ; Aal : Aalénien ; L1-3 : Lias inférieur à supérieur ; L2r : Lias moyen récifal ; L1d : Sinémurien dolomitique ; Tr : Trias ; P : Paléozoïque.

Concerning lithostratigraphy many formations have been previously described in a lot of papers since half a century. Some of these formations are of local interest, many others are synonymous in term of palaeoenvironments. In order to clarify this nomenclature we have selected a transect located in the central part of the High-Atlas where both platforms and basins are well represented. Along this transect we have distinguished in between the formations which are widely distributed in the High-Atlas and the formations which are related to local specific environments and which grade lateraly into formations of more general scope. These formations are presented in two chronological charts along two orthogonal profiles (Figs 3 and 4):

— the N-S one (Fig. 3), shows the platform-basin transition in a direction perpendicular to the axis of the basin (from one margin to the opposite one).

— the other, WSW - ENE (Fig. 4), shows the same platform-basin transition along the axis of a basin bordering the southern platform of the High-Atlas.

The succession of formations presented on Figs 3 and 4 reflects the evolution of the palaeoenvironmental conditions during Jurassic times since the Sinemurian up to the Bathonian. The Late Jurassic has not been identified along this transect however it could be included in the red formations which have been classically attributed to the Bathonian and infra-Cenomanian. At the bottom of the sequence, red fine-grained detritic formations with evaporitic layers and basaltic lava flows are essentially Triassic to Hettangian in age according to K/Ar dating (210 to 196 Ma), but they could reach the Sinemurian (LAVILLE & HARMAND 1982).

THE INITIAL MARINE FLOODING (HETTANGIAN-SINEMURIAN)

The main formations which have been previously described: Idikel (STUDER, 1987), Agoulzi (MILHI, 1992) and Aït Ras (LE MARREC & JENNY, 1980; JENNY, 1988), are synonymous. They represent the first carbonate layers overlying the Palaeozoic basement or the Triassic beds. They are composed of

Source : MNHN, Paris

shallow marine carbonates more or less dolomitized which have been described by BURGESS & LEE (1978), and SEPTFONTAINE (1985). The main facies are pisolitic dolomudstones with fenestral fabric and mud cracks, evaporites and algal laminated boundstones. The palaeoenvironments are those of an internal platform more or even more restricted (intertidal to supra-tidal or sebkha). The age of these formations is poorly constrained in most places. They have been attributed to Hettangian and Sinemurian. They seem to have suddenly covered the entire central and eastern High-Atlas domain, from east to west, possibly by rupture of a natural dam. Faulting was probably active at that time but it is not evident on the field. This period corresponds to a general sea level rise (Fig. 5). We shall see below that the thicknesses vary from one place to another and that subsidence curve show a prominent first maxima.

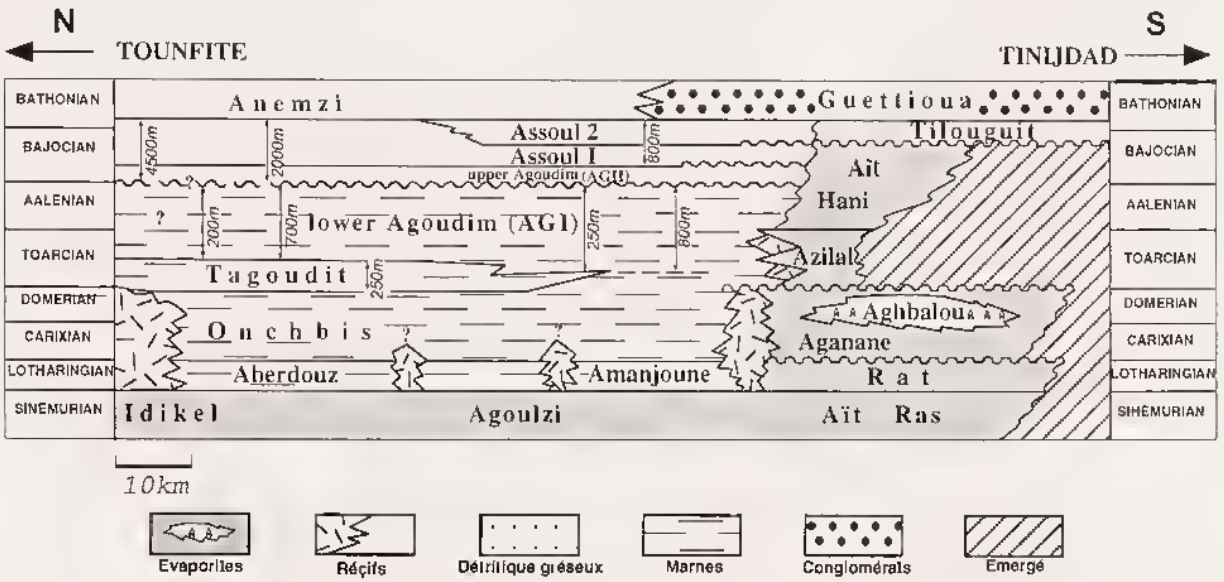

FIG. 3.— Chronological chart of the formations along a N-S section through the central High-Atlas.

FIG. 3.— Charte chronologique des formations le long d'une transversale N-S à travers le Haut-Atlas.

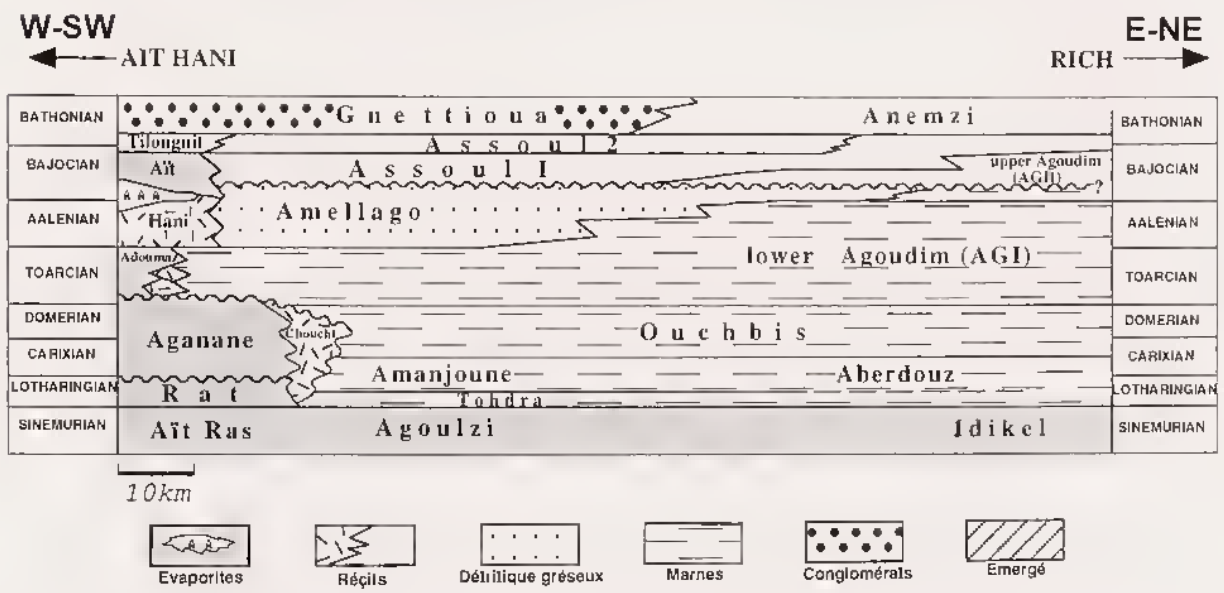

FIG. 4.— Chronological chart of the formations along a WSW-ENE section near the southern High-Atlas platform.

FIG. 4.— Charte chronologique des formations le long d'une section WNW-ESE à la bordure de la plate-forme sud du Haut-Atlas.

Source : MNHN, Paris

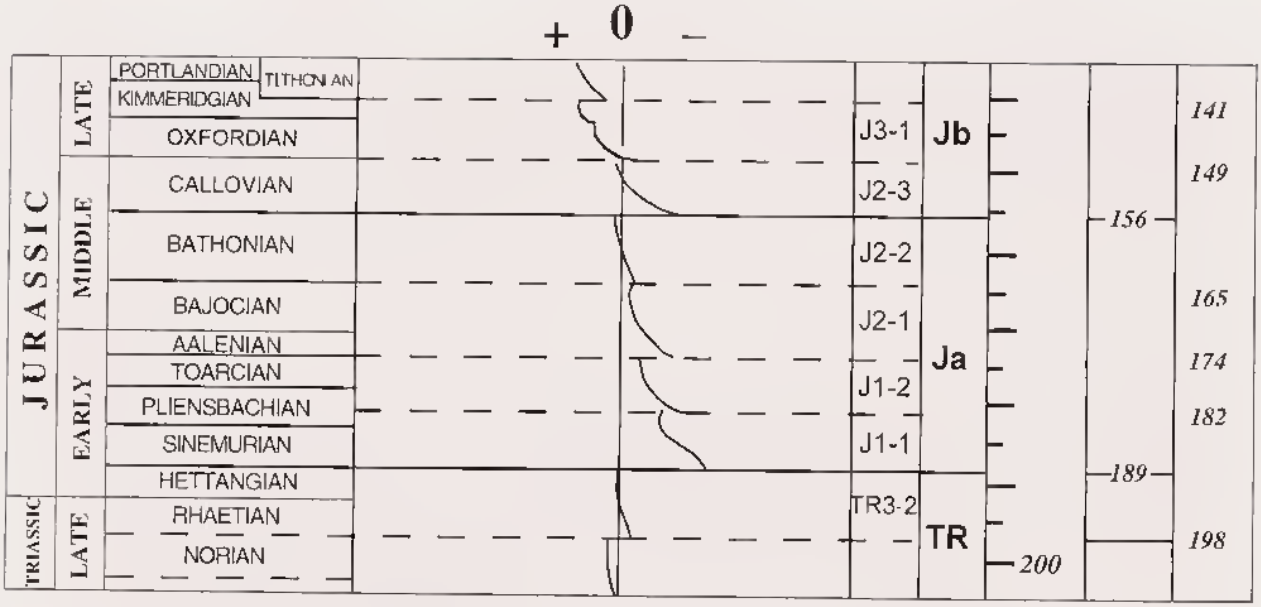

FIG. 5.— Global cycles of relative change of sea level during Jurassic (after HAQ *et al.*, 1988).

FIG. 5.— Cycles globaux des changements relatifs du niveau des mers (d'après HAQ et al., *1988).*

THE SECOND PERIOD: COEXISTENCE OF PLATFORMS AND BASINS (LOTHARINGIAN-BAJOCIAN)

As a result of the continuation of the rifting processes, the initial platform was broken and elongated basins developed in its central part during late Sinemurian (Lotharingian). Unlike the models generally admited which present the central part of the High-Atlas as a single deep basin, there were several basins, separated by shoals which could be the top of tilted blocks in a model of extensional tectonics. These higher parts could have been more or less deeply submerged and as a result they could have been the site of either a shallow marine carbonate deposits (remnant-platforms with coral reefs), or hemi-pelagic marls and carbonate deposits.

THE BASINAL FORMATIONS

EARLY AND MIDDLE LIASSIC TIMES.— The following formations, Aberdouz (STUDER, 1987), Todrha (MILHI, 1992) and Amanjoun (HADRI, 1993), correspond to the first basinal deposits in the central part of the High-Atlas along the main northern and southern platforms but also around the small narrow remnant-platforms. They are restricted to the elongated basins developped as a graben system. The transition between shallow marine and basinal deposits may be progressive though very fast, but sometimes the contact is abrupt and looks like a fault (Fig. 6). Slumps are frequent at a short ditance of the platform (Figs 6 and 7). The main facies are dark coloured cherty limestones with sponge spicules and sponge build-ups which look like reefs. Near Aït Hani these sponge reefs are interstratified in the ammonite bearing limestones which could reach the Carixian. Such reefs are not resedimented blocks as they are undoubtedly at their living emplacement (Fig. 8). WARME (1988) reported such build ups as typical facies of the central part of the High-Atlas trough to the north of Rich. Nevertheless they are not restricted to the central part of the basin. They have actually been observed in other places where they seem to preceed coral reefs along the platform margin (MILHI, 1993). Otherwise, in general, they seem to characterize environments deeper than shallow platforms and they could be used as a good marker of the initiation of subsidence in the whole High-Atlas. Nevertheless the sponge reefs have not yet been studied in detail in the High-Atlas. They have been observed in rather different depositional sequences, and we are not able to conclude about their living environment (unique or diversified and at which depth below sea level they were living during Liassic times). In the elongated basins cherty limestones are surrounded by marls with resedimented blocks near the platforms (frequently these blocks are coral reef

Source : MNHN, Paris

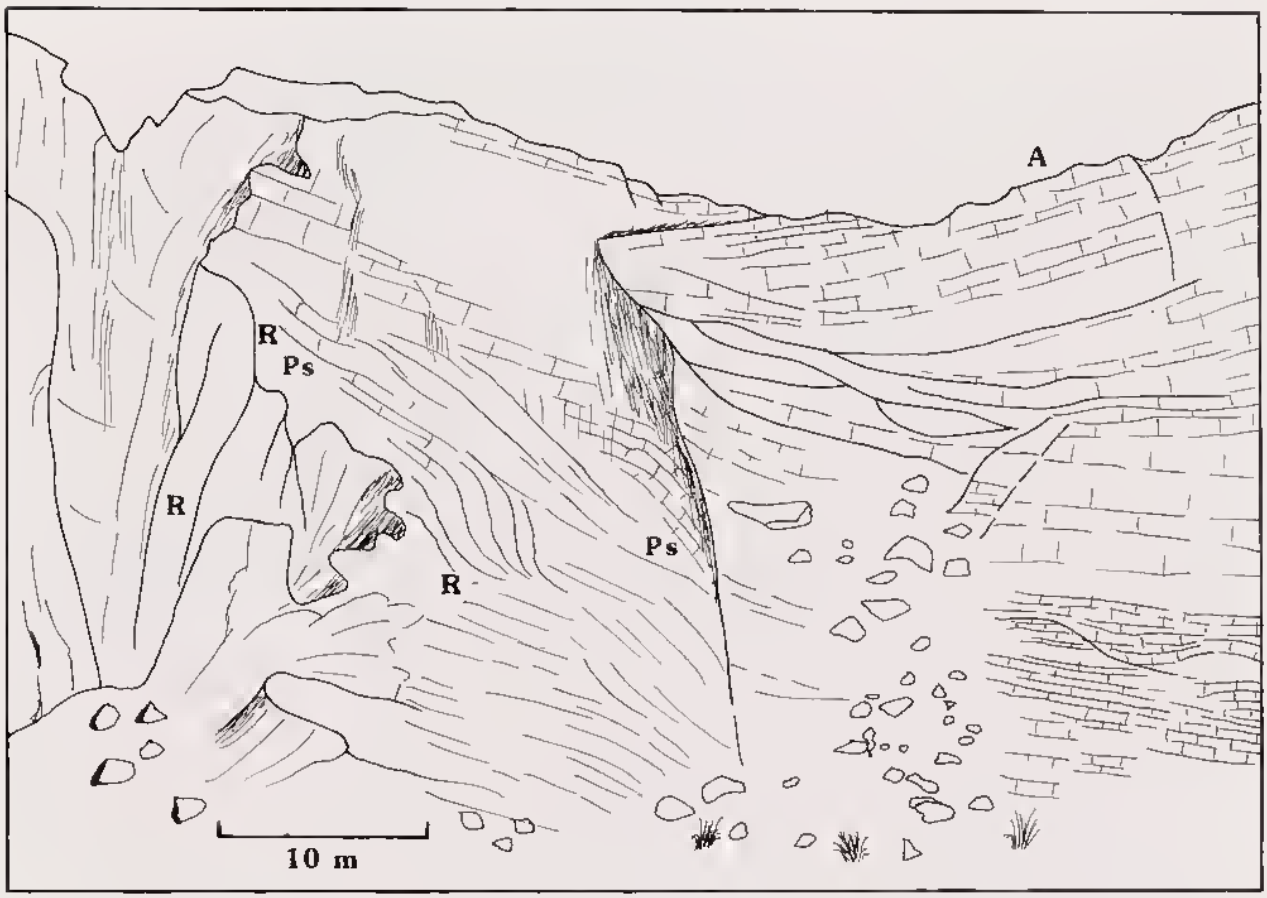

FIG. 6.— Southern platform of the High-Atlas. Road between Goulmina and Amellago. Abrupt of the plaform margin suggesting the morphology of a fault cutting through the Jbel Ikis coral reef (R). (Ps: palaeoslope of the reef; Jbel Choucht formation). The right half part of the picture (A) corresponds to the basinal limestones onlaping the platform with, from bottom to top , Aberdouz and Ouchbis Formations (early and middle Liassic). Faulting occured prohably during Lotharingian time. Notice the mega-slumps near the palaeoslope (see also figure 7; after HADRI, 1993).

FIG. 6.— Plate-forme sud du Haut-Atlas. Piste entre Goulmina et Amellago. Bordure de la plate-forme avec abrupt, pouvant correspondre à une faille, en limite nord du récif d'Ikis (R) ; Ps : paléo-pente du récif, formation du Jbel Choucht. En avant du récif (moitié droite de la photo) (A), les calcaires à ammonites (faciès de bassin), du Lias inférieur à moyen (formations d'Aberdouz et d'Ouchbis) viennent recouvrir progressivement la paléo-pente. Il y a eu effondrement de la plate-forme probablement au cours du Lotharingien. Remarquer les méga-glissements de bancs sur la pente sédimentaire (voir également la figure 7 ; d'après HADRI, 1993).

limestones), and turbidites. Ammonites are locally abundant and provided good stratigraphic data. Rates of subsidence are important and will be discussed below.

TOARCIAN TO BAJOCIAN.— At the end of the Domerian and during the middle Toarcian a significant eustatic rise of sea level occured (Fig. 5). which is approximately contemporaneous in the High-Atlas with a new tectonic event which is not only the reactivation of older faults. The platforms, which correspond to the footwall of reactivated normal faults, were again upheaved. As a result of these antagonist events: rise of sea level and tectonic uplift and compression. the shallow platforms came to near (or complete) emergence. while the basins in general became more subsident. A general discontinuity and local angular unconformities resulted from these events. Erosion on lands provided detritals such that sedimentation in basins became more terrigenous with marls and subordinate sandstones. In more detail, the general morphology of the basinal domain is affected by the persistance of a tectonic instability through the Toarcian: some highs were submerged and were the site of deposits in progressive unconformity along the flanks of the antiformal ridges (Fig. 9), and in complete unconformity on the top of these ridges, while some other came to emergence. STUDER & DU DRESNAY

Source : MNHN, Paris

FIG. 7.— Margin of the southern platform of the High-Atlas. Road between Goulmina and Amellago. Aberdouz limestones with a large slump at a regional scale. Thickness here is 10 m.

FIG. 7.— Bordure de la plate-forme sud du Haut-Atlas (piste entre Goulmina et Amellago). Figure de glissement d'échelle régionale (10 m d'épaisseur sur la photo), dans les calcaires de la formation d'Aberdouz.

(1980) described such unconformity at the western end of Jbel Masker. There an E-W striking antiform has been eroded during the Bajocian. It is suggested that this antiform existed as early as early Toarcian as "an anticline ride", which was the site of a relatively condensed sedimentation.

Similar evolution seems to have prevailed during Aalenian and early to middle Bajocian times. High rates of accumulation characterize some areas located to the northern half of the atlasic domain: Imilchil (SW of Tirrhist), Tounfite and NE of Rich (lower and upper Agoudim formations (STUDER, 1987) which grade laterally into Amellago and Assoul 1 formations of HADRI (1993); these later represent the

Source : MNHN, Paris

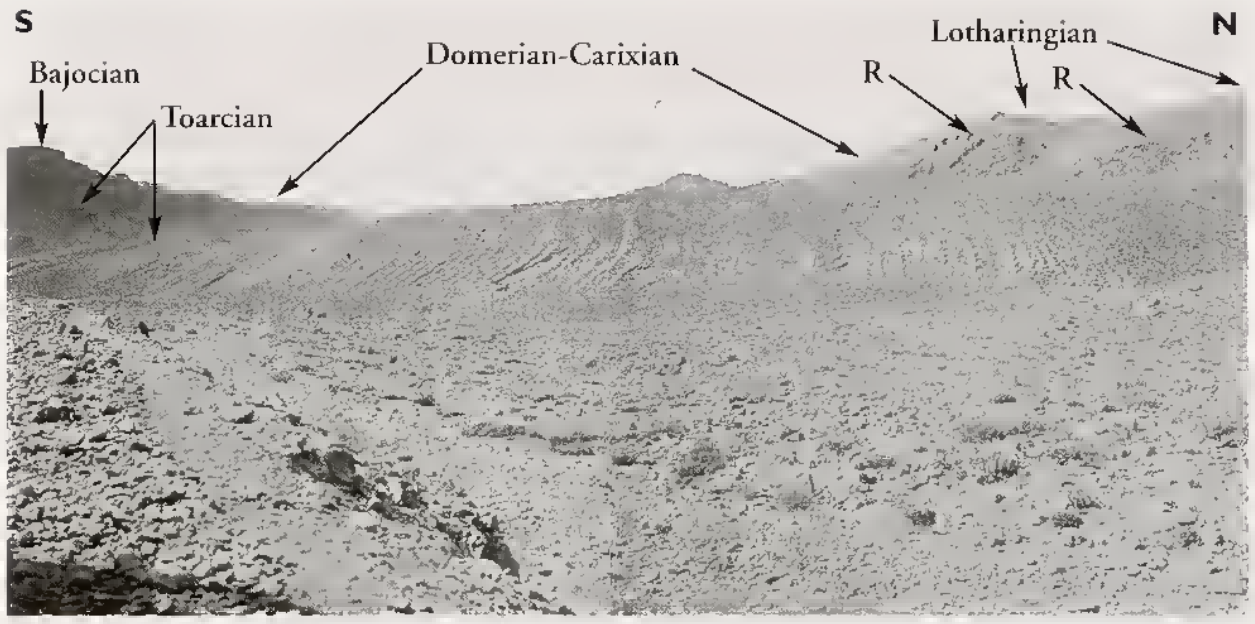

FIG. 8.— Basinal sequence in the region of Assoul. Aberdouz-Amanjoun formation (Lotharingian-Carixian): cherty bedded limestones with sponge reefs (R). Ouchbis formation (Carixian-Domerian): bedded limestones with ammonites. Agoudim formation (Toarcian): marly limestones and marls with ammonites. Amellago formation (Aalenian-Bajocian): oobioclastic limestones caped by the "calcaires corniches" which include small coral reefs.

FIG. 8.— Série de bassin dans la région d'Assoul. Formation d'Aberdouz-Amanjoun (Lotharingien-Carixien) : calcaires lités à silex avec récifs à éponges (R). Formation d'Ouchbis (Carixien-Domérien) : calcaires lités à ammonites. Formation d'Agoudim (Toarcien) : calcaires marneux et marnes à ammonites. Formation d'Amellago (Aalénien-Bajocien) : calcaires oobioclastiques avec la barre des "calcaires corniches" au sommet à petits récifs de coraux.

transitional terms between platform and basin). The maximum being reached during the Bajocian just before the retreat of the sea. Bathonian times are characterized by continental deposits all over the High-Atlas but with important discrepancies concerning thicknesses from one place to another. Nevertheless thicknesses are not always well known due to present day poor chronological data. Investigations are going on.

THE PLATFORM DEPOSITS

EARLY TO MIDDLE LIASSIC TIMES.— As a result of the formation of basins, the platform areas were considerably reduced in width during the Lotharingian, but they prograded northward during the middle Lias. The more important areas where shallow marine deposits persisted during that time are located to the west and along the margins of the High-Atlas, essentially along the southern margin (Figs 9 and 10). In these areas some major formations have been described. Their validity at the scale of the whole High-Atlas is recognized. It is the case for the following formations: Jbel Choucht (SEPTFONTAINE, 1985) (outer platform: bioclastic and oolithic sands with coral reef build up along the platform margin), Jbel Rat (JENNY, 1988), which corresponds to the inner supra-tidal platform (dolomitized algal laminated limestones, dolomudstones with bird-eyes; tepee structures are frequent). Aganane (SEPTFONTAINE, 1985) (shallow marine inner platform, carbonates with benthic foraminifera and giant pelecypods) (Fig. 11). Some other formations are more local but they could represent an original environment. This is the case for the Aghbalou formation (HADRI, 1993), which corresponds to an evaporitic sequence deposited in two subsiding sebkha areas (mainly gypsum and anhydrite, 200 to 500 m in thickness), and which could be considered as a special facies into the Aganane formation. These areas are located on both side of the Goulmina fault. Compared to the basin ones the thicknesses of the platform sequences are reduced, although they are not uniform. Along the southern margin of the High-Atlas, especially from the Dadès valley to the eastern High-Atlas, the basinal area was reduced in width during the middle Lias due to the progradation of the carbonate outer shelf with coral reefs (MILHI, 1992; HADRI, 1993).

Source : MNHN, Paris

FIG. 9.— Southern platform of the High-Atlas to the north of Tinjdad. Northern margin of the Aaddani coral reef. To the left (just outside of the picture), the reef is caped by the Azilal formation (Toarcian, shallow marine facies). To the left side of the picture the basinal early Toarcian marls (Agoudim formation) have covered an abrupt morphology (100 m high), which suggests a fault (pre-Toarcian).

FIG. 9.— Plate-forme sud du Haut-Atlas au nord de Tinjdad. Bordure nord du récif d'Aaddani. Abrupt correspondant probablement à une faille anté-Toarcien. Au sommet du récif (vers la gauche, en dehors de la photo), le Toarcien est de faciès Azilal (plate-forme), alors qu'au pied du récif (à droite), il est de faciès bassin (formation d'Agoudim), marnes à ammonites contenant des blocs récifaux resédimentés.

As a result, during the Lotharingian the southern platform margin was located just to the north of Errachidia, while during Carixian and Domerian times it was located to Foum Zabel (tunnel du Légionnaire), several kilometres to the north.

TOARCIAN TO BAJOCIAN.— During this period, the platforms were the site of important change in rate and type of sedimentation. Despite the eustatic sea level rise, some areas came to emergence and

Source : MNHN, Paris

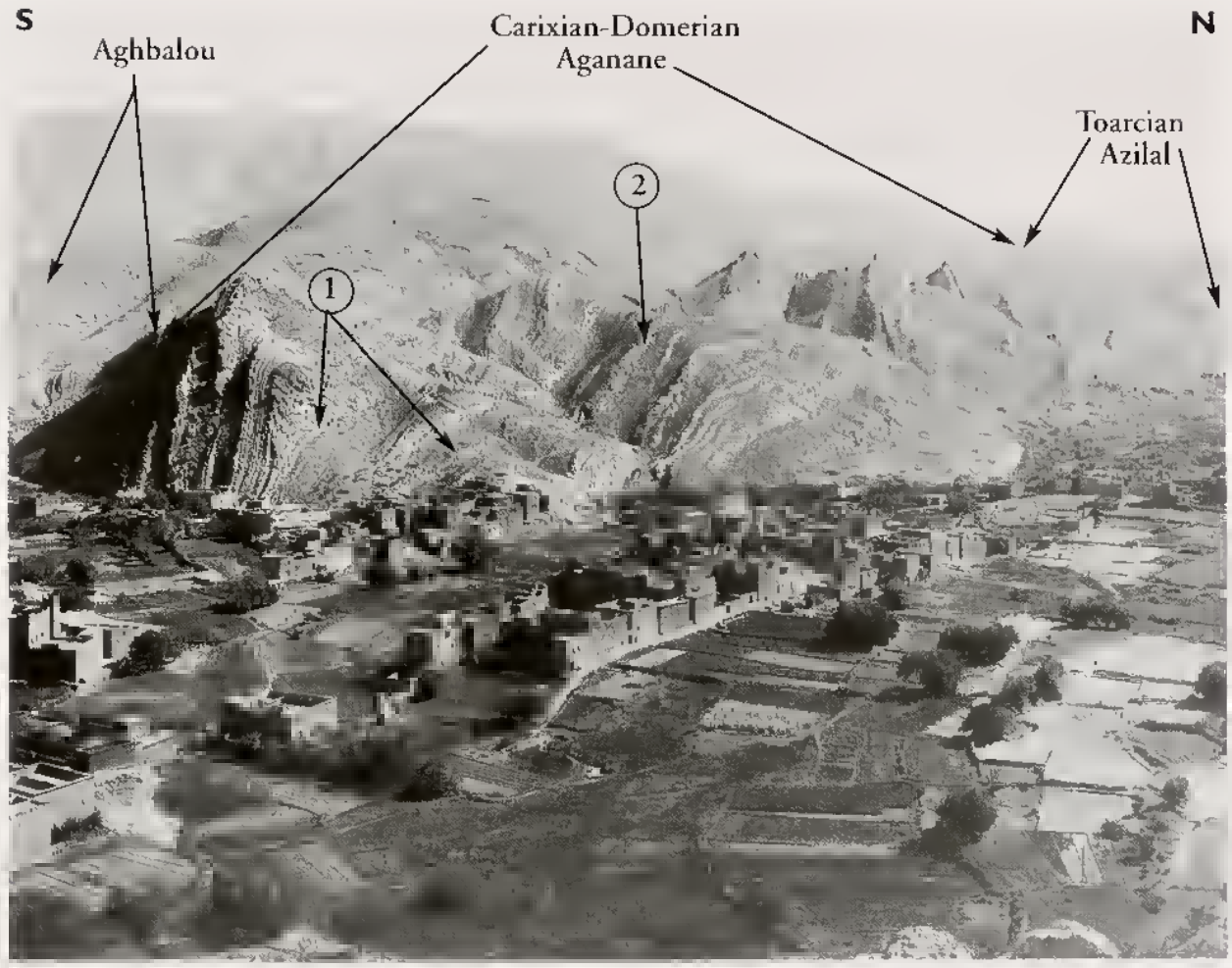

FIG. 10.— Southern platform of the High-Atlas near Aghbalou n'Kerdous (to the north of Tinjdad). Aghbalou formation (Carixian): sequence with gypsum of sebkha type. Aganane formation (Carixian-Domerian): dolomitized limestones with giant pelecypod "reefs" (1), and coral reefs (2). Azilal formation (Toarcian): red shales and marls with small patch reefs and bioclastic limestones.

FIG. 10.— Plate-forme sud du Haut-Atlas à Aghbalou n'Kerdous (au nord de Tinjdad). Formation d'Aghbalou (Carixien) : série gypseuse de sebkha. Formation d'Aganane (Carixien-Domérien) : calcaires dolomitiques avec "récifs" à grands lamellibranches (1), et récifs à coraux (2). Formation d'Azilal (Toarcien) : marnes silteuses rouges avec petits récifs de coraux et calcaires bioclastiques.

were eroded. In some other places crusts developed and open diaclases were filled by detritus and mineralisations, hard grounds are frequent. They correspond to a gap: the early Toarcian (in part or in totality), could be missing. This discontinuity is widely distributed in the High-Atlas and represents the boundary between two main sequences of deposition. DU DRESNAY (1964) and SADKI (1992), following previous authors, pointed out such discontinuity in various places in the High-Atlas and they correlated it with a middle Toarcian transgression (approximately coeval with the eustatic sea level rise). Nevertheless, the existence of angular unconformities below the Toarcian, and more generally below the Dogger, have to be correlated with compressional events which are simply registered in the platforms by gap and discontinuities, and are essentially recognized in the basinal areas as depicted above. The Azilal formation (JENNY, 1988) has been described in the western termination of the High-Atlas. It corresponds to continental and intertidal deposits (red terrigenous clays, sands and conglomerates including patch reefs towards the sea). In the Aït Hani area, in the central part of our transect here, the Aït Hani formation (HADRI, 1993) represents the upper part of the Azilal formation. It is composed of shallow marine to intertidal carbonates with coral patch reefs. Terrigenous sediments are subordinate. The

Source : MNHN, Paris

Amellago formation (HADRI, 1993) is the lateral equivalent of Aït Hani towards the open sea to the east (Fig. 4), and is composed of prograding bodies of oobioclastic sands. These sands are expelled from the adjacent platforms such as Aït Hani, and they correspond to a new development stage during which the basinal areas were contracting. During late Aalenian and Bajocian shallow marine areas predominate and progressively replaced the deeper areas which retreated to the east. As we shall see below these events remain difficult to explain.

FIG. 11.— Example of a bed of giant pelecypods in life position. Aganane formation.

FIG. 11.— Exemple de bancs à grands pélécypodes en position de vie. Formation d'Aganane.

Source : MNHN, Paris

THE THIRD PERIOD: RETREAT OF THE SEA AND EMERGENCE (LATE BAJOCIAN-BATHONIAN)

At the beginning of this period shallow marine areas predominate and the sea progressively retreats towards the east. The general shallowing upwards sequences are capped by continental deposits during the Bathonian which marks the end of the Liassic-Dogger major cycle in the High-Atlas.

SUBSIDENCE AND EUSTATIC SEA LEVEL CHANGE (Figs 12, 13, 14)

During Liassic and Dogger times sea level curve shows a first maxima during the Lotharingian-early Carixian, followed by a small drop during the Carixian, and a second maxima (more important), during the Toarcian (Fig. 5). In the Central High-Atlas the main discontinuities are: 1- the initiation of the basins by drowning of the preexisting platforms (during Late Sinemurian and thus just before the first maxima). This period is characterized by quite purely extensional tectonic events. It can be considered as syn-rift (s.s.) 2- the renewed deepening of these basins which took place during early (?)-middle Toarcian is coeval with the second maxima. This period is also characterized by extensional tectonic events especially in the platform areas (north and south; under preparation), but also by compressional event in the axial part of the belt. So, on a wide scope, the sea level rise is though not to be responsible for the formation of the basins nevertheless provoked an increase of their depth. As a result, subsidence itself may not be directly correlated with the sealevel curve. In fact it varies considerably from place to place and is thus related to tectonic events. The discussion concerns the precise nature of these tectonic events.

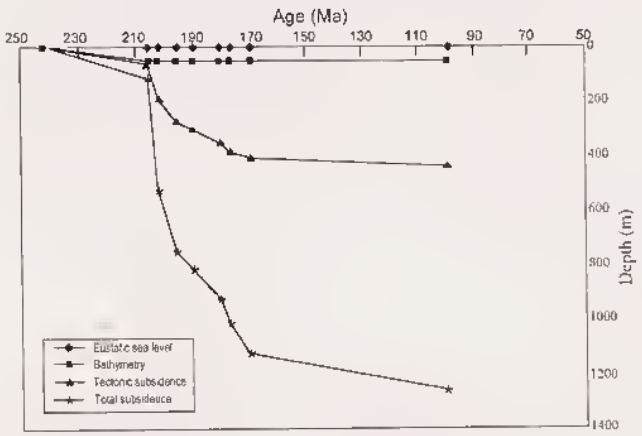

FIG. 12.— Subsidence history for the section of Iffer (southernmost platform).

FIG. 12.— Histoire de la subsidence pour la section d'Iffer (bordure sud de la plate-forme méridionale du Haut-Atlas).

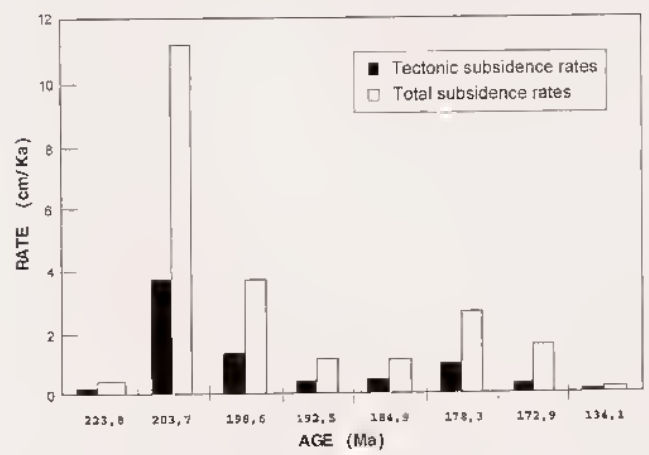

FIG. 13.— Subsidence rates for the section of Iffer.

FIG. 13.— Variation des taux de subsidence au cours du Jurassique pour la coupe d'Iffer.

Important variations in thicknesses have been reported and correlated with subsidence. Table 1 give some data (non decompacted sediments) for the central High-Atlas along a N-S profile (Tinjdad-Tounfite) (data from STUDER, 1987 & HADRI, 1993). From these data two subsidence curve have been prepared. They are given here as preliminary curves, one for the southern platform (Iffer section, Figs 12 and 13), and the other one for a basinal area in the region of Assoul (Fig. 14). The data (Table 1), suggest the following remarks:

— the northern and southern platforms present similar thicknesses during Sinemurian. In the wide southern platform two relatively subsiding areas developed during Middle Liassic time. They were the site of evaporitic deposits: Aghbalou basin, 200 m (HADRI, 1993), and Errachidia basin, 500m for the evaporites only (JOSSEN & FILALI-MOUTEL 1992). This later is essentially known in holes drilled for oil, water and coal prospection;

— the central area was, at the same time the site of an active subsidence. At first (early?-middle Sinemurian), the subsidence rate was compensated by the sediment supply. The facies

Source : MNHN, Paris

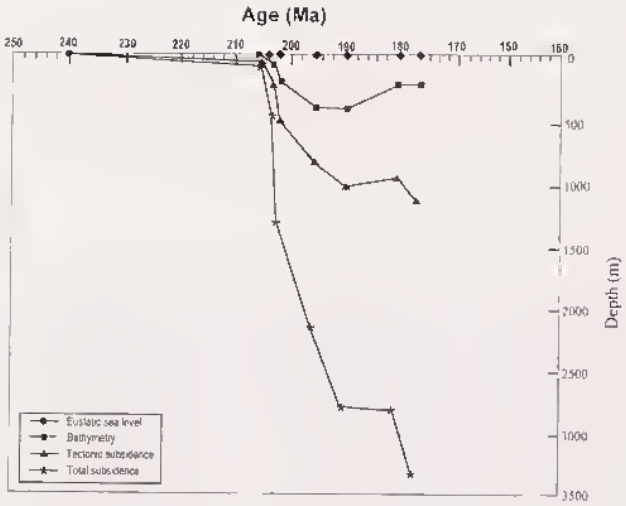

FIG. 14.— Subsidence history for a section (near Assoul), which corresponds to a basinal area to the south of the transect studied here.

Fig. 14.— Histoire de la subsidence pour une coupe (au SE d'Assoul) correspondant à une zone de bassin.

were the same on the platforms and in the central area but they were thicker at the emplacement of the future basin (600 m instead of 400 m). Subsidence remained active and rate of sedimentation increased considerably, and rapidly during the Lotharingian: the Aberdouz and Amanjoun formations reaches 1000 m. As sediment supply did not compensate the deepening of the basin, consequently, facies changed from shallow marine to hemipelagic;

— subsidence remained active in the central area during Liassic and Dogger times but not everywhere at the same rate: the depocenters moved during this period. They were localized at first in the southern part of this area during Liassic times and they migrated northwards during the early Dogger. In such a context of local variations in thicknesses subsidence history would have to be considered from one depocenter to another one, in order to retrace the variations in the rate of subsidence. This work, under preparation, require specific detailed data which are not always available in the published works.

TABLE 1.— Variation in thicknesses in the central High-Atlas. Thicknesses in metres. Non decompacted.

TABLEAU 1.— Variations d'épaisseur des formations dans le Haut-Atlas central. Épaisseurs en mètres. Non décompacté.

	Southern platform (Tounfite)	Central aera	Southern platform (Tinjdad)
BATHONIAN	?	Anemzi 800-1000 Aït Hani 200	
BAJOCIAN	?	Agoudim AGII 2000-5000	
AALENIAN		Agoudim AGI 0-700 Aït Hani 200 — 850 Amellago	170
TOARCIAN	Tagoudite 200	Amellago 800 Amanjoun 750 100	Iffer 0-60 0
DOMERIAN **CARIXIAN**	200	Masker (E) 1000 Aberdouz Amagour 50 N ↑ S	200-500 (evaporites)
SINEMURIAN	Idikel 350	Aberdouz 800 Amanjoun 1000	Iffer 400

The subsidence curves clearly point out, both on platform and basin, the existence of the two separate events which have been depicted above: the first during the Sinemurian and the second during Toarcian-Aalenian times. The first can be considered as syn-rift, but the second is not clearly post-rift.

Source : MNHN, Paris

During the Sinemurian (and more precisely during the late Sinemurian i.e. the Lotharingian), the initiation of several small hasins is associated with a very rapid change of facies. Sometimes Aberdouz deposits lie against cliffs which are probably ancient fault planes. In such a case the change of facies from shallow marine to hemipelagic can be precisely refered to faulting. This seems to be the case in many places during the late Sinemurian, especially along the southern margin of the High-Atlas, even if the faults are not always observed. A model with extensional faults (Figs 9 and 10), could explain the rapid initiation of these basins as well as the sudden facies changes. The existence of NE-SW strike slip faults during this period has not been confirmed by detailed recent studies (EL KOCHRI & CHOROWICZ, 1996, and our data under preparation). The NW-SE faults, such as the fault to the north of Goulmina (Fig. 10), could he interpreted as transfer fault in the model of oblique extension proposed hy EL KOCHRI & CHOROWICZ (1996). The same mechanism could have persisted later and could explain the high rate of subsidence prevailing during middle Liassic times. In conclusion, during early and middle Liassic times, there are evidences of extensional tectonics. After the Triassic magmatic activity which accompanies the initial rifting, extensional tectonic remained active during Liassic times, with a first maxima of subsidence, and the beginning of cooling of the lithosphere.

During Toarcian important changes occur. Globaly, the minor sealevel rise should have provoked a general transgression and, as a result, a general flooding of the platforms and a deepening of the basins would have occured. However, at the scale of the Central High-Atlas in general, this was not at all the case:

— some areas were effectively submerged and open marine deposits transgressed over previous internal platforms, while other areas (for example in the southern platform), became emergent (or near-emergent), and Toarcian could be highly condensed (ferruginous crusts), or restricted to about 60 m of red detritics and shallow marine limestones with patch reefs. Small extensional normal faults have been observed in these platforms.

— on the contrary, in the basin located just to the north of the southen platform (region to the SW of Assoul), the same interval of time could be represented by 800 m of marls with calci-turbidites.

It is also the case in the northern part of the High-Atlas, just to the south of the platform. There, thicknesses vary considerably: from 1250 m to the north (Onchbis), to 150 m (Jebel Masker, western tip, on an ancient high), and to 800 m to the south (between Jebel Masker and Jebel Aberdouz) (STUDER, 1987). In this area Tagoudite formation (STUDER, 1987), records the erosion of the Moulouya high in early Toarcian time. To the western tip of Jebel Masker an important angular unconformity has been observed (STUDER & DU DRESNAY, 1980), which separate the Toarcian and the Bajocian. Thus a compressional event occured, at least after the Toarcian. We have also oberved such stuctures to the west and they seem to characterize the axial part of the High-Atlas. They have been correlated with the emplacement of magmatic bodies (LAVILLE & HARMAND, 1982).

In conclusion, during Toarcian time, global sealevel rise did not provoked, in general, the expected effects of a transgression, and the main change in palaeoenvironments may be related to a renewal of extensional tectonics, accompanied by the second maxima of subsidence.

During Aalenian strong thickness differences have been reported. For example, early and middle Aalenian sediments can be completely missing or at least strongly reduced, for instance in Jebel Masker (western tip), and Jebel Aberdouz. As a result, since Toarcian, Jebel Masker represented a high with no or reduced sedimentation. On the contrary the basins between Jebel Masker and Jebel Aberdouz, and the basins to the north of Jebel Masker, were continuously subsiding (1250 m of sediments), in continuation of the dynamics inherited from Toarcian time.

On the contrary, during late Aalenian and Bajocian times, deposits record a gradual change from deep water marls, micrites and turbidites, to shallower water deposition of benthic shell bearing limestones with coral-algal reefs at the top. This shoaling of the central High-Atlas basins, related to the filling up of the previous troughs, has been described in the area of Rich (STANLEY, 1981), where the Agoudim formation is 1200 m thick (900 m of deep basin deposits capped by 300 m of transitional to shallow marine sediments). Farther to the west, in Jebel Aberdouz, the lower Agoudim formation (deep marine; 800 m; Toarcian) is overcome by the upper Agoudim formation (shallow marine; 1000 m). In the basin, between Jebel Masker and Jebel Aberdouz, the deep marine lower Agoudim formation (1250 m) is also overcome by the upper Agoudim (more than 3000 m; shallower to very shallow water). The

Source : MNHN, Paris

change from deep to shallow marine conditions seems abrupt in Jebel Aberdouz and is possibly more transitional in the basin located just to the north. After a sea level fall during Early Aalenian, Bajocian was characterized by new sealevel rise. Thus the Bajocian shoaling of the High-Atlas sea cannot be related to global eustatic sealevel change, but has a local origin which is tectonic. Compressional events have been proposed as an explanation for the formation of anticline ridges, with low sedimentation rate (STUDER, 1987). Although such events can be responsible for the emergence of large areas, however they cannot explain the subsidence during Bajocian time. According to LAVILLE & HARMAND (1982), synsedimentary deformations such as progressive unconformities, anticline ridges and gravity slidings, could have resulted from subvolcanic intrusions in the context of pull-apart basins. However, the intrusions are not always contemporaneous of the deformation, few of them are Bajocian, the majority are either Triassic to early Lias, or Bathonian to Late Jurassic and Early Cretaceous. According to STUDER (1987), the emplacement of the intrusions (dykes and large bodies), took place after the deposition of the Anemzi formation (which is dated Bathonian), in the area of Tounfite-Rich. Such a renewal of the magmatic activity followed a renewal of the subsidence and both necessitated extensional activity. The new faulting reported by STUDER (1987), in Jebel Masker could be responsible for the near emergence of the central part of the High-Atlas.

In conclusion the high rate of subsidence during Bajocian time, has to be associated with extensional events. Contrarily to the period which ended during Aalenian, emergence preceeded subsidence during Bajocian and was compensated by sediment supply: the subsidence is progressive, probably accompanied by a progressive unconformity related to a progressive deformation such as the uplift of a ridge, and rapid subsidence in the neighbouring areas. In the model of LAVILLE (summarized *in* LAVILLE & FEDAN, 1989), the reactivation of the E-W trending fault system induced multiple releasing and restraining stepover strike-slip basins. During Bathonian (Anemzi formation, STUDER, 1987), subsidence remained very active in some areas (800 to 1000 m of continental deposits), and magmatic activity developed along older faults. The subsidence history during Aalenian and Bajocian-Bathonian appears more complicated in the axial part of the High-Atlas belt and would require new field investigations in order to localize the depot centers and sediment thicknesses fluctuations over the area.

PALINSPASTIC RESTORATION OF SECTIONS FOR LOTHARINGIAN

The palinspastic maps (Figs 15 and 16), correspond to the situation during the Sinemurian, and figure 17 presents five N-S restored sections representing the superposed deposits since the early-middle Sinemurian until the end of the Lotharingian. As a result of field work the restoration is mainly based on

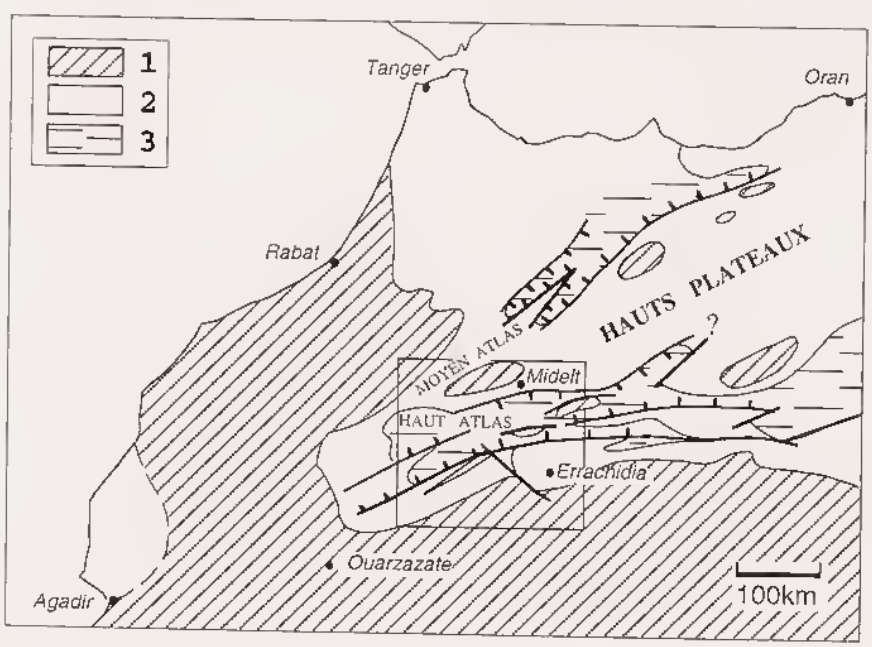

FIG. 15.— Location of the studied area on a palinspastic map corresponding to the Lotharingian. **1**, continental areas; **2**, shallow marine platforms; **3**, deepers basins.

FIG. 15.— Localisation de la région étudiée sur une carte palinspastique correspondant au Lotharingien. 1, zones continentales ; 2, plates-formes marines peu profondes ; 3, bassins.

Source : MNHN, Paris

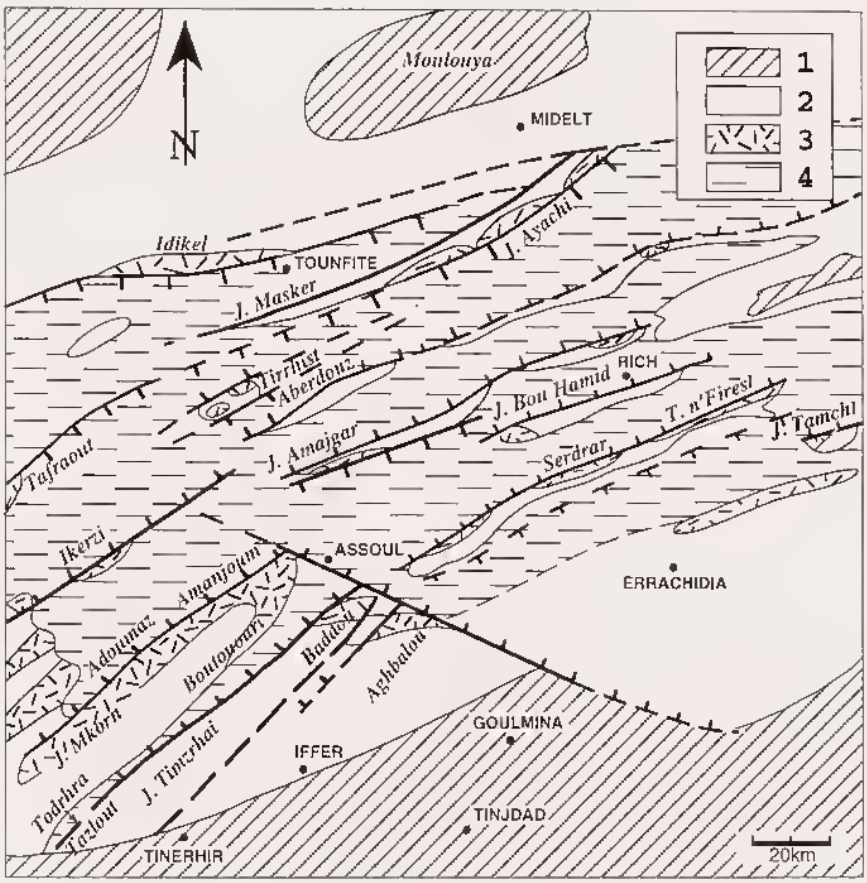

FIG. 16.— Palinspastic map showing the palaeoenvironments during the Lotharingian. **1**, continental areas; **2**, shallow marine platforms; **3**, coral reefs along the margins of the platforms; **4**, deeper basins.

FIG. 16.— Carte palinspastique montrant les palaéoenvironnements pendant le Lotharingien. 1, zones émergées ; 2, plates-formes marines ; 3, récifs de coraux en bordure des plates-formes ; 4, bassins plus profonds.

facies correlations and detailed observation of the transition between shallow marine and basinal carbonate. In such zones of transition, the rapid lateral change of facies from very shallow platform carbonates with coral reefs to deeper facies (ammonite bearing mudstones, bioclastic turbidites) is correlated to contrasted morphologies suggesting the occurrence of faults. In some places, such faults have been observed (HADRI, 1993). As a result our general interpretation favours a model of tilted blocs along normal more or less listric faults. The localization and strike of these faults being guided by older deep seated faults. In this model several elongated semi-graben basins were initiated and as soon as late Sinemurian, were the site of basinal deposits with ammonites. At the same time the highest part of the tilted blocks remained in more or less shallow marine conditions: in many places sponge build-ups could have developped near 200 or 300 m below sea level, while on some other tops corals attest of very shallow conditions. As a result, during late Sinemurian large shallow marine platform areas only persisted along the north and south margins of the basin and to its western end. To the south of the transect this platform remained relatively large: 30 and 60 km respectively to the west and to the east of the Goulmina fault. At that time it became progressively an internal platform where restricted conditions prevailed and an outer platform with sparse coral build up and more generally bioclastic sands. These conditions also prevailed during middle Liassic times when coral reefs attained their maximum extension (several kilometres in width), and when the internal platform evolved to sebkha conditions. By contrast the central part of the High-Atlasbasin was characterized by a succession of highs and basins. These later being the site of an active subsidence.

Source : MNHN, Paris

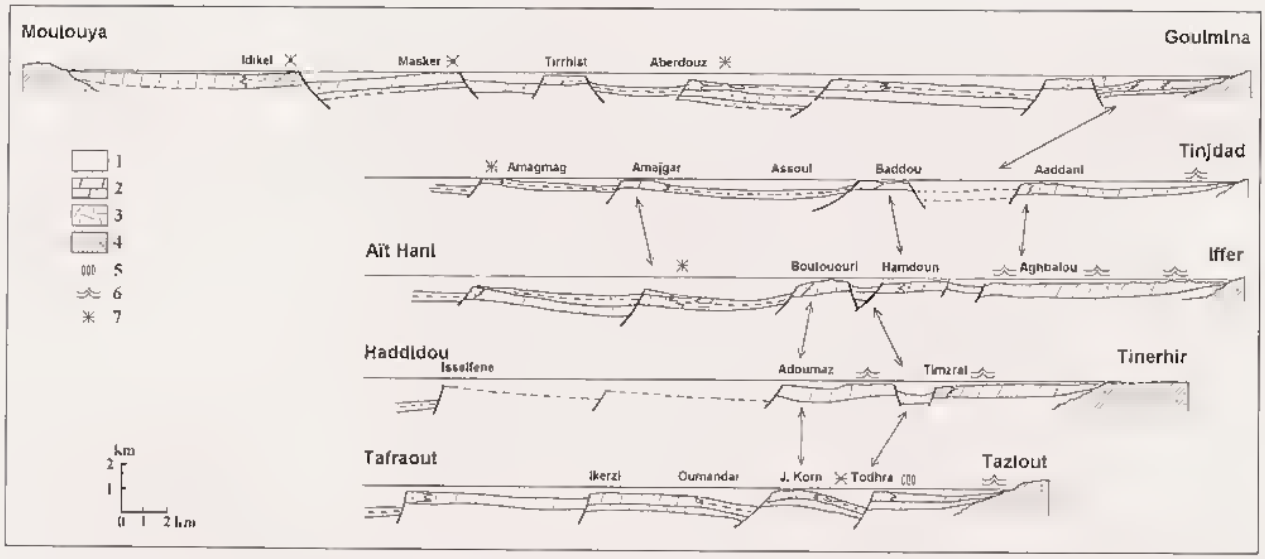

FIG. 17.— Interpretative cross sections through the central High-Atlas corresponding to the Lotharingian. This interpretation favour a model of pure extension. The platforms are restricted to the southern margin and along the crests of the tilted blocks. The elongated basins were the site of an active subsidence mainly at the end of this period. **1**, basinal facies (ammonite bearing marls and limestones); **2**, shallow marine carbonates; **3**, coral reefs; **4**, basement (mainly Palacozoic); **5**, accumulation of molluscs; **6**, lepee structures; **7**, sponge reefs.

FIG. 17.— Sections transversales interprétatives du Haut-Atlas central correspondant au Lotharingien. Cette interprétation reprend le modèle d'extension pure. Des plates-formes résiduelles persistent en bordure de la marge sud et le long des crêtes des blocs basculés. Les bassins étroits ont été subsidents au cours de cette période ; 1, faciès de bassin (marnes et calcaires à ammonites) ; 2, carbonates marins littoraux ; 3, récifs de coraux ; 4, substratum (Paléozoïque essentiellement) ; 5, accumulations de mollusques ; 6, structures en tepee ; 7, récifs à spongiaires.

CONCLUSION

As a conclusion the following points have to be emphasized:

— several general formations have been defined and correlations between facies and palaeoenvironments are possible along this section, and these correlations may be extended at the scale of the High-Atlas;

— an initial shallow marine platform suddenly covered all the High-Atlas during early Liassic time. Open marine basin was to the east (eastern Neotethyan Mediterranean). Subsidence was active;

— basins developed at the expense of this initial platform as early as Sinemurian by faulting (rifting remained active);

— subsidence accompanied the initiation of the basins;

— large platform areas persisted along the northern and (mainly) southern margins of the High-Atlas after the formation of the basins;

— narrow platforms persisted for a time (at least up to late Liassic time), along the crests of tilted blocks;

— two periods of active subsidence can be distinghished: during early-middle Liassic times the basins resulted from syn-rift extensional tectonics; during Toarcian, Aalenian and early Bajocian times. And restricted to some areas only during Bathonian times. Correlated to new extensional tectonic events in the platforms and compressional events in the axial part of the belt which are marked by the begining of a new magmatic stage.

General mechanisms for subsidence history have to be studied in more detail. In this area, eustatic sea level fluctuations have minor influence on subsidence.

Source : MNHN, Paris

ACKNOWLEDGMENTS

This work was funded by Peri-Tethys Program, the Ministère de l'Énergie et des Mines (Rabat) and the Université Paris-Sud (Équipe CNRS Géodynamique Interne et Géophysique). T. JACQUIN help us for subsidence analysis. Two referees gave constructive criticism of the manuscript. We would like to thank Rachel FLECKER for her revision of the English version, Geneviève ROCHE and Laurent DAUMAS for the drawing of the pictures, and Gérard COQUELLE for the photographs.

REFERENCES

BERNASCONI, R., 1983.— Géologie du Haut-Atlas de Rich (Maroc). Thèse, Université de Neuchatel, Suisse. Also published as *Travaux de l'Institut de Géologie*, **158**: 1-107.

BURGESS, C.J. & LEE, C.W., 1978.— The development of a Lower Jurassic carbonate tidal flat, Central High-Atlas, Morocco. 1: sedimentary history. *Journal of Sedimentary Petrology*, **48**, 3: 777-794.

CHOUBERT, G. & FAURE-MURET, A., 1962.— Évolution du domaine atlasique marocain depuis les temps paléozoïques: Livre à la mémoire du Pr P. Fallot. *Mémoire hors série, Société géologique de France, Paris*, **1**: 447-527.

DUBAR, G., 1962.— Notes sur la paléogéographie du Lias marocain: livre à la mémoire du Pr P. Fallot. *Mémoire hors série, Société géologique de France, Paris*, **1**: 529-544.

DU DRESNAY, R., 1964.— Les discontinuités de sédimentation pendant le Jurassique, dans la partie orientale du domaine atlasique marocain, leurs conséquences stratigraphiques et leurs relations avec l'orogenèse atlasique: colloque jurassique, Luxembourg, 1962. *Comptes Rendus et Mémoires de l'Institut grand ducal, Section Sciences naturelles*: 899-912.

DU DRESNAY, R., 1977.— Le milieu récifal fossile du Jurassique inférieur (Lias) dans le domaine des chaînes atlasiques du Maroc. *Mémoires du Bureau de Recherches géologiques et minières*, **89**: 296-312.

EL KOCHRI, A. & CHOROWICZ, J., 1996.— Oblique extension in the Jurassic trough of the Central and Eastern High-Atlas (Morocco). *Canadian Journal of Earth Sciences*, **33**: 84-92.

ERRARHAOUI, K., 1998.— *Structure du Haut-Atlas: plis et chevauchements du socle et de la couverture (interprétation des données géophysiques et géologiques)*. Thèse de Doctorat, Université de Paris-Sud, Orsay, France: 1-328.

FADIL, A., 1987.— *Structure et évolution alpine du Haut-Atlas Central sur la transversale Aghbala-Imilchil (Maroc)*. Thèse de Doctorat Ingénieur, Université P. Sabatier, Toulouse, France: 1-185, 2 cartes HT.

HADRI, M., 1993.— *Un modèle de plate-forme carbonatée au Lias-Dogger dans le Haut-Atlas Central au nord-ouest de Goulmima, Maroc*. Thèse Doctorat, Université Paris-Sud, Orsay, France: 1-272, 1 carte HT. 1/100 000.

HAQ, B.U., HARDENBOL, J. & VAIL, P.R., 1988.— Mesozoic and Cenozoic chronostratigraphy and eustatic cycles. *In*: C.K. WILGUS, B.S. HASTINGS, C.G. KENDAL, H. POSAMENTIER, C.A. ROSS & J. VAN WAGONER (eds), Sea-level changes: an integrated approach. *SEPM Special publication*, **42**: 71-108.

JENNY, J., 1988.— Carte géologique du Maroc au 1/100 000, feuille Azilal (Haut-Atlas central). Mémoire explicatif. *Notes et Mémoires du Service géologique du Maroc*, **339**: 1-104.

JOSSEN, J.A. & FILALI-MOUTEI, J., 1992.— A new look at the structural geology of the southern side of the Central and Eastern High-Atlas mountains. *Geologische Rundschau*, **81**, 1: 143-156.

LAVILLE, E., 1981.— Rôle des décrochements dans le mécanisme de formation des bassins d'effondrement du Haut-Atlas marocain au cours des temps triasiques et liasiques. *Bulletin de la Société géologique de France, Paris*, (7), **23**, 3: 303-312.

LAVILLE, E. & FEDAN, B., 1989.— Le système atlasique marocain au Jurassique: évolution structurale et cadre géodynamique. *Sciences géologiques, Strasbourg, Mémoire*, **84**: 3-28.

LAVILLE, E. & HARMAND, C., 1982.— Évolution magmatique et tectonique du bassin intracontinental mésozoique du Haut-Atlas (Maroc): un modèle de mise en place synsédimentaire de massifs "anorogéniques" liés à des décrochements. *Bulletin de la Société géologique de France, Paris*, **24**, 2: 213-227.

LE MAREC, A. & JENNY, J., 1980.— L'accident de Demnat, comportement synsédimentaire et tectonique d'un décrochement transversal du Haut-Atlas central (Maroc). *Bulletin de la Société géologique de France, Paris*, (7), **22**, 3: 421-427.

MILHI, A., 1992.— Stratigraphie, fazies und paläogeographie des Jura am Südrand des zentralen Hohen Atlas (Marokko). *Berliner geowissenschaften, Abh., Berlin*, (A), **144**: 1-93.

SADKI, D., 1992.— Les variations de faciès et les discontinuités de sédimentation dans le Lias-Dogger du Haut-Atlas central (Maroc): chronologie, caractérisation, corrélations. *Bulletin de la Société géologique de France, Paris*, **163**, 2: 179-186.

SEPTFONTAINE, M., 1985.— Milieux de dépôts et foraminifères (Lituolidés) de la plate-forme carbonatée du Lias moyen du Maroc. *Revue de Micropaléontologie, Paris*, **28**, 4: 265-289.

Source : MNHN, Paris

STANLEY, R.G., 1981.— Middle Jurassic shoaling of the Central High-Atlas sea near Rich, Morocco. *Journal of Sedimentary Petrology*, **51**, 3: 895-907.

STUDER, M.A., 1987.— Tectonique et pétrographie des roches sédimentaires, éruptives et métamorphiques de la région de Tounfite-Tirrhist (Haut-Atlas central mésozoique, Maroc). *Notes et Mémoires du Service géologique du Maroc*, **43**, 321: 65-197.

STUDER, M. & DU DRESNAY, R., 1980. Déformations synsédimentaires en compression pendant le Lias supérieur et le Dogger au Tizi n'Irhil (Haut-Atlas Central de Midelt, Maroc). *Bulletin de la Société géologique de France, Paris*, (7), **22**, 3: 391-397.

WARME, J.E., 1988.— Jurassic carbonate facies of the Central and Eastern High-Atlasrift, Morocco. *In*: V.H. JACOBSHAGEN (ed.), The Atlas system of Morocco. *Lectures and Notes in Earth-Sciences*, **15**: 169-199.

Source : MNHN, Paris

The Permian basins of Tiddas, Bou Achouch and Khenifra (central Morocco). Biostratigraphic and palaeophytogeographic implications

Jean BROUTIN [1], *Habiba* AASSOUMI [1], *Mohammed* EL WARTITI [2]
Pierre FREYTET [1] [3], *Hans* KERP [4], *Cecilio* QUESADA [5]
& *Nadège* TOUTIN-MORIN [6]

[1] Laboratoire de Paléobotanique et Paléoécologie, Université Pierre et Marie Curie
12, rue Cuvier, F-75005 Paris, France

[2] Université Mohammed V, Faculté des Sciences, Laboratoire de Géologie Appliquée, Avenue Ibn Batouta,
B.P. 1014, Rabat, Morocco

[3] 41 rue des Vaux mourants, F-91370, Verrières le Buisson, France

[4] Abt. Paläohotanik, Westfälische Wilhelms-Universität, Hindenburgplatz 57-59, 48143 Münster, Germany

[5] Direccion de Geologia, ITGE, Rios Rosas 23, 28003 Madrid, Spain

[6] Université d'Orléans, Département des Sciences de la Terre, UMR 6530, FRO9 du CNRS, BP 7659,
F-45067 Orléans Cedex 2, France

ABSTRACT

The intramontane deposits of the Tiddas, Bou Achouch, and Khenifra basins (Central Morocco), yielding outsanding palaeofloras from late Early to "Middle" Permian age, have been extensively studied during the last years. Sedimentary facies, lithostratigraphy, occurrence of bimodal magmatic events, macro- and microfloral contents, evidence that these deposits are more or less coeval in the three basins. Our last pluridisciplinary field works, carried out in the central Morocco basins, show they were deposited under tectonic, geographical (latitude, altitude) and climatic conditions quite similar with those observed in the coeval basins of south-western Spain. The palaeoecological study of the fossil material from Tiddas led to suggest a warm humid climate with somewhat irregularly distributed drought periods. Based on all available palaeontological data (macrofloras preserved as impressions-compressions or permineralized structures; microfloras; vertebrate foot-prints), the age of these Spanish and Moroccan continental deposits can be estimated as Kungurian (= Bolorian). The palaeophytogeographical implications are analysed through comparisons with the Permian floras already described in the Niger and Gabon *i.e.* along a

BROUTIN, J., AASSOUMI, H., EL WARTITI, M., FREYTET, P., KERP, H., QUESADA, C. & TOUTIN-MORIN, N., 1998. — The Permian basins of Tiddas, Bou Achouch and Khenifra (central Morocco). Biostratigraphic and palaeophytogeographic implications. *In:* S. CRASQUIN-SOLEAU & É. BARRIER (eds), Peri-Tethys Memoir 4: epicratonic basins of Peri-Tethyan platforms, *Mém. Mus. natn. Hist. nat.*, **179** : 257-278. Paris ISBN : 2-85653-518-4.

Source : MNHN, Paris

North-South transect from Spain to Central Africa. The occurrence of floristical exchanges have been evidenced during the Permian time between the southern margin of the Laurasian domain and the northern part of the Gondwanan floral realm. The main biostratigraphical and palaeogeographical implications of these studies are analysed.

RÉSUMÉ

Les bassins permiens de Tiddas, Bou Achoud et Khénifra (Maroc central). Implications biostratigraphiques et paléophytogéographiques.

Les dépôts intramontagneux des bassins de Tiddas, Bou Achouch et Khénifra (Maroc central), qui ont livré des paléoflores d'âge Permien inférieur-Permien moyen, ont été étudiées intensivement au cours des dernières années. Les faciès sédimentaires, la lithostratigraphie, l'existence d'un magmatisme bimodal et le contenu macro- et microfloristique indiquent que ces dépôts sont plus ou moins contemporains dans les trois bassins. Nos derniers travaux pluridisciplinaires sur le terrain ont permis de montrer que ces trois bassins se sont déposés dans un contexte tectonique similaire, une situation géographique homologue (latitude, altitude) et sous des conditions climatiques identiques aux gisements fossilifères contemporains du Sud Ouest de l'Espagne. Sur la base de l'ensemble des données paléontologiques (macroflores conservées en empreintes, compressions ou structures perminéralisées ; microflores ; empreintes de pattes de vertébrés) un âge Kungurien (= Bolorien) peut être proposé pour les bassins marocains et espagnols. L'étude paléoécologique du matériel fossile de Tiddas suggère un paléoclimat chaud et humide, affecté par des "stations" sèches de périodicité irrégulière. Les implications paléophytogéographiques de ces résultats sont analysées par des comparaisons avec les paléoflores permiennes décrites au Niger et au Gabon, c'est-à-dire le long d'un transect Nord-Sud de l'Espagne à l'Afrique Occidentale. L'existence d'échanges floristiques au cours du Permien entre le Sud du domaine laurasien et le Nord du Gondwana a été mise en évidence. Les principales implications biostratigraphiques et paléogéographiques de ces études sont analysées.

INTRODUCTION

In Morocco, the Permian was a transitional period between the Hercynian orogeny and the Mesozoic distension phase. The former is characterized by strong compression (during the Westphalian); the latter is related to the opening of the Atlantic Ocean in the West and palaeogeographical changes in the eastern Tethys. During this transitional period, until the end of the Palaeozoic, intense fracturing, cutting the Atlas-Mesetian basement into mobile blocks, took place, with subsequent episodic reactivations during the entire Mesozoic and Cenozoic. A compressive phase in the Early Triassic resulted in folding and tilting of the Permian deposits (EL WARTITI & FADLI, 1985). The Permian basins formed on a serie of mainly transverse structures, related to the regional compressive tectonic phase with NNE-SSW strike. These graben structures are considered to be formed during the Asturian phase and deformation eventually took place during the Saalian phase (MICHARD *et al.*, 1978), while a tectonic reactivation resulted in volcanism and the ascent of granitic plutons (CAILLEUX *et al.*, 1986).

The individual, isolated, usually small Permian basins are located around the margin of the central Morocco Hercynian massif (Fig. 1). They are the remnants of intramontane basins characterized by a strong subsidence and filled with detritic, predominantly red-coloured sediments. Carbonates and fine-grained, grey-coloured, lacustrine and palustrine sediments occur locally and are sometimes rich in plant remains. They are part of fining-upward sequences typical for terrestrial environments and consist of conglomerates, sandstones and mudstones. The sequences, showing very strong variations in thickness within a single basin, reflect the depositional history and the decrease of the hinterland relief during the Permian. Extensional tectonics played a fundamental role in the subsidence, through the activity of normal, synsedimentary faults, the elevation of horsts, and particularly the continuous activity of the basin boundary faults leading to a rejuvenation of the hinterland relief which provided detritic material. Large and deep faults, being the continuation of tectonic structures in the basement, favoured the formation of the granitic plutons between the late Visean and the Late Permian (BOUSHABA *et al.*, 1987), and the ascent of a bimodal volcanism, dominated by calc-alkalic magmas, prior (Tiddas), during (Bou Achouch, Chougrane, Mechraâ Ben Abbou), or after the filling of the basins (Khenifra).

The palaeoecological study of the fossil material from the Tiddas basin (impressions-compressions, permineralized woods, vertebrate foot prints, roots-related pedological nodules) led to suggest a warm humid climate with somewhat irregularly distributed drier periods. Their biostratigraphic attribution to the Early-Late Permian is based on the classification of more than sixty taxa of macro- and microfloral plant remains (Table 1 and Figs 8-11).

Source : MNHN, Paris

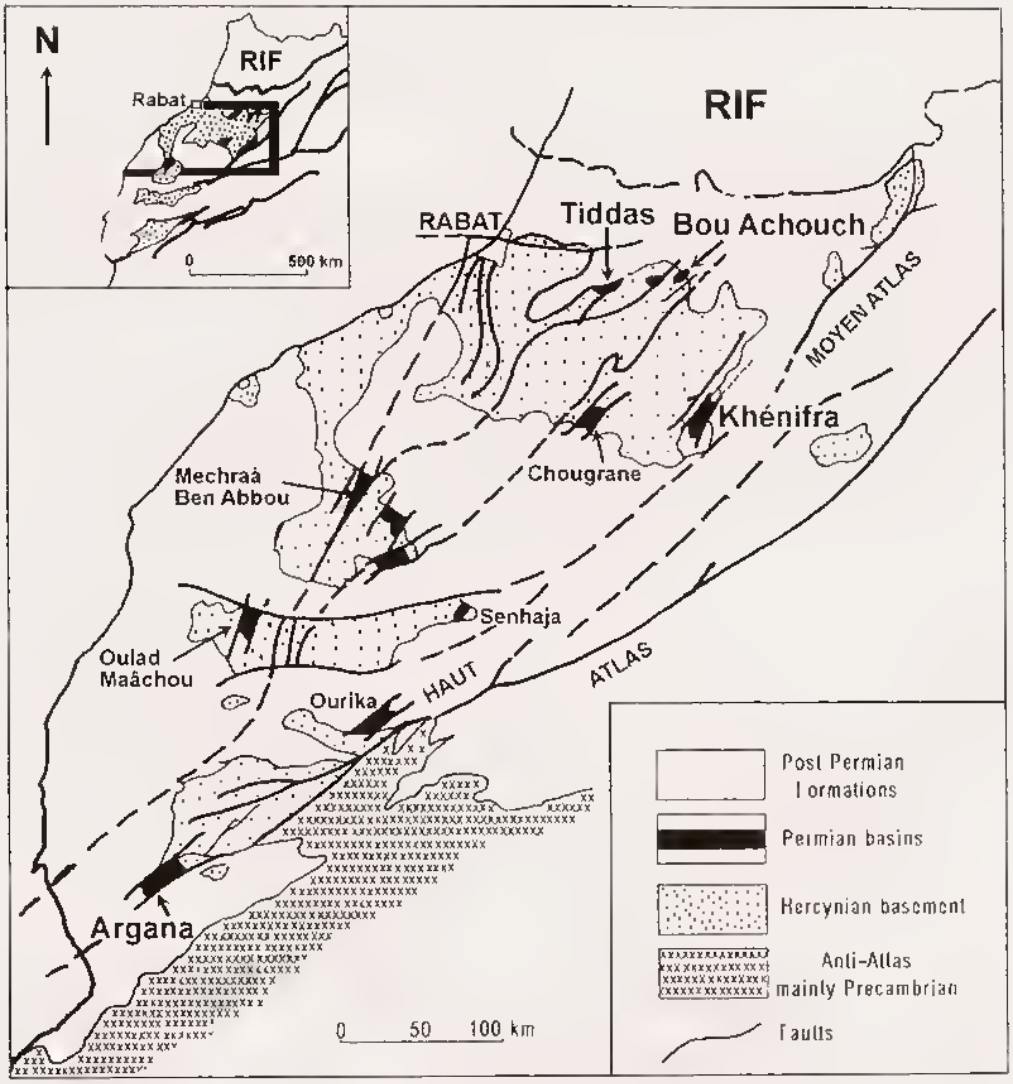

FIG. 1.— Permian basins of Morocco. Modified after MICHARD *et al.*, 1978 and EL WARTITI, 1990.

FIG. 1.— Bassins permiens du Maroc. D'après MICHARD et al., *1978 et* ELWARTITI, *1990.*

The last field investigations by the authors (1994), undertaken within the framework of the Peri-Tethys Program, evidenced the strong similarities between the Moroccan "Khénifra", "Bou Achouch" and "Tiddas" basins themselves, and with the corresponding soutwestern Spanish "Rio Viar" and "Guadalacanal-Urbana- San Nicolas del Puerto" ones. Sedimentary facies, occurrence of bimodal magmatic coeval events, macro- and microfloral contents, suggest that all these basins were built up under very similar tectonic conditions. Geographical (latitude, altitude) and climatical context were also quite similar.

It is clear that the Moroccan basins, on the one hand, and the Spanish ones, on the other hand, represent only residual parts of originally much more widespread intramontane basins (may be even of a single one). But the distance between Moroccan and Spanish areas and, above all, the different basements on which the Moroccan and Spanish Permian strata lie suggests that they did not pertain to a same basin.

Three Permian basins, Tiddas-Souk-es-Seht des Ait Ikkou (or simply "Tiddas"), Bou Achouch and Khenifra, will be described here in more detail, because they show numerous similarities in facies, tectonic setting, and they all contain an abundance of well-preserved plant remains which indicate the same age for all these three basins.

Source : MNHN, Paris

STRATIGRAPHICAL SECTIONS

TIDDAS

The Tiddas basin is located in the northern part of the Hercynian Massif. This elongated basin is 17 km long and up to 2 km wide, and is oriented in NE-SW direction (Fig. 2). In the southwest, the Permian unconformably overlies upper Visean flysch deposits. In the northwest, the Permian is unconformably overlain by Upper Triassic sediments which contain a Carnian flora (Figs 3-4), or by Quaternary sediments.

The Permian succession starts with reddish conglomerates containing boulders and pebbles of basement rocks (predominantly sandstones, quartzites, schists, and rarely crinoidal limestones). These conglomerates are to be interpreted as alluvial fan deposits. These are followed by respectively

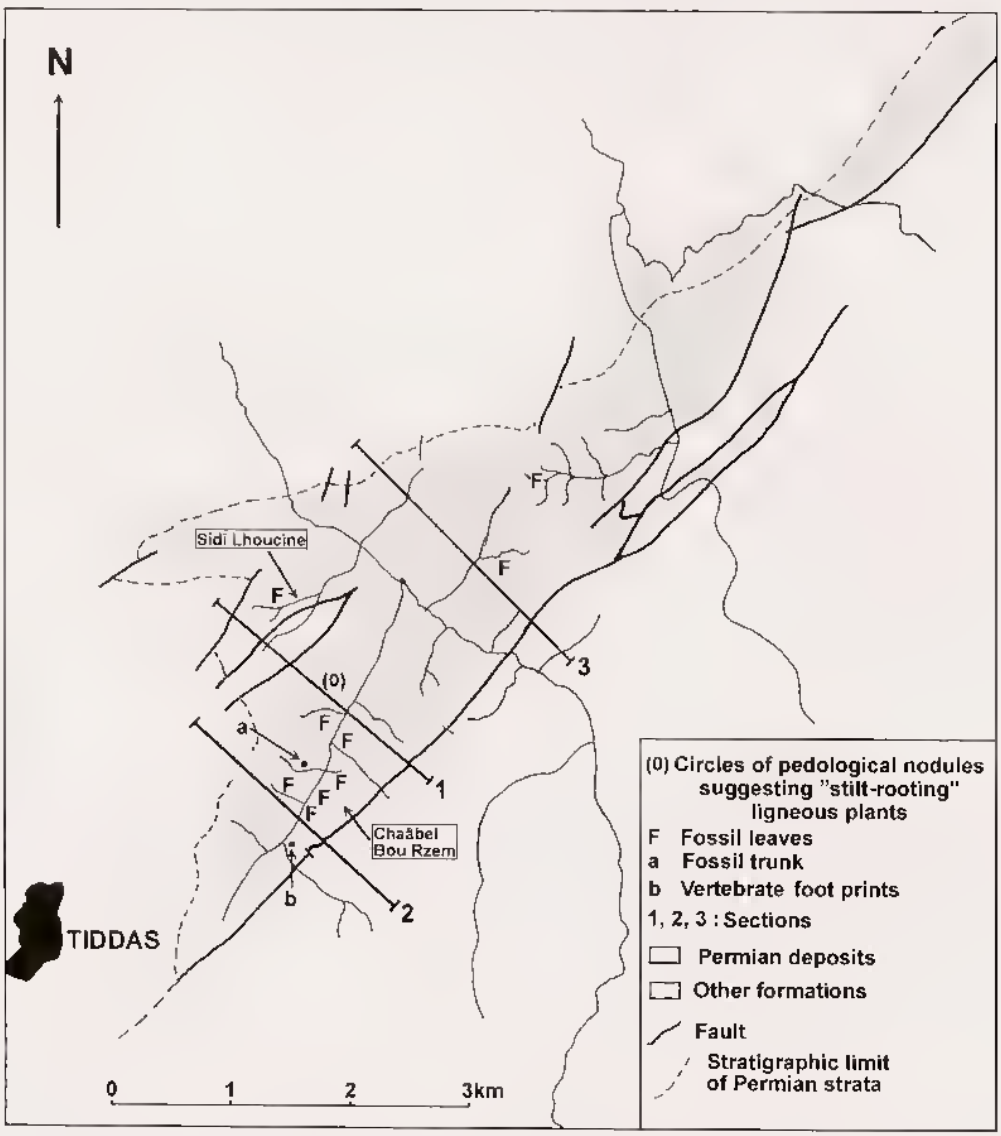

FIG. 2.— Simplified geologic map of the Tiddas-Souk-es-Sebt basin, after EL WARTITI, 1981, completed.

FIG. 2.— Carte géologique simplifiée du bassin de Tiddas-Souk-es-Sebt, d'après EL WARTITI, 1981, complétée.

Source : MNHN, Paris

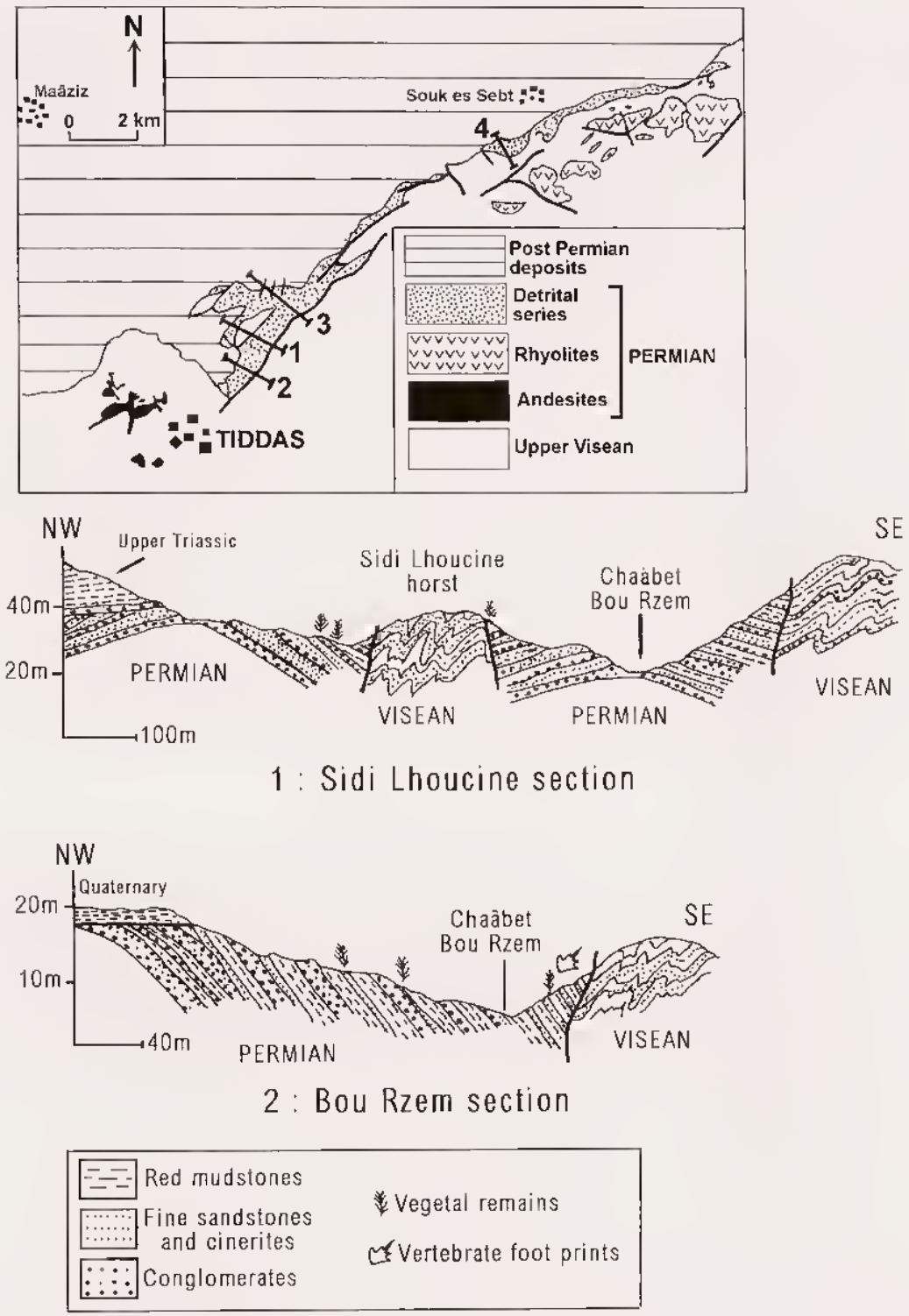

FIG. 3.— Location of the studied sections (1-4) of the Tiddas basin. Modified after EL WARTITI, 1981, Fig. 50; 1990, Fig.49, modified.

FIG. 3.— Localisation des coupes étudiées (1-4) dans le bassin de Tiddas. D'après EL WARTITI, 1981, Fig. 50 ; 1990, Fig. 49, modifiée.

Source : MNHN, Paris

conglomerates with a basal scouring surface, fluvial sandstones and red mudstones, occurring in thin, up to one meter thick but sometimes incomplete fining-upward sequences. The fine-grained sandstones are often rich in invertebrate tracks and burrows. The red mudstones, which are locally indurated and calcified, show ripple marks, desiccation cracks and imprints of rain drops. These thus represent a flood plain facies; in the centre of the basin they are associated with lacustrine and palustrine limestones in the upper part of the sequences. Lens-shaped pedogenic, 0.5-1.0 m thick horizons are locally developed in the red mudstones. These represent hydromorphic soils with carbonate nodules in a more or less circular arrangement (Fig. 2) which are interpreted as encrustations around the stilt roots of certain *Cordaites* (AASSOUMI *et al.*, 1993).

In the upper part of the sequence, vertebrate footprints were discovered (BROUTIN *et al.*, 1987). They mainly belong to *Hyloidichnus*, a taxon that is known from the Lower Permian of Arizona (U.S.A.), Lodève (France) and Thuringia (Germany). Two other forms can be compared respectively with the

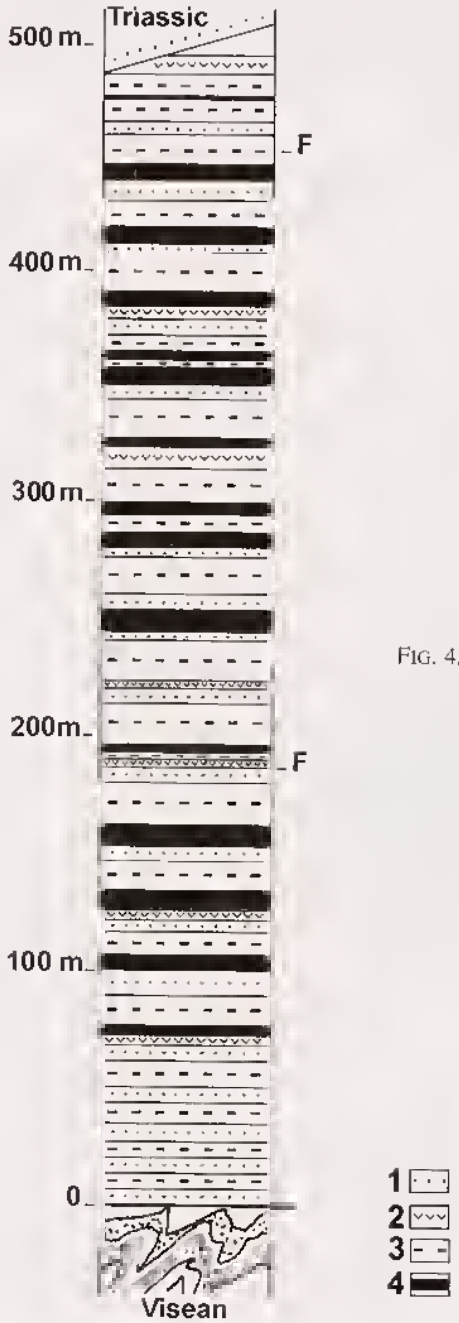

FIG. 4.— Synthetic succession of the Tiddas basin. *Coupe synthétique du bassin de Tiddas.* **1** : conglomerates and sandstones, *conglomérats et grès* ; **2**: volcanic tuffs, *tuffs volcaniques*; **3**: red beds (mudstones with palaeosols, rare vegetal remains and foot-prints), *niveaux rouges (argilites à paléosols, rares débris végétaux et empreintes de pattes)* ; **4**: grey beds (fine sandstones, cinerites and mudstones with vegetal remains, *niveaux gris (grès fins, cinérites et argilites à restes végétaux)* ; **F**: main fossiliferous levels, *principaux lits fossilifères.*

Source : MNHN, Paris

Permian ichnotaxon *Amphisauroides discessus* Haubold, 1970 and the genus *Gilmoreichnus*. The latter form is most similar to the "species" *G. brachydactylus?*, from the Lower Permian of Thuringia (Germany), and *Antichnium salamandroides* (Geinitz) Haubold (Det. G. Gand). A few thin, 20-60 cm thick grey mudstone layers locally occur within the red mudstones; they contain thin coal seams and are rich in well preserved plant remains.

The lower third of the section, or lower member, shows a predominance of coarse-grained sediments; sediments of the overlying upper member are finer and more fossiliferous, and the pebbles are more rounded. Both members show a fining upwards and they represent a positive megasequence; they are estimated 500 m in thickness.

Two main volcanic events, expressed by rhyolitic and andesitic volcanism, affected the Tiddas area (CAILLEUX *et al.*, 1982). Rhyolitic rocks are exposed in the northwestern part of the basin. Lavas are grey-coloured near the emission point, and then subsequently become yellowish red at some distance. Some ignimbritic rhyolites and bedded pyromerides occur locally. A system of intrusive veins in the upper Visean is probably the source of the lavas. Rhyolite pebbles are abundant in Permian deposits of the Souk-es-Sebt area, and fine, chocolate-brown tuffs, are sometimes intercalated in the conglomerates. Andesitic rocks are found in the southwestern part of the basin, forming small domes in the upper Visean. These andesites are massive and dark-grey in colour near their emission point; they locally become dark purple, with white patches or having a brecciated appearance, indicating a considerable release of gasses from the magma fluid. Andesite pebbles and tuffs are present in the conglomerates of this part of the basin. Finally, basic intrusive veins cut through the Permian series in the southwestern part of the basin (Fig. 4).

This calc-alkaline volcanism is related to the compression phase at the end of the Carboniferous and the beginning of the Permian. This volcanism was erupted along a local N 65 E trending, extensionnal fault zone (EL WARTITI, 1990).

The sediment sources do not show a predominant transport direction. The material is of local origin, from the Visean basement, granitic plutons, and Permian volcanic rocks in the northeast and southwest.

BOU ACHOUCH

The Bou Achouch basin is located on the northern side of the Hercynian Massif, approximately 20 km East of Tiddas (Fig. 1). It is a small basin, just 1 km^2, and the outcropping rocks are intersected, displaced and bounded by faults which also affect the basement. The layers generally dip E to ENE (Fig. 5). The Permian unconformably overlies the upper Visean, which consists of grey, folded flysch deposits; in the north and northeast the Permian is covered by Pliocene deposits.

The reddish conglomerates with poorly rounded pebbles of Visean sandstones, quartzites and schists, in the basal part of the sequence are interpreted as alluvial fan deposits (Fig. 5). They are overlain by fluviatile sandstones and red flood plain mudstones, sometimes with lenticular, thin, up to 20 cm thick limestone intercalations, and yellowish-ochrous carbonate nodules in the mudstones, indicating respectively lacustrine and palustrine environments (hydromorphic palaeosols). In the upper part of the sequence, a volcanic acidic phase is represented by a grey rhyolitic intercalation (section 3) and two types of ash tuffs (sections 1, 2, 3). One type is fine-grained, grey-blue, compact and well bedded, showing a fining upwards indicating a slow settling. The other type is yellow, rich in coarse detritic elements and numerous plant remains. Within the basin these ash tuffs with plant remains from the adjacent hinterland form marker horizons. This fining upward succession forms the lower member of the Permian at Bou Achouch.

In the upper part of the sequence, yellowish conglomerates contain pebbles of rhyolite and basement rocks, which are smaller and better rounded than in the lower member. The first layers of these stream deposits show a basal scouring surface, that indicates a new period of erosion. Approximately 30 cm thick, blue green ash tuff layers which show a fining upwards and pass into coal layers where abundant plant remains are common. Restricted environmental conditions are indicated by abundant dolomite in the top of this upper member, that as a whole can be also considered as a fining upwards sequence. A second volcanic episode, also calc-alkaline (SAUVAGE *et al.*, 1983) resulted in the formation of intrusive

Source : MNHN, Paris

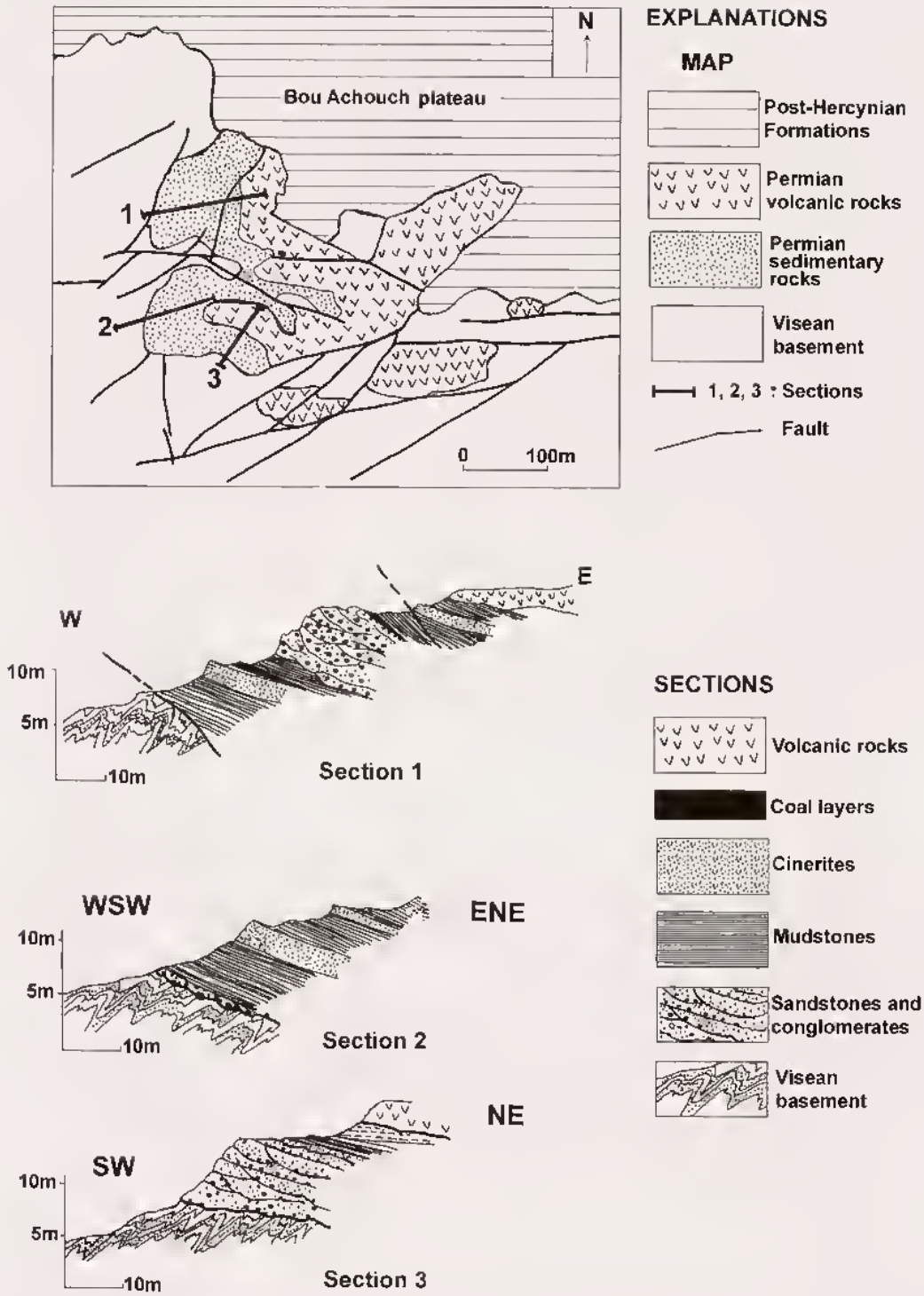

FIG. 5—. Geologic map of the Bou Achouch basin and location of the studied sections. Modified after CAILLEUX *et al.*, 1982 and EL WARTITI, 1990.

FIG. 5—. Carte géologique du bassin de Bou Achouch et coupes étudiées. D'après CAILLEUX et al., *1982 et* EL WARTITI, *1990, modifiée.*

Source : MNHN, Paris

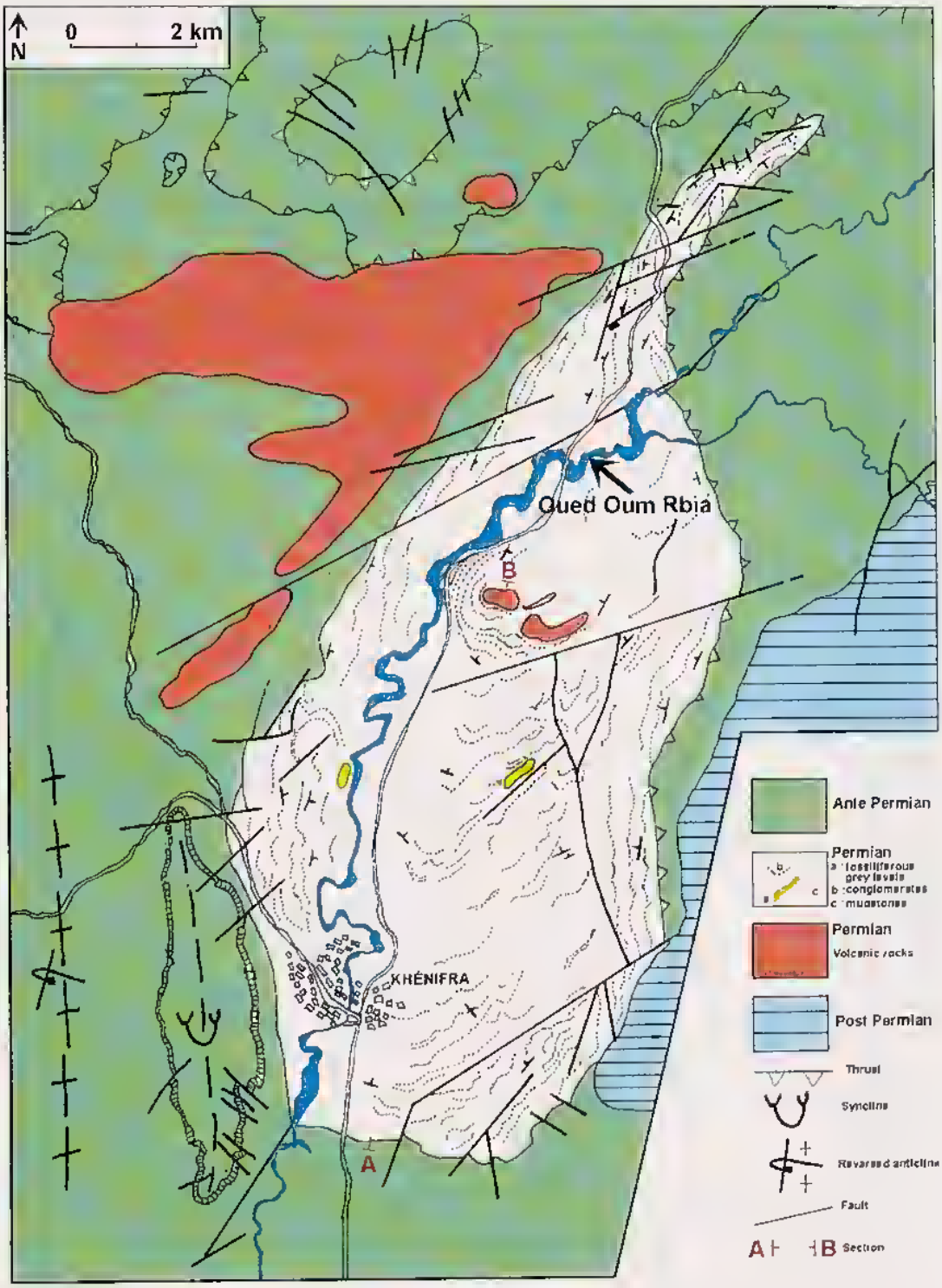

FIG. 6.— Simplified geologic map of the Khenifra Basin. After EL WARTITI, 1990, completed.

FIG. 6.— Carte géologique simplifiée du bassin de Khénifra. D'après EL WARTITI, *1990, complétée.*

Source : MNHN, Paris

veins and plugs of purple-grey rhyodacites and dark-grey to dark-green andesites, found in the eastern and northern parts of the basin.

The whole series is not more than 60 m thick; the sediment source seems to have been located primarily in the east and south-southeast.

KHENIFRA

The Khenifra basin (Fig. 1) is the easternmost one of the Permian basins of central Morocco. This basin is also the largest one regarding its present outcrop area (about 100 km^2). The basin is cut into three parts by transverse faults which run in SSW-NNE direction, the southern part of the basin forms a wide regular synclinal structure (Fig. 6).

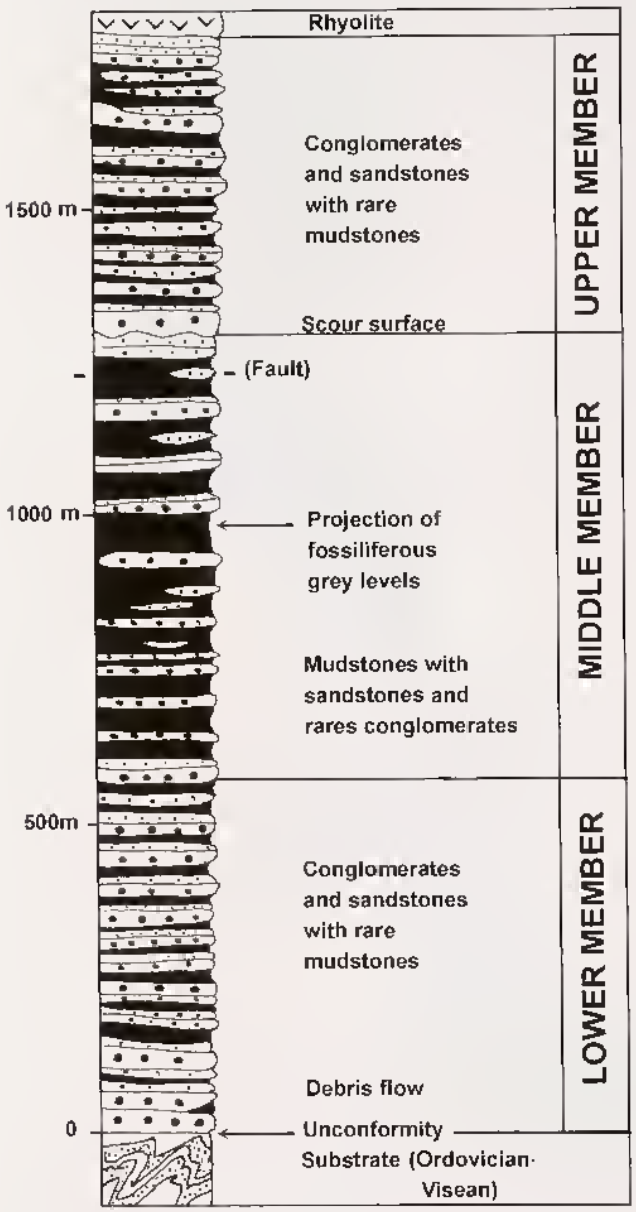

FIG. 7.— Synthetic succession of the Khenifra Basin. ("A - B", Fig. 6). After EL WARTITI, 1990. Fig. 87, completed.

FIG. 7.— Coupe synthétique du bassin de Khénifra ("A - B", Fig. 6). D'après EL WARTITI 1990, Fig. 87, complétée.

The Permian series unconformably overlies Ordovician schists, quartzites and psammites (N, NE and S), Devonian sandstones, siltstones and limestones (N and NW), Visean sandstones, claystones and limestones (W). This folded basement now forms a relief surrounding the Permian basin. Compression took place after the Permian but before the Late Triassic; the normal faults limiting the basin reacted as inverse overthrusts. The Upper Triassic unconformably overlies the Permian (Fig. 6).

The Permian series consists of three members (Fig. 7).

Sedimentation of the lower member starts with conglomerates containing coarse pebbles of Ordovician and Visean sandstones and quartzites, and Visean and Devonian reefal limestones. The lower member consists of a succession of fining upward sequences (conglomerates - sandstones - mudstones), revealing the subsidence of the basin. These materials correspond to alluvial fans deposits, with sometimes debris flow deposits. Toward the basin centre, they become channelised. In the upper part of this member, and in the S of the basin, ripple marks and thin laminations appear in fine grained sandstones and indurated grey mudstones, platy splitted by weathering.

The middle member mainly consists of red mudstones, interbedded with occasional layers of beige sandstones and grey, indurated mudstones, platy splitted by weathering. Plant remains, locally associated with azurite and malachite mineralizations, are frequent in the light-coloured horizons. A few thin lignite horizons, a few cm in thickness, have been reported from the area near Khenifra (TERMIER, 1936). In the area of Bouzouggargh, a lateral transition from red flood plain mudstones to grey lacustrine mudstones can be found; both mudstones are rich in plant remains. Large linguoid ripples (Nkhilat area),

Source : MNHN, Paris

desiccation cracks, invertebrate hurrows and plant remains occur in the grey fine-grained sandstones. This middle member forms, with the lower member, a fining-upwards megasequence.

The upper member consists of coarser material, but the pebbles are well sorted, and, mostly smaller than those in the lower member. This indicates a new phase of erosion, related to a local tectonic phase, and a predominantly fluviatile transport. The fine-grained sandstones sometimes show laminations, ripple-marks and rain imprints. Pedological phenomena, such as marmorisation patches and carbonate nodules locally occur in the red mudstones: the carbonate nodules were formed by the encrustation of plant remains during rain periods. This upper member represents the beginning of an incomplete fining upwards megasequence.

In the northwestern part of the basin (Fig. 6) a thick volcanic unit is exposed, consisting of two types of magmatites (YOUBI, 1990):

— the first, acid and viscous magmatite type, comprises red, yellow or grey rhyolites - reaching a thickness of 150 m and intersecting the Permian in the middle part of the basin ignimbritic rhyolites and purple grey and straw-yellow rhyodacites. The magmas ascended via large faults coming from the basement;

— the second type of magmatite basic, is an explosive magmatite type, which intruded in the former and consists of andesitic domes and black or green dacites.

Several, approximately 10 m thick layers of chocolate-brown ash tuffs and small occurrences of pyroclastites are locally present in the volcanic massif.

This volcanism, which is calc-alkaline (YOUBI & CABANIS, 1995) like in the Tiddas and Bou Achouch basins, is only slightly younger than the basin filling, because pebbles consisting of these volcanic rocks are absent in the coarse sediments, although a radiometric dating indicated a Permian age (264 ± 10 Ma, JEBRAK, 1982).

DEPOSITIONAL ENVIRONMENTS

Field observations and detailed laboratory studies (EL WARTITI, 1990) allowed the reconstruction of the basin history and the sedimentary successions appear to be similar in most of the Moroccan Permian basins, especially in central Morocco, which are all filled with terrestrial, predominantly detritic material.

At the base coarse-grained sediments being the result of the erosion of the adjacent reliefs, are abundant, mainly near the basin margins, where they occur in the form of alluvial fan deposits, or sometimes as mudflows. This lithology reflects a very local origin.

Then the sandstones of fluviatile facies become predominant. With each flooding, meandering channels filled with conglomerates cut into the underlying deposits in the central part of the basin. Braided channels are common in the Tiddas and Khenifra basins, as well as in the Chougrane and Mechraâ Ben Abbou basins that are not described in this paper.

The top of the basin fill (Tiddas), or the top of the megasequences which can consist of several phases (upper part of the middle member in the Khenifra basin), comprises fine sediments, mainly red flood plain mudstones, which were deposited during tectonically calm periods when the surrounding relief was low. During rainy periods small lakes and ponds were formed in these wide, silty plains in which thin lens-shaped carbonate layers were deposited (Tiddas, Bou Achouch, Khenifra, Chougrane). Sometimes (Mechraâ Ben Abbou), stromatolitic encrustations, charophyte remains and ostracod shells indicate the presence of more permanent, somewhat deeper waters (DAMOTTE *et al.*, 1993). The periodical desiccation of the lake edges only resulted in the formation of carbonate nodules. The encrustation of roots can occur during flooding periods (Tiddas). In some cases, the slow settling of fine particles (volcanic ashes in the Bou Achouch Basin, grey platy splitted silts, and clays in the Khenifra Basin) in these lakes is associated with the deposition of plant material which originated from the immediate vicinity or from the adjacent hinterland.

Source : MNHN, Paris

PALAEOBOTANIC BIOSTRATIGRAPHICAL DATA

The Bou Achouch, Tiddas and Khenifra basins have yielded rich and diversified macrofloras. Conversely, our attempt for microfloras extractions have been successful in only one grey pelitic horizon of the Khenifra basin ("Nkilat" locality, on the Oued Oum Rbia right bank: Fig. 6).

MACROFLORA

The "conifer dominated" Bou Achouch, Tiddas and Khenifra floral assemblages are similar enough (as clearly shown in table 1) to suggest that these three basins are more or less coeval.

Looking for the most biostratigraphically relevant forms, we can point out the occurrence of:

— a rich conifer complex characteristic of euramerian Lower Permian "*sensu lato*", including forms such as : *Otovicia hypnoides* Kerp *et al.* (Fig. 8; a,b); *Culmitzschia* (al. *Walchia) laxifolia* Clement-Westerhof (Fig. 8; c); *Culmitzschia* (al. *Walchia) parvifolia* Clement-Westerhof (Fig. 8; d, e, g); *Culmitzschia* (al. *Walchia) speciosa* Clement-Westerhof (Fig. 8; f) and *Feysia minutifolia* Broutin & Kerp (Fig. 8; h);

— a diversified Calliperids assemblage of sterile foliage and reproductive organs: *Rhachiphyllum schenkii* Haubold & Kerp (Fig. 9; a, e), *Lodevia nicklesii* Haubold & Kerp (Fig. 9; c), *Dichophyllum* cf. *flabellifera* Haubold & Kerp (Fig. 9; h). *Autuniopsis* sp.= ovuliferous organs (Fig. 9; b. d), all forms common in the euramerian Lower Permian; *Peltaspermum martinsii* Poort & Kerp vegetative shoots (Fig. 9; f, g) has been found in assocation with numerous very well preserved peltaspermaceous ovuliferous organs (work in progress) : these taxa became common only during the Late Permian;

— a highly diversified Gingophytes association, the occurrence of which, elsewhere in the world, is in latest Early Permian (Fig. 10; a-h).

MICROFLORA

The only one discovered microfloral association is dominated by monosaccates pollen grains pertaining mainly to the genus *Potonieisporites* (Fig. 11; a, b, d, f, g). But bisaccates grains are also represented by non striate forms such as *Gardenasporites* sp. (Fig. 11; k) and striate elements such as *Complexisporites polymorphus* (Fig. 11; o), *Lunatisporites* sp. (Fig. 11; i), *Striatoabieites* sp. (Fig. 11; p).

This microflora is closely similar to the assemblages well known in the "Muse Formation" of the french Autun basin ("lower Autunian": CHATEAUNEUF *et al.*, 1992).

In addition with this palynological association, the macroflora collected, at that time, in the Khenifra basin lacks the Gingkophytes complex. So, we can suppose that the fossiliferous strata of this basin could be slightly older than those of the Bou Achouch and Tiddas basins (see Table 1). We still have to check this more accurately by new collecting in the Khenifra basin.

FIG. 8.— **a**: *Otovicia hypnoides* KERP *et al.* Bou Achouch basin, *Bassin de Bou Achouch* ; **b**: 1, *Otovicia hypnoides* Kerp *et al*; 2, detached conifere seed, Bou Achouch basin; *graine isolée de conifère, Bassin de Bou Achouch.* **c**: *Culmitzschia* (al. Walchia) *laxifolia* Clement-Westerhof, Tiddas basin, sample n° TBR.A20r; *Bassin de Tiddas, éch. n° TBR.A20r.* **d, e**: *Culmitzschia* (al. Walchia) *parvifolia* Clement-Westerhof. Bou Achouch basin, sample n° B1.16a et B1.16b; *Bassin de Bou Achouch, éch. n° B1.16a et B1.16b.* **f**: *Culmitzschia* (al. Walchia) *speciosa* Clement-Westerhof. Khenifra basin, sample n° K.ms8; *Bassin de Khénifra, éch.n° K.ms8.* **g**: *Culmitzschia* (al. Walchia) *parvifolia* Clement-Westerhof. Khenifra basin, sample n° K.ms13; *Bassin de Khénifra, éch.n° K.ms13.* **h**: *Feysia minutifolia-like* ultimate leafy shoot. Khenifra basin, sample n° K.ms1; *rameaux ultimes de type* Feysia minutifolia *BROUTIN & KERP. Bassin de Khénifra, éch.n° K.ms1.* Same scale, *même échelle* : d, f-h.

Source : MNHN, Paris

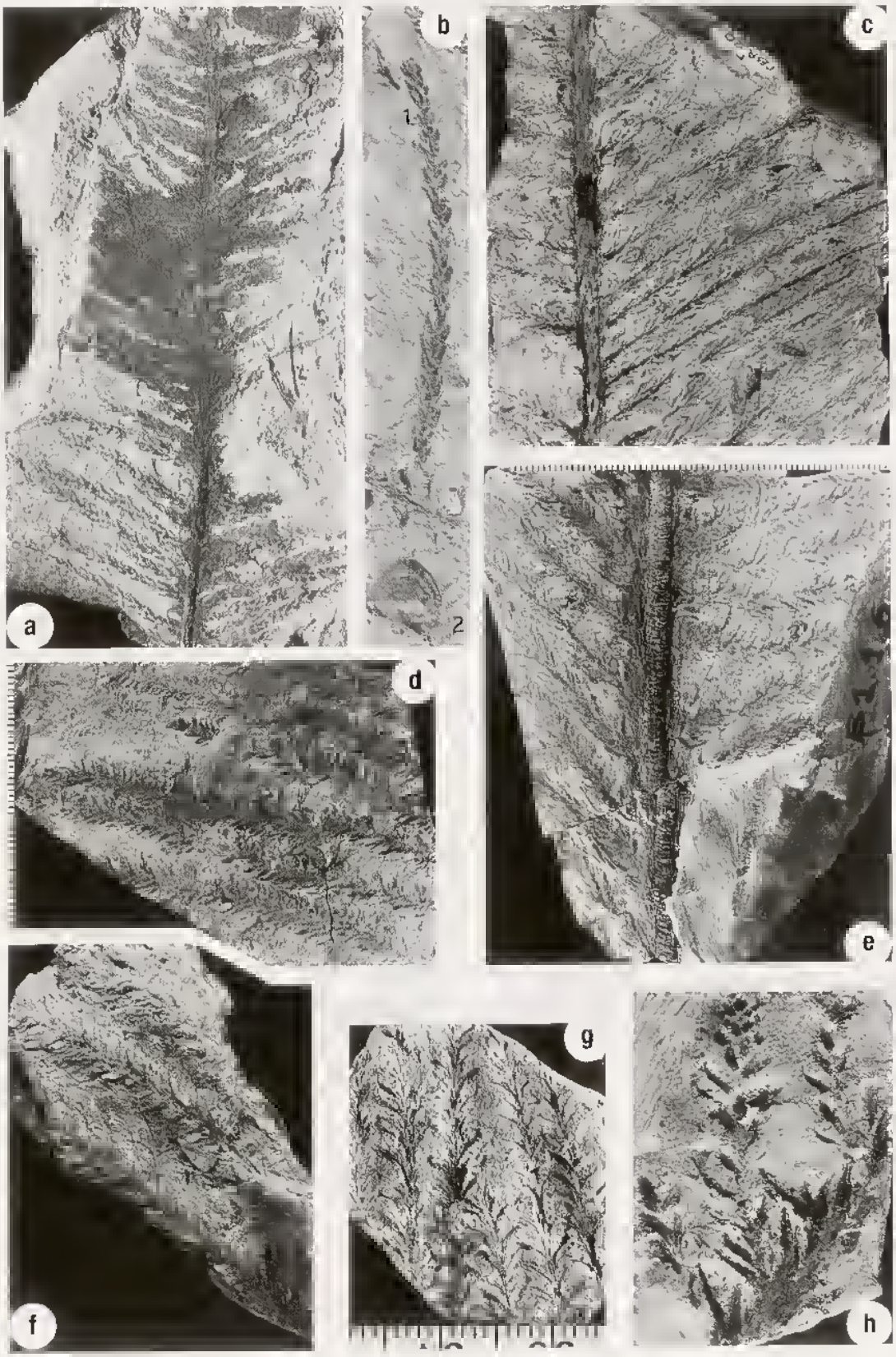

Source : MNHN, Paris

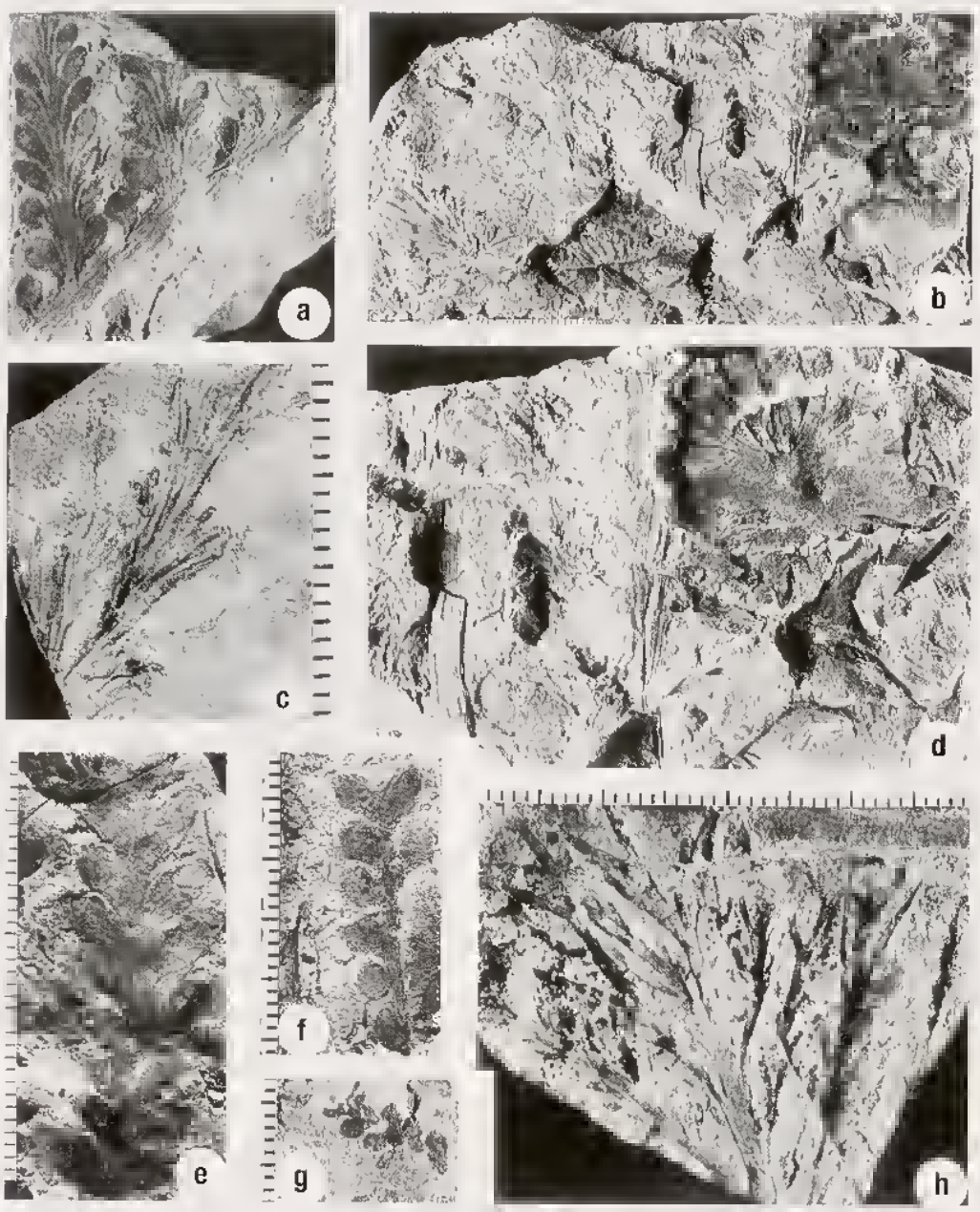

FIG. 9.— **a**: *Rhachiphyllum schenkii* Haubold & Kerp. Pinna fragment showing intercalary pinnules. Bou Achouch basin, sample n° BA88b9; *Fragment d'une penne avec pinnules intercalaires. Bassin de Bou Achouch, éch. n° BA88b9.* Rhachiphyllum schenkii *Haubold & Kerp.* **b, d**: *Autuniopsis* sp.: bilateral ovuliferous dises, see the impression of 2 detached ovules (arrows). Bou Achouch basin, sample n° BA90b9; Autuniopsis *sp. : disques ovilifères à symétrie bilatérale ; remarquer les empreintes de 2 ovules détachées (flèches). Bassin de Bou Achouch, éch. n° BA90b9.* **c**: *Lodevia nicklesii* Haubold & Kerp; Khenifra basin, sample n° Kms6; *Bassin de Khénifra, éch. n° Kms6* ; **e**: *Rhachiphyllum schenkii* Haubold & Kerp.Bou Achouch basin; *Bassin de Bou Achouch.* **f, g**: *Peltaspermum martinsii-like* sterile foliage fragments. Bou Achouch basin, sample n° BA87b24 & BA87s1; *Fragments de pennes ultimes de morphologie similaire à celle du feuillage stérile de* Peltaspermum martinsii. *Bassin de Bou Achouch, éch. n° BA87b24 & BA87s1.* **h**: *Dichophyllum* sp, cf.*D. flabellifera* Haubold & Kerp. *Bou Achouch basin, sample n° BA87s6;* Dichophyllum *sp, cf.* D. flabellifera *Haubold & Kerp. Bassin de Bou Achouch, éch. n° BA87s6.*

Source MNHN, Paris

TABLE 1.— Paleoflora and paleofauna of the Bou Achouch, Tiddas, Khenifra basins. Bold: figured species.

TABLEAU 1.— Paléoflore et Paléofaune des bassins de Bou Achouch, Tiddas, Khénifra. En gras : espèces figurées.

BOU ACHOUCH	TIDDAS	KHENIFRA
« SAXONIAN »	« SAX. »	« SAX. » ?
AUTUNIAN	AUT.	AUT.
Asterophyllites cf.*dumasii*	*Annularia* cf. *hunanensis*	*Calamites cistii*
Calamites cf. *cistii*	*Calamites* cf. *cistii*	*Calamites gigas*
Calamites gigas	*Calamites gigas*	*Calamites suckowii*
Callipteridium marginatum	*Calamites suckowii*	*Sphenopteris pseudogermanica*
Sphenopteris germanica	*Pecopteris* cf. *aspidioides*	*Neuropteris* sp.
Odontopteris gimmi	*Pecopteris* cf. *chihliensis*	*Lodevia nicklesii*
***Autuniopsis* sp.**	*Pecopteris* cf. *densifolia*	*Ginkgophyllum* sp.
Dichophyllum flabellifera	*Pecopteris* cf. *latenervosa*	*Cordaites* cf. *angulosostriatus*
Peltaspermum sp.	*Protoblechnum* cf. *wongii*	*Cordaites principalis*
Rhachiphyllum schenkii	*Odontopteris gimmi*	*Poacordaites* sp.
Rhachiphyllum spp.	***Taeniopteris abnormis***	***Culmitzschia laxifolia***
Ginkgophyllum sp.	*Taeniopteris* sp. 1	***Culmitzschia parvifolia***
***Ginkgoites* spp.**	*Taeniopteris* sp. 2	***Culmitzschia speciosa***
Sphenobaiera digitata	***Rhachiphyllum schenkii***	*Ernestiodendron filiciforme*
***Sphenobaiera* sp.**	*Ginkgophyllum sp.*	***Otovicia hypnoides***
Cordaites cf. *angulosostriatus*	*Cordaites* cf. *angulosostriatus*	*Walchia piniformis*
Cordaites cf. *principalis*	*Cordaites* cf. *principalis*	***Feysia minutifolia***
Poacordaites sp.	*Poacordaites* sp.	
Culmitzschia laxifolia	***Culmitzschia laxifolia***	**MICROFLORA**
Culmitzschia parvifolia	***Culmitzschia parvifolia***	***Endosporites globiformis***
Darneyella gracilis	*Darneyella gracilis*	***Densoisporites* sp.**
Ernestiodendron filiciforme	*Ernestiodendron filiciforme*	***Potonieisporites novicus***
Ortiseia sp	*Walchianthus* sp.	***Nuskoisporites* sp.**
Feysia minutifolia	***Feysia minutifolia***	***Potonieispor. bhadwajii***
Feysia puntii	*Feysia puntii*	***Potonieispor. doubingeri***
Otovicia hypnoides	***Otovicia hypnoides***	***Playfordiaspora crenulata***
Walchia piniformis	*Walchia piniformis*	*Florinites walikalensis*
Walchianthus sp	*Cordaicarpus* sp.	***Divarisaccus latesulcatus***
aff. *Pseudovoltzia* spp.	*Gomphostrobus bifidus*	***Lantzipollenites* sp.**
Gomphostrobus bifidus.	*Samaropsis* sp.	*Cortdallina* sp.
aff. *Glossopteris anatolica*	aff. *Phylladoderma* sp.	*Parasaccites* sp.
aff. *Glossopteris communis*		***Mosulipollenites* sp.**
aff. *Glossopteris communis*	**VERTEBRATE FOOT PRINTS**	***Densipollenites* sp.**
aff. *Venustostrobus*	*Hyloidichnus* sp.	***Gardenasporites* sp.**
aff.*Plagiozamites* sp.	*Gilmoreichnus brachydactylus*	***Complexisporites* sp.**
Dicranophyllum spp.	*Antichnium salamandroides*	***Striatoabieites* sp.**
Mostotchkia sp.	***Figured species***	

Source : MNHN, Paris

PERMIAN PHYTOGEOGRAPHIC SEQUENCE ALONG THE NORTH SOUTH TRANSECT: SOUTH-WESTERN SPAIN - GABON (Fig. 9)

THE SOUTHWESTERN SPAIN "GUADALCANAL-RIO VIAR" LATE EARLY PERMIAN MIXED FLORA

Locally coal-bearing continental strata, yielding fossil plant remains, occur in a few, generally small, outcrops scattered within the Ossa-Morena / South-Portuguese structural zones boundary (BROUTIN, 1983). This boundary was reinterpreted recently (QUESADA, 1991) as a cryptic Variscan suture. The study of the rich macro- and microfloras led to give a "post Autunian - ante Thuringian" age to these strata (BROUTIN, 1986). Among a Euramerian floral assemblage, including *Walchia* spp., Callipterids Ginkgophytes associated with some hygrophilous *"Stephanian"* remnants, a lot of "exotic" elements have been identified.

Cathaysian forms - *Lobatannularia* aff. *L. sinensis* ; *Protoblechnum wongii* Halle, *Protoblechnum* sp., *Sphenopteris pseudogermanica* Halle, *Fascipteris* cf. *robusta* Gu & Zhi ; associated with *Raistrickia* and *Knoxisporites* Cathaysian-like microspores.

The Gondwanan forms appear to be more represented in the microfloral assemblages: *Plicatipollenites* spp., including *P. gondwanensis*, *Sheuringipollenites* spp., *Divarisaccus latesulcatus*, *Schweizerisporites* sp. (= spore monolète n°1, Permian of Gabon, *in* JARDINÉ 1974), *Cannanoropolis* spp, *Crusisaccites* spp. (BROUTIN & DOUBINGER, 1985). Some Macrofloral remains show more disputable Gondwanan affinities (LI, 1986): *Rhipidopsis* spp., *Phyllotheca* spp., *Ginkgophytopsis kidstonii* (BROUTIN, 1982).

THE CENTRAL MOROCCO, LATE EARLY PERMIAN MIXED FLORA

Based on the classification of more than sixty taxa, (Table 1 and Figs 8-11) the palaeoflora recovered from the continental Bou Achouch, Tiddas and Khenifra basins appears to be coeval with the one of south-western Spain and display the same phytogeographic characteristics (EL WARTITI *et al.*, 1990; AASSOUMI, 1994). Again, Cathaysian elements have been found: *Pecopteris chihliensis* Stockmans & Mathieu, *P. latinervosa* Halle, *Protoblechnum wongii* Halle, *Annularia hunanensis* Gu & Zhi, *Sphenopteris pseudogermanica* Halle.

Interestingly, the Gondwanan plants belong to the Glossopterids, as in the Haushi-Huqf area. There: sterile foliage similar to *Glossopteris communis* Feistmantel, *Glossopteris anatolica* Archangelsky & Wagner and scale-leaves related with *Lidgettonia*, *Eretmonia*, *Venustostrobus* fertile organs have been recognized (BROUTIN *et al.*, in prep.).

The palaeoecological study of the recovered fossil material (impressions-compressions, silicified woods, vertebrate foot-prints, roots-related pedological nodules, etc.) led to suggest a warm humid climate with somewhat irregularly distributed drought periods.

Our last pluridisciplinary field works, carried out in the central Morocco basins (1994) showed that sedimentary facies, macro- and microfloral contents and occurrence of bimodal magmatic coeval events, are the same as in the southwestern Spanish basins. Therefore, these Moroccan and Spanish basins were deposited under quite close tectonic, geographical (latitude, altitude) and climatic conditions (= "Cathaysian-like" warm-humid conditions). Based on all the now available palaeontological data, the age of these Spanish and Moroccan continental deposits can be estimated as Kungurian (= Bolorian).

FIG. 10.— **a**: 1, *Sphenobaiera digitata* Florin; 2, 3: Ginkgophyte foliage, Bou Achouch basin, sample n° BA87b8r *Feuillage de Ginkophytes, Bassin de Bou Achouch, éch. n° BA87b8r.* **b**, **d**, **g**, **h**: Various Ginkgophyte foliages Bou Achouch basin, sample n° BA88b10, BA87b21, BA87b13, BA88b17; *Divers feuillages de Ginkgophytes. Bassin de Bou Achouch, éch. n° BA88b10, BA87b21, BA87b13, BA88b17.* **c**: 1, *Sphenobaiera digitata* Florin; 2: Ginkgophyte foliage. Bou Achouch basin, sample n° BA87b17; *feuillage de Ginkgophyte. Bassin de Bou Achouch, éch. n° BA87b17.* **e**, **f**: *Ginkgoites* sp. Bou Achouch basin, sample n° BA87b20 et 20'. *Bassin de Bou Achouch, éch. n° BA87b20 & 20'.* Same scale, *même échelle* : c-g.

Source : MNHN, Paris

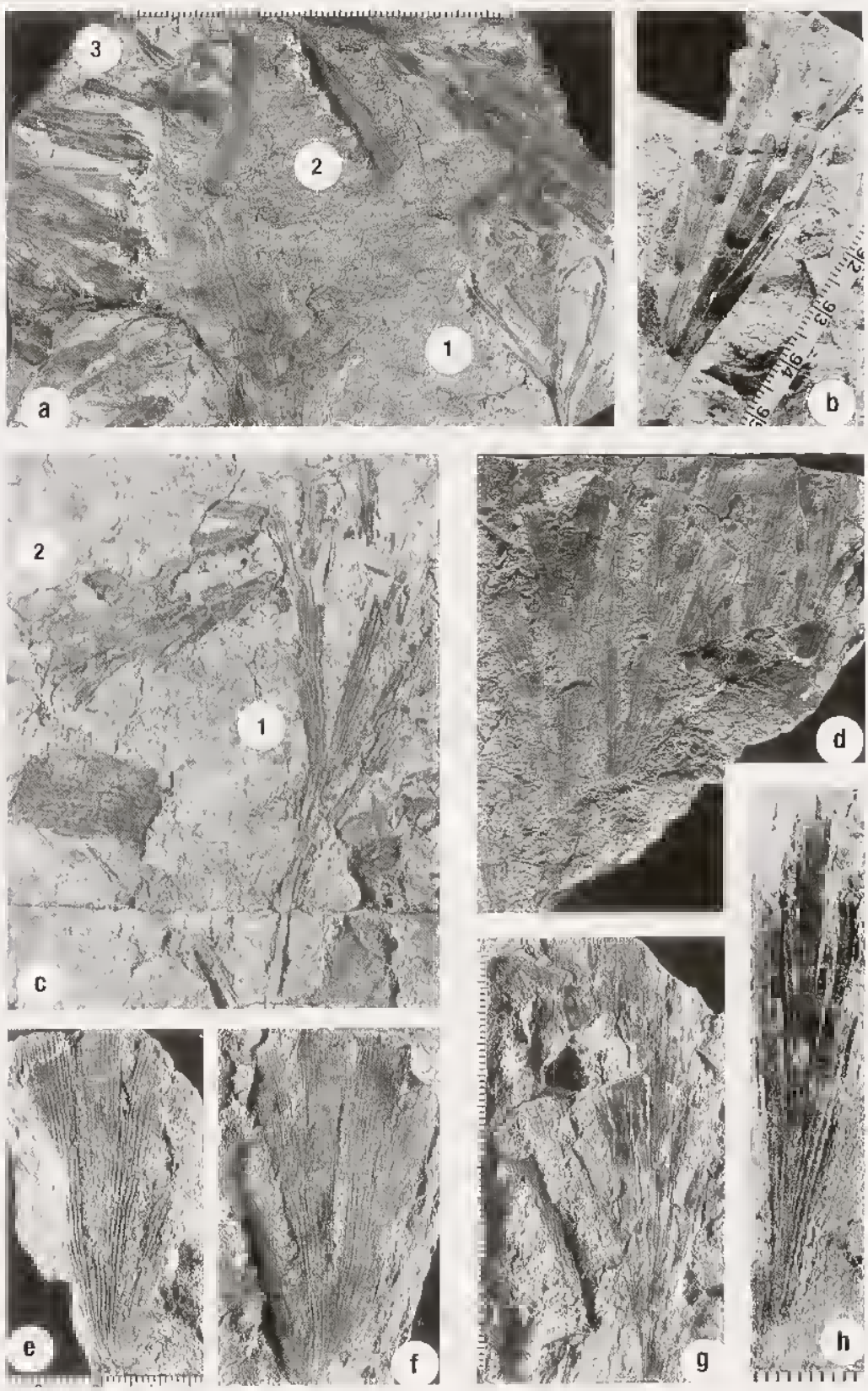

Source : MNHN, Paris

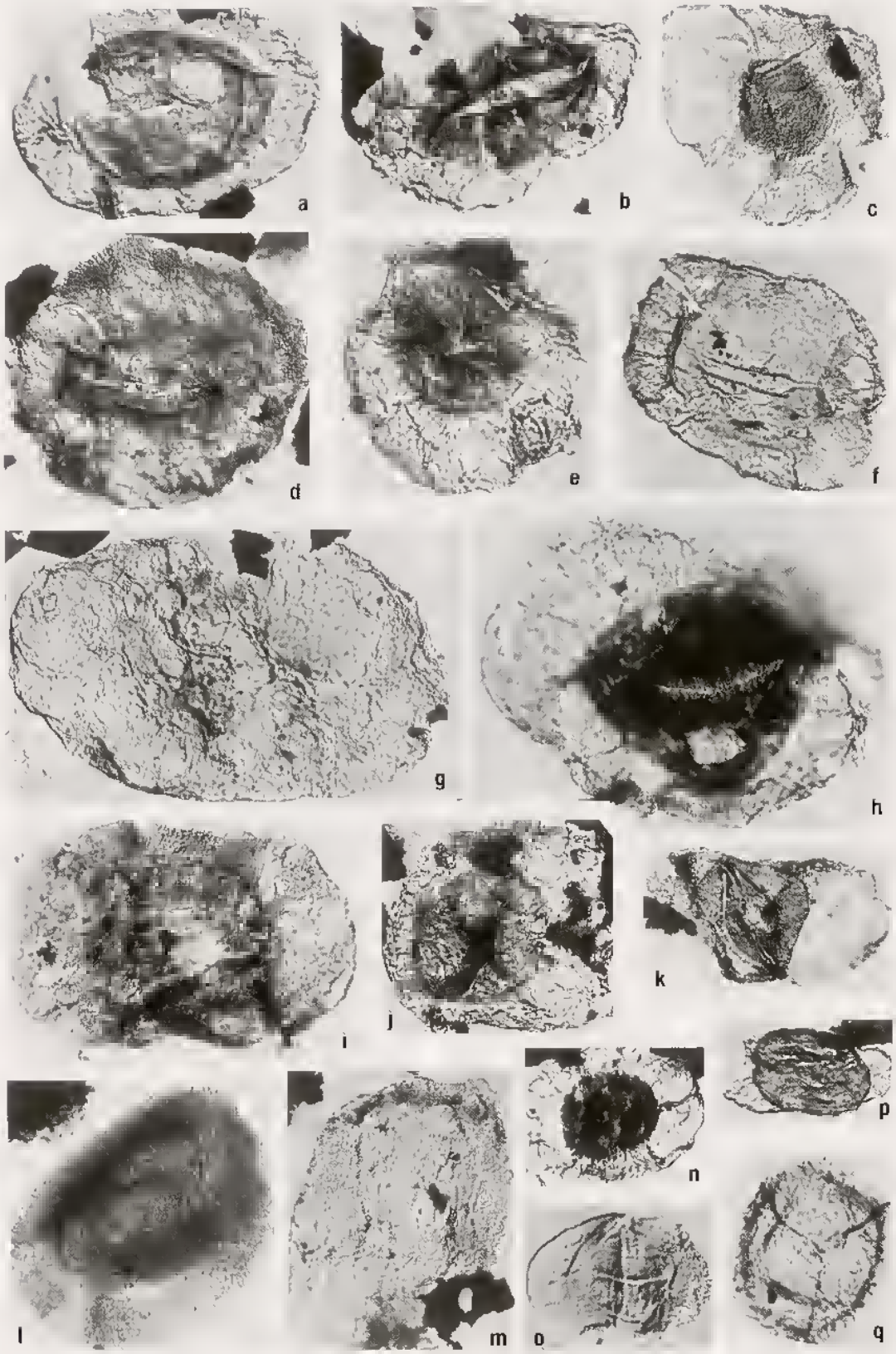

Source : MNHN, Paris

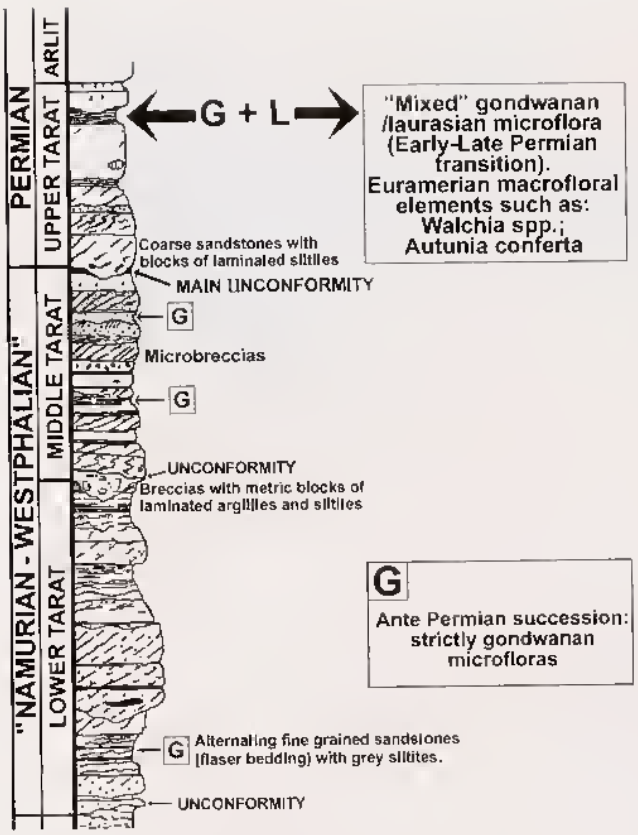

FIG. 12.— Synthetic succession of the Tarat Formation, Arlit area: Niger (modified after BROUTIN *et al.*, 1990).

FIG. 12.— Colonne synthétique de la Formation du Tarat, région d'Arlit : Niger (modifié d'après BROUTIN et al., *1990).*

However, if it emerges that they represent only remnants of much larger intramontane basins, the different nature of the substrata on which Permian Moroccan and Spanish rocks were deposited could suggest that these deposits did not belong to the same single basin.

WESTERN AND CENTRAL AFRICA

The available palaeohotanical and palynological data show that the southernmost limit of Euramerian elements extension, during the Permian, lies in central Africa (Gabon) through western Africa (Niger).

In the upper sequence of the continental Tarat formation (Arlit region, northern Niger) a mixed microflora amalgamates Gondwanan elements and typical Euramerian taxa (Fig. 12).

Based on a comparison with Gondwanan and Euramerian palynological zonation (in the absence of any marine data), the age of this microflora was estimated to be comprised between the Kungurien and the Ufimian or, may be, the early Kazanian (BROUTIN *et al.*, 1990).

Extracted from the same levels, the macrofloral assemblage is dominated by Euramerian plants including, especially : *Autunia (Callipteris) conferta, Lodevia (Callipteris) nicklesii, Walchia piniformis, Walchia* spp. and *Cordaites* spp., assemblage considered as typical of the Lowest Permian (Autunian) in Western Europe. After DE ROUVRE (1985) the associated fructifications have Gondwanan affinities.

In the Tarat succession, all the known ante-Permian (Visean - Namurian) microfloras are typically Gondwanan, similar with those described in Argentina, Zaire, Australia (DOUBINGER *in* EL HAMET 1983).

The microfloral Permian sequence in the Agoula succession (Gabon) has been well characterized by JARDINÉ (1974). In the basal part, the Sakmarian "P II" assemblage is undisputably a Gondwanan one: it is overlain by a "P III" association very similar in composition with the Nigerian upper Tarat microflora and likely more or less coeval. At the top of the succession, JARDINÉ (1974) noticed the occurrence of *Klausipollenites schaubergeri, Lueckisporites virkkiae, Jugasporites* sp. and *Limitisporites* sp. representatives of "a typical north-European Late Permian assemblage".

FIG. 11.— Palynological association from the Khenifra basin ("Nkhilat" locality). *Association palynologique du bassin de Khénifra (localité "Nkhilat").* **a** : *Potonieisporites "novicus"*; **b**: *Potonieisporites "bhardwajii"*; **c**: *Endosporites globiformis*; **d**: *"Potonieisporites bhardwajii"*; **e**: *Nuskoisporites* sp.; **f**: *Potonieisporites "clarus"*; **g**: *Potonieisporites "donbingerii"*; **h**: *Playfordiaspora crenulata*; **i**: *Lunatisporites* sp.; **j**: *Lantzisporites cruciformis*; **k**: *Gardenasporites* sp.; **l**: *Densipollenites* sp.; **m** : *Divarisaccus latesulcatus*: **n** : *Mosulipollenites circularis*: **o**: *Complexisporites polymorphus*; **p**: *Striatoabieites* sp.; **q**: *Densoisporites* sp. All pictures: x 400. *Toutes figures : x 400.*

Source : MNHN, Paris

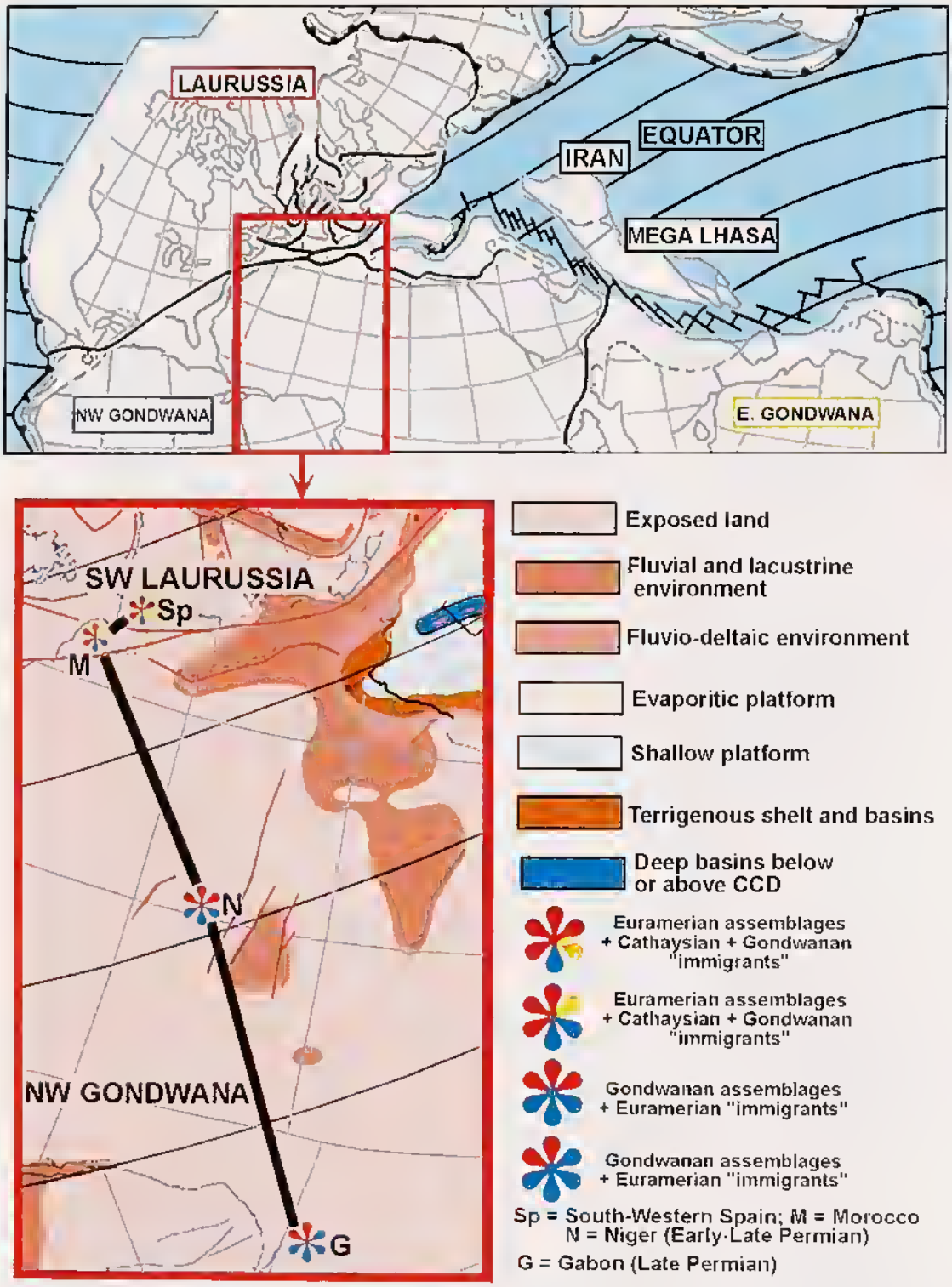

FIG. 13.— Geographical and stratigraphical distribution of the analysed Permian palaeofloras, along the transect south-western Spain - Gabon, plotted on the "late Murgabian" map of BAUD *et al.*, 1993.

FIG. 13.— Distribution géographique et stratigraphique des paléoflores permiennes analysées le long du transect Espagne du Sud-Ouest - Gabon, replacées sur la carte "late Murgabian", BAUD et al., *1993.*

Source : MNHN, Paris

PALAEOPHYTOGEOGRAPHICAL CONCLUSIONS

Along the Permian southwestern Spain-Gabon transect (Fig. 13), one can observe:

— during the Late Early Permian, the incoming of Gondwanan elements into the Euramerian floral province, only up to the Southwestern Spain through North Africa (Gondwanan palynomorphs were also reported from Early Permian of southern Algeria, DOUBINGER & FABRE, 1983);

— the progressive southwards extension of Early Permian Euramerian Gymnosperms and Pteridosperms into the North Gondwana domain.

They are recorded (macro- and microfloras) in the "mid-Permian" of western Africa (Niger) and in the Late Permian microfloras of central Africa (Gabon).

As demonstrated, and well dated, by the occurrence of Walchiacean megafossil forms in the continental Oman Gharif palaeoflora, sandwiched by the Sakmarian Saiwan and early Murgabian Khuff marine Formations, this Early-Late Permian southern phytogeographic band extended Eastwards to the Arabian Peninsula (BROUTIN *et al.*, 1995).

REFERENCES

AASSOUMI, H., 1994.— *Les paléoflores du Permien du Maroc Central. Implications biostratigraphiques, paléoécologiques et paléogéographiques pour le domaine péri-téthysien occidental.* Thèse, Mémoires des Sciences de la Terre de l'Université Pierre et Marie Curie, Paris, France, **94.16**: 1-226.

AASSOUMI, H., BROUTIN, J., EL WARTITI, M., FREYTET, P., KOENIGUER, J. C., QUESADA C., SIMANCAS F. & TOUTIN-MORIN N., 1993.— Pedological nodules with cone in cone structures in the Permian of Sierra Morena (Spain) and Central Morocco. *Carbonates and Evaporites*, **7**, 2: 140-149.

BAUD, A., MARCOUX, J., GUIRAUD, R., RICOU, L.E. & GAETANI, M., 1993.— Late Murgabian (266 to 264 Ma). *In*: J. DERCOURT, L.E. RICOU & B. VRIELINCK (eds), *Atlas Tethys Paleoenvironmental Maps: Explanatory Notes*. Gauthier-Villars, Paris: 9-20.

BOUSHABA, A., CAILLEUX, Y. & EL WARTITI, M., 1987.— Les granitoïdes permiens du domaine mésétien marocain. *Bulletin des Sciences de la Terre de l'Université de Rabat*, **3**: 104-138.

BROUTIN, J., 1982.— Importance paléobiogéographique de la découverte d'une flore continentale mixte dans le Permien inférieur du S.O. de la péninsule ibérique. *Comptes Rendus de l'Académie des Sciences, Paris*, II: 419-422

BROUTIN, J., 1983.— El Pérmico del borde Suroeste de la Meseta. *In*: C. MARTINEZ-DIAZ (ed.), *Carbonífero y Pérmico de España*. Instituto Geologico y Minero de España, Madrid: 441-450.

BROUTIN, J., 1986.— *Étude paléobotanique et palynologique du passage Carbonifère Permien dans le Sud-Ouest de la péninsule ibérique*. Cahiers de Paléontologie, Paris: 1-165, 48 fig.,

BROUTIN, J. & DOUBINGER, J., 1985.— *Intérêt stratigraphique et paléogéographique des palynoflores du Permien inférieur du Nord de la province de Séville (Espagne). Comptes Rendus du 10ème Congrès International de Stratigraphie et Géologie du Carbonifère, Madrid, 1983*. Vol. 2. Instituto Geologico y Minero de España, Madrid: 297-306.

BROUTIN, J., DOUBINGER, J., EL HAMET, M. & LANG, J., 1990.— Palynologie comparée du Permien nigérien (Afrique occidentale) et péri-téthysien. Implications stratigraphiques et paléogéographiques. *Review of Paleobotany and Palynology*, **66**: 243-261.

BROUTIN, J., EL WARTITI, M., FREYTET, P., HEYLER, D., LAHRHIB, M. & MOREL, J.L., 1987.— Nouvelles découvertes paléontologiques dans le bassin détritique carbonaté permien de Tiddas (Maroc Central). *Comptes Rendus de l'Académie des Sciences, Paris*, **305**, II: 143-148.

BROUTIN, J., ROGER, J., PLATEL, J.P., ANGIOLINI, L., BAUD, A., BUCHER, H., MARCOUX, J. & AL HAHSMI, H., 1995.— The Permian Pangea. Phytogeographic implications of new paleontological discoveries in Oman (Arabian Peninsula). *Comptes Rendus de l'Académie des Sciences, Paris*, **321**, IIa: 1069-1086.

CHATEAUNEUF, J.J., FARJANEL, G., PACAUD, G. & BROUTIN, J., 1992.— The Autun Permian basin. The Autunian stratotype. *Cahiers de Micropaléontologie*, N.S., **7**, 1/2: 123-139.

CAILLEUX, Y., LE GUERN, M., SAUVAGE, M. & GONORD, H., 1982.— Taphrogenèse et volcanisme permien dans le Maroc Central. *Bulletin de la Faculté des Sciences de Marrakech, section Sciences de la Terre*, n° spécial **1**: 24-39.

CAILLEUX, Y., DELOCHE, CH., GONORD, H. & ZOUINE, M., 1986.— *Synthèse sur le volcanisme permien du Maroc. Son insertion dans le contexte géodynamique ouest méditerranéen: actes du 111ème Congrès national des Sociétés savantes, Poitiers*. Comité des Travaux historiques et scientifiques, Paris: 221-235.

Source : MNHN, Paris

DAMOTTE, R., EL WARTITI, M., FREYTET, P., KHOUNCH, H., LETHIERS, F. & TOUTIN-MORIN, N., 1993.— *Le bassin de Mechraâ Ben Abbou (Rehamna, Maroc): son insertion dans le contexte permien du Maroc Central et Mésétien: 4ème Colloque de géologie Africaine, Comptes Rendus du 118ème Congrès d'Histoire et Sciences, Pau*. Comité des Travaux historiques et scientifiques, Paris: 53-72.

DOUBINGER, J. & FABRE, J., 1983.— Mise en évidence d'un Autunien à flore mixte dans le bassin de Béchar-Abadla (Sahara occidental algérien). *Pollen et Spores*, **25**, 1: 91-116.

EL HAMET, M.O., 1983.— *Analyse géologique et pétrographique de la Formation Tarat dans les carrières de la Somaïr (Paléozoïque supérieur). Essai d'interprétation paléoclimatique à la lumière de l'épisode glaciaire dévono-carbonifère (région d'Arlit, Niger septentrional)*. Thèse, Université de Dijon, Dijon, France: 1-279.

EL WARTITI, M., 1981.— *Les terrains permo-carbonifères et leur couverture dans la zone de Tiddas-Souk-es-Sebt, bordure NW du Maroc central*. Thèse de 3ème cycle, Université de Rabat, Rabat, Maroc: 1-193.

EL WARTITI, M., 1990.— *Le Permien du Maroc mésétien. Étude géologique et implications paléogéographiques*. Thèse d'État, Université Mohammed V, Rabat, Maroc: 1-501.

EL WARTITI, M., BROUTIN, J., FREYTET, P., LAHRHIB, M. & TOUTIN-MORIN, N., 1990.— Continental deposits in Permian basins of the Mesetian Morocco. Geodynamic history. *Journal of African Earth-Sciences*, **10**, 1/2: 361-368.

EL WARTITI, M. & FADLI, D., 1985.— Relation socle-couverture au cours du Trias dans la zone de ben Slimane-El Gara (Maroc nord mésétien). *Bulletin des Sciences de la Terre de la Faculté des Sciences de Rabat*, **1**: 54-66.

JARDINÉ, S., 1974.— Microflores des formations du Gabon attribuées au Karoo. *Review of Paleobotany and Palynology*, **17**: 75-112.

JÉBRACK, M., 1982.— Les districts à fluorine du Maroc Central. *Bulletin de Bureau de Recherches géologiques et Minières*, **2**, II: 211-221.

LI, X.X., 1986.— The mixed Permian Cathaysia-Gondwana floras. *The Paleobotanist*, **35**, 2: 211-222.

MICHARD, A., HOEPFFNER, C. & JENNY, P., 1978.— Le couloir de cisaillement calédono-hercynien de la Meseta occidentale sur la transversale Mechraâ-Ben-Abbou (Rehamna, Maroc). *Bulletin de la Société géologique de France, Paris*, **20**: 889-894.

SAUVAGE, M., LE GUERN, M. & SAUVAGE, J.F., 1983.— Caractères structurologiques du centre émissif volcanique permien de Bou-Achouch (Maroc Central). *Bulletin de la Faculté des Sciences de Marrakech, section Sciences de la Terre*, n° spécial **1**: 85-100.

QUESADA, C., 1991.— Geological constraints on the Paleozoic tectonic evolution of tectonostratigraphic terranes in the Iberian Massif. *Tectonophysics*, **185**: 225-245.

ROUVRE, I. DE, 1985.— *Contribution à l'étude de la flore paléozoïque de la bordure occidentale de l'Aïr (République du Niger)*. Thèse d'État, Université Paris VI, Paris, France: 1-375.

TERMIER, H., 1936.— Études géologiques sur le Maroc central et le Moyen Atlas septentrional. 1: les terrains primaires et le Permo-Trias. 2: les terrains post-triasiques. 3: paléontologie, pétrographie. 4: Atlas. *Notes et Mémoires du Service des Mines et de la Carte géologique du Maroc*, **33**: 1-1566.

YOUBI, N., 1990.— *Complexe volcanique permien de Khénifra (S.E. du Maroc Central): cartographie, volcanologie, minéralogie, géochimie, considération structurale et implications géodynamiques*. Thèse 3ème cycle, Université de Fès, Fès, Maroc: 1-369.

YOUBI, N. & CABANIS, B., 1995.— *The Permian Volcanic Complex of the Khenifra Basin (Morocco): Volcanology and Geochemistry: Table ronde sur le Permien et le Trias du Maroc: état des connaissances*. Université Mohammed V, Faculté des Sciences, Rabat (Maroc), volume des résumés: 9.

Source : MNHN, Paris

INDEX

A

Aalenian 51; 53; 145; 154; 157; 158; 167; 171; 176; 177; 185; 190; 197; 201; 204; 218; 225; 230; 244; 248; 251; 252
Aalensis Zone 195
Abathomphalus intermedius 66
Abi Adi 134
Acanthicum Zone 24; 31
acritarchs 41; 44; 221
Acracythere dubertreti 226
Acrothentis mosquensis 22
Actinoceramus (Byrostrina) 102
Actinostromarianina lecompti 140
Actinostromarianina praesaleseusis 140
Actostroma dauesini 140
Acuticostites acuticostatus 21; 25; 26
Acuticostites bitrifurcatus 21; 25
Adnatosphaeridium 224
Afghanistan 224
Africa 132; 133; 154; 202; 224; 226; 232; 237; 238; 258; 275; 277
Afrocythereidea faveolata 225
Agbe 134; 136; 137; 138; 140
Aghbalou 245; 249
Aghdarband 49
Aïn Beida 185
Aïn Killoun 180; 182; 192; 195
Aïn Mirid 195
Aïn Ouarka 146; 180; 182; 185; 186; 192; 195; 202
Aït Hani 202; 203; 248
Akchagylian 116; 118; 221
Akmysh 60
Aksu-Dere 98
Aktau 61
Aktubinsk 97
Akusha 96; 103; 105
Albani Zone 27
Albian 40; 42; 95; 96; 97; 98; 100; 102; 103; 104; 105; 107
Alborz 123
algae 47; 138; 221; 224; 227
Algeria 146; 147; 167; 180; 192; 193; 197; 200; 201; 203; 204; 205; 206; 222; 277
Algovianum Zone 190; 195
Alisporites tenuicorpus 43
Alocolytoceras dorcadis 184
Alps 76
Altaid-Hercynian orogeny 49
Alveosepta 137
Alveosepta jaccardi 220; 227; 232
Alveosepta jaccardi personata 221
Alveosepta powersi 140
Amalthens sp. 180
Ammelleretla octoradiata 61
Amijiella amiji 227
Ammnbaculites ? sp. 54
Ammobaculites sp. 195
Ammodiscus siliceus 195
ammonite 9; 10; 12; 14; 16; 18; 19; 21; 22; 23; 24; 25; 31; 96; 98; 100; 101; 103; 105; 107; 112; 133; 134; 138; 140; 143; 146; 147; 157; 162; 167; 171; 176; 177; 180; 182; 184; 185; 186; 190; 192; 193; 195; 200; 203; 205; 218; 219; 221; 222; 230; 231; 242; 243; 253
ammonoid 36; 37; 39; 44; 46; 49; 51; 53; 59; 60; 218
Amoeboceras 23
Amoeboceras (Amoebites) cf. *kitchini* 16
Amoeboceras (Amoebites) cricki 24
Amoeboceras (Amoebites) gr. *kitchini* 16
Amoeboceras (Amoebites) kitchini 24
Amoeboceras (Nannocardioceras) subtilicostatum 19
Amoeboceras (Nannocardioceras) volgae 19
Amoeboceras alternoides 14
Amoeboceras cf. *cricki* 16
Amoeboceras cf. *domoni* 14
Amoeboceras cf. *freboldi* 16
Amoeboceras cf. *glosense* 14; 23
Amoeboceras cf. *koldeweyeuse* 14
Amoeboceras cf. *lineatum* 16
Amoeboceras cf. *ovale* 14
Amoeboceras cf. *talbejeuse* 14
Amoeboceras cf. *tuberculatoalternans* 16
Amoeboceras gerassimovi 16
Amoeboceras gr. *serratum* 14
Amoeboceras ilowaiskii 14; 23
Amoeboceras koldeweyense 16
Amoeboceras leucum 16; 23
Amoeboceras sp. 16; 18; 19; 24
Amoeboceras transitarium 14
Amoeboceras tuberculatoalternans 16; 23
Amphisaurolides discessus 263
Amydropthychus 226
Anarak 43
Anatolide 123; 128
Anchispirocyclina praehsitanica 227
Angulaticeras gr. *dumortieri* 186
Anisian 43
Annularia lunaneusis 272
Antalo limestone 131; 132; 133; 134; 140; 141; 143
Anti-Atlas 238

Source : MNHN, Paris

Antichnium salamandroides 263
Antilebanon 213; 214; 221; 222; 227; 230
Apennines 163; 186
Aporrhais 14; 16
Aporrhais sp. 16
Applanopsis 224
Applanopsis turbatus 224
Applanopsis turbatus Zone 224
Aptian 58; 60; 105; 106; 107
Aptychus 19
Aquitaine 31
Arabia 125; 134; 213; 222; 230; 231; 232
Arabian Peninsula 277
Arabian platform 222; 231
Aratrisporites 43
Araucariaceae 51
Araucariacites australis 51; 216
Arcthoplites 96
Arctic shelf 12
Ardon 214; 216; 217; 218; 224; 225; 227; 230
Argentina 52; 275
Arieticeras sp. 184; 195
Arizona 262
Arkelli Zone 171
Arlit 275
Arnioceras 193
Arnioceras cf. *arnouldi* 186
Arnioceras cf. *flavum* 186
Arnioceras cf. *speciosum* 186
Arnioceras geometricum 186
Arnioceras miserabile 186
Asher 213; 214; 216; 217
Asia 36; 54; 68
Asphinctites cf. *polysphinctus* 168
Aspidoceras 19
Aspidoceras caletanum 18; 24
Aspidoceras gr. *longispinum* 19; 24
Aspidoceras gr. *quercynum* 19; 24
Aspidoceras quercynum 19
Aspidoceras sp. 19; 24
Aspidoceratids 24
Aspidoceratinae 222
Aspidolithus parcus constrictus 61
Aspidolithus parcus parcus 61
Assoul 244; 249; 251
Astacolus compressaeformis 56
Astacolus ectypa castata 56
Astacolus sp. 56
Astacolus spp. 41
Astarte 14
Astarte sp. 13
Asteroceras 186; 193
Asteroceras aff. *confusum* 186; 193
Asteroceras margarita 186
Asteroceras meridionale 186
Asteroceras stellare 186; 193
Asteroceras variatus 186
Asturian 258
Ataxioceras (A.) gr. *discoidale* 140
Ataxioceras (Parataxioceras) gr. *polyplocum* 140
Ataxophragmium nautiloides 101
athleta Zone 219; 222
Atlantic 103; 147; 148; 202; 204
Atlas 146; 147; 149; 180; 184; 186; 192; 193; 196; 197; 200; 201; 202; 203; 204; 205; 237; 258
Atlit 217
Aucellina 102
Aulacostephanids 24
Aulacostephanus 24
Aulacostephanus autissiodorensis 19; 24; 31
Aulacostephanus cf. *ya* 19
Aulacostephanus contejeani 19; 24; 31
Aulacostephanus eudoxus 18; 24
Aulacostephanus kirghisensis 19
Aulacostephanus mudorae 19; 24
Aulacostephanus volgensis 19; 24
Aulacostephanus yo 19; 24; 31
Aulacothyris nov. sp. A 180
Aurigerus Zone 167
Australia 52; 275
Autissiodorensis Zone 19; 24
Autun 268
Autunia (Callipteris) conferta 275
Autunian 268; 272; 275
Autuniopsis sp. 268
Aveyroniceras 190

B

Badenian 84
Bairdia aff. B 225
Bairdia aff. *hilda* 225
Bajocian 51; 52; 107; 145; 146; 154; 157; 163; 164; 167; 168; 176; 177; 178; 182; 185; 190; 192; 195; 196; 201; 204; 218; 224; 225; 226; 227; 230; 231; 239; 243; 244; 245; 251; 252; 254
bakewellids 45
Bakuriani 114
Baksan River 103
Balanocidaris glandifera 220
Baltic Sea 76
Baltica 79
Barbur 218
Barents Sea 43
Barents shelf 12
Barnea 218; 220
Barremian 58; 59
Bathonian 52; 54; 132; 133; 145; 146; 147; 148; 154; 157; 164; 167; 168; 171; 176; 177; 185; 190; 196; 204; 213;

Source : MNHN, Paris

218; 219; 224; 225; 226; 227; 230; 231; 239; 240; 245; 249; 252; 254
Baylei Zone 16
Bechar 204
Beer Yaakov 219
Beersheva 226
belemnite 14; 16; 18; 19; 21; 22; 102; 105
Ben Zireg 197
Béni Bahdel 176; 203
Béni Bou Saïd 167
Béni Mellal 186; 203
Béni Mishel 157
Béni Ouarsous 160; 162
Béni Snassène Mountains 157
Beni Snouss Khemis 205
Béni Yala 180; 203
Béni-Bassia 192
Berberids 149
Berriasella richteri 221
Berriasian 25; 29; 58; 59
Bifrons Zone 167; 176; 184; 195; 204
Bifurcatus Zone 23
Bikfaya 221
Bimammatum Zone 220
Biscutum 49
Biscutum constans 58
Bisulcocypris oertlii 225
bivalve 14; 16; 18; 22; 37; 39; 46; 47; 51; 58; 59; 98; 102; 134; 136; 138; 168; 184; 185; 186; 200; 218; 219; 220; 226; 231
Black Sea 76; 112; 121; 123; 124; 125; 128
Blue Nile Bassin 133
Bohemian Basin 98
Bohemian Massif 98
Bolorian 257; 272
Boqer 218; 220; 226
Bositra 176
Bothriopneustes gallhausenii 196
Botryococcus 51
Bou Achouch 257; 258; 259; 263; 267; 268; 272
Bou Arfa 192
Bou Dahar 192; 200; 230
Bou Lerfahd 182; 190; 192
Boudjenane 162; 203
Bouzouggargh 266
braarudosphaerids 59
brachiopod 18; 19; 41; 49; 53; 58; 101; 132; 134; 136; 138; 146; 157; 162; 167; 168; 180; 185; 192; 193; 197; 200; 203; 218; 219; 220; 221; 226; 231
Bremeri Zone 167; 171
Brightia socini zone 220
Brightia sp.222
Britain 12; 27
Brotzenella berthelini 98; 100
bryozoans 219
Buchia 14
Buchia concentrica 18
Buchia sp. 22
Bullatimorphites 171; 231
Bullatimorphites bullatus 219
Bullatus Zone 171
Burgundia 140
Burgundia ramosa 140
Burgundia trinorchii 140
Burmirhynchia 226
Burmirhynchia ternierae 168

C

caadonia 79
Cadomites deslongchampsi 171; 176
Cadomites gr. *deslongchampsi* 177
Caesarea 219; 220
Calamaspora sp. 43
Calculites obscurus 61
Callialasporites dampieri 52
Callialasporites dampieri zone 52
Callialasporites minus 51; 52
Callialasporites sp. 52
Calliperids 268; 272
Callovian 49; 52; 53; 54; 56; 57; 68; 132; 133; 134; 146; 147; 148; 157; 167; 171; 201; 204; 213; 214; 219; 220; 222; 223; 224; 225; 226; 227; 230; 231; 232
Calloviense Zone 53
Caloceras 146; 185
Cambrian 77
Cauterosporites secatus 46
Campanian 61; 65; 66; 68
Campbeliella striata 221
Cannanoropolis spp. 272
Capillirhynchia ardescica 168
Carboniferous 49; 82
Cardioceratid 23
Cardioceras (Cardioceras) gr. *cordatum* 14; 23
Cardioceras (Cawtoniceras) tenuiserratum 14; 23
Cardioceras (Maltoniceras) koketi 14
Cardioceras (Plasmatoceras) popilanense 14; 23
Cardioceras (Plasmatoceras) tenuicostatum 14
Cardioceras (Plasmataceras) tenuistriatum 14; 23
Cardioceras (Subvertebriceras) densiplicatum 14; 23
Cardioceras (Subvertebriceras) zenaidae 14; 23
Cardioceras cf. *mamutjoi* 14
Cardioceras gr. *cardatum* 23
Cardioceras sp. 14
Cardioceratid 12; 23; 24
Carixian 157; 164; 167; 171; 176; 180; 184; 186; 193; 200; 203; 242; 246; 249
Carmel 218; 219
Carnian 46; 47; 48; 67; 216; 260
Carpathians 76; 81; 113

Source : MNHN, Paris

Caspian Sea 36; 112; 121; 123; 124; 125; 128
Caucasus 96; 102; 103; 104; 105; 106; 107; 108; 112; 113; 116; 121; 122; 124; 125; 126; 128
Cammontisphinctes 176
Cammontisphinctes aplous 176; 177
Celebratum zone 195; 197; 201; 203
Cenomanian 30; 60; 68; 96; 97; 98; 100; 102; 103; 104; 105; 106; 107; 240
Cenozoic 84; 111; 116; 120; 157; 177; 180; 238; 285
Central Asia 49
Central Europe 98
Ceratolithoides aculeus 61
charophytae 45
charophyte 267
Chemarikh 146; 180; 185; 186; 192; 193; 200; 202
Chirkala 61
Chokrakian 116; 118; 121; 125
Chondrites 21; 101; 102; 103; 195
Chott ech Chergui 180
Chougrane 285; 267
Citharina sokalavae 56
Citharinella spatha 56
Claromontanus Zone 23
Classopollis 51
Clypeina jurassica 227
coccolithes 220
Cochlearites 180
Collinites sp. 195; 197
Collotia discus 171
Collotia sp. 222
Caloptoria 226
Complexisporites polymorphus 268
Compositosphaeridium 224
Conarosia 226
Concavum Zone 190
Coniacian 58; 61; 68; 81; 98; 100; 101; 102
Coniopteris spp. 51
conodonts 37; 67
Contusotruncana fornicata 65
Contusotruncana plummerae 65
Coronosphaera mexicana 221
coral 131; 136; 137; 140; 141; 177; 184; 192; 193; 197; 204; 219; 238; 242; 245; 251; 253
Cordaites 262
Cordaites spp. 275
Cordatum Zone 13; 23
Corisaccites alatus 43
Corisaccites stradivarii 39
Corollina 224
Coronatum Zone 219; 222; 227
Cosmetodon sp. 14
Costispiriferina mansfieldi 41
Craspedites 27
Craspedites fragilis 26
Craspedites ivanovi 26
Craspedites jugensis 26
Craspedites kaschpuricus 22; 26
Craspedites krilovi 26
Craspedites kuznetzovi 22; 26
Craspedites milkovensis 22; 26
Craspedites nosqueusis 22; 26
Craspedites nekrassovi 22; 26
Craspedites nodiger 22; 26
Craspedites okensis 22; 26
Craspedites parakaschpuricus 22; 26
Craspedites pseudofragilis 26
Craspedites subditoides 22
Craspedites subditus 22; 26
Craspedites triptychus 26
Crassiceras gradatum 195
Crennoceramus rotundatus 100; 102
Crendonites kuncevi 26
Creniceras renggeri 223
Cretaceous 25; 58; 59; 60; 68; 77; 79; 84; 87; 93; 94; 95; 97; 103; 104; 132; 134; 221; 227
Cretarhabdus spp. 61
Cribrosphaerella ehrenbergii 61
Crimea 79; 94; 96; 97; 98; 100; 101; 102; 103; 104; 105; 106; 107
Crinalites sabinensis 43
crinoids 14; 136
Crusisaccites spp.272
Ctenostreon (= *Lima*) *palati* 185
Ctenostreon palati 185
Culmitzschia (al. *Walchia*) *laxifolia* 268
Culmitzschia (al. *Walchia*) *parvifolia* 268
Culmitzschia (al. *Walchia*) *speciosa* 268
Cunningtoniceras aff. *inerme* 60
Cutch 226
Cycadopites sp. 46
Cyclagelosphaera deflandrei 58
Cyclagelosphaera margerelii 58
Cyclagelosphaera wiedmanni 56
Cylindralithus serratus 61
Cylindralithus sp. 61
Cymodoce Zone 16; 24; 29
Cytherella ? toarcensis 225
Cytherella bashai 225
Cytherella cf. *umbilica* 226
Cytherella index 225
Cytherellaidea atlantolevantina 226

D

Dactylioceras (*Eodactylites*) gr. *mirabile* 184
Dactylioceras (*Orthodactylites*) sp. 184
Dadès 245
Daghanirhynchia 226
Daghestan 96; 103
Dalmatia 43

Source : MNHN, Paris

Danakil Alps 133; 140; 143
Dapsilidinium? deflandrei 224
dasycladacean 47
Daya 214; 218; 224; 225; 230
Debdou 180
Déglène 167; 168; 171; 176; 177; 201
Dehornella crustans 140
Dehornella hurmarensis 140
Demonense Zone 186; 195
Densiplicatum Zone 14; 23
Densoisporites 43
Densoisporites complicatus 43
Densoisporites nejburgii 43; 44
Densoisporites playfordii 43
Densoisporites spp. 41
Dentalina 195
Dentalina nodigera 195
Dentalina obscura 195
Dentalina oppeli 56
Dentalina sp. 56
Dentalina terquemi 195
Dentalina turgida 56
Dentalina sp. 14
Desmosphinctes cf. *umiovnikensis* 16
Devonian 82; 86
Devorah 213; 217; 221; 230
Dichadogonyaulax 224
Dichadogonyaulax sellwoodii Zone 224
Dichophyllum cf. *flabellifera* 268
Dicroloma 14
dinocysts 53; 221; 224
dinoflagellate 53; 220
Diotis 186
"*Diotis*" *janus* 186
Dipoloceras cristatum Zone 60
Divarisuccus latesulcatus 272
Djebel Antar 180
Djebel Chemarikh 186; 192
Djebel es Sekika 157
Djebel Fillaoussène 157
Djebel Gorine 157
Djebel Grouz 180; 192; 193
Djebel Guetob Moulay Mohammed 184
Djebel Gueltaï 182; 184; 196
Djebel Hafid 180
Djebel Kerdacha 192
Djebel Melah 185; 186
Djebel Reha 184
Djebel Selib 171
Djebel Sfissifa 182
Djebel Souiga 185
Djebel Tifkirt 185
Dobrogea 76; 77; 79
Dogger 237; 239; 247; 250
Dolikephalites gracilis 171
Dolnapa 37; 38; 45
Domerian 146; 157; 171; 176; 177; 180; 184; 185; 193; 195; 200; 201; 203; 204; 243; 246
Dorikranites 44
Dorset 30
Dorset Portland 25
Dorsoplanites dorsoplanus 21; 25
Dorsoplanites panderi 21; 25
Dorsoplanites rosanovi 26
Dorsoplanites serus 26
Dubky 12; 18; 19; 24
Dzhamansauran 49; 58
Dzharmysh 49; 51; 52; 53; 54; 58

E

East European Platform 120
echinid 101; 196
Erhysoria 226
Egypt 214; 216; 220; 221; 225; 226; 232
Eiffellithus eximius 61
Eiffellithus turriseiffelii 61
Ein Qinia 221
Ektyphocythere amnhensis 225
Ektyphocythere bneki 225
Ektyphocythere cf. *vitilis* 225
Ektyphocythere shulamitae 225
Ektyphocythere zerqensis 225
Ektyphocythere zoharensis 225
El Abed 167
El Harchaïa 182; 185
Elignus 226; 231
Ellipsoidictyum 224
Emaciaticeras sp. 184
Emaciatum Zone 176; 190
Emileia catamorpha 176
Emilein cf. *brocchi* 192
Emileia polyschides 176
Emmetrocysta 224
Endikurgan 60; 61; 65
Endosporites pupillatus 39; 43; 44
Energlynia 224
England 30; 31; 98; 106; 220
Entolium sp. 13; 14
Enzonalasporites vigens 46
Eocene 116; 120; 123; 128; 132; 157
Eodactylites 192
Eodartylites spp. 177
Eodentata Zone 105
Eogutulina sp. 56
Epiplosphaera reticulospinosa Zone 224
Epistomium sp. 56
Epivirgatites bipliciformis 21; 26
Epivirgatites lahuseni 26
Epivirgatites nikitini 22; 26; 27

Source : MNHN, Paris

Epophioceras 193
Epophioceras sp. 186
Eprolithus floralis 61
Eretmonia 272
Ernoceras 184; 192; 231
Errachidia 146; 249
Estherids 44
Ethiopia 131; 132; 134
Euaptetoceras sp. 190
Euaspidoceras douvillei 223
Euaspidoceras sp. 56; 223
Euaspidoceras subbubeanum 223
Euaspidoceras subcostatum 223
Eucytherura oxfordiana 226
Eudoxus Zone 18; 24; 30
Eumorphotis 37
Eunerinea 219
Europe 43; 52; 54; 60; 78; 93; 95; 98; 100; 101; 103; 106; 107; 125; 203; 204; 206; 219; 222; 223; 224; 226; 227; 230; 232; 275
European platform 76; 78; 81
Eurysites 226
Everticyclammina 137
Everticyclammina virguliana 140
Evoluta Zone 24
Exesipollinites tumulus zone 52
Exophthalmocythere? kidodensis 225; 226

F

Fabanella ramonensis 225
Falsopalmula inaequilaterulis 56
Fascipteris cf. *robusta* 272
Fastigatocythere bakeri 225
Fendi 197
Fernane 167; 168
Feysia minutifolia 268
Figuig 146; 147; 182; 184; 192; 193; 195; 197; 200; 201; 202; 203
Flabellocycloling reissi 219; 227
Fletcherithyris margaritovi 41
foraminifer 37; 39; 41; 45; 46; 49; 53; 56; 61; 65; 66; 68; 98; 100; 101; 103; 107; 133; 134; 136; 137; 138; 140; 143; 186; 193; 195; 214; 218; 220; 221; 227; 231
Fore-Caucasus 111; 112; 113; 114; 118; 122; 124; 125; 128
Forresterin petrocorieuse 100
France 98; 106
Frechiella sp. 176
"*Frondicubaria*" ex gr. *elegantula* 39
Fuciniceras sp. 171; 195
Furloceras 185
Furloceras erbaense 171
Furloceras evolutum 171

G

Ga'ash 216; 218
Gabon 257; 272; 275; 277
Galaticeras cf. *aegoceroides* 186
Galilee 213; 218; 221; 227; 230; 232
Gansserina gansseri Zone 66
Gardenasporites 268
Garniericeras cutemulatum 22; 26
Garniericeras interjectum 26
Garniericeras subclypeiforme 22; 26
gastropod 14; 16; 46; 136; 138; 219; 221
Gavelinella cenomanica 98; 100
Gavelinella cf. *vombensis* 100
Gavelinella moniliformis 100
Gavelinella moniliformis Zone 102
Gavelinella praeinfrasantonica 100
Gebel El-Maghara 225; 226
Gebel Maghara 219; 220; 221; 225; 262; 263
Genizinita ex gr. *crassata* 56
Gerar 219
Germany 31; 98; 104; 106
Gevar Am 213; 214; 219; 220; 221; 230
Gharif 277
Gibbirhynchia curviceps 180
Gilmoreichnus 263
Gilmoreichnus brachydactylus 263
Ginkgophytes 268; 272
Ginkgophytopsis kidstonii 272
Glauconithus Zone 27
Gleviceras gr. *doris* 186
Globigerinelloides 65
Globigerinelloides asper 65
globigerinelloidids 65
Globirhynchia 226
Globirhynchia crassa 226
Globorotalites haugensis 100; 102
Globotruncana aegyptiaca Zone 66
Globotruncana ventricosa 65
Globotruncana ventricosa Zone 66
Globotruncanella havanensis Zone 66
Globotruncanella pschadae 66
Globotruncanita subspinosa 66
Globuligerina sp. 56
Glochiceras 26
Glochiceras (*Paralingulaticeras*) cf. *lithographicum* 19
Glochiceras (*Paralingulaticeras*) cf. *parcevali* 19
Glochiceras aff. *lithographicum* 25
Glochiceras aff. *parcevali* 25
Glochiceras sp. 19; 21; 25
Glomospira sp. 227
Glosense Zone 14; 23; 28
Glossopterids 272
Glossopteris anatolica 272
Glossopteris communis 272
Glyptocythere humiensis 225

Source : MNHN, Paris

Glyptogotocythere magharaensis 225
Glyptogatocythere malzi 225
Gondolella cf. *jubata* 39
Gondwana 133; 200; 231
Gonolkites 167
Gordonispora fossulata 43
Gordonispora sp. 43
Golan 227
Gorine 164
Gorny Mangyshlak 36; 39; 53; 57; 58; 61; 66
Gorodische 12; 21; 26; 29
Goulmina 245; 251; 253
Gracilis Zone 168; 171; 201
Gradata Zone 171; 176; 177; 184; 190; 203; 205
Gradatum Zone 195
Grammatodon sp. 14
Grammoceras 218
"Grandes Rosalines" ex gr. *Marginatmicano coronatmrenzi* 100
Graphoceratids 171
Gravesia 12; 26
Gravesia cf. *gigas* 19; 25
Gravesia cf. *gravesiana* 19
Great Balkhan 94; 97; 102; 103; 105; 106
Great Caucasus 103; 112; 113; 114; 120; 121; 123; 124; 125; 126; 128
Grebeispora concentrica 43
Greenland 12; 52
Grojec 80
Gryphaea dilatata 14
Guadalacanal 259
Guercif 157
Guettaï 184; 185
Gutnicella gr. *cayeuxi* 227
Guttapollenites hannonicus 43

H

Hagere Selam 134
Haifa 213; 217; 218; 219; 221; 224; 225; 230
Halal 214; 216; 217; 218; 219; 220; 227
Haluza 221; 226
Hamakhtesh Hagadol 214; 219; 220; 222; 225; 227
Hammatoceras 146; 171; 177; 205; 206
Hammatoceras roubaudense 146; 171; 177; 205; 206
Hammatoceras speciosum 206
Hammatoceratids 205
Hoploceras aff. *elimatum* 25
Hoploceros cf. *elimatum* 19
Hoploceros sp. 21
Hoplophrogmoides sp. 56
Harar 140
Hassi Ben Khelil 203
Haurania 218
Haushi-Huqf 272
Hauterivian 59; 221; 230
Hazon 221; 226
Hebrides 204
Hecticoceras (Brightia) aff. *salvatori)* 222
Hecticoceras (Chomosia) michalskii 171
Hecticoceras (Hecticoceras) boginense 171
Hecticoceras (H.) posterium 171
Hecticoceras (Kheraites) ferrugineus 222
Hecticoceras (Lunuloceros) cf. *fontei* 56
Hecticoceras (Putealiceras) domvillei 222
Hecticoceras (Putealiceras) intermedium 222
Hecticoceras bonarelli 223
Hecticoceros cf. *guthei* 223
Hecticoceras chotillonense 223
Hecticoceros coelotum 223
Hecticoceras kautzschi 223
Hecticoceras schumacheri 223
Hecticoceras separandum 223
Hecticoceras socini 223
Hecticoceras socini Zone 223
Hecticoceras socinum 223
Hecticoceras solare 223
Hecticoceras syriacum 223
Hecticoceratinae 222
Helez 214; 218; 220; 227; 230
Helvetoglobotruncana helvetica 100
Hercynian 113; 258; 260; 263
Hermon 213; 214; 218; 219; 220; 221; 222; 223; 224; 225; 226; 227; 230
Hesperithyris renierii 184
Hesperithyris sp. 180
Hesperithyris ternieri 180
heterohelicids 65
Heterohelix 65
Heterohelix globulosa 65; 66
Heterohelix labellosa 66
Hettangian 52; 146; 180; 185; 193; 197; 200; 202; 239; 240; 241
Heu River 103
Hibolites sp. 14
Hidoceratids 195
High Atlas 184; 186; 192; 200; 201; 202; 203; 204; 237; 238; 239; 240; 241; 242; 243; 245; 247; 249; 251; 252; 254
High Plains 146; 147; 149; 177; 1180; 184; 197; 202; 203; 204; 205
High Plateaux 177; 180; 197; 203
Hildoceras 167
Hildoceras angustisiphonatum 195
Hildoceras bifrons 195
Hildoceros gr. *semipolitum* 195
Hildoceras snoussi 171
Hildoceras sublevisoni 195
Holcophylloceras 171
Holcophylloceras sp. 168

Source : MNHN, Paris

Holcophylloceras ziguodianum 171
Holy Cross Mountains 75; 76; 77; 78; 79; 83; 84; 85; 86; 87; 88; 89; 90
Homerocythere hermonensis 226
Homoeorhynchia tifritensis 167
Humboldt Range 41
Humphriesianum Zone 157; 176; 201; 204
Hutsouia 226
Hutsouia ahmata 220; 221; 226
Hybonotum Zone 26
Hylaidichnus 262
Hypacanthoplites 105
Hysteroceras orbignyi 96
Hysteroceras orbignyi Zone 105
Hystrichogonyaulax 224

I

Ichthyosaurus 21
Iffer 249
Ilowaiskya klimovi 19; 25
Ilowaiskya pavida 19; 21; 25
Ilowaiskya pseudoscythica 21; 25
Ilowaiskya schaschkovae 21; 25
Ilowaiskya sokolari 19; 21; 25
Imilchil 244
India 134; 226
Indian Ocean 133
Indol-Kuban 112
Indosphinctes gr. *patina* 171
Induan 39; 43; 48
Infraparkinsonia sp.177
Inmar 213; 214; 218; 224; 225; 230; 231
Inoceramid 93; 98; 100; 101; 103
Inoceramus costellatus 102
Inoceramus costellatus Zone 102
Involutina liassica 186
Iran 43; 224
Iranian Block 68
Ischyosporites spp. 52
Isabythocypris avalis 225
Israel 213; 214; 217; 219; 221; 222; 224; 225; 226; 227; 230; 232

J

Jebel Aberdouz 251; 252
Jebel Grouz 197
Jebel Haïmeur 193; 195; 202
Jebel Masker 214; 251
Jebel Nador 180; 184; 197
Jorf Henndia 167
Judea 218; 220; 227; 230
Jugasporites sp. 275
Jurassic 9; 10; 12; 25; 27; 30; 35; 36; 47; 51; 52; 53; 54; 68; 75; 79; 81; 83; 89; 90; 113; 120; 131; 132; 134; 145; 147; 154; 157; 163; 167; 178; 180; 182; 184; 185; 192; 200; 202; 204; 213; 214; 218; 219; 221; 222; 224; 225; 226; 227; 230; 231; 232; 237; 238; 239; 240; 252

K

Kachpurites fulgens 22; 26
Kachpurites subfulgens 22; 26
Kamenyi Ourag 18
Karaduan 45; 46
Karatau 36; 37; 38; 44; 45; 49
Karatauchik 36; 37; 39; 44; 45
Karmon 213; 230
Karpinsky swell 114
Karroo 132; 134
Kashpir 12; 21; 22; 29
Kazakhstan 35
Kazakhstanites 43
Kazanian 275
Kenya 226
Kerberites 27
Kerberus Zone 27
Kerdacha 192
Kfar Darom 219
Kheneg Grou 200; 201
Khenifra 257; 258; 259; 266; 267; 268; 272
Kheraiceras bullatum 167
Khuff 277
Kielce 78
Kilianina 227
Kilianina sp. 218
Kimmeridge 9; 30
Kimmeridgian 9; 10; 12; 16; 18; 23; 24; 26; 29; 30; 31; 52; 27; 58; 59; 131; 132; 134; 140; 143; 147; 154; 202; 205; 214; 220; 221; 226; 227; 230; 232
Kinkelina kadeshensis 225
Kissufim 219
Klausipollenites schaubergeri 275
Klimovi Zone 19; 25; 26
Kuoxisporites 272
Koenigi Zone 54
Kohal 226
Kokhav 220
Korystocysta 224
Kosmoceras annulatum 56
Koudiat el Haïddoura 146
Koudiat el Halfa 176; 195
Krauselisporites 43
Krauselisporites sp. 39; 43
Ksour 147; 149; 167; 182; 185; 196; 201; 204
Ksour El Harchaia 167
Ksour Mountains 146; 147; 168; 180; 184; 186; 192; 193; 203; 204
Kugusem Scarp 44
Kuibyshev reservoir 12

Source : MNHN, Paris

Kuma 105
Kuma High 114
Kungurian 272; 275
Kugusem scarp 44
Kurnub 214; 218; 219; 227
Kurnubia (K.) palastiniensis 227
Kurnubia (K.) variabilis 227
Kurnubia bramkampi 227
Kurnubia cf. *wellingsi* 227
Kurnubia gr. *palastiniensis* 219
Kurnubia palaistiniensis 140
Kurnubiella compressa 222
Kutchithyris 226

L

Labirintodonts 44
Labyrinthina recoarensis 184
Ladinian 46; 67
Laevaptychus 19
Laevicythere sp. 225
Laevinscula 231
Lagena ex. gr. *laevis* 56
Lamberti Zone 56; 219; 222
"Lamberti" Zone 222
Lamplughi Zone 25
Laramide 86; 87; 88; 89; 90
Longeites aenivanovi 21; 26
Langeites stschurowskii 21; 26
Lebanon 213; 22118; 221; 226; 227; 230
Leioceras (Cypholioceras) cf. *comptum* 190
Lenticulina aff. *russiensis* 56
Lenticulina aff. *sumensis* 56
Lenticulina brueckmanni 56
Lenticulina cf. *tumida* 56
Lenticulina conae 56
Lenticulina compressaeformis 56
Lenticulina d'orbignyi 195
Lenticulina deslongchampsi 195
Lenticulina ex gr. *goettingensis* 39; 41
Lenticulina hyalina 56
Lenticulina munsteri 195
Lenticulina sp. 195
Lenticulina spp. 56
Lenticulina subalata 195
Lenticulina sublaevis 195
Leptolepidites spp. 52
Leptosphinctes (Cleistosphinctes) cleistus 171
Leptosphinctes (L.) davidsoni 171
Leptosphinctes (L.) perspicuus 171
Leptasphinctes cf. *perspicuus* 177
Lesser Caucasus 103; 107; 111
Levant 213; 214; 224; 226; 227
Levantinella egyptiensis 218
Levisoni Zone 167; 176; 201; 203
Leymeriella (Leymeriella) 105
Liassic 98; 157; 192; 193; 197; 216; 217; 225; 227; 230; 231; 238; 239; 242; 245; 249; 250; 251; 253; 254
Libya 224
Lidgettonia 272
Limitisporites sp. 275
Limaguella sp. 227
Lingula sp. 18
Lingulina ex gr. *belorussica* 56
Lingulina tenera 195
Lingulogavelinella globosa 98; 100
Liospiriferina praerostrata 197
Liostrea sp. 53
Lirellarina 226
Lithastrinus septenarius 61
Lithiotis 180; 200
Lithraphidites carniolensis 58
Lituotuba ? sp. 39
Lobatannularia aff. *L. sinensis* 272
Lobothyris subpunctata 180
Lodève 263
Lodevia (Callipteris) nicklesii 275
Lodevia nicklesii 268
Lomonossovella blakei 268
Lomonossovella lomonossovi 21; 26
"Lomonossovella" lomonossovi 27
Loripes 19
Loripes sp. 16
Lotharingian 238; 239; 242; 245; 249; 250; 251; 252
Lower Saxony 104
Lublin 79
Luciaporhabdus cayeuxii 61
Luciaporhabdus maleformis 61
Ludwigella cf. *arciteneus* 190
Lueckisporites singhii 43
Lueckisporites virkkiae 275
Lunatisporites noviaulensis 39; 43
Lunatisporites pellucidus 43
Lunatisporites sp. 43; 268
Lunatisporites spp. 39; 43
Lundbladispora 43
Lundbladispora brevicula 43
Lundbladispora echinata 43
Lundbladispora sp. 43
Lunuloceras 171
Lusitanian Basin 192; 193; 206
Lyelli Zone 105
Lyelliceras 105
Lysogory 78
Lytoceras adeloides 176
Lytoceras eudesianum 171
lytoceratids 107

Source : MNHN, Paris

M

Maastrichtian 65; 66; 68; 84
Macrocephalites 167
Maculatisporites sp. 43
Madagascar 134
Maghara 213; 227
Maghreb 147; 186; 193; 200; 203; 204
Maikopian 111; 116; 118; 120; 121; 124; 125; 127; 128
Maïz 192; 195
Majdal Shams 213; 214; 220; 222; 223; 225; 230; 232
Makariev 12; 13; 16; 23; 24; 28
Makhtesh Qatan 218
Makhtesh Ramon 214; 225; 227
Malletia sp. 18
Malopolska Massif 79
Mancodinium semitabulatum 52
Mandelstamia hirschi 225
Manghastia 218
"Mangashtia" egyptiensis 227
Mangyshlak 35; 36; 44; 48; 52; 54; 57; 67; 68; 94; 97; 98; 100; 101; 102; 103; 105; 106; 107
Mantiritella pennatoidea 61
Mantelliceras 100
Manych 116
Marginotruncana 102 ;
Marginotruncana coronatarenzi 100
Marginulina batrakiefornis 56
Marginulina minuta 56
Marginulinopsis aff. *procera* 56
Mariae Zone 220; 223; 232
"Mariae" Zone 220
Matmor 214; 219; 222; 224; 225; 230; 231
Mechraâ Ben Abbou 258; 267
Mediterranean Sea 147; 200
Megalodontids 176; 177; 200; 201; 203
Mekele 134; 140
Mekele outlier 131; 132; 133; 134; 140; 141
Melah 182; 185
Meleagrinella 14; 18
Mellala 162; 203
Mendicodinium umbriense 52
Meneghinii Zone 176
Meotian 116; 121
Merlaites gr. *alticarinatus* 177
Mesozoic 25; 35; 36; 66; 68; 75; 76; 83; 85; 86; 88; 89; 90; 120; 133; 180; 197
Meyendorffina bathonica 227
Miasto 79
Micrantolithus hoschulzii 58
Micrantolithus obtusus 58
Micrhystridium sp. 44
Micramphalites 222; 231
Micromphalites pustuliferus 219
Micropneumatocythere laevireticulata 225
Microrhabdulus decoratus 61
Micula decussata 61
Millioudodinium 224
Millioudodinium nuciformis Zone 224
Mimci 12; 16; 24; 29
Miocene 77; 84; 87; 111; 116; 121; 125; 128
Mirosphinctes aff. *robyi* 223
Mirosphinctes sp. 223
Mishhor 213; 214; 224; 227; 231
Mleta Plain 157
modiolids 45
Modiolus 51
mollusc 132
Monoceratina 225
Monoceratina stimulea 226
Monoceratina striata 225
Montlivaltia 177
Moroccan Meseta 204
Morocco 146; 147; 157; 167; 177; 197; 203; 204; 205; 206; 237; 239; 257; 258; 266; 267;
Morphoceras 171
"Morphoceras" aff. *pingue* 168
"Morphoceras" parvum 168
Morphoceras (Ebrayiceras?) parvum 168; 176
Morphoceratid 168
Mortoniceras inflatum 96
Mortoniceras inflatum Zone 105
Moscow 28
Moscow basin 10
Moulouya 239; 251
Mount Hermon 214; 219; 220; 223
Mountain Crimea 96; 97; 103; 105; 106; 107
Mourhal 197
Mrit-Khouabi 195
Münster Basin 104
Murchisonae Zone 190
Murgabian 277
Mutabilis Zone 24; 30
Myophoriopsis gregariodes 47
Mytiloides hattini 101
Mytiloides hercynicus 102
Mytiloides hercynicus Zone 100
Mytiloides incertus Zone 102
Mytiloides labiatus Zone 100; 102
Mytiloides mytiloides Zone 100
Mytiloides hercynicus - Inoceramus apicalis - Inoceramus lamarcki Zone 102
Mytilus (Falcimytilus) nasai 47

N

Nahar Sa'ar 213; 214; 221; 225; 226; 230
Nakhichevan 113
Namurian 275
Nannoceratopsis gracilis 52; 53
Nannoceratopsis pellucida 224

Source : MNHN, Paris

Nannoceratopsis spiculata 53
nannoconids 59; 61; 65
Nannoconus dauvillieri 65
Nannoconus furrnicciae 61
Nannoconus minutus 61
Nannoconus multicadus 61; 65
Nannoconus spp. 61; 65
Nannoconus steinmannii minor 58
nannofossil 53; 56; 58; 60; 61; 66; 68; 133; 134; 141; 143
Nannogyra sp. 16
Nannolytoceras tripartitum 168; 176
nannoplancton 218; 219; 221
Nastoria 226
Nannovaspora striata 43
Nautiloculina oolithica 140
Negev 213; 214; 218; 219; 220; 221; 224; 225; 227; 230; 232
Neocardioceras juddi 100
Neochetoceras 26
Neochetoceras aff. *sternspis* 25
Neochetoceras cf. *steraspis* 19
Neochetoceras sp. 19
Neospathodus abruptus 39
Neospathodus cf. *N. brevissimus* 39
Neospathodus homeri 39
Neospathodus symmetricus 39
Neostlingoceras 100
Neo-Tethys 230; 232
Neotethys 237
Nerineacea 231
Netherlands 52
Nevada 43
New Zealand 124
Niger 257; 275; 277
Nikitini Zone 21; 25; 26
Nilssonia spp. 51
Niortense Zone 171; 176; 177; 182; 190; 197; 201
Nir'Am 213
Niram 214
Nirim 219
Nodiger Zone 22; 25; 26; 27; 29
Nodosaria aff. *hone* 39
Nodosaria aff. *pseudoprimitiva* 39
Nodosaria cf. *ornlinata* 39
Nodosaria cf. *sluskensis* 39
Nodosaria ex gr. *oxforea* 56
Nodosaria hoae 39
Nodosaria sp. 39
Nodosariids 186
Norian 47; 48
Normannites 176
North America 103
North Sea 10; 30; 31; 163; 204
northern Canada 12
northern Caucasus 94; 96; 102; 103; 105; 106; 107
Nowe Miasto-Ilza 79; 80; 81; 83; 89; 90
Nucula 102
Nuculoma sp. 16
Nuculoma sp. ind. 16

O

Obtusum Zone 186; 193
Oecotraustes cf. *westermanni* 171; 176; 177
Oecotraustes scaphitoides Zone 223
Olenekian 39; 454; 45
Oligocene 116; 120; 121; 123; 124; 128
Oligocythereis aff. *fullonica* 225
Oligocythereis irregularis 226
Oman 134; 277
Opalinum Zone 53; 160; 176; 190; 201; 204
Ophthalmidium sp. 46
Ophthalmidium strumosum 56
Opisoma 180; 197
Oppelia pouyannei 171; 176; 177
Oppressus Zone 25; 26
Oran 148; 157; 177
Oran High Plains 147; 177; 197; 202; 203; 204
Oraniceras 171
Oraniceras hmiyaneuse 167; 185
Orbitammina elliptica 227
Orbitopsella aff. *praecursor* 227
Orbitopsella dubari 184
Orbitopsella praecursor Zone 227
Orbitopsella primaeva 217; 227
Ordovician 266
Orthaspidoceras lallierianum 9; 31
Orthaspidoceras liparum 24
Osperlioceras 171
Ossa-Morena 272
ostracod 39; 180; 214; 218; 219; 221; 225; 226
ostreid 59
Otoites 231
Otoites cf. *sauzei* 192
Otovicia hypnoides 268
Otpan 37; 39
Ouchbis 251
Oued el Hallouf 195
Oued Melah 167
Oued Onm Rbia 268
Oujda 157; 167; 177; 180; 206
Ovalipollis pseudoalutus 46
Oxfordian 10; 12; 13; 14; 23; 28; 30; 35; 56; 57; 131; 1332; 134; 140; 143; 146; 154; 168; 171; 201; 202; 204; 213; 218; 219; 220; 221; 222; 223; 224; 226; 227; 230; 232
Oxycerites yeovilensis 168
Oxynotum Zone 186
Oxytoma sp. 14
oyster 16; 53; 59; 136

Source : MNHN, Paris

P

Pachyerymnoceras kinereusr 22
Pachyerymnoceras levantinense 222
Pachyerymnoceras sp. 222
Pachythentis panderiana 14
Pakistan 134
Palaeocene 58; 61; 74; 83; 120
Palaendasycladus mediterraneus 184
Palaeogene 36; 76; 84; 120
Palaeo-Tethys 67
Palaeozoic 49; 67; 68; 76; 77; 78; 79; 83; 86; 90; 113; 114; 120; 132; 133; 157; 167; 168; 177; 238; 240
Paleupfenderina salernitana 218; 227
Pallasioides Zone 30
Paltarpites gr. *paltus* 177
Paltarpites sp. 184
Paltechioceras 193
Paltechioceras nov. sp. 186
Paltechioceras boehmi 186
Paltechioceras tardecrescens 193
Panderi Zone 21; 25; 27; 29
Paracraspedites appressus 26
Paracraspedites sp. 22
Pararasenia cf. *hybridus* 24
Pararasenia hybridus 18
Paratethys 120; 121
Parathyridina mediterranea 180
Parawedekindia 201 :
Parawedekindia spp. 171
Pareodinia halosa 53
Paris Basin 31
Parkinsania 51
Parkinsonia (Gonolkites) convergens 168
Parkinsonids 176
Partitisporites spp. 46
Partschiceras gr. *viator* 176
Parvocysta 53
Parvocysta ? tricornuta 56
Parvocysta nasuta 53
Patinasporites densus 46
Pavlovia pavlowi 21; 25
Peceneaga-Camena fault 76
Pecopteris chihliensis 272
Pecopteris latinervosa 272
Pectinatites aff. *pectinatus* 25
Pectinatites ianschini 21; 25
Pectinatites tenuicostatus 21; 25
Pectinatus Zone 30
Pediastrum 51
Peltaspermum martinsii 268
Peltoceras solidum 219; 222
Peltoceras sp. 56; 133; 222
Peri-Caspian 95; 97; 98; 103; 105; 106; 107
Perisphinctes (Arisphinctes) gr. *plicatilis* 14; 23
Perisphinctes berneusis 223
Perisphinctes sp. 14; 16
Perisphinctidae 14
Perisphinctids 12; 18; 24
Perisphinctinae 222
Permian 38; 49; 76; 77; 79; 80; 81; 82; 83; 89; 90; 120; 257; 258; 259; 260; 262; 263; 266; 267; 268; 272; 275; 277
Perth Basin 52
Pfenderina gr. *trochoidea* 133
Phanerozoic 76
Phylloceras 171
phylloceratids 107; 171
Phylloceratinae 222
Phyllotheca spp. 272
Physodoceras neuburgense 25
Piarorhynchella mangyshlakensis 41
Pictonia 24
Pictonia baylei 16; 31
Pictonia densicostata 16; 31
Pilica River 80
Plain Crimea 96; 97; 103; 107
Planiinvoluta carinata 45
Planiinvoluta? sp. 39
Planisepta compressa 184; 193
Planisphinctes sp. 168
Planolites 138
Planula Zone 23
Planularia colligata 56
Planularia contracta 56
Planularia sp. 56
Planularia spatulata 56
Planularia subcompressa 56
Planularia tricarinella 56
Platypleuraceras gr. *brevispina* 195
Pleisiosaurus 21
Plenus Zone 100
Plesechioceras 193; 200
Plesechioceras cf. *delicatum* 186
Pleuraceras 177
Pleuracerus solare 176; 190
Pleuromeia 38
Pleuromeia sternbergii 44
Pleuromia sp. 13
Pleurotomaria sp. 14
Plicatilis Zone 23
Plicatipollenites gondwanensis 272
Plicatipollenites spp. 272
Pliensbachian 52; 134; 145; 154; 167; 176; 180; 184; 192; 193; 195; 197; 200; 203; 213; 217; 224; 227; 231
Pliocene 263
"*Podagrosites*" gr. *aratum* 184
Polish Trough 76; 79; 81; 83; 89; 90
pollen 51; 268
Polymorphitids 195
Polymorphum Zone 177; 184; 201; 203

Source : MNHN, Paris

Polystephanephorus 224
Polystephanephorus calathus Zone 224
Pontian 121
Pontides 123
Porporeras sp. 133
Portlandian 25; 27; 31
Portugal 192; 193; 206; 224
Potonieisporites 268
Praeactinocamax plenus 98
Praekurnubia 227
Praekurnubia crusei 227
Praeschmeridea hornei 225
Praeschmeridea innarensis 225
Precambrian 76; 78; 113
Precaucasus 41
Prediscosphaera spp. 61
Preplicomphalus Zone 25; 27
Primitivus Zone 25
Procerites subprocerus 168
Prodactylioceras sp. 184; 195
Progonocythere aff. *parnstilla* 225
Progonocythere honigstrini 225
Prohecticoceras (Zieteniceras) pseudolunula 171
Pramillepora pervinquieri 140
Praperisphinctes sp. 223
Proto-Atlantic 232
Protobeckmum sp. 272
Protobeckmum wongii 272
Protocardioceras cf. *praecordatum* 56
Protodiceras 180
"*Protodiceras*" sp. 180
Protogrammoceras 186
Protogrammoceras celebratum 171; 180; 195
Protogrammoceras gr. *dilectum-pseudodilectum* 186
Protogrammoceras gr. *volubile-pantanelli* 186
Protogrammoceras isseli 171
Protogrammoceras sp. 195
Protohaploxyphus limpidus 43
Protohaploxyphus sp. 43
Pseudobrightia 222
Pseudobrightia s. st. 222
Pseudobrightia sp. 219; 222
Pseudoclypeina 218; 227
Pseudocyclammina sp. 140
Pseudogrammoceras 190
Pseudogrammoceras pinnai 190
Pseudogrammoceras subregale 184; 190
Pseudoscythica Zone 21; 25
Pteridophytae 51
Ptychophylloceras 171
Ptychophylloceras sp. 140
Ptylophyllum spp. 51
Punctatisporites fungosus 43
Purbeck 25
Purpuroidea 219
pyrgosiids 107
Pycnoria 226

Q

Qeren 214; 218; 219; 220; 221; 224; 226; 230
Quadrum gothicum 61
Quadrum sissinghii 61
Quadrum trifidum 65
Quaternary 111; 113; 116; 120; 121; 125; 128; 260
Quenstedoreras cf. *praehumberti* 56
Quenstedoceras sp. 56
Quinqeloculina sp. 56

R

radiolaria 182; 186; 193; 202
radiolarian 56; 65; 66
Radomsko 87; 88; 89
Radotruncana calcarata Zone 66
Raistrickia 272
Raknet el Kahla 190; 192; 204
Ramon 217; 218
Rasenia 24; 31
Rasenia cf. *cymodoce* 16
Rasenia cf. *uralensis* 16
Rasenia gr. *cymodoce* 24
Rasenia gr. *uralensis* 24
Rasenia sp. 16
Rastellum 58
Rawa Mazowiecka Basin 81
Regulare Zone 16; 23
Reha 185
Rehmannia (Rehmannia) spp. 171
Reineckeia nodosa 222
Reinhardtites anthophorus 61
Reinhardtites levis 61
Renggeri Zone 220
Retrocostatum Zone 167
Renssella kelleri 102
Rewinisporn 43
Reynesoceras 190
Reynesoceras gr. *indumense* 184
Reynesocoeloceras sp. 195
Rhachiphyllum schenkii 268
Rhactian 145; 180; 200; 227
Rhar Roubane 147; 167; 176; 177; 192; 201; 203; 205
Rhipidopsis spp. 272
Rhynchonella assymetrica 226
*Rhynchonella fornix*226
"*Rhynchonella*" *maghrebiensis* 180
Rhynchonella nobilis 226
Rhynchonella versabilis 226
rhynchonellid 14; 185; 226
Rhynchonelloidella sp. 53
Rhyzocorallium 138

Source : MNHN, Paris

Rich 238; 242; 244; 251; 252
Rif 200
Rif-Tell 146; 148; 204
Ringsteadia 23
Ringsteadia cf. *frequens* 16
Ringstendia cuneata 23
Ringsteadia frequens 23
Rio Viar 259; 272
Rioni 112
roissyanum Zone 102
Romania 76; 77
Rosenkrantzi Zone 16; 23
Rosh Pinna 218; 231
Rotalipora appenninica 98
Russia 53; 220
Russian Platform 9; 10; 12; 23; 24; 25; 27; 29; 31; 76
Rutlandella transversiplicata 225
Ryasan 96
Ryazanian 22
Ryazinites Zone 59

S

Saalian 258
Safa 219; 230; 231
Sahara 147; 149; 177; 178; 180; 184; 192; 195; 197; 200; 202; 203; 204
Saïda Mountains 167; 192
Sakmarian 275
Salima 221; 226
Samaria 214
San Nicolas del Puerto 259
Santonian 61; 107
Saracenaria cornucopiae 56
Saracenaria inclusa 56
Saratov 96
Sarmatian 116; 118; 121; 125; 128
Satorina apuliensis 227
Saudi Arabia 225; 226
Sauzei Zone 201; 204
Schizoria 226
Schloenbachia 100
Schlotheimiids 186; 193
Schrammeni Zone 105
Schuleridea 226
Schweizerisporites sp. 272
Scythian Platform 94; 103; 113; 114
Sekika 157; 164; 201
Selliporella donzellii 227
Semenoviceras 68
Semenoviceras litschkovi 60
Semenoviceras litschkovi Zone 60
Semenoviceras mangyschlakensis 60
Semenoviceras pseudocoelonodosus 60
Semenoviceras uhligi 60
Semenovites michalskii 60
Semenovites michalskii Zone 60
Semicostatum Zone 180; 186; 200; 202
Senonian 83
Sentusidinium 224
Septaliphoria jordanica 220
Serbarinovella ringstealiaeformis 26
Serbarinovella serburimmi 26
serpulid 136
Serratum Zone 14; 23
Seychelles 134
Shair 37; 47; 48; 49; 51
shark 98
Shekat 143
Sherif 213; 214; 219; 224; 225; 230
Shetpe 60
Sheuringipollenites spp. 272
Shuqraia zuffardi 140
Shyrkala 61
Siberia 12
Sidi el Abed 147; 177; 178; 197; 203
Sidi Jabeur 167
Sidi Mohammed 130
Sidi Yahia ben Sefia 177
Siemiradzkia aurigera 168
Simbirsk 105
Simpheropol 97
Sinai 213; 214; 216; 217; 218; 219; 220; 221; 222; 225; 226; 227; 230; 232
Sinemurian 146; 154; 176; 180; 184; 186; 193; 197; 200; 202; 203; 238; 239; 243; 241; 242; 249; 250; 251; 252; 253; 254
Soaresirhynchia bourkardi 167
Sokolovi Zone 19; 25
Somalia 134; 226
Somalirhynchia 226
Somalirhynchia africana 220
Somalirhynchia somalica 220
Sonninia 218
Sosvaensis Zone 24
Souiga 185
Souiga-Melah 182
Souk-es-Sebt 259; 263
Sowerbyceras helios 223
Spain 224; 272; 277
Spathi 105
Spathian 39; 43; 44; 46; 67
Sphaeroceras 176
Sphaeroceras brongniarti 171
Sphenopteris pseudogermanica 272
Spiraloconulus cf. *perconigi* 227
Spirigerellina pygmaea 41
Spiroceras orbignyi 171; 176
Spitzbergen 12
sponge 136; 137

Source : MNHN, Paris

spores 43; 220; 221
Stacheites 43
Staufenia (=Aucaliaceras) opaliuoides 190
Steinekella cf. *steinekei* 227
Stephanoceras (Sk.) cf. *skolex* 176
Stephanoceras (Sk.) freycineti 176
Stephanoceras (Sk.) thouceni 176
Stephanoceras (St.) deusicastatum 176
Stephanoceras (St.) humphriesianum 176
Stephanolithion bigoti maximum 56
Stephanolithion hexum 56
Stepnoe 114
Stipa tenacissima 177
Stoliczkaia dispar Zone 105
Strenoceras gr. *subfurcatum* 177
Strenoceras subfurcatum 171
Striatoabieites richterii 43
Striatoabieites sp. 268
Strigoceras cf. *puronai* 176
Strigoceras truellei 177
stromatoporoid 131; 1232; 136; 137; 140; 143; 218; 219
Strongylxria 226
Stroudithyris frederici-romani 167
Stroudithyris pisolithica 167
Subditus Zone 22; 25
Sturculospluteridium 224
Susaliinium scrofaides 53
Sutneria aff. *subemmela* 25
Sutneria cf. *subemmela* 19
Sutneria sp. 192
Svalbard 43
Sweden 52
Syria 218; 227; 232
Systematopluru 224
Syzran 12

T

Talghemt 181; 203
Talme Yale 220
Tamlelt 200
Tanzania 226
Taramelliceras cf. *langi* 223
Taranaki 124
Tarat 275
Tarkhankut 97
Tasmanites 51
Tauride 123; 195
Taurometia arethusa 180
Tauramenicerus 184; 190
Teisseyre-Tornquist Zone 75; 76; 79; 83; 88; 89; 90
Teloceras 176
Tendrara 180
Tenouchfi 134; 195
Tenuiplicatus Zone 168
Tenuiserratum Zone 23
Terebrutula psilonoti 185
Terek 112; 114
Terquemula cf. *martini* 226
Terquemula goldbergi 225
Terquemula gublerae 225
Tertiary 124; 238
Tethys 106; 116; 120; 177; 200; 213; 214; 222; 223; 226; 227; 258
Textularia jurassica 54; 56
Thalassinoides 98; 100; 137; 138
Thanbites planus 218; 222
Thaumatoporella parvovesiculifera 227
Thoracosphaera sp. 65
Thuringia 262
Thuringian 272
Tiddas 257; 258; 259; 263; 267; 268; 272
Tigrai 131
Tiniihunella sp. 218; 227
Tinerhir 238
Tinjdad 237; 238; 249
Tiouli 157; 177
Tirrhist 244
Tirrolites 44
Tisseddoûra 157; 171; 176; 177; 205; 206
Tithonian 10; 12; 25; 26; 31; 59; 147; 204; 213; 221; 204; 205
Tizi n'Test 238
Tlemcen 145; 147; 149; 154; 157; 167; 201; 202; 204; 205
Tlela 171; 176; 203
Tinetoceras scissum 176
Toarcian 30; 51; 52; 53; 146; 147; 154; 157; 162; 163; 167; 171; 176; 177; 180; 184; 185; 190; 192; 195; 197; 201; 203; 204; 205; 213; 217; 218; 225; 227; 230; 231; 243; 244; 247; 249; 250; 251; 254
Tobin Range 43
Tolvericeras gr. *sevogodense* 19; 24
Tolvericeras sevagodense 19; 24
Tolypammina ex gr. *gregaria* 39
Tolypammina gregaria 45
Touissit-Bou Beker 167
Tounfite 237; 238; 244; 249; 252
Trauolithus phacelosus 65; 66
Transcaucasus 123; 124; 128
Trans-Caucasus 112; 113
Transversarium Zone 220
Traras 146; 147; 160; 163; 200; 201; 203
Trautscholdia cuvlatu 14
Triassic 35; 36; 38; 39; 43; 45; 46; 47; 48; 49; 51; 67; 68; 75; 80; 81; 82; 83; 89; 90; 98; 113; 120; 132; 180; 192; 197; 202; 203; 217; 230; 237; 238; 240; 251; 258; 260; 266
trigoniids 60
Trigonodus (?) roeperti 47
Trigonodus hornschuchi 47

Source : MNHN, Paris

Tristix tutkowskii 56
Trocholina palusteniensis 218
Tropidoceras 185; 200
Tropidoceras calliplocum 186
Tropidoceras cf. *calliplocum* 200; 201
Tropiloceras sp. 184; 195
Tuarkyr 94
Tunisia 106; 226
Turan 68
Turan Platform 95
Turanian Platform 106
Turkmenia 94
Turneri Zone 200
Turonian 30; 58; 60; 68; 81; 93; 95; 98; 100; 101; 102; 103; 104; 106; 107
Turrilites costatus 100

U

Ufimian 275
Ulianovsk 105
Ulyanovsk 12
Ulyanovsk-Saratov trough 10
Undory 12
Unzha River 12; 23
Urals 97; 106
Urbana 259
Ustyurt Plateau 44
Uvaesparites sp. 39

V

Valanginian 59
Variamussium 102
Venustostrobus 272
"*Vernicera*" *rothpletzi* 193
Veryhachium sp. 41
Virgataxioceras fallax 19; 24
Virgataxioceras sp. 19
Virgatites cf. *sosia* 21
Virgatites crassicostatus 26
Virgatites gerassimovi 21; 26
Virgatites larisae 25; 26
Virgatites pallasianus 21; 25; 26
Virgatites pusillus 21; 25; 26
Virgatites rosanovi 26
Virgatites sosia 25; 26
Virgatites virgatus 21; 26; 26
Virgatus Zone 21; 26; 29
Visean 258; 260; 263; 266; 275
Volga 9; 10; 12; 24; 30
Volgian 12; 19; 21; 22; 25; 26; 27; 29; 30
Volgian basin 12; 23
"Volgian province" 10
Volgograd 113; 118
Voronezh 96

W

Wadi E Shatr 220
Walchia piniformis 275
Walchia spp. 272; 275
Walchiacean 277
Warszawa 79
Watznaueria 56
Watznaueria barnesae 58; 61
Watznaueria britannica 58
Watznaueria sp. 53
Watznaueria spp. 58
Weatleyites arkelli 25
Weatleyites aff. *aestlecottensis* 25
Weatleyites spathi 25
Wessex 30
Westphalian 258
Whiteinella 100
Whiteinella archeocretacea 102
Whiteinella archeocretacea Zone 101
Wola Morawicka 86
Wukro 143

Y

Yorkshire 30; 218

Z

Zaire 275
Zaraiskites michalskii 21; 25
Zaraiskites quenstedti 21; 25
Zaraiskites scythicus 21; 25
Zaraiskites tschernyschovi 21; 25
Zaraiskites zarajskensis 21; 25
Zechstein 80; 81
Zeilleria hierlazica 185
Zeilleria perforata 185
Zeilleria sarthacensis 197
Zeilleria sestii 180
Zeillerids 19
Zekkara 167
Zenaga 195
Zerqacythere subiehensis 225
Zigzag Zone 167
Zohar 214; 219; 220; 224; 225; 230; 231
Zohar-Kidod 220
Zoophycos 137; 171; 176; 177; 184; 195; 201; 204; 206
Zygodiscus diplogrammus 61
Zygoliscus erectus 58; 61
Zygodiscus spp. 58; 61
Zygodyscus 59

Source : MNHN, Paris

Remerciements aux rapporteurs / *Acknowledgements to referees*

La Rédaction tient à remercier les experts extérieurs au Muséum national d'Histoire naturelle dont les noms suivent, d'avoir bien voulu contribuer, avec les rapporteurs de l'Établissement, à l'évaluation des manuscrits (1995/1998) :
The Editorial Board acknowledges with thanks the following referees who, with Muséum referees, have reviewed papers submitted to the Mémoires du Muséum (1995/1998):

Arzelius B.	Stockholm	Suède
Akam M.	Cambridge	Grande-Bretagne
Andersen N.	Copenhague	Danemark
Augelli I.	Milan	Italie
Baba K.	Kumamoto	Japon
Bachmann G. B.	Halle-Wittenberg	Allemagne
Bally A. W.	Houston	USA
Banks T.	Egham	Grande-Bretagne
Baud A.	Lausanne	France
Bellido A.	Paimpont	France
Berggren M.	Fiskebackskil	Suède
Bernet-Rollande M C.	Paris	France
Bernoulli D.	Zürich	Suisse
Bertotti G.	Amsterdam	Pays-Bas
Besse J.	Paris	France
Besseau G.	Rueil-Malmaison	France
Best M.	Leiden	Pays-Bas
Bonavia F.	Paris	France
Bourseau J.P.	Villeurbanne	France
Bruce J.	Helensvale	Australie
Bruce N.	Copenhague	Danemark
Brunton H.	Londres	Grande-Bretagne
Carpenter J.	New York	USA
Cassagneau P.	Toulouse	France
Chace F. A.	Washington	USA
Child C. A.	Washington	USA
Cherix D.	Lausanne	Suisse
Clobert J.	Paris	France
Cloetingh S.	Amsterdam	Pays-Bas
Cohen D.	Los Angeles	USA
Cook P. L.	Victoria	Australie
Cordey F.	Lyon	France
Cornudella L.	Barcelone	Espagne
Cuzin-Roudy J.	Villefranche / Mer	France
Darlu P.	Paris	France
Danchin E.	Paris	France
Davie P.	Brisbane	Australie
Dejean A.	Villetaneuse	France
Delleporte P.	Paimpont	France
Dietrich C.	Champaign	USA
Duffels J. P.	Amsterdam	Pays-Bas
Eldredge L. L.	Hawaii	USA
Elloiz N.	Rueil-Malmaison	France
Fahay M.	Highlands	USA
Fleury A.	Orsay	France
Fodor L.	Budapest	Hongrie
Fransen C.	Leiden	Pays-Bas
Gagné R.	Washington	USA
Gorin G.	Genève	Suisse
Guglielmo L.	Messina	Italie
Gullan P.	Canberra	Australie
Gunzenhauser B.	Zürich	Suisse
Hancock P.	Bristol	Grande-Bretagne
Harmelin J.G.	Marseille	France
Healy J.	Brisbane	Australie
Heemstra P.	Grahamstown	Afrique du Sud
Hodgson C.	Ashford	Grande-Bretagne
Holthuis L. B.	Leiden	Pays-Bas
Horváth F.	Budapest	Hongrie
Ingrisch S.	Frankfurt	Allemagne
Jordan P.	Solothurn	Suisse
Kabat A.	Washington	USA
Kensley B.	Washington	USA
Kerp H.	Munster	Allemagne
Kielan-Jaworowska Z.	Oslo	Norvège
Komai T.	Chiba	Japon
Krapp F.	Bonn	Allemagne
Kristensen N.	Copenhague	Danemark
Lagardère J.P.	La Rochelle	France
Laubscher H.P.	Bâle	Suisse
Ledouaran S.	Paris	France
Lemaitre R.	Washington	USA
Lovelock P. E. R.	La Haye	Pays-Bas
Lowrie J.	Zürich	Suisse
Machida Y.	Kochi	Japon
MacKinnon D.	Christchurch	Nouvelle-Zélande
MacPherson E.	Barcelona	Espagne
Maddison D.	Tucson	USA
Manning R.	Washington	USA
Markle D.	Oregon	USA
Masaki S.	Hirosaki	Japon
Mascle A.	Rueil-Malmaison	France
Masse P.	Paris	France
Mauchline J.	Oban	Grande-Bretagne
McLaughlin P.	Washington	USA
McLennan D.	Toronto	Canada
Merrett N.	Londres	Grande-Bretagne
Messing C.	Dania	USA
Meulenkamp J.	Utrecht	Pays-Bas
Morand S.	Perpignan	France
Mugnier J.L.	Grenoble	France
Nakamura I.	Kyoto	Japon
Naumann C.	Bonn	Allemagne
Newman W. A.	San Diego	USA
Ng P.	Singapore	Singapour
Oliva R.	Barcelone	Espagne
Orousset J.	Paris	France
Packer L.	York	Canada
Platteaux C.	Nancy	France
Poccia D. L.	Amherst	USA
Poore G.	Victoria	Australie
Proust J. N.	Lille	France
Raikova O.	Saint-Pétersbourg	Russie
Ravenne C.	Rueil-Malmaison	France
Rentz D. C. R.	Canberra	Australie
Richards W.	Miami	USA
Roberts C.	Wellington	Nouvelle-Zélande
Roure F.	Rueil-Malmaison	France
Salomon M.	Marseille	France
Sazonov Y.	Moscou	Russie
Scholtz C.	Pretoria	Afrique du Sud
Schmid S. M.	Bâle	Suisse
Schwander M.	La Haye	Pays-Bas
Sheridonov V.	Moscou	Russie
Stampfli G.	Lausanne	Suisse
Stefanescu M. O.	Bucarest	Roumanie
Stewart A.	Wellington	Nouvelle-Zélande
Takeda M.	Tokyo	Japon
Tan C. G. S.	Singapore	Singapour
Tassy P.	Paris	France
Thorne B.	Maryland	USA
Tribovillard N.	Paris	France
Tudge C.	Brisbane	Australie
Van Ameron H. W. J.	Krefeld	Allemagne
Van Baaren J.	Rennes	France
Vernon P.	Paimpont	France
Vickery Vernon R.	Ste-Anne / Bellevue	Canada
Vul M. A.	Lvov	Ukraine
Wagele J. W.	Bielefeld	Allemagne
Warén A.	Stockholm	Suède
Watson N.	Armidale	Australie
Wenzel J.	Colombus	USA
Wiegmann B.	Maryland	USA
Wilson M.	Cardiff	Grande-Bretagne
Wilson S.	Warrensburg	USA
Yeates D.	Brisbane	Australie
Young P.S.	Rio de Janeiro	Brésil
Zappatera E.	Londres	Grande-Bretagne
Zezina O.	Moscou	Russie
Ziegler P. A.	Bâle	Suisse

Source : MNHN, Paris

ACHEVÉ D'IMPRIMER
EN DÉCEMBRE 1998
SUR LES PRESSES
DE
L'IMPRIMERIE F. PAILLART
À ABBEVILLE.

BIBL. DU
MUSÉUM
PARIS

Date de distribution : 23 décembre 1998.
Dépôt légal : décembre 1998.
N° d'impression : 10511.

Source : MNHN, Paris

DERNIERS TITRES PARUS

RECENTLY PUBLISHED MEMOIRS

À partir de 1993 (Tome 155), les *Mémoires du Muséum* sont publiés sans indication de série.
From 1993 (Volume 155), the Mémoires du Muséum *are published without serial titles.*

Tome 178 : Alan G. BEU, 1998.— Indo-West Pacific Ranellidae, Bursidae and Personidae (Mollusca: Gastropoda). A monograph of the New Caledonian fauna and revisions of related taxa. Résultats des Campagnes MUSORSTOM. Volume 19. 256 pp. (ISBN : 2-85653-517-8) 350 FF.

Tome 177 : Sylvie CRASQUIN-SOLEAU & Éric BARRIER (eds), 1998.— Peri-Tethys Memoir 3: Stratigraphy and Evolution of Peri-Tethyan Platforms. 262 pp. (ISBN : 2-85653-512-7) 260 FF.

Tome 176 : Alain CROSNIER (ed.), 1997. — Résultats des Campagnes MUSORSTOM. Volume 18. 570 pp. (ISBN : 2-85653-511-9) 600 FF.

Tome 175 : Isabel PÉREZ FARFANTE & Brian KENSLEY, 1997.— Penaeoid and Sergestoid Shrimps and Prawns of the World: Keys and Diagnoses for the Families and Genera. 233 pp. (ISBN : 2-85653-510-0) 350 FF.

Tome 174 : Bernard SÉRET (ed.), 1997.— Résultats des Campagnes MUSORSTOM. Volume 17. 213 pp. (ISBN : 2-85653-500-3) 245,04 FF.

Tome 173 : Philippe GRANDCOLAS (ed.), 1997.— The Origin of Biodiversity in Insects: Phylogenetic Tests of Evolutionary Scenarios. 356 pp. (ISBN: 2-85653-508-9) 490 FF.

Tome 172 : Alain CROSNIER & Philippe BOUCHET (eds), 1997. — Résultats des Campagnes MUSORSTOM. Volume 16. 667 pp. (ISBN : 2-85653-506-2) 612,60 FF.

Tome 171 : Judith NAJT & Loïc MATILE (eds), 1997. — Zoologia Neocaledonica, Volume 4. 400 pp. (ISBN : 2-85653-505-04) 450 FF.

Tome 170 : Peter A. ZIEGLER & Frank HORVÀTH (eds), 1996. — Peri-Tethys Memoir 2: Structure and Prospects of Alpine Basins and Forelands. 552 pp. + atlas. (ISBN : 2-85653-507-0) 450 FF.

Tome 169 : Jean-Jacques GEOFFROY, Jean-Paul MAURIÈS & Monique NGUYEN DUY-JACQUEMIN (eds), 1996. — Acta Myriapodologica. 683 pp. (ISBN : 2-85653-502-X) 550 FF.

Informations sur les Publications Scientifiques du Muséum national d'Histoire naturelle :
Informations about the Scientific Publications of the Muséum national d'Histoire naturelle:
Internet http://www.mnhn.fr/

Prix TTC, frais de port en sus.
Prices in French Francs, postage not included.

Source : MNHN, Paris

2 3 DEC. 1993

Source : MNHN, Paris

Source : MNHN, Paris

The Peri-Tethys Programme, started in 1993, examines the influence of the Tethyan evolution on the bordering cratons since the birth of the Tethys Sea (through the break-up of the Pangea), its life (by the extension and formation of oceanic seaways) and finally its death (by collision between the main bordering plates which led to inversion within the epicratonic basins).

The Peri-Tethys Memoir 4, as the previous one (Peri-Tethys Memoir 3), is subdivided in two parts which correspond to the two great geographic domains involved in the Program: the Northern Platform and the Southern Platform (5 papers on each). It is mainly devoted to the Mesozoic (one paper on the Permian and one on the Cainozoic). In the first part, the first paper concerns the Jurassic ammonites and the organic matter of the Volga Basin, the second and the third papers are devoted to the Mesozoic evolution of, respectively, the Mangyshlak (Western Kazahkstan) and the Holy Cross Mountains (Poland). The fourth presents the main mid-Cretaceous events in Eastern Europe. The last paper alludes to the Cainozoic modelling of the Fore-Caucasus Basin. In the second part, the four first papers develop Jurassic stratigraphic analysis of, successively, Northern Ethiopia, Western Algeria, Levant and Morocco. Finally, the last paper approaches the Permian phyto-biostratigraphy of the Central Morocco.

Sylvie CRASQUIN-SOLEAU and Éric BARRIER (CNRS - Université Pierre et Marie Curie, Paris) coordinated this volume which follows the International Peri-Tethys Meeting held in Amsterdam (June 1996).

PERI-TETHYS PROGRAMME

PUBLICATIONS
SCIENTIFIQUES
DU MUSÉUM
57, RUE CUVIER
75005 PARIS

ISBN 2-85653-518-4
ISSN 1243-4442

300 FF TTC

Source MNHN, Paris